Diet at Herculaneum in AD 79

A high resolution approach through Compound Specific Stable Isotope Analysis of Amino Acids (CSIA-AA)

Silvia Soncin

Doctor of Philosophy

University of York

Archaeology

June 2021

Abstract

By the 1^{st} century AD, the Roman Empire had almost reached its greatest expansion and the estimated population density was unprecedented in human history. To supply such a vast territory, the state relied on an elaborate system of production and distribution, in which the Bay of Naples had a central role until the AD 79 eruption of Mount Vesuvius. This thesis applies the carbon and nitrogen isotope analysis of amino acids (CSIA-AA) to the bone collagen of the individuals who tragically perished at Herculaneum in AD 79. Indeed, this exceptional assemblage represents a unique opportunity to investigate the life of an ancient community who lived and died together in one of the central economic hubs of the Roman Empire. Carbon and nitrogen stable isotope analysis (SIA) of the bulk bone collagen has been extensively applied in archaeology allowing us to gain meaningful insights into ancient human dietary practices. However, several studies have now exposed the important limitations of SIA regarding how carbon and nitrogen from different food sources and macronutrients are registered in collagen, potentially resulting in misleading interpretations. On the contrary, CSIA-AA allows to distinguish between single signals -the amino acids- whose fractionation mechanisms are better understood. In this thesis, the results obtained by CSIA-AA were investigated using two innovative Bayesian models that incorporate knowledge of amino acid synthesis. Thanks to the joint application of CSIA-AA and Bayesian statistics, it was possible to observe that men at Herculaneum had easier access to C_3 cereals and marine fish, while women were obtaining the majority of their proteins and calories from terrestrial animal products. The high-resolution gained thanks to this approach permitted to compare the estimates obtained with those from modern Mediterranean populations, showing a similar contribution of terrestrial animal products and a three times higher contribution of protein from marine fish at Herculaneum in AD 79.

Ai miei genitori.

Acknowledgements

Firstly, I would like to sincerely thank the White Rose College of the Arts & Humanities (WRoCAH) and the Student Financial Support of the University of York for supporting this work.

I thank Parco Archeologico di Ercolano, Parco Archeologico di Pompei and all the related projects and institutions for entrusting me with such exceptional material and for believing in this study. In particular, many thanks go to Francesco Sirano, Marina Caso, Massimo Osanna, Valeria Amoretti, Luca Bondioli, Steven Ellis, Richard Jones, Andrew 'Bone' Jones and Gill Thompson. A special thanks goes to Peter Garnsey for sharing with me his unparalleled knowledge of the Roman diet and society. I would also like to thank Amy Bogaard, Michelle Alexander and Anita Radini for giving me the possibility to explore the amino acid content of modern experimental and archaeological botanical materials from Çatalhöyük, Hattusa and Roman York.

I would like to express my gratitude to my supervisors: to Professor Oliver Craig for the many advice, the funding and the invaluable support at all the stages of this work but most of all for sharing with me his exceptional enthusiasm. I will cherish the memory of those days when we realised we were getting the first exciting results out of our models; to Dr André Colonese for his interest, motivation and most of all for being my biggest supporter along the course of this journey, especially when I needed it the most. My gratitude is extended to Kirsty Penkman for her supervision and precious comments on the RP-HPLC work, to Michelle Alexander for the advice and fruitful conversations and to Kevin Walsh for chairing the thesis advisory panel. Thank you also to my examiners for taking the energy and time to read this work.

My deepest thanks go to the staff in the Department of Archaeology and especially to the technical support at BioArCh: Matt von Tersch, Krista McGrath, Luke Spindler, Sheila Taylor, Richard Hagan and Sam Presslee, thank you all for your invaluable work and support. A separate and very special thanks goes to Helen Talbot. Her incredible

expertise and dedication made the data out of this work of exceptional quality. I also thank Dr Alison Harris and Rachelle Martyn for their initial guidance with laboratory procedures and Dr Harry Robson and Jan Bakker for their help in classifying the marine specimens from Pompeii.

There are a number of people in BioArCh with whom I have worked with for quite some time and shared many happy moments. Thank you all for being the best family I could have ever wished for away from home.

I would like to express my deepest gratitude to my family, friends and especially Fabrizio for supporting me in all the possible ways. Finally, a special thank you is required for my parents, to whom this thesis is dedicated, for the infinite trust they have in me.

Declaration

This thesis is the original work of the author. This work has not been submitted for any other degree or award at any other institution. The following people contributed to this work:

- Chapter 4: Dr Helen M. Talbot assisted with GC-C-IRMS, developed the current analytical set-up and contributed to the development of data correction strategies. Dr Alison Harris adapted the NAIP derivatisation protocol. Rachelle Martyn adapted the NPIP derivatisation protocol. Matthew von Tersch assisted with EA-IRMS.
- Chapter 5: Ailsa C. Roper analysed the modern and archaeological grains via RP-HPLC.
- Chapters 5, 6 and 7: Dr Harry K. Robson and Dr Jan K. Bakker identified the fish specimens and other small bone elements from the House of the Surgeon, Pompeii and from Porta Stabia, Pompeii, respectively.

Chapter 6 in the form of a scientific article is currently under review with the following reference:

Soncin, Silvia, Talbot, Helen M., Fernandes, Ricardo, Harris, Alison, von Tersch, Matthew, Robson, Harry K., Bakker, Jan K., Ritcher, Kristine K., Alexander, Michelle, Ellis, Steven, Thompson, Gill, Amoretti, Valeria, Osanna, Massimo, Caso, Marina, Sirano, Francesco, Fattore, Luciano, Colonese, André C., Garnsey, Peter, Bondioli, Luca, Craig, Olive E. (in-review). High-resolution dietary reconstruction of victims of the AD79 Vesuvius eruption at Herculaneum by compound specific isotope analysis. *Science Advances*.

The authors contributed to the article as follows: Conceptualization: SS, OEC, LB; Methodology (isotopes): SS, HMT, AH, MVT; Methodology (morphological animal identification): HKR, JKB; Sample access and contextualization: KKR, MA, SE, GT,

VA, MO, LF, MC, FS; Data analysis: SS, OEC with support from RF; Supervision: OEC, ACC, MA; Writing—original draft: SS, OEC; Writing—review and editing: SS, OEC, ACC, PG, LB.

Silvia Soncin
June 2021

Contents

List of Figures **xiv**

List of Tables **xxii**

1 Introduction **1**

1.1 What do we still not know about the Roman diet in the Mediterranean basin? . . . 1

1.2 Why study the human skeletal assemblage from Herculaneum in AD 79? 3

1.3 Why use Compound Specific Stable Isotope Analysis of Amino Acids (CSIA-AA)? . . . 6

1.4 Aims and Objectives . . . 7

1.4.1 Aims . . . 7

1.4.2 Objectives . . . 7

1.5 Thesis Structure . . . 8

2 Diet during the Roman Imperial period and the case study of Herculaneum **10**

2.1 What did the Romans eat in the Mediterranean basin? . . . 10

2.1.1 Sources of evidence . . . 11

2.1.2 Cereals . . . 15

Naked wheats . . . 15

The "inferior" cereals . . . 16

2.1.3 Legumes . . . 18

2.1.4 Terrestrial animals . . . 19

2.1.5 Vegetable and fruits . . . 22

2.1.6 Olive oil and wine . . . 24

2.1.7 Marine resources . . . 26

2.2 The archaeological context: Herculaneum and the Bay of Naples in the 1^{st} century AD . . . 29
2.2.1 Herculaneum . . . 30
The eruption of Mount Vesuvius . . . 32
A brief history of the excavations . . . 34
The town layout . . . 37
Who lived at Herculaneum? . . . 38
2.3 The catastrophic death assemblage . . . 41
2.3.1 The recovery of a scene of human tragedy . . . 41
2.3.2 Not an *osteological paradox* . . . 42
2.3.3 The studies on the individuals from the beachfront . . . 45
2.3.4 The studies on the individuals from the *fornici* . . . 50
2.3.5 Studies around the manner of death . . . 54
2.4 Conclusion . . . 56

3 Dietary studies and stable isotopes analyses: a review 58
3.1 Stable isotopes in Archaeology . . . 58
3.1.1 Carbon stable isotopes and dietary implications . . . 61
Carbon stable isotopes of bone collagen . . . 64
Carbon stable isotopes of bone apatite . . . 65
3.1.2 Nitrogen stable isotopes and dietary implications . . . 66
Nitrogen stable isotopes of bone collagen . . . 69
3.1.3 Application of carbon and nitrogen stable isotope analysis in the Roman Mediterranean basin . . . 70
Rome . . . 72
Campania . . . 77
Outside Italy . . . 78
Sex-based differences . . . 79
Social status-based differences . . . 80
On tracking marine fish consumption in the Roman Mediterranean: AD 79 Herculaneum . . . 81
3.1.4 Quantitative interpretation of carbon and nitrogen stable isotope data: Mixing Models . . . 85
3.2 Compound Specific Isotope Analysis of Amino Acids . . . 87
3.2.1 Previous studies . . . 88
3.2.2 The biochemistry of amino acids . . . 96
The carbon metabolic pool . . . 98

The nitrogen metabolic pool . . . 101
3.2.3 Amino acid composition of bone collagen . . . 102
3.3 Conclusion . . . 104

4 Experimental and analytical protocols for Compound Specific Stable Isotope Analysis of Amino Acids (CSIA-AA) 106
4.1 Experimental . . . 106
4.1.1 Experimental design and sampling strategy . . . 107
4.1.2 Collagen extraction . . . 108
4.1.3 Preparation of amino acid standard mixtures and internal standard 108
4.1.4 Hydrolysis and defatting . . . 109
4.1.5 Derivatisation . . . 110
Preparation of *N*-acetyl-*i*-propyl esters (NAIP) . . . 111
Preparation of *N*-pivaloyl-*i*-propyl esters (NPIP) . . . 112
4.1.6 Extraction of amino acids from grains . . . 113
4.2 Instrumentation . . . 114
4.2.1 Analysis of the bulk material: EA-IRMS . . . 114
4.2.2 Analysis of amino acids: GC-C-IRMS . . . 116
4.3 Data correction and error propagation . . . 118
4.3.1 δ^{15}N data: calibration curve and norleucine correction . . . 118
4.3.2 δ^{13}C data: correction for norleucine and external carbon . . . 118
4.4 Assessing the quality of GC-C-IRMS data . . . 122
4.4.1 Pro-Hyp . . . 122
4.4.2 Mass balance . . . 123
4.4.3 Bovine control sample . . . 124
4.4.4 Derivative stability . . . 125
Carbon isotopes . . . 126
Nitrogen isotopes . . . 126
4.5 Conclusion . . . 129

5 Establishing a baseline for diet at AD 79 Herculaneum 130
5.1 Stable isotope analysis of cereals and pulses . . . 131
5.1.1 Protein and amino acid composition of cereals and pulses - what to expect . . . 132
5.1.2 Experimental design and Materials . . . 134
5.1.3 Methods . . . 134
5.1.4 Results . . . 136

Amino acid content . . . 136
Amino acid racemisation . . . 139
5.1.5 A possible solution: estimation of amino acid δ^{13}C and δ^{15}N values from their bulk values . . . 142
5.1.6 Final considerations on stable isotope analysis of amino acids from archaeological grains . . . 144
5.2 Exploring food webs in the Roman Mediterranean . . . 145
5.2.1 ZooMS analysis to clarify taxonomy of bone samples . . . 146
Method . . . 147
Results . . . 148
5.2.2 SIA and CSIA-AA results and discussion . . . 151
SIA . . . 151
CSIA . . . 154
5.3 Conclusion . . . 163

6 High-resolution dietary reconstruction of victims of the AD79 Vesuvius eruption at Herculaneum by compound specific isotope analysis 165
6.1 Abstract . . . 166
6.2 Main . . . 166
6.2.1 Introduction . . . 166
6.2.2 Results . . . 170
6.2.3 Discussion . . . 176
6.2.4 Materials and Methods . . . 177
Experimental Design . . . 177
Collagen extraction . . . 177
Elemental Analysis Isotope Ratio Mass Spectrometry (EA-IRMS) 178
Preparation of AAs for GC-C-IRMS . . . 178
Gas Chromatography-Combustion-Isotope Ratio Mass Spectrometry (GC-C-IRMS) . . . 179
δ^{15}N measurements of amino acids . . . 180
δ^{13}C measurements of amino acids . . . 180
Analysis of modern and archaeological cereals . . . 181
Statistical Analysis . . . 182
6.3 Supplementary Materials and Methods . . . 183
6.3.1 Quality Control (QC) . . . 183
6.3.2 QC1: Mass Balance of amino acids δ^{13}C and δ^{15}N values . . . 183
6.3.3 QC2: Bovine Control . . . 183

6.3.4 QC3: comparison of proline and hydroxyproline δ^{13}C and δ^{15}N values . . . 184
6.3.5 Description of mixing models and parameters used . . . 184
6.3.6 USDA Standard References . . . 188

7 Results and discussion 189
7.1 Advantages of using CSIA-AA to investigate the Roman Mediterranean diet . . . 189
7.1.1 Problems with interpreting diet at Herculaneum (and in the Roman Mediterranean) using the bulk SIA approach . . . 190
7.1.2 Potential of including δ^{13}C values of bone apatite in the dietary investigations in the Mediterranean: a pilot study . . . 192
Results and discussion . . . 195
7.1.3 Diet at Herculaneum in AD 79: the CSIA-AA approach . . . 201
Marine food consumption revealed . . . 202
Legume consumption at Herculaneum . . . 209
Olive oil calorific contribution at Herculaneum . . . 212
7.2 New pieces to the puzzle: who was living at Herculaneum? . . . 214
7.3 Conclusion . . . 219

8 Conclusions and suggestions for future research 221
8.1 Advantages of using CSIA-AA over bulk SIA in Mediterranean archaeological contexts . . . 222
8.2 Reconstruction of diet at Herculaneum through CSIA-AA . . . 223
8.3 Future directions . . . 226

Bibliography 228

Appendix A Carbon and Nitrogen stable isotope studies from the Roman Mediterranean 261

Appendix B CSIA-AA protocol - BioArCh, University of York 286

Appendix C Standards and Bovine controls 309

Appendix D Bulk SIA and CSIA results 323
D.1 Archaeological grains . . . 323
Cereals from Roman York . . . 323
Grains from Bronze Age and Neolithic Turkey . . . 324

Appendix E Supplementary Material to Soncin *et al.* 2021 - Chapter 6 344

Appendix F Principal Component Analysis 396

List of Figures

2.1 Still life frescoes from the House of the Deer, Herculaneum. From the left: capon with hare; partridge with apple and pomegranate; Song thrushes and mushrooms of the genus *Agaricus*; partridges and morays. Museo Archeologico Nazionale di Napoli, Naples. 13

2.2 Loaf of bread from the territories of the AD 79 eruption. Photo taken by the author at the "Res rustica. Archeologia, botanica e cibo nel 79 d.C." temporary exhibition, 21/09/2018-18/02/2019. Museo Archeologico di Napoli, Naples, Italy. 16

2.3 Triangular graphs showing relative frequencies of cattle, ovicaprid and pig bone remains from different Imperial Roman archaeological sites. Modified after King (1999). 19

2.4 Mammal bones recovered in Italy (a) and in the Provinces (b) through the centuries. Modified after Jongman (2007). 21

2.5 Section of a painted sign at the entrance of a shop of *Insula IV*, Herculaneum, reporting the price of the wines: AD CUCUMAS / A.IIIIS / IIIS / IIIISS/ IIS. Modified after Jebulon, CC0, via Wikimedia Commons. 26

2.6 Mosaic from the House of the Faun in Pompeii representing marine fauna. Central of the scene is the fight between and octopus and a lobster, while various marine species set on the side. Among the others: a crayfish, a mullet, a sea bass, a murex, a moray, a scorpion-fish, a gilt-head bream and a ray. Museo Archeologico Nazionale di Napoli, Naples. 27

2.7 Physical map of the ancient Campania. Modified after Frederiksen and Purcell (1984). 31

2.8 Location of Herculaneum in the Bay of Naples. From Google earth 2020. 33

2.9 Archive photos of Herculaneum under the superintendency of Amedeo Maiuri (1927-1961). The shop of Priapus (a) and the shop of the House of Neptune and Amphitrite (b) with finds on display in an attempt of creating an "open-air" museum. Modified after Camardo (2006)(a) and Maggi (2013)(b). 36

2.10 Archive photo of the recovery of the first skeleton from the ancient Herculaneum seashore on 21^{st} May 1980. Modified after Maggi (2013). 36
2.11 Plan of the ancient town of Herculaneum with differentiation between public spaces (blue), private houses (grey), houses with commercial units attached (white) and commercial spaces (red). Modified after Monteix (2010). 38
2.12 Plan of the ancient town of Herculaneum showing the Theatre (north-west) and the Villa of the Papyri (south-west). Modified after Guidobaldi *et al.* (2014). 39
2.13 Some fragments of the *Album* of Herculaneum. Modified after de Ligt and Garnsey (2012). 40
2.14 View of the ancient town of Herculaneum from the entrance to the archaeological site, with Mount Vesuvius in the background. The vaulted chambers (*fornici*), where a large part of the catastrophic death assemblage was discovered, are visible at the bottom of the photo, below the Suburban Baths (right) and the Sacred Area (left) and divided by the stairs that connect the ancient seashore to the town. Photo by Laura Soncin, 2^{nd} September 2020. 43
2.15 View of the inside of one of the twelve *fornici*. Modified after Maggi (2009). 44
2.16 Photos of the boat recovered from the ancient Herculaneum seashore while being excavated (a, showing Giuseppe Maggi pointing at a skeleton found close to the boat and therefore named "the Helmsman") and after being restored and displayed in the "boat Pavillion" at the entrance of the archaeological site (b). Modified after Maggi (2013)(a) and personal photo by the author (b), 2^{nd} September 2020. 44
2.17 Drawing showing the distribution of the skeletons on the seashore and inside the boat chambers. Modified after Wallace-Hadrill (2011) 45
2.18 Correlation between age at death and ^{19}F content of bones of the individuals from the Herculaneum *fornici*. The clinical phases reported on the graph indicate the degree of skeletal fluorosis. Modified after Petrone *et al.* (2011). The colours were not explained by the authors. 53
2.19 Population pyramids for the Herculaneum assemblage created on the first (a) and second (b) set of excavated individuals and on the whole sample (c). Modified after Fattore *et al.* (2012) 53
2.20 Crystallinity values of the individuals from the vaulted chambers of the ancient Herculaneum seashore (grey) and Velia (black, n=4) with those from controlled charring experiments (from red to blue, as in the legend). Modified after Martyn *et al.* (2020) 55

3.1 Carbon natural cycle. One-way arrows show CO_2 path, while two-way arrows the steady-state of isotopic fractionation. Numbers refer to δ^{13}C ‰ values; numbers associated with two-way arrows refer to the fractionation (Δ) happening during the reaction. POM, particulate organic matter; DOM, dissolved organic matter. Modified after Peterson and Fry (1987). 63

3.2 Correlation between δ^{13}C of bone apatite and δ^{13}C of bulk diet in mice, rats and pigs fed on controlled diet (DeNiro and Epstein 1978; Ambrose and Norr 1993; Tieszen and Fagre 1993; Howland *et al.* 2003; Jim *et al.* 2004; Warinner and Tuross 2009). . 66

3.3 Nitrogen natural cycle. One-way arrows show N_2 and its derivates path, while two-way arrows show the steady-state of isotopic fractionation. Numbers refer to δ^{15}N ‰ values; numbers associated with two-way arrows refer to the fractionation (Δ) happening during the reaction. POM, particulate organic matter; DOM, dissolved organic matter. Modified after Peterson and Fry (1987). 68

3.4 δ^{13}C and δ^{15}N mean values ($\pm 1\sigma$) of Imperial Roman populations and animal and domestic plant remains from the Mediterranean basin (a). Figure b is the same as Figure a but with a focus on the human individuals to help the visualisation of the data. 73

3.5 Location of the human populations in the proximity of Rome subject to carbon and nitrogen stable isotope analysis. CM: Castel Malnome, CE: Castellaccio Europarco, CB: Casal Bertone, PS: Via Padre Semeria, QCP: Quarto Cappello del Prete. From Google earth 2021. 75

3.6 Location of Roman human assemblages from the Mediterranean basin. Herc: Herculaneum, Pom: Pompeii, Pa: Paestum, Ve: Velia. From Google earth 2021. 78

3.7 Carbon isotope values from the human assemblage of Herculaneum against marine protein contribution (%). The models based on 1:1 scrambling of macronutrients and protein routing and total scrambling better explain the isotopic values observed in the individuals from Herculaneum, both when protein contribution from terrestrial animal products is included (A) or not (B). Modified after Craig *et al.* (2013). . . . 83

3.8 Dietary variations across the human assemblage of AD 79 Herculaneum. The kernel density plot (a) shows different marine contribution to dietary carbon in males and females; the boxplot of δ^{15}N values divided by sex and age shows higher values in older adult males, suggesting higher marine consumption. Modified after Martyn *et al.* (2018). 84

3.9 Comparison of the estimates of marine and terrestrial carbon contribution to the diet of nine individuals from AD 79 Herculaneum using a non-routed and concentration independent mixing model (*Scenario 1*) and a routed and concentration-dependent mixing model (*Scenario 2*) with those observed by Craig *et al.* (2013). Modified after Fernandes (2016). 88
3.10 Correlation between δ^{13}C values of alanine in bone collagen and δ^{13}C values of the energy components of diet from three different feeding experiments. Data from Howland *et al.* (2003); Jim *et al.* (2006); Webb *et al.* (2017). 92
3.11 L and D structure of a general amino acid. Black arrows represent bonds coming out of the paper and shaded arrows those coming in. Modified after Lieberman *et al.* (2013). 97
3.12 Overview of the biosynthesis and degradation of amino acids referred as the "carbon metabolic pool" in the text. Amino acids are in bold. Essential amino acids are highlighted with a grey background. Dotted lines identify reactions that do not directly involve amino acids. 99
3.13 Overview of the main pathways of nitrogen exchange of amino acids (modified after O'Connell (2017) and Braun *et al.* (2014)). 101
3.14 The nonhemo iron enzyme 4-hydroxylase (P4H) catalyses the hydroxilation reaction of Pro in $Y_{(aa)}$ position to form 4-hydroxyproline. Modified from Shoulders and Raines (2009) 103

4.1 GC-C-IRMS profiles of collagen amino acid from a modern bovine sample prepared following the NPIP (a) and the NAIP techniques (b). 111
4.2 GC-C-IRMS profiles of amino acid from a modern grain prepared following the NAIP techniques in nitrogen (a) and carbon (b) mode, without using a cation-exchange resin for amino acid purification. 115
4.3 GC-C-IRMS profiles of hydroxyproline and phenylalanine from collagen NAIP derivatives using a 30 M (a) and a 60 M (b) DB-35 column. 118
4.4 True and raw δ^{15}N mean values and standard deviation of the amino acid international standards ($n = 181$) and Sigma Nle ($n = 175$) used to normalise the data. 119
4.5 Correlation between the corrected amino acid standard δ^{13}C values of the "carbon mixture" by the mean correction factors calculated from the standard amino acid of the "nitrogen mixture" and the true δ^{13}C values of the amino acid standards measured in-house via EA-IRMS. 120
4.6 Correlation of estimated and measured bulk collagen δ^{13}C values without (a) and with (b) internal standard correction prior that for single correction factors. 121

4.7 Cross plots of δ^{13}C (a) and δ^{15}N (b) values of proline and hydroxyproline of the samples analysed for this thesis. 122
4.8 Correlation of estimated and measured bulk collagen δ^{13}C (a) and δ^{15}N (b) values. The estimated collagen values were obtained by mass balance calculation considering the single amino acid isotope values and their relative contribution to collagen carbon and nitrogen. 124
4.9 δ^{13}C values of collagen amino acids from two modern bovine derivatives (BVCR117 and BVCR7117) analysed within (week 9) and outside (week 33) the suggested 12 weeks storage period (Corr *et al.* 2007b,a). The δ^{13}C values have been divided in two separate graphs containing non-essential (a) and essential (b) amino acids to facilitate visualisation. 127
4.10 GC-C-IRMS profiles of modern bovine collagen amino acids from the same NAIP derivative analysed within (a) and outside (b) the suggested 12 weeks storage period (Corr *et al.* 2007b,a). 127
4.11 δ^{15}N values of collagen amino acids from three bovine controls derivatives run after 21 (light blue diamonds), 30 (red diamonds) and 49 (green and purple diamonds) weeks and compared to the average ($\pm$ 2σ) of bovine controls (n = 12) analysed within the suggested 12 weeks storage period (black circles). 128
4.12 GC-C-IRMS profiles of modern bovine collagen amino acids from analysed within 12 weeks (black profile) and after 49 weeks (blue profile) from derivatisation. 128

5.1 Examples of RP-HPLC profiles of a modern uncharred (a) and of an archaeological charred (b) sample. In b it is visible the baseline rise at *ca.* 54 *min* onwards characteristic of all the charred samples here analysed. 137
5.2 Absolute (a) and relative (b) content of amino acids in modern uncharred, modern charred and archaeological grains analysed via RP-HPLC. 138
5.3 D/L values of glutamic acid (Glx) and aspartic acid (Asx) of modern uncharred, modern charred and archaeological grains (a) and D/L values of glutamic acid and aspartic acid of only archaeological grains (b). Asx D/L values of three of the samples from Roman York (b) are *ca.* half of the Glx D/L values, perhaps indicating a different decay mechanism. 140
5.4 MALDI-TOF-MS profile of the three samples from Porta Stabia identified as *Gallus gallus* by morphological analysis. 149
5.5 Bulk δ^{13}C and δ^{15}N of plant and fauna remains from Herculaneum and comparable archaeological contexts: a, divided by groups; b, only terrestrial animals; c, only marine fish. 152

5.6 $\delta^{15}N_{Phe}$ and $\delta^{15}N_{Glx}$ values of cereals, terrestrial herbivores, terrestrial omnivores and marine fish from Herculaneum and comparable archaeological contexts. Dashed lines identify terrestrial trophic levels, dotted lines identify marine trophic levels . . 155

5.7 $\delta^{15}N_{Phe}$ and $\delta^{15}N_{Glx}$ (b) and $\delta^{13}C_{Val}$ and $\delta^{13}C_{Phe}$ values of cereals and terrestrial animals from Herculaneum and comparable archaeological contexts. Dashed lines identify terrestrial trophic levels. The line in b identifies y= x. 156

5.8 $\delta^{15}N_{Phe}$ and $\delta^{15}N_{Glx}$ (a) and $\delta^{15}N_{Phe}$ and $\delta^{15}N_{Asx}$ (b) values of marine fish from Pompeii in the 1^{st} century AD and comparable archaeological contexts. Dashed lines identify marine trophic levels. 159

5.9 $\delta^{13}C$ values of essential amino acids in marine fish from 1^{st} century AD Pompeii and comparable archaeological contexts. 162

6.1 View of skeletal remains in one of the vaulted chambers (*fornici*) during excavation. Photo Credit: Luciano Fattore, Sapienza Università di Roma. 167

6.2 Rationale for metabolic model parameters. Carbohydrates, lipids and proteins all contribute to the "Metabolic Carbon Pool": carbon in alanine, serine and glycine has a glycolytic origin which is directly linked to carbohydrate digestion; glutamic acid and aspartic acid are synthesised via transamination through the TCA cycle from all macronutrients (Howland *et al.* 2003). Dietary protein is considered to be the only source of nitrogen, with glutamic acid the source of nitrogen for other trophic AAs (O'Connell 2017). "Source" AAs incorporated directly from diet with negligible isotopic fractionation are indicated by dashed circles. Isotope values for AAs labelled M1, M2 are used in *Model 1* and *Model 2* respectively. Ala: alanine, Gly: glycine, Val: valine, Leu: leucine, Ile: isoleucine, Thr: threonine, Ser: serine, Pro: proline, Asx: aspartic acid/asparagine, Glx: glutamic acid/glutamine, Phe: phenylalanine, Lys: lysine, Tyr: tyrosine, His: histidine, Arg: arginine. 169

6.3 Dietary estimates for 17 individuals from Herculaneum under different scenarios. Estimates were obtained using a concentration dependent Bayesian mixing model. a) *Model 0p* - SIA, protein routed model. b) *Model 1* – CSIA, protein model. c) *Model 0wd* – SIA, whole diet model. d) *Model 2* – CSIA, whole diet model. Boxes represent a 68% credible interval (corresponding to the 16^{th} and 84^{th} percentiles) while the whiskers represent a 95% credible interval (corresponding to the 2.5^{th} and 97.5^{th} percentiles). The horizontal continuous line represents the estimated median (50th percentile). Orange = females, blue = males, grey = outcomes based on average AAs isotopic values of the 17 individuals. Equivalent proportions of protein and calorie supplied to modern Mediterranean populations between 1961-1963 (grey circles) and 1998-2000 (black circles) are shown, with bars representing 1σ (Balanza *et al.* 2007). 172

6.4 'Raincloud' plots of dietary estimates for 17 individuals from Herculaneum grouped by sex. Estimates were obtained using a concentration dependent Bayesian mixing model. a) *Model 1* – CSIA, protein model. b) *Model 2* – CSIA, whole diet model. The rainclouds show the raw outputs of each model alongside the means and standard deviations and the probability density of the distribution. Non-parametric Wilcox test (two-sided) shows statistical differences for all the food sources across sex when applied to both *Model 1* and *Model 2* (p-values < 0.05, Table S5). 174

7.1 δ^{15}N and δ^{13}C values of human individuals from Herculaneum (only the nineteen individuals analysed in this study) compared with mean values of cereals, legumes and animals from comparable archaeological contexts. Error bars represent 1σ. . . 192

7.2 $\delta^{13}C_{collagen}$ and $\delta^{13}C_{apatite}$ values of eight individuals from Herculaneum and nine fauna remains plotted against experimental animal regression lines and their 95% confidence intervals (a) and discriminant function F1 and F2 scores calculated using $\delta^{13}C_{collagen}$, $\delta^{15}N_{collagen}$ and $\delta^{13}C_{apatite}$ values against clusters of animals from feeding experiments and archaeological populations (b) (Froehle *et al.* 2010, 2012). Mean $\delta^{13}C_{collagen}$, $\delta^{15}N_{collagen}$ and $\delta^{13}C_{apatite}$ values ($\pm$ 1σ) from other Mediterranean Roman context are also included (Prowse *et al.* 2004, 2005; Keenleyside *et al.* 2009; Killgrove and Tykot 2013, 2018; Dotsika and Michael 2018). 197

7.3 $\delta^{13}C_{apatite}$ values of human individuals from Herculaneum and nine animals from comparable contexts against collagen $\delta^{13}C_{Ala}$ (a) and $\delta^{13}C_{Glx}$ (b) values. 199

7.4 δ^{13}C values of glycine from Herculaneum human individuals, cereals, animals and marine fish from comparable contexts against the δ^{13}C values of the essential amino acids phenylalanine (a) and leucine (b). 203

7.5 δ^{13}C values of glycine from Herculaneum human individuals, cereals, animals and marine fish from comparable contexts against the δ^{13}C values of the essential amino acids phenylalanine (a) and leucine (b). 204

7.6 δ^{15}N values of glutamic acid against the δ^{15}N values of phenylalanine (a) and δ^{15}N values of threonine against the offset $\delta^{15}N_{Glx-Phe}$ values (b) from Herculaneum human individuals, cereals, animals and marine fish from comparable contexts. . . 205

7.7 Principal component analysis of δ^{15}N and δ^{13}C of source (PCA-SAA, a, b, c and d) and source and trophic (PCA-TAA, e, f, g and h) amino acids of the human, animal and cereal samples object of this study. The principal component 1 (PC1) values are plotted against those of principal component 2 (PC2) (Figures a and b for PCA-SAA and e and f for PCA-TAA) and those of principal component 3 (PC3) (Figure c and d for PCA-SAA and g and h for PCA-TAA). To facilitate the visualisation of the data, the vectors have been plotted in separate graphs (Figures b, d, f and h).) . . 208

7.8 Violin plots describing the protein contribution (%) of C_3 cereals, legumes, terrestrial animals and marine fish to seventeen individuals from Herculaneum grouped by gender. The violin represents the kernel density mirrored on each side. Circles represent the mean; bars represent 1σ. 211

7.9 Violin plots describing the calorific contribution (%) of C_3 cereals, marine fish, olive oil and terrestrial animals to seventeen individuals from Herculaneum grouped by gender. The violin represents the kernel density mirrored on each side. Circles represent the mean; bars represent 1σ. 213

7.10 Violin plots describing the protein contribution (%) of C_3 cereals, terrestrial animals and marine fish to female, male under 30 year old and male above 30 year old individuals from Herculaneum. The violin represents the kernel density mirrored on each side. Circles represent the mean; bars represent 1σ. 217

E.1 GC-C-IRMS chromatograms of amino acids from archaeological bone collagen, in nitrogen mode (a) and carbon mode (b). See section 6.2.4 "Materials and Methods" for details. Ala: alanine, Gly: glycine, Val: valine, Leu: leucine, Ile: isoleucine, Nle: norleucine, Thr: threonine, Ser: serine, Pro: proline, Asp: aspartic acid, Glu: glutamic acid, Hyp: hydroxyproline, Phe: phenylalanine, Lys: lysine, Tyr: tyrosine. 345

E.2 GC-C-IRMS chromatograms of amino acids from modern grains, in nitrogen mode (a) and carbon mode (b). See section 6.2.4 "Materials and Methods" for details. Ala: alanine, Gly: glycine, Val: valine, Leu: leucine, Ile: isoleucine, Nle: norleucine, Thr: threonine, Ser: serine, Pro: proline, Asp: aspartic acid, Glu: glutamic acid, Hyp: hydroxyproline, Phe: phenylalanine, Lys: lysine, Tyr: tyrosine. 346

E.3 Scatter plot of nitrogen isotope ratios of phenylalanine and glutamic acid. Predicted values for terrestrial and marine trophic levels are shown. 347

E.4 Comparison of dietary marine contribution estimates from CSIA and AMS dating. Orange - % contribution of dietary calories derived from marine source, estimated using Model 2 above. Blue - % contribution of collagen carbon derived from a marine source, estimated from the measured and predicted marine reservoir ages (Craig *et al.* 2013; Martyn *et al.* 2018). Error bars represent 1σ. The errors for the marine carbon estimations are based on the error of the maximum marine reservoir age for the region (*i.e.*, 390 ± 30 years from Craig *et al.* (2013). 347

E.5 Quality control assessment. Bivariate plots showing correlations between bulk collagen stable isotope values estimated (EST) based on the proportional contribution of each amino acid determined by GC-C-IRMS and observed (OBS) by bulk EA-IRMS for $\delta^{15}N$ (a) and $\delta^{13}C$ (b). Bivariate plots showing the relationship between proline and hydroxyproline measured in the same samples for $\delta^{15}N$ (c) and $\delta^{13}C$ (d). 348

List of Tables

3.1 Observed $\Delta^{13}C_{collagen-diet}$ values from feeding experiment studies (Hare *et al.* 1991; Ambrose and Norr 1993; Tieszen and Fagre 1993; Howland *et al.* 2003; Jim *et al.* 2004; Warinner and Tuross 2009; Webb *et al.* 2017). Bottom three lines represent mean and 1σ of the three groups of diets discussed in the text. Here, the source indicated in the dietary fraction (*e.g.*, C_3) represents either the totality (*e.g.*, 100% C_3) or the majority (*e.g.*, $\geq 50\% C_3$) of that fraction. Modified from Froehle *et al.* (2010) after inclusion of Webb *et al.* (2017). 67

3.2 Observed $\Delta^{15}N_{collagen-diet}$ values from feeding experiment studies (DeNiro and Epstein 1981; Hare *et al.* 1991; Ambrose 2000; Young 2003; Warinner and Tuross 2009; Webb *et al.* 2016b; Kendall *et al.* 2017). Bottom two lines represent mean and 1σ of all the experiments and of swine only experiments. 71

3.3 Descriptive statistics (dplyr, R version 4.0.2) of Imperial Roman populations and of domestic herbivores, wild herbivores, domestic omnivores, marine fish, C_3 cereals and legumes from the Mediterranean basin. References: 1= Prowse *et al.* (2004), 2= Prowse *et al.* (2005), 3=Lagia (2015), 4= Rissech *et al.* (2016), 5= Killgrove and Tykot (2013), 6= De Angelis *et al.* (2020a), 7=Lightfoot *et al.* (2012), 8=Dotsika and Michael (2018), 9= Killgrove and Tykot (2018), 10=Martyn *et al.* (2018), 11= Crowe *et al.* (2010), 12= Keenleyside *et al.* (2009), 13=Tafuri *et al.* (2018) 14= Ricci *et al.* (2016), 15= Pate *et al.* (2016), 16=Baldoni *et al.* (2019) 17= De Angelis *et al.* (2020b), 18= Craig *et al.* (2009), 19=O'Connell *et al.* (2019). 74

3.4 Amino acid occurrence in collagen type I. Alpha-1 (CO1A1_HUMAN, P02452) and Alpha-2 (CO1A2_HUMAN, P08123) type I collagen sequences from the Swiss-Prot database (Boeckmann *et al.* 2003) using ProtParam (Gasteiger *et al.* 2005). Ala: alanine, Arg: arginine; Asx: aspartic acid/asparagine, Cys: cysteine, Glx: glutamic acid/glutamine, Gly: glycine, His: histidine, Ile: isoleucine, Leu: leucine, Lys: lysine, Met: methionine, Phe: phenylalanine, Pro: proline, Hyp: hydroxyproline, Ser: serine, Thr: threonine, Trp: tryptophan, Tyr: tyrosine, Val: valine. 104

5.1 Macronutrient composition of cereal and legume grains expressed as dry weight (%). Data collected and elaborated from USDA National Nutrient Database for Standard Reference (which can be accessed at this link). *NDB* is the identifier for the item in the USDA Database. 133
5.2 List of modern and archaeological samples analysed via RP-HPLC. 135
5.3 Relative amino acid contribution in modern uncharred, modern charred and archaeological charred grain samples. 139
5.4 $\Delta^{15}N_{AA-bulk}$ and $\Delta^{13}C_{AA-bulk}$ values of modern C_3 and C_4 cereals and legumes analysed for this project (referred to as "this study") and from two previous studies (Styring *et al.* 2014a; Paolini *et al.* 2015). The error associated to the measurements from this study where $n > 1$ is the error propagated that accounts for the highest analytical error among the samples from the GC-C-IRMS analysis and 1σ of the AA-bulk values of the samples. 143
5.5 ZooMS identification of the terrestrial animal remains included in this study on the basis of collagen peptide markers. 150
5.6 Trophic levels of archaeological marine fish remains according to the FishBase database and those estimated with equation 3.6 using the β_{T-S} and the Δ_{T-S} values at the bottom of the marine food web reported by Chikaraishi *et al.* (2009) and by Nielsen *et al.* (2015) for Glx-Phe and Asx-Phe, respectively. The morphological identification of the marine fish and the estimation of their total length (cm) were carried out by Dr H. K. Robson for the remains from the House of the Surgeon (Pompeii) and by Dr J. K. Bakker for those from Porta Stabia (Pompeii). See Appendix D Table 5.2.2 for sample provenance and chronology. 161

7.1 Descriptive statistics (dplyr, R version 4.03) of the nineteen human individuals from Herculaneum included in this thesis and of the herbivore and omnivore animals, marine fish, C_3 and C_4 cereals and the legumes analysed as a reference for the human data. *: Only one millet sample was analysed as representative of the C_4 cereal group. 193
7.2 Preservation indices values (IRSF and C/P) of the pre- and post-treated human samples and $\delta^{13}C_{Ap}$ and $\delta^{18}O_{Ap}$ values of the post-treated samples analysed by CF-IRMS. *Samples excluded from the discussion. 196
7.3 Relative protein and calorific contribution of cereals, terrestrial animals, legumes and marine fish to the diet of modern Mediterranean populations (Balanza *et al.* 2007) and Herculaneum, the latter estimated using two Bayesian mixing models as described in the text. 212

A.1 $\delta^{13}C$ and $\delta^{15}N$ values of the human individuals from Imperial Roman Mediterranean contexts. AN: ANAS, At: Athens, Ba: Barcelona; CB: Casal Bertone, CM: Castel Malnome, CE: Castellaccio Europarco, Cr: Croatia, Ed: Edessa, Ga: Gabii, He: Herculaneum, IS: Isola Sacra, Le: Leptiminus, LF: Lucus Feroniae, Pa: Paestum, Pom: Pompeii; Pr: Praeneste, QCP: Quarto Cappello del Prete, Ve: Velia, VPS: Via di Padre Semeria. 278

A.2 p-values obtained by applying the non-paramentric Pairwise Wilcoxon Rank Sum Test (R version 4.0.3) adjusted by Bonferroni for multiple testing to the $\delta^{13}C$ values. Results were considered significant when $p \leq 0.05$ (highlighted in bold). AN: ANAS, At: Athens, Ba: Barcelona; CB: Casal Bertone, CM: Castel Malnome, CE: Castellaccio Europarco, Cr: Croatia, Ed: Edessa, Ga: Gabii, He: Herculaneum, IS: Isola Sacra, Le: Leptiminus, LF: Lucus Feroniae, Pa: Paestum, Pom: Pompeii; Pr: Praeneste, QCP: Quarto Cappello del Prete, Ve: Velia, VPS: Via di Padre Semeria. 279

A.3 p-values obtained by applying the non-paramentric Pairwise Wilcoxon Rank Sum Test (R version 4.0.3) adjusted by Bonferroni for multiple testing to the $\delta^{15}N$ values. Results were considered significant when $p \leq 0.05$ (highlighted in bold). AN: ANAS, At: Athens, Ba: Barcelona; CB: Casal Bertone, CM: Castel Malnome, CE: Castellaccio Europarco, Cr: Croatia, Ed: Edessa, Ga: Gabii, He: Herculaneum, IS: Isola Sacra, Le: Leptiminus, LF: Lucus Feroniae, Pa: Paestum, Pom: Pompeii; Pr: Praeneste, QCP: Quarto Cappello del Prete, Ve: Velia, VPS: Via di Padre Semeria. 280

A.4 $\delta^{13}C$ and $\delta^{15}N$ values of animal and wheat remains analysed from Imperial Roman Mediterranean contexts. Ba: Barcelona; CM: Castel Malnome, Col: Colosseum, Cr: Croatia, IS: Isola Sacra, Le: Leptiminus, LF: Lucus Feroniae, Po: Portus Romae, Pod: $V^{th} - VI^{th}$ centuries AD Portus Romae, Pom: Pompeii, Ve: Velia, VPS: Via di Padre Semeria. Horse and donkey specimens were not included in the statistical analyses since these species were probably not preferentially consumed. 283

A.5 p-values obtained by applying the non-paramentric Pairwise Wilcoxon Rank Sum Test (R version 4.0.3) adjusted by Bonferroni for multiple testing to the $\delta^{13}C$ values of the animals divided by group. Results were considered significant when $p \leq 0.05$ (highlighted in bold). Ba: Barcelona; CM: Castel Malnome, Col: Colosseum, Cr: Croatia, IS: Isola Sacra, Le: Leptiminus, LF: Lucus Feroniae, Po: Portus Romae, Pod: $Vth - VIth$ centuries AD Portus Romae, Pom: Pompeii, Ve: Velia, VPS: Via di Padre Semeria. 284

A.6 p-values obtained by applying the non-paramentric Pairwise Wilcoxon Rank Sum Test (R version 4.0.3) adjusted by Bonferroni for multiple testing to the $\delta^{15}N$ values of the animals divided by group. Results were considered significant when $p \leq 0.05$ (highlighted in bold). Ba: Barcelona; CM: Castel Malnome, Col: Colosseum, Cr: Croatia, IS: Isola Sacra, Le: Leptiminus, LF: Lucus Feroniae, Po: Portus Romae, Pod: $Vth - VIth$ centuries AD Portus Romae, Pom: Pompeii, Ve: Velia, VPS: Via di Padre Semeria. 285

C.1 List of the standards used for GC-C-IRMS analysis and their "true" values. The $\delta^{13}C$ and $\delta^{15}N$ (‰) values of the international standards are those provided by the supplier. The $\delta^{13}C$ and $\delta^{15}N$ (‰) values of the Sigma standards were measured at BioArCh by EA-IRMS. Three Sigma L-Norleucine were opened and used as internal standards for the duration of this project. 310

C.2 International standards' raw $\delta^{15}N$ values. Norleucine (Nle) International was only used in the first run (17/11/17). For all the other runs, the Nle used was the one purchased from Sigma-Aldrich. 313

C.3 Sigma standards' raw $\delta^{13}C$ values. 319

C.4 Carbon amino acid values ($\delta^{13}C_{AA}$) of modern cattle samples used as controls during the analysis (referred to as "bovine controls")."Err." refers to the measurement uncertainty as explained in the main text. The bulk values were measured by EA-IRMS. The estimated bulk values were derived by mass balance calculations as explained in the main text and the error associated (Err.) is the error propagated from all the amino acid measurements. 321

C.5 Nitrogen amino acid values ($\delta^{15}N_{AA}$) of modern cattle samples used as controls during the analysis (referred to as "bovine controls")."Err." refers to the measurement uncertainty as explained in the main text. The bulk values were measured by EA-IRMS. The estimated bulk values were derived by mass balance calculations as explained in the main text and the error associated (Err.) is the error propagated from all the amino acid measurements. 322

D.1 Information about the material analysed in this thesis. Sex and age determination of the human remains from AD79 Herculaneum were provided by Dr Luca Bondioli. The classification of the terrestrial animals by their Latin name is the one obtained using ZooMS while the common name is sometimes more specific depending on the morphological identification or archaeological context. The morphological identification of the marine fish and the estimation of their total length (cm) was carried out by Dr H. K. Robson, for the remains from the House of the Surgeon (Pompeii), and by Dr J. K. Bakker, for those from Porta Stabia (Pompeii). 330

D.2 Bulk carbon and nitrogen values from human and animal collagen and plant material ($\delta^{13}C$ ‰ and $\delta^{15}N$ ‰) and carbon and oxygen isotope values of bone apatite ($\delta^{13}C_{apa}$ ‰ and $\delta^{18}O_{apa}$ ‰) from a small sub-sample of human and faunal remains. From only two human individuals the collagen was extracted and measured via EA-IRMS (*F12i28* and *F7i10*) for this thesis. For all the others, the data are those generated by Craig *et al.* (2013) and Martyn *et al.* (2018). $\delta^{13}C$ ‰ and $\delta^{15}N$ ‰ values of the barley samples from Pompeii (*BarleyP*) and the grains from *Portus Romae* (*LBCFA16F*, *LBCFD16E*, *LBTA1012I*, *LBTD1012H&I*) are from Pate *et al.* (2016) and O'Connell *et al.* (2019), respectively, and they are corrected for charring after Nitsch *et al.* (2015). 334

D.3 Carbon amino acid values ($\delta^{13}C_{AA}$) of human and animal collagen and plant material. The amino acid values of archaeological plant material (*1703b*, *1703w*, *1895e*, *723w*, *200b*, *2314c*, *2317p*, *692l*, *LBCFA16F*, *LBCFD16E*, *LBTA1012I*, *LBTD1012H&I*) were estimated using calculated $\Delta^{13}C_{AA-bulk}$ offsets determined by measuring the bulk and amino acid values of modern grains and pulses. The *Err.* associated to the estimated amino acid values of the archaeological plant material is the propagated error which accounts for the highest measurement uncertainty of the modern samples and their standard deviation. The estimated bulk values were derived by mass balance calculations as explained in the main text; in this case, Err. is the error propagated from all the amino acid measurements. 338

D.4 Nitrogen amino acid values ($\delta^{15}N_{AA}$) of human and animal collagen and plant material. *Err.* represents the measurement uncertainty. The amino acid values of archaeological plant material (*1703b*, *1703w*, *1895e*, *723w*, *200b*, *2314c*, *2317p*, *692l*, *LBCFA16F*, *LBCFD16E*, *LBTA1012I*, *LBTD1012H&I*) were estimated using calculated $\Delta^{15}N_{AA-bulk}$ offsets determined by measuring the bulk and amino acid values of modern grains and pulses. The *Err.* associated to the estimated amino acid values of the archaeological plant material is the propagated error which accounts for the highest measurement uncertainty of the modern samples and their standard deviation. The estimated bulk values were derived by mass balance calculations as explained in the main text; in this case, Err. is the error propagated from all the amino acid measurements. 343

E.1 *Model 0*$_{wd}$ input parameters and the generated estimates. 372
E.2 *Model 0*$_{p}$ input parameters and the generated estimates. 374
E.3 *Model 1* input parameters and the generated estimates. 376
E.4 *Model 2* input parameters and the generated estimates. 381
E.5 Input parameters and the generated estimates of *Model 2* with olive oil included. . 386
E.6 *Model 1* input parameters and the generated estimates with legumes included. . . . 389
E.7 Input parameters and the generated estimates of *Model 2* with legumes included. . 395

F.1 Principal component analysis output using source amino acids (PCA-SAA). 397
F.2 Principal component analysis output using source and trophic amino acids (PCA-TAA). 400

Chapter 1

Introduction

This first chapter introduces the interconnected research questions that lead to the aims of this thesis, presented in the first three paragraphs (1.1, 1.2, 1.3), followed by an outline of the aims and objectives of the thesis (1.4). Finally, the structure of the thesis and the outline of the chapters will also be presented (1.5).

1.1 What do we still not know about the Roman diet in the Mediterranean basin?

There seems to be a paradox in archaeology when it comes to study the diet of people living in complex and evolved societies as the Imperial Roman civilization was. Although when investigating prehistoric populations there is a lack of non direct and direct dietary evidence of food consumption, in the extent that the smallest finding becomes an exceptional recovery, the incredible amount of information we generally have from historical times can sometimes lead us to misreading, magnification or, on the contrary, underestimation of the available evidence.

The Imperial Roman time (27 BC to AD 395) was the period of the largest expansion of the Roman civilization. During this period, and particularly during the first two centuries of the Empire, the so-called *Pax Romana* (transl. from Latin: *Roman Peace*), the Roman civilization was a fortunate fusion of different cultures, organised in a non static social hierarchical model (Saller 2008). The territories were organized in *Provinciae* (transl. from Latin: *provinces*), each of them with its own governor in charge of specialized activities, ranging from land use specialization, as in the case of North Africa, to industries or commercial activities which made the Empire economy probably the largest in scale and the most advanced before the industrialization (Mattingly

2006). Intense trade networks across the Mediterranean and beyond permitted to make the most out of this heterogeneous regional system, and a variety of commodities were moved inside and outside the territories of the Empire (Paterson 2005). This all implies that the inhabitants of the Empire could access a variety of foodstuffs, as well as local resources secured by the Mediterranean temperate to warm climate and geography (Garnsey 2008).

What we know today about diet in the Roman Empire can be briefly summarised as follows. According to some studies of the ancient economy, the diet of people around the Empire was mainly composed of cereals (according to Foxhall and Forbes (1982), around 70 % of the total caloric intake came from cereals), followed by legumes, vegetables and fruits, while primary and secondary animal products were only secondary, although meat was probably more important in temperate Europe. Therefore, the consumption of wild animals, including freshwater and marine fish, was probably only complementary (Garnsey 2008).

This concise outline comes from centuries of study and collection of ancient texts, decorative elements such as frescoes and mosaics, and archaeological findings, especially epigraphies, pottery, botanical, animal and even food remains, as well as human skeletons. However, each of these sources only bears a partial knowledge. The numerous references to diet in the Roman literature refer to the elite, and in particular to feasts, among which the Trimalchio's episode (*Sat* 26-35) by Petronius written at the half of the 1^{st} century AD, certainly stands out (Grimm 2006), and the same can be said about the luxurious frescoes and mosaics found in the urban *domus* or countryside *villae*. Pottery vessels are likely to be recovered from archaeological sites. Several insights about diet can be deduced from ceramics in different ways; for example, the style and typology of a vessel give an information about its role in the kitchen or on the table (*e.g.*, King 1983; Bruno 2005), while the residues analysis of preserved food crusts and fats absorbed inside the ceramic is informative about the food that was once cooked inside of it or contained in it (Roffet-Salque *et al.* 2017). However, ceramic remains are only representative of a fraction of the entire ceramic production and usage. Moreover, as for residue analysis, the recovered lipids have been accumulating through time, so that if the usage of a specific vessel changed with time, this cannot be detected by the scientific approach (Lis 2015). Similarly, the study of botanical and animal remains from archaeological contexts can only give a partial view of the plants and animal products that were produced and consumed, mainly because of their state of preservation, selective recovery (*e.g.*, from dumps or sewers) as well as recovery techniques and species identification issues (Peres 2010; Wright 2010).

All these sources of evidence have one main limitation in common which is that they are *non-direct* testimony of what was once eaten. On the contrary, skeletal human remains can provide *direct* evidence of the diet at the individual level. Although the osteological investigation of the skeleton can sometimes be by itself informative about the general nutritional status, stable isotope analysis (SIA) of both the inorganic and organic components of the skeleton is nowadays the most straightforward approach to study the diet of ancient human societies (Roberts *et al.* 2017). Carbon and nitrogen SIA in particular, has been extensively applied to identify dietary habits of human individuals living in the Roman Empire (Prowse *et al.* 2004, 2005; Keenleyside *et al.* 2009; Craig *et al.* 2009; Crowe *et al.* 2010; Lightfoot *et al.* 2012; Killgrove and Tykot 2013; Lagia 2015; Pate *et al.* 2016; Ricci *et al.* 2016; Rissech *et al.* 2016; Dotsika and Michael 2018; Martyn *et al.* 2018; Killgrove and Tykot 2018; Tafuri *et al.* 2018; O'Connell *et al.* 2019; Baldoni *et al.* 2019; De Angelis *et al.* 2020a,b). However, there are important methodological limitations that make the SIA data difficult to interpret; these will be briefly introduced in the following section 1.3 and reviewed and discussed in chapter 3.

All of this provides an extensive knowledge about which food products were available to the people living in the territories of the Empire and how these products were moving inside and outside the Empire. However, it is still not possible to know for certain in which proportions individuals living in the Empire were consuming such foodstuffs, therefore in quantitative terms, although some scholars in the last years have been trying to with some difficulties (*e.g.*, Foxhall and Forbes 1982; Allen 2009; Craig *et al.* 2013; Fernandes 2016). Moreover, it is still not known whether these proportions varied among different groups of individuals, such as males and females, children and adults, indigent and wealthy groups. Most importantly, it can be questioned whether the commonly accepted 70% contribution of cereals to diet was also followed by the humans living in geographical areas that allowed easy access to other kinds of resources, as it could have been fish for people living in the Bay of Naples in AD 79 .

1.2 Why study the human skeletal assemblage from Herculaneum in AD 79?

Between 1980 and 1982 some archaeologists who were working on a new trench on the AD 79 ancient bay of Herculaneum, Italy, made a discovery that was recognised as one of the most exceptional in the entire history of archaeology (Maggi 2013).

340 exceptionally well preserved human skeletons were recovered during four excavation campaigns, first from 1980 to 1985, then in 1988 and from 1996 to 1999, and finally from 2008 to 2012 (Capasso 2001; Fattore *et al.* 2012; Martyn *et al.* 2020). Only fifty-four of the individuals were found on the ancient shore, while the remaining were recovered under some vaults, the so-called *fornici*, probably used as boat chambers (Lazer 2009).

This human assemblage owes its importance to multiple reasons. First of all, it is a rare scene of human tragedy emerged from the past. These individuals were all trying to escape the eruption of Mount Vesuvius, either by getting ready to shove off or hiding under the *fornici*. Unlike the human remains from Pompeii and from the other sites hit by the eruption, the Herculaneum assemblage is the only testimony of a group of individuals, which permits the study of group dynamics during a catastrophic event as it has never been possible to do before from archaeological contexts (Fattore *et al.* 2012). Secondly, this large assemblage is fortunate to be well inserted into the context of one of the most well preserved towns of the Roman Empire. Thanks to its spectacular preservation, a lot has been studied from Herculaneum, such as its luxurious private buildings, the public and commercial activities, the food items available at the time of the eruption and even the social status and professional occupation of its inhabitants (e.g., Wallace-Hadrill 1994; de Ligt and Garnsey 2012; Rowan 2014). All of this makes the study of the human skeletal remains well supported by other evidence. Last but not least, the Herculaneum human assemblage represents a snapshot of a living population frozen in time. This has major implications in archaeology. To begin with, it is possible to overcome the well-known *osteological paradox* which is one of the greatest limitations of paleodemography and paleopathology analyses of human remains from archaeological contexts (Wood *et al.* 1992). In fact, individuals from cemeteries are hardly representative of a living population. On the contrary, the Herculaneum human assemblage is composed of people that were not likely going to encounter death in the near future if it was not for the Vesuvius eruption. Moreover, these individuals were all living in the same place at the same time, meaning that they all had the same resources available. Therefore, any difference in dietary habits among the individuals of Herculaneum is likely to be driven by economic, social or personal reasons, as Martyn *et al.* (2018) and colleagues pointed out.

The study of this unique assemblage has already allowed us gaining new information about the diet of people living in the Bay of Naples during the Imperial time. A few years ago, Craig *et al.* (2013) published the first attempt of quantifying the marine contribution to the diet of nine individuals of the dead Herculaneum assemblage. The

authors applied radiocarbon dating to determine a date offset from the real date of death for each of the individuals and one sheep (*i.e.*, AD 79). Since any older date would be caused by the consumption of marine products which contains more "old" ^{13}C, it was possible to determine marine contribution to diet from both carbon and nitrogen isotope ratios values using linear interpolations. Following this, Fernandes (2016) elaborated the results obtained by Craig and colleagues (2013) using Bayesian statistics; this validated the marine foodstuff contribution to diet determined by Craig *et al.* (2013) and it was used by Fernandes (2016) as an exceptional case study to propose a novel statistical approach for the study of ancient diet in archaeology. More recently, Martyn *et al.* (2018) applied the equations derived by Craig *et al.* (2013) to the carbon and nitrogen SIA values from all the other available individuals and they evaluated gender- and age-related differences, also in comparison with other populations from Imperial Roman central Italy.

This assemblage has also been at the center of a debate around the temperature of death. Indeed, while some authors have previously proposed that the individuals from the Herculaneum assemblage had died immediately as a consequence to the high temperature (around 500°C) (Mastrolorenzo *et al.* 2001, 2010; Petrone 2011; Petrone *et al.* 2018), two more recent experiments by Schmidt *et al.* (2015) and Martyn *et al.* (2020) suggest that much lower temperatures, most likely between 270°C and 190°C, caused the slow death of the individuals. The different techniques and the results obtained by these studies will be the focus of section 2.3.5.

The Herculaneum death assemblage has still much more to reveal. For example, the relative contribution of cereals and animal products to the diet, as well as that of legumes, is still very uncertain and the SIA of bulk collagen seems to be unhelpful in this direction. Moreover, as it will be introduced in the next section, SIA has some important limitations which can make the detection of marine food consumption extremely challenging outside of the exceptional case of Herculaneum. In particular, this thesis aims to apply compound specific stable isotope analysis of the amino acids (CSIA-AA) from the collagen of some randomly selected individuals, taking care of representing both biological sexes, among the collagen previously extracted, as it will be explained in section 4.1.1. In addition to this, a richer baseline based on the collection of animal and botanical remains will be included, helping to overcome the bulk stable isotope limitations and disclose more high-resolution dietary information from Herculaneum in AD 79.

1.3 Why use Compound Specific Stable Isotope Analysis of Amino Acids (CSIA-AA)?

When it comes to study diet and migratory patterns of ancient human populations, SIA is certainly the most applied tool, as proven by the exponential increase of articles published in the last fifty years mentioning the words 'archaeology' and 'stable isotopes' (Roberts *et al.* 2017). Carbon and nitrogen SIA of bone collagen, a protein extremely well preserved in most archaeological contexts, is the most applied method for dietary studies, followed by sulphur in collagen and carbon isotope analysis of enamel and sometimes bone apatite.

However, the carbon and nitrogen isotope values obtained by the analysis of collagen actually represent average values of the stable isotopes ratios of every single molecule composing the collagen: the amino acids. Each amino acid fraction can have isotope values that are different from those of the others, depending on its own metabolic pathway. Therefore, bulk SIA - as isotope analyses are named when applied to heterogeneous materials - can be useful to visualize a distributional trend of environmental and nutritional data, particularly when numbers of samples are considered, but they can hide important information about food consumption. Moreover, while nitrogen can only be routed from the protein components of diet, carbon can derive from proteins as well as carbohydrates and lipids.

Despite the limitations, over the years several scholars have offered different solutions to *quantifying* the different food sources consumed by an individual or a group of individuals, for example by using mixing models that consider the chemical signal registered in the sample, the chemical signals of the possible sources and an assumption about nitrogen and carbon fractionation from food to consumer. So far, one of the most applied methods has been the Bayesian mixing model FRUITS, with its related user-friendly open source application. FRUITS was proposed by Fernandes *et al.* (2014) stimulated by the partially unsatisfactory attempts of previous methods (*e.g.*, Phillips 2001; Phillips and Gregg 2003; Moore and Semmens 2008; Parnell *et al.* 2010).

Statistical models have made an important contribution to the application of bulk SIA in archaeology. However, the estimates generated are often not able to discriminate between dietary sources with similar carbon and nitrogen isotopes values, for example when differences in contribution from terrestrial animals and terrestrial plants need to be explored, which might be the case of Herculaneum in AD 79. Moreover, the models rely on diet-to-consumer offsets that are derived from feeding experiments which are often very different from one to another (*inter alia*, Krueger and Sullivan

1984; Ambrose and Norr 1993; Tieszen and Fagre 1993; Ambrose 2000; Howland *et al.* 2003; Passey *et al.* 2005; Warinner and Tuross 2009; O'Connell *et al.* 2012; Webb *et al.* 2016b, 2017). The discrepancy between the offset values is to some extent due to the different dietary compositions of the animals used in the studies, something that it is difficult to predict from archaeological contexts (Webb *et al.* 2017).

The joint application of CSIA-AA (for which fractionation mechanisms are better understood) and Bayesian statistics have the potential to provide higher resolution estimates of dietary intakes, while at the same time to reduce the number of assumptions about how nitrogen and carbon isotopes fractionate from diet to consumer. When applied to the exceptional death assemblage of Herculaneum in AD 79, it will provide a better understanding of the diet of who was living in a coastal town at the heart of the Empire. Moreover, the Herculaneum assemblage, since being a unique case of an archaeological living population, represents the perfect model on which to test the reliability of CSIA-AA used in conjunction with Bayesian mixing models.

1.4 Aims and Objectives

Following on the research questions presented above, aims and objectives of this PhD are presented in this section.

1.4.1 Aims

There are two aims to this thesis both made possible by the exceptional nature of the human assemblage of Herculaneum in AD 79. First, to compare the results obtained through bulk SIA and CSIA-AA to demonstrate the advantages of the latter both qualitatively and quantitatively when applied in a Mediterranean archaeological context. Second, to use the high resolution obtained thanks to the application of CSIA-AA and Bayesian mixing models to answers some of the questions around the diet of people living at Herculaneum in AD 79 and to explore differences across the assemblage.

1.4.2 Objectives

In order to fulfil these two aims, this PhD will complete the following objectives:

- To explore what is known of the diet of the Romans living in the Mediterranean basin during the Empire looking at historical accounts, economic studies, archaeological findings, and bioarchaeological evidence, and what remains to be explored as it will be examined in chapter 2 and chapter 3;

- To develop a laboratory and analytical procedure for the determination of carbon and nitrogen isotopic signatures of amino acids from bone collagen and plant material at BioArCh (Department of Archaeology, University of York) using a GC-C-IRMS system. This will be outlined in chapter 4;
- To create a solid dietary baseline for the area of the Gulf of Naples in the 1^{st} century AD. To do so, first, the protein and amino acids preservation from archaeological charred grains and pulses will be evaluated (via RP-HPLC), and the attribution of the faunal remains to specific *taxa* will be confirmed and/or corrected using Zooarchaeology by Mass Spectrometry (ZooMS). Finally, the bulk and amino acid carbon and nitrogen stable isotope values of both plant and animal remains will be discussed considering different crop management systems and farming and herding practices. This will be the focus of chapter 5;
- To propose two novel mixing models for the analysis of CSIA-AA results. The estimates will allow quantifying the protein and calorie intakes from different food sources at Herculaneum in AD 79, which is the focus of chapters 6 and 7.

1.5 Thesis Structure

This PhD thesis is a combination of traditional thesis chapters and one scientific article which is currently under review. The thesis is structured as follows:

- Chapter 2 "Diet during the Roman Imperial time and the case study of Herculaneum" outlines what is known about the diet of the Romans who were living in the Mediterranean area. This chapter also presents the geographical, political and economic context of the Bay of Naples in the 1^{st} century AD with a focus the town of Herculaneum, its layout, the history of the excavations, its inhabitants and the extraordinary death assemblage recovered from the ancient seashore.
- Chapter 3 "Dietary studies and stable isotopes analyses: a review" is a review chapter of the scientific literature produced in the last decades on stable isotope analysis applied to dietary investigations. The aim of this chapter is to provide the reader with the state of the art of bulk SIA and CSIA-AA, with a focus on previous studies carried out in Roman Mediterranean contexts.
- Chapter 4 "Experimental and analytical protocols for Compound Specific Stable Isotope Analysis of Amino Acids (CSIA-AA)" illustrates the steps that were

necessary to develop the protocol currently in use for CSIA-AA at BioArCh, Department of Archaeology, University of York. The quality of the data is also presented and evaluated using different methods.

- Chapter 5 "Establishing a baseline for diet at Herculaneum in AD 79" presents the botanical and animal remains analysed by SIA and CSIA-AA to be used as a dietary baseline for the interpretation of the human data. However, some limitations were faced, such as the poor understanding of protein degradation in archaeological plant material and the erroneous identification of the animal remains. Therefore, the first part of this chapter will focus on the discussion of such limitations and provide solutions for this thesis and future work. Then, the SIA and CSIA-AA will be presented and discussed.

- Chapter 6 is an article currently under review in *Science Advances* with the title "High-resolution dietary reconstruction of victims of the AD79 Vesuvius eruption at Herculaneum by compound specific isotope analysis". The aim of this chapter is to present high-resolution dietary estimates obtained for seventeen human individuals from the AD 79 catastrophic death assemblage. To do so, two novel mixing models which incorporate previous knowledge of amino acid synthesis were used and are here presented. The data obtained were also compared to those of modern Mediterranean populations.

- Chapter 7 "Discussion" begins with a critical evaluation of the limitations and advantages of using the bulk SIA approach by exploring the results obtained from the Herculaneum case study. The potential of including carbon isotope analysis of the bone apatite will be also discussed presenting the results from a pilot study. Then, the results obtained by CSIA-AA will be presented more extensively compared to chapter 6, by exploring different valuable proxies. Finally, the data obtained will be discussed considering what is known of the people who where living at Herculaneum at the time of the eruption with the aim to add a new piece of evidence to the overall picture.

- Chapter 8 "Conclusions and suggestions for future research" summarises the work, reconsidering the aims of the thesis and evaluating if and how these were met. The major findings will be outlined, and the limitations will be discussed, proposing future directions.

Chapter 2

Diet during the Roman Imperial period and the case study of Herculaneum

This chapter offers an overview on the state of the art on the Roman diet in the Mediterranean basin, the archaeological site of Herculaneum and its catastrophic death assemblage, which are the main focus of this thesis. First, the main categories of foodstuff available to the Romans will be presented, drawing information from the ancient texts and the archaeological findings with examples from the Bay of Naples (2.1). Then, the historical context of the Bay of Naples in the 1^{st} century AD will be briefly introduced with the aim to contextualise Herculaneum, which will be then explored focusing on the discovery, the economic role and the social structure of the town and on the AD 79 eruption of Mount Vesuvius (2.2). The last paragraph (2.3) will be dedicated to the exceptional human assemblage of the ancient seashore of Herculaneum and the discovery of the skeletons and the studies conducted on them will be reviewed.

2.1 What did the Romans eat in the Mediterranean basin?

In the 1^{st} century AD the Roman Empire had almost reached its greatest extension and population density. Although the size of the Roman population keeps being under debate (Scheidel 2008), the low estimates suggest that it increased from 45 to 60 million between the time of Augustus (27 BC - AD 14) and the half of the 2^{nd} century AD

(Scheidel 2004). In order to supply such a vast territory, the state had to rely on an accurate system of production and distribution, also considering the unpredictability of the climate and variety of environments in the Mediterrenean area and beyond (Horden and Purcell 2000). In this setting, the agricultural production, in particular of wheat, olive oil and wine, the so-called "Mediterranean triad", became central in the economy of the Empire and consequently in the diet of the Romans (Kehoe 2007). Although written accounts, archaeological evidence and historical studies suggest that cereals were the first source of calories for the inhabitants of the Empire, other foodstuffs seem to have played a significant role in their diets, in particular vegetables and fruits, eggs and dairy products but also small quantities of meat and fish. In the following sections, different categories of foodstuff available to the Romans will be presented relying on different kinds of evidence, with examples mainly from the Gulf of Naples, which is most relevant for the scope of this thesis.

2.1.1 Sources of evidence

Undoubtedly, the main evidence about Roman diet comes from the ancient literary sources. Since the Punic Wars (3^{rd} - 2^{nd} centuries BC), different authors described Roman agricultural and farming practices in texts that have been passed down to this day with only minor lacunae. Among others, the agronomists Cato, Varro, Columella and Pliny the Elder provided a wealth of information.

Marcus Porcius Cato (234 - 149 BC) was the first to collect his knowledge about agriculture into a manual composed of 162 chapters called *De agri cultura*. *De agri cultura*, which also represents the oldest surviving example of Latin prose, was written around the first half of the 2^{nd} century BC, when Cato returned to his small estate a few kilometres south of Rome to dedicate his time to the work of the land. Therefore, the manual is a collection of his personal experience written in a direct and lacking of form prose.

One century later, Marcus Terentius Varro (116 - 27 BC) was witness and reporter of the agricultural and husbandry practices of the 1^{st} century BC, the time of the Late Republic. *Rerum rusticarum libri tres* (or *De re rustica*) is a three volume manual based on his experience as a landowner, Greek and Roman authors' texts and information provided by technical consultants. He was the first to divide agricultural practices according to the seasons.

However, it is in the 1^{st} century AD that agronomic science got the highest contribution with *De re rustica* by Columella. Although little is known of his life, Lucius Junius Moderatus Columella (1^{st} century AD), the author of *De re rustica*,

probably dedicated most of his life to the management of his estates in *Latium*. His purpose, that he clearly states in the introduction to the manual, was to reestablish the socio-economic role of agriculture which he believes is, with no doubt, close to and own sister of *sapientia* ("sine dubitatione proxima et quasi consanguinea sapientiae est", *De re rustica* 1 *prefatio*). The text is articulated into twelve volumes, each dedicated to a specific topic.

The suggestions provided by Cato and Columella were used and re-elaborated by Pliny in his *Naturalis historia*, published in AD 77. Gaius Plinius Secundus (AD 23 – 79), better known as Pliny the Elder, was a wealthy landowner, commander, author and philosopher that lived in the Imperial time and died during the tragic event of the AD 79 eruption of Mount Vesuvius. The *Naturalis historia* is the first example of an encyclopaedic text and it has been used as a model by following authors of encyclopaedias. In the text, Pliny also criticizes the previous agricultural calendar advanced by Cato and he proposed a new crop schedule based on the practical needs of the land and of the farmers (Malossini 2011). The *Naturalis historia* is particularly relevant to this thesis. Pliny the Elder spent a large part of his life in Campania and he often refers to this region to make examples of specific crops and culinary habits, as it will be noted in the following sections.

Apicius, or *De re coquinaria*, is worthy of a separate mention. *Apicius* is a collection of gourmet recipes traditionally attributed to Marcus Gavius Apicius, a Roman cook who lived in the 1^{st} century AD. However, the compilation that was passed down to this day is dated to the end of the 4^{th} century AD and it probably contains only a few original Apicius' recipes. The book is organized in ten chapters, going from "the secrets of the chef" (*Epimeles*), through the preparation of legumes, predominantly in the form of *puls* or soups, to chapters dedicated to birds' recipes (*Aeropetes*) and gourmet dishes (*Politeles*)(Introna 2018).

Last but not least, *The Edict of Diocletian*, or *Edict on Maximum Prices*, is a later (AD 301) piece of evidence providing with a long list of goods, including food and drink, and services in an attempt to assign them to maximum prices (Kropff 2016).

Unfortunately, information about diet derived from the written sources is subject to a number of biases. First of all, the ancient agronomists were writing for the elite, while the ordinary people most likely did not have access at all to these manuals. Therefore, it is impossible to tell whether the descriptions on agricultural and husbandry practices provided by Cato, Varro, Columella and Pliny among others, also apply to rural contexts and subordinate classes in addition to the large-scale commercial estates and their respective elites. Secondly, one can only extrapolate dietary information

Figure 2.1 Still life frescoes from the House of the Deer, Herculaneum. From the left: capon with hare; partridge with apple and pomegranate; Song thrushes and mushrooms of the genus *Agaricus*; partridges and morays. Museo Archeologico Nazionale di Napoli, Naples.

from these texts, where the authors' aims are somewhere else directed. This means that apart from information upon specific foodstuffs that were available in the Italian peninsula and in the provinces, the texts lack evidence about how food was distributed on a geographical and social scale. A separate note needs to be made on *Apicius*, a collection of gourmet recipes for special occasions, therefore not really indicative of the daily Roman cuisine. Ultimately, the ancient texts were passed down through countless transcripts, which were inevitably filled-in (if lacunae were present) or even adapted according to the tradition and the customs of following historical periods.

Roman wall paintings and mosaics often represent banquets and still lives. However, they are frequently recovered from sumptuous villas, therefore their role was mainly decorative and declarative of the social status of the owner of the property. Game or exotic and expensive items are often at the forefront of these depictions, but it is unlikely that they represented the daily meal, even for the richest (Figure 2.1).

The archaeological record usually preserves direct and non-direct evidence of past human diet. The location itself of a settlement is informative of the most likely food sources for its inhabitants. For example, one could assume that the Romans living in the Bay of Naples, with easy access to the sea, were eating in proportion more fish than those living in the hinterland. Further palaeo-environmental surveys of the area can provide information about the climate and surrounding natural vegetation and crops. This is usually performed through a macroscopic and microscopic screening of the sediments and the proxies collected can also be used to drive hypotheses about food availability (See section 2.1.5 and 2.1.6 for examples).

Certainly, the most explicit evidence of food is the presence of the food itself. Animal remains are a common finding in archaeological stratigraphies. Their presence is evidence of the animals that were raised at (or imported to) at the site and possibly used for dietary purposes. Moreover, livestock bones can be analysed in order to

provide an age at death profile, which can lead to the use that past people made of those animals, considering that meat is most likely obtained from younger animals and that secondary products (milk, wool but also labour) are derived from the animals for a longer period of life. Butchery marks on the bones can also carry important information (an example of this can be seen in section 2.1.4). Traces of food can also be found charred associated with fireplaces and it is not unlikely that large quantities are found in specific structures, such as shops and warehouses. In extraordinary circumstances, food can even be recovered in its original shape (such as the bread loaves from Pompeii and Herculaneum mentioned in section 2.1.2).

Although all these approaches are of great help in identifying the presence of specific foodstuff in Roman archaeological contexts, they are only partially informative. The conservation of botanical and faunal remains is selective. Only specific remains are destined to survive through time, depending on the context, the chemical nature of the sediments and of the material itself. A striking example comes from the study of the remains from the *Cardo V* Sewer at Herculaneum, that will be often mentioned in the following sections for the extraordinary amount of information that the analysis provided (Robinson and Rowan 2015; Rowan 2017a). The small number of wheat grains recovered from the sewer does not indicate low consumption of wheat. On the contrary, since wheat was usually processed into flour, it is unlikely to be found in such a context, as pointed out by Rowan (2017a). Therefore, it is impossible to confidently quantify to which extent some food sources were consumed compared to others or among different socio-economic groups using as evidence the food, botanical or faunal remains. Most importantly, these approaches cannot be considered a *direct* evidence of diet, even in the case of sewer, since the latrines were often collocated near kitchens to be used as toilet and waste bin which might have served to dispose items not meant to be eaten (Robinson and Rowan 2015).

A quantitative approach has been often proposed by the historians of the ancient economy (Tchernia 2016, 188-200). These studies meticulously review the archaeological record, literary sources and epigraphes providing precise estimates of the energy intakes from diet, with a main focus on cereals, olive oil and wine (*e.g.,* Foxhall and Forbes 1982; Amouretti 1986; Garnsey and Scheidel 1998). However, these studies can only provide average estimates on food economies that apply to the Empire as a whole, lacking the resolution to explore geographical or socio-cultural differences, as well as individual dietary intake. Moreover, Greco-Roman economists base their assumptions upon evidence, namely the archaeological remains and ancient sources, that can be largely biased, as aforementioned.

In the next chapter (3) stable isotopes from collagen will be presented as a unique tool to directly quantify caloric intakes and explore differences across space, time and social groups. Nevertheless, literary sources, decorative elements and archaeological remains provide an extraordinary insight into the diet of ancient Romans, summarised in the following sections, and they are essential in the interpretation of the data presented in the result chapters (5, 6, 7).

2.1.2 Cereals

The Mediterranean climate must have played a dominant role in influencing the diet of the Romans. For example, the unpredictability of rainfalls made it impossible for the local Roman farmers to live by cultivating a single crop. Therefore, they adopted a "polyculture" strategy that allowed them mixing the cultivation of cereals with that of other crops, notably olive trees and vines. Thanks to this, and also by rotating the cultivation of cereals with that of legumes, farmers were able to minimise the risks and even to produce a small surplus for the market (Kehoe 2007). However, the majority of the population was densely packed into cities, primary Rome, with no access, if limited, to the land (Garnsey 1999, 24-26). To sustain the city of Rome, the army and other major cities, the state adopted a system of free wheat distribution.

Naked wheats

Every thirty days in Rome the so-called *frumentationes* took place. 33 kilograms of *frumentum publicum* (free wheat) were distributed to 200,000 adult male citizens from the Late Republic, providing *ca.* 3,700 kcals per person per day. This amount corresponds to around twice the daily requirements of an average person (Garnsey and Scheidel 1998, 226-252). Such an enormous amount of wheat was produced in the provinces of Sicily and Sardinia first and from those of Egypt and North Africa later. It is estimated that Egypt, where the annual floods of the Nile ensured the right conditions for the cultivation of wheat, produced wheat in the order of 1,000 kg/ha (Kehoe 2007). As a consequence, in the 1^{st} century AD, the main two naked wheats, bread wheat (*Triticum aestivum*) and hard wheat (*Triticum durum*), had almost completely replaced husked wheats such as emmer (*Triticum dicoccum*), einkorn (*Triticum monococcum*), oats (*Avena sativa*) and millet (*Panicum miliaceum*), that were now considered "inferior" cereals (Garnsey 1999, 121). The large-scale production of bread became of commercial importance in the Republican and Imperial times. This is testified not only by the numerous written accounts but also from the archaeological

evidence, for example by the thirty-nine bakeries that have been excavated at Pompeii that make around the 60 % of the total workshops in town (Monteix 2017).

While soft wheat was preferred for bread production, hard wheat was most likely used to obtain flat and unleavened cakes (Garnsey 1999, 121). Remains of charred bread have been occasionally recovered in Roman archaeological sites (Heiss *et al.* 2015). However, again, the main example come from the territories of the AD 79 eruption, where numerous loaves have been discovered, such us in the case of the eighty-one bread loaves in only one oven of the Bakery VII 1, 36–7 in Pompeii (Monteix 2017), sometimes exceptionally well preserved (Figure 2.2).

Figure 2.2 Loaf of bread from the territories of the AD 79 eruption. Photo taken by the author at the "Res rustica. Archeologia, botanica e cibo nel 79 d.C." temporary exhibition, 21/09/2018-18/02/2019. Museo Archeologico di Napoli, Naples, Italy.

The "inferior" cereals

However, it is most likely that the Roman farmers of the countryside in the 1^{st} century AD were still relying on various "inferior" cereals that could be easily adapted to different environments and climates. Indeed, the naked wheats, where produced, were intended to be exported rather than consumed locally (Garnsey 1989).

Pliny the Elder reports that emmer, called *far* by the Romans, is able to resist very cold weather, under-cultivated lands and also in hot and arid conditions (*HN* 18.83). This is probably why emmer was the most consumed wheat for over three hundred years (*HN* 18.62). Emmer was used to make *puls*, a meal prepared with ground cereals boiled in water (Garnsey 1999, 78), similar to *polenta* or porridge. *Puls* was a staple of the Roman cuisine, at least until bread became commercially available

in the 2^{nd} century BC (Garnsey 1999, 120). Interestingly, Pliny distinguishes between *far* and *zea*, pointing out that *zea* was abundant in Campania where it was called *semen* (*HN* 18.82). It is not an easy matter to distinguish among cereals from the ancient written sources and some historians believe that it is possible that the word *far* refers instead to *Triticum spelta* (spelt) and *zea* to *Triticum dicoccum* (emmer)(Segrè 1950). Interestingly, to our knowledge, archaeobotanical studies in the territories of the eruption have not reported remains belonging to the *Triticum spelta* species so far (*e.g.,* Meyer 1980; Murphy *et al.* 2013; Rowan 2017a).

It seems that millet and foxtail millet (*Setaria italica*) were also welcomed in Roman cuisine. For example, Columella reports that millet could be used to make bread and that both millet and foxtail millet, the latter after being processed to remove the external skin, could be used to make *puls*, even better if mixed with milk (*Rust.* 2.9). This might explain why, in the *Edict of Diocletian*, millet has the highest price together with wheat compared to the other cereals (100-150 *denarii*, while barley and rye 60 and oat only 30)(Kropff 2016). In addition, Pliny informs that millet grows well in Campania (*HN* 18.100). This seems to be confirmed by the high number (around three hundred units) of millet and foxtail millet grains recovered from the Herculaneum *Cardo V* sewer, located in a commercial non-elite area of the town (Robinson and Rowan 2015; Rowan 2017a). Rowan (2017a) here notes that large quantity of millet had also been previously identified in a modest house in Pompeii, while lower numbers of millet grains were found in the sumptuous House of the Vestals, which suggests that millet might have had an important role in the diet of non-elite individuals, at least in that area of the Empire.

Other cereals were not particularly appreciated. Pliny for instance informs that one can try to mitigate the bitter taste of rye (*Secale cereale*) by mixing it with *far*, but that the taste would still be unpleasant. Rye can be cultivated everywhere and it can be used to manure the soil (*HN* 18.141). Oat is generally suggested to be used as animal fodder by the ancient authors (*e.g.*, Columella, *Rust.* 2.10). Ancient sources also report that barley was a low status cereal and that it was only consumed in the countryside, and also used as a fodder for the livestock (Garnsey 1999, 120). This does not mean that barley consumption was rare. Notably, barley is one of the most common botanical species recovered from the territories of the AD 79 eruption (De Simone 2017; Robinson and Rowan 2015; Rowan 2017b).

2.1.3 Legumes

The cultivation of legumes and their uses are often reported and discussed by the ancient authors. Legume consumption has for long been neglected but it is nowadays believed that they were a staple in the Roman diet. Legumes could provide the nutrients that cereals lack, notably proteins, and although the rich could afford to replace them with more expensive sources of proteins, pulses were still largely consumed by the elite, as testified by the numerous Apicius' recipes that include legumes (Garnsey 1999, 15, 121).

The rotation of cereal crops with that of legumes could improve the fertility of the soil and the pulses could be used for human consumption, as a fodder or to further fertilize the soil by green manuring (Kehoe 2007; Rowan 2017b). Broad beans, chickpeas, lentils and peas were all species intended for human consumption. Broad beans (*Vicia faba*) were often ground to obtain a flour called *lomentum* which could be used to make bread, as many other leguminous flours were, or mixed with wheat or foxtail millet to make *puls* (Pliny, *HN* 18.117). Vases containing *lomentum* have also been found in Pompeii (Spurr 1986). Broad beans were also used as animal fodder, although it is possible that the pulses themselves were only used for human consumption and that the stalks and pods were given to the livestock (Spurr 1986).

Broad beans, peas (*Pisum sativum*), chickpeas (*Cicer arietinum*) and lentils (*Lens culinaris*) have all been found as macro or micro remains in Roman archaeological context in the Mediterranean area (*e.g.*, Meyer 1980; Murphy *et al.* 2013; Bowes *et al.* 2015; Bosi *et al.* 2017; Robinson and Rowan 2015; Rowan 2017a; O'Connell *et al.* 2019). However, except for a few cases due to exceptional circumstances (*e.g.*, Meyer 1980; Murphy *et al.* 2013), they are commonly recovered in small quantities, probably due to their soft texture once cooked (Rowan 2017a).

It is also known that legumes were shipped from Egypt and North Africa, suggesting that their consumption was not only reserved to peasants in the countryside (Casson 1980; Spurr 1986; Rowan 2017b). The commercial value of legumes is also attested by the *Edict of Diocletian* where the maximum price is fixed between 60 and 100 *denarii* (Kropff 2016). Lupins are also often mentioned by ancient authors, for example Pliny refers to them as a food suitable both for humans and animals (*HN* 18.133). However, their presence in the archaeological record is rare (Spurr 1986).

2.1.4 Terrestrial animals

In the Mediterranean, the few fertile lands available were exploited for the cultivation of crops and the rest of the territories, namely scrublands, wetlands, hillsides and woodlands were instead dedicated to animal farming. Some landscapes are better suited for some animals than others.

Ovicaprids can be left grazing on scrubs and on the vegetation of wetlands, while pigs can feed on acorns, chestnuts, mushrooms and roots in the forest (Horden and Purcell 2000). Columella also identifies these landscapes as the most appropriate for ovicaprid and pig husbandry (*Rust.* 7.2, 6, 9). Interestingly, sheep, goats and pigs are the species that represent the majority of animal remains from many Roman archaeological sites of the Mediterranean basin (Figure 2.3)(*e.g.*, King 1999; MacKinnon 2001). Although cattle also had a central role in the Roman economy, it was most likely only used as a work animal for the cultivation of the land. Furthermore, the decline of relative frequencies of cattle bone from Mediterranean sites in the Imperial time (MacKinnon 2010a), seems to confirm that ovicaprids and pigs better adapted to the economical development of the Empire, where the cultivation of the available land was maximised for grain production.

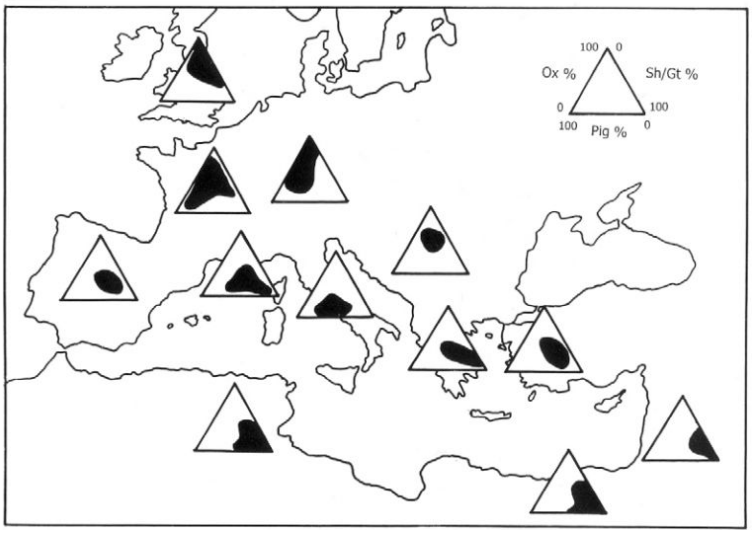

Figure 2.3 Triangular graphs showing relative frequencies of cattle, ovicaprid and pig bone remains from different Imperial Roman archaeological sites. Modified after King (1999).

As a consequence, meat only represented a supplement to the diet, rather than a staple. It is also clear that when destined for meat consumption, the animal was used in all of its parts by the Romans, as testified by the numerous recipes from the Apicius' book, mentioning different kinds of meat cuts but also the most varied parts

of the body, such us the skin, sex organs, feet and the liver. Evidence of this practice was found for example in the marks of butchery and bone marrowing in the sub-elite area of *Regio I* and *Regio VIII* in southern Pompeii, and not only on bones associated with higher-quality meat (upper limbs, ribs and vertebrae). This made the author believe that lower socio-economic groups of people living in the *Regio I* and *VIII* were consuming all of the animal, probably by chopping it in small pieces to be used in stews (Moses 2012).

Sheep and goat were used for their wool and hair and for their milk, ultimately for their meat and skin. This could allow the farmer obtaining the maximum profit out of a single animal. Pigs only were used exclusively for meat consumption but it should be noted that they were also easy for anyone to raise since they could feed on whatever was available and they could even live in confined urban space (Garnsey 1999, 122-127).

Although the consumption of animal products was secondary to that of cereals, vegetables and legumes, the number of mammal bones recovered by zooarchaeologists rises dramatically in the Late Republic levels reaching a peak in the Early Empire (Figure 2.4). This, together with the change in size of livestock, suggests an increase of animal product consumption in the Roman Empire compared to the previous and following periods (Figure 2.4)(Jongman 2007).

Columella, when questioning whether farmers should possess animals at all, refers to poultry as the only animal that is important to keep in the farm according to tradition (*Rust.* 8.2). Chickens could provide eggs as well as meat. Geese and ducks were also farmed, although these animals, unlike chickens, needed access to water, which was not always easy to provide (*Rust.* 8.13-15). The presence of domestic fowl bones also in urban sites, although in modest proportions, confirms the role of poultry and eggs in the diet of ancient Romans. Indeed, chickens could be easily raised in an urban setting, where they could be kept in courtyards or household coops (MacKinnon 2018). The measurement of the thickness of 100 eggshell fragments from the Herculaneum *Cardo V* sewer confirmed chicken as the most common bird used for egg consumption (only two fragments were identified as belonging to goose), at least in this area (Rowan 2014).

The *Edict of Diocletian* also includes the maximum prices for game meat and wild birds, suggesting a commercial role of these animals (Kropff 2016). The presence of wild animals on the market suggest the practice of breeding of, at least some of, these animals (Chandezon 2015). Indeed, Varro reports the presence of enclosed spaces for the breeding of hares (*leporaria*), dormice (*glilaria*), snails (*cocliaria*) and bees

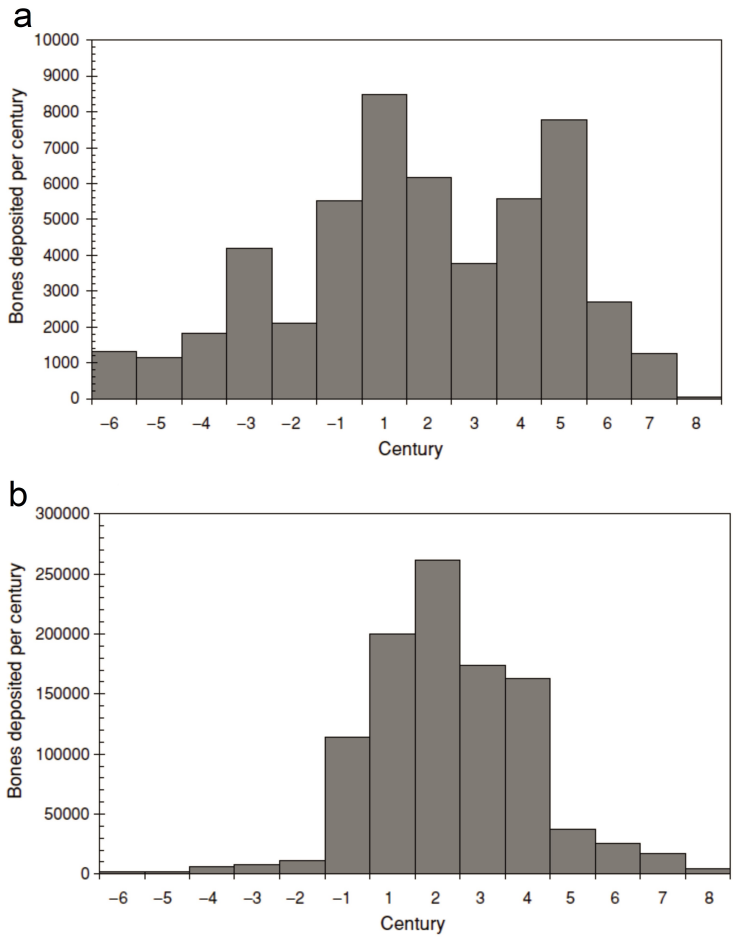

Figure 2.4 Mammal bones recovered in Italy (a) and in the Provinces (b) through the centuries. Modified after Jongman (2007).

(*alvaria*), as well as extensive enclosed hunting parks (that he calls *therotrophium*, meaning "breeding place of fairs") with deers, roe deers, mouflons and boars, either captured in the wild or bred in captivity (*Rust.* 3.12-13). These parks were later referred to as *vivaria* by Columella (*Rust.* 9.1). The practice of keeping wild animals in captivity in enclosed spaces seem to be confirmed by some zooarchaeological data collected on fallow deer (*Dama dama*) remains from Roman Mallorca (Valenzuela *et al.* 2016). However, the presence of wild animal bones in Mediterranean Roman sites is often of modest proportion compared to that of ovicaprids, pigs and cattle, although they seem to increase in some later contexts (3^{rd}-4^{th} century AD)(*e.g.*, Van Neer and De Cupere 1993; Wilson 2000; Chandezon 2015; Valenzuela *et al.* 2016). Wild animal bones represent less than 1 % of the remains in Pompeii from the 4^{th} century BC to AD 79 (King 2002) and they are equally insignificant in other urban sites such as Ostia, Rome and Athens (MacKinnon 2018). As for wild birds and other small wild animals, they are equally underepresented in the archaeological record, although this might be additionally biased by difficulties in the recovery and identifications of these animals (MacKinnon 2018). Indeed, doves, pigeons and song thrushes were either captured or bred in captivity, following the precise instructions for fattening provided by the ancient literary sources (Malossini 2011).

2.1.5 Vegetable and fruits

There is no doubt that vegetable and fruit consumption was of great importance to the Romans. The *Edict of Diocletian* mentions around forty-five different varieties of vegetables and fruits, all very cheap, with only a few exceptions (Kropff 2016). The large variety of species available and their low market price made this food category a common element of the Mediterranean Roman diet.

Although people could benefit from a variety of products all the year around, greenhouses were also used, made of selenite first and of double-glaze later, sometimes even heated with hot water, that made it possible to grow vegetables off-season (Kron 2015). Large-scale horticulture, such as that in the *suburbium* of Rome, was made possible by a sophisticated system of irrigation. Indeed, while smaller *horta* (transl. vegetable gardens) could have been hand watered from wells or cisterns, larger cultivated areas needed to be irrigated using stream diversions or connections to the nearby aqueducts (Thomas and Wilson 1994). The cultivation of vegetables was possible also in urban areas. Notably, 17.7 % of the excavated city of Pompeii are market gardens, vineyards, domestic gardens and courtyards (Kron 2015; van der Veen 2018). Root vegetables were probably the most consumed because they could be stored

for longer periods. Onions, garlic, leeks, shallots, turnips, carrots and parsley could be left drying in the sun and then covered with vinegar, brine, honey or oil or a mixture of these liquids (Thurmond 2006). This was a procedure that allowed farmers either selling the products at the market or consuming them during winter. Leafy vegetables such as cabbage, beets leaves, lettuce, rocket, endive, chicory, chards, broccoli, kale and asparagus were more difficult to conserve and therefore they were mainly consumed fresh (Thurmond 2006).

Varro refers to the Italian peninsula as a vast orchard for the high number of fruit trees cultivated there (*Rust.* 1.2). Certainly, the majority of arboriculture was destined to olive oil production, but there is a large body of evidence that other fruit and nut trees had a commercial value (Kron 2015). For some fruits there were many varieties, as reported for example by Pliny, therefore suggesting that behind the practice of arboriculture there was scrupulous work to optimise and standardise the taste and production of these products (Kron 2015). Leaving aside olives and grapes, figs, pears and apples were without doubt among the most widely produced, in such a degree that they are often suggested for feeding the pigs by the ancient sources (Kron 2015). However, the more recent cherries, pomegranates, carobs and peaches were also widely spread in the Mediterranean basin (Thurmond 2006). Pinenuts, hazelnuts, walnuts, almonds and chestnuts were among the most available nuts in Roman times and there is no doubt that they were commonly included into the diet of ancient Romans (Thurmond 2006).

Apart from ancient literary sources, wall painting and mosaics, confirmation of the consumption of these species can be gained from the archaeological record. Charred remains of fruits and nuts have been found in the territories of the AD 79 eruption (*e.g.*, Meyer 1980). However, when such exceptional circumstances of preservation are not available, the analysis of macro and micro botanical remains is of great help to understand the natural landscape and agricultural practices in ancient times. For instance, Sadori *et al.* (2010) evidenced the presence of numerous charred remains of pine nuts and peach stones, as well as pollen belonging to hazelnut and legumes, in a basket dated to the second half of the 1^{st} century AD found in a *domus* located 70 km south-west of Rome. The drainage system was also analysed and seeds belonging to species used for the production of mustard (*Sinapis* sp. and *Brassica nigra*) were evidenced (Sadori *et al.* 2010). In the same way, the pollen analysis of the ancient harbour of Neapolis revealed an abundance of Brassicacae (most likely broccoli, cabbage and raddish), walnuts, chestnuts and grapevines in the area between the 1^{st} century BC and the 5^{th} century AD, with a drastic decrease in the 3^{rd} century AD and an

increase in Mediterranean shrublands and deciduous forest, probably concomitant with a socio-economic decline (Ermolli *et al.* 2014).

2.1.6 Olive oil and wine

Roman economic studies suggest that it was the large scale production of olive oil and wine that influenced positively the general agricultural productivity of the Roman Empire. Monte Testaccio in Rome, an artificial hill made entirely of broken amphorae once containing olive oil, is clear evidence of the commercial importance of this product in the Roman Empire. Almeida (1984, 116-119) estimated that Monte Testaccio is composed of around 50,000,000 amphorae, predominantly Spanish Dressel 20s (around 80 %) but also African amphorae. There is no doubt that the Guadalquivir valley in Spain and North Africa were both important centres of olive oil production (*e.g.*, De Vos *et al.* 2013). However, it is also known that a large part of the demand was covered by the agricultural production of the Italian peninsula. In the *suburbium* of Rome, in an area measuring 5,500 km^2, 169 presses have been counted, either for the production of oil or that of wine (Marzano 2013a). Therefore, Marzano (2013a) estimated that in the Roman hinterland there was one press every 32.5 km^2, which is not impressive when compared to the density of olive oil presses in the North African provinces, where in some areas it reaches that of one press every 2 km^2. However, in the Guadalquivir valley there is "only" one press every 23 km^2 (Marzano 2013a). It should be noted that a quantitative approach based on the number of archaeological findings is largely biased by the preservation, the recovery and the study of the sites. Nevertheless, such a high number of presses suggests a large-scale production even in the surroundings of Rome, comparable to that of the main trade routes (Marzano 2013a).

Amouretti (1986) first suggested that the Romans consumed around 20 liters per head of olive oil per annum. This estimate does not account for the other uses the Romans made of olive oil, such as fuel and for cosmetic purposes. This figure is accepted by many historians, who provided further evidence based on the number and distribution of amphorae and presses around the Empire (*e.g.*, Mattingly 1988; Foxhall 2007). Such a quantity would account for almost a quarter of the total energy requirements (Jongman 2007). On the contrary, it has been estimated that modern Mediterranean populations derive only *ca.* 5 % of their energy from olive oil (Balanza *et al.* 2007). The difference is impressive. Modern consumption of olive oil might be more similar, if not higher, to that of the Romans in some rural areas of the Mediterranean, for example that of some communities in Greece (Foxhall 2007).

Botanical remains can also provide the evidence of large-scale olive oil and olive consumption (van der Veen 2018, 59). For example, Rowan (2014) found that the carbonized material from the *Cardo V* sewer in Herculaneum was composed for almost its entirety of olive stone fragments (*ca.* 95 %). The fragmentary nature of the material and its abundance made the author believe that the olive stones were most likely used as a fuel together with other leftovers of the production of olive oil (Rowan 2014, 2015). Since olive oil production centres have not been recovered in the ancient town, the production of oil must have taken place in the surrounding countryside. Previous pollen and wood analyses in the harbour of Neapolis already attested olive arboriculture in the area during the 1^{st} century AD (Allevato *et al.* 2010). Moreover, Rowan (2015) noted that the choice of using this fuel instead of charcoal suggests a high availability of production waste, therefore of a large-scale production. The consumption of the fruit itself is also supported by the additional presence of mineralized olive stones (Rowan 2014, 2015).

Together with cereals and olive oil, wine represented the most traded good in the Roman Empire. The commercial scale of its production boomed in the Republican period and it is testified by the numerous amphorae with the name of the wine stamped on, villas with presses and cellars scattered around the Mediterranean basin, as well as by the countless details provided by the ancient agronomists about wine production and grape varieties. Moreover, the Mediterranean climate is ideal for viniculture, since grapes (*Vitis vinifera*) flourish during warm and dry summers (Thurmond 2006). Wine was probably accessible by many, depending on the quality and price of the wine. Columella suggests that the farmer would earn, as a minimum price, one *as*[1] per *sextarius* (a Roman measurement unit corresponding to *ca.* half a litre)(*Rust.* 3.3). This is in line with the inscriptions found in Pompeii and Herculaneum. For example, the sign at the entrance of a shop at Herculaneum *Insula IV* reports that the price went from four *asses* per *sextarius* to as little as two *asses* per *sextarius* (Figure 2.5)(Santamato 2014). Different prices according to the quality and provenance of the wine are also reported in the *Edict of Diocletian* (Kropff 2016).

De Simone (2017) estimated that the area around Mount Vesuvius produced four times the local demand of wine, by considering the number of *dolia* per cellar from the excavated farms and the capacity of the *dolia* (*ca.* 786 litres). It is possible that the majority of the countryside was indeed dedicated to the cultivation of grapevine

[1] One *as* is equivalent to 1/16 *denarius*.

Figure 2.5 Section of a painted sign at the entrance of a shop of *Insula IV*, Herculaneum, reporting the price of the wines: AD CUCUMAS / A.IIIIS / IIIS / IIIISS/ IIS. Modified after Jebulon, CC0, via Wikimedia Commons.

and ancient sources report that two-thirds of Mount Vesuvius was used for viniculture (De Simone 2017).

Further pollen analyses of the sediments of the ancient harbour of Neapolis suggest that viticulture was the main local crop together with that of chestnut, just after that of walnut, between the 1^{st} century BC and the 5^{th} century AD (Sadori *et al.* 2015).

Interestingly, grape represents the main fruit species found in the *Cardo V* sewer at Herculaneum (pips and stalks, $n = 221$), just after fig (achenes, thousands) attesting the large consumption of the fruit itself (Rowan 2017a).

2.1.7 Marine resources

The importance of marine fish for the Romans is well attested. In Rome there was a specific market specialized in the sale of fish called *Forum Piscarium* (Livy, 26.27.2-3). However, Cato complains about the high price of the fish from this market, saying that it is far higher than that of meat (Plutarch, *Quaest. Conv.* 4.4.2.9). The Mediterranean provided a large variety of fish and shellfish, which is documented by some astonishing Roman mosaics (an example is reported in Figure 2.6). However, the majority of these species were gourmet products usually served during banquets, while the most popular marine fish, often farmed, where the gilt-head bream (*Sparus aurata*), the common dentex (*Dentex dentex*) and the sea bass (*Dicentrarchus labrax*)(Marzano 2013b).

It is important to note that the ancient Mediterranean coast was largely characterised by marshy lagoons (perhaps 6500 km^2, Horden and Purcell, 2000). Juvenile individuals belonging to the families Sparidae, Anguillidae, Solidae and Moronidae

Figure 2.6 Mosaic from the House of the Faun in Pompeii representing marine fauna. Central of the scene is the fight between and octopus and a lobster, while various marine species set on the side. Among the others: a crayfish, a mullet, a sea bass, a murex, a moray, a scorpion-fish, a gilt-head bream and a ray. Museo Archeologico Nazionale di Napoli, Naples.

all enter the lagoons in spring - where they can find shelter and food - and leave in autumn to reproduce (Marzano 2013b). As a consequence, lagoons are at least twice as productive as the open-sea (Horden and Purcell 2000; Marzano 2013b). The Romans used to trap the fish in the lagoons that were trying to return to the open-sea by sophisticated systems of fences, nets and wickers, and by doing so, they could also control the growth and therefore the size of the fish, practising an actual form of fish farming (Marzano 2013b). Therefore, it is not a coincidence that the most consumed species belonged to the families of fish that most adapt to the lagoon environment. These activities were often on a large commercial scale. Interestingly, in Lattes, in southern Gaul, the zooarchaeological analysis of the remains belonging to *Dicentrarchus labrax* has evidenced a decrease in size and weight of the fish from 150 BC to AD 100, which could suggests an over-exploitation of the marine environment (Marzano 2013b).

However, the Mediterranean is also ideal for the fishing of pelagic migratory fish, notably tuna but also mackerel and bonito, that enter in large schools the warm waters of the Mediterranean from the Atlantic to reproduce. When the fish in search of food were close to the sea-shore, the Roman fishermen would capture them by using a long net fixed to the seabed to block the fish route and by encircling them with a net

released from the boat, an anticipation of the later more sophisticated system known in Italy with the name *tonnara* (Marzano 2013b).

The best way to preserve such large catches was by salting them. Indeed, the marine marshy coasts were also ideal for the production of salt and therefore for fish salting. Large-scale production installations of fish-salting were excavated around the Black Sea, the Strait of Gibraltar and North Africa but smaller establishments are ubiquitous in the Mediterranean basin, also in urban contexts (Curtis 1991). The commercial role of fish-salting products is well attested by the numerous mentions in the ancient texts. Strikingly, the majority of Apicius' recipes are prepared with *liquamen*, a product of the fish salting practice. Some other ancient literary sources provided a wide variety of recipes for the preparation of fish sauces. Briefly, meat of large pelagic fish (as well as their interiors and other waste parts) or whole small fish, such as anchovies and pilchards, are added into a container and mixed with large quantity of salt, sometimes also with wine and/or herbs; weights were placed on the mixture which is then left for several months in the sun. At the end of this period, the so-formed liquid, called *garum*, was separated and stored in vessels for sale. The *allec* was the name of the remaining fish at the bottom, while the *liquamen* was probably a secondary product of the *garum* production, obtained by washing the *allec* once again with a salty solution. However, the term *liquamen* replaced that of *garum* in late antiquity (Curtis 2009).

Apart from salting, the only way for the Romans to provide fresh fish was to keep them alive as much as possible. Some ancient authors refer to fish holding tanks that could be transported by ship thanks to a system of holes that allowed the exchange of sea water throughout the trip. A boat with these characteristics, known as *navis vivaria*, was for example found at Ostia (Boetto 2010). The most convenient way, however, was to farm the fish in artificial ponds. Many fishponds have been attested in Tyrrenian coastal villas, that extend from 700 to 1300 m^2. Columella recommends to provide the fishpond with a series of openings and channels to allow a constant exchange of water between the pond and the open sea (*Rust.* 8.17.1-6). Marzano and Brizzi estimated that fishponds with a size of *ca.* 1300 m^2 could contain up to five tonnes of fish, which would largely exceed the fish consumption inside the villa. Therefore, it is most likely that the majority of the fish produced in the fishponds was destined for commercialization (2009). From there, fish were probably transferred into small tanks or vessels and transported to the local market (Marzano and Brizzi 2009).

Fishing was probably a valuable commercial activity in the Bay of Naples. This area could in fact benefit from coastal lagoons and by the salt production at the *salinae Herculeae* (Marzano 2013b). Fragments of fish nets have been found at Herculaneum as well as a long line used to catch deep-sea fish (Marzano 2013b). Some fish-salting workshops have been found in Pompeii but it is most likely that the large-scale production of the Pompeian *garum* mentioned by Pliny (*HN* 31.94) was produced outside the city (Marzano 2013b). In total, *ca.* 200 fish sauce vessels were recovered from Pompeii and Herculaneum from both elite and more modest contexts suggesting that fish sauces were available to many (Curtis 2009). Rowan (2017a) registered a total of 98 different taxa of shellfish and fish from the Herculaneum *Cardo V* sewer, attesting to a wide range of species at Herculaneum, also available to the lower social classes. Cumae also appears to be involved in fish-salting activity from ancient literary sources (Marzano 2013b). It would therefore appear that a great part of the population of the Gulf of Naples was involved in fishing or fishing related activities (Rowan 2017b).

2.2 The archaeological context: Herculaneum and the Bay of Naples in the 1^{st} century AD

Campania was referred to by Pliny as "the lucky land" (*Campania felix*), who was referring to its hills covered in vines for the production of the famous wine, the cereal crops, the high quality olive oil and the renowned marine species that can be found along its sea-shore (*HN* 3.60). Geographically, Campania consists of the coastline between Mons Massicus in the north and the peninsula of Sorrento in the south, the volcanic area of the Campi Flegrei and Mount Vesuvius, and the plain behind them up to the first ridges of the Apennines (Figure 2.7).

The fertile soil and the high water availability of this region made it an ideal setting for human settlements long before the Roman domination (Cerchiai 2010). The Graeco-Italic amphorae containing a high quality wine had originated in Campania, and more specifically in the area of the Gulf of Naples, with a peak in production between the late 4^{th} and the early 3^{rd} century BC (Olcese 2017). By then, local vine-growers and merchants had already attested their production and distribution in the Mediterranean (Olcese 2017). Rome was most likely interested in this rich industrial activity and affirmed maritime trade in its plans of southward expansion (Olcese 2017).

By the 2^{nd} century BC, the area of the Bay of Naples had reached a population density and an intensity of land use which had few other parallels in the ancient world (Frederiksen and Purcell 1984). Between the second and the third Punic war (241

- 218 BC), the state placed new colonies along the coastline that would protect the area against further invasions by Carthage. Among others, Puteoli, with its sheltered harbour, could offer both protection and connection with the hinterland and across the Mediterranean, becoming one of the finest cities of the Italian peninsula (Polyb. 3.91). Puteoli remained for centuries the main harbour of the Roman Empire in the Italian peninsula. The coast of Ostia, at the mouth of the river Tiber, was in fact low and flat and inhospitable, and the sea there was rough, making it difficult for the ships to approach land (Tchernia 2016, 207). Until Trajan built the new harbour of Rome, the first man-made artificial harbour, which was inaugurated indicatively in AD 112/113 (Bellotti *et al.* 2009), Puteoli was the main offloading point of all the goods coming from the Provinces (Tchernia 2016, 208).

That the area was involved into commercial activities already in the 2^{nd} century BC is testified by an inscription found at Delos which reports a list of names of Italian traders, of which a great proportion are Campanian (Frederiksen and Purcell 1984). Many famous figures, such as Cicero, and rich landowners moved into this region and invested in the economy of the area by running large-scale farm estates, benefiting from the massive importation of slaves from the new provinces, arriving at the harbour of Puteoli. By the 1^{st} century BC, the area was a mixture of locals, Roman settlers and foreigner slaves that would quickly become freedmen, which created not a few social turbulences in the area. It would appear therefore that it was the Roman colonization which determined the agricultural importance of the area as reported by the ancient authors (Arthur 1991).

While its commercial importance for the Empire would remain unaltered for long, the social and political role of Campania, and in particular of the Bay of Naples, started to decline around the 2^{nd} century AD, for which probably the AD 79 Mount Vesuvius eruption was a main cause (Frederiksen and Purcell 1984). In this setting, we find the town of Herculaneum.

2.2.1 Herculaneum

The ancient town of Herculaneum was located on a promontory overlooking the sea at the middle of the Bay of Naples, around 6 km from Mount Vesuvius, 10 km from Neapolis and 20 km from Puteoli (Figure 2.8). The town was probably located between two rivers, as it has been passed down by the Roman historian Cornelius Sisenna (Sisenna, 4, fr. 53), although excavations did not identify any sign of their presence[2].

[2]Rowan (2014) identified only three taxa belonging to freshwater environments (Percidae and Anguillidae), outnumbered compared to the 42 assigned to marine species.

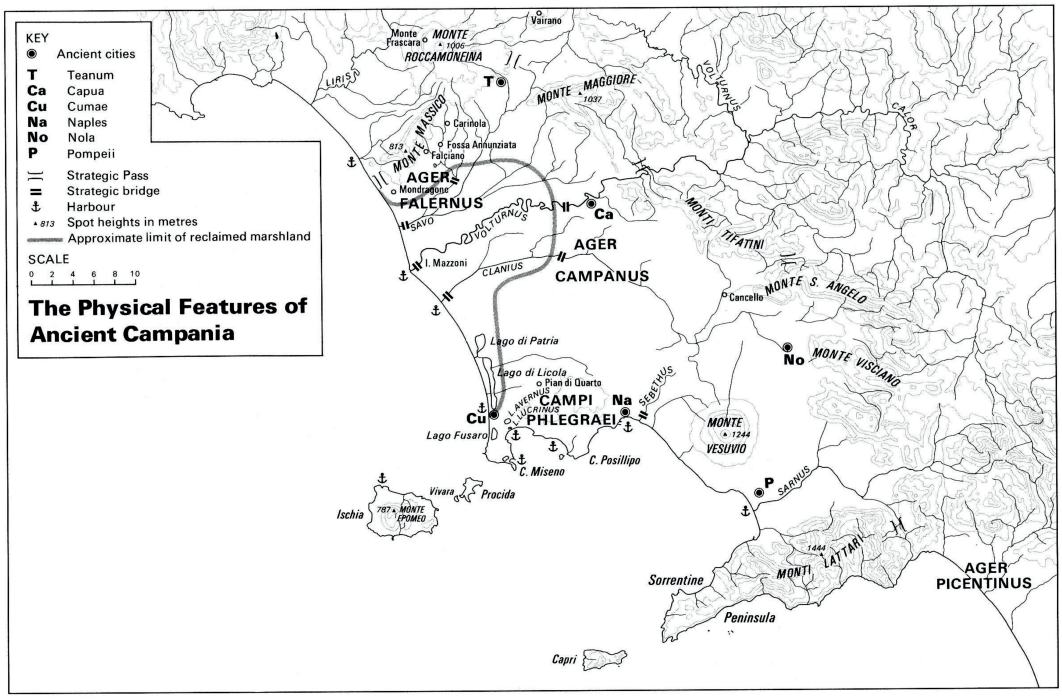

Figure 2.7 Physical map of the ancient Campania. Modified after Frederiksen and Purcell (1984).

According to a myth reported by the writer Dionysius of Halicarnassus, the town was founded by Hercules, to whom the name is attributed (*Ant. Rom.* 1.44). Although the legend was welcomed by the ancient inhabitants that adorned both private and public spaces with frescoes and statues of the Greek God (Cooley and Cooley 2013, 10), it is possible that the town was never occupied by the Greeks. Indeed, the geographer Strabo reports that the town was held by the Osci first and then by the Etruscans and the Samnites (Strab. 5.4), therefore suggesting that Herculaneum was already there when the Etruscans came into Campania between the 7^{th} and the 6^{th} centuries BC to react to the Greek colonisation of the area. By that time, the Greeks had already founded Cumae (8^{th} century BC) but not yet Neapolis, which would have only come in the 5^{th} century BC. Interestingly, excavations at Herculaneum have so far shown no sign of substantial human activity before the 4^{th} century BC and the only evidence supporting the hypothesis that the town was under the influence of the Oscans, is a single inscription in the Oscan language. If Strabo's account is accepted, by being the northernmost Etruscan settlement in the Bay of Naples before the Greek colonisation block, there is no doubt that Herculaneum was also under the influence of the Greek culture which also resulted in the adoption of the Greek language (Wallace-Hadrill 2011, 89-122). Nevertheless, the Social Wars represented a turning point in the identity

of the people from Herculaneum and more in general of those living in the Campanian territories (Wallace-Hadrill 2008, 81).

During the Social Wars (91-89 BC) Herculaneum battled alongside Pompeii against Rome and it was eventually conquered by a legate of Sulla, Titus Didius, becoming a *municipium* of Rome (Cooley and Cooley 2013, 25-26). By that time, Rome had already conquered the Greek colony of Puteoli (194 BC) and made it the central pole of the Empire trade across the Mediterranean. In the following decades Herculaneum was invested by the wealth of the area and its protective walls were transformed into luxurious private and public buildings overhanging the sea to be admired from a distance. However, the role of Herculaneum in the busy political and economic scenario of the Bay of Naples remains unclear but some hints can be obtained by comparing it to its neighbour Pompeii (Wallace-Hadrill 2011, 287-305).

Herculaneum was a small town, only a quarter of the size of Pompeii. Graffiti of electoral propaganda (called *programmata*) are absent at Herculaneum, with the only exception of one possible electoral notice (Pagano 1987), perhaps suggesting that the political life of the town was much less competitive than that of Pompeii, where *programmata* have been found in large number (Wallace-Hadrill 2011, 287-305). There is no doubt that Pompeii was a center of large-scale production of many commodities, such as that of *garum* (see section 2.1.7) and probably that of wool since numerous fulleries have been found in the city (Cooley and Cooley 2013, 227). On the contrary, the shops of Herculaneum seem to be dedicated to the local market, although some products of its hinterland, in particular figs (Pliny, *HN* 15.70), vines and wood were renowned in the area (Wallace-Hadrill 2011, 287-305). A further indication of the limited involvement of Herculaneum in the economy of the area can perhaps be seen in the absence of the wheel ruts in the paving of the streets left by carts that are visible in Pompeii, suggesting that fewer carts passed on the streets of Herculaneum. The architectural and decorative elements of the buildings in Herculaneum are also very different from those in Pompeii, in a way that made numerous scholars believe that Herculaneum was a holiday town or a retirement place (Wallace-Hadrill 2011, 287-305).

The eruption of Mount Vesuvius

The eruption of Mount Vesuvius in AD 79 is without doubt one of the most famous historical natural disasters. Its popularity is mainly due to the numerous accounts of the event reported in the ancient literary sources and of course to the exceptional recovery of the sites hit by the eruption which provide a unique evidence of Roman life at the time of the Empire.

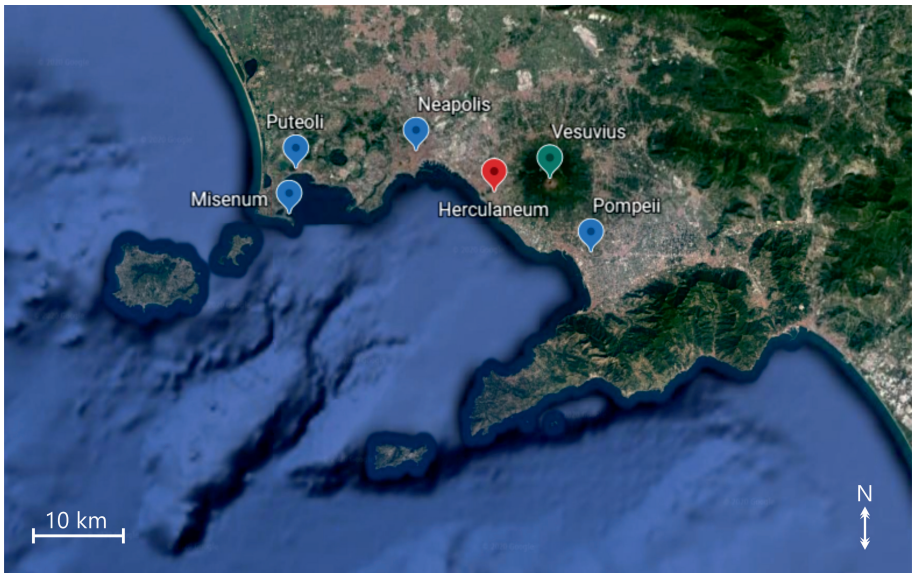

Figure 2.8 Location of Herculaneum in the Bay of Naples. From Google earth 2020.

The most remarkable details about the event comes from two letters (*epistulae*) that Pliny the Younger, nephew of Pliny the Elder, addressed to the historian Tacitus who was asking about the death of his uncle (*Ep* 6.16, 20). In these letters, Pliny reports that at the time of the eruption he was living with his uncle at Misenum, where Pliny the Elder was in charge of the Roman navy. From here, Pliny the Elder sailed towards the coast just below Mount Vesuvius' slopes to offer aid to the people living the area that could have escaped the eruption only by sea (*Ep* 6.16). It is clear from the letters that the eruption was not sudden and unanticipated, since a series of events happening between 24^{th} and 25^{th} of August are reported. The two letters are so vivid in the description of the eruption that are still used by volcanologists in the interpretation of the event and the term "Plinian eruption" is used to describe eruptions similar to that of AD 79 (*e.g.*, Sigurdsson *et al.* 1982).

The stratigraphy of the eruption levels have been extensively studied and recent investigations from different spots in Herculaneum confirmed the previous evidence (Gurioli *et al.* 2002). Briefly, the first event consisted of a fallout of ashes caused by the opening of the conduit, which is probably the event that made Pliny the Elder decide to sail to offer help just after noon on the 24^{th}. Following, the actual Plinian phase took place, with a high erupting column that deposited a thick layer of pumice lapilli in the south-east, affecting the sites of Pompeii, Oplontis, Boscoreale and Stabiae. This event probably lasted for seven hours, followed by the collapse of the column resulting in a dilute pyroclastic flow that hit Herculaneum causing the death of its inhabitants.

Two pyroclastic flows rich in pumice debris followed during the night that covered Herculaneum for the largest part. The day after, some more flows and surges would have buried the city completely (Gurioli *et al.* 2002).

The dates of 24^{th} - 25^{th} August have been often questioned since multiple evidence suggest instead that the eruption occurred later in autumn. Modern data collected over 20 years from two meteorological stations at Pratica di Mare (Rome) and Brindisi, show that high-altitude winds blow toward the northeast and southeast in autumn-winter, while those blowing toward west-northwest are typical of the summer period. Therefore, the dispersion of the pumice lapilli towards the southeast, in the direction of Pompeii, would suggest an autumn-winter date (Rolandi *et al.* 2008). This would be in accordance with the well-attested presence of autumnal fruits, such as fig, grape, pomegranate, chestnut and walnut recovered from the layers of the eruption, although it cannot be ruled out that these food items were preserved as discussed in section 2.1.5. Moreover, a coin with the image of the emperor Titus found in Pompeii reporting Titus being emperor for the fifteenth time (Rolandi *et al.* 2008). According to Cassius Dio, Titus received the title in the summer of AD 79, therefore, for it to be found in Pompeii, the coin should have been first given the time to be minted and then circulated. Two epigraphies dated to the 7^{th} and 8^{th} September AD 79 report Titus being emperor for the fourteenth time, therefore, the eruption would have happened after this date (Rolandi *et al.* 2008). Recently, the recovery from Pompeii of a charcoal inscription dated to 17^{th} October further supports a later date for the AD 79 eruption of Mount Vesuvius (Borgongino and Stefani 2021).

A brief history of the excavations

The discovery of Herculaneum is partially steeped in legend. According to local contemporary sources, in 1709, Prince d'Elbeuf, who had recently moved to Naples, came to know that many locals were recovering precious marbles from some wells they were excavating at Resina[3]. Interested in using the marbles to decorate his nearby villa, he bought from a local farmer, called Enzecheta, his land, with the aim to access the marbles himself (De Jorio 1827). During this period, through the excavation of tunnels (*cunicoli*), part of the theatre of Herculaneum was recovered. However, the work was arrested in 1711.

In 1738, King Charles VII of Naples began a systematic excavation that continued intermittently until 1780. However, his only intent was to recover statues, frescoes and

[3]Resina was the name of the town built over the ancient Herculaneum ruins whose name was later changed to Ercolano in 1969 (Wallace-Hadrill 2011, 114).

mosaics to be used to decorate his palace at Portici. The system of tunnels adopted by the engineers ruined a great part of the ancient city and it was only in 1828 that the first attempt of an open-air excavation took place, on the example of those at Pompeii. It was the time of the *Grand Tour*, when many upper-class young students, scholars and amateurs came to Italy to see the ancient ruins and learn about history and art (Bowersock 1978). However, the hard nature of the sediments made the procedure slow and difficult, resulting in the collapse of many of the ancient buildings and the works therefore halted in 1855.

After a brief campaign between 1869 and 1875, under the direction of Giuseppe Fiorelli, the excavation stopped once again. Later, the fascist ideology of glorifying ancient Rome brought up a new interest into the territories of the AD 79 eruption and in 1927 a systematic excavation at Herculaneum took place under the superintendency of Amedeo Maiuri. The excavations proceeded undisturbed until 1943, with the start of the fighting on the Italian Peninsula during the Second World War. The work of Maiuri was organised in a way that each building after being excavated would have also been propped, restored and decorated with various contextualised remains, ready to be visited by the public, making Herculaneum an open-air museum (Figure 2.9)(Camardo 2006).

After the war, Maiuri proceeded with his campaign of excavation and restoration until 1958. In the 1970s, under the direction of Giuseppe Maggi, a series of intermittent excavations took place in the area of the Suburban Baths. At the end of the 70s, Maggi was given permission to explore the area south of the entrance to the suburban baths with the aim to drain the groundwater which was causing major problems to that area of the site (Maggi 1998). On this occasion, on the 21^{st} May 1980, three human skeletons emerged, deposited in a stratigraphy composed of marine sand and seashells (Figure 2.10). Without at first realising it, Maggi was just beginning to expose the extraordinary death assemblage of the Herculaneum seashore and from that moment almost all the future excavations at Herculaneum have focused on that area (Maggi 1998).

Between 1996 and 1999, the atrium of the Villa of the Papyri was excavated, just outside the wall of the town on the south-west (Wallace-Hadrill 2011, 118). From 2001, conservation and research projects as well as out-reach programs related to the archaeological site are managed by the Herculaneum Conservation Project (HCP), a partnership between the Packard Humanities Institute, Parco Archeologico di Ercolano and the British school at Rome, under the direction of Andrew Wallace-Hadrill (Camardo 2006).

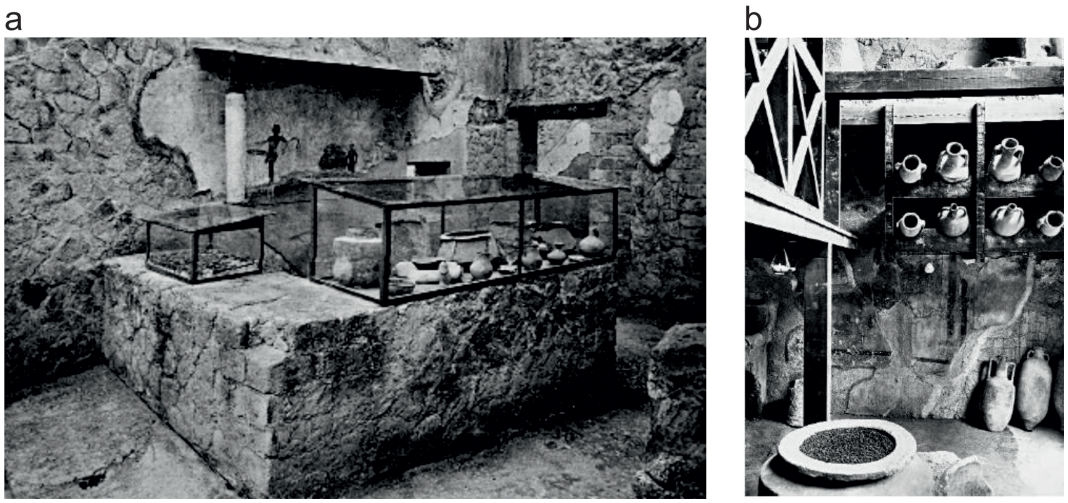

Figure 2.9 Archive photos of Herculaneum under the superintendency of Amedeo Maiuri (1927-1961). The shop of Priapus (a) and the shop of the House of Neptune and Amphitrite (b) with finds on display in an attempt of creating an "open-air" museum. Modified after Camardo (2006)(a) and Maggi (2013)(b).

Figure 2.10 Archive photo of the recovery of the first skeleton from the ancient Herculaneum seashore on 21^{st} May 1980. Modified after Maggi (2013).

The town layout

Only the southern part of the town of Herculaneum has been excavated so far and the visible ruins today extends for 4.5 hectares. However, it is estimated that the total extension of the town is between 15-20 hectares (Wallace-Hadrill 2011, 105).

The town is articulated into eight blocks (*insulae*) defined by the main streets running west-east (*decumani*) and those cutting the town north-south (*cardines*)(Figure 2.11). The excavated portion of the town reveals three *cardines* (from west to east, *Cardo III*, *IV* and *V*) and two *decumani* (from north to south, *Decumanus Maximus* and *Decumanus Inferiore*). The southern excavated portion of the town is completely dedicated to private houses with the only exception of the Suburban Baths and of the Sacred Area that overlook the sea by the cliff. The most luxurious and largest houses are located here, including the House of the Telephus, the House of the Mosaic Atrium and the House of the Stag. From the Sacred Area and the Suburban Baths, a stair leads to the seashore area, where some vaulted chambers sustain the terraces above. According to Wallace-Hadrill (2011, 103), the harbour of the town should be located further east, at the mouth of one of the rivers mentioned by Sisenna, as suggested by some signs of damage caused by the sea on the southernmost side of the House of Telephus.

The other public spaces are located in the northern part of the town. The central baths have been excavated in *Insula VII*, while the *Palestra* (only partially excavated) is located in the north-east of the site. The north-west corner seems to be almost entirely dedicated to the political life of the town, with the College of the *Augustales*, which is now believed to be the *Curia*, an open space with colonnades called *Basilica* and the *Basilica Noniana*, the last two only explored through the Bourbon tunnels. The location of the *Forum*, the centre of the political life in every Roman town, is still unknown, if present at all (Wallace-Hadrill 2011, 151-157). From here, the theatre is located in the northernmost portion of the town (Figure 2.12). Commercial spaces, either independent or associated to private houses, are restricted to the northern part of the town, the majority of them facing the two *decumani* and the *Cardo V* next to the *Palestra* (Figure 2.11).

Just outside the town, on the south-west, a sumptuous villa stood along the coastline, today still only partially explored through the Bourbon tunnels. The side of the villa facing the sea runs for more than 200 meters, which is approximately the total length of the seafront of Herculaneum. The villa, organised on four levels, is called Villa of the Papyri for the exceptional discovery of around 1800 charred papyrus scrolls found in its library (Wallace-Hadrill 2011, 114-118). Further excavations of the ancient town

of Herculaneum and of the Villa of the Papyri are hampered by the presence of modern buildings. Moreover, at the moment the priority of the Herculaneum Conservation Project is the maintenance of what has already been recovered and to promote its cultural significance (Wallace-Hadrill 2011, 333-336).

Figure 2.11 Plan of the ancient town of Herculaneum with differentiation between public spaces (blue), private houses (grey), houses with commercial units attached (white) and commercial spaces (red). Modified after Monteix (2010).

Who lived at Herculaneum?

Rich families of benefactors were living at Herculaneum, notably that of Marcus Nonius Balbus and that of Lucius Mammius Maximus, whose names are recurrent in inscriptions and to whom statues around the town were dedicated to celebrate them

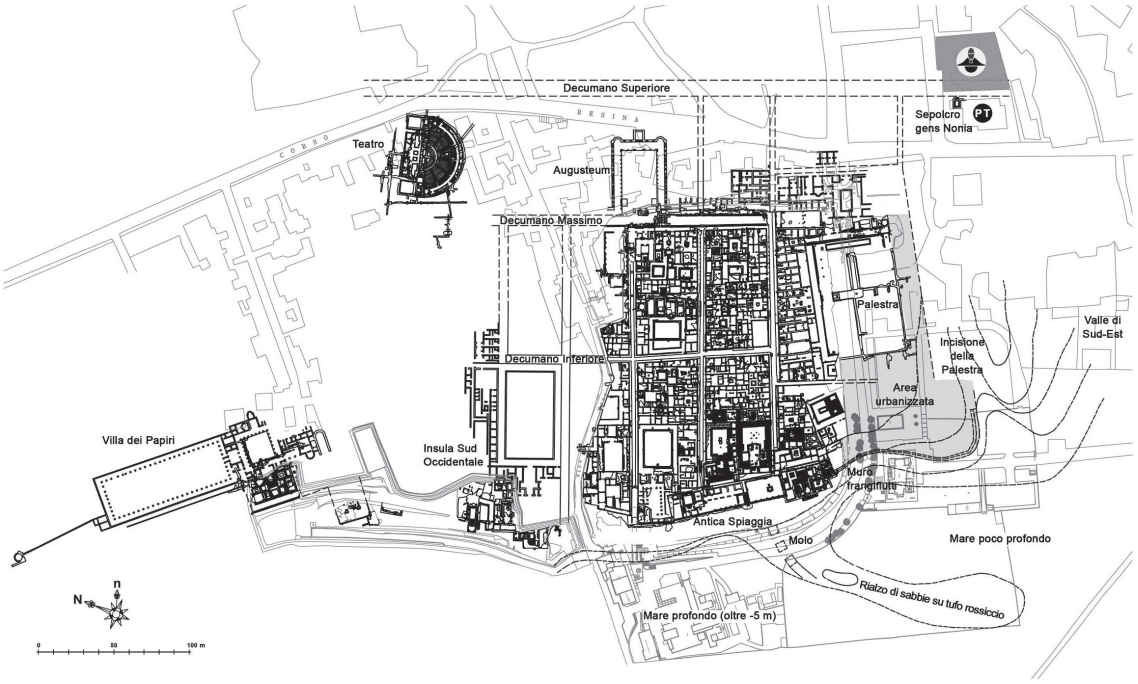

Figure 2.12 Plan of the ancient town of Herculaneum showing the Theatre (north-west) and the Villa of the Papyri (south-west). Modified after Guidobaldi *et al.* (2014).

for their contribution in the construction of public buildings (Wallace-Hadrill 2011, 130-134). The figure of Nonius Balbus is commemorated with an altar built on the site where his ashes were collected after his funeral took place (Frischer 1984).

Apart from the elite, Herculaneum was inhabited by a new generation of freeborn citizens (*ingenui*), whose parents or grandparents were ex slaves of Roman citizens, the new freedmen (*liberti*), who gained the Roman citizenship after being manumitted from the role of slave. The slaves (*servi*) were also living in town, owned by the elite as well as by the freeborns and freedmen (Wallace-Hadrill 2011, 123-145). The discovery over the centuries of several marble fragments belonging to the so-called *Album of names* allowed gaining a new understanding of the town (Figure 2.13). Initially believed to be a list of members of the college of *Augustales* (an order dedicated to the cult of the Emperor), this assumption has now been set aside since the 500 names reported in the fragments would be too many to be all part of a small group of devotees. Indeed, new studies have estimated that the panels originally reported around 1200 names, with the possibility that more panels exist but have never been excavated. It appears that this is instead a list of freeborn citizens, freedmen and of a third group of men that were promoted to citizenship by some merit, that were entitled to vote. The majority of the names reported belong to ex-slaves and de Ligt and Garnsey (2012)

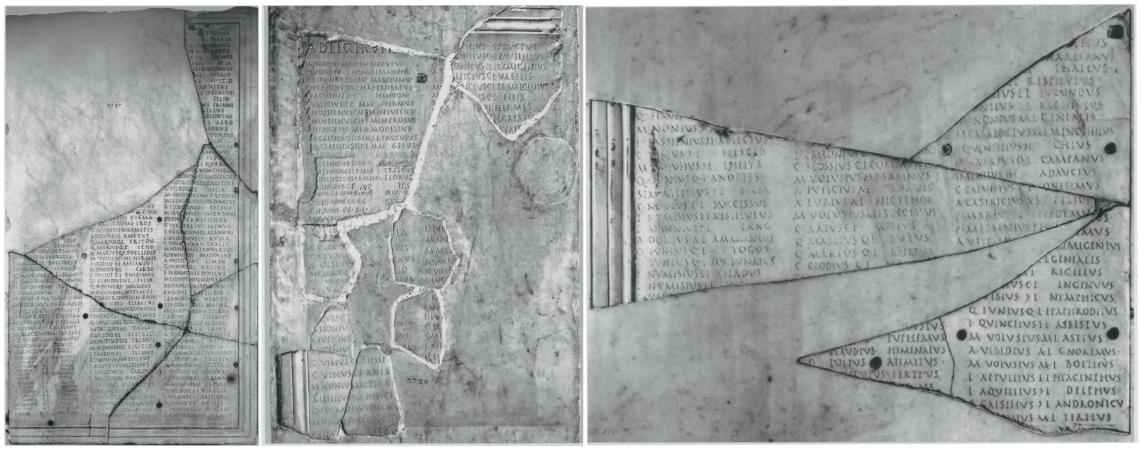

Figure 2.13 Some fragments of the *Album* of Herculaneum. Modified after de Ligt and Garnsey (2012).

have advanced a conservative estimation of 850 names of ex-slaves originally in the *Album*. Since freedwomen are not included in the list because they were not entitled to vote, the authors further estimated that ex-slaves in total in the town and hinterland of Herculaneum must have been at least 1550, considering that female slaves were manumitted later in life compared to men (de Ligt and Garnsey 2012). Taking into account the age limit of 30 years-old for manumission introduced by Augustus, de Ligt and Garnsey (2012) estimated that at least 2200 slaves were living in the area by the time the *Album* was compiled. By assuming that the total number of inhabitants of Herculaneum at the time of the AD 79 eruption was 4000, that at least four fifth of ex-slaves were living inside the town walls and that the slaves that had higher chances to be manumitted were those living in-town, de Ligt and Garnsey (2012) calculated that around 40 % of the population consisted of slaves and that more than 20 % was composed of freedmen and freedwomen.

It is clear therefore that the town of Herculaneum was sustained by a slave-driven urbanism, therefore by involuntary immigration, different from other Italian towns, first and foremost Rome (Garnsey and de Ligt 2016). According to recent estimates, Rome was in fact composed of around 30 % of slaves and exslaves, while freeborns accounted for the highest proportion of the population of Rome. This is believed to be linked to the grain dole, since the male recipients of the frumentationes would have most likely also had a job which would have ensure the access to other essential items, such such other food sources and textiles (Garnsey and de Ligt 2016).

The *Album of names* of Herculaneum helps to elucidate the social structure of a Roman town deeply influenced by the surrounding economic and political scenario,

presented in the introduction of this section (de Ligt and Garnsey 2012, 2019). Wallace-Hadrill (1994) suggested that the spread luxury of the houses in Herculaneum (but also in Pompeii) mirrors the social reality, where ex-slaves and freedmen by a few generations were looking for ways to affirm their newly acquired identity of Roman citizens.

The study of the catastrophic death assemblage of the Herculaneum seashore provides new insights into the life of these people.

2.3 The catastrophic death assemblage

2.3.1 The recovery of a scene of human tragedy

Before the accidental discovery of the skeletons from the ancient Herculaneum seashore, it was believed that the city was completely evacuated before the eruption. Very differently from Pompeii, only a few bodies were in fact recovered from the town (Lazer 2009). Therefore, the beachfront became immediately the main focus of the excavations at Herculaneum.

Here, archaeologists revealed the presence of some vaulted chambers, referred to as *fornici*, that support the terraces of the Suburban Baths on one side and those of the Sacred Area on the other (Figure 2.14). Maggi (2013) hypothesised that these chambers were used as boat houses for small fishing boats that needed a shelter during off-season, as they are still used in the coastal towns of the area. On 11^{th} January 1982, new excavations focused on the *fornici*, starting from *fornice* 3 and just a few days later, on the 16^{th}, a scene of human tragedy was revealed to the archaeologists. Maggi (2013) remembers the day of the recovery of the first group of skeletons from *fornice* 3 with excitement and deep feeling. It was clear to him that those individuals were desperately seeking shelter in the chambers. The scene was a snapshot of last movements of people from almost two thousand years before, that were reacting in many different ways to the inevitable death (Figure 2.15)(Maggi 2013).

The exceptional discovery brought up the attention of the media from all over the world and that summer, the National Geographic Society decided to fund further excavations on the area and the conservation and research on the skeletons (Maggi 2013). From summer 1982 until 1985 the excavation, conservation and study of the human assemblage from the seashore and the *fornici* was handed to the American anthropologist Sara Bisel. In that period, a boat was also recovered from the seashore, supporting the hypothesis that the habitants of Herculaneum were trying to escape

the eruption by sea (Figure 2.16). The public interest in the assemblage probably influenced Bisel to provide interpretations about the life of some of these individuals that were often poorly supported by the evidence. Some of the skeletons were even assigned appellations or names, such as "the Ring Lady", "Portia", "the Helmsman", "the Soldier" and "the Pretty Lady" that became the protagonists of a children's book titled *The Secrets of Vesuvius* and were also presented in two articles of the *National Geographic* journal (Lazer 2009, 28-32).

A total of 162 skeletons were recovered at the end of the collaboration with the National Geographic Society, 54 from the ancient beach and the remaining from the chambers under the suburban baths (*fornici* 3, 4 and part of 5) although their original location has now been lost, as well as that of numerous archaeological finds found in the proximity of some skeletons (Fattore *et al.* 2012). In 1988 the excavations of the *fornici* located on the opposite side of the stairs, under the Sacred Area, continued but the removal of the skeletons would only begin between 1997 and 1999 (*fornici* 5, 10 and 12)(Capasso 2001). Ultimately, the skeletons from fornici 7, 8, 9, 11 and from a niche of 10 were excavated between 2008 and 2012 (Martyn *et al.* 2020). In total, 340 individuals have been recovered (Figure 2.17)(Martyn *et al.* 2020).

2.3.2 Not an *osteological paradox*

Apart from the scene of human tragedy, another factor added to the cultural value of the assemblage. Indeed, the exceptional death circumstances made (and still do) scholars to carrying out paleodemographic and paleodietary investigations without having to deal with the typical biases of the study of archaeological populations. In cemeteries, infants, juveniles and older adults are commonly over-represented compared to the younger adults (DeWitte and Stojanowski 2015, 406-408). This most likely does not mirror the demographic profile, which is instead composed of those individuals which are less likely to perish, typically the younger adults. In the same way, assessing the health status of a cemetery population is contradictory in its definition, as certainly the majority of those who died were ill before their death. Nutritional studies are similarly affected by the latter since sick individuals might have changed dietary habits during the period of illness or rather, deficiencies in their diets lead to their death. Furthermore, dietary habits might change with age and therefore nutritional studies might not reflect mid age people diet, who are usually under-represented in cemeteries as stated above. In any case, nutritional data from cemetery populations hardly reflects the dietary habits of the living population. Last but not least, burial grounds are typically used over a certain period of time, a time during which the social, cultural,

Figure 2.14 View of the ancient town of Herculaneum from the entrance to the archaeological site, with Mount Vesuvius in the background. The vaulted chambers (*fornici*), where a large part of the catastrophic death assemblage was discovered, are visible at the bottom of the photo, below the Suburban Baths (right) and the Sacred Area (left) and divided by the stairs that connect the ancient seashore to the town. Photo by Laura Soncin, 2^{nd} September 2020.

Figure 2.15 View of the inside of one of the twelve *fornici*. Modified after Maggi (2009).

Figure 2.16 Photos of the boat recovered from the ancient Herculaneum seashore while being excavated (a, showing Giuseppe Maggi pointing at a skeleton found close to the boat and therefore named "the Helmsman") and after being restored and displayed in the "boat Pavillion" at the entrance of the archaeological site (b). Modified after Maggi (2013)(a) and personal photo by the author (b), 2^{nd} September 2020.

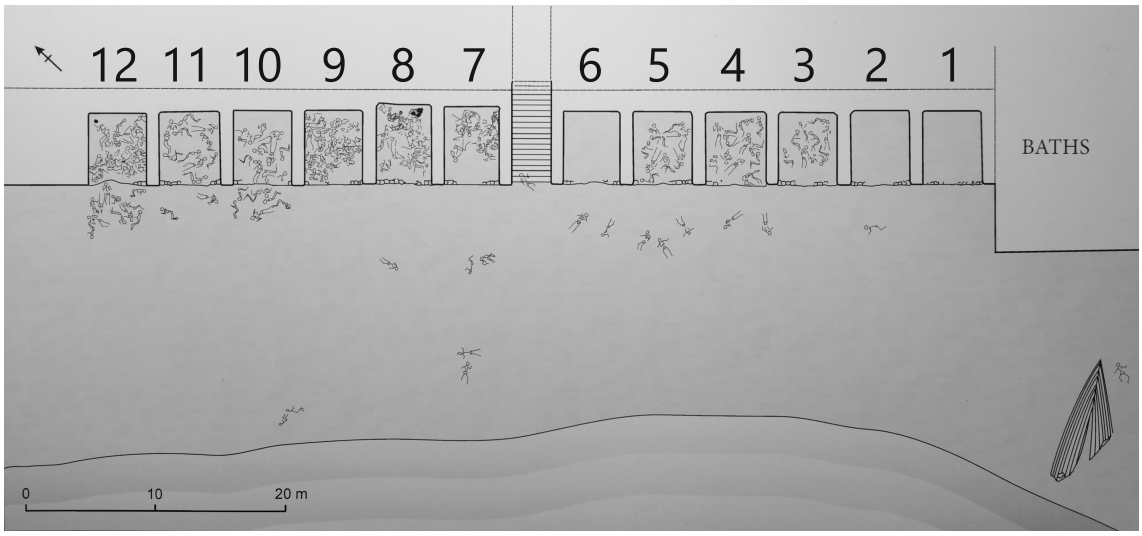

Figure 2.17 Drawing showing the distribution of the skeletons on the seashore and inside the boat chambers. Modified after Wallace-Hadrill (2011)

environmental and economic scenarios might have changed, making it difficult to address the group of individuals analysed as a single population. These aspects - presented here in the simplest terms - and many others have been fully discussed in a landmark article published in 1992 by Wood *et al.* titled: *The Osteological Paradox. Problems of Inferring Prehistoric Health from Skeletal Samples* and in following papers (*e.g.*, Pinhasi and Bourbou 2007; Jackes 2011; DeWitte and Stojanowski 2015).

The simultaneous death of the individuals recovered from the ancient Herculaneum beach and *fornici* makes them an archaeological *living* population (Martyn *et al.* 2018). That is, the demographic and the health status profiles are carried out on individuals that were not at risk of death if it was not for the eruption of Mount Vesuvius. Moreover, the food sources were potentially the same for all the individuals and therefore any difference in diet must be dependent upon cultural and social differences.

2.3.3 The studies on the individuals from the beachfront

Soon after the first excavation campaign, Sara Bisel published preliminary results derived from the anthropological investigation that she was carrying out on the assemblage from the beachfront. In an attempt to reconstruct the health and nutritional status of the assemblage, on a total of 98 individuals, Bisel (1988) calculated an average stature of 155.2 cm for female and of 169.1 cm for men, taller than 1960's Neapolitans and she explained this difference as a sign of better nutrition than that of modern Neapolitans. It was later noted that the results could also suggest that the individuals

from Herculaneum are not genetically related to modern Neapolitans. However, since the difference is only of a few centimetres and that the error associated with the measurements overlaps with the average stature of modern Neapolitans, regional continuity seems more plausible (Lazer 2009, 183).

Bisel (1988) also observed flattening of the pelvis and long bones, suggesting that the ancient inhabitants were used to heavy labor. Almost half of the male individuals presented vertebral arthritis, slightly lower in the female group (36.4 %), again explained as a symptom of heavy exercise. She interpreted the low incidence of caries, abscesses and antemortem teeth loss as an evidence of low sugar consumption, that historically was still not introduced in the Mediterranean basin. Enamel hypoplasia (linear defects of the enamel) was on the contrary frequently detected (30 %) and interpreted as evidence of nutritional stress in early childhood. The presence of porotic hyperostosis (anomalous porosity in the outer table of the skull and/or in the orbital roof), representing 34.1 % of the assemblage was linked to possible iron deficiency, nutritional debilitating disease or presence of parasites. The elemental analysis of the bones through Atomic Absorption Spectroscopy (AAS) evidenced a lower concentration of zinc (Zn) compared to modern Americans, which was interpreted as a lack of consumption of red meat at Herculaneum, while slightly higher strontium to calcium ratio (Sr/Ca) was explained as indicative of either a diet high in fish or in vegetables (Bisel 1988).

Other 43 skeletons were later analysed and the new results presented in a following publication (Bisel 1991). In here, Bisel noted a few infants and juveniles ($\leq$ 20 years-old) in the assemblage. This was explained suggesting a low birth rate at Herculaneum, supported by the low number of births per female older than 15 years (mean = 1.69), measured by looking at the destruction of the dorsal rim of the pubic symphysis (Bisel 1991). However, it should be noted that the link between lesions of the pelvis and parturition has been frequently questioned by scholars since they have been detected in both sexes and they seem rather influenced by weight and pelvis stability (*e.g.*, Maass and Friedling 2016). Bisel also observed extreme variability of the skulls measurements suggesting a mixture of genetic heritage in the assemblage. Concentrations of calcium, strontium and zinc in bones and soil samples were investigated again through AAS leading to the same results reported in the previous publication (Bisel 1988, 1991). The author also relied on the pelvic brim index as indicative of nutritional status, since the bone tends to flatten if it can not sustain the weight of the upper body, concluding that the individuals from Herculaneum had poorer nutrition profile compared to modern Americans (Bisel 1991).

After Bisel's untimely death, Luigi Capasso proceeded with the analysis of the 162 individuals excavated until then, with the main goal to create a collection of osteo-biographies, which resulted in the publication of an Italian monograph containing separate detailed descriptions for each individual titled *I fuggiaschi di Ercolano. Paleobiologia delle vittime dell'eruzione vesuviana del 79 d.C.* (2001). In doing this, Capasso was probably influenced by the popular culture around the assemblage in the same way that Bisel was. He considered the assemblage an exceptional opportunity to obtain not only a paleodemographic profile of an archaeological living population, but also to perform palaeoepidemiological studies on each skeleton (Lazer 2009, 64). One of the most famous examples is that of the individual called "E52". *E52* was identified as an eight months pregnant woman being 20-25 years old when she died, who was found with a melted metallic pin on her scalp that allowed the exceptional preservation of part of the cornrowed hair (Capasso 2001, 460-472). By microscopically observing the hair, Capasso and Di Tota (1998) found what seemed to be a louse egg, which could explain the depression due to bone remodelling found on one side of her skull, probably caused by the continuous scratching of the area that caused an inflammation. The authors also noted that similar depressions on the skull were observed in about 22 % of the individuals, therefore suggesting a lice infestation in the group (Capasso and Di Tota 1998)(also discussed in Capasso 2001, 1004-1006).

Of the 162 individuals analysed by Capasso (2001), 83 were male and 61 were female, with an unbalanced M:F ratio towards males (1.38:1). However, the author admitted that this was probably not an actual representation of the demography of the town, since several factors might have contributed to the gathering of these individuals on the beachfront (Capasso 2001, 956-957). The measurements of the long bones, that were only possible on 96 of the individuals, indicated an average stature of 163.8 cm in the males and 151,7 cm in the females, surprisingly very close to those of contemporary Neapolitans (Capasso 2001, 927). It is unclear why these results do not match with those from Bisel (1988) but it could be explained by a different use of the *Trotter and Gleser formulae* (Lazer 2009, 183).

The author also examined the distribution of the individuals according to their age and compared them with census data from modern populations. The distribution resembled that of an *expansive* model, since juvenile individuals (0-14.9 years old) represent more than 30 % of the assemblage, while older adults (>50 years old) only 10 %, suggesting that the population of Herculaneum was growing at the time of the eruption (Capasso 2001, 959-969). Interestingly, Capasso and Capasso (1999) observed a lower number of individuals aged between 15 and 20 years old compared to the other

classes, suggesting a birth rate crisis between AD 59 and 64, probably linked to the earthquake of AD 62 (also discussed in Capasso 2001, 967-969).

The author showed the presence of different skeletal lesions that could be linked to work activities (Capasso 2001). In a separate publication, Capasso and Di Domenicantonio (1998) discussed the signs on the bones caused by the syndesmopathy of the costoclavicular ligaments observed in 41.3 % of the male individuals, 6.5 % of the female and 11.5 % of the children. According to the authors, this would suggest the engagement of a large part of the population, five years-old and over children included, in heavy work related activities that involved the continuous movement of the head and of the upper limbs (Capasso and Di Domenicantonio 1998). Moreover, since the lesions where predominant on the right side of the skeleton, the authors hypothesised that this could be linked to rowing, therefore implying the involvement of a large part of the assemblage into fishing related activities (Capasso and Di Domenicantonio 1998)(also discussed in Capasso 2001, 1026-1028). (Capasso 2001, 994) suggested that the presence of the Poirier's facet on the femoral head in 15 adult individuals (11 of which are male) could further support the engagement of these individuals in activities that were carried out in the beachfront area. Indeed, according to the author, the Poirier's facet would be often caused by walking uphill, therefore suggesting that the individuals affected walked frequently uphill from the seashore area to the town. Other skeletal lesions were also interpreted as evidence of work activities. For example, the author observed periostitis in the lower limbs linked to venous stasis in 15.1 % of the adults (M:F = 2.5:1), probably caused by standing for long periods of time (Capasso 2001, 1003). Moreover, the extremely high occurrence (74.2 % of the adults over 20 years old) of osteoarthritis, even in the younger individuals, was interpreted as a sign of heavy excercise/work in which the majority of the population was involved, regardless of gender (Capasso 2001, 1018-1024).

Other evidence from the skeletons was linked by the author to the living conditions of the individuals. For example, periostitis caused by sinusitis and other inflammation of the respiratory system were found to be abundant in the assemblage (17.5 %). The author suggested that the frequent inflammations of the respiratory system was caused by indoor pollution, created by fireplaces and oil lamps (Capasso 2001, 1003-1004).

Capasso (2001) also evidenced the presence of pathologies indicative of food consumption. For example, vertebral lesions compatible with brucellosis, were found on 16 adult individuals (Capasso 1999). Brucellosis is a disease caused by the *Brucella* sp. bacteria that infect animals, including ovicaprines, cattle, pigs and dogs. In humans,

brucellosis is mainly associated with the consumption of dairy products that have not been pasteurised, but also with occupational exposure or consumption of raw meat (*e.g.*, Corbel 1997). Capasso (1999) explained the high frequency of affected individuals with the consumption of milk and cheese derived from sheep and goats, as reported by the ancient literary sources, which was not sterilised prior to consumption (also discussed in Capasso 2001, 1006-1011). It should be noted that some sheep[4] were found sporadically inside the *fornici*, testifying to the importance of these animals for, at least some of, the individuals that were trying to save them from the eruption, as part of their precious belongings. However, it cannot be ruled out that these bone remains were part of possible garbage hidden inside the *fornici*. Later, Capasso (2002) detected the presence of bacteria with a shape consistent with that of the *Brucella* sp., in a carbonized cheese found in Herculaneum. However, the author admitted that the shape could also be compatible with that of the more common group of streptococci (Capasso 2002).

A correlation between porotic hyperostosis with other lesions that occur during the development of the skeleton were also observed by Capasso (2001). In particular, 41 % of the individuals with porotic hyperostosis were also found with enamel hypoplasia, often (1/3) in association with the Harris lines on the tibia. The combination of these lesions were interpreted as a nutritional/health crisis during the development of the skeleton diffuse among the assemblage (Capasso 2001, 1012-1013).

Capasso (2001) evidenced a peculiar extramasticatory dental wear of the anterior teeth in 18 individuals, 15 of which being male. In addition to this, the author noted a peculiar recurrent loss of the central incisors, probably linked to the same extramasticatory use of the mouth (Capasso 2001, 1040-1042, 1047-1049). Caries were found to be frequent in the assemblage, with 56 individuals presenting at least incidence of one caries, in contrast with what reported by Bisel (1988)(Capasso 2001, 1044-1047). Dental calculus was also reported to be common (30.2 % of the individuals with teeth, *i.e.* 139) although only in four individuals the accumulation of calculus was severe (Capasso 2001, 1042).

Trace elemental analysis had been already carried out by Bisel (1988, 1991) but repeated by Capasso *et al.* (2001) on 56 adult individuals and 36 children, arriving to similar conclusions. Slightly higher Zn/Ca ratio and slightly lower Sr/Ca (both included in their standard deviation) were observed in children compared to the adult

[4]To my knowledge, a list of animal remains found on the seashore or under the *fornici* has not been published yet. For this thesis, I have analysed collagen from bone fragments belonging to: 3 ovicaprines (one from *fornice* 7, one from *fornice* 8 and one from *fornice* 10), one cow from *fornice* 8, and two dogs (one from *fornice* 11 and one from *fornice* 12). See chapter 5.

group, interpreted by the authors as higher consumption of animal products, milk in particular, in children (Capasso *et al.* 2001).

Mariani Costantini and Capasso (2001) also attempted the extraction of ancient mitochondrial DNA from the bones of eight individuals. For only two individuals the extraction was successful and led to the PCR amplification of 180 bases, proving the presence of endogenous DNA in at least some individuals from the assemblage (Mariani Costantini and Capasso 2001). However, the authors do not indicate from which bone they performed the extraction as it is nowadays well-attested that only specific skeletal districts have a better chance of preservation of endogenous non-contaminated DNA, notably teeth and Petrous bone (*e.g.*, Pinhasi *et al.* 2015).

More recently, Viciano *et al.* (2011) measured the permanent dentition of 87 adults from the assemblage whose sex was previously confidently attributed with the aim to detect dimorphic characters. They concluded that the permanent canine is the most dimorphic tooth and therefore they used it to determine the sex of children and juveniles in the assemblage (n=30). The group resulted composed by 5 males and 17 females, while the sex attribution was not obtained from 8 individuals (Viciano *et al.* 2011).

2.3.4 The studies on the individuals from the *fornici*

While Bisel first and Capasso later were analysing the skeletons recovered from the seashore, Torino and Fornaciari carried out preliminary studies *in situ* of the victims that were emerging from the vaulted chambers.

The first results from *fornice* 7 and *fornice* 8 showed low incidence of caries and of other dental disorders (*ca.* 30 %) compared to modern and other ancient populations, as well as diffused enamel hypoplasia that the authors refer to as possibly caused by fluorosis (Torino and Fornaciari 1993). This possibility was further explored by analysing thin-sections of the teeth of eight individuals by Scanning Electron Microscopy with Energy Dispersive Spectroscopy (SEM-EDS). Fluorine was found to be high in 6 out of 8 teeth suggesting access to a water rich in fluorine at the time of enamel formation. The groundwater of Herculaneum was also analysed, reporting high levels of fluorine. According to the authors, endemic fluorosis might also explain the low incidence of caries. The authors noted a recurrent tooth wear of the front teeth in all the individuals analysed which suggest a more intense use of the front teeth compared to modern populations, that might have also been used as a third hand (Torino and Fornaciari 1993). The analysis *in situ* gave to the authors the opportunity

to focus on the evidence of kinship, not only by observing the depositional connection between individuals, but also by noticing skeletal hereditary traits, as for two female individuals close to each other, both around 20 years old and both with impacted canine (individuals *F8i2* and *F8i9*)(Torino and Fornaciari 1993).

Later, Torino and Fornaciari (1995) focused on a subgroup of individuals from *fornice* 9 (n=10), *fornice* 10 (n=23), *fornice* 11 (n=18) and 3 individuals from a *fornice* called "fornice della famiglia" (transl. *fornice* of the family) providing the first palaeodemographic analysis of the skeletons excavated from the vaulted chambers. They showed a prevalence of adult individuals between 15 and 25 years old, the majority of which were females, in contrast to what is usually observed from burial grounds (Torino and Fornaciari 1995). They suggest that the almost complete absence of individuals older than 40 years-old is related to the possible high social status of older individuals, that probably had the chance to escape the eruption earlier than the rest of the inhabitants (Torino and Fornaciari 1995). However, this is not the only possible explanation for the lack of individuals older than 40 years across the assemblage. The elderly people might have been limited in flying away from the eruption as a consequence of their poorer health conditions, or might have died while trying to do so. However, if the possibility that the elderly individuals were not hampered in reaching the town's seashore is accepted, one may suspect that the lack of individuals older than 40 years-old could be a sign of seasonal mortality. Shaw (1996) suggested that the death rates in Imperial Rome were higher during the wetter and colder months, therefore this could be used as an additional evidence for an autumnal date of the eruption.

As in their previous publication, Torino and Fornaciari (1995) observed evidence of kinship in the group of individuals. They suggested that it was clear from the disposition of the skeletons that many of the female individuals were hiding under the vaulted chambers with their children. This would be not only suggested by those cases of young women holding infants (this is the case of *F10i8*, *ca.* 25 years-old that hugs *F10i9*, 2 years-old and of *F11i1*, 17-25 years old, that holds *F11i2*, 3 months-old), but also from the peculiar stratigraphy that sees the skeletons of infants and juveniles below those of females, probably in an attempt to use their bodies as a shield to protect their children (this is for example the case of the children *F11i4*, 4 years-old and *F11i17*, 11 years-old, found below the skeletons of the women *F11i5*, 17-25 years old, and *F11i16*, 25-25 years-old, respectively)(Torino and Fornaciari 1995).

First investigations on some of the individuals from *fornici* 5 (n=3), 10 (n=40), 11 (n=5) and 12 (n=32) were presented by Mastrolorenzo *et al.* (2001) focusing on the manner of death of these individuals (Mastrolorenzo *et al.* 2001). Later, Petrone *et al.* (2011) published a more detailed discussion around the osteological investigation of this almost identical group of skeletons (from *fornici* 5 (n=3), 6 (n=1), 10 (n=41) and 12 (n=31)). The authors evidenced a diffuse calcification of ligaments, tendons and interosseous membranes (73.5 % of individuals aged $\geq$ 15 years) more frequent in the chest area, but also in the vertebrae and pelvis, often associated with osteosclerosis (*i.e.*, elevation of bone density) as well as recurrent osteophytes (*i.e.*, bone spurs) also found in children (91.8 % of the entire group). Lesions linked to osteoarthritis was also reported to be frequent (47.2 % of individuals aged $\geq$ 15 years) and ankylosis (*i.e.*, fusion of bones of the joint) affected 39.2 % of the individuals. 96.1 % of the individuals were also found to be affected by linear hypoplasia of the enamel and 54.9 % of all the teeth shown pitting, staining and mottling. Caries were also frequent as they affected 78.6 % of the assemblage. Petrone *et al.* (2011) suggested that the high occurrence of all these lesions on a rather young assemblage (mean = 30.2 years) are most likely evidence of endemic skeletal fluorosis.

Interestingly, although the lesions and traits evidenced by the authors are in agreement with what reported by Capasso (2001) on the assemblage from the seashore, the interpretation by Petrone *et al.* (2011) is very different. The hypothesis of endemic fluorosis, already suggested by Torino and Fornaciari (1993), appeared to be further supported by the results obtained by Instrumental Neutron Activation Analysis (INAA) that showed correlation between fluorine (^{19}F) content in bones and age of the individual (Figure 2.18)(Petrone *et al.* 2011). As reported by the authors, skeletal fluorosis increases the risk of bone fractures, which could explain the presence of healed fractures found to be frequent (35.7 %) in the assemblage. Dental fluorosis in the Mount Vesuvius area was later further confirmed by analysing five teeth of the Herculaneum eruption's victims, one tooth from a AD 14-37 burial from Pompeii and one tooth from 4^th century AD Nocera Inferiore (Salerno) by applying Particle Induced Gamma-ray Emission (PIGE) technique for the determination of fluoride concentration (Petrone *et al.* 2019).

Fattore *et al.* (2012) examined the last excavated skeletons from *fornici* 7, 8, 9, 10 and 11 and revised the previous studies in light of the new sex and age profiles. By doing so, the authors turned the previous male to female ratio that was unbalanced towards male (M:F = 1.4:1), into a new more balanced ratio only slightly unbalanced towards females (M:F = 1:1.2)(Fattore *et al.* 2012). Moreover, the new discovery of a substantial amount of infants and juveniles among the assemblage, allowed revising the

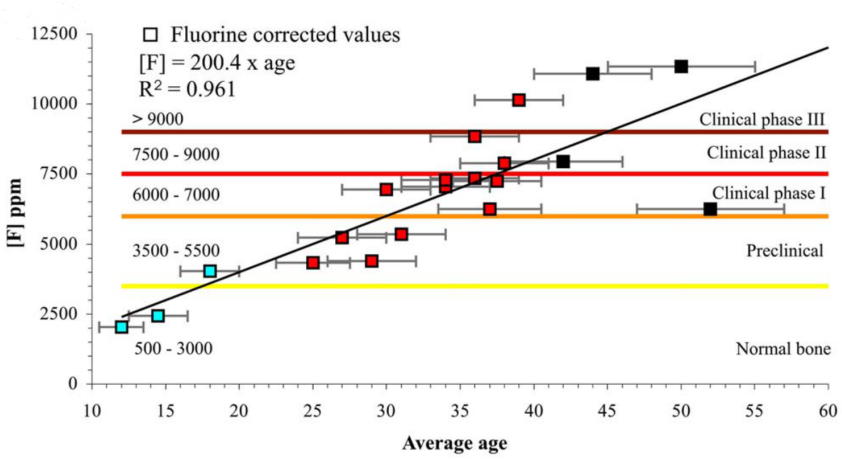

Figure 2.18 Correlation between age at death and ^{19}F content of bones of the individuals from the Herculaneum *fornici*. The clinical phases reported on the graph indicate the degree of skeletal fluorosis. Modified after Petrone *et al.* (2011). The colours were not explained by the authors.

population pyramid and possibly to exclude a birth-rate crisis as a consequence of the AD 62 earthquake (Figure 2.19)(Fattore *et al.* 2012). Therefore, it seems that previous examinations of parts of the assemblage were biased not only by the excavation strategy but also by the escape strategies adopted by the individuals both between *fornici* and between *fornici* and the beach. The authors therefore urge for a unified analysis of the entire assemblage that has still not taken place to this date (Fattore *et al.* 2012).

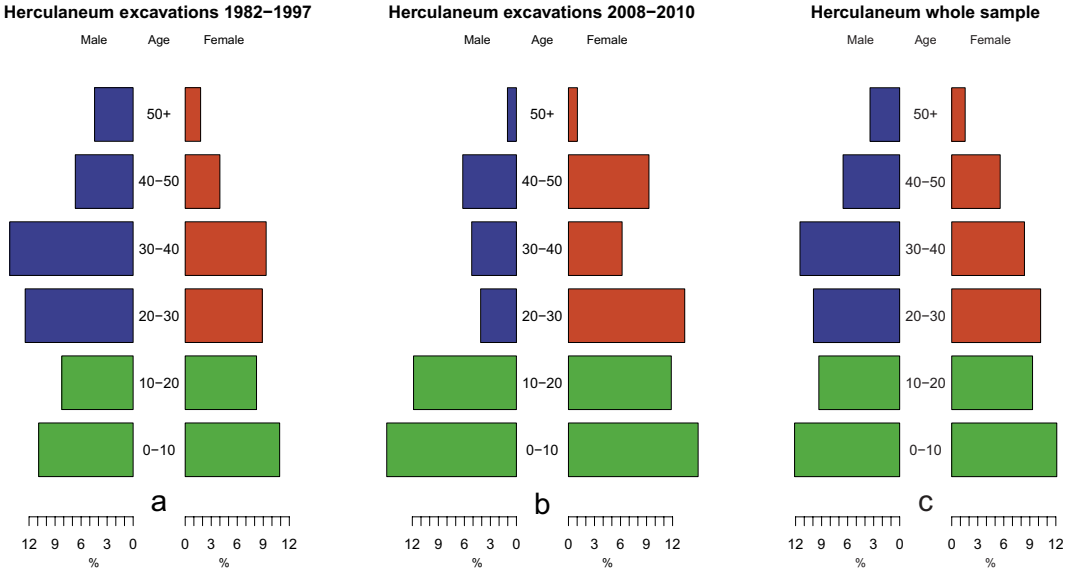

Figure 2.19 Population pyramids for the Herculaneum assemblage created on the first (a) and second (b) set of excavated individuals and on the whole sample (c). Modified after Fattore *et al.* (2012)

2.3.5 Studies around the manner of death

Concurrently, great attention was given to the exploration of the manner of death of the Herculaneum death assemblage. Mastrolorenzo *et al.* (2001) suggested that the individuals recovered from the *fornici* were killed instantly by the high temperature (at least 500 °C) of the first surge, basing their hypothesis on the absence of self-protective positions or contortions due to agony and the presence of bone and enamel fracture and bone blackening. The life-like postures of the casts of the individuals killed in Pompeii were also considered as an evidence of instantaneous death caused by thermally induced shock at around 250-300°C (Mastrolorenzo *et al.* 2010). In contrast, the authors estimated a temperature of death of 500°C at Herculaneum and 600°C at Oplontis by observing bone discolouring, cranial fractures caused by increased cranial pressure, incipient recrystallisation of hydroxyapatite and absence of DNA using a light microscope and a Scanning Electron Microscope (SEM) and comparing them with modern bones experimentally exposed to temperature ranging from 100°C to 800°C (Mastrolorenzo *et al.* 2010; Petrone 2011).

Later, Petrone *et al.* (2018) highlighted that the fractures are always found on bones with a charred aspect. Petrone *et al.* (2018) also observed the presence of dark stains on the inner surface of the skulls and they suggest that pale-yellow colouring is indicative of exposure to a lower temperature ($\leq$ 200°C) while the brown-black stain would be caused by higher temperatures (300-500°C). The authors also noted that these signs are more frequent on the skeletons coming from the less crowded *fornici* (Petrone *et al.* 2018). Red and black residues and incrustations found on several cranial and post-cranial bones but also on the ashes that were filling the intra-cranial space or those that embedded the bones where analysed through Inductively Coupled Plasma Mass Spectrometry (ICP-MS) in order to explore iron (Fe) content (Petrone *et al.* 2018). The detection of high Fe levels were interpreted as possible evidence of degradation products of body fluids, confirmed by the revelation through Raman spectroscopy of iron oxides. According to the authors this would further sustain the hypothesis of instant death by thermal shock (Petrone *et al.* 2018).

In the meantime, Schmidt *et al.* (2015) were analysing the group of 162 individuals from the beach coming to a higher temperature at death estimation (*i.e.*, 700-900°C). They rejected some of Mastrolorenzo *et al.*'s (2010) interpretations, in particular that the skulls exploded as a consequence of increased cranial pressure and that soft tissues evaporated suddenly, while Schmidt *et al.* (2015)'s analysis showed that the less charred bones were those where the tissues are deepest, therefore in contrast suggesting that soft tissues held up protecting the bones.

Recently, Martyn *et al.* (2020) analysed 152 individuals from the vaulted chambers by Fourier Transform Infrared Spectroscopy-Attenuated Total Reflectance (FTIR-ATR) to explore the crystalline structure of the bones that could be altered by the temperature and by the time of exposure to this. The crystallinity values obtained suggest an exposure to a low-intensity burning event (Figure 2.20)(Martyn *et al.* 2020). The authors also observed variation of collagen yields (*i.e.*, collagen content in a portion of bone reported as a percentage) according to the distribution of the individuals into the *fornici*. Notably, the individuals that reported the highest collagen yields are

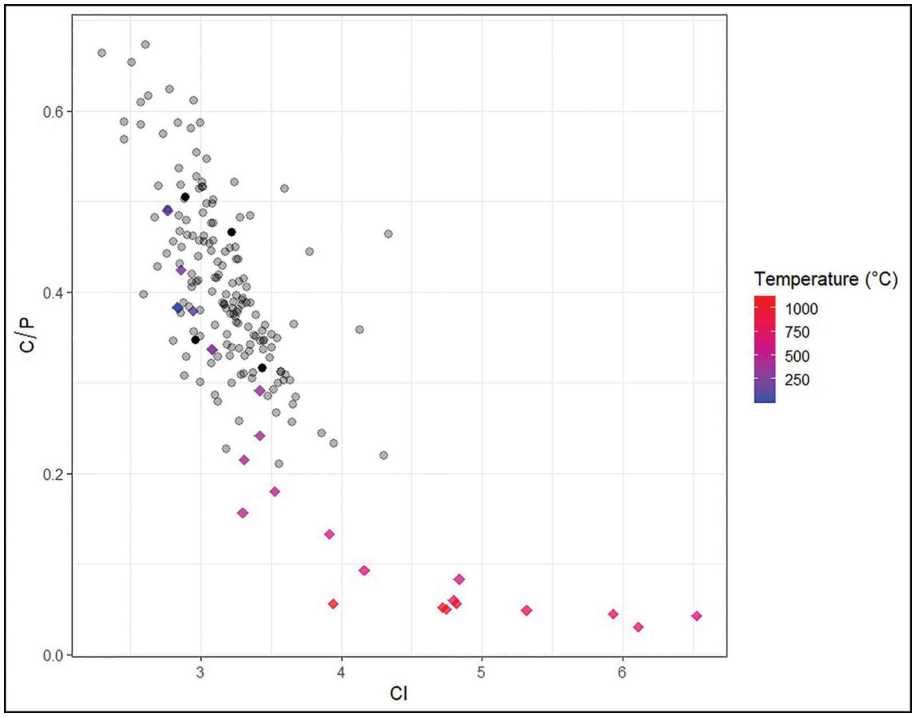

Figure 2.20 Crystallinity values of the individuals from the vaulted chambers of the ancient Herculaneum seashore (grey) and Velia (black, n=4) with those from controlled charring experiments (from red to blue, as in the legend). Modified after Martyn *et al.* (2020)

those from *fornice* 10, which is also the chamber with the highest number of victims, while individuals from *fornice* 7, which is the one with the lowest number of skeletons, reported the lowest collagen yields (Martyn *et al.* 2020). A subsample of this assemblage (81 individuals) was analysed for stable carbon and nitrogen analysis (Martyn *et al.* 2018)(See chapter 3), and their carbon to nitrogen (C:N) ratio was indicative of diagenetically unaltered collagen (Martyn *et al.* 2020). The results obtained by exploring the collagen yield and the crystallinity values disagree with Mastrolorenzo *et al.* (2001), Mastrolorenzo *et al.* (2010), Petrone *et al.* (2018) and Petrone (2019) but they are in line with a recent study on Villa of the Papyri (Giordano *et al.* 2018),

which suggests a temperature of the pyroclastic flow of around 350°C and that the temperatures generated by the interaction of the flow with debris and the sea water are estimated to be much lower, of 270°C and 190°C, respectively. This would largely support the FTIR-ATR data of the skeletons recovered from the *fornici*, since the interaction of the pyroclastic flow with the sea, the structure of the chambers and the proximity of the bodies all resulted into lower temperatures at death. Moreover, Martyn *et al.* (2020) suggests that a further factor that led to lower exposure temperature was the presence of the soft tissues that acted as a protection to the bones, thanks to the movement of water towards the central portion of the body.

What emerges from this review is that there is often a disparity in the results obtained from the analysis of the skeletal assemblage of Herculaneum. This seems most likely caused by the lack of uniformity in the strategies of analysis carried out by different scholars. A few years ago, Lazer (2009) was already calling for a re-analysis of the entire assemblage following standard techniques, which is to this date yet to happen.

2.4 Conclusion

There is no doubt that there is plenty of information about the diet of the ancient Romans, as it has been reviewed in section 2.1. However, the ancient texts and the archaeological findings are not able on their own to shed light into the complex socio-cultural aspects that are mirrored in the dietary habits of who was living at the time of the Roman Empire. Herculaneum certainly represents the best opportunity to explore such dynamics.

The AD 79 eruption of Mount Vesuvius and the resulting burying of the town, has permitted scholars the study of a wealth of information in the last three centuries of explorations. For example, thanks to the recovery of the *Album of names*, it is known by whom the town was inhabited (section 2.2.1). Moreover, the botanical and faunal remains recovered from the *Cardo V* sewer are extremely instructive about the foodstuff available to and consumed by the "ordinary" people living in the commercial area of Herculaneum (section 2.1.1). Thanks to the analysis of these remains, it was possible to observe that lower socio-economic groups living in the Imperial Roman time could afford daily meals certainly above subsistence (Robinson and Rowan 2015; Rowan 2017b). Last but not least, the discovery of over three hundreds skeletons from the Herculaneum beachfront, represents a unique opportunity to explore the diet of those

who were living at Herculaneum by interrogating the people themselves. Indeed, the simultaneous death of this numerous assemblage makes any demographic, nutritional and dietary study comparable to a survey carried out on a modern living population (section 2.3.2). Bisel (1988, 1991); Capasso (2001) first tried to investigate the diet of these individuals but unfortunately, trace elemental analysis is largely biased by soil contamination, therefore the diet reconstruction provided by the authors can not be considered reliable (Lazer 2009, 214). So far, the only way to directly look into the diet of past human populations, in quantitative terms and at the individual level, is represented by the stable isotope analysis of the atoms that compose human remains. In the next chapter, stable isotope analysis will be reviewed, with a focus on previous studies on Roman contexts, including Herculaneum.

Chapter 3

Dietary studies and stable isotopes analyses: a review

The aim of this chapter is to provide an overview of carbon and nitrogen stable isotope research in archaeology. First (3.1), stable isotopes will be introduced, focusing on the natural cycles of carbon and nitrogen in the atmosphere and water environments. Here, attention will be given to the isotopic fractionation mechanisms and how these can be applied to the study of ancient human diets (3.1.1 and 3.1.2). Carbon and nitrogen stable isotope studies carried out in the Roman Mediterranean will be then reviewed (3.1.3) and the results discussed, also in light of the limitations that they encountered. Mixing models represent a powerful tool for the quantitative interpretation of stable isotope analysis, and therefore they will be presented with an example from AD 79 Herculaneum (3.1.4). Then, the review will move on to relevant pioneering and more recent applications of carbon and nitrogen isotope analysis of amino acids (3.2.1), highlighting crucial evidence for the interpretation of the data. By doing so, it appears essential to draw the metabolic pathways of the amino acids in the human body; these will be outlined in section 3.2.2, discriminating between the carbon and nitrogen routes. Finally, the collagen structure and composition will be briefly presented (section 3.2.3).

3.1 Stable isotopes in Archaeology

Isotopes are nuclides of the same element that have different atomic mass numbers related to their different number of neutrons. Isotopes are commonly distinguished between stable and radioactive (or unstable) isotopes (Hoefs 2008). The number of

nuclides discovered up to this date is 3386[1] and, among these, only 254 are stable (or, at least, no decay has ever been observed)(Thoennessen 2016).

The concept of "isotope" was introduced with the discovery of radioactivity, made unexpectedly by Henry Becquerel in 1896 while studying uranium light adsorption (Thoennessen 2016). Subsequently, many substances were studied to explore different radiations effects, as Marie and Pierre Curie made with thorium and radium, focusing on the comprehension of the source of the radiation (Radvanyi and Villain 2017). However, the connection between radioactivity and isotopes was not initially made and only acquainted two decades later, in 1913, when Francis Aston revealed "...evidence has now been obtained that atmospheric neon is not homogeneous, but consists of a mixture of two elements of approximate atomic weights, 19.9 and 22.1 respectively... The two elements appear to be identical in all their properties except atomic weight" (Aston 1913). In the same year, the term *isotope* was introduced for the first time, composed by the two Greek words ἴσος (isos, 'equal') and τόπος (topos, 'place') "[...]because they occupied the same place in the periodic tables." (Soddy 1913).

Research on stable isotopes later benefited by the invention of mass spectrometers (Dempster 1918). In only five years, Aston discovered 100 new isotopes of 47 different elements, including ^{12}C (Aston 1919) and ^{14}N (Aston 1920). Mass spectrometers were implemented and later on, in 1929, King discovered ^{13}C and Naude recognized ^{15}N (Thoennessen 2016).

Many scientific research fields owe their progresses to the development of the Isotope Ratio Mass Spectrometer (IRMS), first proposed by Nier in 1940, which allowed determination of relative abundances of light elements isotopes in small samples (*i.e.*, usually lower than 1 mg of material). IRMSs allowed analysis of solid materials by being simply combusted or converted in gases obtaining high resolution results at low costs (Brenna *et al.* 1997). Becoming therefore a routine analysis, it enabled revolutionary breakthrough discoveries from the natural world.

Isotope abundances are expressed in ratio (R) as:

$$R = \frac{X_h}{X_l} \tag{3.1}$$

where X is the element, h is the heavier isotope and l the lighter isotope. Concentration of isotopes are reported referring them to international standards, as first proposed by McKinney and colleagues (1950). These are Vienna Pee Dee Belemnite

[1]The Chart of Nuclides of the National Nuclear Data center is available at this link.

(VPDB) for the isotopic ratio $^{13}C/^{12}C$ and air (AIR) for $^{15}N/^{14}N$. Concentrations are expressed in "parts per mil" (‰) with the δ symbol, as reported in the following equation:

$$\delta\,(‰) = \left(\frac{\frac{h}{l} X_{sample}}{\frac{h}{l} X_{standard}} \right) - 1 \tag{3.2}$$

That, for carbon and nitrogen are:

$$\delta^{13}C\,(‰) = \left(\frac{\frac{13}{12} C_{sample}}{\frac{13}{12} C_{VPDB}} \right) - 1 \tag{3.3}$$

$$\delta^{15}N\,(‰) = \left(\frac{\frac{15}{14} N_{sample}}{\frac{15}{14} N_{AIR}} \right) - 1 \tag{3.4}$$

The difference between the δ of a sample from a given baseline is indicated with the symbol Δ and expressed as:

$$\Delta_{sample-baseline} = \delta_{sample} - \delta_{baseline} \tag{3.5}$$

(Coplen 2011). Archaeology relies on the analysis of the stable isotopes of multiple elements to explore several questions. A variety of archaeological materials can be investigated with stable isotope analysis. Among these, human and animal bones and teeth are studied in both their organic and inorganic matrices to evaluate past dietary habits and migratory patterns. The organic component of bones and teeth mainly consists of the protein collagen. All the elements which make up collagen have been explored in varying degrees in their isotopic composition to investigate diet in more or less extent. Carbon and nitrogen are certainly the most exploited as they are applied more consistently and for longer, benefiting from a feasible and well defined extraction and analytical protocol that can easily been reproduced in different laboratories (Brown *et al.* 1988) and by a wide database that allow comparison across time and space (Fernandes *et al.* 2017). Carbon and nitrogen stable isotope research owes its success to the abundance of these two elements in collagen, thus requiring a small amount of material to be analysed, usually between 0.5 and 1 mg. Sulphur has also been proved to be a powerful tool, particularly to detect marine consumption (Richards *et al.* 2003) but this analysis has been less applied because of the low concentration of sulphur in collagen (< 0.3 %). Recently, a new Elemental Analyser (EA) source (EA IsoLink™ by Thermo Fisher Scientific, Bremen, Germany) allowed the simultaneous analysis of carbon, nitrogen and sulphur isotopes by only using 1.5 mg of collagen (Sayle *et al.*

2019). Therefore, there is no doubt that sulphur isotope analysis will become a routine approach for dietary studies in the future. Hydrogen and oxygen isotopes also show patterns relative to dietary and physiological characteristics but they still need to be further investigated (*e.g.*, Reynard and Hedges 2008; Reynard *et al.* 2015; Tuross *et al.* 2017; Reynard *et al.* 2020). Bioapatite, which constitutes the inorganic matrix of bones and teeth, is also commonly investigated in its isotopic composition. Again, carbon isotopes of bioapatite are highly informative about dietary patterns (Ambrose and Norr 1993), as well as calcium, the latter possibly linked to dairy consumption (Reynard *et al.* 2010, 2011, 2013; Tacail *et al.* 2021). On the other hand, oxygen (Lightfoot and O'Connell 2016) and strontium (Bentley 2006) in apatite are commonly analysed to investigate the migratory history of a single or groups of individuals. Last, carbon and nitrogen isotopic ratios can also be studied with dietary implications from other organic materials in archaeological sites, such as seeds (Bogaard *et al.* 2007), food crusts (Morton and Schwarcz 2004), organic residues from ceramic or cooking tools (Evershed 2008) and dental calculus (Scott and Poulson 2012).

The working principle of the research based on stable isotopes consists in detecting the existing differences of isotopic ratios among environments, organisms and their tissues. This is owed to a phenomenon known as Kinetic Isotope Effect (KIE), where normally, lighter isotopes are preferred over heavier isotopes when the element is required to diffuse or to react in chemical, physical and physiological processes (Fry 2006; Coplen 2011). The next two sections will focus on the natural carbon and nitrogen isotopes cycles in order to understand the dynamics behind δ^{13}C (‰) and δ^{15}N (‰) in human bone collagen.

3.1.1 Carbon stable isotopes and dietary implications

The study of isotopic fractionation of carbon was first applied in geochemistry with the aim to evaluate correlation between different inorganic and organic, fossil and modern, materials (*e.g.*, Nier and Gulbransen 1939; Craig 1953), also with archaeological implication, as in the Greek marbles provenance study proposed by Craig and Craig (1972). It was not long before scholars realized that fractionation of carbon was linked to its natural cycle. First, Park and Epstein (1961) demonstrated evidence for carbon isotopes fractionation mechanisms during photosynthesis. Later on, several studies observed the similarity of δ^{13}C (‰) values in terrestrial, marine and freshwater animals compared to the plants from their respectively environments (*e.g.*, Degens *et al.* 1968; Sackett *et al.* 1965; Smith and Epstein 1970). This acquired knowledge was soon

used to propose dietary investigations of modern and fossil animals, first presented by DeNiro and Epstein in a very brief abstract (1976) and discussed in the two year later publication (DeNiro and Epstein 1978). In the same year, Van der Merwe and Vogel (1978) were the first to apply the analysis of carbon stable isotopes in human bone collagen to study ancient human dietary practices.

The $\delta^{13}C$ (‰) of modern and fossil remains depends on the interaction the organism (and its tissues) had in life with the environment. Carbon is present in the atmosphere predominantly as carbon dioxide (CO_2) (Figure 3.1). $\delta^{13}C$ of atmospheric CO_2 was measured to -7.4 ‰ in 1974 (Keeling *et al.* 1979) but this value is constantly changing mainly depending on anthropogenic emissions of CO_2 (Hellevang and Aagaard 2015). Autotrophic organisms, therefore plants, algae and photosynthetic bacteria, use the atmospheric CO_2 and water (H_2O) to produce glucose ($C_6H_{12}O_6$) and molecular oxygen (O_2) by a chain of endothermic reduction–oxidation reactions, commonly known as *photosynthesis*. Photosynthesis is a classic example of KIE, as the biochemical reactions that lead to $C_6H_{12}O_6$ and O_2 production all favour the lighter carbon against ^{13}C, with an important role played by ezymes. As a result, photosynthetic organisms are enriched in ^{12}C and depleted in ^{13}C compared to the atmosphere. However, different photosynthetic mechanisms cause differences in carbon fractionation. In particular, plants are classified as C_3 plants, C_4 plants and Crassulacean Acid Metabolism (*CAM*) plants, depending on their photosynthetic pathways. In C_3 plants, the carboxylating enzyme (RuBisCO) uses ribulose bisphosphate as substrate to fix atmospheric CO_2, forming a compound composed of three carbon atoms, the so-called 3-phosphoglycerate, from which the plants category is named; C_4 plants rely on phosphoenolpyruvate (PEP) as a substrate for the fixation of atmospheric CO_2, which will then lead to the synthesis of malate (or, sometimes, aspartic acid), a compound with four atoms of carbon.

The difference in the carbon isotopic fractionation in these two pathways lies on the fixation of CO_2 by C_4 plants, which takes place in two steps: first, CO_2 is fixed to form malate or aspartic acid, then, when the latter enters the vascular bundle sheath cells, it is decarboxylated to form CO_2 again, which will be further fixed through the same cycle (Calvin cycle) of C_3 plants. This allows the back diffusion of CO_2 to the atmosphere compared to C_3 plants, explaining why the relative concentration of ^{13}C is higher than ^{12}C in C_4 plants than in the C_3 ones. *CAM* plants have an unusual photosynthetic pathway that fixes CO_2 in the dark into organic acids which is similar to the C_4 one, therefore resulting in a similar isotopic signature to the latter (Lambers *et al.* 2008). C_3 plants are the most diverse group of plants on earth, growing in condi-

tions of moderate sunlight, temperate climate and plentiful groundwater; this group includes grasses, trees, shrubs, vegetables, legumes, numerous dicotyledonous plants, wheat and rice. On the contrary, C_4 plants developed their photosynthetic system to survive arid climate with low water supply; this group includes grasses of tropical climates, sugar cane, sorghum, maize and millets. Finally, *CAM* carbon fixation is typical of plants like cacti, agaves, bromeliads and euphorbias (Ambrose and Norr 1993).

The organic components of soils usually reflect carbon isotopic values of the local vegetation. On the other hand, the carbon in ocean waters is mainly present in the form of dissolved CO_2. At the surface, carbonates are in equilibrium with atmospheric CO_2 and the reaction only causes little isotopic fractionation. Plankton are autotrophic organisms that operate photosynthesis using the inorganic carbon dissolved in water. $\delta^{13}C$ values of plankton are usually between those of C_3 and C_4 plants. On a different note, isotopic signatures of carbonates dissolved in freshwater basins is affected by the isotopic composition of the carbonate rocks on which waters flow dissolving carbonates and they are usually more depleted in ^{13}C compared to C_3 plants.

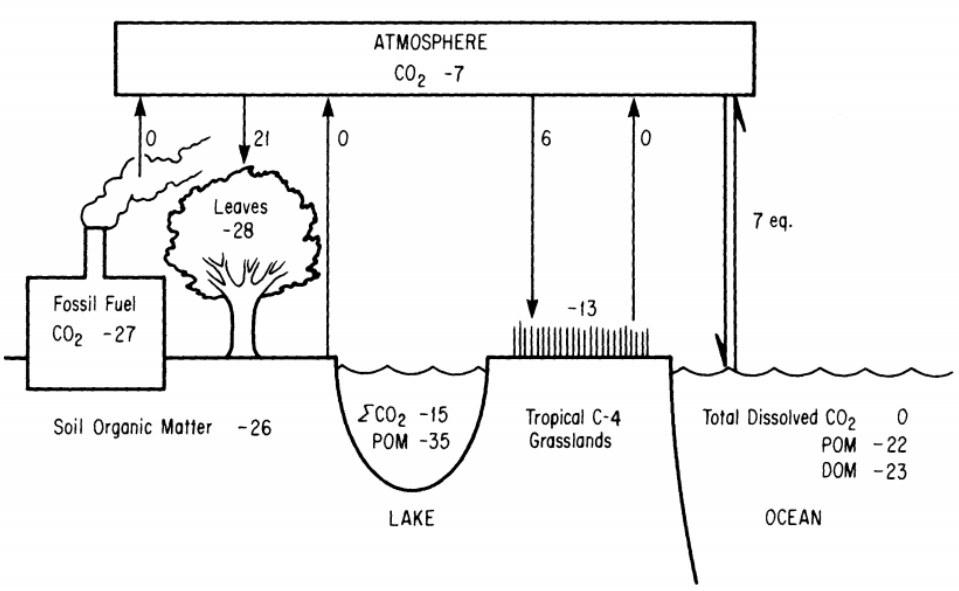

Figure 3.1 Carbon natural cycle. One-way arrows show CO_2 path, while two-way arrows the steady-state of isotopic fractionation. Numbers refer to $\delta^{13}C$ ‰ values; numbers associated with two-way arrows refer to the fractionation (Δ) happening during the reaction. POM, particulate organic matter; DOM, dissolved organic matter. Modified after Peterson and Fry (1987).

Carbon stable isotopes of bone collagen

Once plants are eaten by animals, the carbon atoms composing plant tissues are used by the animals to build up their own tissues through biochemical reactions. It has been observed that carbon is enriched in its heavier isotope at each step of the food web. This progressive enrichment is known as *trophic level effect* and it is regulated by metabolic reactions in the body. More specifically, it was initially noted that animals are enriched by +1 ‰ compared to their diet (DeNiro and Epstein 1978). However, subsequently feeding experiments and controlled field studies have shown more diversified offsets from diet to consumer tissues ($\Delta^{13}C_{tissue-diet}$). At that time scholars were debating whether carbon in collagen was directly routed from the protein fraction (*e.g.*, Krueger and Sullivan 1984) or "scrambled" from all parts of diet (*i.e.*, carbohydrates, lipids and protein)(Van der Merwe 1982). It was also noted that $\Delta^{13}C_{tissue-diet}$ was highly affected by the diet composition. For example, Hare *et al.* (1991) observed in their feeding experiment conducted on pigs that pigs raised on a 100 % C_3 diet where enriched by +1.4 ‰ in their bone collagen compared to their diet, while pigs raised on a 100 % C_4 diet showed a higher enrichment of +3 ‰ (Table 3.1.1). The effect of dietary composition on the $\Delta^{13}C_{tissue-diet}$ offset was further explored by Ambrose and Norr (1993) with the aim to detect whether carbon in collagen and bioapatite are preferentially routed or scrambled from diet. In their experiments, Ambrose and Norr (1993) raised two generations of laboratory rats on seven different diets. One diet was composed of 100% C_3 components (A), two of the diets consists of carbohydrates and lipids coming from a C_3 source while protein was C_4 (B and D), and the remaining three had carbohydrates and lipids composed of a C_4 source while protein was C_3 (C, E, F and G) (Table 3.1.1). The results showed that carbon in collagen of rats raised on diets with carbohydrates and lipids from a C_4 source and protein a C_3 source (*i.e.*, C, E, F and G) showed a much lower $\Delta^{13}C_{tissue-diet}$ offset (-0.9 ± 1.6 ‰) compared to those raised on diets with carbohydrates and lipids being a C_3 source and protein a C_4 source (*i.e.*, B and D) ($\Delta^{13}C_{tissue-diet}$ = +8.5 ± 1.6 ‰). On the contrary, the rats fed on a mono-isotopic (*i.e.*, fractions coming all from C_3 source, diet A) diet showed a $\Delta^{13}C_{tissue-diet}$ offset of +3.8 ‰ (Table 3.1.1)(Ambrose and Norr 1993).

Similarly, Tieszen and Fagre (1993) fed two generations of mice with eight different diets of known isotopic composition). The eight diets were composed of a 100% C_3 source, a 100% C_4 source, or of a mixture of the two in different proportions. In addition, one of the diets had double the amount of the protein content of the others and another one only one-fourth. The results showed that mice fed on diets composed of C_3 sources but with the protein fraction being a C_4 source, were on average enriched

by +7.6 ± 0.4 ‰, while those fed on a mono-isotopic diet were only enriched by +2.7 ± 1.4 ‰, and the mice raised on diets where C_4 sources represented the non-protein fraction of the diet were less enriched of all, on average by +1.7 ± 1.5 ‰ (Tieszen and Fagre 1993). Following feeding experiments confirmed this pattern, as reported in Table 3.1.1 (Howland *et al.* 2003; Jim *et al.* 2004; Warinner and Tuross 2009; Froehle *et al.* 2010; Webb *et al.* 2017).

Froehle *et al.* (2010) reviewed all studies of feeding experiments conducted up to that time and showed that when the $\delta^{13}C_{protein}$ in diet is higher than the $\delta^{13}C$ of the overall diet, the offset $\Delta^{13}C_{collagen-diet}$ is larger and that, on the contrary, when the $\delta^{13}C_{protein}$ in diet is lower than the $\delta^{13}C$ of the overall diet, $\Delta^{13}C_{collagen-diet}$ is smaller. This effect is caused by the dual dependency of carbon in collagen to both protein and non-protein components of diet (Froehle *et al.* 2010). More specifically, Fernandes *et al.* (2012) calculated that ∼ 75 % of carbon in bone collagen has a protein origin and that the remaining ∼ 25 % comes from carbohydrates and lipids. However, these proportions might change in case of a diet rich or, on the contrary, poor in protein (*e.g.*, Jim *et al.* 2006). Therefore, $\delta^{13}C$ values of bone collagen cannot on their own help to elucidate the animal diet unless the composition of the diet is known *a priori*, which is obviously unknown for archaeological contexts (Froehle *et al.* 2010; Webb *et al.* 2017). Furthermore, it was noted that marine protein consumption is difficult to detect when this is less than 20 % of total diet since this would produce $\Delta^{13}C_{collagen-diet}$ offsets close to 0 ‰ (Hedges 2004; Webb *et al.* 2017). This has a major implication in the investigation of ancient human dietary practices, particularly in the Mediterranean basin, where marine consumption is often secondary to other sources but its quantification has major socio-economic implications (See the following section 3.1.3 and chapter 6).

Carbon stable isotopes of bone apatite

In contrast to collagen, a very high correlation between the $\delta^{13}C$ values of apatite of bone and the $\delta^{13}C$ values of the whole diet has been observed (Figure 3.2). DeNiro and Epstein (1978) observed a $\Delta^{13}C_{apatite-diet}$ offset of + 9.5 ‰ and + 9.7 ‰ in two groups of mice fed on distinct diets. Ambrose and Norr (1993) showed comparable offsets from their experiment on rats, again with no differences across groups of diets ($\Delta^{13}C_{apatite-diet}$ = + 9.5 ± 0.6 ‰), and Tieszen and Fagre (1993) obtained a similar offset from their experiments on mice ($\Delta^{13}C_{apatite-diet}$ = + 9.0 ± 1.6 ‰). Later, a similar offset was also reported by Howland *et al.* (2003) ($\Delta^{13}C_{apatite-diet}$ = + 10.2 ± 1.3 ‰) and by Jim *et al.* (2004) ($\Delta^{13}C_{apatite-diet}$ = + 9.6 ± 0.5 ‰), the latter using

unpublished values from the experiment carried out by Ambrose and Norr (1993), while Warinner and Tuross (2009) observed a slightly higher offset ($\Delta^{13}C_{apatite-diet} = +$ 12.1 $\pm$ 0.6 ‰). The high correlation between δ^{13}C values of the consumer's bioapatite and the bulk diet subsists because of the formation pathways of bioapatite in bones. Indeed, bone apatite is derived from dissolved carbonates (HCO_3^-) in the blood. HCO_3^- in the blood is in constant equilibrium with the CO_2 produced by respiration from all the macronutrients ingested. Therefore, the δ^{13}C values of apatite should reflect the weighted average of all the macronutrients in the diet (Schwarcz 2002).

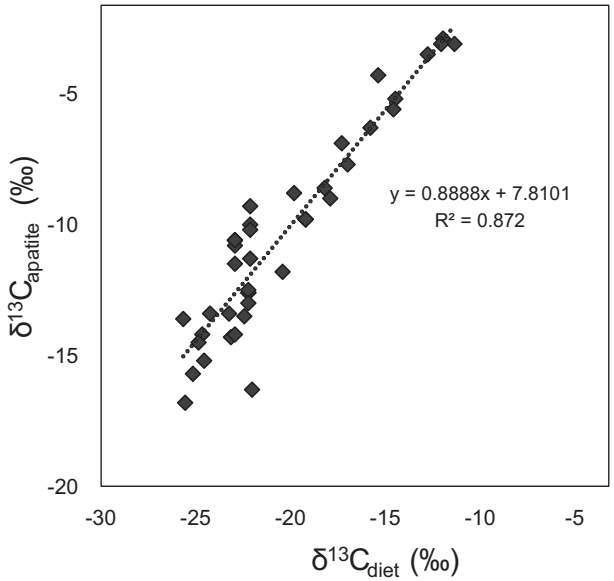

Figure 3.2 Correlation between δ^{13}C of bone apatite and δ^{13}C of bulk diet in mice, rats and pigs fed on controlled diet (DeNiro and Epstein 1978; Ambrose and Norr 1993; Tieszen and Fagre 1993; Howland *et al.* 2003; Jim *et al.* 2004; Warinner and Tuross 2009).

3.1.2 Nitrogen stable isotopes and dietary implications

Three years after their first paper on the $^{13}C/^{12}C$ ratio investigation in animals and their diets, DeNiro and Epstein (1981) explored the potential of nitrogen signatures in the same direction. Similarly to what happened for carbon, nitrogen isotopic composition of natural substances also started to be explored in the 50s (Hoering 1955), and it was not long before scientists realized that it was connected to the different strategies that autotrophic organisms have to fix nitrogen in terrestrial and aquatic environments (*e.g.*, Hoering and Ford 1960; Cheng *et al.* 1964; Miyake and Wada 1967; Wada *et al.* 1975; Pang and Nriagu 1977). As a result, the δ^{15}N (‰) value of modern and fossil remains is caused by the interaction of the organism with the environment. The natural cycle

Experiment	Animal	Diet ID	Diet composition (weight %)		$\Delta^{13}C_{collagen-diet}$
			Protein	**Non-protein**	
Hare et. Al 1991	Swine	C_3	100% C_3	100% C_3	1.4
		C_4	100% C_4	100% C_4	3.2
Ambrose and Norr 1993	Rats	1A	100%C_3(20%)	100% C_3	3.8
		2B	100% C_4 (5%)	100% C_3	9.6
		3C	100% C_3 (5%)	30% C_4,70% C_3	-1.6
		4D	100% C_4 (70%)	100% C_3	7.4
		5E	100% C_3 (70%)	100% C_4	1.8
		6F	100% C_3 (20%)	100% C_4	-1.4
		12,13G	100% C_3 (20%)	100% C_4	-2.2
Tieszen and Fagre 1993	Mice	1	100%C_3(18.2%)	100% C_3	3.7
		2	100% C_3 (18.1%)	25% C_4, 75% C_3	0.6
		3	100% C_3 (18.1%)	70% C_4, 30% C_3	1.8
		4	100% C_3 (18.4%)	5% C_4, 95% C_3	2.9
		5	mix C_3/C_4 (18.4%)	100% C_3	7.4
		6	mix C_3/C_4 (36.1%)	100% C_3	8.1
		7	mix C_3/C_4 (4.7%)	100% C_3	7.5
		8	85% C_4, 15% C_3 (12%)	92% C_4, 8% C_3	1.7
Howland et al. 2003	Swine	3	%5C_4, %95C_3(20%)	10%C_4, 90%C_3	4.1
		4	15% C_4, 85% C_3 (20%)	30% C_4, 70% C_3	1.8
		5	25% C_4, 75% C_3 (20%)	50% C_4, 50% C_3	1.1
		6	35% C_4, 65% C_3 (20%)	70% C_4, 30% C_3	0.5
		8	100% C_3 (20%)	100% C_3	6.1
		10	35% C_4, 65% marine (20%)	98%$C_4/marine$	4.0
Jim et al. 2004	Rats	d2a4	100% C_3 (20%)	100% C_3	5.0
		d4h	100% C_4 (20%)	100% C_4	4.3
		d5i	100% C_4 (20%)	100% C_3	10.0
		d6j2	100% marine (20%)	100% C_3	8.8
		d7k2	100% marine (20%)	100% C_4	3.2
		d8l2	100% marine (20%)	50% C_4, 50% C_3	6.1
Warinner and Tuross 2009	Swine	raw 7	23% C_4, 77% C_3 (13%)	29% C_4, 71% C_3	3.5
		raw 8	23% C_4, 77% C_3 (13%)	29% C_4, 71% C_3	2.5
		raw 9	23% C_4, 77% C_3 (13%)	29% C_4, 71% C_3	3.5
		raw 10	23% C_4, 77% C_3 (13%)	29% C_4, 71% C_3	3.6
		nix 2	18% C_4, 82% C_3 (13%)	23% C_4, 77% C_3	4.5
		nix 3	18% C_4, 82% C_3 (13%)	23% C_4, 77% C_3	3.7
		nix 4	18% C_4, 82% C_3 (13%)	23% C_4, 77% C_3	3.9
		nix 5	18% C_4, 82% C_3 (13%)	23% C_4, 77% C_3	4.3
		nix 6	18% C_4, 82% C_3 (13%)	23% C_4, 77% C_3	4.4
Webb et al. 2017	Swine (1^{st} gen.)	1	100% C_3 (20%)	terrestrial (C_3)	3.1
		2	87.5% C_3, 12.5% marine (20%)	terrestrial (C_3)	3.5
		3	75% C_3, 25% marine (20%)	C_3	3.8
		4	50% C_3, 50% marine (20%)	C_3	4.6
		5	100% marine (20%)	C_3	6.5
	Swine (2^{st} gen.)	1	100% C_3 (20%)	C_3	3.4
		2	87.5% C_3, 12.5% marine (20%)	terrestrial (C_3)	3.6
		3	75% C_3, 25% marine (20%)	C_3	4.3
		4	50% C_3, 50% marine (20%)	C_3	5.2
		5	100% marine (20%)	C_3	6.5
			$C_4/marine$	**C_3**	7.4 ± 1.7
			C_3	**$C_4/marine$**	0.6 ± 1.5
			same as non-protein	***same as protein***	3.4 ± 1.2

Table 3.1 Observed $\Delta^{13}C_{collagen-diet}$ values from feeding experiment studies (Hare *et al.* 1991; Ambrose and Norr 1993; Tieszen and Fagre 1993; Howland *et al.* 2003; Jim *et al.* 2004; Warinner and Tuross 2009; Webb *et al.* 2017). Bottom three lines represent mean and 1σ of the three groups of diets discussed in the text. Here, the source indicated in the dietary fraction (*e.g.*, C_3) represents either the totality (*e.g.*, 100% C_3) or the majority (*e.g.*, $\geq 50\%C_3$) of that fraction. Modified from Froehle *et al.* (2010) after inclusion of Webb *et al.* (2017).

of nitrogen is summarised in Figure 3.3.

Atmospheric nitrogen (N_2) has a $\delta^{15}N$ value of 0 ‰, and this is also used as International Standard for $\delta^{15}N$ measurements (Brand *et al.* 2014). Among all the organisms, diazotrophs are the only ones capable of fixing molecular nitrogen from the atmosphere. All the other organisms can only absorb nitrogen from different compounds. More specifically, terrestrial plants can obtain nitrogen from nitrates, nitrites and ammonium salts naturally present in soils from degraded organic matter, from precipitations or from diazotrophs in symbiotic relation with their roots (*e.g.*, in Leguminosae plants). Degradation of organic matter in soils is caused by the nitrifying bacteria, while denitrifying bacteria are able to restore N_2, which then enters again the atmosphere. Bacterial decomposition causes accumulation of ^{15}N in soils with different rates depending on several factors, such as temperature and dryness and age of the soil (*e.g.*, Ambrose 1991). The same happens in ocean waters, for which it has also been observed an additional increment of ^{15}N proceeding with depth (Peterson and Fry 1987).

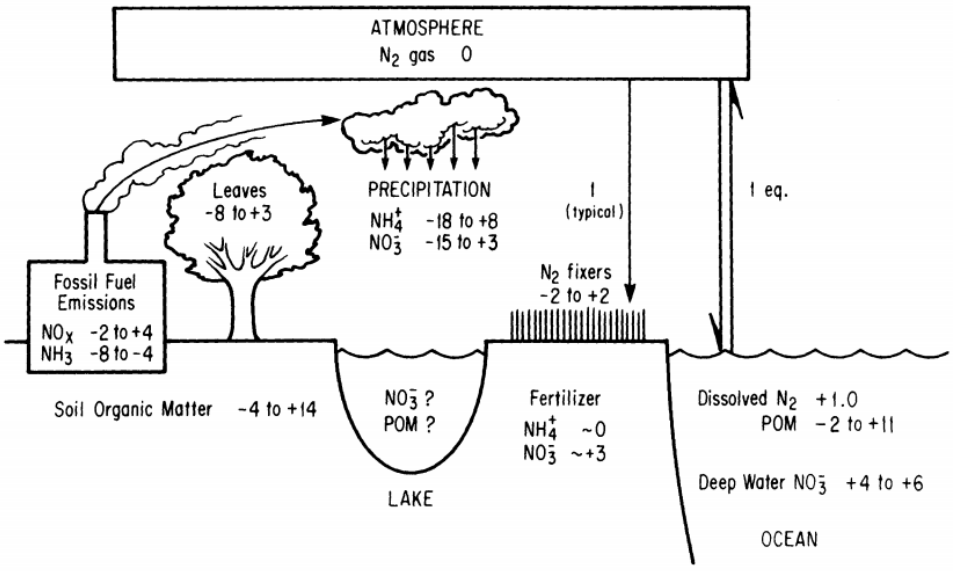

Figure 3.3 Nitrogen natural cycle. One-way arrows show N_2 and its derivates path, while two-way arrows show the steady-state of isotopic fractionation. Numbers refer to $\delta^{15}N$ ‰ values; numbers associated with two-way arrows refer to the fractionation (Δ) happening during the reaction. POM, particulate organic matter; DOM, dissolved organic matter. Modified after Peterson and Fry (1987).

Nitrogen stable isotopes of bone collagen

Proteins are the only significant source of nitrogen in diet. Food proteins are digested in the body and nitrogen atoms are used for the synthesis, among other tissues, of bone collagen. Therefore, the $\delta^{15}N$ values of bone collagen are directly linked to protein consumption and the $\Delta^{15}N_{collagen-diet}$ offset values are not affected by total dietary composition. As a result, feeding experiments have shown much less variable $\Delta^{15}N_{collagen-diet}$ offset values compared to carbon. DeNiro and Epstein (1981) first explored the $\Delta^{15}N_{collagen-diet}$ of three groups of mice raised on three different diets, varying from +1.4 ‰ to +3.4 ‰. Following, Hare *et al.* (1991) observed a consistent $\Delta^{15}N_{collagen-diet}$ offset in the bone collagen of pigs fed on a 100% C_3 and on a 100% C_4 diet (+2.2 ‰ and +2.3 ‰, respectively). On the contrary, numerous field studies from various ecosystems at that time were observing more variable $\Delta^{15}N_{collagen-diet}$ offset values (*e.g.*, Minagawa and Wada 1984; Schoeninger and DeNiro 1984; Sealy *et al.* 1987). Therefore, Ambrose (2000) analysed $\delta^{15}N$ values from different tissues of the rats used in his previous carbon experiment (Ambrose and Norr 1993), which were fed on diets with different protein proportions (*i.e.*, 5%, 20% and 70%) and that had different access to water (*i.e.*, water provided *ad libitum* or on restricted access) and different temperatures (*i.e.*, 20 °C or 36 °C), in order to explore the effect of different dietary and living condition on nitrogen fractionation from diet to the consumer's tissues. The author did not evidence any statistically significant difference in the $\Delta^{15}N_{collagen-diet}$ values among groups of rats. However, Ambrose (2000) later observed lower $\Delta^{15}N_{flesh-diet}$ and higher $\Delta^{15}N_{collagen-diet}$ and $\Delta^{15}N_{hair-diet}$ with age (rats were sacrificed at 91, 131, 171, 211 and 251 days after birth).

While further feeding experiments supported the previous evidence with an average $\Delta^{15}N_{collagen-diet}$ value of +3.4 ± 1 ‰ (Table 3.1.2), a controlled dietary study on humans (O'Connell *et al.* 2012) proposed a higher offset of *ca.* +6 ‰. The offset was obtained by measuring the $\delta^{15}N$ values of red blood cells (RBC) from eleven individuals under controlled diet for 30 days, to which they added previously proposed $\Delta^{15}N_{keratin-RBC}$ and $\Delta^{15}N_{collagen-keratin}$ offsets (O'Connell *et al.* 2012). O'Connell *et al.* (2012) also noted that the offset was in line with previously observed $\Delta^{15}N_{keratin-diet}$ values based on food consumption surveys and diaries (Yoshinaga *et al.* 1996; Hedges *et al.* 2009). The *ca.* +6 ‰ offset might be biased by the estimation made upon published $\Delta^{15}N_{RBC-keratin}$ and $\Delta^{15}N_{keratin-collagen}$ values. However, O'Connell *et al.* (2012) highlighted that a very conservative approach to their data, would still provide a $\Delta^{15}N_{collagen-diet}$ value of *ca.* +4.6 ‰, higher than that proposed by previous feeding experiments (Table 3.1.2). Pigs are commonly used in feeding experiments because

they present similarities to humans in their digestive and metabolic processes (*e.g.*, Heinritz *et al.* 2013). Therefore such a difference in $\Delta^{15}N_{collagen-diet}$ might be surprising and future controlled dietary studies on groups of humans might help to support the evidence presented by O'Connell *et al.* (2012).

Notably, numerous studies have shown that $\Delta^{15}N_{tissue-diet}$ also responds to nutritional stress or physiological and pathological conditions, such as growth, pregnancy and starvation (*e.g.*, Fuller *et al.* 2005; Mekota *et al.* 2006; Warinner and Tuross 2010; Webb *et al.* 2016b). This could bias data obtained from archaeological individuals, that are often recovered from cemeteries. Indeed, if the individuals died after a long period of illness or other nutritionally stress related causes, this can interfere with the original dietary signal.

In conclusion, although nitrogen fractionation should not be influenced by diet composition as explained at the beginning of this paragraph, minor differences might be caused by the amino acid composition of the protein fraction. In particular, the data obtained from the feeding experiment by Webb *et al.* (2016b) seem to suggest that, when the protein fraction is optimal (*i.e.*, 20 %), the $\Delta^{15}N_{collagen-diet}$ increases with increasing % marine protein in diet (Table 3.1.2). It is possible that the synthesis of non-essential amino acids is inhibited when these are abundant in diet: for example, the non-essential amino acid glycine is higher in fish than in soy, and since glycine composes around one-third of collagen, a switch from enzymatic synthesis to direct routing might be visible at the bulk level. This would explain the increased $\Delta^{15}N_{collagen-diet}$ with increasing % marine protein in Webb *et al.*(2016b), and it will be further discussed in the next paragraph.

3.1.3 Application of carbon and nitrogen stable isotope analysis in the Roman Mediterranean basin

In the last few years, several scholars have applied bulk carbon and nitrogen stable isotope analysis (SIA) to investigate the dietary habits of Imperial Roman populations from the Mediterranean basin. The results of these studies are reported in Figure 3.4 as mean values ($\pm$ 1σ) only for those individuals aged $\geq$ 13 years-old. Descriptive statistics (dplyr, R version 4.0.3) is reported in Table 3.1.3. The results from animal remains and domestic plants (cereals and legumes) are also included to guide the description and discussion around the diet of these Roman communities. Domestic herbivores from Leptiminus are statistically significantly different in their $\delta^{15}N$ values

Experiment	**Animal**	**Diet ID**	**Protein**	$\Delta^{15}N_{collagen-diet}$
DeNiro and Epstein 1981	Mice	P	NA	1.4
		W	NA	2.5
		J	NA	3.4
Hare et al. 1991	Swine	C_3	100% C_3	2.2
		C_4	100% C_4	2.3
Ambrose 2000	Rats	1A	100% C_3 (20%)	3.4
		2B	100% C_4 (5%)	3.3
		3C	100% C_3 (5%)	3.4
		4D	100% C_4 (70%)	3.6
		5E	100% C_3 (70%)	3.4
		6F	100% C_3 (20%)	3.1
		12/13G	100% C_3 (20%)	3.1
		9A	100% C_3 (20%)	2.9
		10A	100% C_3 (20%)	2.6
		14A	100% C_3 (20%)	3.1
		11E	100% C_3 (70%)	3.8
Young 2003	Swine	1	C_3/C_4 (15%)	5.3
		2	C_3/C_4 (30%)	4.0
		3	C_3/C_4 (20%)	3.5
		4	C_3/C_4 (20%)	3.9
		5	C_3/C_4 (20%)	4.0
		6	C_3/C_4 (20%)	4.6
		7	C_3/C_4 (20%)	5.4
		8	C_3/C_4 (20%)	3.7
		9	C_3/C_4 (20%)	5.0
		10	marine/C_4 (20%)	3.6
		11	C_3/C_4 (20%)	4.4
		12	C_3/C_4 (20%)	4.5
Warinner and Tuross 2009	Swine	control	C_3/C_4	1.8
Webb et al. 2016	Swine	1	100% C_3 (20%)	1.9
		2	87.5% C_3, 12.5% marine (20%)	2.1
		3	75% C_3, 25% marine (20%)	2.4
		4	50% C_3, 50% marine (20%)	2.6
		5	100% marine (20%)	3.0
Kendall et al. 2017	Cattle	grass	C_3	4.9
			all	3.4 ± 1.0
			only Swine	3.5 ± 1.2

Table 3.2 Observed $\Delta^{15}N_{collagen-diet}$ values from feeding experiment studies (DeNiro and Epstein 1981; Hare *et al.* 1991; Ambrose 2000; Young 2003; Warinner and Tuross 2009; Webb *et al.* 2016b; Kendall *et al.* 2017). Bottom two lines represent mean and 1σ of all the experiments and of swine only experiments.

from the domestic herbivores from the other sites, therefore they have been treated as a separate group (Pairwise Wilcoxon Rank Sum Test, R version 4.0.3, Table A.6). In the following paragraphs differences across the populations will be discussed referring to the outcome of the non-parametric Pairwise Wilcoxon Rank Sum Test (R version 4.0.3, Tables A.2 and A.3) and p-values Bonferroni-adjusted to correct for multiple testing. Results were considered significant when $p \leq 0.05$. The list of human and animal δ^{13}C and δ^{15}N values can be found in Appendix A.

Following, the bulk SIA data are discussed: first, by the geographic location of the sites, with the aim to detect similarities which might be indicative of the direct engagement of some of these communities with the main productive and commercial routes of the Empire; then, by exploring gender- and status-related dietary differences; finally, by moving the focus to one of the main methodological issues of bulk SIA in Mediterranean contexts: the detection of marine food consumption.

Rome

Up to this date, several Imperial cemetery populations in the surroundings of Rome have been analysed through bulk SIA (Figure 3.5). These are: Casal Bertone (2^{nd}-3^{rd} centuries AD)(Killgrove and Tykot 2013; De Angelis *et al.* 2020a), Casal Malnome (2^{nd}-3^{rd} centuries AD)(De Angelis *et al.* 2020a), Castellaccio Europarco (1^{st}-3^{rd} centuries AD)(Killgrove and Tykot 2013), Quarto Cappello del Prete (1^{st}-3^{rd} centuries AD)(De Angelis *et al.* 2020a,b), Via Padre Semeria (2^{nd}-3^{rd} centuries AD)(De Angelis *et al.* 2020a), Gabii (1^{st} centuries AD)(Killgrove and Tykot 2018), Isola Sacra (1^{st}-3^{rd} centuries AD)(Prowse *et al.* 2004, 2005; Crowe *et al.* 2010), ANAS (Roman period)(Prowse *et al.* 2004, 2005), Praeneste (1^{st}-3^{rd} centuries AD)(Baldoni *et al.* 2019) and Lucus Feroniae (1^{st}-3^{rd} centuries AD)(Tafuri *et al.* 2018). The individuals buried just outside the city walls are more likely to have spent their life living and working in the Capital of the Empire while the burial grounds from the hinterland of Rome are mainly associated with rural communities involved in agricultural activities or productive sites. The authors of the SIA analyses from these communities all agree that C_3 plants (notably cereals) played a pivotal role in the diet of the humans analysed. However, some differences can be outlined.

For example, the individuals from Via Padre Semeria, a farming-based community, as suggested by a nearby *villa rustica* and by the stress marks found on the skeletons, were found with higher δ^{15}N values compared to the assemblage from Casal Bertone, interpreted by De Angelis *et al.* (2020a) with a higher consumption of higher trophic level products, such as terrestrial animal products but also freshwater fish, since the

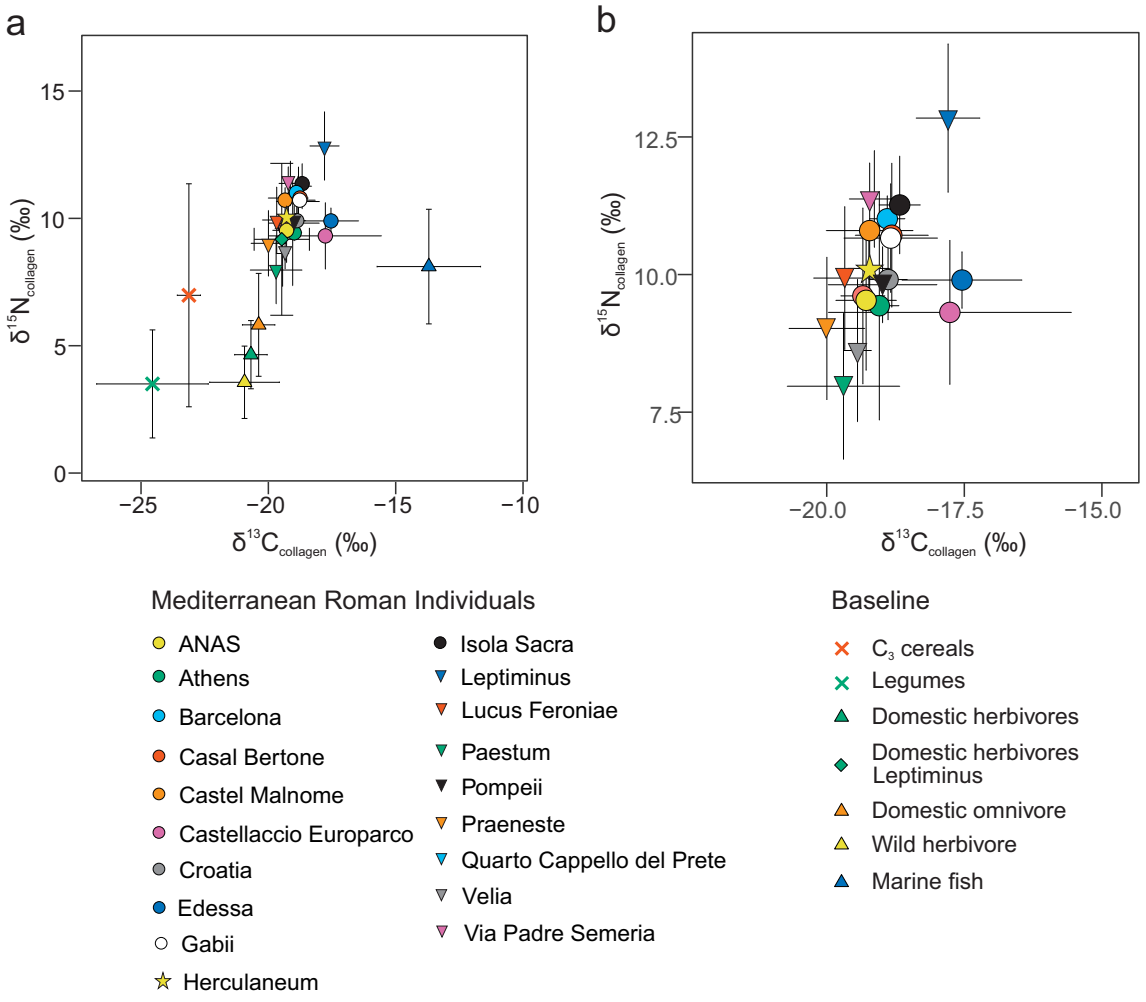

Figure 3.4 δ^{13}C and δ^{15}N mean values ($\pm 1\sigma$) of Imperial Roman populations and animal and domestic plant remains from the Mediterranean basin (a). Figure b is the same as Figure a but with a focus on the human individuals to help the visualisation of the data.

		$\delta^{13}C$				$\delta^{15}N$			
Group	***n***	$\overline{X}$	1σ	***min***	***max***	$\overline{X}$	1σ	***min***	***max***
ANAS[1,2]	14	-19.34	0.40	-19.90	-18.57	9.61	1.60	6.90	11.30
Athens[3]	9	-19.04	0.36	-19.80	-18.70	9.43	2.07	4.00	10.70
Barcelona[4]	15	-18.90	0.32	-19.50	-18.40	11.01	0.42	10.40	11.70
Casal Bertone[5,6]	75	-18.82	0.66	-20.40	-16.50	10.71	1.31	7.00	12.60
Castel Malnome[6]	72	-19.22	0.79	-20.80	-14.80	10.80	1.23	7.20	12.90
Castellaccio Europarco[5]	8	-17.76	2.21	-19.50	-12.50	9.31	1.31	7.80	11.50
Croatia[7]	63	-18.89	0.35	-19.62	-17.84	9.91	0.73	8.51	12.90
Edessa[8]	19	-17.54	1.09	-21.00	-16.20	9.90	0.51	8.80	10.80
Gabii[9]	16	-18.84	0.85	-19.30	-15.80	10.66	0.99	8.50	11.50
Herculaneum[10]	69	-19.23	0.38	-20.17	-18.21	10.11	0.77	8.17	11.72
Isola Sacra[1,2,11]	176	-18.67	0.37	-19.90	-17.30	11.26	0.88	8.30	12.90
Leptiminus[12]	56	-17.79	0.58	-19.00	-16.50	12.84	1.35	10.00	15.70
Lucus Feroniae[13]	31	-19.67	0.56	-20.49	-17.88	9.94	1.30	6.61	12.15
Paestum[14]	21	-19.70	1.02	-22.10	-18.40	7.97	1.33	4.70	11.40
Pompeii[15]	27	-18.99	0.99	-20.10	-15.80	9.81	0.69	8.10	10.60
Praeneste[16]	33	-20.00	0.69	-22.50	-18.90	9.02	1.29	6.50	12.20
Quarto Cappello del Prete[6,17]	19	-19.28	0.55	-20.50	-18.20	9.53	1.27	7.70	12.30
Velia[18]	114	-19.44	0.25	-20.00	-18.70	8.62	1.29	6.40	14.10
Via Padre Semeria[6]	26	-19.13	0.45	-20.00	-18.10	11.37	0.88	10.00	13.20
Domestic Herbivores	58	-20.68	0.64	-22.60	-19.10	4.65	1.34	1.90	9.50
Domestic Herbivores Leptiminus[12]	6	-19.68	1.17	-21.10	-18.30	8.78	2.82	6.00	12.90
Domestic Omnivores	30	-20.38	0.64	-21.50	-18.60	5.82	2.02	3.00	10.30
Wild Herbivores	14	-20.94	1.37	-23.00	-18.20	3.56	1.42	2.00	6.00
Marine fish	19	-13.70	2.03	-17.80	-7.60	8.11	2.25	4.90	12.10
C_3 Cereals[15,19]	5	-23.12	0.45	-23.70	-22.50	6.98	4.38	0.80	10.90
Legumes[15]	2	-24.55	2.19	-26.10	-23.00	3.50	2.12	2	5

Table 3.3 Descriptive statistics (dplyr, R version 4.0.2) of Imperial Roman populations and of domestic herbivores, wild herbivores, domestic omnivores, marine fish, C_3 cereals and legumes from the Mediterranean basin. References: 1= Prowse *et al.* (2004), 2= Prowse *et al.* (2005), 3=Lagia (2015), 4= Rissech *et al.* (2016), 5= Killgrove and Tykot (2013), 6= De Angelis *et al.* (2020a), 7=Lightfoot *et al.* (2012), 8=Dotsika and Michael (2018), 9= Killgrove and Tykot (2018), 10=Martyn *et al.* (2018), 11= Crowe *et al.* (2010), 12= Keenleyside *et al.* (2009), 13=Tafuri *et al.* (2018) 14= Ricci *et al.* (2016), 15= Pate *et al.* (2016), 16=Baldoni *et al.* (2019) 17= De Angelis *et al.* (2020b), 18= Craig *et al.* (2009), 19=O'Connell *et al.* (2019).

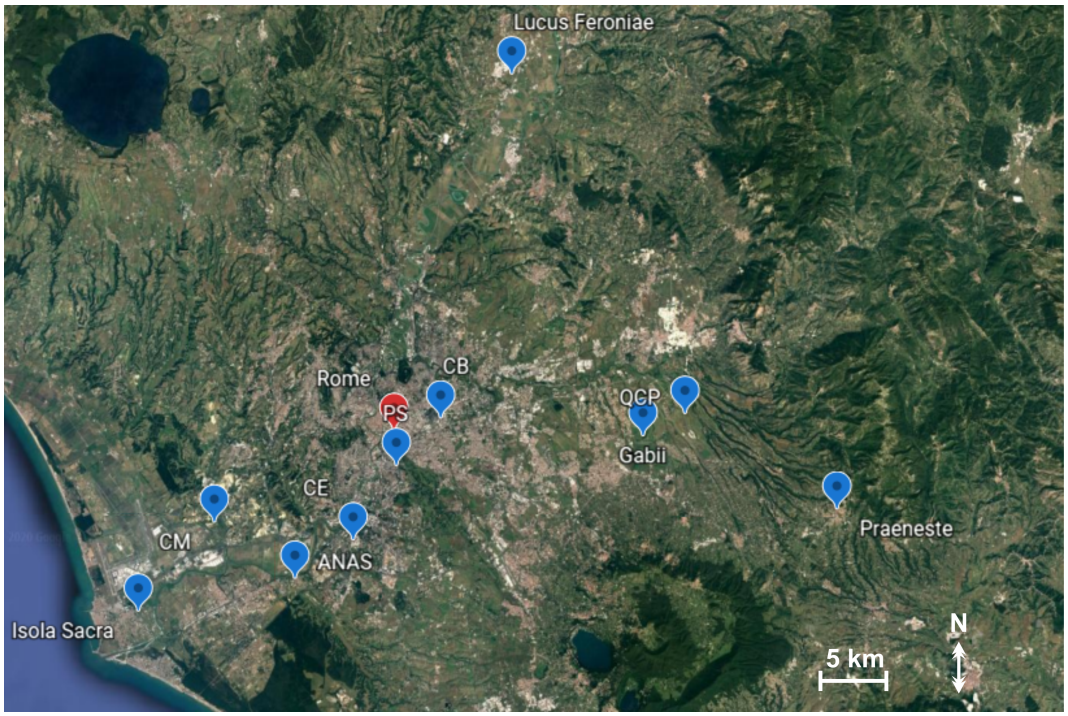

Figure 3.5 Location of the human populations in the proximity of Rome subject to carbon and nitrogen stable isotope analysis. CM: Castel Malnome, CE: Castellaccio Europarco, CB: Casal Bertone, PS: Via Padre Semeria, QCP: Quarto Cappello del Prete. From Google earth 2021.

cemetery is located close to the Almone river. On the contrary, Casal Bertone and Castel Malnome were both involved in manufacturing activities, in particular that of tanning and that of salt flats, respectively. The distribution of $\delta^{13}C$ and $\delta^{15}N$ values does not evidence any statistically significant difference between the two groups, suggesting that their diet was very similar even though Castel Malnome is located *ca.* 15 km to the south-west of Rome, while Casal Bertone is located just outside the city walls (Tables A.2 and A.3). Surprisingly, Castellaccio Europarco, a small human assemblage from the southern *suburbium ca.* 10 km from Rome whose community was probably involved in agricultural activities, show strikingly less negative carbon values and at the same time lower nitrogen values, although the differences are not statistically significant due to the limited number of samples representing this group (Killgrove and Tykot 2013)(Tables A.2 and A.3). The $\delta^{13}C$ values led the authors to suggest a diet rich in C_4 plants, millet in particular, as also evidenced by the apatite $\delta^{13}C$ values (Killgrove and Tykot 2013). Quarto Cappello del Prete and Gabii are two nearby communities located *ca.* 20 km to the east of Rome. Their location makes them less likely to access products from the Roman market as well as marine resources. The two assemblages do not show statistically significant differences in their isotopic values (it

must be acknowledged the limited number of samples of both distributions)(Tables A.2 and A.3). However, Killgrove and Tykot (2018), when comparing the δ^{15}N values of the humans from Gabii with those from Isola Sacra, suggested a significant consumption of terrestrial animal products and marine fish in Gabii, comparable to that of Isola Sacra, although the latter comes from a very different economic and cultural context, since it was the necropolis associated with Portus Romae, the harbour of Rome, an area intensely involved in commercial activities and marine resource exploitation (Killgrove and Tykot 2018). On the contrary, Gabii was an important religious site that started to decline during the Imperial period. The individuals analysed by Killgrove and Tykot (2018) were buried inside the city walls, something unusual for the Romans, suggesting that the city was already going through a progressive abandonment at that time, as reported by the authors. Quarto Cappello del Prete was also a religious site characterised by a population turnover (De Angelis *et al.* 2020a,b), but the δ^{13}C and δ^{15}N values from this assemblage appear to be much closer to those of ANAS, a small human assemblage from a rural context of farmers (Prowse *et al.* 2004, 2005) and Lucus Feroniae, located around 30 km north-east of Rome, a rural commercial and religious town (Tafuri *et al.* 2018), rather than to Gabii. Archaeological evidence and anthropological studies carried out on the skeletons suggested that people from Lucus Feroniae were labourers of humble origins. The authors suggested that the isotopic signatures are characteristic of a diet certainly rich in cereals but also in terrestrial animal products (Tafuri *et al.* 2018). On the contrary, the rural site of Praeneste, *ca.* 30 km to the south-east of Rome, shows the lowest δ^{13}C and δ^{15}N values among all the assemblages from the hinterland of Rome (Baldoni *et al.* 2019). The authors proposed a diet mainly based on terrestrial foodstuff and, although millet was detected in the calculus of some of the individuals, C_4 plants were probably not a major component of diet. It seems likely that people living in the area were relying mainly on the products of the land such as cereals and legumes and that animal products were only supplementary, although lactose was detected in the dental calculus of two individuals (Baldoni *et al.* 2019).

What emerges from these data is an heterogeneous picture of the dietary habits of people living in the proximity of Rome. Some rural communities (Via Padre Semeria, Casal Bertone, Castel Malnome) exhibit values which are surprisingly similar to those of the individuals from Isola Sacra. Isola Sacra is the Roman community showing the highest mean δ^{13}C and δ^{15}N values from the Italian peninsula, perhaps indicative of a diet with a significant inclusion of higher trophic level food items (*i.e.*, animal products and marine fish). This would suggest that, although of humble origins, the individuals

from these rural communities were able to access food sources above the subsistence level, which is perhaps indicative of the economic involvement with the Capital. On the contrary, Lucus Feroniae, ANAS and particularly Praeneste, which are also rural communities from the surroundings of Rome, do not seem to be invested either by the same wealth or influence.

Campania

Further south in the Italian peninsula, in Campania, δ^{13}C and δ^{15}N values from four populations have been published so far (Figure 3.6) (Craig *et al.* 2009, 2013; Pate *et al.* 2016; Ricci *et al.* 2016; Martyn *et al.* 2018).

Paestum (2^{nd}-4^{th} centuries AD), a small rural community, represents the human assemblage with the lowest δ^{15}N values among all the populations considered in this review (Tables A.2 and A.3)(Ricci *et al.* 2016). The isotopic values were interpreted by the authors as indicative of a diet rich in C_3 cereals and other products of the land while fish, if eaten, was probably only consumed in the form of *garum* made with lower trophic level fish (Ricci *et al.* 2016).

The population of Velia (1^{st}-2^{nd} centuries AD) also shows significantly lower ^{15}N compared to many of the other assemblages (Table A.3)(Craig *et al.* 2009). The authors suggested a diet largely based on C_3 plants, although they also observed the presence of a small group of individuals (called by the authors "Velia II") that probably consumed more terrestrial animal products and marine fish compared to the rest of the population. The statistically significant differences of both δ^{13}C and δ^{15}N values between Velia and Isola Sacra were explained as influenced by the economy of the two areas (Tables A.2 and A.3): while Isola Sacra was located in the proximity of one of the most important harbours of the Roman Empire, Velia, although with quite a large port, had an economy based on agriculture (Craig *et al.* 2009).

The δ^{13}C and δ^{15}N values of the human individuals from AD 79 Pompeii were interpreted by Pate *et al.* (2016) with a diverse diet composed of cereals, fruits, vegetables, animal products and fish, as suggested by the archaeological evidence from the site.

When compared with the communities from the surroundings of Rome, the δ^{13}C and δ^{15}N values of the human individuals from 79 AD Pompeii and Herculaneum appear to be closer to those from rural communities such as Lucus Feroniae and ANAS than to those more economically active such as Isola Sacra (Tables A.2 and A.3). This is somehow surprising, since the Bay of Naples in the the 1^{st} century AD was probably as equally productive and commercially active as Portus Romae (see section

2.2). However, the δ^{13}C and δ^{15}N values of the human individuals from 79 AD Pompeii and Herculaneum are also different from those some exhibited by Paestum and Velia, both sites being more rural and probably less influenced by the main production and trade routes of the Empire in the Mediterranean (Tables A.2 and A.3).

Outside Italy

Only a few Roman Empire populations outside Italy have been analysed through carbon and nitrogen stable isotope analysis in the Mediterranean (Figure 3.6). Edessa (2^{nd}-4^{th} centuries AD) was an inland town located in northern Macedonia, Greece (Dotsika and Michael 2018). The δ^{13}C and δ^{15}N values obtained from the individuals were interpreted by the authors as indicative of a diet composed of C_4 plants (millet) and/or of animals fed on millet or C_4 grasses, alongside C_3 cereals (Dotsika and Michael 2018). In contrast, the few individuals from Roman Athens show δ^{13}C and δ^{15}N values closer to those of the hinterland of Rome, interpreted as a diet mainly based on C_3 products (Tables A.2 and A.3)(Lagia 2015).

Figure 3.6 Location of Roman human assemblages from the Mediterranean basin. Herc: Herculaneum, Pom: Pompeii, Pa: Paestum, Ve: Velia. From Google earth 2021.

The Roman colony of Barcelona (1^{st}-4^{th} centuries AD), called *Barcino*, was an important harbour town involved in intense agricultural exploitation but also in the exportation of products such as cereals, wine, iron and clay (Rissech *et al.* 2016). Archaeological and anthropological evidence suggested that the individuals analysed

belong to low socio-economic groups (Rissech *et al.* 2016). The human assemblage from this cemetery reported δ^{13}C and δ^{15}N values interpreted as typical of a terrestrial diet with contribution of marine fish, similar to Isola Sacra (Tables A.2 and A.3)(Rissech *et al.* 2016). The lower δ^{15}N values detected in Roman individuals from three archaeological sites located on the coast of the Dalmatia region, Croatia, (2^{nd}-4^{th} centuries AD), compared to other Roman populations, led the authors to suggest only limited marine contribution to a diet mainly based on C_3 plants and animal products (Lightfoot *et al.* 2012).

Leptiminus (2^{nd}-4^{th} centuries AD), modern Lamta, on the Mediterranean coast of Tunisia, was an important harbour city renowned for the production of *garum* (Pliny, *HN* 31.94)(Keenleyside *et al.* 2009). By comparing the δ^{13}C and δ^{15}N values of the humans with those of the local fauna, the authors proposed that people living in Roman and Late Roman Leptiminus had a diet rich in cereals and other C_3 plant products (e.g, olive oil and wine) with a high marine fish contribution. The consumption of marine resources appears significant when the authors compare the δ^{13}C and δ^{15}N values of the individuals from Leptiminus with those from Isola Sacra and Roman Britain, suggesting regional variability of diet in the Roman period (Keenleyside *et al.* 2009).

Although limited in number, it is clear that these Mediterranean communities present some differences in their dietary habits from each other and also from the communities of the Italian Peninsula. Of course, the observed differences can be largely explained by their different geographic location, and therefore by the environment and climatic conditions and their cultural histories. It is interesting to note however, that the higher δ^{13}C and δ^{15}N values of the individuals from the harbour town of Barcino are close to those from Isola Sacra and other communities from the surroundings of Rome (Tables A.2 and A.3). This seems to suggest that the deep involvement of the area with the main production and commercial routes of the Empire in the Mediterranean, had perhaps a cultural influence on the local communities.

Sex-based differences

According to ancient medical treatises, such as those written by Galen, Rufus of Ephesus and Athenaeus of Attaleia (Garnsey 1999, 100-102), the diet of women was strictly regulate, suggesting for example small portions of food and no access to meat and wine (Garnsey 1999, 100-112). However, it is easy to believe that these restrictions were loosened in contexts where there was no food shortage or where women engaged in working activities that required a more nutritious diet compared to that of women that

were spending most of their time at home (Garnsey 1999, 100-112). Moreover, these treatises were written by men and they are most likely not representative of the reality. As Garnsey (1999) was expecting, the carbon and nitrogen isotope analysis of different Imperial assemblages from the Mediterranean basin do not suggest a homogeneous picture.

Statistically significant sex-based differences were only detected at Isola Sacra, Velia, Pompeii and Herculaneum. At Isola Sacra, Prowse *et al.* (2005) observed consistently higher δ^{15}N values and higher δ^{13}C in males compared to females in all the age classes, concluding that males had a larger access to marine food than females. Similarly, at Velia, differences in δ^{13}C and δ^{15}N values between males and females are statistically significant (Craig *et al.* 2009). The authors interpreted the values with occupational-related differences in males and females but also with exclusion of women from consuming some types of food (Craig *et al.* 2009). As suggested above however, there is no evidence for exclusion of women from eating some type of food with the exception of medical treatises, and therefore the differences observed by Craig *et al.* (2009) should be further investigated.

No statistically significant sex variations were detected in all the other assemblages (Keenleyside *et al.* 2009; Lightfoot *et al.* 2012; Killgrove and Tykot 2013; Lagia 2015; Rissech *et al.* 2016; Killgrove and Tykot 2018; Tafuri *et al.* 2018; De Angelis *et al.* 2020a,b). Although it needs to be acknowledged the limited number of individuals from some of these assemblages, it is worth noting that most of these sites were communities involved in productive or commercial activities that could have required an equal involvement of women and men in working activities.

The fact that gender-related significant differences were only observed at Isola Sacra, Velia and Herculaneum, does not necessarily imply that women and men from the other communities had the same diet. Indeed, more subtle differences might simply not be visible at the bulk SIA level.

Social status-based differences

Variations of diet related to social status have been addressed in some of the studies included here. Interestingly, Keenleyside *et al.* (2009) reported higher δ^{13}C values of bone hydroxyapatite in adult individuals buried in pit coffins at Leptiminus that they interpreted with higher consumption of marine fish. The authors also suggested that individuals buried in simple pits should be of a lower social status than those buried with ceramic covers or cut stone, therefore the higher consumption of marine fish by this group of individuals remains to be explained. It is possible that marine fish was

a low status food in this population or perhaps that simple pits were not only used to bury low social status individuals. The authors also observed higher δ^{15}N values in individuals resting in *cupula* burials but no differences in any of the other types of burials, including the *mauseolea* and hypogea that belonged to higher social status individuals, suggesting that diet at Leptiminus was probably not influenced by social status, at least not in the way one might expect (Keenleyside *et al.* 2009).

Similarly in Rome, although a few individuals from the *Mausoleum* context of Casal Bertone show higher δ^{15}N values, the group is not significantly separated from the other two Casal Bertone necropolis (De Angelis *et al.* 2020a).

Studies of this type are still limited, mainly because it is not always easy to confidently identify the social status of an individual from its burial. However, from the few articles where social-status based differences were detectable (Keenleyside *et al.* 2009; De Angelis *et al.* 2020a), it would appear that in the same community, status-based differences were not reflected into the diet.

Although not related to differences in funerary practices, (Prowse *et al.* 2005) noted that both $\delta^{13}C_{ap-co}$ offset values and δ^{15}N values of bone collagen were correlated with age (the former negatively and the latter positively), suggesting that both males and females changed their dietary habits with age, probably consuming more terrestrial products such as animal products, olive oil and wine as well as marine fish. They also pointed out that it must be acknowledged that individuals of higher social status were more likely to reach older ages (Prowse *et al.* 2005).

On tracking marine fish consumption in the Roman Mediterranean: AD 79 Herculaneum

Prowse *et al.* (2004) first observed a possible different response of carbon and nitrogen in bone collagen to marine fish consumption. They suggested that a diet rich in C_3 products such as bread and olive oil, as the Roman diet was, would account for a great part of the carbon atoms of the amino acids present in collagen, since the carbon skeleton can also be derived from carbohydrates and lipids; on the contrary, nitrogen, which is necessarily introduced with proteins, is more sensitive to the consumption of foodstuff that are rich in proteins, notably fish, even if in limited quantities compared to other components of diet (Prowse *et al.* 2004). They found their hypothesis confirmed in the mean δ^{13}C values of bone apatite, since these would reflect a diet based on C_3 sources with only a minor input from marine fish (Prowse *et al.* 2004). Later on, Prowse *et al.* (2005) concluded that δ^{13}C of bone apatite reflects the terrestrial components of the diet of the Romans while δ^{15}N and, to a lesser extent δ^{13}C, of bone collagen that

of proteins, in this case marine fish.

To quantify marine carbon and nitrogen in bone collagen from Mediterranean contexts, Craig *et al.* (2013) obtained radiocarbon dates and δ^{13}C and δ^{15}N values of the bone collagen from nine individuals and one sheep from the AD 79 Herculaneum assemblage. The authors considered that dates older than AD 79 would be caused by the marine reservoir effect (which is, a lower concentration of ^{14}C in marine environments as a consequence of the slow mixing of waters that can only incorporate new CO_2 from the atmosphere when at the surface (Ascough *et al.* 2005)), therefore, by higher consumption of marine foodstuff. Assuming that a 100 % marine consumer should have a date offset of 390 years (which is the marine reservoir age observed in the Mediterranean by Reimer and McCormac (2002)), it was possible to extrapolate from the regression lines of the δ^{13}C and δ^{15}N values and the date offsets of each individual (obtained by subtracting the date of the sheep, which is most likely a 100 % terrestrial consumer, from the date of each individual) the isotopic values of a 100 % terrestrial and a 100 % marine human consumers.

The equations of the regression lines for the δ^{13}C and δ^{15}N values obtained from a 100 % terrestrial and a 100 % marine consumer were used to derive the percentage of marine carbon and marine nitrogen in the collagen of each individual (Craig *et al.* 2013). However, the authors observed that while the extrapolation of the regression equation to the estimated δ^{13}C value of a 100% marine consumer produces a date offset value of 430 years, in line with the measured marine reservoir effect for the Mediterranean, the extrapolation to the estimated δ^{15}N value produces instead a much lower date offset of 127 $\pm$ 24 years. To explain this discrepancy Craig *et al.* (2013) modelled three different dietary scenarios: one where carbon in collagen can only derive from carbon in proteins (routed), one where carbon in collagen derives equally from carbohydrates/lipids and proteins (scrambled) and one which is a mixture of the previous two (routed:scrambled=1:1). The authors concluded that either a scrambled or a scrambled:routed model could better explain the isotopic values observed at AD 79 Herculaneum, rather than a routed model, confirming that the non-protein fraction of diet needs to be accounted for when interpreting carbon stable isotope results from bone collagen (Figure 3.7).

Martyn *et al.* (2018) detected statistically significant sex-related differences both in carbon and nitrogen isotopic values at Herculaneum suggesting a higher consumption of higher trophic level fish by men. Using the regression equation for δ^{15}N from Craig *et al.* (2013), Martyn *et al.* (2018) calculated that at least 70 % of diet at Herculaneum

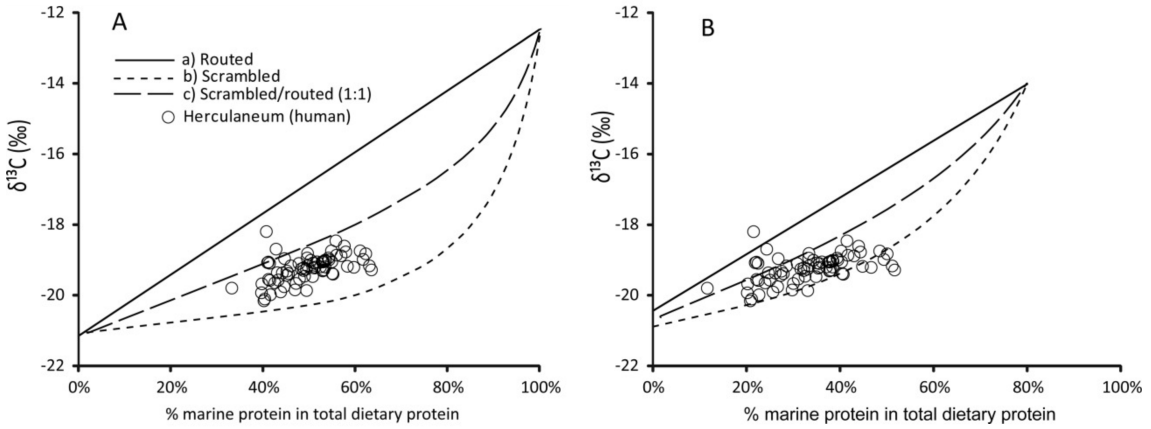

Figure 3.7 Carbon isotope values from the human assemblage of Herculaneum against marine protein contribution (%). The models based on 1:1 scrambling of macronutrients and protein routing and total scrambling better explain the isotopic values observed in the individuals from Herculaneum, both when protein contribution from terrestrial animal products is included (A) or not (B). Modified after Craig *et al.* (2013).

was made of terrestrial sources and that marine protein accounted for up to 50 % of total dietary protein (Figure 3.8 a). The authors also observed statistically significant differences of δ^{15}N values between younger adults (10-30 years-old) and older male adults (> 30 years-old), suggesting that older males were consuming more marine fish than younger male and female adults. The authors suggest that by that age men would have obtained the role of *pater familias* (*i.e.*, head of the household) or manumission by their owners when slaves (Figure 3.8 b), therefore by that age they were more likely to access more expensive food sources such as perhaps fresh marine fish, in addition to the more familiar fish-sauces (Garnsey 1999, 122-127).

In conclusion, the results from previous stable isotope studies have provided a complex picture that can only partially resolve the questions around dietary habits in the Mediterranean basin under the rule of the Roman Empire. Populations from the hinterland of Rome show a diet somehow homogeneous with some differences possibly related to the role of these communities in the economy right at the center of the Empire. Only three Italian Roman settlements have been analysed for stable isotope analysis farther away from Rome. While Paestum and Velia show isotopic values significantly depleted both in ^{13}C and in ^{15}N (Tables A.2 and A.3), possibly indicating a more rural diet largely based on the consumption of the products of the land, Herculaneum would appear much more similar to the communities living in the proximity of Rome. As for outside Italy, it seems clear that the dietary habits of people

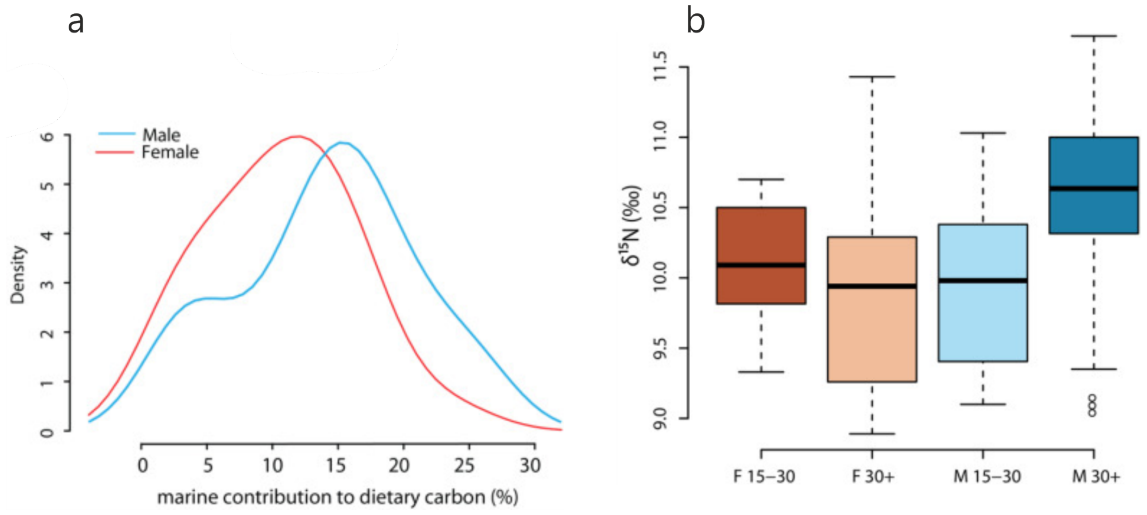

Figure 3.8 Dietary variations across the human assemblage of AD 79 Herculaneum. The kernel density plot (a) shows different marine contribution to dietary carbon in males and females; the boxplot of δ^{15}N values divided by sex and age shows higher values in older adult males, suggesting higher marine consumption. Modified after Martyn *et al.* (2018).

living in newly acquired territories reflected some degree of continuity with the local products and traditions despite the influence of the Roman culture, as observed at Edessa and Leptiminus. It should be noted however that the qualitative interpretation of the isotopic values can be easily questioned. For example, high marine consumption was proposed at Leptiminus. However, high δ^{13}C and δ^{15}N values were also observed in the terrestrial local fauna, probably due to the effect of the local climatic conditions, therefore the human isotopic values could also be interpreted with a terrestrial local diet with only a minor degree of marine foodstuff consumption. Most importantly, it would appear that all these studies have underestimated the contribution of cereals that, when manured, can have δ^{15}N values higher than those of herbivores, although the latter are in principle one trophic level higher in the trophic web (Bogaard *et al.* 2007).

Linking it back to the discussion around carbon and nitrogen isotopic fractionation from diet to collagen from the previous sections 3.1.1 and 3.1.2, these studies appeared to be severely limited by the large degree of uncertainty around the prediction of a given fractionation value from diet to consumer. The Roman diet was a diet rich in C_3 carbohydrates (cereals) and lipids (olive oil). Therefore, it is likely that the proteins in cereals, since these were eaten in abundance, accounted for a great part of the amino acid requirement; therefore, a small contribution from an isotopically distinguished

protein source (notably marine in the Mediterranean basin) would be largely (if not completely) hidden in the overall δ^{13}C values of bone collagen, as observed by Prowse *et al.* (2004, 2005) and Craig *et al.* (2013). However, even "small" (*i.e.*, < 20 % (Hedges 2004; Webb *et al.* 2017)) contribution of marine consumption could have major socio-cultural implications in the Roman period, and it seems therefore important to be able to confidently detect it. The limited resolution of carbon and nitrogen stable isotope analysis could have major implications in the interpretation of the results in many other directions. For example, sex-based differences have been detected only at Isola Sacra, Velia and Herculaneum. Although this could suggest that men and women had a more similar diet compared to what reported by the ancient literary sources, it is possible that differences, if present, are not always detectable by this type of analysis.

3.1.4 Quantitative interpretation of carbon and nitrogen stable isotope data: Mixing Models

Compared to other types of evidence, the application of carbon and nitrogen stable isotope analysis on human, animal and botanical remains provides a *direct* direct evidence of the consumption of certain food sources by past human populations. Furthermore, since the isotopic signal of carbon and nitrogen isotopic values in the consumer tissue is correlated to that from the foodstuff consumed, carbon and nitrogen analysis lead to a new level of knowledge by answering to the question "*How much* of this source did they eat?".

Initially, Linear Mixing Models (LMMs) were proposed to offer a quantitative approach, however, although mathematically solid, they are limited by the number of food sources, that can be maximum equal to the number of proxies (*e.g.*, δ^{13}C and δ^{15}N) used plus one and, most importantly, they cannot be realistically applied to a system where at least one of the proxies is linked to more than a single fraction in diet and in different proportions (a mechanism previously referred to in this section as "scrambling" and typical of δ^{13}C values of collagen (see section 3.1.1) (*e.g.*, Phillips and Koch 2002). Moreover, the result of the application of a LMM is a single value which clearly underestimates the degree of uncertainty associated with the estimation. A more sophisticated simple probabilistic model called IsoSource[2] was later proposed, which gives permission to use more dietary sources and which reports the estimation as a range of values, accounting for the uncertainty of the prediction (Phillips and

[2]IsoSource is vailable at this link.

Gregg 2003). However, IsoSource lacks the possibility to account for macronutrient concentrations of the food sources.

Parnell *et al.* (2010) first relied on the Bayes' theorem to circumvent the limitations of LMMs and simple mixing models such as IsoSource. Briefly, Bayesian Mixing Models describe the probability that an event has to occur by taking into account some prior conditions that the user has to provide. This provides a certain degree of uncertainty associated with the estimates. The two most applied BMMs are MixSIAR (Parnell *et al.* 2010; Stock and Semmens 2017; Stock *et al.* 2018) and FRUITS (Fernandes *et al.* 2014) and they both adopt the Markov chain Monte Carlo (MCMC) method to simulate the probabilistic events. Compared to MixSIAR, FRUITS additionally considers possible scrambling mechanisms that involve the proxies (*e.g.*, δ^{13}C that receives contribution from all proteins, carbohydrates and lipids) and the concentration of the dietary fractions in the food sources. FRUITS comes in the shape of a user-friendly interface that can be easily downloaded[3] but a more recent online application has been developed (ReSources[4]) that offers the possibility to aggregate the food sources *a posteriori* (*i.e.*, after the model has been run), aggregating sources with different concentrations. The aggregation of sources *a posteriori* has been shown to provide a better accuracy than that carried out *a priori* when applied to different case studies (Cheung and Szpak 2020).

Fernandes (2016) applied FRUITS on the nine individuals radiocarbon dated from the AD 79 Herculaneum assemblage with the aim to observe the agreement of the estimates from two possible scenarios with those obtained previously by Craig *et al.* (2013). By doing so, Fernandes (2016) considered only two possible food sources, namely terrestrial herbivores and marine fish, taking the δ^{13}C and δ^{15}N values from Craig *et al.* (2009). *Scenario 1* corresponded to a simplified non-routed and concentration-independent model, therefore with δ^{13}C only receiving contribution from protein with an estimated $\Delta^{13}C_{collagen-diet} = +5 \pm 2.3$ and a $\Delta^{15}N_{collagen-diet} = +5.5 \pm 0.5$, and variation of protein concentration in the two food groups not considered. On the contrary, *Scenario 2* was a routed and concentration-dependent model, therefore accounting for the contribution of both proteins (74 ± 4 %) and carbohydrates and lipids (26 ± 4 %) (these last two under the same category called "energy") to carbon with an estimated offset that account for the two $\Delta^{13}C_{collagen-diet} = +4.8 \pm 0.5$. Since the estimates derived by the application of the two scenarios were within the error of the observed values and they showed agreement with the estimates from Craig *et al.*

[3]FRUITS can be downloded from the SourceForge platform at this link.
[4]ReSources is available at this link.

(2013), Fernandes (2016) concluded that they can be both reliably applied to similar archaeological contexts (Figure 3.9). However, the model only considers terrestrial herbivores as terrestrial food sources, notably neglecting the contribution of C_3 cereals. Although it was argued by the author that the isotopic values of cereals would be reflected in those of terrestrial animals, the $\delta^{13}C$ value of lipids derived by Fernandes (2016) of terrestrial animals ($-29.3 \pm 1‰$), that notably accounts for 70 % of the source $\delta^{13}C$ value, is considerably depleted compared to the $\delta^{13}C$ value that cereals would contribute. Moreover, $\delta^{15}N$ values of C_3 cereals can be higher than those of domestic herbivores due to manuring practices (*e.g.*, Bogaard *et al.* 2007), as it has also been observed at Portus Romae (Figure 3.4 and Table 3.1.3)(O'Connell *et al.* 2019). Ancient texts and archaeological evidence further suggest that pork meat was likely consumed by Romans in the Mediterranean, therefore omnivores also seem to be important to be included in the dietary model. However, this last group has $\delta^{13}C$ and $\delta^{15}N$ values similar to those of the terrestrial herbivores, therefore they should be better grouped with the herbivores under a "terrestrial animals" category. Most importantly, as discussed in the previous sections 3.1.1 and 3.1.2, larger conservative uncertainties should be used for both $\Delta^{13}C_{collagen-diet}$ and $\Delta^{15}N_{collagen-diet}$ offsets. When a new BMM FRUITS model that considers three food sources (C_3 cereals, terrestrial animals and marine fish) is applied to the assemblage, the estimates related to C_3 cereals and terrestrial animals are not satisfactorily resolved and, most importantly, marine fish contribution is underestimated (see chapter 6 and Appendix E for the model parameters, estimates and further discussion). BMMs are not able to discriminate between food sources that are isotopically homogeneous, therefore in this case C_3 cereals and terrestrial animals. In conclusion, their application on $\delta^{13}C$ and $\delta^{15}N$ values of bulk collagen is severely limited by the large degree of uncertainty around the fractionation mechanisms of both carbon and nitrogen from diet to collagen. A better understanding of amino acids metabolism can help in this direction.

3.2 Compound Specific Isotope Analysis of Amino Acids

As introduced previously (1.3 and 3.1), although stable isotope analysis of carbon and nitrogen of collagen has many advantages in the study of dietary habits of ancient human populations, scholars are nowadays aware of some important limitations of this approach. One of the most important issues when dealing with "traditional" isotope analysis is that the isotopic values obtained are average values of the isotopic signature

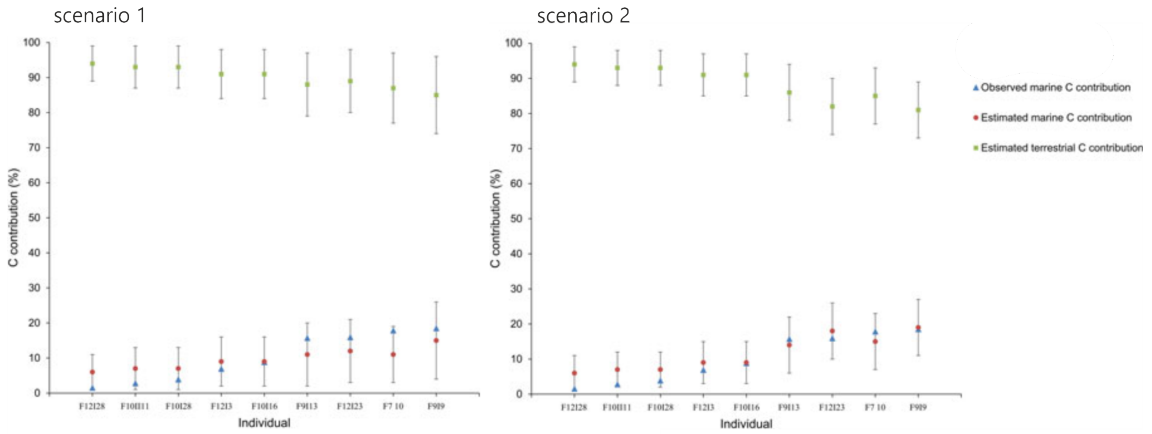

Figure 3.9 Comparison of the estimates of marine and terrestrial carbon contribution to the diet of nine individuals from AD 79 Herculaneum using a non-routed and concentration independent mixing model (*Scenario 1*) and a routed and concentration-dependent mixing model (*Scenario 2*) with those observed by Craig *et al.* (2013). Modified after Fernandes (2016).

of the single molecules composing it, which are, in the case of collagen, amino acids. Amino acids in proteins present different nitrogen and carbon isotope ratios depending on the metabolic and catabolic pathways that they follow, as it is going to be outlined in section 3.2.2. Depending on its metabolic route, each amino acid is bearer of a different information about the food ingested. These metabolic mechanisms have been widely explored and used to interpret the archaeological data, obtaining a much higher resolution than with the bulk stable isotope analysis alone. The main steps of the carbon and nitrogen isotope research on amino acids with application in archaeology will be retraced in the following section.

3.2.1 Previous studies

The analysis of isotope ratios of elements composing macromolecules is called "Compound Specific Isotope Analysis" (CSIA). In archaeology, CSIA is mostly applied to lipids and amino acids, two macromolecules likely to be found in archaeological contexts (Brown and Brown 2011). While CSIA of lipids has been applied to archaeological material, particularly in potsherds, extensively and steadily since 1994 (Evershed *et al.* 1994), CSIA of amino acids has a more turbulent history.

Compound specific isotope analysis of amino acids (CSIA-AA) was applied for the very first time in 1961 by Abelson and Hoering, to the study of carbon isotope fractions in amino acids of photosynthetic organisms (Abelson and Hoering 1961). More studies followed, but only in the 90s of the past century, CSIA-AAs started to be exploited becoming a conventional technique, thanks to the commercial introduction

of GC-C-IRMS first (Hayes *et al.* 1990; Meier-Augenstein 1999) and of LC-IRMS then (McCullagh *et al.* 2006; Smith *et al.* 2009). In this scenario, its application in archaeology is relatively recent. Soon after the publication of *You are what you eat (plus a few ‰)* (DeNiro and Epstein 1976), indeed, several scholars wondered whether the assumption that stable isotopic composition of animal tissues is a direct function of the diet was really valid. With this respect, researchers compared isotopic signatures of amino acids from modern collagen to those from fossil material belonging to the same species, with the aim to assess collagen preservation through time.

The first study in this direction was published by Hare and Estep (1983) and it was not long before some others realised that differences in isotope ratio among individuals belonging to the same species could depend on differences in diet rather than on diagenesis (Tuross *et al.* 1988). This awareness came from the results of contemporary ecological studies, among which that from Macko *et al.* (1987) surely stands out. The authors compared carbon and nitrogen fractionation in single amino acids from controlled growth microorganisms (Macko *et al.* 1987). The study showed that all the amino acids of the microorganisms were depleted in ^{15}N relative to glutamic acid, which was also similar in its isotopic composition among the different microorganisms. The authors explained this depletion due to the dependence of the other amino acids on glutamic acid, from which they obtain nitrogen through enzymatic dependent reactions that prefer lighter isotopes (Macko *et al.* 1987). They also observed a ^{15}N and ^{13}C enrichment of aspartic acid compared to glutamic acid in blue-green algae, thus suggesting a different metabolic pathway for this amino acid in these organisms (Macko *et al.* 1987). The authors further suggested more complex pathways for carbon isotopic fractionation, because each amino acid contains more than one carbon coming from different sources, supported by a general trend: acidic amino acids (aspartic acid and glutamic acid) were enriched in ^{13}C, while neutral (glycine, alanine, isoleucine, valine, leucine, phenylalanine, serine, threonine, tyrosine) and basic (arginine, lysine and histidine) amino acids were depleted in ^{13}C (Macko *et al.* 1987). The enrichment of ^{13}C in acidic amino acid was suggested to be related to the direct addition of the carbon of the carboxyl group directly from the growth substrate. Again, further depletions of ^{13}C in leucine, isoleucine, lysine and tyrosine were explained as depending on further enzymatic dependent reactions.

The following year, Tuross and colleagues, partly inspired by Macko and colleagues' study, published the results obtained from the analysis of bulk collagen and amino acids from modern and fossil specimens, including humans, in order to investigate collagen diagenesis and to explore dietary intakes through carbon and nitrogen fractionation

at the amino acid level (Tuross *et al.* 1988). This study highlighted that the isotopic signatures in single amino acids of fossil bones mirror the ones from modern material, suggesting absence of diagenetic processes at the amino acid resolution (Tuross *et al.* 1988). The authors also underlined the wide differences in isotope values of glycine, serine and threonine from the other amino acids and the collagen bulk values and, since glycine is the most abundant amino acid in collagen, they also warn that its degradation could greatly perturb the bulk collagen values (Tuross *et al.* 1988).

In 1991, Hare and colleagues, aware of the dangers of isotopic studies in evaluating past diets of fossil organisms, depending on the mixture of organic compounds in bones, diagenetic processes, different synthetic pathways of amino acids and additional fractionation at the tissue level, proposed the first feeding experiment applied in archaeology. The aim of this study was to understand carbon and nitrogen isotopic fractionation mechanisms in modern and controlled-fed pigs in order to understand carbon and nitrogen isotopic values from fossil bones. The authors observed that glutamic acid is always greatly enriched in δ^{15}N compared to the bulk value, since the molecule loses one nitrogen into the urea cycle (Hare *et al.* 1991). In general, δ^{15}N of amino acids in the consumer's collagen are always enriched compared to its diet, with the only exception of threonine, an essential amino acid, that is always depleted in ^{15}N, probably in relation to its degradation pathways (Hare *et al.* 1991). The study also suggests caution in estimating the bulk value through mass balance calculation of fossil samples as the amino acid composition of collagen could be modified by diagenetic processes.

Fogel *et al.* (1997) further deepened the subject, observing that carbon signatures in four non-essential amino acids (aspartic acid, glutamic acid, proline and hydroxiproline) are *uniformly labelled* in vertebrates with carnivore or herbivore diets, while they vary greatly in plants. Most importantly, they introduced the potential of discriminating herbivores, omnivores and carnivores using amino acid isotopic values rather than the bulk ones (Fogel *et al.* 1997).

Considering the carbon backbone of essential amino acids coming uniquely from protein in diet, Fogel and Tuross (2003) evaluated δ^{13}C values of individual amino acids of modern C_3 and C_4 plants and herbivores and humans from prehistoric North American sites. Interestingly, in all the plant samples, the authors evidenced a high consistency in leucine, isoleucine and phenylalanine values with their photosynthetic groups (Fogel and Tuross 2003). Moreover, the authors highlighted a linear relationship between δ^{13}C of plants and herbivores amino acids, because all of their *de novo* carbon and essential amino acids come from their unique dietary source, which is plants (Fogel

and Tuross 2003). As expected, the same relation was not present between humans and plants, confirming that the $\delta^{13}C$ values of humans and other animals depend on a wide range of dietary sources (and macromolecules)(Fogel and Tuross 2003). Indeed, Fogel and Tuross (2003) suggested that the nitrogen isotopic analysis of amino acids is an helpful tool in the investigation of marine dietary intakes, whilst carbon is likely unhelpful.

At that time, the Organic Geochemistry Unit of the University of Bristol was exploring the carbon isotopic composition of amino acids in rats and pigs from two feeding experiments whose bulk isotopic signatures had already been examined (Ambrose and Norr 1993; Ambrose 2000; Young 2003). The goal of these follow-up studies was to outline the metabolic pathways of the amino acids in bone collagen and other tissues and use the acquired knowledge for the interpretation of archaeological material (Jones 2002; Howland 2003; Howland *et al.* 2003; Jim *et al.* 2004, 2006). These studies highlighted the non-negligible role of lipids and carbohydrates on the carbon isotopic composition of non-essential amino acids. In particular, they evidenced a correlation between $\delta^{13}C$ of the energy components of diet, carbohydrates in particular, and $\delta^{13}C$ of alanine, linked to the metabolic pathways of this amino acid (Figure 3.10, see section 3.12). Furthermore, they supported previous hypotheses based on bulk values, for example that in high protein consumers the direct dietary protein intake of non-essential amino acids is preferred to the *de novo* synthesis route.

Alongside, the same research group proposed a new dietary indicator to determine marine consumption based on carbon isotope values of bone collagen amino acids (Corr *et al.* 2005). The new approach was applied to South African populations where it is difficult to distinguish between C_4 plant consumers or marine consumers because of the arid climate that causes high nitrogen isotope values of the C_4 plants. The authors observed differences in $\delta^{13}C$ values of individual amino acids of three reference human individuals defined as a predominantly C_3 consumer, C_4 consumer and high marine protein (HMP) consumer (Corr *et al.* 2005). The amino acid $\delta^{13}C$ values of the C_3 consumer were as expected the most depleted among the three individuals. On the contrary, the C_4 consumer was enriched in ^{13}C in all the amino acids and, interestingly, the C_3 consumer and HMP consumer had similar $\delta^{13}C$ values in all the amino acids with the only exception of glycine, which was highly enriched in ^{13}C in the HMP consumer. The higher glycine $\delta^{13}C$ value in this individual explained its higher bulk $\delta^{13}C$ values, as glycine contributes to around 20 % of carbon in bone collagen. To rationalize this pattern, the authors related glycine $\delta^{13}C$ values to those

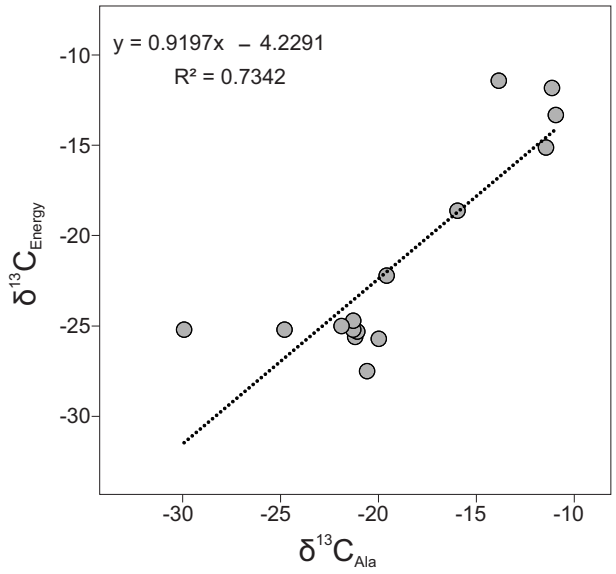

Figure 3.10 Correlation between δ^{13}C values of alanine in bone collagen and δ^{13}C values of the energy components of diet from three different feeding experiments. Data from Howland *et al.* (2003); Jim *et al.* (2006); Webb *et al.* (2017).

of phenylalanine, as the latter reflects the isotopic composition at the bottom of the food web and it is not expected to fractionate further. The $\delta^{13}C_{Gly-Phe}$ index showed, distinctive differences among HMP consumers ($+12.0 \pm 1.9$), C_3 ($+5.1 \pm 1.8$) and C_4 ($+4.0 \pm 1.6$) consumers (Corr *et al.* 2005). The authors concluded that glycine is greatly dependent on dietary intake rather than on *de novo* synthesis and that this needs further studies (Corr *et al.* 2005). Indeed, an earlier feeding experiment on rats (Jones 2002) already outlined an increase of non-essential amino acids inclusion from diet when protein in diet is high (*i.e.*, 70 %). However, the authors also proposed that it is possible that glycine is particularly reactive to marine foodstuff as this category has a relatively higher glycine composition compared to terrestrial sources (Corr *et al.* 2005).

Later on, Styring and colleagues (2010) further explored the diet of the individuals presented in Corr *et al.* (2005), this time looking at the nitrogen isotope values of amino acids. The authors evidenced a ^{15}N-enrichment in all the amino acids of HMP consumers compared to the others (Styring *et al.* 2010). In particular, glutamic acid and its derived amino acids, alanine, proline and hydroxyproline, showed similar δ^{15}N values, also mirroring that of the bulk. Threonine represented the only exception, being highly depleted compared to that from terrestrial consumers. The threonine's singular pattern, already evidenced in the pig feeding experiment by Hare *et al.* (1991), was highly pronounced in the marine animal group, and this was explained by Styring

and colleagues as being related to the higher number of trophic levels in the marine food web, which would cause each time an additional isotopic fractionation (Styring *et al.* 2010). To determine marine consumption, the authors applied the $\delta^{15}N_{Glu-Phe}$ index, first proposed by McClelland and Montoya (McClelland and Montoya 2002; Styring *et al.* 2010). The use of this index relies on the assumption that glutamic acid is a trophic indicator, since it is enriched in ^{15}N at each step of the food chain; on the contrary, phenylalanine, an essential amino acid, remains mostly unaltered through the food web (McClelland and Montoya 2002). The authors here evidenced significant correlation between bulk δ^{15}N values and $\Delta^{15}N_{Glu-Phe}$ in both animals and humans ($P = 0.01$ and $P = 0.02$, respectively) but also between $\Delta^{15}N_{Glu-Phe}$ and $\Delta^{13}C_{Gly-Phe}$ ($P = 0.000$)(Styring *et al.* 2010).

At that time, the $\Delta^{15}N_{Glu-Phe}$ index was emerging as a powerful tool to determine the trophic level of an organism. This application was proposed in a series of studies published by a Japanese team (Chikaraishi *et al.* 2007, 2009; Naito *et al.* 2010b). The team, involving mainly the Japan Agency for Marine-Earth Science and Technology of Yokosuka and the Department of Integrated Biosciences and the Department of Earth and Planetary Sciences, both of the University of Tokyo, were analysing variations of the nitrogen isotope compositions of some amino acids of organisms from natural marine environments. They presented the application of a simple equation to determine the trophic level (TL) of an organism (3.6):

$$TL_{x/y} = \left(\delta^{15}N_x - \delta^{15}N_y + \beta_{x/y}\right) / \left(\Delta_x - \Delta_y\right) + 1 \tag{3.6}$$

where $\beta_{x/y}$ is the difference of δ^{15}N in the amino acids x and y in the primary producers and Δ_x and Δ_y are the fractionation at the additional trophic level for the amino acids x and y, respectively. Amino acids x and y should be two amino acids showing different metabolic behaviours, such as glutamic acid and phenylalanine, as suggested by McClelland and Montoya (2002) (Chikaraishi *et al.* 2009). In a marine ecosystem, using the δ^{15}N values of glutamic acid and phenylalanine, the trophic level of an organism can be estimated with the following equation:

$$TL_{glu/phe} = \left(\Delta^{15}N_{glu-phe} - 3.4\right) / 7.6 + 1 \tag{3.7}$$

where -3.4 is the difference in the isotopic composition of glutamic acid and phenylalanine at the bottom of the marine ecosystems ($\beta_{x/y}$, in Eq. 3.6) and $+7.6$ is the enrichment at each step of the food web in the same ecosystem ($\Delta_x - \Delta_y$ in Eq. 3.6), as derived by Chikaraishi *et al.* (2009) using macroalgae representing the bottom of

the food web (producer, TL from 0.8 to 1.2), gastropods being the primary consumer (herbivore, TL from 1.7 to 2.0), crabs the secondary consumer (omnivore, TL = from 2.3 to 2.6) and fish the tertiary consumer (carnivore, TL = from 2.9 to 3.3). The authors also evidenced how these trophic levels better estimated the actual trophic level compared to the ones determined using bulk values, with only a small error associated ($1\sigma = 0.12$)(Chikaraishi *et al.* 2009). The same approach was later tested in terrestrial ecosystems (Chikaraishi *et al.* 2010). Here, the authors investigated the isotopic composition of amino acids in C_3 and C_4 plants and caterpillars being the primary consumers (Chikaraishi *et al.* 2010). As expected, Eq. 3.7 could not work with the two terrestrial systems, since isotopic fractionation happens with different enzymatic mechanisms in the different classes (Chikaraishi *et al.* 2010). Basing their assumptions on the results obtained, the authors proposed the use of $+8.4$ and -0.4 as the $\beta_{x/y}$ terms in the C_3 and C_4 plants based food webs, respectively (Chikaraishi *et al.* 2010). The error associated with the TLs derived with these equations from the known actual levels was 0.20 (1σ)(Chikaraishi *et al.* 2010). The application of the method on terrestrial ecosystems was further investigated by Chikaraishi *et al.* (2011) on different species of bees, wasps and hornets, confirming the reliability of the TLs attribution. Later on, Naito *et al.* (2010a) and Naito *et al.* (2010b) first tested the method on archaeological human individuals from two different populations in order to assess marine food consumption. In Naito *et al.* (2010b), they also proposed a quantitative approach based on CSIA-AAs, as an alternative solution to mixing models strategies.

Following on this, some scholars explored the use of other amino acids to discriminate food sources from the consumer's tissues with an application on archaeological populations.

By using LC-IRMS, Choy *et al.* (2010) examined the $\delta^{13}C_{AA}$ values from humans and animal remains from two prehistoric sites from South Korea. They observed that the $\delta^{13}C$ values of the essential amino acids of the humans from the site of Tongsamdong were closer to those of the marine animals, while the essential amino acids of the humans from the second site (Nukdo), were closer to those of the terrestrial animals. Since essential amino acids should not go through significant fractionation from diet to consumer, the authors suggested that the result was indicative of different access to protein sources at the two sites (Choy *et al.* 2010). The authors also showed that the $\Delta^{13}C_{Gly-Phe}$ values proposed by (Corr *et al.* 2005) to identify HMP, C_3 and C_4 consumers, did not directly apply to the South Korean assemblage and therefore they concluded that it is important to rely on a local dietary baseline to interpret

the $\delta^{13}C_{AA}$ values of human individuals (Choy *et al.* 2010). Since the $\delta^{13}C$ values of threonine had a large difference (*ca.* 8 ‰) between marine and terrestrial animal, the authors proposed it as a valuable tool to detect the consumption of marine sources, even more helpful when used associated with the $\Delta^{13}C_{Ser-Phe}$ offset, which allowed the authors in making a clear distinction between the terrestrial and marine groups (Choy *et al.* 2010).

Later, Webb *et al.* (2016a) showed that the $\Delta^{13}C_{Gly-Phe}$ proxy, previously proposed by Corr *et al.* (2005), was also useful in detecting freshwater consumption. A few years before, Honch and colleagues collected CSIA-AAs values from populations defined as "pure terrestrial C_3 consumers" (C_3), "pure terrestrial C_4 consumers" (C_4), "high freshwater protein consumers" (HFP) and "high marine protein consumers" (HMP) and observed that while for terrestrial C_3 and C_4 consumers $\delta^{13}C_{Phe}$ and $\delta^{13}C_{Val}$ are similar, $\delta^{13}C_{Val}$ is enriched compared to $\delta^{13}C_{Phe}$ in HFP and HMP (2012). By using this method, Colonese *et al.* (2014) also confirmed high marine proteins consumption in two South American pre-Columbian populations. More recently, the $\Delta^{13}C_{Val-Phe}$ index has been used to observe the trophic level of the Les Cottés Neanderthal, which came out being the same of the ones of the other carnivores found at the same site Jaouen *et al.* (2019). Jaouen *et al.* (2019) also found very ^{15}N-depleted $\delta^{15}N$ values of threonine in the Neanderthals from Les Cottés and Grotte du Renne, in line with the other carnivores. Interestingly, a previous study by Fuller and Petzke (2017) suggests that $\delta^{15}N_{Thr}$ values might be more than a simple trophic level indicator. Indeed, their feeding experiment on rats showed a significant dependency of $\delta^{15}N_{Thr}$ to the amount of protein in diet, proposing it as a new biomarker to evaluate protein consumption (Fuller and Petzke 2017).

Worthy of attention is an experimental study on pigs carried out by the University of Bristol, UK, and published by Webb *et al.* (2016b) and Webb *et al.* (2017). The authors here explored nitrogen Webb *et al.* (2016b) and carbon Webb *et al.* (2017) isotopic signatures of bulk Webb *et al.* (2016b) but also single amino acids Webb *et al.* (2017) from several tissues (*i.e.*, blood, urine, faeces, plasma, muscle, liver, collagen, hair) of two generations of pigs (in total, 10 sows from the first generation and 19 piglets, aged 4 weeks, and 39 pigs, sacrificed in adolescence, from the second generation) fed with different proportions of terrestrial and marine food keeping a fixed amount of protein (20%), to overcome the limitations of previous controlled feeding experiments. Webb *et al.* (2017) presented preliminary amino acids carbon data from which the authors derived important suggestions about protein routing. Here, they showed that $\Delta^{13}C_{collagen-diet}$ offsets of non-essential amino acids decrease when marine protein in

diet increases, contradicting what was earlier believed, which is that the direct routing of non-essential amino acids from diet is preferential under a higher consumption of protein regardless of the type of protein consumed. This would confirm what Corr *et al.* (2005) suspected for glycine: since glycine is higher in concentration in marine fish, with high marine protein diet, glycine is preferentially directly routed from diet and metabolic reactions do not start for *de novo* synthesis, in particular when the contribution is $\geq$50 % (Webb *et al.* 2017).

Nowadays, CSIA-AA is still not applied as a routine analysis in dietary investigations with application in archaeology. However, the better understanding of the metabolic mechanisms that lead to the synthesis of the amino acids (that will be outlined in the following section 3.2.2), also thanks to the the number of feeding experiments that have been carried out, has gradually increased its application to a variety of archaeological contexts (*e.g.*, Cooper *et al.* 2016; Jarman *et al.* 2017; Mora *et al.* 2018, 2021; Ma *et al.* 2021; Choy *et al.* 2021). Due to the limitations of bulk SIA, which have been explored in the previous sections, it is likely that the application of CSIA-AA on archaeological populations will keep increasing in the near future.

3.2.2 The biochemistry of amino acids

Amino acids are monomeric compounds constituting proteins. More than five hundred amino acids have been identified so far, but only 21 of these constitute proteins on Earth (Wagner and Musso 1983). Each amino acid is composed of a carbon atom (called α-carbon) which is bonded to a carboxylic group, an amino group and a side chain (called the R group)(Figure 3.11). The amino acids differ from each other by their R group. The presence of four different groups linked to the α-carbon atom makes the α-carbon a stereocenter and, for this reason, amino acids are considered chiral molecules, with the exception of glycine, in which the R group is composed of one hydrogen atom, which makes it a symmetric structure. Like all the other chiral compounds, amino acids can exist in both their D and L configuration, although all the amino acids in living organisms (with a few exceptions) are in their L configuration, with their carboxylic group on the top and the amino group on the left (as shown in Figure 3.11)(Bada 1985). Amino acids are connected through the *peptide bond*, a covalent bond between the amino group of an amino acid and the carboxylic group of another, to form polypeptide chains of hundreds of amino acids which constitute the primary structure of proteins. The type and order of amino acids in the primary structure are genetically encoded and determine protein function. The α-carbon and

the carboxylic and the amino groups form the backbone of the polypeptides, while the side chains interact in different ways determining the three-dimensional structure of proteins.

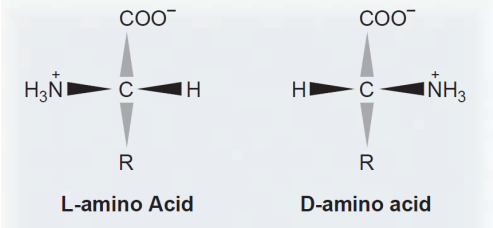

Figure 3.11 L and D structure of a general amino acid. Black arrows represent bonds coming out of the paper and shaded arrows those coming in. Modified after Lieberman *et al.* (2013).

In order to perform a successful protein synthesis, all the amino acids need to be in the cell when the synthesis begins; this process starts with the food ingestion. When proteins arrive in the stomach, the acidic pH condition of the gastric juice allows the denaturation of proteins (*i.e.*, the loss of quaternary, tertiary and secondary structures) and the optimal condition for pepsin to operate. Pepsin is the first enzyme to play a fundamental role in protein digestion, hydrolysing the peptide bonds of aromatic and hydrophobic amino acids in the acidic pH condition of the gastric juice. When what is left of the proteins arrives into the small intestine, pepsin is inhibited due to the alkaline environment and other enzymes (trypsin, chymotrypsin and carboxypeptidase) break down the longer polypeptide chains into smaller peptides. The final small peptides are hydrolised by the proteolytic digestive enzymes of the brush border of lumen and the single amino acids, together with a small portion of dipeptides and tripeptides (*i.e.*, peptides formed by two or three amino acids, respectively) pass through the enterocytes to enter the blood vessels. From here, amino acids are transported around the body and the protein synthesis will start with different modalities depending on the tissue in which it will take place (Lieberman *et al.* 2013).

The amino acids can either be directly routed from proteins in diet or synthesised *de novo* in the body. With this in mind, for over a century, amino acids have been classified in three groups: *nutritionally essential* amino acids, *nutritionally non-essential* amino acids, *conditionally nutritionally essential* amino acids (Lieberman *et al.* 2013). Essential amino acids are those amino acids which cannot be synthesised in the body and therefore they need to be introduced through diet. On the contrary, non-essential amino acids are those amino acids that the body is able to synthesise *de novo*; therefore, if they are not sufficiently available in the diet, this do not affect the synthesis/degradation

balance of proteins. The conditionally essential amino acids are those that can be both synthesised *de novo* and also come from the diet; the body usually forms these amino acids by *de novo* synthesis but there are several situation in which it might require a greater intake coming from the diet, as in the case of arginine and histidine in children and pregnant women. Tyrosine and cysteine are also considered conditionally essential amino acids, as they are synthesised from phenylalanine and methionine, respectively, which are essential amino acids (Lieberman *et al.* 2013).

Some scholars are nowadays trying to dismiss the essential/non-essential classification after reviewing several studies that prove that the *de novo* synthesis of non-essential amino acids is not enough in many physiologic functions and that a nutritional income for these is fundamental to the optimus growth and health of animals, humans included (*e.g.*, Hou and Wu 2017). Furthermore, this classification can only refer to the carbon backbone of the amino acids, as transamination reactions regulate the exchange of nitrogen atoms also in the majority of the essential amino acids (Braun *et al.* 2014).

In this thesis the standard nomenclature (*i.e.*, essential, non-essential and conditionally essential) will be used to refer to carbon stable isotopes, and the terms *trophic* and *source* will be used instead when referring to nitrogen stable isotopes, to discriminate the degree of nitrogen interchangeability of amino acids (O'Connell 2017). In the following two sections, amino acids metabolic pathways will be traced distinguishing between reactions that involve carbon and those that involve nitrogen. To do so, the concept of "metabolic pool" suggested for nitrogen by O'Connell (2017) will be adopted and extended to carbon.

The carbon metabolic pool

While proteins in diet are the only source of essential amino acids, carbohydrates, lipids and proteins, can all provide the carbon atoms for the synthesis of non-essential amino acids. Figure 3.12 outlines the main carbon routes in the synthesis and degradation of amino acids in the human body. In order to describe the mechanisms of synthesis of the amino acids, the exchange of nitrogen will also be mentioned, although these reactions do not contribute to the carbon metabolic pool.

Dietary carbohydrates, lipids and proteins are all involved into the tricarboxylic acid (TCA) cycle, a series of chemical reactions that generate two thirds of the total adenosine triphosphate (ATP) from fuel oxidation. α-ketoglutarate and oxaloacetate are two intermediates of the TCA cycle that are used for the synthesis of glutamic acid and aspartic acid, respectively. Glutamic acid, the ionic form of glutamic acid, derives from α-ketoglutarate through two, both possible, reversible reactions, one

involving transaminases and one glutamic acid dehydrogenase. Glutamine, proline, ornithine and arginine are all synthesised from glutamic acid. Glutamine requires an ammonium cation (NH_4^+) to be formed from glutamic acid, which is provided by glutamine synthetase. The synthetic pathway of proline consists of three passages; first, the carboxylic group of glutamic acid is reduced to an aldehyde, producing glutamic acid 5-semialdehyde. Then, glutamic acid 5-semialdehyde sets in a cyclic conformation through the joint of the α-amino group and the aldehyde. Ultimately, the compound is reduced to form proline. The process is reversible. Arginine can also be synthesised from the glutamic acid semialdehyde. This is then converted through transamination to ornithine from which arginine will be produced. The arginase enzyme acts to degrade arginine back to urea and ornithine. aspartate, the ionic form of aspartic acid is synthesised from oxaloacetate. However, carbons of aspartic acid can also be used to form fumarate. Asparagine is formed from aspartic acid with the contribution of nitrogen from glutamine. Asparagine frees (NH_4^+) to restore aspartic acid with the action of asparaginase (Lieberman *et al.* 2013).

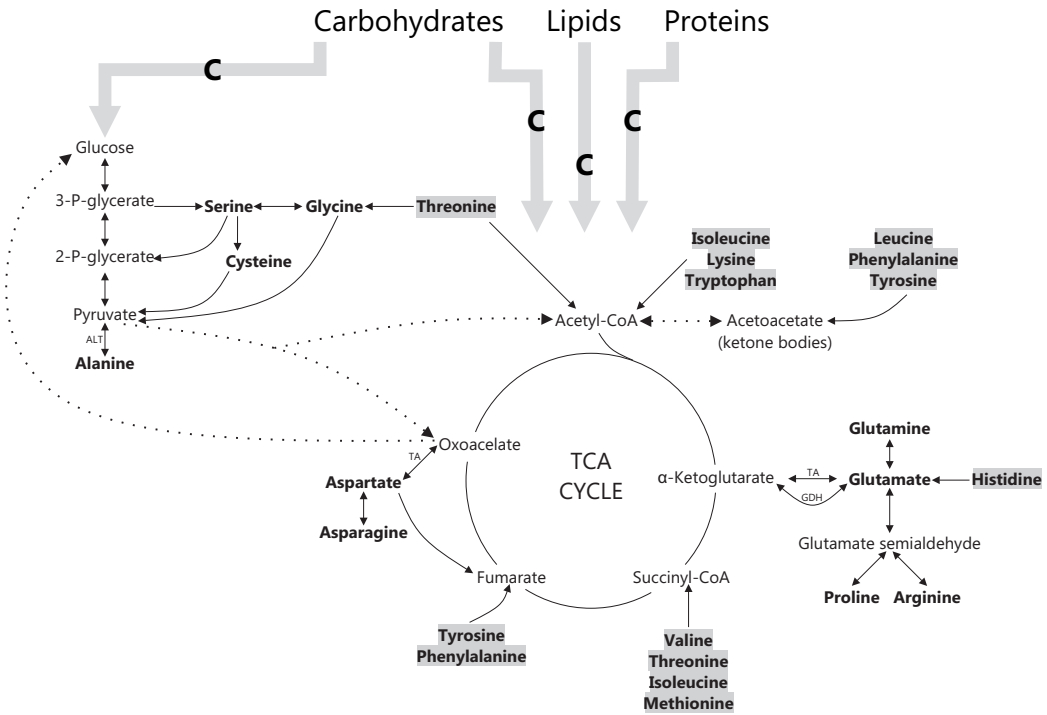

Figure 3.12 Overview of the biosynthesis and degradation of amino acids referred as the "carbon metabolic pool" in the text. Amino acids are in bold. Essential amino acids are highlighted with a grey background. Dotted lines identify reactions that do not directly involve amino acids.

Outside the TCA cycle, carbohydrates alone provide the carbon to four non-essential amino acids through glycolysis. These are alanine, glycine, serine and cysteine.

Glycolysis is the metabolic pathway that leads to the formation of pyruvate from glucose. Pyruvate can eventually enter the TCA cycle by forming acetyl-CoA or oxaloacetate. Alanine can be synthesised from pyruvate by a reversible transamination reaction catalysed by alanine aminotransaminase. An intermediate of glycolysis, the 3-phosphoglycerate is used for the synthesis of serine. 3-phosphoglycerate is oxidised into 3-phosphohydroxypyruvate and then transaminated. The transaminated product, called phosphoserine, is then hydrolised to serine. Serine is degraded by transamination to hydroxypyruvate and then by reduction and phosphorylation to another intermediate of glycolysis, 2-phosphoglycerate. Serine can also be degraded directly into pyruvate by β-elimination of the hydroxyl group. Glycine can be synthesized from serine thanks to the action of the tetrahydrofolate (FH_4) coenzyme or from degradation of threonine operated by the pyridoxal phosphate (PLP) cofactor. The first reaction is reversible, which means that also serine can be formed from glycine. Degradation of glycine can also occur with the oxidation of glycine into ammonia, CO_2 and a carbon atom that is donated to FH_4 or by forming glyoxylate by the enzyme D-amino acid oxidase (Lieberman *et al.* 2013).

The essential amino acids also contribute to the carbon metabolic pool through their degradation. The carbon skeleton of all the non-essential amino acids degrades into intermediates of gluconeogenesis. Depending on the amino acid degradation outcome, amino acids can be categorised as gluconeogenic, when they determine the formation of glucose, or ketogenic, when they degrade into acetyl-CoA which then forms ketone bodies. Among the essential amino acids, histidine donates five of its carbon atoms to form glutamic acid, therefore contributing to gluconeogenesis. Phenylalanine is used for the synthesis of tyrosine by hydroxylation and tyrosine can be converted into acetoacetate and fumarate. Since fumarate is then converted into malate, tyrosine contributes with carbons to be used for gluconeogenesis. However, the other product of the degradation of tyrosine, acetoacetate, is a ketone body, therefore, phenylalanine and tyrosine are categorised as both gluconeogenic and ketogenic. Valine, isoleucine, methionine and threonine degrade to form propionyl-CoA and then succinyl-CoA which is ultimately involved into glucose synthesis. However, isoleucine and threonine can also form acetyl-CoA. Tryptophan is also both gluconeogenic and ketogenic, since its degradation leads to the formation of both alanine and acetyl-CoA. Leucine and lysine, through degradation, can only produce acetyl-CoA and acetoacetate and are therefore categorized as ketogenic (Lieberman *et al.* 2013).

The nitrogen metabolic pool

The ammonium ion (NH_4^+) liberated from amino acids during catabolism is a toxic compound not tolerated by the body. Therefore, NH_4^+ requires conversion to an organic compound, which is carbamide. Carbamide is an amide composed of two amino groups joined by a carbonyl group, with chemical formula $CO(NH_2)_2$ and better known as *urea*. In the amino acid catabolism, first the amino group has to be removed from the amino acid through transamination. All the amino acids are theoretically able to undergo transamination with the exception of lysine and threonine. With the transamination, an α-ketoglutarate accepts the amino group of an amino acid to form glutamic acid. glutamic acid is then deamidated, catalysed by glutamic acid dehydrogenase, to form again an α-ketoglutarate and NH_4^+. The process is reversible (Lieberman *et al.* 2013).

The trophic *vs* source classification of amino acids was adopted to differentiate amino acids that show different nitrogen fractionation behaviour. Recently, O'Connell (2017) suggested that the dichotomy can be realistically explained with the degree of interchangeability of the amino-nitrogen with the nitrogen metabolic pool. Figure 3.13 summarises the main routes of nitrogen exchange between amino acids and free NH_4^+.

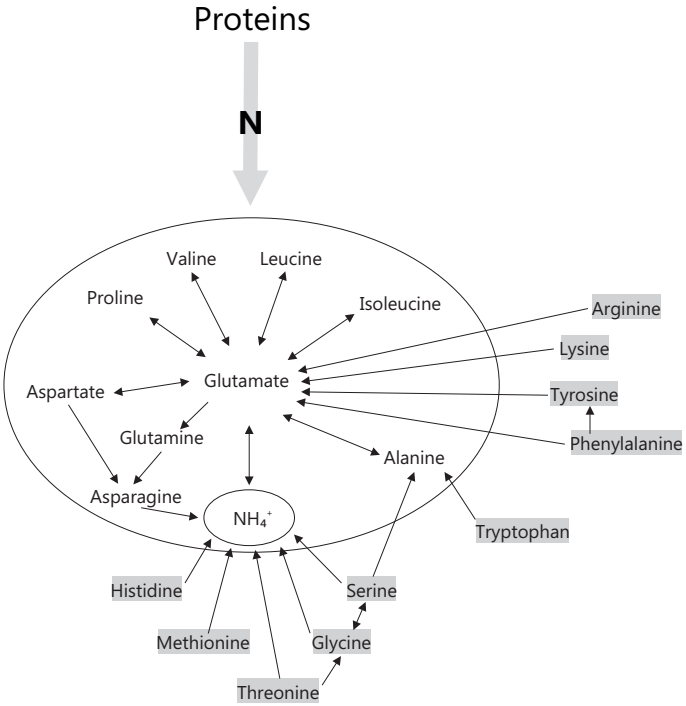

Figure 3.13 Overview of the main pathways of nitrogen exchange of amino acids (modified after O'Connell (2017) and Braun *et al.* (2014)).

Alanine, aspartic acid, leucine, isoleucine, valine and glutamine are able to exchange their nitrogen with glutamic acid through transamination with an α-ketoglutarate. Proline also exchanges its nitrogen with glutamic acid, although not by undergoing transamination as seen in the previous section. Therefore, these amino acids, together with the temporarily free NH_4^+, constitute the "nitrogen metabolic pool" (Figure 3.13)(O'Connell 2017). These amino acids are categorised as trophic. All the other amino acids have not been observed to undergo transamination *in vivo* and therefore they are catabolised according to specific pathways. As described in the previous section, glycine and serine are closely linked, which makes them interchange nitrogen. Threonine can be transformed into serine. Lysine catabolism instead determines the incorporation of both its nitrogen atoms into glutamic acid. Phenylalanine mainly degrades forming tyrosine, as reported in the previous section. The nitrogen in tyrosine will eventually undergo transamination forming glutamic acid. Asparagine is deamidated by asparaginase, yielding aspartic acid and NH_4^+. Tryptophan is converted into alanine through oxidation (Lieberman *et al.* 2013).

3.2.3 Amino acid composition of bone collagen

Collagen is the most abundant structural protein in animals. The name collagen refers to a family of twenty-eight proteins, all having the same helix structure but different functions, domain architecture and supramolecular organisation (Bella 2016; Veit *et al.* 2006). Collagen proteins are an association of three polypeptide chains, called a trimer. Each trimer is identified with roman numerals, while each polypeptide chain with the greek letter α and arabic numeral. For example, type I collagen, which represents the most abundant bone protein, consists of two $\alpha_1(I)$ chains and one $\alpha_2(I)$ (Bella 2016). Collagen proteins owe their stable and packed structure to the presence of the smallest amino acid, glycine (Gly), every three positions in the amino acid sequence which allows the interstrand bond $N - H_{(Gly)} \cdots O = C_{(X_{aa})}$(Cowan *et al.* 1955). The repetitive $(\text{Gly-X-Y})_n$ sequence allows the close-packing triple helix conformation.

Another element increasing the stability of the triple helix is the hydroxyproline (Hyp) in the $\text{Y}_{(aa)}$ position. Original proline (Pro) in $\text{Y}_{(aa)}$ position in protocollagen is converted to 4-hydroxyproline prior to triple-helix formation. The reaction is catalyzed by the enzyme 4-hydroxylase (P4H) which allows the hydroxylation of the γ-carbon of proline from 2-oxoglutarate and O_2, as shown in Figure 3.14 (Shoulders and Raines 2009).

Hydroxylated human type I collagen has been proved to have a higher thermal stability than the same but un-hydroxylated one (*e.g.*, Perret *et al.* 2001). Since the

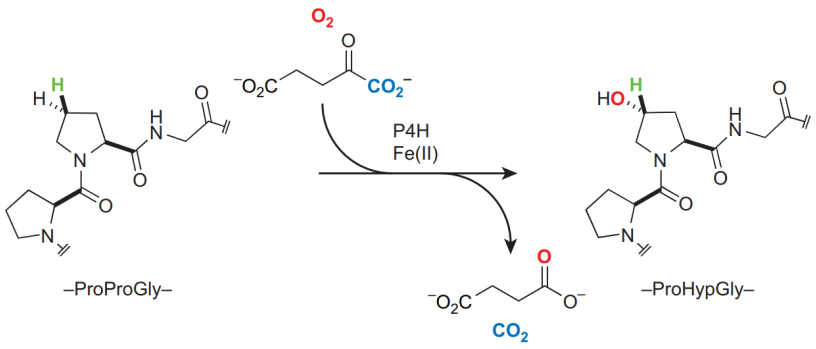

Figure 3.14 The nonhemo iron enzyme 4-hydroxylase (P4H) catalyses the hydroxilation reaction of Pro in $Y_{(aa)}$ position to form 4-hydroxyproline. Modified from Shoulders and Raines (2009)

thermal stability for non-hydroxylated human type I collagen is 27 °C, this can not be tolerated by the human body and the hydroxylated form is necessary (Bella 2016). Amino acid composition of type I collagen is reported in Table 3.4. Since glycine is placed every three residues, it represents 33 % of the total residues. The second most abundant residues are those composing the most recurring triplet, hydroxyproline and proline, that together compose 22 % of collagen type I. Notably, collagen type I does not contain tryptophan and cysteine (Table 3.4).

Hydrolysis and derivatisation procedures determine the partial or total degradation of some amino acids, something that needs to be considered before carrying out any CSIA-AA analysis.

	Residues (%)	C atoms (%)	N atoms (%)
Ala	11	9	9
Arg	5	8	17
Asx	4	5	4
Cys	-	-	-
Glx	7	9	6
Gly	33	17	28
His	1	1	1
Ile	1	2	1
Leu	2	4	2
Lys	3	5	6
Met	1	1	1
Phe	1	3	1
Pro/Hyp	22	28	18
Ser	3	3	3
Thr	2	2	1
Trp	-	-	-
Tyr	0	1	0
Val	3	3	2

Table 3.4 Amino acid occurrence in collagen type I. Alpha-1 (CO1A1_HUMAN, P02452) and Alpha-2 (CO1A2_HUMAN, P08123) type I collagen sequences from the Swiss-Prot database (Boeckmann *et al.* 2003) using ProtParam (Gasteiger *et al.* 2005). Ala: alanine, Arg: arginine; Asx: aspartic acid/asparagine, Cys: cysteine, Glx: glutamic acid/glutamine, Gly: glycine, His: histidine, Ile: isoleucine, Leu: leucine, Lys: lysine, Met: methionine, Phe: phenylalanine, Pro: proline, Hyp: hydroxyproline, Ser: serine, Thr: threonine, Trp: tryptophan, Tyr: tyrosine, Val: valine.

3.3 Conclusion

Carbon and nitrogen stable isotope analysis of human bone collagen has revolutionised, among the others, the way to look into ancient dietary practices by providing a direct and both qualitative and quantitative approach (section 3.1). However, in the last few decades, numerous studies and feeding experiments have warned about the large degree of uncertainty about carbon and nitrogen isotope fractionation from diet to consumer, which can easily lead to the misinterpretation of the data (sections 3.1.1 and 3.1.2). As a consequence, studies carried out on human populations from the Mediterranean basin living under the Roman Empire, although precious, have provided a fragmentary picture and opened the way to new questions (section 3.1.3). Lately, several scholars have shown the potential of compound specific carbon and nitrogen stable isotope analysis of amino acids (CSIA-AA) from human bone collagen which allows gaining a much higher resolution compared to the standard bulk approach (SIA) (section 3.2.1). However, to this date, only a few studies have explored the potential of a quantitative approach based on CSIA-AA (*e.g.*, Jarman *et al.* 2017). By following the

mechanisms of synthesis and catabolism by distinguishing between those that involve carbon (here referred to as "carbon metabolic pool") and nitrogen (nitrogen metabolic pool, after O'Connell (2017))(section 3.2.2), it is now possible to make use of a new level of knowledge in the quantitative interpretation of δ^{13}C and δ^{15}N values of amino acids. This will be the focus of chapter 6.

Chapter 4

Experimental and analytical protocols for Compound Specific Stable Isotope Analysis of Amino Acids (CSIA-AA)

The aim of this chapter is to present the experimental design and the materials analysed which are the focus of this thesis (section 4.1.1), as well as to inform about the analytical procedure applied (section 4.2). The analysis of carbon and nitrogen isotopes of amino acids from the human remains of AD 79 Herculaneum were analysed at BioArCh in a period of method development (section 4.2.2). During this period, a new derivatisation technique was also put in place (section 4.1.5) and the instrumentation went through multiple adjustments to maximise the performance. For this reason, this chapter represents not only a description of the protocols deployed but also a discussion around the development of the method and the quality of the data obtained.

4.1 Experimental

This section describes the design of the experiment, the laboratory techniques deployed and the set-up of the instruments. The BioArCh protocol for hydrolysis and derivatisation of amino acids is reported in Appendix B.

4.1.1 Experimental design and sampling strategy

Extracted collagen was already available for the majority of the AD 79 Herculaneum human individuals as a consequence of previous bulk δ^{13}C and δ^{15}N analysis (Craig *et al.* 2013; Martyn *et al.* 2018) and evaluation of bone diagenesis (Martyn *et al.* 2020). The analyses, carried out by Prof. Oliver Craig and Rachelle Martyn, were part of a collaboration with Dr. Luca Bondioli, former head of the Section of Bioarchaeology at the *Museo Nazionale Preistorico Etnografico Luigi Pigorini*, Rome Italy and the former *Soprintendenza Speciale per i beni archeologici di Napoli e Pompei* (today named *Parco Archeologico di Ercolano*), Naples, Italy. For the purposes of this thesis, priority was given to the nine human individuals and one sheep previously subjected to radiocarbon dating, that allowed Craig *et al.* (2013) to quantify marine fish consumption at AD 79 Herculaneum. Where there was no collagen left from these individuals, collagen extraction was performed again from the bone fragments available according to the protocol presented in the following section (4.1.2). Other individuals were selected among those for which there was enough collagen left, with the aim to avoid performing new destructive sampling.

Terrestrial animal and marine fish remains and cereals and legumes from Pompeii and Herculaneum were collected with the aim to reconstruct a local and coeval dietary baseline for the human individuals. Besides a few ovicaprine and dog samples from the Herculaneum *fornici*, which had been already sampled as part of the previous investigations, the faunal remains were provided by Dr. Richard Jones, Dr. Andrew Jones and Dr. Gill Thompson as part of the *Anglo-American Project in Pompeii* (AAPP) and by Prof. Steven Ellis, head of the *Pompeii Archaeological Research Project: Porta Stabia* (PARP:PS). Permission to analyse the samples was granted by *Parco Archeologico di Pompei*. Charred cereals and legumes from AD 79 Herculaneum were sampled *in loco* with the permission of *Parco Archeologico di Ercolano*.

Preliminary analysis via RP-HPLC to assess protein degradation and amino acid composition of charred archaeological grains were performed on samples from two Roman contexts in York, UK, and from two prehistoric sites from Turkey, with the aim to represent different environmental and preservation conditions. In addition to this, modern cereals and legumes purchased in Italy were analysed for CSIA-AA and the data used to estimate amino acid carbon and nitrogen isotope values from archaeological material. Information on the animal and botanical samples and their contexts will be provided in chapter 5.

Faunal and botanical materials were photographically documented prior to laboratory analysis.

4.1.2 Collagen extraction

Collagen was extracted following the Longin (1971) protocol modified by Brown *et al.* (1988). Starting bone masses were usually between 300-500 mg, sometimes higher if the bone looked highly degraded and often lower in marine fish and small terrestrial animal elements. A modern bovine homogenised bone sample was included with every collagen extraction batch to assess the quality of the analysis.

The bones were cleaned mechanically with a scalpel from any visible contaminant such as soil. More resistant bone fragments, such as those belonging to domestic herbivores and omnivores, were mechanically cleaned from dirt and soil residues with a sandblaster. Weights were registered before proceeding with demineralisation.

Bone fragments were demineralised into sterile borosilicate test tubes at +4 °C with 8 mL of 0.6 M HCl aqueous solution, changing it every two days until the samples resulted flexible and translucent. More fragile elements such as marine fish were treated with a weaker acidic solution (0.1 M HCl). The demineralisation process took a couple of days up to three weeks, depending on the animal species, the bone sampled and its degradation. Once demineralised, samples were washed three times with deionised water. Further 8 mL of 0.001 M HCl solution were added to each sample and then held at +80 °C for 48 h to perform collagen gelatinisation. At the end of the process, the liquid was preliminary filtered using Ezee-filte™ separators (Elkay Laboratory Products Ltd., pore size: 60-90 μm) in order to remove insoluble residues, and subsequently using Amicon® Ultra-4 Millipore™ filter centrifuge tubes (Merk Millipore, MWCO: 30 kDa) in order to analyse only molecule fractions bigger than 30 kDa. Samples were then frozen at -20 °C for at least 48 h and freeze-dried for additional 48 h. Lyophylised collagen was then weighed out and collagen yield calculated in relation to the start mass of the sample.

4.1.3 Preparation of amino acid standard mixtures and internal standard

Standards mixtures for GC-C-IRMS analysis were prepared ahead and processed together with the collagen and grain samples. Nine amino acid international standards with known δ^{15}N were purchased from Indiana University (USA) and SHOKO Science (Japan) to be used in "nitrogen mode" runs. International standard norleucine (Nle) was only used in the run with the first batch of samples that followed a different derivatisation technique, as explained in paragraph 4.1.5. A new Nle standard was purchased from Sigma-Aldrich Company Ltd.(UK) and used in the following prepara-

tions. The "true" value of Sigma Nle was measured in-house by EA-IRMS. A known quantity of international standards and Sigma Nle were dissolved into 0.1 M HCl to get a concentration of 2000 ng/μL for each standard. 50 μL from each stock standard solution were poured into a new sterile test tube, blown down under a gentle stream of N_2 and stored at at -20 °C until required for derivatisation. Information about the standards are reported in Appendix C Table C.11.

As for "carbon mode" runs, sixteen amino acid standards supplied by Sigma-Aldrich were used, since for the correction of the δ^{13}C values, a standard is required for each of the amino acids that are of interest in the study, as explained in the following paragraph 4.3.2. Their "true" δ^{13}C and δ^{15}N values were determined in-house by EA-IRMS. 10 mg of each Sigma standard amino acid was added into a sterile scintillation vial and dissolved in 16 mL of 0.1 M HCl. From this stock solution, 40 μL were added into a new sterile test tube, blown down under a gentle stream of N_2 and stored at -20 °C until required for derivatisation.

The Sigma Nle used in both the nitrogen and carbon standard mixture was also used as internal standard as this amino acid is not present in both collagen and plant material. The stock solution containing Sigma Nle internal standard was prepared by adding 5 mg of Sigma Nle into a sterile scintillation vial and dissolving it in 1 mL of 0.1 M HCl. The internal standard volume required was then calculated depending on the starting collagen or plant material mass.

All the amino acid standard solutions were stored under N_2 by flushing N_2 into the vials.

4.1.4 Hydrolysis and defatting

When possible, 4 mg of collagen samples were introduced into sterile Reacti-Vials™ (Thermo Scientific™) with phenolic caps with previously prepared internal standard (Nle, 50 μL for 4 mg of collagen). Preliminary tests showed that 4 mg of collagen can produce sufficient aliquots of derivatives to be run in both nitrogen and carbon mode, also in case of required re-runs. However, when this was not possible, smaller amounts of collagen were used, up to a minimum of 1 mg, modifying the Nle concentration accordingly. 200 μL of 6 M HCl prepared with HPLC grade water were poured into each vial. The vials were then introduced into a pre-heated oven at 110 °C for 24 h with caps closed tightly. At the end of the treatment, the hydrolysates were filtered to remove any insoluble deposit through centrifugation (11000 x g, 1 min) using Nanosep™ devices (Pall Laboratory, pore size: 0.45 μm).

The liquids were transferred into new sterile Reacti-Vials™. In order to extract any lipidic compounds from the hydrolysates, a mixture of *n*-hexane/DCM (1 mL, 3:2 v/v) was poured into each vial and shaken vigorously for around 10 sec. Once the organic and acidic layers were clearly separated, the organic phase was discarded and the procedure repeated two times more by adding new *n*-hexane/DCM (1 mL, 3:2 v/v) into the Reacti-Vials™. The defatted hydrolysates were finally transferred into new sterile borosilicate test tubes and blown down gently under N_2 at room temperature, re-dissolved into 100 μL 0.1 M *HCI* and stored at -20 °C until required for the derivatisation step. Before derivatisation, the acidic solution was completely blown down under a gentle stream of N_2 at room temperature.

4.1.5 Derivatisation

Gas chromatography-combustion-isotope ratio mass spectrometry (GC-C-IRMS) has been extensively used in the last few decades for the measurement of stable isotopes of single amino acids. Compared to LC-IRMS, GC-C-IRMS allows the measurement of both δ^{13}C and δ^{15}N (Dunn *et al.* 2011). The main challenge in the use of GC-C-IRMS is represented by the derivatisation step. Indeed, the amino acids need to be converted into volatile compounds before being injected in the gas chromatograph. Derivatisations are time-consuming procedures and the obtained derivatives contain new carbon atoms added by the reagents that cause KIE. Consequently, the δ^{13}C values must be corrected, which adds a large degree of uncertainty to the isotopic values (see the following section, 4.3.2 for carbon correction and the error propagation). This makes LC-IRMS "the optimal method" (Dunn *et al.* 2011) for δ^{13}C values measurements. Nevertheless, several derivatisation techniques have been developed with the aim to simplify the laboratory procedure and reduce the number of carbon atoms added during the derivatisation (Corr *et al.* 2007a,b). Among different derivatisation techniques, the acetylation-esterification ones are the most deployed for GC-C-IRMS analysis (Yarnes and Herszage 2017). They consist of a two step reaction: first, the esterification of the carboxylic group is performed using an acidified alcohol; then, an anhydride determines the acetylation of the amine, hydroxyl and thiol groups (Corr *et al.* 2007b). Although *N*-acetylmethyl (NACME) esters are considered the ideal esters for determining δ^{13}C values, since the procedure introduces only three external carbon atoms and thus reduces analytical error, *N*-acetyl-*i*-propyl (NAIP) esters were preferred for this study since this technique has been more broadly applied, particularly for δ^{15}N values determination (Yarnes and Herszage 2017), and it is considered the propylated homologue of the NACME esters

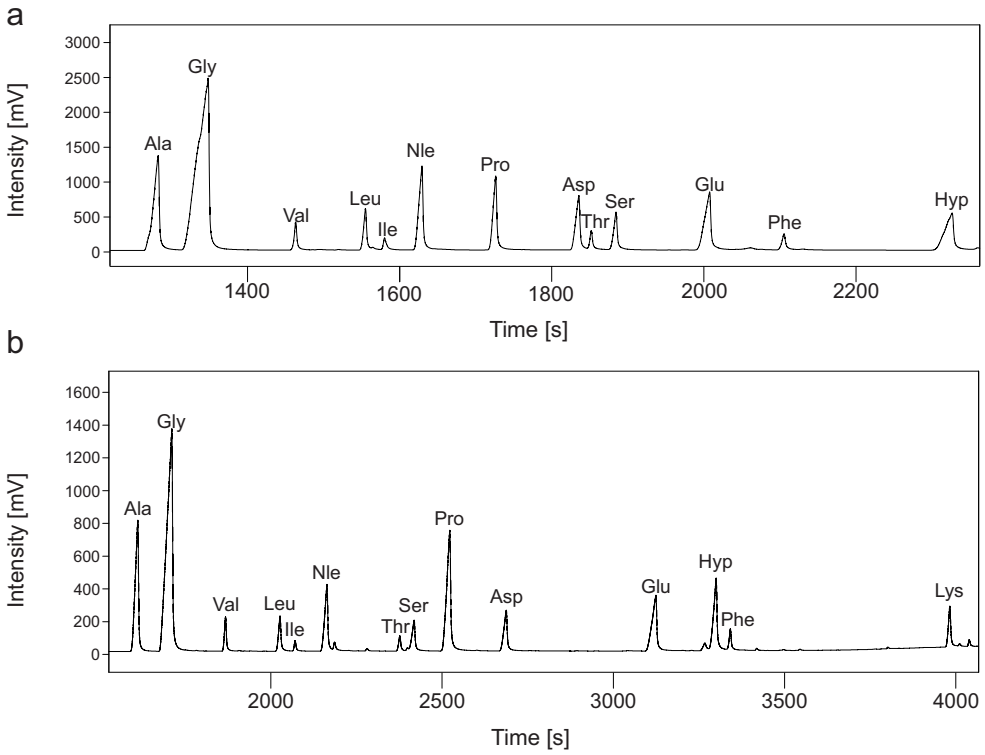

Figure 4.1 GC-C-IRMS profiles of collagen amino acid from a modern bovine sample prepared following the NPIP (a) and the NAIP techniques (b).

in terms of derivatisation yield, instrumentation performance, KIE caused by acylation, analytical errors and stability (Corr *et al.* 2007a).

The first batch of sample (run date: 17/11/2017) was derivatised using the pivaloyl-*i*-propyl esters (NPIP) technique. However, this method introduces up to 13 derivative carbon atoms, making it difficult to confidently determine δ^{13}C values and therefore it was subsequently abandoned (Corr *et al.* 2007b). Figure 4.1 shows two GC-C-IRMS chromatograms of a modern bovine collagen sample prepared following the NPIP (a) and the NAIP techniques (b) analysed in "nitrogen mode". The following paragraphs describe the two adopted procedures.

Preparation of *N*-acetyl-*i*-propyl esters (NAIP)

The following procedure was adapted from Metges *et al.* (1996); Corr *et al.* (2007b); Styring (2012); Philben *et al.* (2018). The protocol is reported in Appendix B. Esterification of amino acids was achieved with acidified propanol. The acidified propanol was prepared by adding dropwise in an ice bath acetyl chloride into isopropanol (isopropanol:acetyl chloride, 4:1 v/v). The mixture was added (1 mL) into each sample, the meniscus marked with a pen to check for evaporation and the culture tubes sealed

and heated at 100 °C for 1 h into a block heater kept under the fumehood. At the end of the treatment, the culture tubes were transferred at -20 °C for a few minutes to stop the reaction. The reagents were blown down under a gentle stream of N_2 at room temperature. To remove excess reagents, samples were washed with dichloromethane (DCM) (2 x 0.5 mL), which was then removed under a gentle stream of N_2. A mixture of acetic anhydride, triethylamine and acetone (1 mL; 1:2:5, v/v/v) was used to perform acetylation. The reagents were added and the samples left at 60 °C for 10 min. The reaction was quenched by transferring the samples at -20 °C for a few minutes and the mixture evaporated under a gentle stream of N_2 at room temperature but with the aluminium blocks still cold. The *N*-acetyl-*i*-propyl esters were redissolved in ethyl acetate (EtAc, 2 mL) and saturated *NaCl* solution (1 mL) for phase separation. The liquids were mixed using a vortex for 20 sec. Once the organic and inorganic phases were separated, the organic phase containing the *N*-acetyl-*i*-propyl esters was transferred into new culture tubes. The phase separation was repeated a second time by adding new EtAc (1 mL) into the tubes containing the saturated NaCl solution. Any trace water was removed by addition of molecular sieves (Merk Millipore, sodium aluminium silicate 0.3 nm). Samples were transferred into GC vials and evaporated completely under a gentle stream of N_2. DCM (1 mL) was added to remove any excess of water and blown down under a gentle stream of N_2. The samples were redissolved in a known quantity of EtAc depending on the original collagen start mass and then split into several aliquots for GC-C-IRMS analysis. One aliquot was further diluted with a known quantity of EtAc and split in aliquots for analysis in carbon mode.

Preparation of *N*-pivaloyl-*i*-propyl esters (NPIP)

The following protocol was adapted from Metges *et al.* (1996); Corr *et al.* (2007b); Chikaraishi *et al.* (2007). Isopropanol was acidified adding dropwise thionyl chloride (isopropanol:thionyl chloride, 4:1 v/v). The mixture (0.2 mL) was added to the samples and the tubes transferred into a block heater at 100 °C for 2 h to perform esterification. The reaction was quenched by transferring the samples at -20 °C for a few minutes and the mixture evaporated under a gentle stream of N_2 at room temperature. DCM (0.5 mL) was added and blown down under N_2 three times to remove any remaining reagent. Pivaloylation, a type of acetylation, of the esters was obtained by pouring into the vials a mixture of pivaloyl chloride and toluene (1:4, v/v, 0.2 mL per sample) and heating up the tubes at 110 °C for 2 h. The samples were then transferred at -20 °C for a few minutes to stop pyvaloylation and then evaporated under a gentle stream of N_2 at room temperature. DCM (0.5 mL) was added and blown down under N_2

three times. The *N*-pivaloyl-*i*-propyl esters were redissolved in *n*-hexane/DCM (3:2, v/v, 0.5 mL per sample) and HPLC grade water was added (0.2 mL). The liquids were mixed using a vortex for 10 sec approximately and the organic phase containing the *N*-pivaloyl-*i*-propyl esters transferred into a $MgSO_4$ column created by pugging a glass sterile pipette with glass wool and by adding a small quantity of $MgSO_4$ on top. Phase separation and filtration were repeated twice. The filtrates were collected into sterile GC vials and the liquids evaporated under N_2. A known quantity of previously dried and degassed DCM was added into the vial and then split into aliquots into new GC vials for analysis. The samples were stored at -20 °C until required for analysis.

4.1.6 Extraction of amino acids from grains

Protein extraction from cereals and legumes was performed following a modified protocol by Styring (2012). Charred archaeological grains were previously cleaned from visible contamination with the use of a blade. Both modern and archaeological samples were then washed with deionised water by ultrasonication (3 x 3 min). Once dry, grains were grounded with a mortar to a fine homogeneous powder, frozen at -20 °C for at least 48 h and freeze-dried for additional 48 h.

Around 50 mg of powder were isolated from each sample into new vials for lipids extraction. 10 μL of n-tetratriacontane (C_{34}, 1 μg μL^{-1} in *n*-hexane) was added as an internal standard to each sample. 10 mL of dichloromethane/methanol (2:1 v/v) were poured into each vial and lipids extracted by ultrasonication (2 x 20 min). Supernatants were transferred to new glass tubes, blown down to dryness under a gentle stream of N_2 at room temperature and then stored at -20 °C until required for lipid analysis. The powdered samples were left open under the fume hood until dry.

Samples were transferred into Reacti-Vials™ in order to proceed to the hydrolysis. 2 mL of 6 M HCl prepared with HPLC grade water were poured into each vial, together with 50 μ L of Nle as internal standard. Samples were then transferred to the oven previously heated to reach 110 °C and left there for 24 h.

At the end of 24 h, samples were allowed to cool down at room temperature and the supernatants transferred into Nanosep™ (Pall Laboratory, pore size: 0.45 μm) and centrifuged to remove remaining insoluble material (2 x 11000 x g, 1 min). The filtered hydrolysates were then transferred to sterile borosilicate test tubes, blown down gently under N_2 at room temperature, re-dissolved into 100 μL 0.1 M HCl and stored at -20 °C until required for derivatisation.

After the hydrolysis, Styring (2012) used cation-exchange chromatography to purify the hydrolysates from non-protein compounds that can possibly co-elute with amino

acids in the GC-C-IRMS and therefore interfere with the carbon and nitrogen signatures of the amino acids. It has been reported previously in the literature that ion-exchange chromatography can cause nitrogen isotopic fractionation (Macko *et al.* 1987; Hare *et al.* 1991). However, the same was not observed by Takano *et al.* (2010) and Styring (2012) and minimally and in only a few amino acids by Metges and Petzke (1997) when using a different type of resin, specifically Bio-Rad AG 50W-X8. 200-400 mesh cation-exchange resin used by Takano *et al.* (2010) and Dowex 50WX8, 200-400 mesh ion-exchange resin used by Metges and Petzke (1997) and Styring (2012). As for carbon, Abelson and Hoering (1961) and Macko *et al.* (1987) observed a significant fractionation in some amino acids, while the same was not observed by Hare *et al.* (1991). To my knowledge, there is no more complete and recent data available on the effect of the use of a ion-exchange resin in the fractionation of carbon isotope of amino acids, which is of interest for the output of this thesis. Therefore, a preliminary test was carried out to observe the derivative composition of plant material without the purification step using a GC-MS with a DB-23 column. Since the GC-MS profiles obtained only showed the presence of amino acids and only occasionally of other compounds, the derivatives were analysed via GC-C-IRMS. Co-elution with other compounds was only observed in serine (only in nitrogen mode) and lysine (only in carbon mode) (Figure 4.2). Since the isotopic composition of the affected amino acids was not considered essential for the purpose of this thesis, the purification step was also avoided in the following extractions of amino acids from plant material.

4.2 Instrumentation

4.2.1 Analysis of the bulk material: EA-IRMS

An Sercon continuous flow 20-22 Isotope Ratio Mass Spectrometer interfaced with a Universal Sercon GSL was used for bulk δ^{13}C and δ^{15}N values determination of collagen, plant material and individual amino acid standards. Each sample was weighed out twice in tin capsules to be run in duplicate. The required collagen mass was between 0.5-0.9 $\pm$ 0.1 mg depending on the condition of the instrument. As for plant material, 2 $\pm$ 0.1 mg were required. 1 $\pm$ 0.1 mg of each amino acid standard was weighed out and run in triplicate.

Tin capsules containing the samples were introduced into the combustion chamber of the elemental analyser through a carousel and burnt in an oxygen atmosphere. The combustion tube contains CrO_3, CuO and silver wool producing CO_2, NO_x and

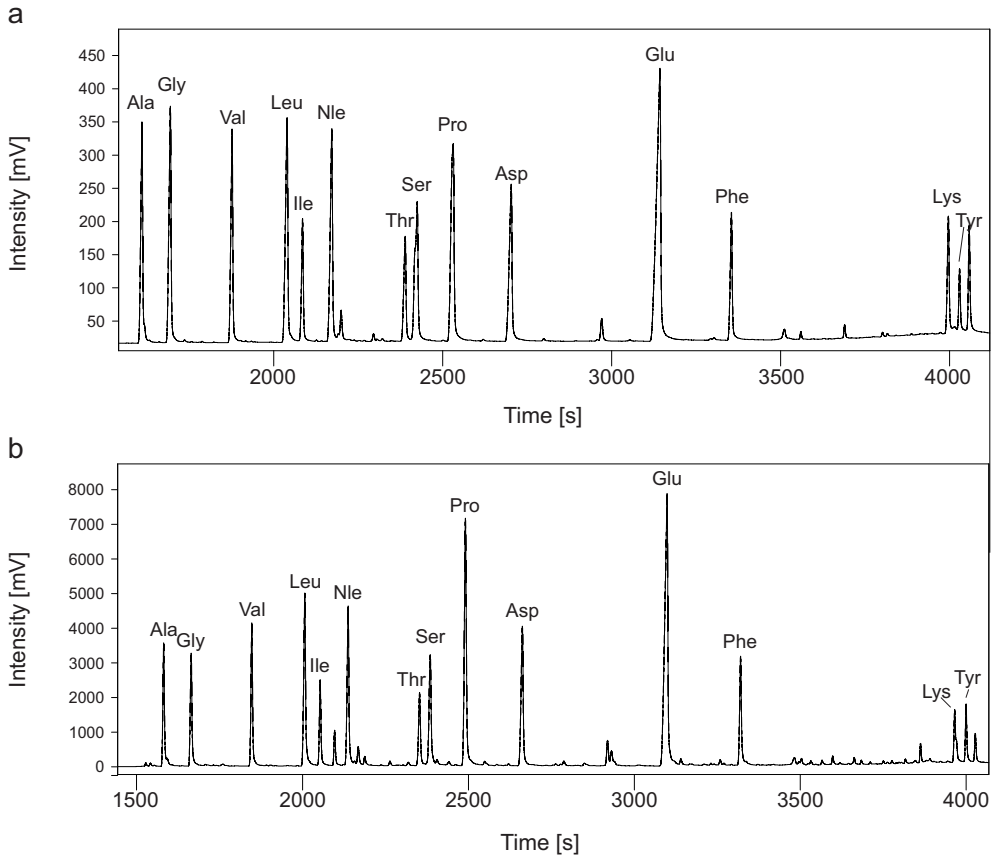

Figure 4.2 GC-C-IRMS profiles of amino acid from a modern grain prepared following the NAIP techniques in nitrogen (a) and carbon (b) mode, without using a cation-exchange resin for amino acid purification.

H_2O. A copper reactor reduces NO_x to NO_2. A $MgClO_4$ trap removes H_2O and CO_2 and NO_2 enter the GC column which separates them. CO_2 and NO_2 are transferred into the ion source inside the mass spectrometer, where the electron beam ionises the gas molecules. A magnetic field drives the ions, accelerated through a high voltage, towards the detector. The detector consists of a universal Faraday triple collector which measures simultaneously m/z 28, 29 and 30 or m/z 44, 45 and 46, corresponding to $^{14}N_2$, $^{14}N^{15}N$, $^{15}N_2$ and $^{12}C^{16}O_2$, $^{13}C^{16}O_2$ e $^{12}C^{16}O^{18}$, respectively. The results were reported using the δ (‰) notation relatively to $\delta^{13}C_{VPDB}$ and $\delta^{15}N_{AIR}$ international standard values.

Each run included a set of standards of known isotopic composition to determine the accuracy: caffeine (IAEA-600, $\delta^{13}C_{TRUE}$ = -27.77 ± 0.04 ‰ and $\delta^{15}N_{TRUE}$ = +1 ± 0.2 ‰), ammonium sulphate (IAEA-N-2, $\delta^{15}N_{TRUE}$ = +20.3 ± 0.2 ‰), and cane sugar (IA-Cane, $\delta^{13}C_{TRUE}$ = -11.64 ± 0.03 ‰). The mean and standard deviation measured across all the runs were: Caffeine, IAEA-600 $n = 43$, $\delta^{13}C_{MEAS}$ = -27.70 ± 0.14 ‰ and $\delta^{15}N_{MEAS}$ = +0.95 ± 0.23 ‰; ammonium sulphate, IAEA-N-2 $n = 43$, $\delta^{15}N_{MEAS}$ = +20.34 ± 0.16 ‰; cane sugar IA-Cane $n = 42$, $\delta^{13}C_{MEAS}$ = -11.68 ± 0.15 ‰.

The sample raw values were normalised according to the true and measured standard values and the sample uncertainty calculated using the method proposed by Kragten (1994). Across all runs, the maximum uncertainty for all the samples ($n = 127$) was 0.4 for $\delta^{13}C$ and 0.6 for $\delta^{15}N$.

The mean bulk values of the bovine control samples across all run and standard deviation ($n = 8$) were $\delta^{13}C$ = -22.88 ± 0.12 ‰ and $\delta^{15}N$ +6.37 ± 0.23 ‰. These values were within those from 50 measurements carried out at the BioArCh facility using the same instrument ($\delta^{13}C$ = -22.97 ± 0.13 ‰ and $\delta^{15}N$ +6.22 ± 0.31 ‰).

4.2.2 Analysis of amino acids: GC-C-IRMS

A Delta V Plus™ isotope ratio mass spectrometer (Thermo Scientific™) linked to a Trace Ultra™ gas chromatograph (Thermo Scientific™) with a GC Isolink II™ interface (Thermo Scientific™) was used for the amino acid $\delta^{13}C$ and $\delta^{15}N$ values determination. Helium was used as the carrier gas at a flow rate of 1.4 mL min^{-1}.

Samples (1 μL), blanks (1 μL) and standard mixtures (2 μL) were injected at 240 °C in triplicate into the chromatograph fitted with a custom DB-35 fused-silica column (60 M x 0.32 mm x 0.50 μm supplied by Agilent J&W, USA). At this point, a small fraction of the flow was diverted towards the Flame Ionisation Detector (FID: temperature 250 °C, hydrogen flow 35 mL min^{-1}, air flow 350 mL min^{-1}). The oven

temperature programme was set as following: 40 °C (hold for 5 min) to 120 °C at 5 °C min^{-1}, then to 180 °C at 3 °C min^{-1}, then to 210 °C at 1.5 °C min^{-1} and finally to 280 °C at 5 °C min^{-1} (hold for 8 min). The combustion reactor was maintained at 1000 °C and the High Temperature Conversion (HTC) reactor at 400 °C. The compounds were either combusted or reduced to CO_2 and N_2, respectively, and sent to the mass spectrometer. A Nafion™ membrane was employed to remove H_2O. A cryogenic trap was additionally used to remove CO_2 in nitrogen mode. In the ion source, the electron beam ionised the gases and the ions were driven towards the Faraday cup collectors for m/z 44, 45 and 46 (carbon mode) and m/z 28, 29, 30 (nitrogen mode).

Data were processed using the Isodat software version 3.0 (Thermo Scientific™) according to repeated measurements of reference gas (CO_2 and N_2). The results were reported using the δ (‰) notation relatively to $\delta^{13}C_{VPDB}$ and $\delta^{15}N_{AIR}$ international standard values.

During the duration of this PhD project, some changes have been made to the instrumentation with the aim to improve the performance of the analysis. In particular, although the chromatographic column used to analyse the NAIP derivatives was always a DB-35 by Agilent with 0.32 mm internal diameter and 0.50 μm film thickness (all supplied by Agilent J&W) the length of the column and/or the assembly has changed three times: first, a single DB-35 with length 30 m (Agilent J&W, code: 123-1933) was used until 15/11/2018. However, the fronting and tailing of the peaks made it difficult to separate hydroxyproline from phenylalanine, both amino acids considered to be relevant for this thesis either for quality assessment (hydroxyproline, see paragraph 4.4.1) and for data analysis (phenylalanine). To better separate the peaks, two 30 M DB-35 (Agilent J&W, code: 123-1933) columns were connected together using a press-fit connector and this setting was used for a few months, until 05/02/2019. During this period many of the NAIP derivatives have been analysed in carbon mode while the measurement of nitrogen isotopes had to be arrested as the runs were affected by a small leak where the two columns were connected. For this reason, in February 2019 a new DB-35 column with custom length 60 M (Agilent J&W by request) was assembled and used for the rest of the project. Figure 4.3 shows the achieved better definition and separation of the hydroxyproline and phenylalanine peaks using the 60 M DB-35 column.

The only batch of samples prepared using the NPIP derivatisation technique was run instead using a HP-Ultra-2 with 0.32 mm internal diameter and 0.52 μm film thickness and 50 M long (supplied by Agilent J&W).

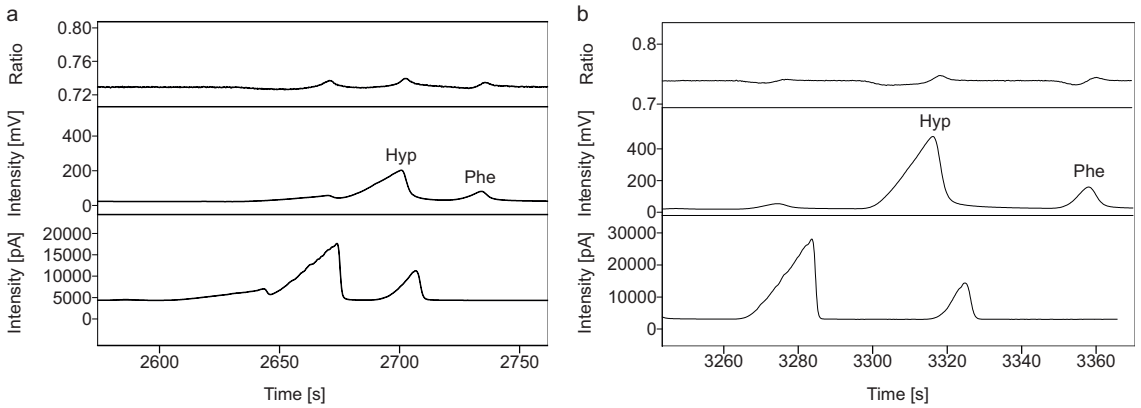

Figure 4.3 GC-C-IRMS profiles of hydroxyproline and phenylalanine from collagen NAIP derivatives using a 30 M (a) and a 60 M (b) DB-35 column.

4.3 Data correction and error propagation

4.3.1 δ^{15}N data: calibration curve and norleucine correction

The international standard amino acid mixture was injected after every three sample runs to monitor instrument performance and drift. A calibration curve was used to normalise the samples and the data then further corrected by the internal standard true (measured via EA-IRMS) value (Figure 4.4). Measured mean δ^{15}N raw values of the international standards ($n = 181$), international Nle ($n = 6$) and Sigma Nle ($n = 175$) across all runs and standard deviation were: Ala, +42.64 ± 2.83 ‰ (true: +43.25 ± 0.07 ‰); Gly, +1.43 ± 1.89 ‰ (true: +1.76 ± 0.06 ‰); Val, −3.95 ± 1.55 ‰ (true: −5.21 ± 0.05 ‰); Leu, +6.47 ± 1.14 ‰ (true: +6.22 ‰); Sigma Nle, +14.59 ± 1.41 ‰ (true: +14.31 ± 0.23 ‰); international Nle, +17.65 ± 0.54 ‰ (true: +18.96 ‰); Asp, +33.92 ± 1.40 ‰ (true: +35.2 ‰), Glu, −3.50 ± 1.05 ‰ (true: −4.52± 0.06 ‰); Hyp, −8.40 ± 1.16 ‰ (true: −9.17 ‰); Phe, +1.75 ± 0.68 ‰ (true: +1.70 ± 0.06 ‰). The raw values are reported in Appendix C Table C.2.

The normalised δ^{15}N values were then corrected by the true (measured in house via EA-IRMS) value of the internal standard.

The standard deviation of the three measurements was used as the error associated with the sample mean isotopic value.

4.3.2 δ^{13}C data: correction for norleucine and external carbon

Similarly to δ^{15}N values determinations, the standard mixture containing sixteen amino acid standards was run every three sample injections to check instrument performance

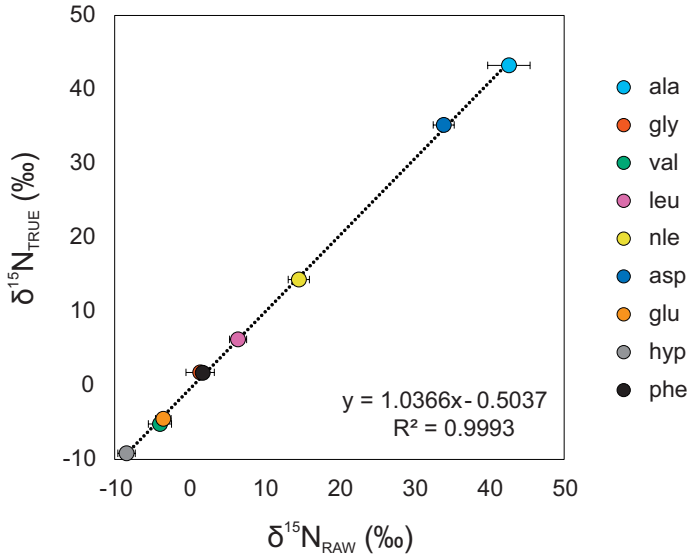

Figure 4.4 True and raw δ^{15}N mean values and standard deviation of the amino acid international standards (n = 181) and Sigma Nle (n = 175) used to normalise the data.

and drift. Since the δ^{13}C values measured are those of the carbon atoms from both the amino acids and the reagents used for the derivatisation, the raw values needed to be corrected by specific correction factors related to the number of external carbon atoms added and the resulting KIE. To do so, the following equation was used, as reported by Docherty *et al.* (2001):

$$\delta^{13}C_{CORR} = \delta^{13}C_D = \frac{[(n_{DC}\delta^{13}C_{DC}) - (n_C\delta^{13}C_C)]}{n_D} \tag{4.1}$$

Where $CORR$ stands for "correction", n represents the number of carbon atoms, DC is the derivatised compound (i.e., the ester), C the original compound (i.e., the amino acid) and D the derivative group.

After each run, the mean correction factors were calculated from the standard mixture injections using the true amino acid δ^{13}C values measured via EA-IRMS and the so-obtained correction factors were used to determine the actual amino acid δ^{13}C values of the samples. The mean correction factors δ^{13}C values across all runs (n = 154) and standard deviation were: Ala, −40.46 ± 1.22 ‰; Gly, −39.73 ± 1.02 ‰; Val, −45.57 ± 1.39 ‰; Leu, −45.03 ± 2.10 ‰; Ile, −46.31 ± 1.81 ‰; Nle, −43.43 ± 1.63 ‰; Thr, −48.52 ± 1.25 ‰; Ser, −46.56 ± 1.19 ‰; Pro, −42.27 ± 1.41 ‰; Asp,−37.27 ± 1.09 ‰; Met, −41.82 ± 2.12 ‰; Glu, −36.73 ± 1.10 ‰; Hyp, −47.97 ± 1.13 ‰; Phe, −45.36 ± 1.46 ‰; Lys, −48.29 ± 2.29 ‰; Tyr, −48.71 ± 1.23 ‰. The raw values are reported in Appendix C Table C.3.

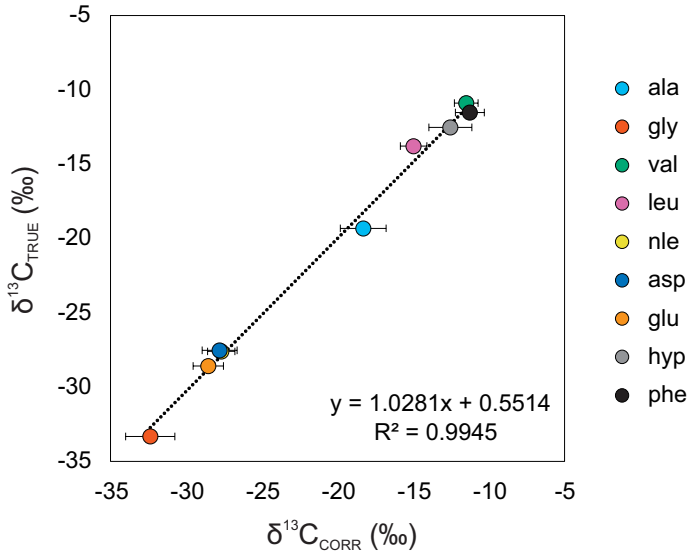

Figure 4.5 Correlation between the corrected amino acid standard δ^{13}C values of the "carbon mixture" by the mean correction factors calculated from the standard amino acid of the "nitrogen mixture" and the true δ^{13}C values of the amino acid standards measured in-house via EA-IRMS.

To check the reliability of the correction applied, the amino acid standards δ^{13}C values of the "carbon mixture" were corrected by the mean correction factors calculated from the standard amino acids of the "nitrogen mixture" which was also included in every run (Figure 4.5).

The correlation between the estimated bulk collagen values (calculated as explained in the following paragraph 4.4.2) and the actual collagen values measured via EA-IRMS (Figure 4.6 a) showed a consistent enrichment of ^{13}C in the estimated bulk values compared to the measured ones ($\Delta^{13}C_{EST-MEAS} = +2.28 \pm 1.42$, $n = 101$). The offset was significantly reduced by applying a preliminary correction of the data by their internal standard true value ($\Delta^{13}C_{EST-MEAS} = +0.76 \pm 1.37$, $n = 101$)(Figure 4.6 b). Moreover, by applying the preliminary correction by the internal standard, it was possible to include a much higher number of samples that would have otherwise been discarded as falling outside $\pm\ 2\sigma$ of the distribution (35 should have been discarded, while only 3 with the additional correction for the internal standard) (Bland and Altman 2003). Although a slightly higher δ^{13}C estimated collagen value has been previously explained by the lack of detection of amino acids that are ^{13}C-depleted (in this case, arginine and minimally histidine), the distribution seems to suggest that samples with higher δ^{13}C measured collagen values are more affected then the others (Figure 4.6 b). Notably, these samples belong almost entirely to marine species.

One reason could be that the collagen sequence used to calculate the relative contribution of carbon according to its amino acid composition for these samples is not

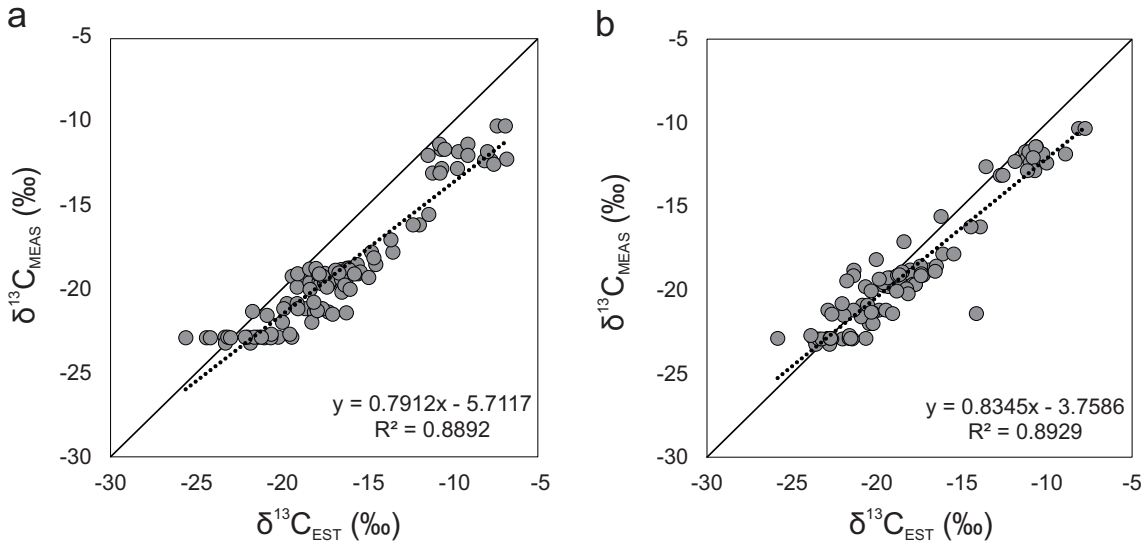

Figure 4.6 Correlation of estimated and measured bulk collagen δ^{13}C values without (a) and with (b) internal standard correction prior that for single correction factors.

adequate. Indeed, the collagen sequence used for calculating the mass balance of marine species was that of Atlantic cod (*Gadus morhua*) (Ensembl ENSGMOP00000009077, ENSGMOP00000014420, ENSGMOP00000016465), one of the few collagen sequences from marine fin fish available for computation (Richter *et al.* 2011; Buckley 2018; Harvey *et al.* 2018; Richter *et al.* 2020). However, due to the rapid evolution of the collagen chains in fish, amino acids sequence in collagen is highly variable in this group across species (Buckley 2018), and it was therefore expected that the Atlantic cod collagen sequence would have not been satisfactory when applied to other marine species. When the marine fish samples are removed from the distribution, the offset is further lowered ($\Delta^{13}C_{EST-MEAS} = +0.63 \pm 1.42$, $n = 81$). However, it should be noted that the number of marine fish samples is significantly lower compared to that of humans and other mammals and it is therefore possible that this trend will not be confirmed in the future if more marine fish samples are included.

To account for the additional errors introduced with the two step correction of data, the following equation was applied, as reported by Docherty *et al.* (2001):

$$\sigma^2 = \sigma_S^2 \left(\frac{n_S}{n_C}\right)^2 + \sigma_{DS}^2 \left[\frac{(n_S + n_D)}{n_C}\right] + \sigma_{DC}^2 \left[\frac{(n_D + n_C)}{n_C}\right] \tag{4.2}$$

Where σ is the standard deviation, n the number of carbon atoms, S the non-derivatised standard, DS the derivatised standard, C the original compound, DC the derivatised compound.

4.4 Assessing the quality of GC-C-IRMS data

4.4.1 Pro-Hyp

Cross plots showing δ^{15}N and δ^{13}C values of proline and hydroxyproline have recently been proposed (Roberts *et al.* 2017; O'Connell and Collins 2018) to assess the quality of the analysis and since then applied by some scholars (*e.g.*, Jaouen *et al.* 2019; Ma *et al.* 2021; Choy *et al.* 2021). The hydroxylation of proline to form hydroxyproline does not involve the exchange of nitrogen or carbon atoms (see Chapter 3, section 3.2.3) therefore the δ^{13}C and δ^{15}N values of proline and hydroxyproline in collagen should be the same. The δ^{13}C and δ^{15}N values of proline and hydroxyproline of the samples analysed for this thesis were compared and the values resulted highly correlated for both carbon and nitrogen analyses ($R^2 = 0.95$ for carbon and $R^2 = 0.96$ for nitrogen) and both the trend-lines close to $y = x$ (Figure 4.7).

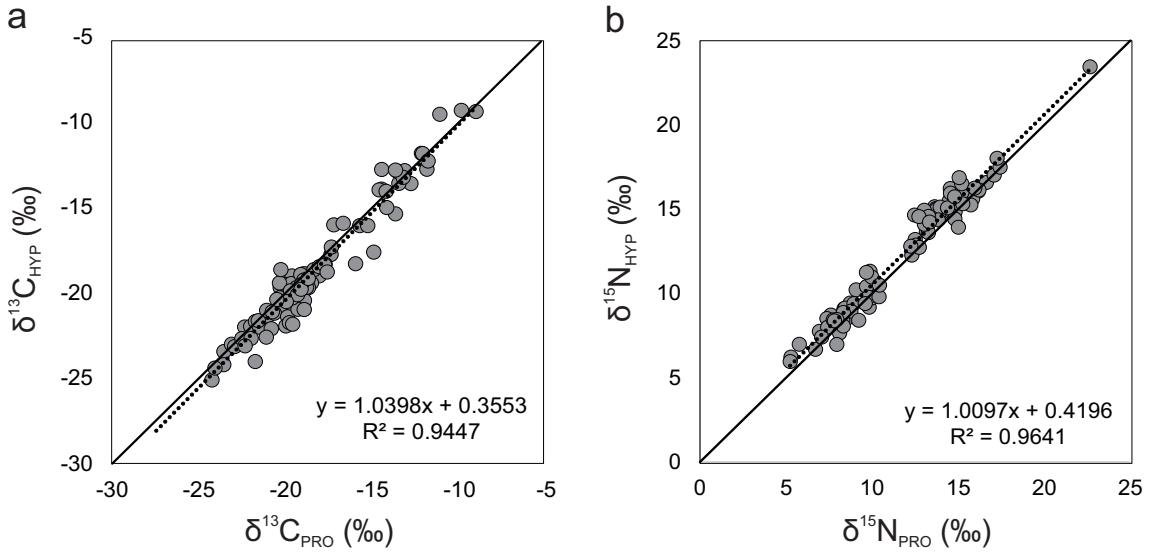

Figure 4.7 Cross plots of δ^{13}C (a) and δ^{15}N (b) values of proline and hydroxyproline of the samples analysed for this thesis.

Although this method represents a valuable means of evaluation of the quality of the data, it must be acknowledged that it is limited to only two amino acid isotope values determinations out of the 13 or 12 we measured in carbon and nitrogen mode, respectively. For this reason, in this thesis, "failed" runs were identified by the raw values of the standard mixtures injections, while single "failed" samples by mass balance calculations, excluding those samples falling outside $\pm$ 2σ of the $\Delta^{13}C_{EST-MEAS}$ and $\Delta^{15}N_{EST-MEAS}$ distributions, as outlined in the following paragraph.

4.4.2 Mass balance

The amino acids detected by GC-C-IRMS account for the 90.37 % of carbon and 80.69 % of nitrogen in human collagen. The relative contributions of carbon and nitrogen from each amino acid was used for mass balance calculations to estimate the bulk collagen δ^{13}C and δ^{15}N values. For a few samples, either the isoleucine, threonine or lysine peaks were too small to be confidently included in the results. For those samples, the mass balance was calculated by excluding the contribution of nitrogen from those amino acids. The amino acid sequences used for computation were those of *Homo sapiens* for all the mammals (Uniprot P02452 and P08123), *Gadus morhua* for marine specimens (Ensembl ENSGMOP00000009077, ENSGMOP00000014420, ENSGMOP00000016465) and *Gallus gallus* (Uniprot P02457 and P02467) for the three chicken samples. The collagen sequences were processed using the ProtParam tool on the ExPASy server (Gasteiger *et al.* 2005). Although it must be acknowledged that the estimated bulk collagen values are mostly affected by the isotopic values of the most numerous amino acids in collagen (first among all, glycine, proline and hydroxyproline), the mass balance calculations represent the best opportunity to assess the overall quality of the amino acid isotope measurements from a single sample. For this reason, the mean offset between the estimated bulk collagen values and the measured via EA-IRMS bulk collagen values was calculated for both carbon and nitrogen and those data falling outside $\pm$ 2σ of the distribution were considered outliers and therefore excluded from the study (Bland and Altman 2003). The samples excluded were in total 3 for carbon and 2 for nitrogen. Two more samples (SSF2 and SSF5) should have been excluded from the nitrogen group as their offsets (both being -1.78) fall outside $\pm$ 2σ of the distribution. However, these two samples belong to marine species for which the collagen sequence used for mass balance calculation might not be representative of the actual amino acid relative contribution. Therefore, since both the raw values of the internal standard and the chromatograms were not found to be anomalous, they have been included in the results. The mean $\Delta^{13}C_{EST-MEAS}$ offset and standard deviation after exclusion of outliers was +0.71 $\pm$ 1.14, n = 98. The mean $\Delta^{15}N_{EST-MEAS}$ offset and standard deviation after exclusion of outliers was +0.15 $\pm$ 0.71 (n = 92). Both carbon and nitrogen estimated and measured bulk values resulted highly correlated (R^2 = 0.92 and R^2 = 0.90 for carbon and nitrogen, respectively)(Figure 4.8).

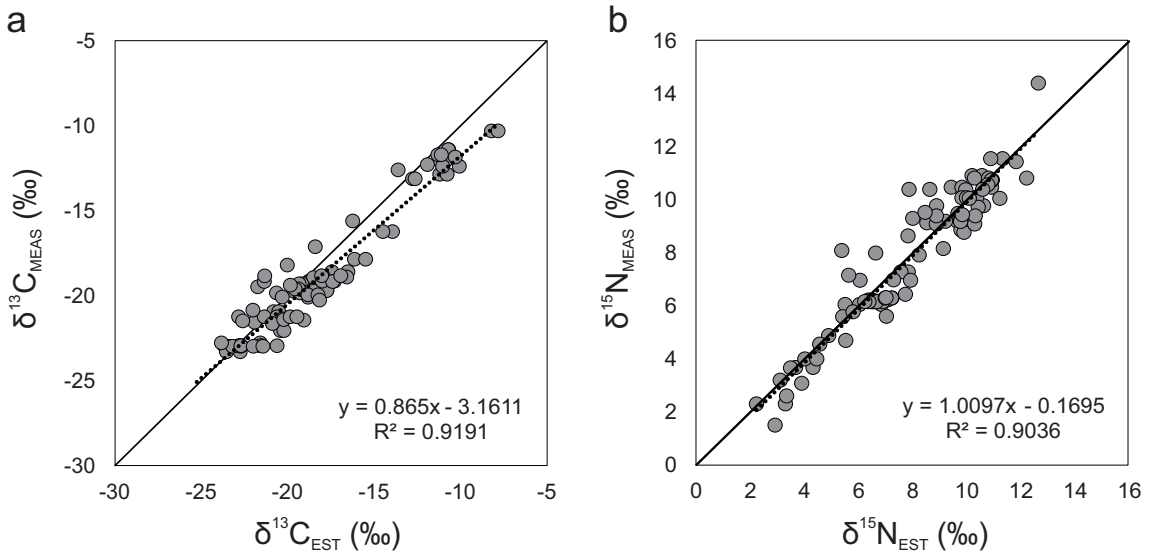

Figure 4.8 Correlation of estimated and measured bulk collagen δ^{13}C (a) and δ^{15}N (b) values. The estimated collagen values were obtained by mass balance calculation considering the single amino acid isotope values and their relative contribution to collagen carbon and nitrogen.

4.4.3 Bovine control sample

A collagen extract from the same bovine control specimen used for EA-IRMS analysis was included with every batch of samples to be analysed via GC-C-IRMS. Although the analysis of amino acid standards represent a valuable tool to assess the quality of one analytical run, the inclusion of a repetitive measurement of collagen from the same specimen was believed to be essential to monitor the reproducibility of isotope values determinations from a "unusual" mixture of amino acids such as that of collagen, where the relative contribution of some of the amino acids (glycine, proline and hydroxyproline in particular) prevails over the others.

The mean δ^{13}C values across all runs (n = 17) and ± 1σ were: Gly, −18.26 ± 1.67 ‰; Ser, −14.17 ± 1.46 ‰; Glx, −21.41 ± 0.77 ‰; Ala, −26.93 ± 1.27 ‰; Asx, −22.80 ± 1.13 ‰; Pro, −22.10 ± 1.36 ‰; Hyp, −22.33 ± 1.40 ‰; Val, −28.53 ± 1.76 ‰; Leu, −31.99 ± 0.73 ‰; Ile, −28.00 ± 0.68 ‰; Thr, −15.41 ± 1.89 ‰; Met, −26.42 ± 1.47 ‰; Lys, −21.26 ± 1.51 ‰; Phe, −31.29 ± 1.23 ‰; Tyr, −28.57 ± 1.09 ‰. The mean estimated bulk δ^{13}C value and 1 σ were −22.51 ± 0.92 ‰ ($\delta^{13}C_{MEAS}$ = −22.92 ± 0.14 ‰). The single values are reported in Appendix C Table C.4.

The mean δ^{15}N values across all runs (n = 16) and ± 1σ were: Gly, +3.99 ± 0.49 ‰; Ser, +4.49 ± 0.78 ‰; Glx, +9.86 ± 0.64 ‰; Ala, +7.57 ± 0.78 ‰; Asx, +9.71 ± 0.71 ‰; Pro, +8.88 ± 0.79 ‰; Hyp, +9.44 ± 0.87 ‰; Val, +14.40 ± 1.53 ‰; Leu, +10.95 ± 1.04 ‰; Ile, +12.06 ± 0.97 ‰; Thr, −3.42 ± 1.10 ‰; Lys, +2.96 ± 0.57 ‰;

Phe, +9.33 ± 0.49 ‰. The mean estimated bulk δ^{15}N value and standard deviation was +6.63 ± 0.44 ‰ ($\delta^{15}N_{MEAS}$ = +6.18 ± 0.08 ‰). The single values are reported in Appendix C Table C.5.

A preliminary test was carried out to observe the differences of the amino acid δ^{13}C values between bovine control samples from different collagen extracts derivatised at the same time. The samples included were: two derivatives from the same collagen extraction where collagen was ultra-filtrated using Ultra-4 Millipore™ filter centrifuge tubes (BVCR71117_1 and BVCR71117_2), two derivatives from another collagen extract where collagen was also ultra-filtrated (BVCR231018_1 and BVCR231018_2), two derivatives from another collagen extract where collagen was not ultra-filtrated and provided by Dr Alison Harris (BVC7_1 and BVC7_2).

The δ^{13}C values of serine, hydroxyproline, phenylalanine, lysine and threonine of sample BVCR71117_2 skewed from the values of the amino acid from the other bovine control samples. Since the raw δ^{13}C value of BVCR71117_2 was also higher than that of the other bovine controls, this sample was excluded as probably affected by some problem occurred during the derivatisation. The mean δ^{13}C values (n = 6) and ± 1σ were: Gly, −19.39 ± 1.08 ‰; Ser, −14.84 ± 0.80 ‰; Glx, −21.61 ± 0.34 ‰; Ala, −26.46 ± 0.47 ‰; Asx, −22.37 ± 0.58 ‰; Pro, −23.59 ± 0.51 ‰; Hyp, −23.89 ± 0.82 ‰; Val, −26.53 ± 0.35 ‰; Leu, −31.97 ± 0.39 ‰; Ile, −28.23 ± 0.31 ‰; Thr, −15.31 ± 0.66 ‰; Met, −25.75 ± 0.47 ‰; Lys, −21.81 ± 0.59 ‰; Phe, −32.06 ± 0.32 ‰; Tyr, −28.83 ± 0.40 ‰. The mean estimated bulk δ^{13}C value and standard deviation was −23.15 ± 0.42 ‰($\delta^{13}C_{MEAS}$ = −23.01 ± 0.18 ‰).

4.4.4 Derivative stability

During the duration of this PhD project, the instrumentation set-up has gone through multiple adjustments, as outlined in section 4.2.2. To verify the quality of the analysis, some derivatives have been run more than once. The results have all been used to discuss the overall quality of the data over a period of two years (section 4.4), with the exception of "bad" runs and outliers. Only one measurement for each archaeological sample needed to be selected for the purpose of this thesis. Nevertheless, duplicate measurements can be used to drive a preliminary discussion about the stability of the derivatives.

Carbon isotopes

Many of the derivative batches prepared for GC-C-IRMS analysis of carbon isotopes were measured both within and outside the 12 weeks period, which is the suggested maximum storage time by Corr *et al.* (2007a,b). Therefore, this dataset represents a precious opportunity to observe the stability of δ^{13}C values beyond the established 12 weeks period. However, it must be acknowledged that stability should better be assessed by observing correlation of more than two repeated measurements through time. Therefore, the following observations must be considered preliminary.

Systematic increase or decrease of δ^{13}C values was not observed in any of the measured amino acids and the δ^{13}C values from the second analysis were generally within the associated uncertainties. As an example, Figure 4.9 shows δ^{13}C values of two pairs of bovine control derivatives (BVCR117 and BVCR7117) run within (week 9) and outside (week 33) the suggested storage period (Corr *et al.* 2007b,a). Occasionally, the δ^{13}C values were not found within the uncertainties associated with the two measurements, as in the case of $\delta^{13}C_{val}$ for sample BVCR117 and $\delta^{13}C_{thr}$ for both samples from Figure 4.9. However, it was not possible to detect a specific pattern and therefore the different value was not considered to be related to storage period. Moreover, both $\delta^{13}C_{val}$ and $\delta^{13}C_{thr}$ are within $\pm$ 1σ of all the measurements carried out on bovine control samples (see previous section 4.4.3). The GC-C-IRMS profiles of derivatives run outside the suggested storage period were also found to be equivalent to those run within 12 weeks and an example is reported in Figure 4.10.

Since none of the amino acid δ^{13}C value determinations seems to be systematically affected by storage time up to a maximum of 34 weeks, for the purposes of this thesis, in the following chapters, where a sample has duplicate measurements, will be used that with the lowest $\Delta^{13}C_{EST-MEAS}$ regardless of the time they were stored before being run. Where applicable, measurements carried out using a single 30 M DB-35 column were excluded *a priori* for the reasons explained in section 4.2.2.

Nitrogen isotopes

As for nitrogen stable isotope determinations, none of the samples has been run both within and outside the 12 weeks storage period and therefore any discussion around derivative δ^{15}N value stability through time would be unsound. However, since some of the samples were run after the 12 weeks suggested storage period, up to a maximum of 52 weeks, it seemed important to verify any substantial change possibly related to the time of storage. Repetitive measurements of modern bovine control collagen (although

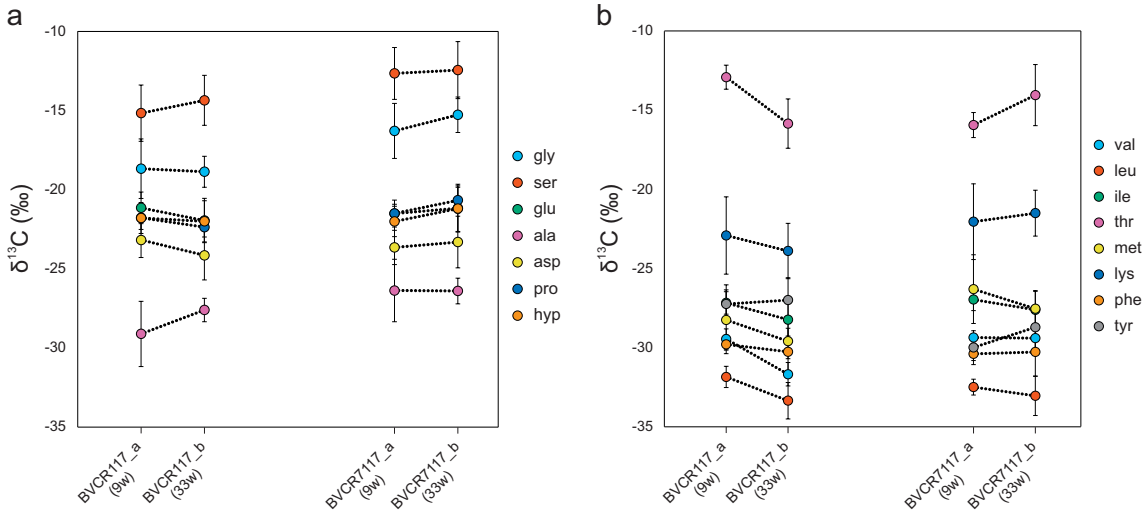

Figure 4.9 δ^{13}C values of collagen amino acids from two modern bovine derivatives (BVCR117 and BVCR7117) analysed within (week 9) and outside (week 33) the suggested 12 weeks storage period (Corr *et al.* 2007b,a). The δ^{13}C values have been divided in two separate graphs containing non-essential (a) and essential (b) amino acids to facilitate visualisation.

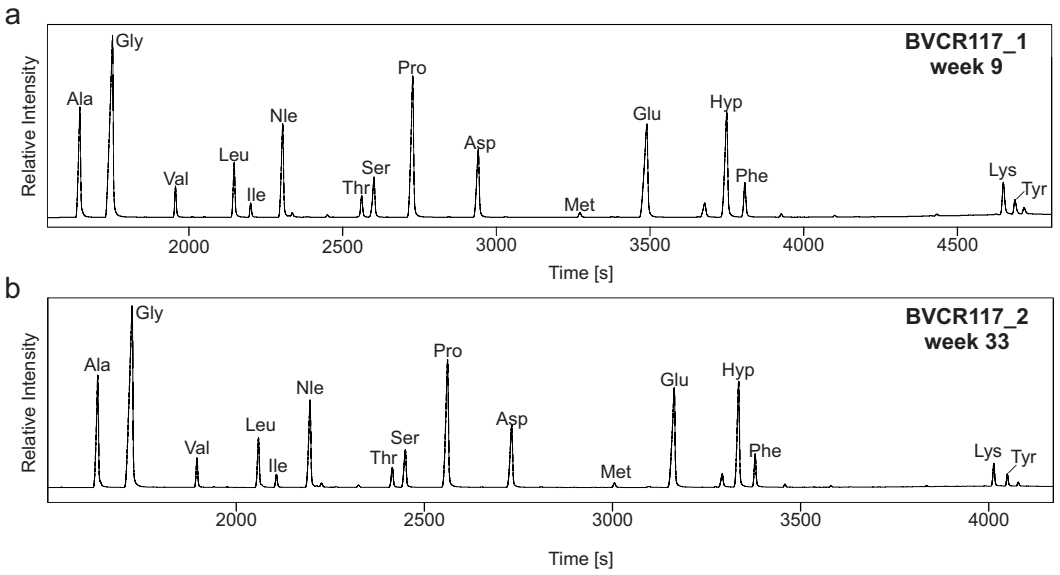

Figure 4.10 GC-C-IRMS profiles of modern bovine collagen amino acids from the same NAIP derivative analysed within (a) and outside (b) the suggested 12 weeks storage period (Corr *et al.* 2007b,a).

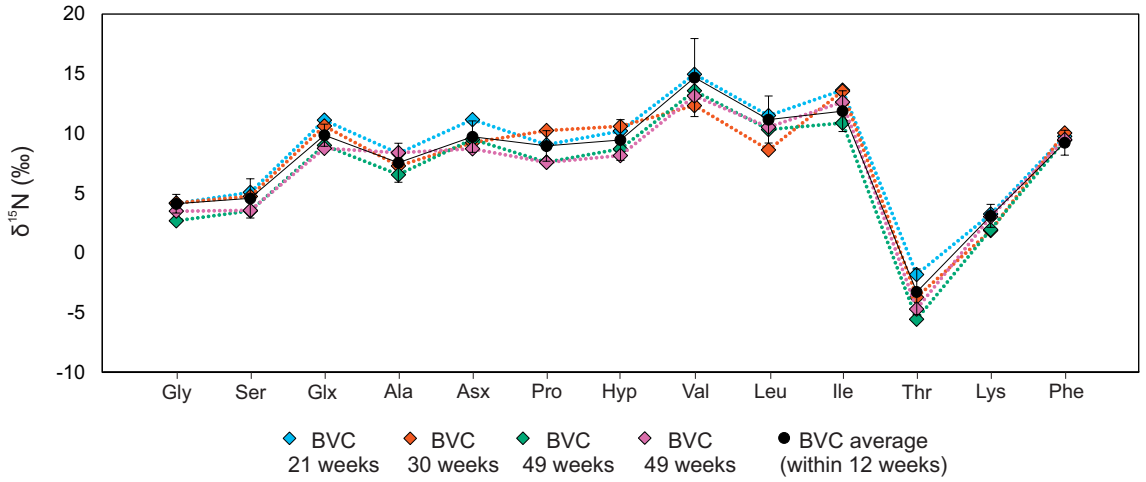

Figure 4.11 δ^{15}N values of collagen amino acids from three bovine controls derivatives run after 21 (light blue diamonds), 30 (red diamonds) and 49 (green and purple diamonds) weeks and compared to the average ($\pm$ 2σ) of bovine controls (n = 12) analysed within the suggested 12 weeks storage period (black circles).

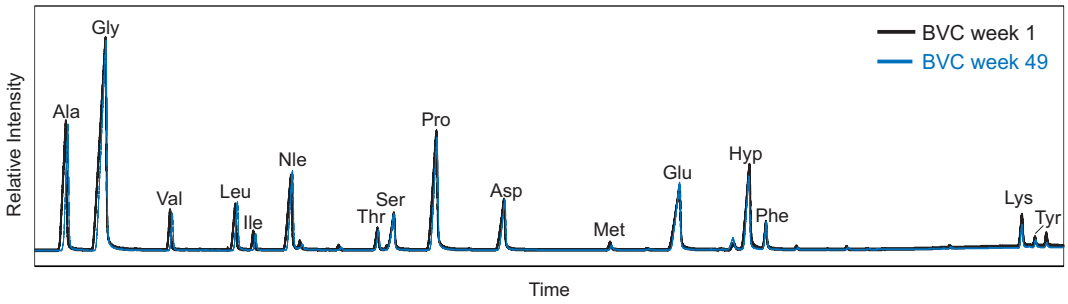

Figure 4.12 GC-C-IRMS profiles of modern bovine collagen amino acids from analysed within 12 weeks (black profile) and after 49 weeks (blue profile) from derivatisation.

not from the same derivative) seems to suggest that if present, any fractionation through time is included in the overall measurement variability, as shown in Figure 4.11.

Furthermore, the relative intensity of the GC-C-IRMS profiles of bovine control amino acids run after the 12 weeks suggested that, despite the storage period, these were not different from those run within 12 weeks, as shown in Figure 4.12

Since nitrogen fractionation with time cannot be excluded, the following approach has been followed in excluding one of the duplicate measurements: first, priority was given to those samples run using a 60 M column for the reasons explained in section 4.2.2; second, if both samples were run using a 60 M column, it would be prioritised the run within the suggested 12 weeks storage period; last, if both the samples were

run using the 60 M column and they were both analysed after the 12 weeks period, it was chosen the sample with the better $\delta^{15}N_{MEAS}$ offset.

4.5 Conclusion

In this Chapter, the design of the research was introduced as a follow-up to a previous research conducted in collaboration with *Museo Nazionale Preistorico Etnografico Luigi Pigorini* and *Parco Archeologico di Ercolano* and the sampling strategies of old and newly acquired material described (section 4.1.1). After a first brief explanation of the protocol used for the isolation of collagen from human and animal bones (section 4.1.2), a more detailed description was provided for the extraction of amino acids (section 4.1.4) and the preparation of the standard (section 4.1.3) used for GC-C-IRMS analysis. In order to be analysed through a GC-C-IRMS system, the amino acids were derivatised to their respective esters using two different techniques outlined in section 4.1.5. For the first time at BioArCh, the analysis of amino acids from botanical material was attempted and the experiment described in section 4.1.6. The instrumentation used for the analysis of carbon and nitrogen of bulk material (section 4.2.1) and of amino acids (section 4.2.2) was also outlined as well as some changes the latter went through during the duration of this project. The correction of the amino acid data and the calculation of the associated uncertainty was also presented (section 4.3) with a focus on the improvement obtained by applying a preliminary correction for the internal standard on carbon data. To conclude, the quality of the data was discussed by looking at different parameters (section 4.4) and the stability of the derivatives assessed by comparing duplicate measurements of the same samples (section 4.4.4).

Chapter 5

Establishing a baseline for diet at AD 79 Herculaneum

Agricultural and husbandry practices in the Roman imperial time were highly organized with the aim to ensure food production and distribution in all parts of the Empire. Some items in particular were extensively produced and distributed from specific geographical locations across the Empire, and this is definitely the case of the "Mediterranean triad" (cereals, olive oil and wine) but also of other products that were commonly traded, such as legumes, cured meat and *garum*. Of course, local production was also important, especially in rural communities distant from the main trade routes, and this was adapted according to the natural environment (see Chapter 2). From a stable isotope point of view, interpreting human values with inputs from such a variety of food items and possible geographical locations is extremely challenging, since the isotopic composition of the food items is influenced by many factors, such as the environment, herding practices and crop management strategies, as will be outlined in the following sections. Therefore, in this Chapter, the isotopic signatures of the food categories that were most likely the major contributors of proteins and calories to the people living in Herculaneum in the 1^{st} century AD, namely cereals and legumes and animal and fish products, will be explored as extensively as possible, with the aim to compare the isotope values of the human individuals to those collected from a reliable dietary baseline.

However, each of these food categories has its own specific methodological challenges when it comes to measuring its bulk and/or amino acid isotopic composition that may seriously jeopardise the outcome of any dietary investigation. More specifically, cereals and legumes (and more in general botanical material) undergo diagenetic mechanisms that make it difficult to measure the isotopic signatures of endogenous amino acids and

therefore their preservation was first evaluated using RP-HPLC (section 5.1). As for terrestrial animals and fish remains, the dangers of attributing fragmentary remains to the wrong *taxon* are often underestimated in the field, as it will be pointed out in section 5.2.1 by comparing the results obtained using ZooMS with those from the morphological identification.

Finally, the carbon and nitrogen isotope bulk and amino acid values of cereals, legumes, animals and fish will be presented and discussed considering the implication for dietary and economic studies of the Roman Mediterranean (section 5.2.2).

5.1 Stable isotope analysis of cereals and pulses

Plants represent one of the major food sources in many past and contemporary human diets. Cereals and legumes in particular, can provide the calories that are required by the metabolism, thanks to their high carbohydrate content and significant amounts of proteins. Therefore, plant consumption should be easy to detect with the analysis of carbon and nitrogen stable isotopes from the consumer's bone collagen. Cereals and legumes can be found in many archaeological contexts, often charred, and their carbon and nitrogen isotopic content has been measured in the past for the investigation of crop growing conditions (*e.g.*, Bogaard *et al.* 2007; Fiorentino *et al.* 2015; Mueller-Bieniek *et al.* 2019) and only occasionally as reference for the interpretation of carbon and nitrogen isotope analysis of human bone collagen (Fraser *et al.* 2013b; Gismondi *et al.* 2020). One of the main reasons why stable isotopes from plant remains are not commonly measured for the investigation of past human diets is that it is not possible to isolate a single component as is done with bone collagen, since plant remains are an heterogeneous material consisting of a mixture of proteins, carbohydrates and a small portion of lipids. Moreover, there is a certain degree of uncertainty about how plant components degrade with time and under other conditions, in particular that of charring and burial environment, including humic acid contamination, which have the potential to alter the original isotopic composition of the material (Hedges and Reynard 2007). Many of the concerns about charring have now been dissipated as several studies have shown that the isotope fractionation is minimal and predictable and it can therefore be corrected from the measured values (Bogaard *et al.* 2007; Aguilera *et al.* 2008; Fraser *et al.* 2013a; Nitsch *et al.* 2015). As for burial and humic acid contamination, these do not seem to have significant effect on the carbon and nitrogen isotope values of plant bulk material (Fraser *et al.* 2013a). Moreover, it is believed that the melanoidins (the Maillard reaction products) that are formed during charring

between amino acids and starches in grains, are resistant to bacterial degradation (Fraser *et al.* 2013a; Styring *et al.* 2013).

Now that many scholars are turning to CSIA-AA to study ancient human dietary practices it seems important to assess the state of preservation of amino acids in cereals and legumes so that they can potentially be included in the investigation (Styring *et al.* 2015). Styring *et al.* (2013) were the first to observe that amino acids in einkorn charred grains from two distinct archaeological sites were only 0.4 % of the total hydrolysable amino acid content of their modern counterparts. This is indicative of the loss of the majority of the original amino acids, which might have determined the isotopic fractionation of the remaining portion, but it could also suggest that they are not even endogenous, making the application of CSIA-AA on ancient cereals challenging (Styring *et al.* 2015). In this section the results from an exploratory study on amino acid preservation in modern and ancient cereals and legumes using Reverse Phase High-Performance Liquid Chromatography (RP-HPLC) will be presented. By relying on RP-HPLC, it will be possible to observe the content of amino acids in their D and L isomers, providing a helpful insight into the preservation status of amino acids in archaeological grains.

5.1.1 Protein and amino acid composition of cereals and pulses - what to expect

The edible part of cereals is the grain, the common name used to refer to the caryopsis, which is the fruit of the Poaceae family. In the caryopsis, the fruit and the seed are fused into a single unit. The term legume refers instead to the fruit of the Leguminosae family which on the inside contains the seeds, also called beans or grains. Generally, the seeds of cereals and pulses are characterized by a high content of polysaccharides (mainly starch), small but significant amounts of proteins (higher in pulses) and a low lipid content. However, differences between different species either in the cereal or legume group are significant (Lasztity 1996).

Very differently from animal bones, where the protein fraction is almost entirely represented by collagen, seeds contain a large variety of proteins which can be classified as cytoplasmic (metabolically active, such as albumins and globulins) and storage proteins, on the basis of their biological function (Lasztity 1996). In terms of amino acid composition, cytoplasmic and storage proteins are very different: storage proteins have a larger proportion of glutamic acid and proline and a smaller proportion of lysine, arginine, threonine and tryptophan, while cytoplasmic proteins have lower glutamic

Grain or grain product	NDB Number	Protein (%)	Carbohydrates (%)	Lipids (%)
		Cereals		
Barley, hulled	20004	14.14%	83.25%	2.61%
Barley, pearled	20005	7.31%	91.27%	1.42%
Millet	20031	12.51%	82.7%	4.79%
Oat bran	20033	19.11%	73.13%	7.76%
Sorghum	20067	12.32%	83.66%	4.02%
Rye	20062	11.77%	86.37%	1.86%
Durum wheat	20076	15.67%	81.5%	2.83%
Wheat, sprouted	20087	14.6%	82.92%	2.48%
Wheat plain flour	20481	11.79%	87.09%	1.12%
Spelt	20140	16.71%	80.5%	2.79%
		Legumes		
Broadbeans	16052	30.39%	67.83%	1.78%
Chickpeas	16056	22.88%	70.37%	6.75%
Lupins	16076	41.92%	46.79%	11.29%
Lentils	16069	27.66%	71.15%	1.19%
Green peas	16085	26.08%	69.53%	4.39%

Table 5.1 Macronutrient composition of cereal and legume grains expressed as dry weight (%). Data collected and elaborated from USDA National Nutrient Database for Standard Reference (which can be accessed at this link). *NDB* is the identifier for the item in the USDA Database.

acid and proline content and higher proportion of lysine and arginine (Lasztity 1996). In cereal grains, storage proteins are abundant in the endosperm, metabolically active proteins are more concentrated in the aleurone layer and in the germ. It must also be considered that different parts of the seed have a different protein content. The germ is about 30% protein, the aleurone layer has a relatively high concentration as well (about 20%) whilst the endosperm has the lowest. The highest content of essential amino acids is found in the aleurone layer and in the germ. The amount of proteins is also variable according to the life cycle of the plant and as a reaction to environmental factors. For example, the synthesis of proteins in the seeds is enhanced during the fruiting period but also as a reaction to drought or to certain diseases (Lasztity 1996).

In conclusion, the amount and type of protein and amino acid that cereal and legume grains can provide to the consumer varies depending on the species consumed, its life stage, environmental conditions and how the grains have been processed. For example, flour, which is obtained by grinding the grains, is mainly composed of the endosperm and it is therefore low in protein (mainly of the storage type) and high in starch. Some other examples are reported in Table 5.1.1.

5.1.2 Experimental design and Materials

In order to evaluate the amino acid composition of archaeological grains, the RP-HPLC experiment was designed to include measurements from modern material and archaeological grains from different locations (Table 5.1.2). These included four samples from Roman York (Rougier Street and Coney Street), provided by Dr Michelle Alexander, archaeological charred material from the sites of Hattusha and Çatalhöyük and modern experimentally charred samples provided by Professor Amy Bogaard from the University of Oxford, and a small group of modern grains from Italy purchased by the author of the thesis in 2017.

Samples were prepared for analysis by Silvia Soncin, while the hydrolysis and RP-HPLC analysis were performed by Ailsa Roper under the supervision of Professor Kirsty Penkman and Dr Kirsty High. These data have been previoulsy reported in Ailsa Roper's MSc by Research final report (Roper 2019).

The modern Italian cereals were all grown organically and purchased from an organic supermarket in Rome (EcorNaturaSì Spa). The modern durum wheat sample (MDW) was already processed, specifically cracked, when purchased while the others were whole grains. The modern experimentally charred (24 h at 230 °C) samples consisted of pea (*Pisum sativum*), lentil (*Lens culinaris*), einkorn, barley, emmer (*Triticum dioccum*) and bread wheat (*Triticum aestivum*). The archaeological group was composed of barley and spelt (*Triticum spelta*) from two archaeological Roman sites in York, UK, and by emmer, barley, a type of *Triticum* sp. named "new type" and pea from Bronze Age Hattusa and Neolithic Çatalhöyük, Turkey (Table 5.1.2). Brief information about the archaeological sites from which the grains were recovered are reported in Appendix D, section D.1.

5.1.3 Methods

Both modern and archaeological grains were homogenised into a powder using a mortar. The Italian modern grains and the archaeological samples from Roman York have been preliminary washed by ultrasonication with deionized water multiple times before being ground into a powder. No prior chemical treatment was applied since these were shown to lead to significant sample loss (Brinkkemper *et al.* 2018). Preparation of the seed samples for RP-HPLC analysis using the methods reported by Roper (2019). Briefly, a portion of powder (*ca.* 1 mg) was isolated from each sample and added into a sterile hydrolisis vial. 200 μL of 6 M *HCl* were pipetted into the vial, the vials flushed with nitrogen, the caps closed tightly and the samples left at 110 °C for 24 h.

		Species				
ID	**Group**	**Common Name**	**Latin Name**	**Provenance**	**Modern/ Archaeological**	**State**
MDW	C_3	Durum wheat	*Triticum durum*	Italy	Modern	Uncharred
MB	C_3	Barley	*Hordeum vulgare*	Italy	Modern	Uncharred
MF	C_3	Einkorn	*Triticum monococcum*	Italy	Modern	Uncharred
MO	C_3	Oat	*Avena sativa*	Italy	Modern	Uncharred
MM	C_4	Millet	*Panicum miliaceum*	Italy	Modern	Uncharred
C5NB	C_3	Barley	*Hordeum vulgare*	UK	Modern	Charred
C5LEN	Legume	Lentil	*Lens culinaris*	UK	Modern	Charred
C5PEA	Legume	Pea	*Pisum sativum*	UK	Modern	Charred
C5EIN	C_3	Einkorn	*Triticum monococcum*	UK	Modern	Charred
C5EM	C_3	Emmer	*Triticum dicoccum*	UK	Modern	Charred
C5BW	C_3	Bread wheat	*Triticum aestivum*	UK	Modern	Charred
SRG	C_3	Spelt	*Triticum spelta*	Rougier Street	Archaeological	charred and waterlogged
BRS	C_3	Barley	*Hordeum vulgare*	Rougier Street	Archaeological	charred and waterlogged
SCS	C_3	Spelt	*Triticum spelta*	Coney Street	Archaeological	Charred
BCS	C_3	Barley	*Hordeum vulgare*	Coney Street	Archaeological	Charred
HATEM245	C_3	Emmer	*Triticum dicoccum*	Hattusha	Archaeological	Charred
HATB245	C_3	Barley	*Hordeum vulgare*	Hattusha	Archaeological	Charred
HATEM71	C_3	Emmer	*Triticum dicoccum*	Hattusha	Archaeological	Charred
HATB71	C_3	Barley	*Hordeum vulgare*	Hattusha	Archaeological	Charred
CH6020	C_3	Barley	*Hordeum vulgare*	Çatalhöyük	Archaeological	Charred
CH6081	Legume	Pea	*Pisum sativum*	Çatalhöyük	Archaeological	Charred
CH6181	Legume	Pea	*Pisum sativum*	Çatalhöyük	Archaeological	Charred
CH8415	C_3	"New type"	*Triticum* sp.	Çatalhöyük	Archaeological	Charred
CH8453	C_3	"New type"	*Triticum* sp.	Çatalhöyük	Archaeological	Charred
CH8454	C_3	"New type"	*Triticum* sp.	Çatalhöyük	Archaeological	Charred

Table 5.2 List of modern and archaeological samples analysed via RP-HPLC.

After 24 h, the liquids were removed using a centrifugal evaporator under vacuum and the amino acids rehydrated in a solution made with 0.01 M *HCl* and 1.5 mM sodium azide. A known quantity of internal standard (0.01 mM L-homo-arginine) was added at this stage. The Italian modern samples were rehydrated in 500 μL/mg of rehydration solution and then diluted 1 in 10 before analysis, the modern charred samples in 100 μL/mg then diluted 1 in 4, and the archaeological samples in 20-30 μL/mg and not further diluted. Analysis via RP-HPLC (Agilent 1100 Series HPLC) was performed following the method of Kaufman and Manley (1998) modified by Penkman (2005): 2 μL from each sample were injected and mixed online with 2.2 μL of derivitising reagent prepared with 260 *mM* N-Iso-L-butyryl L-cysteine (IBLC), 170 mM o-phthaldialdehyde (OPA) in 1 M potassium borate buffer, adjusted to pH 10.4 with potassium hydroxide pellets. The amino acids were separated on a C18 HyperSil BDS column (5 mm x 250 mm) at 25 °C using a gradient elution of 3 solvents: sodium acetate buffer (solvent A made of 23 mM sodium acetate tri-hydrate, 1.5 mM sodium azide, 1.3 μL EDTA, adjusted to pH 6.00 $\pm$ 0.01 with 10 % acetic acid and sodium hydroxide), methanol (solvent C) and acetonitrile (solvent D). First, 95 % A and 5 % C were used at a flow rate of 0.56 m L/min, grading to 50 % C and 2 % D after 95 minutes. Prior to the injection of the next sample, the column was flushed with 95 % C and D for 15 minutes, followed by equilibration of 95 % A and 5 % C for 5 minutes. A xenon-arc flash lamp was used in the fluorescence detector at a frequency of 55 Hz, with a 280 nm cut-off filter and an excitation wavelength of 230 nm and emission wavelength of 445 nm. A standard mixture made of the following amino acids was used: L-Asp, D-Asp, L-Glu, D-Glu, L-Thr, L-His, L-Ser, D-Ser, L-Arg, D-Arg, L-Ala, L-hArg, D-Ala, L-Tyr, D-Tyr, L-Val, L-Met, D-Met, D-Val, L-Phe, L-Ile, D-Phe, L-Leu, D-Ile and D-Leu. Figure 5.1 reports an example of the RP-HPLC profiles of a modern uncharred (a) and of an archaeological charred (b) sample.

5.1.4 Results

Amino acid content

First, the absolute and relative amino acid content of the different grain categories (*i.e.*, modern uncharred, modern charred and archaeological) was explored to evaluate the effect of charring and burial on the potential loss of amino acids (Figure 5.2 a and b).

The chromatographic profiles of modern charred and archaeological samples resulted affected by the co-elution of other compounds that made the baseline increase from

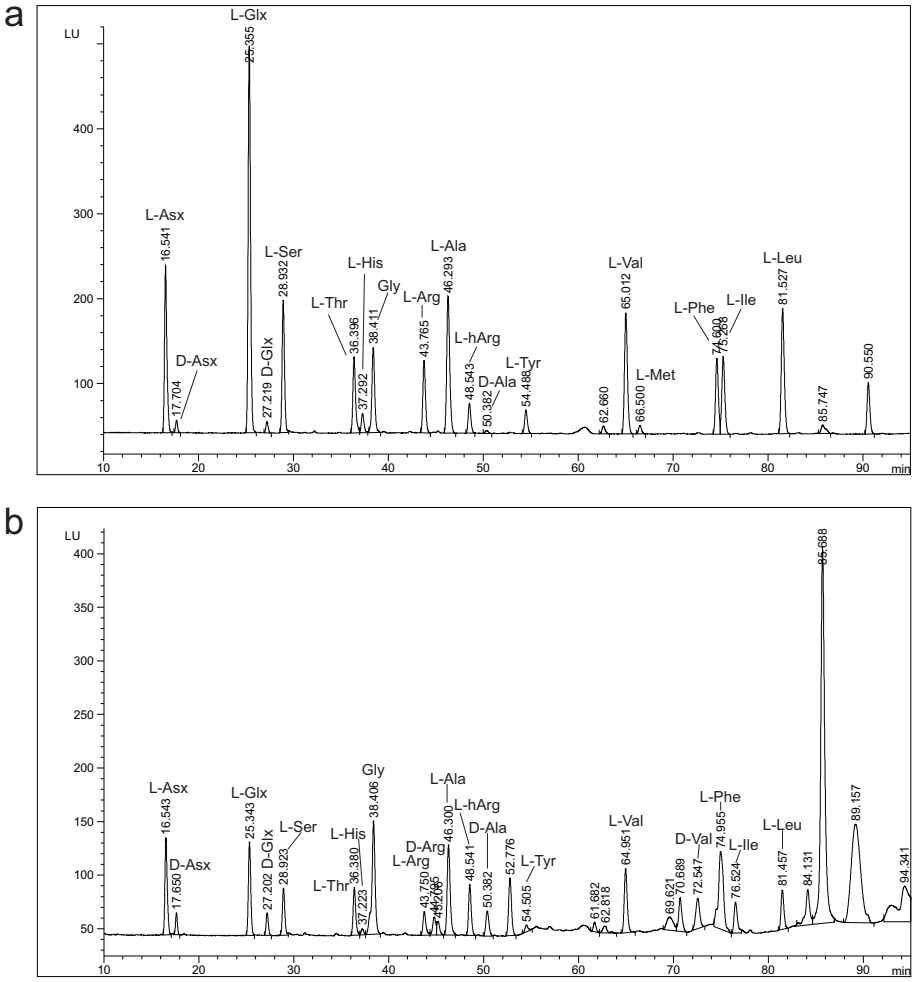

Figure 5.1 Examples of RP-HPLC profiles of a modern uncharred (a) and of an archaeological charred (b) sample. In b it is visible the baseline rise at *ca.* 54 *min* onwards characteristic of all the charred samples here analysed.

ca. 54 min onwards (Figure 5.1 b). This made it difficult to confidently integrate the amino acid peaks from the affected region, namely L-Tyr, L-Val, D-Val, L-Phe, L-Ile and L-Leu, and therefore they have not been included in the results. In this section, these amino acids have also been excluded from the modern uncharred samples for comparative purposes. Concentration, expressed as *pmol* mg^{-1} of amino acids in the samples have been determined thanks to the use of an internal standard (L-hArg) at a known concentration and the overall amino acid content referred to as total hydrolysable amino acid fraction (THAA). As expected, modern uncharred samples yield the highest [THAA], while experimentally charred modern and archaeological grains grains contain only 20 % and 1 % of the modern uncharred, respectively (Figure 5.2 a). Styring (2012)

suggested that the lower content of amino acids in the archaeological grains compared to the experimentally charred ones can be due to three possible reasons: i) exposure of the archaeological samples to temperature higher than 230 °C, determining a higher condensation of amino acids and carbohydrates in melanoidins; ii) continuation of the Maillard reaction over time, since the reaction can also take place at room temperature, although at a lower rate; iii) caused from microbial attack.

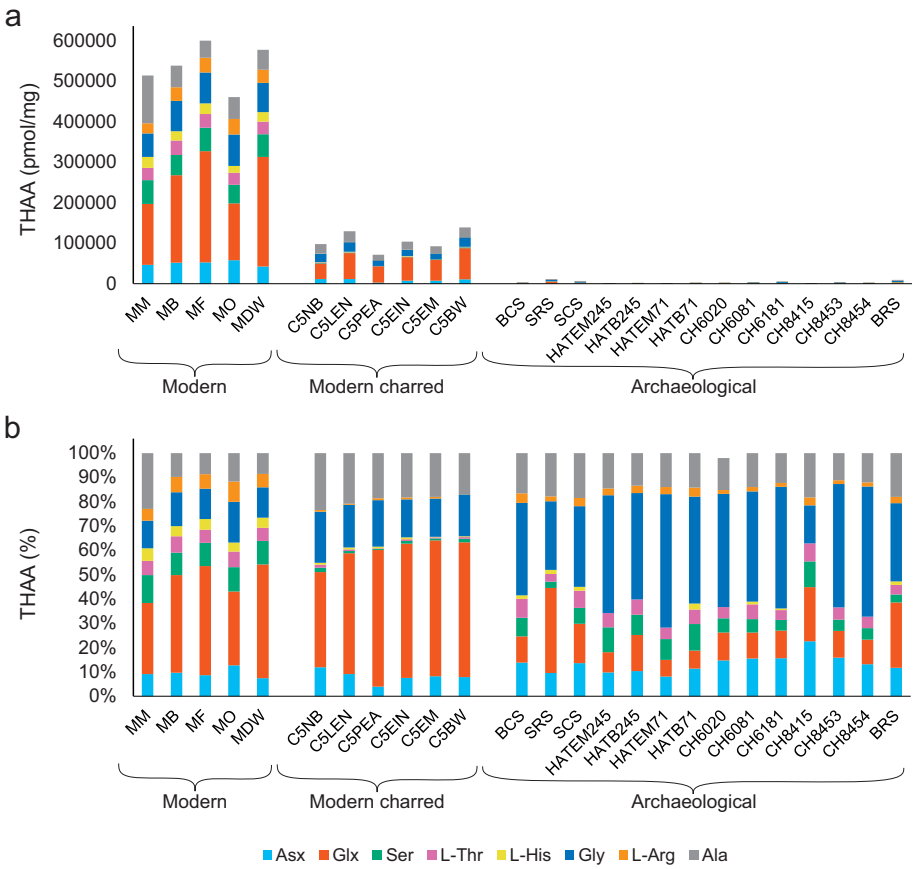

Figure 5.2 Absolute (a) and relative (b) content of amino acids in modern uncharred, modern charred and archaeological grains analysed via RP-HPLC.

To compare the relative contributions of amino acids, the concentrations have been normalised (Figure 5.2 b and Table 5.1.4). Glx represents the most abundant fraction in all the modern samples and it appears to be higher in the charred modern samples compared to the uncharred ones (∼40 % and 50 %, respectively). There is an evident reduction of Ser (from ∼10 % to ∼1 %), Thr (from ∼6 % to ∼1 %), L-His (from ∼4 % to ∼1 %) and L-Arg (from ∼6 % to ∼1 %) in modern charred grains compared to the uncharred ones. Ser, His and Arg have shown to be the first to degrade into new products due to their chemical instability (*e.g.*, Penkman 2005; Demarchi *et al.* 2013). Gly is formed by the decomposition of both Thr and Ser, which could explain its small

	Asx (%)		**Glx** (%)		**Ser** (%)		**L-Thr** (%)		**L-His** (%)		**Gly** (%)		**L-Arg** (%)		**Ala** (%)	
	$\overline{X}$	1σ	$\overline{X}$	1σ	$\overline{X}$	1σ	$\overline{X}$	1σ	$\overline{X}$	1σ	$\overline{X}$	1σ	$\overline{X}$	1σ	$\overline{X}$	1σ
Modern uncharred	9.5	2.0	38.3	8.1	10.0	0.9	6.0	0.6	4.3	0.5	13.4	2.1	6.2	1.3	12.4	6.1
Modern charred	8.1	2.6	51.9	6.7	1.1	0.5	0.7	0.3	0.6	0.3	17.7	2.1	0.6	0.3	19.3	2.4
Archaeological	13.3	3.7	14.5	8.1	6.7	2.7	5.5	1.4	0.8	0.9	41.7	11.1	2.6	0.8	14.9	2.5

Table 5.3 Relative amino acid contribution in modern uncharred, modern charred and archaeological charred grain samples.

relative enrichment in the charred modern samples (from ∼13 % to ∼18 %)(Demarchi *et al.* 2013).

Archaeological charred samples do not mirror the amino acid composition of their modern charred counterparts with Gly being the most abundant amino acid (∼42 %)(Table 5.1.4). Glx, Ala and Asx all contribute similarly (Glx: ∼15 %, Ala: ∼15 %, Asx: ∼13 %), followed by Ser and L-Thr (Ser: ∼7 %, L-Thr: ∼6 %) and finally by L-Arg and L-His (L-Arg: ∼3 %, L-His: ∼1 %). Glx is a particularly stable amino acid, so the loss of Glx in archaeological grains supports the hypothesis of microbial attack since glutamic acid is preferentially degraded by microorganisms (Balzer *et al.* 1997). The same pattern was previously observed by Styring *et al.* (2013). Some differences across the samples are however visible. For example, sample CH8415 from Çatalhöyük has the lowest content of Gly of the group, balanced by an increased amount of Asx and Ala. On the other hand, both barley and spelt from Rougier Street, York, have the highest content of Glx across the group, which might suggest that the material was somehow better protected from microbial attack. The samples from Rougier Street, after charring, went through partial if not complete waterlogging (Allison *et al.* 1990) and this could have helped to better preserve the remaining proteins. The higher concentration of THAAs in the samples from Rougier Street compared to the other archaeological grains seem to confirm that.

Amino acid racemisation

Next, the degree of amino acid racemisation was assessed and compared across the three grain groups since this is a powerful method to detect amino acid decomposition. As outlined in chapter 3, section 3.2.2, amino acids are chiral molecules and their two isomeric forms are denoted as L and D. In nature, almost all living organisms synthesize their proteins from L-amino acid (Bada 1985). When an organism is no longer biologically active, L-amino acids tend to decay into their D-isomer until there

is an equal amount of each; this reaction is known as racemisation. The rate of racemisation is influenced by the temperatures at which the material is exposed, its chemical nature and that of the environment. The more D-amino acids, the more degraded the material is. The experimental exposure to increasing temperatures simulate the degradation mechanisms of archaeological material (*e.g.*, Penkman *et al.* 2008; Crisp *et al.* 2013; Demarchi *et al.* 2013, 2016). Therefore, it is expected that the modern uncharred samples will have a degree of racemisation (expressed as THAA D/L) close to 0 for all the amino acids, whilst charred material should exhibit higher D/L values. Following, the degree of racemization will be evaluated looking at the D/L values of Glx and Asx.

As expected, both Glx and Asx in modern uncharred samples have an average D/L value close to 0 (0.026 ± 0.002 and 0.053 ± 0.001, respectively)(Figure 5.3 a). Charred modern grains show the highest degree of racemisation (Glx: 0.894 ± 0.045; Glx: 0.843 ± 0.068) whilst archaeological material is between the two (Glx: 0.338 ± 0.144; Glx: 0.276 ± 0.083)(Figure 5.3 a). The high degree of racemisation shown by the modern charred material indicates that the experimental technique used to observe variations in the δ^{13}C and δ^{15}N values after charring (24 h at 230 °C) is probably not representative of the charring of archaeological material, as it is inducing far greater levels of racemisation than have been experienced by the archaeological material.

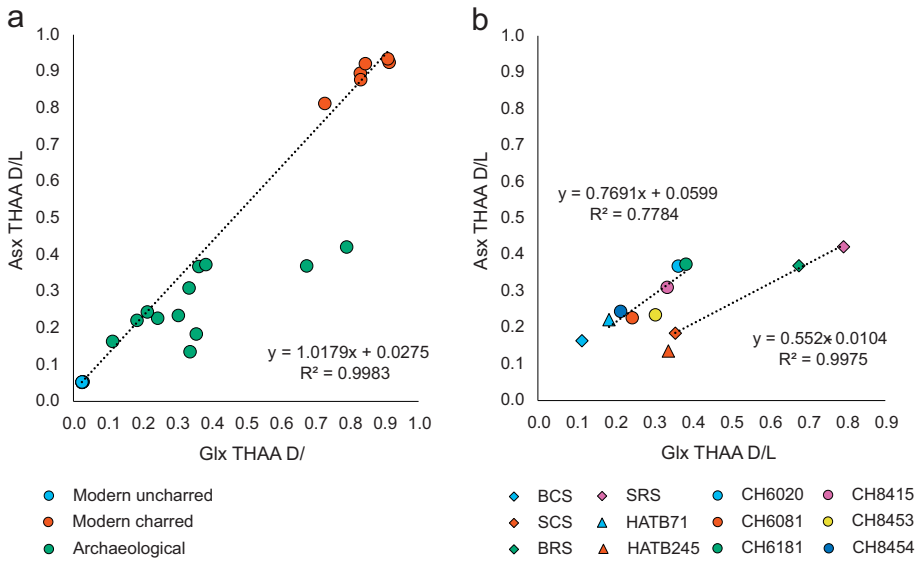

Figure 5.3 D/L values of glutamic acid (Glx) and aspartic acid (Asx) of modern uncharred, modern charred and archaeological grains (a) and D/L values of glutamic acid and aspartic acid of only archaeological grains (b). Asx D/L values of three of the samples from Roman York (b) are *ca.* half of the Glx D/L values, perhaps indicating a different decay mechanism.

The archaeological grains seem to follow two separate trajectories (Figure 5.3 b): in three samples from Roman York, Asx D/L values are *ca.* half of the Glx D/L values. On the contrary, in all the samples from Turkey (with the only exclusion of HATB245) Glx and Asx seem to show similar levels of racemisation, in accordance with the degradation patterns exhibited by modern charred grains. It is well known that Asx has an atypical pattern of racemisation which tends to be faster than that of other amino acids (Collins *et al.* 1999). It is therefore unexpected that the racemisation of Asx is slower than Glx in these samples, as Glx is a much slower racemiser in closed systems of protein. However, it is interesting to note that three out of four come from two archaeological contexts, Rougier Street and Coney Street from Roman York, with similar environmental and burial conditions. Spelt and barley from Rougier Street are the most degraded samples of the group, despite being younger than those from Çatalhöyük and Hattusha. This is also in contradiction with that observed in the previous section, where samples from Rougier Street appeared to be better preserved (Figure 5.2). Interestingly, the samples from Hattusha appear to be less degraded than those from Çatalhöyük which might suggest that when environmental, chemical and burial conditions are comparable, degradation of plant material could potentially be related with age, although more samples would be needed to confirm the trend. It is clear that a similar assumption can not be sustained when grains were recovered from environmentally distinguished archaeological sites, since remains from Hattusha and Coney Street show a similar degradation path, although chronologically distinct.

This pilot study has shown that a more extensive study is needed to explore the pattern and mechanisms of protein and amino acid degradation in grains. Concentrations of amino acids in charred archaeological material is significantly lower than that in experimentally charred modern grains, suggesting that archaeological grains cannot be considered a closed system. Moreover, the D/L values of Glx and Asx suggest that the degradation mechanisms are also highly unpredictable and possibly related to environmental, chemical and burial conditions. For these reasons, changes to the original isotopic composition can not be ruled out and therefore, the direct measurement of δ^{13}C and δ^{15}N of grain amino acids does not appear to be a viable route.

5.1.5 A possible solution: estimation of amino acid δ^{13}C and δ^{15}N values from their bulk values

From the results obtained via RP-HPLC analysis of modern and archaeological grains and from previous observations (Styring *et al.* 2013) any attempt of CSIA-AA from archaeological material is not advisable for two main reasons: i) the concentration of amino acids in archaeological grains is very low and the analysis cannot be considered micro-destructive, unless the grains come from a special archaeological unit such as that of Hattusha; ii) the amino acids in the archaeological grains seem to be, at least partially, what remains of microbial attack which, together with amino acid leaching can lead to an unknown degree of isotope fractionation. Future RP-HPLC analysis of more significant numbers of archaeological material, together with kinetic experiments to observe amino acid leaching at different temperatures and pHs, will be of help to understand amino acid degradation in grains. Nevertheless, the amino acid content in archaeological grains was shown to be minimal (Figure 5.2) and therefore their contribution is considered irrelevant to the overall bulk δ^{13}C and δ^{15}N values.

As for CSIA-AA, the amino acid synthesis in cereal grains follows predictable routes and therefore the δ^{13}C and δ^{15}N values can be theoretically estimated from the bulk δ^{13}C and δ^{15}N values (Styring *et al.* 2014a). For this reason, four of the modern Italian grains (MDW, MB, MF and MM) were prepared and analysed via GC-C-IRMS and the results were used to calculate amino acid to bulk isotope offsets both for carbon and nitrogen. The $\Delta^{15}N_{AA-bulk}$ and $\Delta^{13}C_{AA-bulk}$ values from MDW, MB and MF (all C_3 plants) were compared with those from two previous publications and they were found in accordance despite a certain degree of uncertainty (Table 5.1.5)(Styring *et al.* 2014a; Paolini *et al.* 2015).

C_4 plants exhibit a different metabolism which lead to a different isotope fractionation, at least for carbon (see chapter 33 section 3.1.1). As expected, $\Delta^{15}N_{AA-bulk}$ and $\Delta^{13}C_{AA-bulk}$ values of modern millet (MM), a C_4 plant, varied from those of the C_3 group, in some amino acids more than others (Table 5.1.5). In the future, the inclusion of new CSIA-AA of C_4 plants will confirm or not whether the observed AA-bulk offset values from MM are reproducible and, if so, be used to estimate δ^{13}C and δ^{15}N amino acid values from those of bulk C_4 archaeological material.

		$\Delta^{15}N_{AA-bulk}$																					
		Gly	**Err.**	**Glu**	**Err.**	**Ala**	**Err.**	**Asp**	**Err.**	**Pro**	**Err.**	**Val**	**Err.**	**Leu**	**Err.**	**Ile**	**Err.**	**Thr**	**Err.**	**Lys**	**Err.**	**Phe**	**Err.**	**Tyr**	**Err.**
C_3	**This study** ($n = 3$)	0.7	1.8	2.5	0.9	2.2	0.9	4.5	1.0	3.7	0.7	4.9	1.1	1.3	1.1	2.1	1.1	-4.7	1.2	-0.8	1.3	10.9	1.1	-0.8	1.3
	Styring et al. 2014	-1.4	1.1	0.3	1.1	0.9	0.6	1.7	0.9	2.2	0.8	1.3	0.9	-1.9	0.8							8.1	1.4		
	Paolini et al. 2015	-2.9	1.8	3.6	1.5	-0.1	1.2	-0.4	1.1	4.4	1.3	1.8	1.1	-2.6	1.2	-1.2	1.3	-7.1	1.8			7.8	0.9		
C_4	**This study** ($n = 1$)	2.5	0.2	2.2	0.1	2.4	0.5	4.2	0.3	4.2	0.4	5.7	0.9	1.2	0.4	2.4	0.4	1.2	0.4	1.6	0.6	7.4	0.6	1.6	0.6
Legumes	**This study** ($n = 2$)	1.1	1.2	3.9	0.9	3.5	1.1	4.8	0.9	9.4	1.1	7.0	1.7	1.7	1.1	2.4	1.3	-3.7	1.4	0.5	2.0	8.2	3.5		
	Styring et al. 2014	4.4	2.5	0.9	0.8	-0.3	0.9	1.9	1.1	3.7	0.7	0.3	0.5	-3.6	0.5							0.8	1.6		

		$\Delta^{13}C_{AA-bulk}$																							
		Gly	**Err.**	**Ser**	**Err.**	**Glu**	**Err.**	**Ala**	**Err.**	**Asp**	**Err.**	**Pro**	**Err.**	**Val**	**Err.**	**Leu**	**Err.**	**Ile**	**Err.**	**Thr**	**Err.**	**Phe**	**Err.**	**Tyr**	**Err.**
C_3	**This study** ($n = 3$)	9.4	1.7	11.9	1.9	-0.5	1.3	0.0	1.7	-1.6	1.2	0.4	1.0	-5.3	1.3	-8.4	1.2	-2.0	1.2	14.4	1.1	-3.0	2.0	-1.1	1.4
	Paolini et al. 2015	12.0	1.3			1.0	1.1	1.6	0.7	1.3	1.4	-1.5	0.9	-4.6	1.1	-7.9	0.7	-0.5	1.2	12.5	2.0	-0.8	1.6		
C_4	**This study** ($n = 1$)	5.2	1.0	13.0	1.8	0.9	0.9	0.0	1.6	1.5	0.8	1.9	0.8	-4.0	0.6	-7.6	0.4	0.1	0.5	12.7	1.2	-3.6	0.6	0.5	1.4
Legumes	**This study** ($n = 2$)	7.0	3.1	13.1	3.7	-0.5	0.6	1.2	1.7	0.5	0.9	2.4	1.2	-5.9	2.0	-9.4	1.4	-3.8	0.6	10.7	1.0	-4.2	0.6	-4.8	1.8

Table 5.4 $\Delta^{15}N_{AA-bulk}$ and $\Delta^{13}C_{AA-bulk}$ values of modern C_3 and C_4 cereals and legumes analysed for this project (referred to as "this study") and from two previous studies (Styring *et al.* 2014a; Paolini *et al.* 2015). The error associated to the measurements from this study where $n > 1$ is the error propagated that accounts for the highest analytical error among the samples from the GC-C-IRMS analysis and 1σ of the AA-bulk values of the samples.

CSIA-AA was additionally performed on two modern legume samples from Italy, chickpeas (MC, *Cicer arietinum*) and lentils (ML, *Lens culinaris*). The samples were purchased from a farm located in an area of the Lazio region known as *Viterbese*. As expected, the calculated $\Delta^{15}N_{AA-bulk}$ and $\Delta^{13}C_{AA-bulk}$ offset values varied considerably between the two samples, and also from published values (Styring *et al.* 2014a). It is difficult to tell if the higher observed variability compared to the C_3 group is related to the species (chickpea and lentil from this study and broadbean and pea from Styring *et al.* (2014a)) or to other factors. Nevertheless, it is clear that a more extensive research work on legumes seems to be needed before bulk isotope data of archaeological material can be used to predict their corresponding amino acid values.

5.1.6 Final considerations on stable isotope analysis of amino acids from archaeological grains

The importance of including edible plants in the reconstruction of past human dietary habits is essential for the central role they had in the diet of many human populations. Their caloric contribution has been often overlooked in stable isotope analysis applications, mainly due to previous doubts about the authenticity of $\delta^{13}C$ and $\delta^{15}N$ values of archaeological plants. As a result, many scholars have used $\delta^{13}C$ and $\delta^{15}N$ values of bone collagen from terrestrial animals to estimate those of plants by applying a known diet to tissue offsets. This is dangerous for two main reasons: i) there is a lot of uncertainty around the predictability of diet to tissue offsets values and this uncertainty tends to be underestimated when using mixing models (see chapter 3 sections 3.1.1 and 3.1.2); ii) plants destined for human consumption and to livestock are often different, which makes them members of distinct trophic webs. If the growing conditions and/or cultivation strategies are different between the two, plants destined to human consumption can exhibit $\delta^{13}C$ and $\delta^{15}N$ values different from those eaten by the animals. Despite the extensive work on the effect of manuring in the investigation of past human dietary habits (*e.g.*, Bogaard *et al.* 2007; Fraser *et al.* 2011; Szpak 2014; Styring *et al.* 2014b), this is often overlooked and could lead to erroneous conclusions about past human diets. It is commonly accepted in the field that a higher $\delta^{15}N$ of human collagen corresponds to a higher consumption of higher trophic level organisms, such as omnivores and marine fish. However, if the cereals were extensively manured, their values can be equal or even higher than those of animal products. The production of cereals in the Roman Empire was on a large scale and different cultivation strategies are reported by the ancient sources, such as manuring and crop rotation. Moreover,

cereals were likely to have come from different geographical regions in the Empire, following a complex system of distribution around the Mediterranean and beyond (see chapter 2, section 2.1). A recent publication by (O'Connell *et al.* 2019) on SIA applied to grains from Roman *Portus* confirms the existence of a wide variability of both δ^{13}C and δ^{15}N values of cereals at the heart of the Empire, most likely reflecting different environments and/or crop strategies.

In addition, when using the SIA bulk approach, the contribution of cereals is difficult to distinguish from that of terrestrial animal products, and therefore they are often excluded from the investigation. This is a methodological limitation that has to be accepted. However, CSIA-AA has the potential to help in this regard (Styring *et al.* 2015).

Although the results from the RP-HPLC preliminary study have shown that endogenous amino acids are present in low concentrations and that they are diagenetically altered, therefore suggesting that their isotopic composition might not reflect the one they had prior to deposition, it was also shown that δ^{13}C and δ^{15}N values from at least C_3 cereals can be predicted from their bulk values, accepting a certain degree of uncertainty. It is hoped that in the future this approach can be applied to other nutritionally relevant plants, such as C_4 plants and legumes, once more data from modern material has been analysed.

5.2 Exploring food webs in the Roman Mediterranean

In this section, the carbon and nitrogen isotopic signatures of cereals, legumes, animals and marine fish from Herculaneum and comparable archaeological contexts will be discussed with the aim to detect possible husbandry and crop management strategies which would be of help not only to better interpret the data from the human assemblage but also for the study of the ancient economy from a specific geographic area of the Empire.

Four charred C_3 cereal samples, four charred legume samples and one charred C_4 representative from Herculaneum were analysed via EA-IRMS analysis to be included in the study. These were: *1703b* barley, and *1703w* wheat, identified with archive numbers 1703/76981; *1895e* emmer, identified with archive numbers 1895/77175; *723w* wheat, identified with archive numbers 723/76000; *200b* broadbeans, identified with archive numbers 200/75476; *692l* lentils, identified with archive numbers 692/75969; *2314c*, chickpeas identified with archive numbers 2314/77610; *2317p* peas, identified

with archive numbers 2317/77613; *2327m* millet, identified with archive numbers 2327/76000.

Only a few animal remains, specifically dogs and sheep, were found associated with the Herculaneum human assemblage. All the other animal remains following discussed have been provided by the Pompeii Archaeological Research Project: Porta Stabia (PARP:PS)(2005–) and by the Anglo-American Project in Pompeii (AAPP), that is now concluded (1994–2006), from two different area of the ancient city of Pompeii, Naples. The PARP:PS project explores the sub-elite area of *Regio I* and *Regio VIII*, focusing on the excavations of *Insulae VIII.7* and *I.1*. The samples sent for analysis consisted of domestic herbivores, marine fish and other terrestrial species mainly from the 1^{st} century AD levels of the excavations. The AAPP project was focused instead on the investigation of *Insula* VI.1, a commercial and residential block near the Herculaneum gate, on the northern-west side of the ancient town. The marine fish assemblage analysed for this thesis comes from the House of the Surgeon, considered to be one of the oldest buildings in Pompeii, constructed between 200 and 130 BC (Anderson and Robinson 2018). Some marine specimens from Medieval Spain and Medieval Santa Severa, Italy, were also included, kindly provided by Dr K. K. Richter and Dr M. M. Alexander, respectively. The species identification of the marine and small animal samples, where missing, was conducted by Dr Harry Robson (samples from AAPP) and by Jan Bakker (samples from PARP:PS). Information and isotope values of the plant and animal remains are provided in Appendix D.

5.2.1 ZooMS analysis to clarify taxonomy of bone samples

Zooarchaeology by Mass Spectrometry (ZooMS) is a proteomic method recently developed which allows the identification of animal species by some peptides in their collagen (Buckley *et al.* 2009). ZooMS was applied to the terrestrial animal assemblage from this study after first ambiguous results from SIA. In particular, the cat sample from Pompeii Porta Stabia (*PSFE1*) exhibited very low δ^{15}N values, which is in contradiction with the trophic level of this carnivore animal and one dog from Herculaneum *fornice* (*EF7DOG*) showed lower bulk δ^{15}N and δ^{13}C values compared to those of other dogs from the same context.

As previously discussed (see chapter 4 sections 4.3.2 and 4.4.2), the amino acid sequence of collagen can vary to a more or less extent from one species to another, depending on their evolutionary history (Buckley 2018). The extensive comparison of collagen sequences from different animal species in the last few years allowed the detection of amino acid substitution in specific peptides which can distinguish some *taxa*

from others. The detection of these "markers" is made easy by the utilisation of a Matrix Assisted Laser Desorption Ionization (MALDI) mass spectrometer in conjunction with the Time of Flight (ToF) mass analyzer, which determines the charge ratio (m/z) of the peptides by measuring the time that each peptide ion takes to traverse the flight tube in relation to the ionisation energy (Buckley 2018). ZooMS is often applied in conjunction to SIA investigations, particularly when the animal samples are fragmentary and therefore difficult to identify using classical zooarchaeological approaches. Moreover, some species are difficult to discriminate because of their phylogenetic proximity. This is often the case of sheep and goat, which often end up being classified as "ovicaprid". However, these two species are often managed differently by humans and therefore their identifications can have important repercussions in the interpretation of SIA data (Buckley *et al.* 2010).

Method

Briefly, a small portion of the extracted collagen (less than 1 mg) was added into a new sterile eppendorf tube together with 50 μL of 50 mM ammonium bicarbonate buffer (NH_4HCO_3, AmBic, pH 8) and 1 μL of trypsin (0.4 μg/μL). Samples were incubated at 37 °C overnight to perform collagen digestion using a heating block. The day after, samples were centrifuge at maximum speed and 1 μL of 5 % v/v trifluoroacetic acid (TFA) was added to each sample to stop the trypsin action. Peptide extraction was performed by using C_{18} resin ZipTip® pipette tips (Millipore) previously conditioned using 50 μL of 50 % acetonitrile (ACN) and 0.1 % v/v TFA (conditioning solution) to remove possible contaminants. The peptides were then eluted into a new eppendorf containing new conditioning solution. 1 μL of eluted peptides mixed with 1 μL of matrix solution (α-cyano-hydroxycinnamic acid) were spotted in triplicates on a ground steel plate. The plate was analysed using a Bruker Ultraflex III mass spectrometer (MALDI-TOF system) at the Centre of Excellence in Mass Spectrometry facility of the University of York.

Species were identified manually by screening the mass spectra for peptide m/z markers using the open-source software mMass[1] (Strohalm *et al.* 2010). The signal-to-noise threshold was set at 3.0 and the relative intensity threshold at 0.3. The identification was performed using previously published markers (*e.g.* Buckley *et al.* 2010; Buckley and Kansa 2011; Kirby *et al.* 2013; Stewart *et al.* 2013; Welker *et al.* 2015; Buckley 2016; Buckley *et al.* 2017; McGrath *et al.* 2019).

[1]mMass can be downloaded at this link.

Results

The results from the ZooMS analysis of the terrestrial animals from this study are worrying. Of a total of 35 samples, 10 were assigned to a different *taxon* than the one identified through the classical morphological identification. One of these was from the Herculaneum *fornici* context, one from the assemblage from Velia, and the remaining 8 from that of Porta Stabia. The attribution of a faunal skeletal element to the wrong species can have serious implications in the interpretation of the human diet, particularly when the remain is classified to the wrong animal group (*e.g.*, wild herbivore instead of domestic herbivore or domestic herbivore instead of domestic omnivore). Therefore, it is recommended that, unless the morphological identification is carried out on morphologically identifiable bone elements, any isotopic investigation should rely on a preliminary screening of the animal remains via ZooMS or any other biomolecular approach. In other cases, ZooMS allowed the attribution of those remains that were of dubious identification to a *taxon*; this is the case of two ovicaprids from the Herculaneum *fornici*, which were identified via ZooMS as *Ovis* and of one herbivore tooth from the same context assigned via ZooMS to *Bos*.

In other cases however, it was not possible to assign the samples to a precise species using ZooMS. It is accepted that ZooMS has some limitations due to the similarity of the collagen amino acid sequence in closely related *taxa*, which make it often difficult to classify further than the genus (*e.g.*, Buckley *et al.* 2017). This is the case of the horse (*Equus caballus*) samples from Velia and from *Villa dei Papiri* at Herculaneum, identified thanks to morphological analysis but not via ZooMS, which can only attribute these remains to the level of the genus (*i.e.*, *Equus*). Moreover, the identification via ZooMS can sometimes be challenging depending on the degradation of collagen. This is the case of sample *PSG2*, morphologically classified as goat and instead assigned to either the *Ovis*, *Cervus* or *Dama* genus, or that of sample *PSP2* which was not possible to assign via ZooMS to any *taxa*.

As for the three samples morphologically identified as chickens, it has to be acknowledged that collagen fingerprinting identification of birds is made challenging by the high conservation of the amino acid sequence of collagen Buckley (2018). Nevertheless, identification between families seems to be achievable by observing the presence of three m/z markers named A (1578.8 m/z) B (1604.8 m/z) and C (1620.8 m/z) by Eda *et al.* (2020). 1578.8 m/z was observed in pheasant (*Phasianus*) samples while the same was not detected in chickens (*Gallus*), which instead exhibit the 1604.8 m/z and 1620.8 m/z markers, that are absent in pheasants (Buckley 2018; Eda *et al.* 2020). Ducks (*Anas*) on the contrary can be potentially identified by the absence of 1578.8 m/z

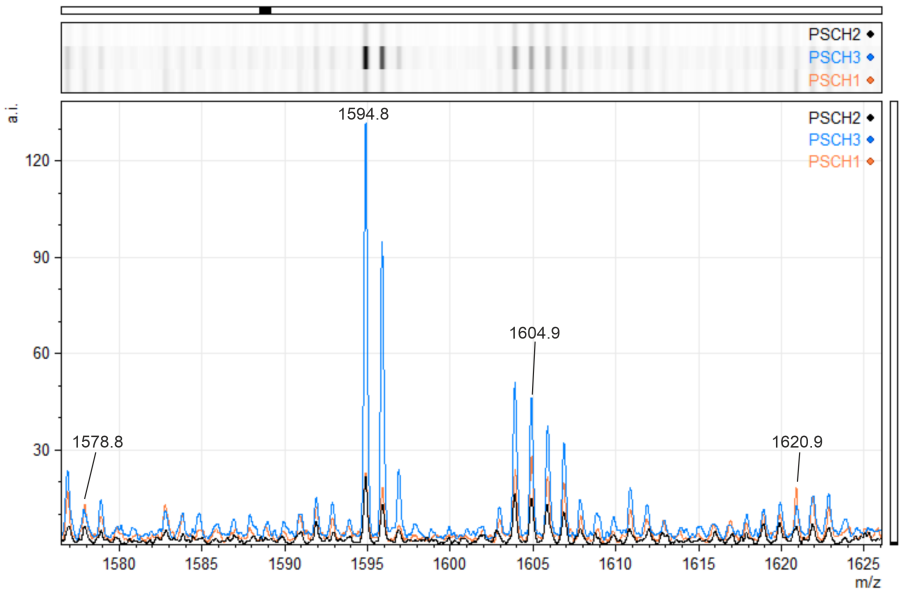

Figure 5.4 MALDI-TOF-MS profile of the three samples from Porta Stabia identified as *Gallus gallus* by morphological analysis.

and the presence of two markers at 1616.8 m/z and 1632.8 m/z (Buckley 2018). The three chicken samples from Porta Stabia could potentially be assigned to the *Gallus* genus (Figure 5.4). However, peaks at 1604.8 m/z and 1620.8m/z are lower in intensity compared to those from the *Gallus* profile reported by Buckley (2018) and, although marker 1578.8 m/z is barely detectable, its hydroxylated counterpart at 1594.8 m/z is very high in intensity, while the same it is absent in Buckley (2018). Therefore, the ZooMS identification of these three samples remains dubious.

Thanks to the application of ZooMS to the animal assemblage used in this study, it was possible to avoid their attribution to the wrong animal food category. This could have caused major problems in the interpretation of the human isotopic signals both at the bulk and amino acid level. With a more confident assignment to specific *taxa*, it is also possible to observe any relevant pattern in the δ^{15}N and δ^{13}C values that can be indicative of husbandry practices in the Roman Mediterranean, which is discussed in the following section.

ID	Provenance	Age	Element	Morphological identification	ZooMS identification	Peptides												
						P1	A1	A2	B	C	P2	D	E	F1	F2	G1	G2	Other
EF12DOG2	*fornici*	AD 79	vertebra	*Canis familiaris*	*Canis*	1106			1454	1567		2131	2820	2853		2984	3000	1577
EF12DOG1	*fornici*	AD 79	atlante	*Canis familiaris*	*Canis*	1106			1454	1567		2131	2820	2853		2984	3000	1577
EF11DOG	*fornici*	AD 79	vertebra	*Canis familiaris*	*Canis*	1106			1454			2131	2820			2984	3000	1577
EF7DOG?	*fornici*	AD 79	fragments	possible *Canis familiaris*	*Bos*	1106	1193	1209	1428	1581	1649	2131	2792	2853		3018	3034	1577
EF7OC	*fornici*	AD 79	vertebra	Ovicaprid	*Ovis*	1106			1428	1581	1649	2131	2792	2883		3018	3034	
EF8BOS?	*fornici*	AD 79	tooth	Herbivore	*Bos*	1106	1193	1209	1428		1649	2131				3018	3034	
EF10OC	*fornici*	AD 79	vertebra	Ovicaprid	*Ovis*	1106			1428	1581	1649	2131	2792	2883		3018	3034	
EF8SG	*fornici*	AD 79	long bone	*Ovis aries*	*Ovis*	1106	1181	1197	1428	1581	1649	2131	2792	2883		3018	3034	
VEHO1	Velia	I - II AD	NA	*Equus caballus*	*Equus*	1106			1428	1551		2145		2884		2984	3000	
VEHO2	Velia	I - II AD	NA	*Equus caballus*	*Equus*	1106			1428	1551		2145	2820	2884		2984	3000	
VEHO3	Velia	I - II AD	NA	*Equus caballus*	*Equus*	1106			1428	1551		2145	2820	2884		2984	3000	
VEHO4	Velia	I - II AD	NA	*Equus caballus*	*Equus*	1106			1428	1551		2145		2884		2984	3000	
VEDE1	Velia	I - II AD	NA	*Capreolus capreolus*	*Capreolus*	1105			1428		1649	2131					3059	
VESH1	Velia	I - II AD	NA	*Ovis aries*	*Capra*	1106	1181		1428	1581	1649	2131	2792	2883		3078	3094	
VPHO	Villa dei Papiri	AD 79	NA	*Equus caballus*	*Equus*	1106	1183		1428	1551		2145	2820	2884		2984	3000	
PSFE1	Porta Stabia	I AD	rib	*Felis catus*	*Capra*	1106	1181	1197	1428	1581	1649	2131	2792	2883	2899	3078	3094	
PSSG1	Porta Stabia	I AD	pelvis	ovicaprid	*Sus*	1106			1454			2131	2820	2883		3018	3034	
PSSG2	Porta Stabia	I AD	phalanx	ovicaprid	*Sus*	1106		1197	1454		1648	2131					3034	
PSSG3	Porta Stabia	I AD	phalanx	ovicaprid	*Capreolus*	1105		1197	1428		1649	2131				3043	3059	
PSG1	Porta Stabia	I AD	femur	*Capra hircus*	*Sus*	1106			1454	1551	1648	2131	2820	2883		3018	3034	
PSG2	Porta Stabia	I AD	metacarpal	*Capra hircus*	*Ovis/ Cervus/Dama*	1106			1428		1649	2131	2792	2883	2899	3018	3034	
PSG3	Porta Stabia	I AD	tibia	*Capra hircus*	*Sus*	1106			1454	1551	1648	2131	2820	2883		3018	3034	
PSS1	Porta Stabia	I AD	humerus	*Ovis aries*	*Sus*	1106	1181	1197	1454	1551	1648	2131	2820	2883		3018	3034	
PSC1	Porta Stabia	I BC	phalanx	*Bos taurus*	*Bos*	1106	1193	1209	1428	1581	1649	2131	2792	2853		3018	3034	
PSC2	Porta Stabia	I BC	phalanx	*Bos taurus*	*Bos*	1106	1193	1209	1428		1649	2131	2792	2853		3018	3034	
PSP1	Porta Stabia	I AD	tibia	*Sus scrofa*	*Sus*	1106			1454	1551	1648	2131						
PSP2	Porta Stabia	I AD	tibia	*Sus scrofa*	no ID													
PSP3	Porta Stabia	I AD	tibia	*Sus scrofa*	*Sus*	1106			1454	1551		2131						
PSP4	Porta Stabia	I AD	jaw	*Sus scrofa*	*Sus*	1106			1454	1551		2131	2820	2883		3018	3034	
PSP5	Porta Stabia	I AD	jaw	*Sus scrofa*	*Sus*	1106	1181	1197	1454	1551	1648	2131	2820	2883		3018	3034	
PSP6	Porta Stabia	I AD	radius	*Sus scrofa*	*Sus*	1106	1181	1197	1454			2131	2820			3018	3034	
PSP7	Porta Stabia	I AD	radius cap	*Sus scrofa*	*Sus*	1106	1181	1197	1454	1551	1648	2131	2820	2883	2899	3018	3034	
PSCH1	Porta Stabia	I AD	humerus	*Gallus gallus domesticus*	possible *Gallus*													1605 + 1621
PSCH2	Porta Stabia	Early I AD	tibio tarsus	*Gallus gallus domesticus*	possible *Gallus*													1605 + 1621
PSCH3	Porta Stabia	Early I AD	femur	*Gallus gallus domesticus*	possible *Gallus*													1605 + 1621

Table 5.5 ZooMS identification of the terrestrial animal remains included in this study on the basis of collagen peptide markers.

5.2.2 SIA and CSIA-AA results and discussion

Following, the results obtained by bulk SIA and CSIA will be discussed separately. The bulk values of charred cereals and legumes were corrected for charring by subtracting 0.31 ‰ and 0.11 ‰ to the measured δ^{15}N and δ^{13}C values, respectively (Nitsch *et al.* 2015).

SIA

The bulk δ^{13}C and δ^{15}N values obtained from the analysis of the cereal, legume and fauna remains allow the clear distinction of the terrestrial and marine food webs (Mann-Whitney U Test, p-value = 6.453e-10 for δ^{15}N and p-value = 5.585e-13 for δ^{13}C)(Figure 5.5 a).

The C_3 cereals from Herculaneum (*1703b, 1895e, 723w, 1703w*) exhibit variability in their isotopic values, particularly in their δ^{15}N ones (mean and 1σ, n = 4, δ^{15}N = +4.08 ± 2.58 and δ^{13}C = -23.33 ± 1.16). The bulk values of five additional C_3 cereal samples from comparable contexts previously published (Pate *et al.* 2016; O'Connell *et al.* 2019) were also included with the aim to consider a larger variability of values in this food category, since it is believed that in Imperial Italy C_3 cereals, even if partially locally grown, were extensively produced in the Provinces and then distributed around the Empire (see chapter 2 section 2.1 and 2.1.2). The additionally included C_3 cereals are one barley sample from Pompeii (*BarleyP*)(Pate *et al.* 2016) and four wheat samples from the early 2nd century AD *Portus Romae* (*LBCFA16F, LBCFD16E, LBTA1012I, LBTD1012H&I*)(O'Connell *et al.* 2019) and they were also corrected for charring after Nitsch *et al.* (2015). After the inclusion of these samples (n = 9), the mean bulk values of C_3 cereals are δ^{15}N = +5.69 ± 3.8 and δ^{13}C = -23.27 ± 0.78 (Figure 5.5 a). The consistency of the δ^{13}C values suggest that these cereals were all produced under similar growing conditions and perhaps in the same geographical region (O'Connell *et al.* 2019), while the high δ^{15}N values of some of the cereals suggest intensive manuring of these crops (Bogaard *et al.* 2007). Four pulse samples from Herculaneum (*200b, 692l, 2314c, 2317p*) were also included and the results represent, to my knowledge, the first evidence of legume bulk δ^{13}C and δ^{15}N values from Imperial Italy. As expected from this plant category, the δ^{15}N values are ^{15}N-depleted since they are able to fix the nitrogen from the atmosphere (mean and 1σ, n = 4, δ^{15}N = +0.35 ± 0.6)(*e.g.*, Styring *et al.* 2014a). The δ^{13}C values are homogeneous in three of the samples, while the broadbean (200b) value results more ^{13}C-depleted (mean and 1σ, n = 4, δ^{13}C = -23.03 ± 2.38) probably reflecting a different crop management strategy

or a different growing location (Figure 5.5 a). One millet sample from Herculaneum (*2327m*) was also analysed to represent the C_4 plant group and this shows $\delta^{13}C$ and $\delta^{15}N$ values typical of C_4 plants (see chapter 3 section 3.1.1)(Figure 5.5 a).

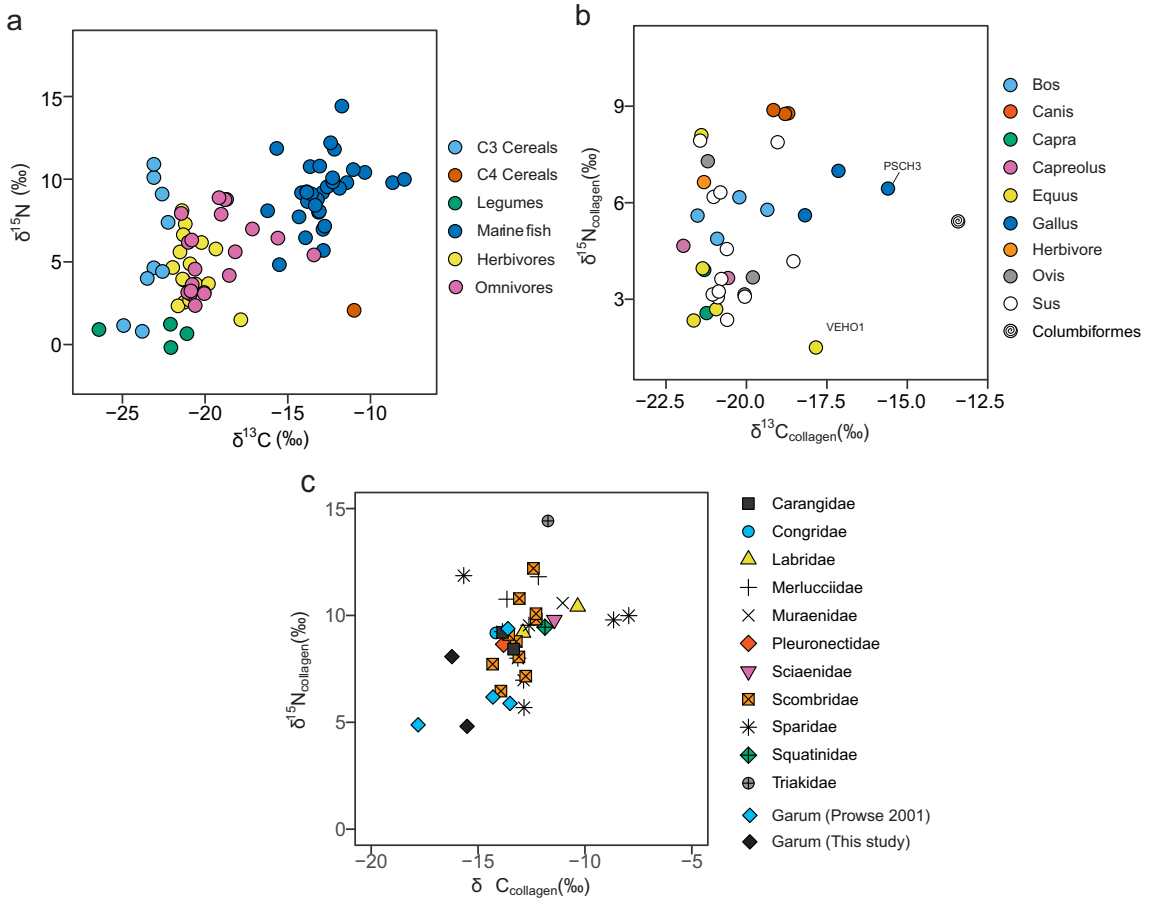

Figure 5.5 Bulk $\delta^{13}C$ and $\delta^{15}N$ of plant and fauna remains from Herculaneum and comparable archaeological contexts: a, divided by groups; b, only terrestrial animals; c, only marine fish.

Terrestrial herbivores and terrestrial omnivores from this assemblage are statistically discriminated only by their $\delta^{13}C$ values (Mann-Whitney U Test, p-value = 0.1681 for nitrogen and p-value = 0.006428 for carbon)(Figure 5.5 a). Clearly, the *Sus* samples exhibit a high degree of variability of bulk $\delta^{15}N$ and $\delta^{13}C$ values (Figure 5.5 b). Pigs are the most versatile animals in terms of where they can be raised and what they can eat. According to Columella, pigs should better be farmed in woodlands where they can feed from different fruits throughout the year; if there is no woodland in the area, he conveys that grazing is a possibility and, in this case, marshland areas, with worms and roots that pigs can eat, are preferred (*Rust.* 7.9). Lower bulk $\delta^{15}N$ and $\delta^{13}C$ values perhaps suggest that the animals were feeding on low trophic level organisms (such as plants and fungi)(this could be the case of samples *PSG1, PSG3,*

PSP4, PSP6, PSP7, PSS1, PSSG1 and *PSSG2*). The three chicken samples from Porta Stabia (*Gallus*, *PSCH1*, *PSCH2*, *PSCH3*) exhibit bulk carbon and nitrogen signatures that reflect a diet composed of multiple sources including C_3 and C_4 plants (Figure 5.5 b). Sample *PSCH3* exhibits the highest bulk δ^{13}C values of the three, suggesting that C_4 consumption was high in this animal. This would appear to be the case also of one of the horses from Velia (*Equus*, VEHO1)(Figure 5.5 b). The most ^{13}C-enriched value is the one exhibited by the sample identified with the Columbiformes order, therefore a pigeon or a dove (*PSB1*). According to the ancient sources, millet should be preferred to feed these animals when bred, and this seems to be the case of the individual here analysed (Malossini 2011)(Figure 5.5 b). Two of the dog samples exhibit almost identical δ^{13}C and δ^{15}N values (*Canis*, *EF12DOG1*, *EF12DOG2*); since these two bone fragments were recovered from the same *fornice*, it is possible that they belong to the same individual.

The bulk δ^{13}C and δ^{15}N values of the marine fish samples are highly variable across the group and they do not seem to be related to the sample trophic position, with the only exception of the school shark sample (*SSF2*, family Triakidae)(Figure 5.5 c). However, some differences in their isotope signature were expected, since some of the specimens here considered exhibit different dietary habits. For example, fish of the family Scombridae are carnivore predators, while fish from the family Sparidae, although carnivore, are opportunistic feeders and mainly bottom-dwellers. However, these different feeding habits are not reflected in their δ^{13}C and δ^{15}N values using the SIA approach (Mann-Whitney U Test, p-value = 0.894 for δ^{15}N and p-value = 0.6893 for δ^{13}C). Fish in the Roman Mediterranean were caught and farmed in different ways and from different ecosystems, which can in part explain the wide range of δ^{13}C and δ^{15}N values. More negative δ^{13}C values, such as that of *HSSP3*, one of the Sparidae samples from the House of the Surgeon and those of two *garum* samples made of remains of the Clupeidae family from the same archaeological context, could perhaps reflect an ecosystem partially influenced by terrestrial inputs, such as an estuary (Figure 5.5 c). Fish farming in coastal lagoons was common in the Roman Mediterranean (see chapter 2, section 2.1.7). However, the majority of the fish here analysed exhibit higher δ^{13}C values, suggesting either that the farming of fish in lagoons was not so common as previously thought or that freshwater discharges were not enough to determine a clear change in the δ^{13}C values (Vizzini *et al.* 2005). As for the two *garum* samples, it is possible that at least part of the fish destined for the production of *garum* was farmed into fishponds or coastal lagoons partially supplied with freshwater, which would explain the more negative δ^{13}C values of these two samples (Marzano 2013b,

100). However, when the samples analysed by Prowse (2001) are also included in the discussion, it appears that there is a certain degree of variability of δ^{13}C and δ^{15}N values also in the fish used for the production of *garum* in Roman Italy, although they tend to have on average lower δ^{15}N values, probably for the small dimension of the fish, at least in the samples here considered (Figure 5.5 c). The variability of δ^{13}C values instead confirm the utilisation of different fish catching/farming strategies adopted by the Romans. On the other hand, it is more difficult to explain the differences observed in the δ^{15}N values, which does not seem to be related either to the species or to the total length of the sample, when the latter could be estimated (Appendix D Table D.1). It is possible however that the variability of the ecological backgrounds, and therefore of the fishing/farming strategies adopted by the Romans, is reflected in the δ^{15}N values of the trophic baseline. Nevertheless, the average bulk δ^{15}N value (+ 9.25 ± 1.94 ‰, $n = 32$) is in line with that observed in other archaeological Mediterranean contexts (Craig *et al.* 2009; Vika and Theodoropoulou 2012; Craig *et al.* 2013; Alexander *et al.* 2015; O'Connell *et al.* 2019) and lower than that from Atlantic fish (Jay and Richards 2007; Müldner and Richards 2007; López-Costas and Müldner 2016; Cubas *et al.* 2019). It has been observed that nitrates in the Mediterranean sea are depleted in ^{15}N (δ^{15}N = + 3.4 ± 0.5 ‰, in the western Mediterranean basin) compared to those from deep world ocean (δ^{15}N = +5 ‰)(Pantoja *et al.* 2002). This is only one of the possible explanations for the lower δ^{15}N values of fish in the Mediterranean sea compared to those from the Atlantic, for which more studies are needed. Notably, the δ^{15}N values of fish in the Mediterranean can be lower than those of cereals, as shown in Figure 5.5 a. For this reason, and also considering the high consumption of cereals which contribute to the synthesis of non-essential amino acids, it is difficult, if not impossible, to observe marine consumption in Mediterrenean contexts using the bulk SIA approach (Prowse *et al.* 2004, 2005; Craig *et al.* 2013).

CSIA

The results obtained by CSIA, which was carried out on a sub-sample of the assemblage analysed by bulk SIA, allow a better distinction of the trophic levels inside each food web and also to observe interesting patterns which could be indicative of animal and crop management strategies.

The comparison of $\delta^{15}N_{Phe}$ and $\delta^{15}N_{Glx}$ values allows the determination of the trophic position of specimens from both terrestrial and marine ecosystems (see chapter 3 section 3.2.1). When the data from this study are visualised using the $\delta^{15}N_{Phe}$-$\delta^{15}N_{Glx}$ cross plot, a more high-resolution insight into the trophic relationships of the remains is

achieved (Figure 5.6). The trophic level lines were calculated using equation 3.7, using the $\beta_{Glx-Phe}$ and the $\Delta^{15}N_{Glx-Phe}$ values determined by Chikaraishi *et al.* (2009, 2010), specifically $\beta_{Glx-Phe}$ = -3.4 ‰ and $\beta_{Glx-Phe}$ = +8.4 ‰ for aquatic and terrestrial ecosystems, respectively, while it is assumed that $\Delta^{15}N_{Glx-Phe}$ at each trophic transfer is +7.6 ‰ in both ecosystems.

Unfortunately, as explained in the previous section 5.1.5, amino acid $\delta^{13}C$ and $\delta^{15}N$ values could only be estimated for the C_3 cereal samples and not for C_4 plants and legumes (Figure 5.6).

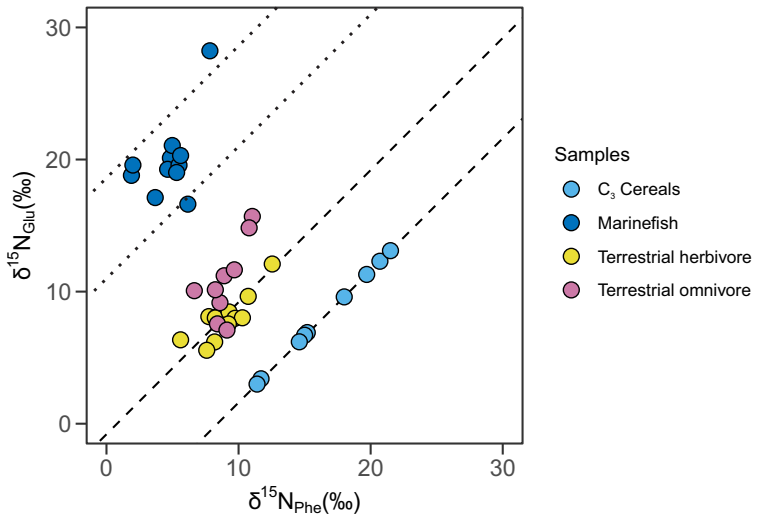

Figure 5.6 $\delta^{15}N_{Phe}$ and $\delta^{15}N_{Glx}$ values of cereals, terrestrial herbivores, terrestrial omnivores and marine fish from Herculaneum and comparable archaeological contexts. Dashed lines identify terrestrial trophic levels, dotted lines identify marine trophic levels

The distribution of $\delta^{15}N$ values of Glx and Phe in the C_3 cereals suggests that at least part of the C_3 cereals consumed at the heart of the Empire belonged to a food web that is different from that of the terrestrial animals. In particular, the majority of the terrestrial animals exhibit $\delta^{15}N_{phe}$ values that are lower than those of the estimated $\delta^{15}N_{Phe}$ values in the cereals (terrestrial animals: median = +9.28, Q1 = +8.27, Q3 = +12.55; C_3 cereals: median = +15.2, Q1 = +14.6, Q3 = +19.7). This indicates that the production of cereals followed specific strategies (and/or was carried out in geographically distinct regions) that make them isotopically different from the terrestrial animals, thus confirms the economic and nutritional role that the Romans were giving to this food category (Figure 5.6).

The $\delta^{15}N_{Phe}$ values of the two roe deer samples (*Capreolus*, *PSSG3* and *VEDE1*) are similar ($\delta^{15}N_{Phe}$ = +8.74 ± 0.77 ‰) although they come from two archaeological sites that are *ca.* 100 km distant from each other, suggesting an isotopic homogeneity

of the wild vegetation in the area (Figure 5.7 a). The fact that the two dogs (*Canis*, *EF11DOG* and *EF12DOG2*) from the Herculaneum *fornici* exhibit higher $\delta^{15}N_{Phe}$ values compared to the other terrestrial omnivores, suggest that their diet might have included the same C_3 cereals destined to human consumption, as it has to be expected due to the role that these animals had in the Roman society (MacKinnon 2010b)(Figure 5.7 a). Indeed, Varro suggests to give the dogs bread made with barley flour soaked in milk (*Rust.* 2.9) and Columella to feed them with the same barley flour destined to the sheep, or with bread made with wheat or *farro* and soaked in the water used to cook broadbeans (*Rust.* 7.12). Curiously, higher $\delta^{15}N_{Phe}$ values are also observed in sheep *EF8SG* from *fornice* 8 (Figure 5.7 a). It is clear that the animals recovered from the Herculaneum *fornici* must have had a certain importance, either economical or sentimental, for the humans that decided to try to save them in such a tragic circumstance. The *EF8SG* sheep was perhaps living in close contact with humans, which is not unlikely in an urban context, and therefore probably fed with what was available in the house. Slightly ^{15}N-enriched $\delta^{15}N_{Phe}$ values could perhaps suggest a small C_3 cereals contribution to the diet of other animals from the assemblage (*EF7OC, EF10OC, PSC2, PSG2*).

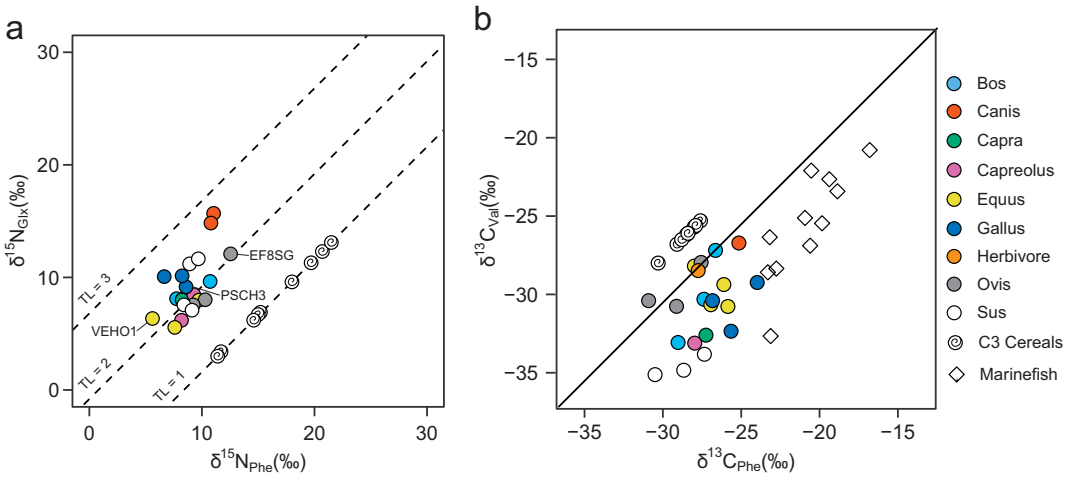

Figure 5.7 $\delta^{15}N_{Phe}$ and $\delta^{15}N_{Glx}$ (b) and $\delta^{13}C_{Val}$ and $\delta^{13}C_{Phe}$ values of cereals and terrestrial animals from Herculaneum and comparable archaeological contexts. Dashed lines identify terrestrial trophic levels. The line in b identifies y= x.

The δ^{13}C values of the essential amino acids can also be of help in observing differences in the dietary habits of the terrestrial animals since these will reflect the δ^{13}C values of the primary producers with only minimal fractionation. The graph in Figure 5.7 b, based on what proposed by Honch *et al.* (2012), clearly separates the C_3 cereals with less ^{13}C-depleted $\delta^{13}C_{Phe}$ values compared to the $\delta^{13}C_{Val}$ ones. On

the contrary, the marine fish and the majority of the terrestrial animals exhibit an opposite trend (less ^{13}C-depleted $\delta^{13}C_{Val}$ values compared to the $\delta^{13}C_{Phe}$ ones). Some of the animals appear to be closer to the C_3 cereal line, with more ^{13}C-enriched $\delta^{13}C_{Phe}$ values, sometimes equal to the $\delta^{13}C_{Val}$ ones. This is the case of all the sheep (*Ovis*, *EF8SG, EF7OC, EF10OC*) and the dog *EF11DOG* (the other dog, *EF12DOG2*, was not analysed in carbon mode) from the *fornici*, one of the horse from Velia (*VEHO2*) and one *Bos* sample (PSC2) and a herbivore sample no further classified (*PSG2*) from from Porta Stabia. This would reinforce the hypothesis that the sheep *EF8SG* and the dog *EF11DOG* from the *fornici* were partially fed with C_3 cereals and it further suggests that this was also the case of some other herbivores from the assemblage, although probably to a lesser extent (Figure 5.7 b).

The ancient literary sources provide valuable information around Roman husbandry practices. Varro explains that goats should be preferentially left grazing in forested areas and that, since their tendency to eat shoots, farmers should not permit them grazing on cultivated fields (*Rust.* 2.2). Indeed the only goat from the assemblage (*Capra*, *VESH1* from Velia) exhibits amino acid δ^{15}N and δ^{13}C values close to those of wild animals (*Capreolus*, *PSSG3* and *VEDE1*), suggesting that this animal was feeding on wild vegetation (Figure 5.7 a and b). On the contrary, sheep were allowed grazing on cultivated fields with the secondary purpose of preparing the soil for the next year's harvest. Moreover, the diet of sheep was often supplemented with other products, such as hay, bran, grapeseeds and fig leaves (*Rust.* 2.2). Similarly, Varro reports that the cattle was also under some sort of controlled diet, usually consisting of hay, on its own or mixed with other elements such as grapeseed, macerated millet and legumes, but also acorns, tree leaves and stems of legume plants (*Rust.* 2.5). The more variegated diet of sheep and cattle seems to be reflected by their amino acid carbon and nitrogen isotope values (Figure 5.7 a and b).

The different dietary habits of pigs suggested by the bulk δ^{15}N and δ^{13}C values seem to be confirmed by the $\Delta^{15}N_{Glx-Phe}$ offsets which are lower in samples *PSG1* and *PSP4* compared to *PSP3* and *PSP5*, which identifies the first two with the herbivorous trophic level (Figure 5.7 a). It has been recently proposed that pigs in Imperial Italy were mainly raised on herbivorous diets which makes them similar to sheep and goats in their isotope values (O'Connell *et al.* 2019; Trentacoste *et al.* 2020; Trentacoste 2020). The results from this study add a piece to the picture, showing that this was perhaps the case for some of the samples here analysed but that others were rather under an omnivorous diet. Moreover, it needs to be acknowledged that the *Sus* samples used in this thesis were not further classified and therefore some wild boars might be

included. When the carbon isotopes of amino acids are also explored, the three *Sus* samples analysed (*PSP3, PSP4* and *PSP5*) curiously exhibit the lowest $\delta^{13}C_{Phe}$ values among the terrestrial animal group (particularly *PSP3* and *PSP5*)(Figure 5.7 b). It is possible that the more negative values reflect a trophic baseline not represented by the dataset, perhaps that of the fungi. However, it is also possible that these three bone samples belong to animals that were not local. Pigs were the only animals bred merely for meat consumption and pork meat was often stored with salt, dried or cured to obtain cold cuts (Malossini 2011). Therefore, it cannot be ruled out that pork, in the form of cured meat, was imported from a different geographical region with distinct background carbon isotopic signals (Trentacoste 2020).

As for chicken, Columella reports that hens should be fed with barley, vetch, peavine, millet and foxtail millet but, in case these comestibles were not available or too expensive, cooked grasses of the genus *Lolium*, brooms, bran and grapeseeds can also be used (*Rust.* 8.2-7). Varro also suggests, when hens are kept to be eaten, to feed them with a dough of bread and water together with wine, or made with barley flour or flour made from the Lolium genus grass and lineseed oil (*Rust.* 3.9). The bulk $\delta^{13}C$ values suggest that these animals were at least in part fed on C_4 plants. If this is the case, the background C_4 isotopic signal does not appear to be distinguishable using the $\delta^{15}N_{Phe}$ values. On the contrary, the horse *VEHO1*, who also has a ^{13}C-enriched bulk $\delta^{13}C$ value compared to the majority of the terrestrial animals (Figure 5.5 b), exhibits the lowest $\delta^{15}N_{Phe}$ value (+ 5.61 ± 0.8 ‰) among all the terrestrial animals (Figure 5.7 a). If these animals were fed on C_4 plants, their $\delta^{13}C_{Phe}$ and $\delta^{13}C_{Val}$ values are also not clearly distinguished from those exhibited by the other animals and the C_3 cereals (Figure 5.7 b).

It is also essential to note that, according to the ancient texts, many of the animals here discussed were at least partially fed with legumes. It is therefore expected that Leguminosae plants would have source ($\delta^{15}N$) and essential ($\delta^{13}C$) amino acid values within those exhibited by the terrestrial animals analysed.

The $\delta^{15}N_{Phe}$ and $\delta^{15}N_{Glx}$ values are here also explored from the marine fish group with the aim to identify their trophic positions. By doing so, it is possible to observe a more homogeneous distribution of the marine samples, with the exception of two Sparidae samples from the House of the Surgeon (*HSSP1* and *HSSP2*), the two Labridae samples (*HSLA* and *SSF5*) and the school shark (*SSF2*) (Figure 5.8 a). The trophic level (TL), calculated according to the equation 3.6, is between 2 and 3 in all the samples (Table 5.2.2). These are strikingly lower than the TLs reported

in the FishBase[2] database (for those samples for which it was possible to obtain an identification at the species level), where trophic levels are estimated according to stomach contents (Froese and Pauly 2000). The underestimation of the fish trophic levels using nitrogen SIA compared to those estimated by evaluating the stomach contents was also observed in a modern Mediterranean lagoon ecosystem by Mancinelli *et al.* (2013), although the latter does not provide any satisfactory explanation, which is outside the aims of the publication. It seems likely that the marine fish here analysed were all accessing the same type of resources, for which fish farming in limited and controlled environments such as coastal lagoons or fishponds is a possible explanation.

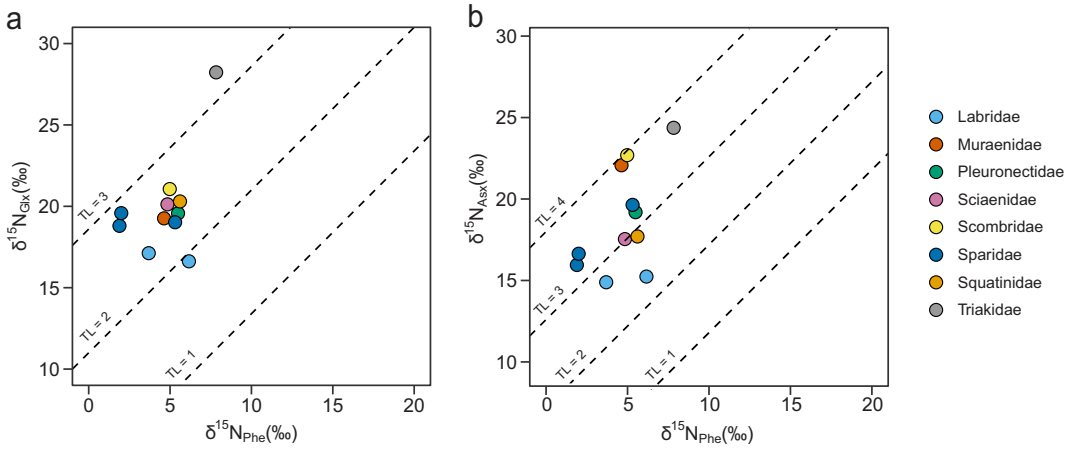

Figure 5.8 $\delta^{15}N_{Phe}$ and $\delta^{15}N_{Glx}$ (a) and $\delta^{15}N_{Phe}$ and $\delta^{15}N_{Asx}$ (b) values of marine fish from Pompeii in the 1^{st} century AD and comparable archaeological contexts. Dashed lines identify marine trophic levels.

However, when Asx is used instead of Glx as the trophic amino acid in TLs calculation, the trophic levels seem to be better discriminated despite still lower than the theoretical ones from the FishBase database, at least in some cases (Figure 5.8 b and Table 5.2.2). The $\beta_{Asx-Phe}$ and $\Delta_{Asx-Phe}$ values here used are those reported in the meta-analysis carried out by Nielsen *et al.* (2015). The two members of the Labridae family are still the lowest of the group (TL = 2.3 for *SSF5* and TL = 2.7 for *HSLA*) while the Mediterranean eel (*HSMU1*) and the Scombridae (*HSCC2*) exhibit the highest trophic level in the group (TL = 3.9), followed by the school shark *SSF2* (TL = 3.7). It is unclear why Asx is more powerful in discriminating the trophic level of the marine fish from these contexts compared to Glx but it is possible that the β_{t-s} and Δ_{t-s} here used to calculate the trophic levels do not apply well to Mediterranean ecosystems. Before drawing any conclusion about trophic hierarchy in the Roman Mediterranean,

[2]Fishbase can be accessed at this link.

it would be important to explore both SIA and CSIA-AA of the primary producers and fractionation mechanisms of modern Mediterranean sea food webs. Nevertheless the consistency of the nitrogen isotope values of the source amino acids ($\delta^{15}N_{Phe}$ = +4.77 ± 1.73 ‰, n = 11, and $\delta^{15}N_{Lys}$ = +3.30 ± 1.71 ‰, n = 11) suggest that there is a certain continuity of the baseline in the Mediterranean despite possible different background environments (*e.g.*, open-sea, coastal lagoon and fishponds). Moreover, the $\delta^{15}N$ of the majority of the trophic amino acids here considered (Glx, Asx, Ala, Val, Leu, Ile) are significantly higher than those from the terrestrial food web, making it simpler to distinguish marine food sources in the Roman Mediterranean diet. It is important to note however that this is not the case of proline and hydroxyproline (see Table D.4).

On the contrary, the $\delta^{13}C$ values of the essential amino acids are more variable. The *garum* sample *HSG1* in particular exhibits the lowest $\delta^{13}C$ values of the group in leucine, isoleucine, phenylalanine and lysine, probably affected by some terrestrial inputs, as previously discussed in relation to the SIA results (see Table D.3). However, it is unclear why this ^{13}C depletion does not affect the other essential amino acids. Unfortunately, the collagen extracted from *HSG1* was not enough to be analysed in nitrogen mode, which could have confirmed the attribution of this sample to a distinct environment. Similarly, the other marine sample that exhibited ^{13}C-depleted bulk collagen value (*HSP3*, Sparidae) did not provide enough collagen to be explored using CSIA-AA.

In conclusion, thanks to the application of CSIA-AA, it was possible to observe trophic hierarchies that were hardly visible using the SIA approach. As for the terrestrial samples, it was confirmed that at least part of the C_3 cereals represent a trophic web which is separated from that of the terrestrial animals. This confirms the nutritional and economic value that C_3 cereals had in the Roman times, which followed specific crop management strategies. Nevertheless it would appear that C_3 cereals also contributed to the diet of some of the animals here analysed, suggesting that part of the cereal production was also used for feeding the animals, as also reported by the ancient sources, but overall only minimally. The estimated carbon and nitrogen amino acid values of C_3 cereals are clearly separated from that of the animal terrestrial baseline and this needs to be taken into consideration when interpreting the diet of the ancient Romans using a stable isotope approach. As for the marine fish group, the SIA and CSIA-AA dataset here discussed confirms the complexity behind the marine food-source category in the Mediterranean. The determination of marine food consumption in the Roman Mediterranean only using the SIA approach is made difficult if not

ID	**Taxa**		**Element**	**Total length** (cm)	**Trophic level** (**FishBase**)	**Trophic level** $\Delta^{15}N_{Glx-Phe}$	**Trophic level** $\Delta^{15}N_{Asx-Phe}$
	Latin name	**Common name**					
ABF3	Sciaenidae	Meagre	vertebra		4.3	2.6	3
HSLA	Labridae	Wrasses	Premaxilla	30-40		2.3	2.7
HSSP1	Sparidae	Sea breams and porgies	Caudal vertebra	20-30		2.8	3.3
HSSP2	Sparidae	Sea breams and porgies	Posterior abd. vertebra	30-40		2.9	3.4
HSSSQ	Squatinidae	Angelshark	Posterior abd. vertebra	70-80	4.1	2.5	2.9
PSMU1	Muraenidae	Mediterranean moray	mandibola		4.2	2.5	3.9
PSPL1	Pleuronectidae	European plaice	Preopercular	50-60	3.2	2.4	3.2
PSSC2	Scombridae	Bonito or frigate tuna	vertebra	>50	4.5	2.7	3.9
PSSP1	Sparidae	Sea breams and porgies	vertebra	20-30		2.4	3.3
SSF2	Triakidae	School shark			4.3	3.2	3.7
SSF5	Labridae	Ballan wrasse			3.2	1.9	2.3

Table 5.6 Trophic levels of archaeological marine fish remains according to the FishBase database and those estimated with equation 3.6 using the β_{T-S} and the Δ_{T-S} values at the bottom of the marine food web reported by Chikaraishi *et al.* (2009) and by Nielsen *et al.* (2015) for Glx-Phe and Asx-Phe, respectively. The morphological identification of the marine fish and the estimation of their total length (cm) were carried out by Dr H. K. Robson for the remains from the House of the Surgeon (Pompeii) and by Dr J. K. Bakker for those from Porta Stabia (Pompeii). See Appendix D Table 5.2.2 for sample provenance and chronology.

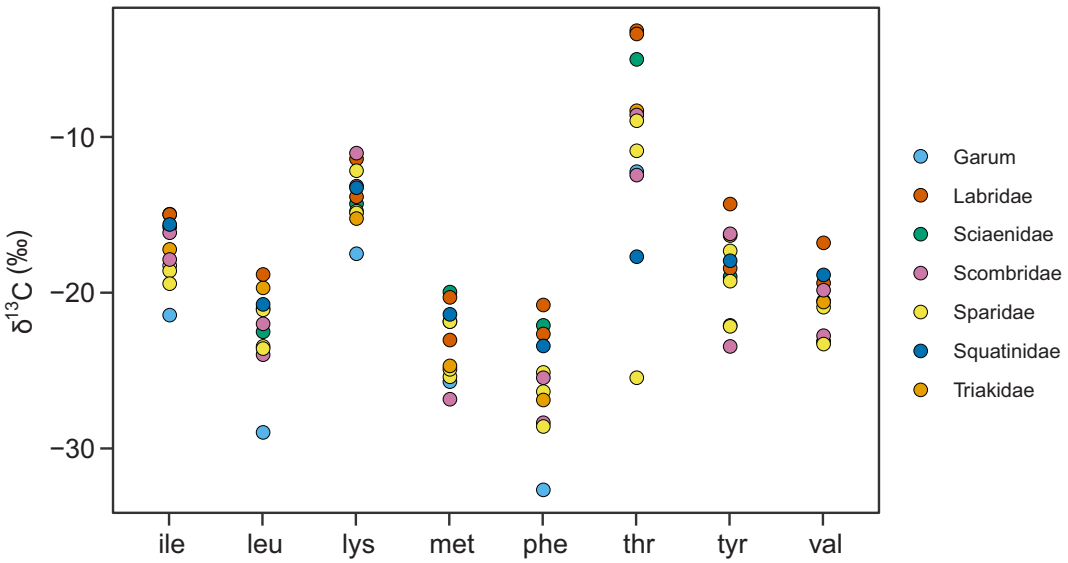

Figure 5.9 δ^{13}C values of essential amino acids in marine fish from 1^{st} century AD Pompeii and comparable archaeological contexts.

impossible by two main factors: i) the average δ^{15}N values of bulk collagen of marine Mediterranean fish are often equal and even lower than those of terrestrial animals and cereals; ii) marine fish were caught or farmed in different ways and this is likely to be reflected in their tissue carbon and nitrogen isotopic signatures. Thanks to the CSIA-AA approach it was possible to overcome these difficulties by: i) distinguishing between food webs at a higher resolution, clearly differentiating between the terrestrial and the marine isotopic signal (Figure 5.6 and 5.7); ii) discriminating groups from the same ecosystem, providing precious insights into the strategies adopted by the Romans to secure the supply of marine resources.

5.3 Conclusion

The exploration of cereal, legume, animal and marine fish isotopic signatures both at the SIA and CSIA-AA level in this chapter was proven to be essential to better understand the differences inside each food category in the Roman Mediterranean.

First, archaeological and modern cereals and legumes were analysed using RP-HPLC to observe amino acid content and degradation (Section 5.1). Since the profiles suggest that the amino acids from archaeological material are highly degraded, the amino acid isotope values of the cereals from Herculaneum and other published samples were estimated from their bulk values using the offsets measured from modern material.

At the bulk SIA level, it was evidenced that bulk δ^{15}N values of C_3 cereals in the Imperial Mediterranean are often higher than those of terrestrial animals and marine fish. The Roman diet was notoriously rich in C_3 cereal consumption (see chapter 2 section 2.1). When cereal products are abundant in diet, they can easily cover the protein requirements (Garnsey and Scheidel 1998, 226-252). Therefore, high δ^{15}N collagen values in human collagen from Roman Mediterranean contexts do not necessarily reflect a consumption of higher trophic level organisms, such as animal products or marine fish. It is therefore recommended to not underestimate the contribution of cereals to the bulk δ^{13}C and δ^{15}N values in humans from similar contexts. Although cereals, terrestrial animals and marine fish are more difficult to distinguish relying on the bulk SIA approach, the dataset discussed in this chapter has shown that the same is not true when using the amino acid isotope analysis. Indeed, the δ^{13}C and δ^{15}N values of source and essential amino acids of C_3 cereals are quite well distinguished from those of terrestrial animals and marine fish.

Both bulk SIA and CSIA-AA values of terrestrial animals suggest that husbandry practices were varied and not always pertinent to the nature of the animal. For example, some of the pigs exhibit isotopic values typical of a herbivorous diet, close to that of sheep and cattle and even wild animals. Some domestic herbivores were also probably fed partially with C_3 cereals, while others were more likely left grazing on local wild vegetation. In this direction, it was essential to identify the animal remains using ZooMS which avoided the allocation of the remains to the wrong animal group and therefore drive erroneous discussion around their dietary habits (Section 5.2.1). Unfortunately, if some of the animals were fed on C_4 plants, as it seems to be suggested by the bulk values of at least one horse and three chicken samples, these do not present distinct isotopic signatures that can be easily detected at the CSIA-AA level, at least from this specific assemblage.

As for marine fish, the dataset collected has shown that it is difficult to observe dietary patterns in fish that could be related to the species or to the size of the specimen, although this seems to be better achieved using the δ^{15}N values of amino acids. The δ^{15}N values of the source amino acids appear to be quite consistent, suggesting a certain homogeneity of the baseline isotopic signatures in the Mediterranean. The bulk δ^{13}C values suggest that some of the fish might have spent a great part of their life in a marine environment partially influenced by terrestrial inputs, such as estuaries, coastal lagoon with freshwater supplies or artificial fishponds. This appears to be the case of at least one Sparidae and two *garum* samples from this assemblage and it seems to be confirmed by the δ^{13}C values of the essential amino acid explored in one of the *garum* samples.

The analysis of this dataset will be used to better guide the discussion of the results from the catastrophic death assemblage of Herculaneum. In addition, it has put forward new evidence for agricultural and husbandry practices in the Roman times with possible interesting implications for socio-economic studies.

Chapter 6

High-resolution dietary reconstruction of victims of the AD79 Vesuvius eruption at Herculaneum by compound specific isotope analysis

This chapter explores the potential of using Bayesian Mixing models to interpret the CSIA-AA results obtained from the AD 79 Herculaneum death assemblage and comparative dietary baseline. By incorporating previous knowledge of amino acid synthesis into the models, it was possible to obtain high-resolution dietary information about this exceptional human assemblage and compare the results with those from modern Mediterranean populations.

This chapter is currently under review with the reference: Soncin, Silvia, Talbot, Helen M., Fernandes, Ricardo, Harris, Alison, von Tersch, Matthew, Robson, Harry K., Bakker, Jan K., Ritcher, Kristine K., Alexander, Michelle, Ellis, Steven, Thompson, Gill, Amoretti, Valeria, Osanna, Massimo, Caso, Marina, Sirano, Francesco, Fattore, Luciano, Colonese, André C., Garnsey, Peter, Bondioli, Luca, Craig, Oliver E. (in-review). High-resolution dietary reconstruction of victims of the AD79 Vesuvius eruption at Herculaneum by compound specific isotope analysis. *Science Advances*.

The authors contributed to the article as follows: Conceptualization: SS, OEC, LB; Methodology (isotopes): SS, HMT, AH, MVT; Methodology (morphological animal identification): HKR, JKB; Sample access and contextualization: KKR, MA, SE, GT, VA, MO, LF, MC, FS; Data analysis: SS, OEC with support from RF; Supervision: OEC, ACC, MA; Writing—original draft: SS, OEC; Writing—review and editing: SS, OEC, ACC, PG, LB.

The supplementary figures and tables as they have been submitted to the journal are in Appendix E. The input parameters and the obtained estimates of the Bayesian mixing models used in this chapter are adapted in the form of tables and can be found in Appendix E.

6.1 Abstract

The remains of those who perished at Herculaneum in AD79 offer a unique opportunity to examine lifeways across an ancient community who lived and died together. Historical sources often allude to differential access to foodstuffs across Roman society but provide no direct or quantitative information. By determining the stable isotope values of amino acids from bone collagen and deploying Bayesian models that incorporate knowledge of protein synthesis, we were able to reconstruct the diets of 17 adults from Herculaneum with unprecedented resolution. Significant differences in the proportions of marine and terrestrial foods consumed were observed between males and females, implying that access to food was differentiated according to gender. The approach also provided dietary data of sufficient precision for comparison with assessments of food supply to modern populations, opening up the possibility of benchmarking ancient diets against contemporary settings where the consequences for health are better understood.

6.2 Main

6.2.1 Introduction

The human remains found at Herculaneum represent a sample of a "living" population who died trying to escape from the eruption of the Vesuvius volcano in AD79. In total, 340 individuals have been excavated from the beach and from nine adjacent *fornici* (stone vaults) that run parallel to the seashore, where they sought shelter (Figure 6.1)(Martyn *et al.* 2020). This remarkable assemblage of victims of a natural

catastrophe is of huge public interest, but also offers an opportunity to significantly advance our knowledge of Roman society through the application of bioarchaeological approaches. The skeletal sample at Herculaneum is not constrained by the biases usually faced by osteoarchaeologists when dealing with attritional cemetery assemblages, such as selective mortality and burial, rather it provides a 'snapshot' of an ancient population rarely afforded in archaeology. And although some selectivity between the few who failed to evacuate the town of *ca.* 3,000-4,000 inhabitants and the majority who escaped may be expected, males, females, the old and young are all well represented (Sperduti *et al.* 2018; Martyn *et al.* 2020). No evidence has emerged as yet of biases toward any particular social class, although we know from other evidence, namely the so-called *Album* of Herculaneum, that freedmen and slaves made up a significant proportion of the residents of the town (de Ligt and Garnsey 2012, 2019).

Figure 6.1 View of skeletal remains in one of the vaulted chambers (*fornici*) during excavation. Photo Credit: Luciano Fattore, Sapienza Università di Roma.

Here, we sought to reconstruct the diets of 17 individuals from this catastrophic death assemblage through compound specific stable isotope analysis of amino acids

directly obtained from bone collagen. The aim of this study was to quantify and examine dietary variability within this unique sample of Roman society at much higher resolution than has previously been achievable (Craig *et al.* 2013; Fernandes 2016; Martyn *et al.* 2018), particularly by deploying a new Bayesian model that incorporates prior knowledge of amino acid metabolism. We examine the capacity of this method to provide nutritional information regarding major food classes that were available and compare their consumption across the sample. In doing so we hoped to create an approach for dietary reconstruction that would be suitable for much wider application.

Despite its importance for assessing health and well-being, quantitative data regarding food supply and diet is rarely available to historians, leaving only impressionistic accounts of consumption. Literature, epigraphy and other documentary evidence, including papyri, can be a useful source of information for social and economic historians, but they are often anecdotal, difficult to quantify and far from complete, and even the most detailed accounts of consumption practices usually only refer to a narrow stratum of society (Sperduti *et al.* 2018). Faunal and botanical remains recovered from archaeological excavations provide detailed evidence of the range of the foods available and quantitative analysis can reveal major economic changes through time (Trentacoste *et al.* 2021) but both are subject to sample and taphonomic biases and only rarely they can be reconciled with specific household activities (*e.g.*, Rowan 2017b) let alone individual diets. These gaps in our knowledge limit our ability to meaningfully compare diets either through time or by geographical location. In addition, we have only limited knowledge of how diets may have varied within an ancient society, for example by social standing, gender or between households, villages or towns or over the course of an individual's life. Without accurate quantification, we are unable to make fruitful comparisons among ancient populations or with modern societies, where more robust and detailed nutritional data are available. Such comparisons are essential for studying the long-term relationship between diet, health, disease, environmental change and social inequality, and the origin and changing nature of food cultures.

Following its first application over four decades ago (Van der Merwe and Vogel 1978), stable isotope analysis (SIA) of bone collagen offered a way to circumvent these problems by providing dietary estimates that can be compared across time and space. The approach has penetrated all aspects of archaeology and anthropology offering dietary information regarding specific individuals, from Neanderthals to historical figures (Richards and Trinkaus 2009; Lamb *et al.* 2014) and insight into differential access to foodstuffs within populations (Privat *et al.* 2002). The carbon and nitrogen in adult bone collagen derive from foods typically consumed over a period of at least

10 years prior to death (Hedges *et al.* 2007) and their respective collagen isotope ratios, expressed as δ^{13}C and δ^{15}N values, are related to those in the foodstuffs consumed over this period. Atoms in collagen are derived from amino acids (AAs) either incorporated directly from dietary proteins (source AAs) or synthesised *de novo* (trophic AAs), the latter using additional carbon from proteins, carbohydrates and lipids (Jim *et al.* 2006), and nitrogen from transamination reactions with the metabolic pool of amino nitrogen (O'Connell 2017). This integrated bulk isotopic signal is immensely powerful at providing long-term dietary records, but the approach relies on knowledge of the proportion of AAs routed to collagen directly from the diet against those synthesised *de novo* by the body. While source AAs undergo negligible isotopic fractionation, trophic AAs are synthesised by a series of transamination and deamination reactions leading to significant isotopic fractionations (Ohkouchi *et al.* 2017). Understanding the magnitude of these isotopic changes under different dietary scenarios is a major challenge still outstanding in this field, severely limiting the accuracy of the approach.

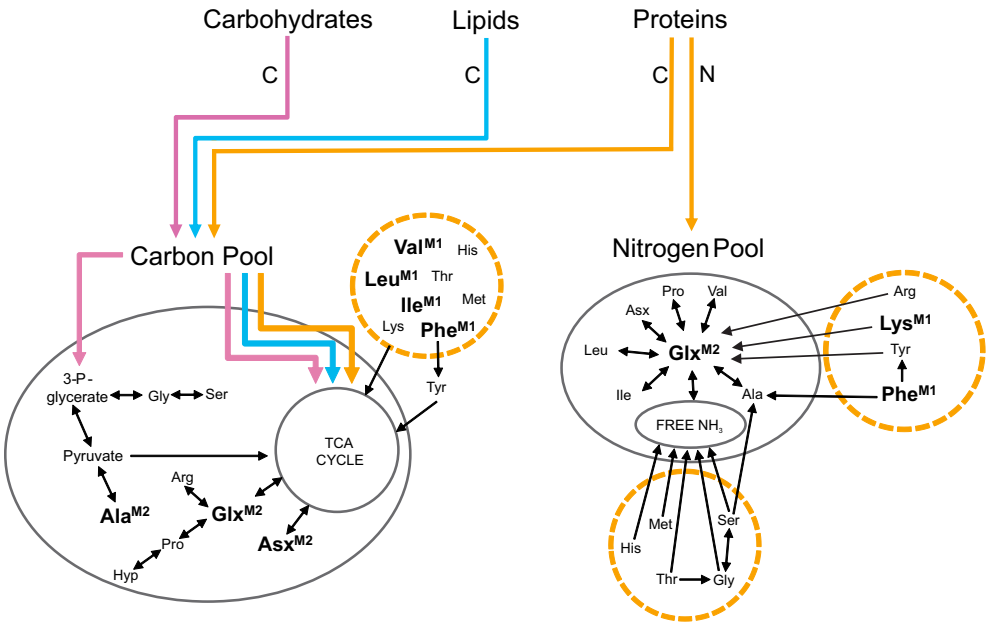

Figure 6.2 Rationale for metabolic model parameters. Carbohydrates, lipids and proteins all contribute to the "Metabolic Carbon Pool": carbon in alanine, serine and glycine has a glycolytic origin which is directly linked to carbohydrate digestion; glutamic acid and aspartic acid are synthesised via transamination through the TCA cycle from all macronutrients (Howland *et al.* 2003). Dietary protein is considered to be the only source of nitrogen, with glutamic acid the source of nitrogen for other trophic AAs (O'Connell 2017). "Source" AAs incorporated directly from diet with negligible isotopic fractionation are indicated by dashed circles. Isotope values for AAs labelled M1, M2 are used in *Model 1* and *Model 2* respectively. Ala: alanine, Gly: glycine, Val: valine, Leu: leucine, Ile: isoleucine, Thr: threonine, Ser: serine, Pro: proline, Asx: aspartic acid/asparagine, Glx: glutamic acid/glutamine, Phe: phenylalanine, Lys: lysine, Tyr: tyrosine, His: histidine, Arg: arginine.

A range of controlled studies and feeding experiments have been undertaken to understand both the degree of fractionation and the extent of amino acid routing. It has more recently emerged that the latter is likely to be itself dependent on dietary composition (Webb *et al.* 2017), further reducing the reliability of dietary reconstructions based on bulk carbon and nitrogen isotopic values. Moreover, the degree of fractionation between food and consumer tissues has also been found to be variable in animal feeding experiments and controlled dietary studies of humans (O'Connell *et al.* 2012). To overcome these sources of uncertainty, isotope ecologists and archaeological scientists are turning to measurements of the isotopic signatures of individual AAs (Ohkouchi *et al.* 2017; Jaouen *et al.* 2019; Commendador *et al.* 2019; Ma *et al.* 2021), which can be more easily traced to specific dietary sources. Such compound specific isotope analysis (CSIA) approaches are beginning to reveal additional dietary information that is often obscured in bulk stable isotope data sets, allowing population level dietary patterns to be tracked through time and space at much greater resolution (Ma *et al.* 2021). However, here, we focus on the utility of CSIA to explore intra-population dietary differences. Rather than using amino acid isotope proxies to distinguish dietary groups, we use prior knowledge of the amino acid metabolic pathways, their dietary isotope values, and their dietary concentrations to quantify individual diets using probabilistic models (Fernandes *et al.* 2014). We aimed to examine whether the differences between individuals at Herculaneum, as shown from bulk SIA (Martyn *et al.* 2018), could be refined and quantified at higher precision.

6.2.2 Results

Collagen was extracted and the δ^{13}C and δ^{15}N values of AAs measured by Gas Chromatography-Combustion-Isotope Ratio Mass Spectrometry (GC-C-IRMS) from the ribs and one tarsal bone (individual *F10i22*) of eleven adult males and six adult females whose remains were found within the vaulted chambers (*fornici*) next to the Herculaneum beachfront (see section 6.2.4 "Materials and Methods" and Table S1). We considered three potential food groups (C_3 cereals, terrestrial animals and marine fish) as the most likely dietary sources for people living in Herculaneum in 79 AD, based on archaeological finds from the site (Rowan 2017b) and historical records (Garnsey 1999). We obtained baseline $\delta^{13}C_{AA}$ and $\delta^{15}N_{AA}$ values from the collagen of terrestrial animals (omnivores and herbivores) and marine fish bones, the majority from 1^{st} century AD contexts at Herculaneum and Pompeii (Table S2). As endogenous AAs cannot be reliably extracted from archaeological plant remains, which are often charred, an alternative strategy was used. Bulk and AA stable isotope values were first

measured in modern grains to derive an offset for each AA. Amino acid stable isotope values of archaeological cereal grains were then predicted by applying the offsets to bulk measurements of cereal grains from Herculaneum and previously reported values from comparable Roman contexts (see section 6.2.4 "Materials and Methods" and Table S3)(Pate *et al.* 2016; O'Connell *et al.* 2019). Finally, Bayesian mixing models were applied to explore the data considering uncertainties in the isotope measurements and the concentration of AAs and macronutrients in the different potential foodstuffs.

In *Model 1*, we considered only nitrogen and carbon isotope values of source AAs (leucine, valine, isoleucine and phenylalanine for δ^{13}C and phenylalanine and lysine for δ^{15}N) that we were able to reliably measure in ancient bone collagen (Figure E.1) and modern cereals (Figure E.2). As these AAs show negligible (<1 ‰) isotopic fractionation between diet and consumer and are derived only from dietary protein (Figure 6.2), they offer the most robust approach for estimating the composition of ancient human diets since the major assumptions regarding fractionation and routing are negated. Using this approach, we were able to easily discriminate the three different food groups, implying fundamental isotopic differences in the AAs of primary producers in their respective food sources (*i.e.*, cereals, animal forage, marine phytoplankton). The estimates obtained from *Model 1* (Figure 6.3 b) represent % component contribution to total dietary protein consumed (by dry weight). Using this approach we achieve far higher dietary resolution compared to previous approaches that rely on bulk collagen stable isotope data alone (Figure 6.3 a, Table E.2 and Table E.3)(Fernandes 2016), with individual estimates of each food group typically ± 10 % at the 68 % credible interval. Importantly, we show that the bulk isotope data underestimate the marine protein component of diet (Figure 6.3 a, Table E.2), leading to an erroneous interpretation of the importance of fish to the inhabitants of this coastal town. When the amino acid data are considered, the marine contribution is shown to be significant (mean = 26 ± 6 %) for all individuals in line with estimations based on ^{14}C marine reservoir ages (Craig *et al.* 2013) and supported by other assessments of the economy of the Bay of Naples during the 1^{st} century AD (Rowan 2017b). The estimated marine protein consumption at Herculaneum is strikingly higher than the relative amounts of marine protein supplied to mid- and late- 20th century Mediterranean populations (Craig *et al.* 2009), which are consistently below 10 % (Figure 6.3).

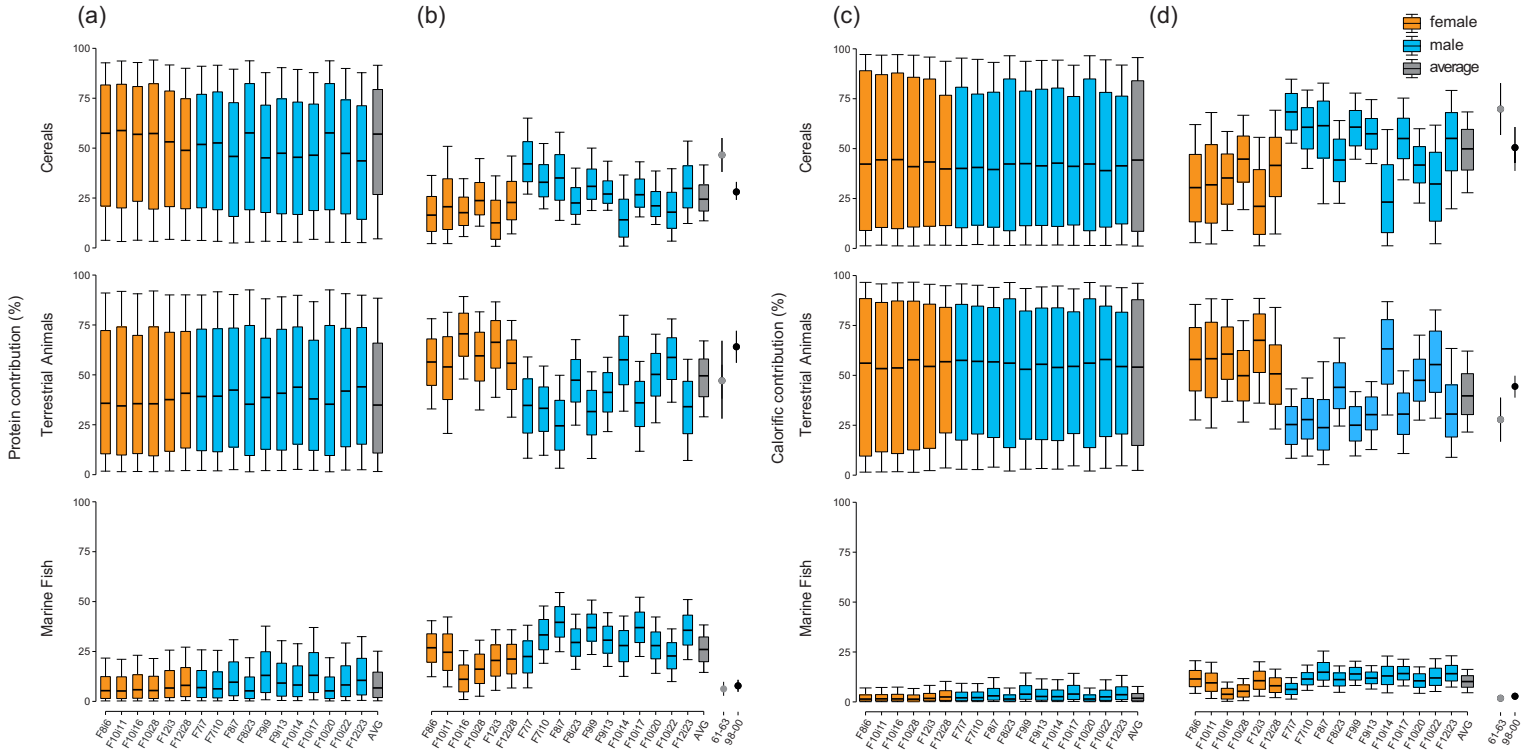

Figure 6.3 Dietary estimates for 17 individuals from Herculaneum under different scenarios. Estimates were obtained using a concentration dependent Bayesian mixing model. a) *Model 0p* - SIA, protein routed model. b) *Model 1* – CSIA, protein model. c) *Model 0wd* – SIA, whole diet model. d) *Model 2* – CSIA, whole diet model. Boxes represent a 68% credible interval (corresponding to the 16^{th} and 84^{th} percentiles) while the whiskers represent a 95% credible interval (corresponding to the 2.5^{th} and 97.5^{th} percentiles). The horizontal continuous line represents the estimated median (50th percentile). Orange = females, blue = males, grey = outcomes based on average AAs isotopic values of the 17 individuals. Equivalent proportions of protein and calorie supplied to modern Mediterranean populations between 1961-1963 (grey circles) and 1998-2000 (black circles) are shown, with bars representing 1σ (Balanza *et al.* 2007).

The source AAs also show significant sex based dietary differences throughout the group for all food sources (Figure 6.4 and Table S5) with females generally obtaining less of their total dietary protein from fish and cereals than males but relatively more from terrestrial animal products (*i.e.*, meat, eggs and dairy). This last category could theoretically also include protein from a broad range of locally produced foods, including pulses, legumes and nuts, as these foodstuffs are likely to have had similar isotope values of source AAs to animal forage. It has previously been demonstrated from bulk isotope data sets that males eat relatively more marine fish at Herculaneum (Martyn *et al.* 2018), and more broadly in Roman Italy (Prowse *et al.* 2005; Craig *et al.* 2009). It is possible that males were directly engaged in fishing activities or that they occupied more privileged positions in society. Furthermore, males were freed from slavery at an earlier age compared to females, who were on the contrary unlikely to be freed until the end of their reproductive period (de Ligt and Garnsey 2012, 86). This would have given males the opportunity to become economically independent joining the economic development of the area of the Bay of Naples and therefore accessing more expensive commodities, such as fresh fish. However, this explanation remains tentatively. In fact, we should also consider that females were also possibly involved in fishing or fishing-related activities and that they could have also occupied privileged positions in society. However, here we were able to quantify the gender difference more accurately within the group, with males on average obtaining 1.6 times more dietary protein from seafood compared with females (Figure 6.4 a). Males also obtained a higher proportion of protein from cereals compared with their female contemporaries, whereas females obtained a greater proportion of protein from terrestrial animal products or locally grown plant foods. Although these estimates do not reflect the absolute quantities of protein consumed, which also may of course have varied considerably by gender, such a quantitative approach is likely to be immensely useful for studying nutritional health in ancient societies, especially when used in conjunction with historical sources.

Next, we estimated the contribution of each source to the total diet by dry weight, broadly equivalent to the contribution to total calorific value. To do so we considered the additional contribution of carbon from dietary carbohydrates and lipids. We adapted the concept of "metabolic pools" (O'Connell 2017) from which carbon and nitrogen are drawn for amino acid synthesis. This model (*Model 2*) additionally considers trophic AAs; alanine (Ala), glutamine/glutamic acid (Glx) and asparagine/aspartic acid (Asx) as sources of carbon. The carbon in Ala is considered to have a glycolytic origin and therefore to have been obtained from the digestion of carbohydrates via pyruvate (Figure 6.2). Conversely, the carbon in Glx and Asx are derived from

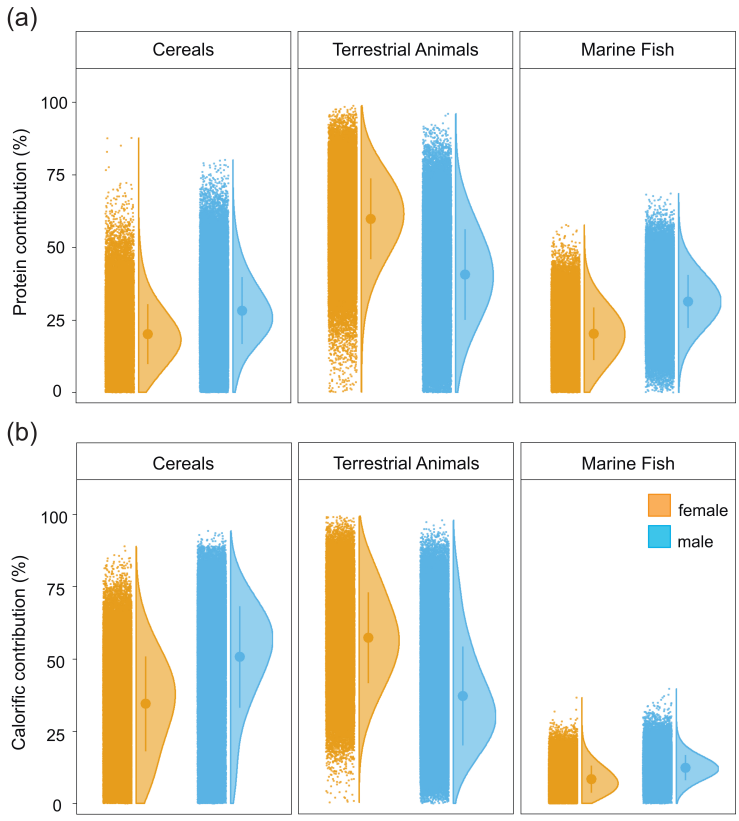

Figure 6.4 'Raincloud' plots of dietary estimates for 17 individuals from Herculaneum grouped by sex. Estimates were obtained using a concentration dependent Bayesian mixing model. a) *Model 1* – CSIA, protein model. b) *Model 2* – CSIA, whole diet model. The raincloud show the raw outputs of each model alongside the means and standard deviations and the probability density of the distribution. Non-parametric Wilcox test (two-sided) shows statistical differences for all the food sources across sex when applied to both *Model 1* and *Model 2* (p-values < 0.05, Table S5).

intermediates of the TCA cycle and therefore to have been derived from the pool of carbon from all macronutrients including protein (Figure 6.2). These proxies are confirmed by the high correlations observed in δ^{13}C values between AAs and dietary macronutrients from controlled feeding experiments (Jones 2002; Howland *et al.* 2003; Jim *et al.* 2006). The δ^{13}C values of dietary protein, carbohydrates and lipids are estimated from the bulk δ^{13}C values of faunal collagen or plant remains using previously established macronutrient "offsets" updated after more recent studies (see section 6.2.4 "Materials and Methods") (Fernandes *et al.* 2015; Webb *et al.* 2016b, 2017; Bownes *et al.* 2017). Finally, *Model 2* also considered Glx as an additional source of nitrogen. The difference in δ^{15}N of Glx and Phe have been used to study an organism's trophic position (Ohkouchi *et al.* 2017) but alone they fail to resolve more complex diets, as in

this case, when there are multiple sources (Figure E.3). As glutamic acid is involved in transamination of other AAs, its nitrogen is considered to derive from the total pool of nitrogen and therefore is estimated from the bulk δ^{15}N value of each protein source (Figure 6.2)(O'Connell 2017). The estimation of nitrogen isotopic fractionation associated with interchange of nitrogen between glutamic acid/glutamine and the nitrogen pool was obtained from studies of a range of consumers and their food sources (see section 6.2.4 "Materials and Methods").

Compared to *Model 1*, *Model 2* introduces additional sources of uncertainty regarding the degree of trophic amino acids fractionation, energy macronutrient source values and the flux of both carbon and nitrogen from dietary pools to collagen AAs. Nevertheless, even by using conservative estimations of these errors (see section 6.3 "Supplementary Materials and Methods" and Table E.1), the output of the *Model 2*, shows much greater dietary resolution compared to using bulk data alone (Figure 6.3 c and Table E.4)(Fernandes 2016) with a non-negligible contribution of marine foods to total calories for the majority of individuals and a statistical difference between sexes for all foodstuffs (Figure 6.3 and Table S5). The estimations of calorific value provided by *Model 2* also correspond well with previous estimations of % marine carbon in diet based on their marine reservoir ages (Figure E.4)(Craig *et al.* 2013; Martyn *et al.* 2018). The % dietary protein contribution estimated from *Model 2* is also within the error of those from *Model 1* providing further cross-validation (Table S4). The results of *Model 2* show that on average individuals at Herculaneum obtained the majority of their energy from terrestrial resources, *i.e.* cereals (49 $\pm$ 10%) and terrestrial animal products (40 $\pm$ 10 %). However, other high energy products such as olive oil, and potentially wine, are not considered as dietary sources and therefore missing in the outputs provided in Figure 6.3. Olive oil, for example, contributes *ca.* 5% of the calories in contemporary Mediterranean populations (Balanza *et al.* 2007). By using the δ^{13}C value of modern Mediterranean olive oils (Dudd 1999; Spangenberg and Ogrinc 2001; Steele *et al.* 2010) corrected for the Suess Effect (Hellevang and Aagaard 2015), *Model 2* permits a contribution of 29 $\pm$ 17% to total diet, when it is included as an additional source (see section 6.3 "Supplementary Materials and Methods" and Table E.5). Although even the lowest estimation would be much higher than most modern Mediterranean populations, this value is consistent with estimations of oil consumption in Rome during the 1^{st} century AD (*ca.* 20L/year, De Sena (2005)), directly attesting to the importance of the olive as one of the triads of the Roman Mediterranean diet, along with cereals and wine (Garnsey 1999).

6.2.3 Discussion

By applying the compound specific isotope analysis approach to the Herculaneum sample, here we are able to reconstruct the diets of people who lived contemporaneously with unprecedented resolution compared to previous studies (Craig *et al.* 2013; Fernandes 2016; Martyn *et al.* 2018). We show with much greater certainty that adult males and females drawn from the sample population had different diets during their lifetime. This must be attributable to differential access to foodstuffs, perhaps related to the different occupations held by men and women, cultural prohibitions, as reported by ancient medical treatises (Garnsey 1999, 100-102), or evidence of the uneven distribution of power that restricted certain foods to the latter (Garnsey 1999). A clear distinction by sex, however, is not observed in all cases. The dietary estimates from the male sample were more variable than the female with some males consuming less cereal based foods than the others (Figures 6.3 b and d), perhaps related to differences in their occupation or social standing, aspects difficult to directly assess given the nature of the assemblage. It is significant that such subtle dietary differences are not observable from the lower resolution reconstructions based on the bulk isotope data alone (Figures 6.3 a and c).

The paleodietary data obtained from CSIA are also of sufficient quality for comparison with records of food supplied to modern populations. Indeed, we found that proportionally more marine foods were consumed by the inhabitants of 1^{st} century Herculaneum compared to 20th century Mediterranean populations, while cereals were of lower overall dietary significance compared to the typical 'Mediterranean diet', as defined in the 1960s (Balanza *et al.* 2007). Whether this pattern is reflected more broadly in ancient Mediterranean societies or is peculiar to coastal settlements, such as Herculaneum, remains to be determined. Such high-resolution data also opens up the possibility of 'benchmarking' ancient diets against modern records, where, for example, the nutritional consequences for health are better understood (Kromhout *et al.* 1985).

More broadly, we show that CSIA of collagen AAs combined with probabilistic modelling, as presented above, offers a robust approach for dietary reconstruction at unprecedented resolution. This is an important advance that is likely to transform paleodietary research, not least by providing data that are of adequate quality to be of interest to the broader community of nutritional and environmental scientists. For example, quantification of seafood consumption by past communities could be used to study long-term anthropogenic impacts on marine ecosystems (Pauly and Zeller 2016) or help assess health inequalities (Brunner *et al.* 2009). Dietary accuracy is greatly enhanced by our knowledge of the $\delta^{13}C_{AA}$ and $\delta^{15}N_{AA}$ values of the main food groups

under consideration and so obtaining these data from a broader range of non-osseous sources, such as legumes, nuts, fungi and wild plant foods, would be a fruitful focus for future research. Finally, we show that using bulk stable isotope data alone to reconstruct an individual's diet can lead to erroneous conclusions regarding the relative quantities of different foodstuffs consumed and the extent of dietary variability within ancient populations.

6.2.4 Materials and Methods

Experimental Design

The ribs and one tarsal bone (individual *F10i22*) of 17 adult individuals were obtained from vaulted chambers (*fornici*) next to the Herculaneum beachfront. Nine had previously been subjected to radiocarbon dating and all had had a full osteological assessment (Table S1). Further samples that previously yielded the highest amounts of collagen (Martyn *et al.* 2020) were preferentially selected for analysis. Collagen was extracted and analysed by EA-IRMS and prepared for GC-C-IRMS following hydrolysis to release amino acids. The same procedure was applied to faunal remains from the study area (Table S2). Stable carbon and nitrogen isotope measurements were obtained for at least nine individual amino acids for each extract. Procedures were made for assuring quality control (see section 6.2.4 "Materials and Methods"). Amino acid stable isotope values were also obtained from modern cereals and these data were used to estimate the values for ancient cereals based on their bulk isotope values (Table S3). Several mixing models were constructed using the knowledge of the bulk and amino acids stable isotope values in the source foodstuffs, the concentrations of amino acids in the foodstuffs and their associated uncertainties (see section 6.2.4 "Materials and Methods"). The outputs of the models were used to create Figure 6.3 and Figure 6.4 and derive inferences.

Collagen extraction

Collagen was extracted from bone fragments following the modified Longin method (Brown *et al.* 1988). Briefly, small human and animal bone fragments (*ca.* 100-500 mg) were mechanically cleaned to remove exogenous residues and demineralized at + 4 °C in 8 mL *HCl* 0.6 M for at least 48h. A homogenized modern bovine bone sample was included with each batch of sample to serve as a control. More fragile fish elements were demineralized with a more diluted *HCl* solution (0.1 M). Once completely demineralized, collagen was gelatinized at 80 °C for 48h in *HCl* 0.001 M.

Gelatinized collagen was filtered (60-90 μm Ezee-filters™), ultrafiltered (Amicon® Ultra-4 Millipore™ 30 kDa of Ultracel® membrane) and then freeze-dried.

Elemental Analysis Isotope Ratio Mass Spectrometry (EA-IRMS)

Collagen (0.9-1.1 mg) was analysed in duplicate using a Sercon continuous flow 20-22 Isotope Ratio Mass Spectrometer interfaced with a Universal Sercon GSL to determine the carbon and nitrogen isotopic values. The obtained values were corrected from the isotopic ratio of the international standards, Vienna Pee Dee Belemnite (VPDB) for carbon and air (AIR) for nitrogen, using the standard δ (‰) notation.

Uncertainties on the measurements were calculated by combining the standard deviations of the sample replicates and those of reference material according to Kragten (Kragten 1994). Caffeine (IAEA-600), ammonium sulphate (IAEA-N-2), and cane sugar (IA-Cane) international standards were used as reference material in each analytical run. International standards average values and standard deviation across the runs were: IAEA-600 (n = 25), δ^{13}C raw = -27.69 ± 0.15 ‰ (δ^{13}C true = -27.77 ± 0.04 ‰) and δ^{15}N raw = +0.99 ± 0.26 ‰ (δ^{15}N true = 1 ± 0.2 ‰); IAEA-N-2 (n = 25), δ^{15}N raw = +20.32 ± 0.15 ‰ (δ^{15}N true = 20.3 ± 0.2 ‰); IA-CANE (n = 24), δ^{13}C raw = -11.67 ± 0.11 ‰ (δ^{13}C true = -11.64 ± 0.03 ‰). The maximum uncertainty across all samples (n = 83) was ± 0.41‰ for δ^{13}C and 0.32 ‰ for δ^{15}N.

Preparation of AAs for GC-C-IRMS

Collagen was hydrolyzed (6M *HCl*, 200 μL, 110°C, 24 h) after addition of 250 μL of an internal Norleucine standard (Sigma Aldrich) of known isotopic composition. The hydrolysates were centrifuged (11,000 x g, 1 min) using Pall Nanosep® filters (0.45 μm) in order to remove remaining insoluble material. The hydrolysates were gently dried at room temperature under N_2, redissolved in 0.1 M *HCl* (100 μL) and stored at -20°C until required for analysis. Samples were again evaporated to dryness prior to derivatization. AAs were then derivatized to form N-acetyl-*i*-propyl (NAIP) esters (Philben *et al.* 2018).

Briefly, isopropanol and acetyl chloride (1 mL; 4:1 v/v) were added, tubes were sealed, and heated at 100 °C (1 h). After 1 h, sample mixtures were cooled (at -20 °C) and the solution dried under a gentle stream of N_2. Dichloromethane (DCM) was added (2 x 0.5 mL) and blown down under a gentle stream of N_2 to remove excess reagents. Next, a mixture of acetic anhydride, triethylamine and acetone (1 mL; 1:2:5, v/v/v) was added to the tubes and heated at 60 °C (10 min). The mixture was cooled and evaporated to dryness under a gentle stream of N_2. NAIP esters were then dissolved

in ethyl acetate (EtAc; 2 mL) and a saturated NaCl solution (1 mL) was added to separate polar and/or inorganic components from the organic phase and transferred into a new culture tube. The phase separation was repeated with additional EtAc (1 mL). Trace water was removed from the organic phase with molecular sieves (Sodium aluminium silicate 0.3 nm, Merck KGaA, Darmstadt, Germany). The EtAc containing the NAIP esters was blown down under a gentle stream of N_2, then DCM (1 mL) was added and dried to remove excess water. Samples were redissolved in known quantities of EtAc and stored at -20 °C until required for analysis by GC-C-IRMS. The same derivatization procedure was used for preparing mixtures of international reference standards (Indiana, USA and SHOKO Science, Japan) and standards purchased from Sigma-Aldrich (Sigma-Aldrich Company Ltd., UK).

Gas Chromatography-Combustion-Isotope Ratio Mass Spectrometry (GC-C-IRMS)

GC-C-IRMS measurements of the AAs were conducted using a Delta V Plus isotope ratio mass spectrometer (Thermo Fisher, Bremen, Germany) linked to a Trace Ultra gas chromatograph (Thermo Fisher, Bremen, Germany) with a GC Isolink II interface fitted with a Cu/Ni combustion reactor maintained at 1000 °C. Ultra high-purity-grade helium with a flow rate of 1.4 mL min-1 was used as the carrier gas, and parallel acquisition of Flame Ionization data was achieved by diverting a small part of the flow to an integrated FID (Thermo Fisher). Ethyl acetate was used to dilute the samples, and 1 μL of each sample and 2 μL of each standard was injected at 240 °C with a 3.5s pre-injection dwell time, onto a custom DB-35 fused-silica column (60 m × 0.32 mm × 0.50 μm; Agilent J&W Scientific Technologies, Folsom, CA, USA). All samples were injected in triplicate. The oven temperature programme used for samples and standards was as follows: 40 °C (hold 5 min) then increasing by 15 °C min-1 up to 120 °C, then by 3 °C min-1 up to 180 °C, then by 1.5 °C min-1 up to 210 °C, then by 5 °C min-1 up to 280 °C (hold 8 min). A nafion membrane removed water and a cryogenic trap was employed in order to remove CO_2 from the oxidized and reduced sample when operated in nitrogen mode. In carbon mode, eluted products were combusted to CO_2 and ionized in the mass spectrometer by electron impact. Ion intensities of m/z 44, 45, and 46 were monitored in order to automatically compute the $^{13}C/^{12}C$ ratio of each peak in the samples. In nitrogen mode ion intensities of m/z 28, 29, and 30 were monitored in order to automatically compute the $^{15}N/^{14}N$ ratio of each peak in the samples. Computations were made with Isodat (version 3.0; Thermo Fisher) and were based on comparisons with a repeatedly measured high purity standard reference gas

(CO_2 or N_2). The results from the analysis are reported in parts per mil (‰) relative to international standards using the δ notation.

δ^{15}N measurements of amino acids

Each reported value is a mean of triplicate δ^{15}N measurements. An AA international standard mixture of known isotopic composition was run after every three sample injections in order to monitor instrument performance and drift. The AA standard mixture used for δ^{15}N determinations comprised eight international standards (Indiana and SHOKO Science) and L-Norleucine (Sigma Aldrich). δ^{15}N true values of L-Norleucine were determined in-house by EA-IRMS. International standards average raw values and standard deviation ($n = 124$) across the runs were: Ala, 42.22 ± 3.07 ‰ (true: +43.25 ± 0.07 ‰); Gly, +1.09 ± 2.02 ‰ (true: +1.76 ± 0.06 ‰); Val, -4.07 ± 1.73 ‰ (true: -5.21 ± 0.05 ‰); Leu, +6.39 ± 1.27 ‰ (true: +6.22 ‰); Nle, +14.46 ± 1.42 ‰ (true: +14.31 ± 0.23 ‰); Asp, +33 ± 1.50 ‰ (true: 35.2 ‰), Glu, -3.52 ± 1.10 ‰ (true: -4.52 ± 0.06 ‰); Hyp, -8.19 ± 1.08 ‰ (true: -9.17 ‰); Phe, +1.73 ± 0.69 ‰ (true: +1.70 ± 0.06 ‰). Samples δ^{15}N raw values were corrected by the calibration curve and the L-Norleucine internal standard true value.

δ^{13}C measurements of amino acids

Each reported sample value is a mean of triplicate δ^{13}C measurements. AAs in the samples were first corrected for the isotopic difference between L-Norleucine in the standard mixture and L-Norleucine in the sample. δ^{13}C amino acids measurements were then corrected by specific correction factors to account for the derivatizing carbon and the kinetic isotope effect (Docherty *et al.* 2001), according to the following equation:

$$\delta^{13}C_{CORR} = \delta^{13}C_D = \frac{[(n_{DC}\delta^{13}C_{DC}) - (n_C\delta^{13}C_C)]}{n_D} \tag{6.1}$$

Where n is the number of carbon atoms, DC indicates the derivatized compound, C the original compound and D the derivative group.

A standard AA mixture was run after every three sample injections and the average correction factors from the standard mixture used for the correction of the samples (Sigma Aldrich, UK). True δ^{13}C values of standards were measured by EA-IRMS: Ala, -19.31 ± 0.02 ‰; Gly, -33.31 ± 0.02 ‰; Val, -10.89 ± 0.02 ‰; Leu, -13.78 ± 0.06 ‰; Ile, -24.89 ± 0.07 ‰; Nle, -27.59 ± 0.02 ‰; Thr, -10.46 ± 0.01 ‰; Ser, -12.54 ± 0.09 ‰; Pro, -12.33 ± 0.02 ‰; Asp, -27.52 ± 0.12 ‰; Met, -29.88 ± 0.14 ‰; Glu, -28.57 ± 0.09 ‰; Hyp, -12.52 ± 0.03 ‰; Phe, -11.52 ± 0.05 ‰; Lys, -13.7 ± 0.11 ‰; Tyr,

-24.85 ± 0.02 ‰. The standards δ^{13}C average correction factor values and standard deviation ($n = 154$) across the runs were: Ala, -40.46 ± 1.22 ‰; Gly, -39.73 ± 1.02 ‰; Val, -45.57 ± 1.39 ‰; Leu, -45.03 ± 2.10 ‰; Ile, -46.31 ± 1.81 ‰; Nle, -43.43 ± 1.63 ‰; Thr, -48.52 ± 1.25 ‰; Ser, -46.56 ± 1.19 ‰; Pro, -42.27 ± 1.41 ‰; Asp,-37.27 ± 1.09 ‰; Met, -41.82 ± 2.12 ‰; Glu, -36.73 ± 1.10 ‰; Hyp, -47.97 ± 1.13 ‰; Phe, -45.36 ± 1.46 ‰; Lys, -48.29 ± 2.29 ‰; Tyr, -48.71 ± 1.23 ‰. Correction factors induce a new source of error, therefore the error propagated for each amino acid was calculated according to the following equation (Docherty *et al.* 2001):

$$\sigma^2 = \sigma_S^2 \left(\frac{n_S}{n_C}\right)^2 + \sigma_{DS}^2 \left[\frac{(n_S + n_D)}{n_C}\right] + \sigma_{DC}^2 \left[\frac{(n_D + n_C)}{n_C}\right] \tag{6.2}$$

Where σ is the standard deviation, n the number of carbon atoms, S represents the non-derivatized standard, DS the derivatized standard, DC the derivatized compound, C the original compound and D the derivative group.

Analysis of modern and archaeological cereals

Modern C_3 cereals were collected from Italian organic productions. Three species were selected for the analysis: barley (*Hordeum vulgare*), einkorn wheat or farro (*Triticum monococcum*) and durum wheat (*Triticum durum*). Grains were homogeneously powdered, washed three times with deionized water and freeze-dried. Around 2 mg were weighed out in duplicate and analysed by EA-IRMS to measure bulk carbon and nitrogen isotopic values following the approach described above. A portion of the original powdered material was prepared for compound specific analysis following a slightly modified protocol from Styring *et al.* (2012, 2014b). Lipids were first extracted from the powdered samples with dichloromethane/methanol (2:1 v/v, 10 mL) by ultrasonication and the extracts stored at -20 °C until required for analysis. Around 40 mg of dry lipid extracted residues were hydrolysed (6M *HCl*, 2 mL, 110 °C, 24 h). A known quantity of internal standard was added at this stage (Norleucine, Sigma Aldrich). The hydrolysed samples were centrifuged (11,000 x g, 1 min) twice using Nanosep® filters in order to remove the insoluble matter left. The hydrolysed samples were blown to dryness under N_2, redissolved in 0.1 M *HCl* and stored at -20 °C until required for analysis. Four charred cereals (ca. 300 mg) from excavations at Herculaneum (Table S3) were sampled for EA-IRMS analysis, including *Hordeum vulgare* (archive #1703/76981), *Triticum* sp. (#1703/76981 & #723/76000) and *Triticum dicoccum*, (#1895/77175). The samples were treated with *HCl* 0.5 M for 20 mins at room temperature to remove external carbonates and then rinsed three times with deionised water. The samples

were then frozen and lyophilized, grounded and weighed into tin capsules for EA-IRMS analysis of both carbon and nitrogen stable isotopes, as described above. The offset in the δ^{13}C and δ^{15}N values of each amino acid and the bulk value was calculated for each of the three modern C_3 cereal samples (Table S3). All AAs in plants are synthesised *de novo* by following specific metabolic reactions (Styring *et al.* 2014a). Therefore, we assumed that the degree of fractionation of nitrogen and carbon in C_3 cereal AAs can be predicted relative to their total nitrogen and carbon. Our $\Delta^{15}N_{AA-bulk}$ values were observed to be similar to those of barley and bread wheat (only grains) published by Styring *et al.* (2014a) and to those of bread wheat published by Paolini *et al.* (2015).

Next, we predicted AAs δ^{13}C and δ^{15}N values by applying the measured $\Delta^{13}C_{AA-bulk}$ and $\Delta^{15}N_{AA-bulk}$ offsets to the bulk δ^{13}C and δ^{15}N values from four samples of C_3 cereals from Herculaneum, a barley sample from AD79 Pompeii (Pate *et al.* 2016) and four 2^{nd} century AD cereal samples from the Imperial Roman harbour, Portus Romae (O'Connell *et al.* 2019). The bulk values of the archaeological grains were corrected for charring after (Nitsch *et al.* 2015). From this we obtained an average value for each amino acid with an associated uncertainty derived from propagating all errors from the measurements made on charred archaeological cereal grains and the errors associated with the $\Delta^{15}N_{AA-bulk}$ offset (Table S3).

Statistical Analysis

Bayesian mixing models were performed using FRUITS version 3.0 beta (available at http://sourceforge.net/projects/fruits/). Markov chains were obtained in FRUITS using the Markov Chain Monte Carlo (MCMC) method with the BUGS software (https://www.mrc-bsu.cam.ac.uk/software/bugs/). The BUGS software applies the Metropolis-Hastings algorithm and automatically discards the first 5000 iterations of the Markov chains and then additionally runs them for 10000 iterations. Convergence was assessed by examining the trace autocorrelation plots generated. Finally, the model outputs (Markov chains) were summarised, plotted and statistically analysed in R (version 4.0.3) using ggplot2 and the raincloud plot function (https://github.com/RainCloudPlots/RainCloudPlots)(Allen *et al.* 2019). Parameters and the rationale for the four models deployed (*Model 0p*, *Model 0wd*, *Model 1* and *Model 2*) are described in 6.2.4 Materials and Methods and the FRUITS files used to generate the outputs are also provided. A non-parametric two-sided Wilcox test was used to test whether distribution of median predicted contributions differed between sex for each food group at the 0.05 significance level. This test was used due to the low sample of independent observations (17 individuals).

6.3 Supplementary Materials and Methods

6.3.1 Quality Control (QC)

Three quality control measures were used. Firstly, the bulk collagen δ^{13}C and δ^{15}N values were estimated from the CSIA data and compared with the corresponding measured values (QC1), secondly a sample of bovine bone was extracted and analysed with every batch of samples to check for variability between runs (QC2), finally, the correlation between Pro and Hyp values was monitored (QC3). These are described below.

6.3.2 QC1: Mass Balance of amino acids δ^{13}C and δ^{15}N values

The AAs measured by GC-C-IRMS represent 90.4 % and 80.7 % of total carbon and nitrogen, respectively, in human collagen. We calculated the estimated bulk collagen δ^{13}C and δ^{15}N values by mass balance equations considering the relative contribution of each amino acid to collagen and compared the obtained values with those measured via EA-IRMS. Collagen sequences from human (UniProt P02052, P02058) and Atlantic cod (Gadus morhua) (Ensembl ENSGMOP00000009077, ENSGMOP00000014420, ENSGMOP00000016465) were processed with the ProtParam tool (Gasteiger *et al.* 2005) to obtain AAs composition and the number of carbon and nitrogen atoms. We excluded samples where the estimated to observed offset was greater than 2σ of the average (Bland and Altman 2003). The $\Delta^{13}C_{est-obs}$ and $\Delta^{15}N_{est-obs}$ of samples used in this study were on average 0.43 ± 0.99 ‰ and -0.13 ± 0.77 ‰ respectively (Figures E.5 a and b).

6.3.3 QC2: Bovine Control

Extracted collagen from a modern cattle (*Bos taurus*) bone that had been homogenized was included within each extraction batch and referred to as "Bovine control". The average bulk collagen values and one standard deviation ($n = 12$) from the EA-IRMS analysis of the Bovine Controls from the same batch of the samples were δ^{13}C = -22.89 ± 0.13 ‰ and δ^{15}N = +6.33 ± 0.2 ‰. These values were within those from fifty measurements obtained from different extracts (δ^{13}C = -23.04 ± 0.16 ‰ and δ^{15}N = +6.29 ± 0.3 ‰).

Bovine Control collagen extracts were also hydrolyzed and derivatized as described above and run on GC-C-IRMS together with the samples from the same batch. Bovine Control AAs δ^{15}N average values and standard error ($n = 10$) run together with the

samples used in this study were: Ala, +7.84 ± 0.21 ‰; Gly, +4.03 ± 0.42 ‰; Val, +14.40 ± 1.53 ‰; Leu, +10.95 ± 1.04 ‰; Ile, +12.06 ± 0.97 ‰; Thr, -3.42 ± 1.10 ‰; Ser, +4.49 ± 0.78 ‰; Pro +8.88 ± 0.79 ‰; +Asp, 9.71 ± 0.71 ‰; Glu, +9.77 ± 0.22 ‰; Hyp, +9.44 ± 0.87 ‰; Phe, +9.33 ± 0.49 ‰; Lys, +2.96 ± 0.0.57 ‰. Nitrogen bulk collagen value estimated from these AAs average values was +6.63 ± 0.44 ‰with an average offset from the observed (EA-IRMS) collagen value of +0.44 ± 0.39 ‰(δ^{15}NEA-IRMS = +6.18 ± 0.08 ‰).

Bovine Control AAs δ^{13}C average values and standard error ($n = 8$) run together with the samples used in this study were: Ala, -27.58 ± 1.37 ‰; Gly, -18.03 ± 1.47 ‰; Val, -29.57 ± 0.89 ‰; Leu, -31.82 ± 0.73 ‰; Ile, -27.92 ± 0.93 ‰; Thr, -15.76 ± 2.68 ‰; Ser, -14.16 ± 1.66 ‰; Pro -21.37 ± 0.87 ‰; Asp, -23.70 ± 0.51 ‰; Glu, -21.93 ± 0.39 ‰; Hyp, -21.59 ± 0.72 ‰; Phe, -31.17 ± 1.46 ‰; Lys, -20.72 ± 1.70 ‰; Tyr, -28.73 ± 1.37 ‰. Carbon bulk collagen value estimated from these AAs average values was -22.32 ± 0.81 ‰ with an average offset from the observed (EA-IRMS) collagen value of +0.53 ± 0.84 ‰ (δ^{13}CEA-IRMS = -22.86 ± 0.08 ‰).

6.3.4 QC3: comparison of proline and hydroxyproline δ^{13}C and δ^{15}N values

The relationship between proline and hydroxyproline stable isotope values is valuable tool to assess the quality of the analysis since hydroxylation of proline to form hydroxyproline via post-translational modification does not involve the exchange of nitrogen or carbon atoms and therefore the δ^{13}C and δ^{15}N values of both amino acids in collagen should be the same (O'Connell and Collins 2018). The δ^{13}C and δ^{15}N values of proline and hydroxyproline from this study were highly correlated ($R^2 = 0.94$ and $R^2 = 0.97$ for carbon and for nitrogen, respectively) and the regression lines close to $y = x$ (Figures E.5 c and d).

6.3.5 Description of mixing models and parameters used

***Model 0wd* - Whole Diet**. *Model 0wd* is a routed and concentration-dependent model based on bulk δ^{13}C (‰) and δ^{15}N (‰) proxies to estimate dry weight contribution to the whole diet from C_3 cereals, terrestrial animals and marine fish. *Model 0wd* was adapted from *Scenario 2* described by Fernandes (2016). The δ^{13}C (‰) and δ^{15}N (‰) values of human individuals from the Herculaneum *fornici* are those already reported by Craig *et al.* (2012) and Martyn *et al.* (2018) or extracted again from the same bone fragment when there was no collagen left and analysed by EA-IRMS as described

above (Table S1). A conservative uncertainty of 0.5 ‰is considered for both proxies (5). Terrestrial animal and marine fish source bulk values were collected from the same samples analysed for compound specific analysis (Table S2). C_3 cereal values were selected among published values from early II^{nd} C AD Portus Romae (O'Connell *et al.* 2019). To estimate the actual δ^{13}C (‰) and δ^{15}N (‰) of protein and energy components ingested from measured collagen, the values obtained were corrected by offsets reported by Fernandes (2016) and corrected after more recent studies (Webb *et al.* 2016b, 2017; Bownes *et al.* 2017)(*i.e.*, terrestrial animals: $\Delta^{13}C_{muscle-collagen}$ = -2 ‰, $\Delta^{13}C_{lipids-collagen}$ = -8 ‰, $\Delta^{15}N_{muscle-collagen}$ = 0 ‰; marine fish: $\Delta^{13}C_{muscle-collagen}$ = -1 ‰, $\Delta^{13}C_{lipids-collagen}$ = -7 ‰, $\Delta^{15}N_{muscle-collagen}$ = +1.5 ‰). Similarly, to estimate δ^{13}C (‰) values of protein and energy components from bulk C_3 cereals measurements, the following offsets were applied: $\Delta^{13}C_{protein-bulk}$ = -2 ‰, $\Delta^{13}C_{carb-bulk}$ = +0.5 ‰, considering the lipids contribution to be negligible (Fernandes 2016). Uncertainties associated with sources values are standard errors. However, a more conservative uncertainty was used that accounts for the corrections applied. Following Fernandes (2016), $\Delta^{15}N_{collagen-diet}$ was set at +5.5 ± 0.5 ‰, with 100 % contribution from protein, and $\delta^{13}C_{collagen-diet}$ was set to +4.8 ± 0.5 ‰, with 74 ± 4 % contribution from protein and 26 ± 4 % from lipids and carbohydrates. Macronutrient concentrations were collected from USDA National Nutrient Database for Standard Reference (available at https://fdc.nal.usda.gov/) and expressed as dry weight (%) with uncertainties being standard error (Table S6). The input values and the generated estimates are reported in Table E.1.

***Model 0p* - Protein**. *Model 0p* is a non-routed and concentration-independent model based on bulk δ^{13}C (‰) and δ^{15}N (‰) proxies to estimate dry weight contribution to protein in diet from C_3 cereals, terrestrial animals and marine fish. *Model 0p* is adapted from *Scenario 1* described by Fernandes (2016). Parameters used in *Model 0p* are the same as those used in *Model 0wd* - Whole diet but here carbon is only linked to protein consumption (100% contribution from protein) and $\Delta^{13}C_{tissue-diet}$ set to +5.0 ± 2.3 ‰. C_3 cereals, terrestrial animals and marine fish are considered to contribute equally to total protein in the consumer. The input values and the generated estimates are reported in Table E.2.

Model 1. *Model 1* is a concentration dependent model. δ^{13}C (‰) and δ^{15}N (‰) values of source AAs in human collagen are used to estimate relative contribution of protein to diet from C_3 cereals, terrestrial animals and marine fish. The isotopic proxies

used are: $\delta^{15}N_{Phe}$, $\delta^{15}N_{Lys}$, $\delta^{13}C_{Phe}$, $\delta^{13}C_{Val}$, $\delta^{13}C_{Leu}$ and $\delta^{13}C_{Ile}$. $\Delta^{15}N_{tissue-diet}$ and $\Delta^{13}C_{tissue-diet}$ were set close to 0 ‰, depending on individual cases as explored from experimental and field controlled studies (Hare *et al.* 1991; Howland *et al.* 2003; Jim *et al.* 2006; McMahon *et al.* 2010, 2015; McMahon and McCarthy 2016; Webb *et al.* 2016b; Fuller and Petzke 2017; Kendall *et al.* 2017; Webb *et al.* 2017). Terrestrial animals and marine fish are average values from the samples analysed and reported in Table S2. Uncertainties associated with source values are reported as standard errors. C_3 cereal AAs values were estimated from four charred grains from Herculaneum, one barley sample from Pompeii (Pate *et al.* 2016) and four early 2^{nd} century AD Portus Romae grains (O'Connell *et al.* 2019) by applying calculated bulk-offsets from measured modern cereals as described above (Table S3). The uncertainty associated to C_3 cereal values in the model is the standard error of the propagated uncertainty (*i.e.*, 1σ of the measured offsets of the three modern samples plus 1σ of the estimated amino acid values across the nine archaeological samples), rounded to the next higher multiple of five in order to use a more conservative estimation of uncertainty that accounts for possible variation from the estimated values to the true values. AA concentrations in the three sources were collected from USDA National Nutrient Database for Standard Reference (available at https://fdc.nal.usda.gov/) and reported as a percentage of total protein. The associated uncertainty is the standard error. The input values and the generated estimates are reported in Table E.3.

Model 2. *Model 2* is a concentration dependent model that accounts for the same source AAs isotopic values in the target as *Model 1*, with the addition of selected trophic AAs.

The following parameters were used to estimate the fractionation between dietary source and each amino acid using data derived from feeding experiments.

$\Delta^{15}N_{Glx-wholeN} = +9.7 \pm 2.5$ ‰, $\Delta^{13}C_{Glx-wholeC} = +8.7 \pm 3$ ‰, $\Delta^{13}C_{Asx-wholeC} = +4.7 \pm 1.5$ ‰and $\Delta^{13}C_{Ala-carbC} = +4.0 \pm 1.5$ ‰. $\Delta^{13}C_{Glx-wholeC}$, $\Delta^{13}C_{Asx-wholeC}$ and $\Delta^{13}C_{Ala-carbC}$ were derived from data collected only from feeding experiment studies conducted on pigs (Hare *et al.* 1991; Howland *et al.* 2003; Jim *et al.* 2006; Webb *et al.* 2017). To our knowledge, only one feeding experiment on pig nitrogen AAs values has been published so far (Hare *et al.* 1991). Therefore, $\Delta^{15}N_{Glx-wholeN}$ was derived from published feeding experiments on various mammals (Hare *et al.* 1991; McMahon *et al.* 2010; Fuller and Petzke 2017; Kendall *et al.* 2017). The conservative uncertainties associated with these offsets account for possible differences in isotope fractionation in humans compared to the species used in the experiments and possible direct routing of

these non-essential AAs when at high concentration in diet (Fuller and Petzke 2017). The "Whole N", and "Whole C" fractions in terrestrial animals and marine fish were estimated from bulk collagen values as following:

$$\delta^{15}N_{wholeN} = \delta^{15}N_{muscle} \tag{6.3}$$

$$\delta^{13}C_{wholeC} = \left[\left(\delta^{13}C_{energy}\, x\, \%C_{energy}\right) + \left(\delta^{13}C_{muscle}\, x\, \%C_{protein}\right)\right]/100 \tag{6.4}$$

Where: $\delta^{15}\mathrm{N}_{muscle}$ is estimated from the measured $\delta^{15}\mathrm{N}_{collagen}$ by adding the $\Delta^{15}\mathrm{N}_{muscle-collagen}$ offset; $\delta^{13}\mathrm{C}_{energy}$ is estimated from measured $\delta^{13}\mathrm{C}_{collagen}$ by adding the $\Delta^{13}\mathrm{C}_{energy-collagen}$ offset; $\delta^{13}\mathrm{C}_{muscle}$ is estimated from measured $\delta^{13}\mathrm{C}_{collagen}$ by adding the $\Delta^{13}\mathrm{C}_{muscle-collagen}$ offset; Energy %C and Protein %C represent the carbon content (%) of the energy components (lipids and carbohydrates) and protein calculated by multiplying the dry weight of the macronutrient components from each foodstuff by the carbon content factors (*i.e.*, 0.52 for protein, 0.44 for carbohydrate and 0.77 for lipid (Morrison *et al.* 2000)).

$\Delta^{13}\mathrm{C}_{energy-collagen}$ and $\Delta^{15}\mathrm{N}_{muscle-collagen}$ have the same values used in *Model 0* (*i.e.*, terrestrial animal: $\Delta^{13}\mathrm{C}_{muscle-collagen}$ = -2 ‰, $\Delta^{13}\mathrm{C}_{lipids-collagen}$ = -8 ‰, $\Delta^{15}\mathrm{N}_{muscle-collagen}$ = 0 ‰; marine fish: $\Delta^{13}\mathrm{C}_{muscle-collagen}$ = -1 ‰, $\Delta^{13}\mathrm{C}_{lipids-collagen}$ = -7 ‰, $\Delta^{15}\mathrm{N}_{muscle-collagen}$ = +1.5‰).

As for C_3 cereals, $\delta^{15}\mathrm{N}_{wholeN}$ is represented by the bulk δ^{15}N value, $\delta^{13}\mathrm{C}_{wholeC}$ by the bulk δ^{13}C and the $\delta^{13}\mathrm{C}_{carb}$ by applying the offset $\Delta^{13}\mathrm{C}_{carb-bulk}$ = +0.5 ‰(Tieszen 1991). Concentrations were reported as dry weight (%). The input values and the generated estimates are reported in Table E.4.

***Model 2* with olive oil**. This is a concentration dependent model that accounts for the same source and trophic AAs as *Model 2*, with the addition of olive oil as a source. It uses the same parameters as *Model 2* and it is assumed that carbon from olive oil is entirely routed to the Whole C fraction. The δ^{13}C value used for olive oil (-30 ± 1.3 ‰) is an average of the δ^{13}C values of modern samples previously reported (Dudd 1999; Spangenberg and Ogrinc 2001; Steele *et al.* 2010) corrected for the Suess effect (Hellevang and Aagaard 2015). The input values and the generated estimates are reported in Table E.5.

6.3.6 USDA Standard References

We obtained AAs and macronutrients food composition from USDA National Nutrient Database for Standard Reference (available at https://fdc.nal.usda.gov/). We selected from the database those food items most likely present in Herculaneum in AD 79 as reported by archaeological evidence and historical accounts. Moreover, we selected the highest variability of items to account for possible difference in macronutrient concentration of products belonging to the same food group (*e.g.*, whole cereal and flour, different cuts of meat, fresh and mature cheese, finfish and shellfish) and avoiding any processed foods or those with additives. The food items selected were (NDB Numbers): C_3 Cereals, 20004, 20005, 20033, 20038, 20062, 20076, 20087, 20140, 20466, 20481; Terrestrial animal products, 10020, 10070, 10192, 13019, 13147, 13235, 23095, 05001, 05011, 05023, 05057, 05075, 05135, 01123, 01109, 01106, 01089, 01145, 01036, 01156, 01157, 01159, 01019, 0108; Marine fish, 15001, 15091, 15039, 15117, 15025, 15028, 15046, 15057, 15110, 15157, 15163, 15166, 15270. Macronutrient composition of the three food groups is reported in Table S6.

Chapter 7

Results and discussion

The goal of this chapter is to present the results obtained by CSIA-AA and discuss the advantages of using this approach to study ancient diet in the Mediterranean. To do so, the discussion will be divided in two main sections: the first one (section 7.1) will focus on the methodological achievements, while the second one (section 7.2) will synthesise the new evidence derived by using CSIA-AA to contextualise the catastrophic human assemblage of Herculaneum.

7.1 Advantages of using CSIA-AA to investigate the Roman Mediterranean diet

The aim of this section is to explore the advantages of using CSIA-AA in the investigation of the Roman Mediterranean diet by presenting and discussing the results obtained from the analysis of the nineteen human individuals from the Herculaneum *fornici* and a comparable dietary baseline. First, the bulk carbon and nitrogen stable isotope values of the human individuals will be discussed once again, but this time comparing the results with those from a new dietary baseline, adding new evidence to previous publications (Craig *et al.* 2013; Fernandes 2016; Martyn *et al.* 2018)(section 7.1.1). Then, since the isotopic analysis of the single amino acids might not be available to many researchers yet, the potential of including bulk carbon isotopic measurements of bone apatite in dietary investigations in the Mediterranean will be evaluated, in light of the results obtained from a pilot study on a small number of samples (section 7.1.2). Finally, the carbon and nitrogen CSIA-AA results will be discussed focusing on some of the central questions around the diet of the Romans in the Mediterranean, namely

marine product consumption and the protein and calorific contribution of legumes and olive oil (section 7.1.3).

7.1.1 Problems with interpreting diet at Herculaneum (and in the Roman Mediterranean) using the bulk SIA approach

The inclusion of a local and contemporary baseline (with the exception of a few marine fish from Medieval Santa Severa and Spain) provides new evidence to the work previously carried out by Craig *et al.* (2013), Fernandes (2016) and Martyn *et al.* (2018).

Indeed, the bulk isotope results of the human individuals were previously compared to terrestrial herbivores from Velia and Isola Sacra and to fish remains from Velia and Pompeii only in part identified to a specific *taxon* (Craig *et al.* 2013; Fernandes 2016). Therefore, terrestrial omnivores, which might have played an important role into the Roman diet (see chapter 2 section 2.1.4) and that usually exhibit more ^{15}N- and ^{13}C-enriched isotopic signatures than the herbivores (see Table 3.1.3 and Figure 3.4 from chapter 3) were not included in the analysis. Most importantly, the contribution of terrestrial plants was either estimated from the isotope values of the terrestrial animals (Craig *et al.* 2013), assuming that the plants eaten by the humans and by the herbivores were the same, which is most likely not the case in the Roman Mediterranean, or completely neglected (Fernandes 2016). Figure 7.1 shows the δ^{15}N and δ^{13}C bulk collagen values of the nineteen humans analysed in this thesis and the averaged ($\pm$ 1σ) bulk δ^{15}N and δ^{13}C values from possible dietary resources divided by group. Descriptive statistics for the humans, the animals and the plant material is reported in Table 7.1.1. For the purpose of this section, the three dog samples (*EF11DOG*, *EF12DOG1* and *EF12DOG2*) were excluded from the terrestrial omnivore group since dogs are unlikely to be human prey.

When compared to the new baseline, the δ^{15}N and δ^{13}C of the nineteen humans from Herculaneum appear to be indicative of an omnivorous diet mainly based on products with a C_3 signature, perhaps with a minor C_4/marine contribution, as already proposed by Craig *et al.* (2013), Fernandes (2016) and Martyn *et al.* (2018). Craig *et al.* (2013) and Martyn *et al.* (2018) interpreted the slightly higher δ^{15}N and δ^{13}C in the male group with a higher consumption of high trophic level marine fish. There is a tendency in the field to interpret higher bulk collagen δ^{15}N and δ^{13}C values in Roman Mediterranean communities with an increased consumption of marine products (see chapter 3 section 3.1.3). However, higher bulk collagen δ^{15}N is not necessarily

indicative of a richer diet in marine (or terrestrial animal) products, but rather it indicates inclusion of any dietary protein showing a ^{15}N-enrichment, which might also include C_3 cereals. Indeed, some of the C_3 cereals from Herculaneum and early 2^{nd} century *Portus Romae* show enriched δ^{15}N values, probably as a consequence of intensive manuring or environmental and climatic conditions (Figure 7.1 and Table 7.1.1) and they cannot be distinguished from those of terrestrial animals (Mann-Whitney U Test, p-value = 0.5049). Therefore, if an averaged $\delta^{15}N_{collagen-diet}$ of +3.4 ± 1 ‰ from feeding experiments is accepted (see chapter 3 section 3.1.2), the δ^{15}N values of the humans can be explained with the consumption of only ^{15}N-enriched C_3 cereals. If, on the contrary, a larger $\delta^{15}N_{collagen-diet}$ offset of *ca.* +6 ‰ as suggested by O'Connell *et al.* (2012) is considered, the δ^{15}N values of the humans would be indicative of a diet largely based on ^{15}N-depleted proteins, perhaps mainly legumes mixed with cereals and cereal products.

It is probably even more difficult to interpret the δ^{13}C values of the Herculaneum individuals and more in general from archaeological populations. The low δ^{13}C bulk collagen values in Roman individuals was previously explained with the contribution of carbohydrates from C_3 cereals and lipids from olive oil to the synthesis of non-essential amino acids in collagen (Prowse *et al.* 2004, 2005)(see chapter 3 section 3.1.3). The fact that carbon in collagen comes, although preferentially from proteins, from a mixture of all the macronutrients, makes the identification of a $\delta^{13}C_{collagen-diet}$ offset extremely challenging. Moreover, if the protein fraction in the diet is low, the carbon from carbohydrates and lipids can contribute to *ca.* 50 % of the total carbon in collagen, making the marine protein contribution invisible when this is lower than 20 %, which might be the case in the Roman Mediterranean. It is nowadays accepted that it is impossible to trace back the diet of an individual from its collagen δ^{13}C value without knowing the composition of the diet *a priori*, which is contradictory in its sense (see chapter 3 section 3.1.1). Therefore, it is difficult to predict the cause of the slight ^{13}C-enrichment of the bone collagen of the male individuals from Herculaneum. However, in this specific context, the radiocarbon dating of nine individuals from Herculaneum allowed Craig *et al.* (2013) and Martyn *et al.* (2018) the confident attribution of increased δ^{13}C values to marine resources consumption. This remains an exceptional case which might not be reflected by other Roman Mediterranean communities.

This certainly does not imply that the SIA approach has to be set aside from its application for dietary investigations. Indeed, although it has to be accepted that the *reasons* behind the bulk δ^{15}N and δ^{13}C collagen values can not be confidently identified, SIA is extremely helpful to explore intra- and inter-populations differences.

The fact that women and men from Herculaneum exhibit slightly different bulk δ^{15}N and δ^{13}C collagen values is indicative of the preferential access to different food sources by the two groups, which is a valuable information about social and cultural differences *per se*. The SIA approach also gives the opportunity to observe the economic role of Herculaneum when compared to other Roman Mediterranean contexts. Indeed, the averaged bulk δ^{15}N and δ^{13}C values from the human individuals of Herculaneum appear to be closer to those from the communities located in the proximity of Rome rather than to Velia and Paestum, two archaeological sites from Campania (see chapter 3, Figure 3.4 and section 3.1.3). This supports the existing evidence that the Bay of Naples was an important area of production and trade in the Mediterranean which is reflected in the diet of the people living in the area.

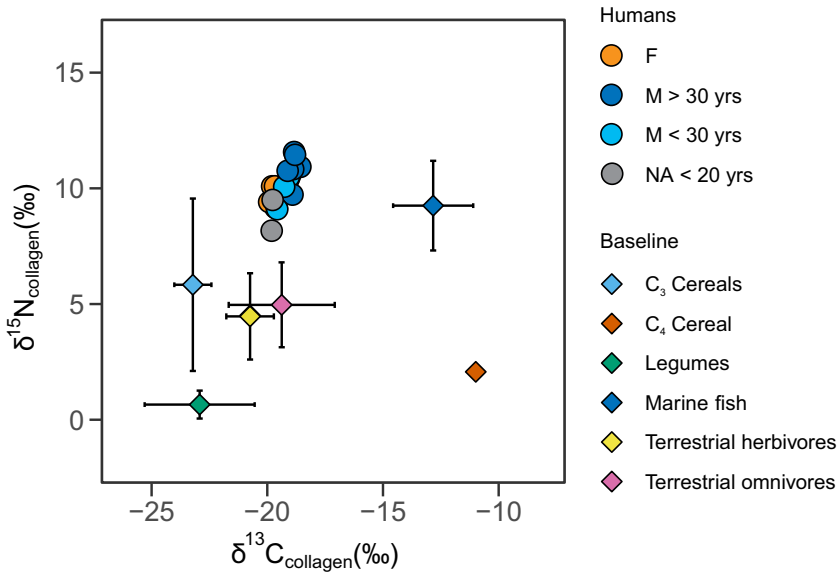

Figure 7.1 δ^{15}N and δ^{13}C values of human individuals from Herculaneum (only the nineteen individuals analysed in this study) compared with mean values of cereals, legumes and animals from comparable archaeological contexts. Error bars represent 1σ.

7.1.2 Potential of including δ^{13}C values of bone apatite in the dietary investigations in the Mediterranean: a pilot study

One of the main methodological limitations of the SIA approach applied to collagen is the difficulty of predicting the carbon isotope composition of the diet considering the $\delta^{13}C_{collagen}$ values, since bulk $\delta^{13}C_{collagen-diet}$ offset values are highly influenced by dietary composition (Webb *et al.* 2017). On the contrary, $\delta^{13}C_{apatite}$ are strongly

		$\delta^{15}N$					δ^{13}C				
	n	*mean*	*median*	1σ	*min*	*max*	*mean*	*median*	1σ	*min*	*max*
Humans											
F	6	9.74	9.75	0.51	9.16	10.39	-19.64	-19.69	0.29	-19.92	-19.08
M	11	10.42	10.54	0.83	9.10	11.57	-19.06	-19.02	0.32	-19.59	-18.57
NA	2	8.84	8.84	0.94	8.17	9.50	-19.79	-19.79	0.03	-19.81	-19.77
Baseline											
C_3 Cereals	9	5.69	4.30	3.80	0.80	10.90	-23.27	-23.10	0.78	-25.00	-22.40
C_4 Cereals*	1	1.76					-11.10				
Legumes	4	0.35	0.48	0.60	-0.49	0.92	-23.03	-22.20	2.38	-26.53	-21.21
Marine fish	32	9.25	9.23	1.94	4.83	14.42	-12.83	-12.99	1.73	-16.22	-7.95
Terrestrial herbivores	17	4.50	3.96	1.86	1.50	8.10	-20.74	-21.20	1.03	-21.96	-17.84
Terrestrial omnivores	16	5.00	1.83	2.36	2.36	7.93	-19.38	-20.61	2.29	-21.44	-13.42

Table 7.1 Descriptive statistics (dplyr, R version 4.03) of the nineteen human individuals from Herculaneum included in this thesis and of the herbivore and omnivore animals, marine fish, C_3 and C_4 cereals and the legumes analysed as a reference for the human data. *: Only one millet sample was analysed as representative of the C_4 cereal group.

correlated with the overall $\delta^{13}C_{diet}$ signal, precisely by $\delta^{13}C_{apatite-diet} = +10.09 \pm 1.43$ ‰, as calculated from feeding experiment studies ($n = 42$, see chapter 3 section 3.1.1).

It was decided therefore to explore $\delta^{13}C_{apatite}$ values in a small number of samples with the aim to explore the potential of this proxy in identifying marine consumption at Herculaneum.

Although the measurement of δ^{13}C of bone apatite represents a valuable tool in the investigation of dietary habits, there are some limitations linked to its diagenesis and laboratory procedures. Bioapatite can dissolve and recrystallise during burial as a consequence of active hydrology, soil pH and microbial attack (*e.g.*, Kontopoulos *et al.* 2019). If the bone sample is contaminated with diagenetic carbonates, the measured δ^{13}C value will be influenced by their presence and therefore possibly mislead the interpretation of the results.

The nine individuals from Herculaneum radiocarbon-dated by Craig *et al.* (2013) were selected for the analysis of their carbonate isotope values. Although these samples were already screened via Fourier Transform Infrared spectroscopy in conjunction with an Attenuated Total Reflection accessory (FTIR-ATR) to observe the exposure to high temperature that would have altered the bone microstructure (Martyn *et al.* 2020), here FTIR-ATR was applied again to detect changes in the structure before and after

the chemical treatment used for the carbonate isotope analysis. Ten animal remains were also included in the analysis.

FTIR-ATR has been widely adopted to explore collagen and apatite molecular bonds and evaluate their preservation relying on specific indices (France *et al.* 2020). The indices are calculated considering the infrared spectrum of absorption at a given wavelength. Among others, the Infrared Splitting Factor (IRSF) also called Crystallinity Index (CI) and the Carbonate to Phosphate ratio (C/P) are the most deployed and therefore those for which there are more reference values in the literature (France *et al.* 2020). The IRSF is used to observe the order/disorder and size of the apatite crystals: the larger and/or more ordered crystals will determine a higher IRSF value. The C/P instead informs about any diagenetic change comparing the carbonate content with the phosphate one (Kontopoulos *et al.* 2019). These two indices are calculated as following:

$$IRSF = \frac{600cm^{-1} + 560cm^{-1}}{590cm^{-1}} \tag{7.1}$$

$$C/P = \frac{1410cm^{-1}}{1010cm^{-1}} \tag{7.2}$$

Small bone fragments from the samples were ground to a fine powder and divided in two portions. One, referred to as "pre-treatment" was analysed via ATR-FTIR to explore carbonate composition of the original sample. The second one, referred to as "post-treatment" was processed after Pellegrini and Snoeck (2016) to remove possible diagenetic carbonates and salts as follows: briefly, the samples were soaked in 1 M calcium acetate ($(CH_3COO)_2Ca$) buffered solution (pH 4.7) for 30 min. The solution was removed and the samples washed five times with deionised water. The samples were then frozen and placed into a freeze-drier to remove water.

The FTIR-ATR system adopted was a Bruker Alpha Platinum instrument set to: spectrum range, 4000-400 cm^{-1}; Number of scans, 144; zero filling factor, 4; resolution, 4 cm^{-1}; mode: absorbance) and the indices were calculated using the OPUS 7.5 software (Kontopoulos *et al.* 2019).

The treated samples were sent to Iso-Analytical Limited to be analysed in their carbon and oxygen isotope composition by Continuous Flow-Isotope Ratio Mass Spectrometry (CF-IRMS). The samples had a replicate precision ≤ 0.3 ‰ for carbon and < 0.4 ‰ for oxygen. Carbon content was calculated by comparing the total ion beam data for the samples against the pure calcium carbonate references.

Results and discussion

None of the post-treated samples exhibits IRSF values above 4.3 and C/P values above 0.32, which would be indicative of bad apatite preservation (France *et al.* 2020). However, it was not possible to carry out the FTIR screening for all the treated samples due to lack of material. For these cases, the indices obtained from the pre-treated powders were used instead and sample *SSF5* was excluded from the result discussion since the C/P value of the pre-treated powder was higher than 0.32. Sample *F10i28* was also excluded for its low carbonate content. Results are reported in Table 7.1.2.

The results obtained were compared with reference values from feeding experiments and archaeological populations as suggested by Froehle *et al.* (2010, 2012)(Figure 7.2). The two lines (with 95 % confidence intervals) from Figure 7.2 a represent diets with a mostly-C_3 (dashed line) and C_4/marine (dotted line) protein fraction. It is essential to note that these models were not tested against collagen and apatite isotope values from the Mediterranean area and therefore might not be accurate. For comparison purposes, $\delta^{13}C_{collagen}$, $\delta^{15}N_{collagen}$ and $\delta^{13}C_{apatite}$ mean values ($\pm$ 1σ) of other Imperial Roman Mediterranean communities were also included (Prowse *et al.* 2004, 2005; Keenleyside *et al.* 2009; Killgrove and Tykot 2013, 2018; Dotsika and Michael 2018). The distribution of the human values, which is close to the mostly-C_3 protein line, suggest that the eight individuals from Herculaneum were consuming mainly C_3 proteins, likewise the other Roman communities. The $\delta^{13}C_{apatite}$ values however, particularly in the female individuals and in one of the males (*F12i23*), are higher than those exhibited by the other Roman individuals, suggesting that the non-protein fraction of diet was ^{13}C-enriched compared to the protein one (Mann-Whitney U Test, p-value = 1.027e-12) (Froehle *et al.* 2010). Among products that have ^{13}C-depleted protein isotope values there are terrestrial primary producers and primary/secondary consumers, in line with other archaeological evidence and the bulk $\delta^{13}C$ values of C_3 cereals, legumes and terrestrial animals from Herculaneum and comparable contexts presented in chapter 5, Figure 5.5 a. The slightly lower $\delta^{13}C_{collagen}$ values at Herculaneum compared to the other individuals (Mann-Whitney U Test, p-value = 3.313e-08) suggest that at least part of the terrestrial sources consumed had a slightly more ^{13}C-depleted baseline than that consumed by the other Mediterranean Roman communities here considered, and this could be the case of C_3 cereals from outside the main extensive production chain from the Provinces, legumes, higher consumption of other vegetables, or even a modest consumption of freshwater resources. The male and female individuals from Herculaneum turn out to be better distinguished by their $\delta^{13}C_{apatite}$ values than by

ID	Group	Sex	Age	Treatment	IRSF	C/P	Carbonate content (%)	$\delta^{13}C_{Ap}$ (‰)	$\delta^{18}O_{Ap}$ (‰)
F10i11	Human	F	30-40	Pre	4.19	0.18			
				Post	3.64	0.18	6.4	-8.65	-5.25
F10i16	Human	F	30-40	Pre	4.10	0.16			
				Post	4.11	0.15	5.3	-9.23	-5.30
F10i128*	Human	F	30-40	Pre	4.37	0.12			
				Post	3.53	0.22	1.1	-6.66	-3.91
F12i3	Human	F	20-30	Pre	3.87	0.18			
				Post	3.76	0.17	5.1	-7.50	-4.22
F12i28	Human	F	30-40	Pre	3.61	0.22			
				Post	3.44	0.30	3	-8.44	-3.40
F7i10	Human	M	30-40	Pre	3.64	0.20			
				Post	3.70	0.17	7.8	-10.71	-2.81
F9i9	Human	M	40-50	Pre	3.76	0.19			
				Post	3.83	0.16	8.4	-10.22	-4.34
F9i13	Human	M	40-50	Pre	3.72	0.18			
				Post	3.68	0.19	4.9	-10.24	-3.99
F12i23	Human	M	40-50	Pre	4.25	0.13			
				Post	3.96	0.13	4.2	-8.61	-5.29
EF8SG	Herbivore			Pre	3.47	0.25			
				Post	3.48	0.25	4.8	-10.24	-0.17
PSC2	Herbivore			Pre	3.42	0.28			
				Post	3.62	0.20	6.8	-4.61	-1.25
PSSG3	Herbivore			Pre	3.23	0.36			
				Post	3.34	0.28	4.3	-5.36	1.05
PSCH1	Omnivore			Pre	3.39	0.28			
				Post	3.45	0.27	6.6	-5.68	-1.44
PSG1	Omnivore			Pre	3.31	0.31			
				Post	3.44	0.25	6.9	-8.11	-1.34
PSP3	Omnivore			Pre	3.44	0.34			
				Post	3.42	0.28	7.8	-7.92	-1.24
ABF3	Marine fish			Pre	3.25	0.28			
				Post			2.0	-5.96	-0.05
HSSSQ	Marine fish			Pre	3.47	0.21			
				Post	3.44	0.22	8.5	-1.55	0.06
SSF2	Marine fish			Pre	3.52	0.21			
				Post			6.4	-5.36	-0.31
SSF5*	Marine fish			Pre	3.42	0.72			
				Post			3.6	-7.80	-0.99

Table 7.2 Preservation indices values (IRSF and C/P) of the pre- and post-treated human samples and $\delta^{13}C_{Ap}$ and $\delta^{18}O_{Ap}$ values of the post-treated samples analysed by CF-IRMS. *Samples excluded from the discussion.

their $\delta^{13}C_{collagen}$ ones, although this can not be confirmed by any statistical test due to the low number of samples.

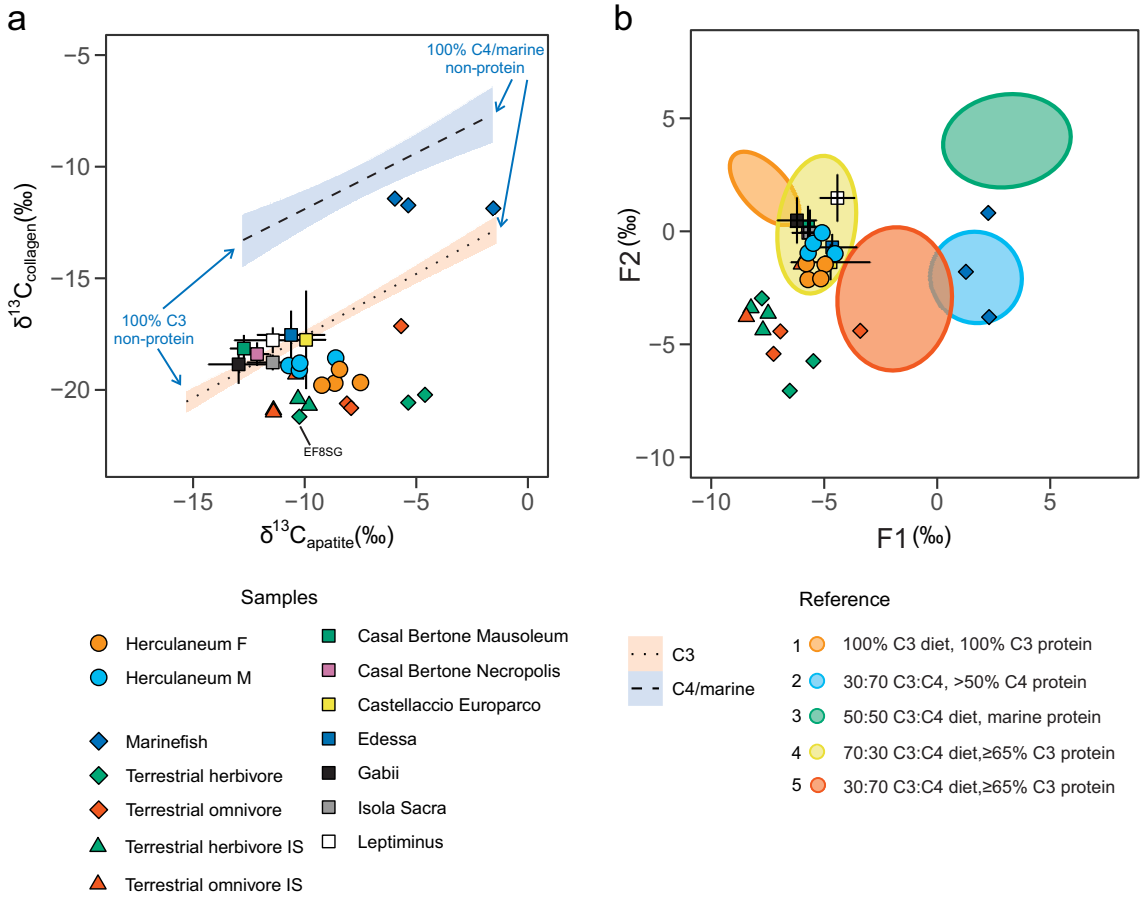

Figure 7.2 $\delta^{13}C_{collagen}$ and $\delta^{13}C_{apatite}$ values of eight individuals from Herculaneum and nine fauna remains plotted against experimental animal regression lines and their 95% confidence intervals (a) and discriminant function F1 and F2 scores calculated using $\delta^{13}C_{collagen}$, $\delta^{15}N_{collagen}$ and $\delta^{13}C_{apatite}$ values against clusters of animals from feeding experiments and archaeological populations (b) (Froehle *et al.* 2010, 2012). Mean $\delta^{13}C_{collagen}$, $\delta^{15}N_{collagen}$ and $\delta^{13}C_{apatite}$ values ($\pm$ 1σ) from other Mediterranean Roman context are also included (Prowse *et al.* 2004, 2005; Keenleyside *et al.* 2009; Killgrove and Tykot 2013, 2018; Dotsika and Michael 2018).

It is more difficult to explain the more ^{13}C-enriched contribution of non-protein components in the diet of the individuals at Herculaneum, particularly of the female ones. A food source that has a C_4/marine isotopic signature and a high non-protein component content could be represented by the C_4 cereals. Millet was certainly consumed at Herculaneum, as reported by Pliny and documented by archaeobotany studies (see chapter 2 section 2.1.2). However, if the consumption of C_4 cereals such as millet was so high to contribute to the bone apatite isotopic signal, they would have also, if minimally, participate to the $\delta^{13}C_{collagen}$ values, such as in the case of

the individuals from Edessa and Castellaccio Europarco (Figure 7.2 a)(Killgrove and Tykot 2013; Dotsika and Michael 2018), unless the contribution from a ^{13}C-depleted protein source is so high to obscure that from the C_4 cereals, which might be the case if ^{13}C-depleted products with a high content of proteins, such as animal products and legumes, are consumed. This would reflect a poorer and more "rural" diet composed by products such as "inferior" cereals (including millet, see chapter 2 section 2.1.2), legumes and dairy products (Garnsey 1999, 100-112).

Another option might be the consumption of marine products that are low in protein and high in non-protein components. Fish sauces such as *garum* were prepared using all the parts of the fish and often by only using the innards discarded by the fish salting industry (Marzano 2013b, 89-98). The innards, and more specifically the guts, facilitate the fermentation process due to their higher quantity of proteolytic enzymes and are therefore considered essential in the fish sauce production (Mouritsen *et al.* 2017). Guts, liver, and skin are richer in fatty acids compared to the fish muscle (Pateiro *et al.* 2020). The consumption of fatty fish sauces or of fish fatty tissues could contribute to the ^{13}C-enriched apatite values of the humans here analysed. However, it should also be noted that lipids are ^{13}C-depleted relative to proteins and carbohydrates by *ca.* -7 ‰ (Fernandes 2016) and therefore this possibility does not entirely explain the observed $\delta^{13}C_{apatite}$ values. Moreover, fish sauces and fish fatty tissues are expected to also contain proteins and free amino acids, and therefore their consumption should have been reflected by the $\delta^{13}C_{collagen}$ values as well (*e.g.*, Curtis 2009).

Froehle *et al.* (2012) proposed a multivariate model that included $\delta^{15}N_{collagen}$ values in addition to the $\delta^{13}C_{collagen}$ values and $\delta^{13}C_{apatite}$ ones with the aim to better discriminate C_4 and marine sources since the latter are expected to exhibit higher $\delta^{15}N$ values. This could theoretically be of help in this specific case, where it is difficult to explain which source (or rather mixture of sources) is responsible for the higher observed $\delta^{13}C_{apatite}$ values. The 8 human individuals overlap, together with the other Mediterranean Roman communities, with the cluster number 4, which identifies a diet mainly consisting of C_3 sources but also with a C_4 input ($C_3 : C_4 = 70 : 30$) also in the protein fraction (total protein consumed is $\geq$ 65 % C_3)(Figure 7.2 b). However, it should be noted that this model was not tested for marine input values from the Mediterranean, where fish $\delta^{15}N_{collagen}$ values are lower than those from the Atlantic (see chapter 5 section 5.2.2)(Froehle *et al.* 2012). Therefore, this model most likely underestimates the marine consumption at Herculaneum and more in general in the Mediterranean.

Carbon amino acid data can be of help in confirming whether the ^{13}C-enriched $\delta^{13}C_{apatite}$ values of the female plus the *F12i23* male are caused by an increased consumption of C_4s or marine fatty tissues (Figure 7.3). If the $\delta^{13}C_{apatite}$ values in this group are caused by a higher consumption of C_4 carbohydrates, this should be in theory reflected by the carbon isotopes of alanine, a non-essential amino acid whose carbon is derived from the digestion of carbohydrates via the pyruvate synthesis (see chapter 3 section 3.12). The $\delta^{13}C_{Ala}$ values do not appear to be different between the two groups and therefore a significant contribution from C_4 carbohydrates seems unlikely, unless hidden by the $\delta^{13}C_{Ala}$ measurement uncertainty (max $\delta^{13}C_{Ala}$ uncertainty between these eight humans is 1.1 ‰)(Figure 7.3 a). On the other hand, if the apatite ^{13}C-enrichment is instead caused by the consumption of fatty fish components, the $\delta^{13}C$ values of non-essential amino acids synthesised from the overall digestion of macronutrients via the TCA cycle, such as glutamic acid, would be expected to be ^{13}C-enriched in this group of individuals (see chapter 3 section 3.12). However the $\delta^{13}C_{Glx}$ values do not support this hypothesis and they also seem to be slightly higher in the male group (with the exception of one male, *F7i10*)(Figure 7.3 b).

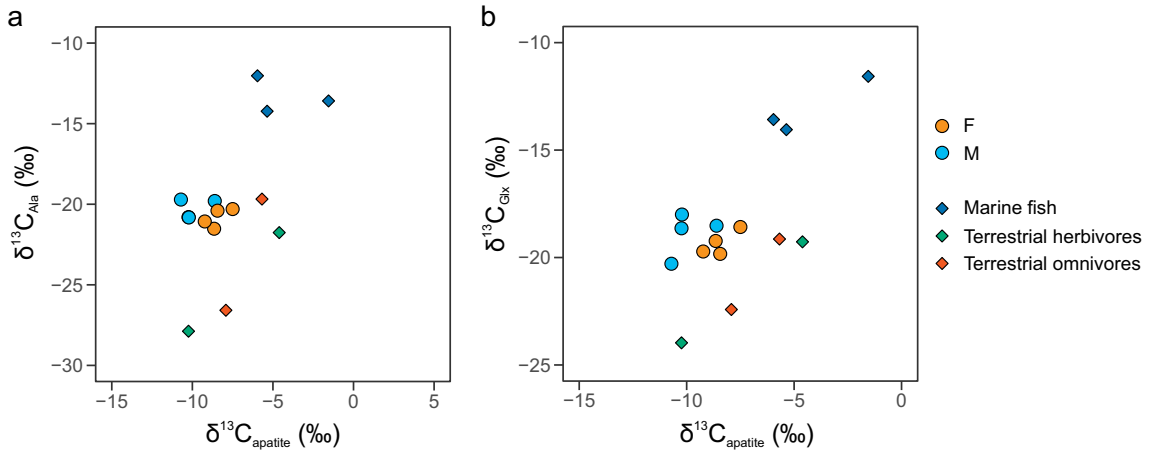

Figure 7.3 $\delta^{13}C_{apatite}$ values of human individuals from Herculaneum and nine animals from comparable contexts against collagen $\delta^{13}C_{Ala}$ (a) and $\delta^{13}C_{Glx}$ (b) values.

The inclusion of the terrestrial and marine fauna can be of help in this specific context. Interestingly, all the terrestrial animals, with the only exception of the *EF8SG* sheep from the *fornici*, exhibit $\delta^{13}C_{apatite}$ values that are equal or above those of the female and one male from Herculaneum (Figure 7.2 a) and of the animals from Isola Sacra. Although it is possible that these animals were at least in part fed with C_4 sources, a more general ^{13}C enrichment at the bottom of the local terrestrial C_3 baseline seems a more plausible explanation, probably caused by the injection of "old"

magmatic CO_2 into the local groundwater as a consequence to volcanic activity in the area (Holdaway *et al.* 2018).

Therefore, the most likely explanation behind the different $\delta^{13}C_{apatite}$ values between the two groups from Figure 7.2 a is that the women (and the *F12i23* male) were consuming a higher proportion of local products compared to the males. The sheep *EF8SG* shows $\delta^{13}C_{apatite}$ values that are in line with the male group from Herculaneum, other Roman communities and the animals from Isola Sacra. As discussed in chapter 5 section 5.2.2, the amino acid isotope data suggest that the sheep *EF8SG* was in great part fed with sources different from those of the other animals and closer to the majority of the C_3 cereals analysed. If the C_3 cereals were imported from elsewhere, and this seems to be the case in the Roman Mediterranean, this would explain why the $\delta^{13}C_{apatite}$ values of the sheep *EF8SG* are not ^{13}C-enriched like other animals. However, it is not clear why the emission of magmatic CO_2 has an effect on the inorganic component of bone and not on the collagen. This does not seem to be related to the turnover rates of collagen and apatite, since the mineralisation process appears to be slower than the collagen turnover (Tsutaya and Yoneda 2013). Moreover, the cereals and legumes from Herculaneum are not equally ^{13}C-enriched in their bulk values (see Figure 7.1 and Table 7.1.1), although it can not be ruled out that all the legumes and cereals analysed were imported from elsewhere, which is attested by the historical and archaeological evidence (see chapter 2 section 2.1.2 and 2.1.3).

It can also not be ruled out that the $\delta^{13}C_{apatite}$ values are ^{13}C-enriched as an effect of exposure to the high temperature caused by the volcanic eruption at Pompeii and Herculaneum (Surovell 2000). However, this does not explain why this would affect preferentially the female individuals (and the *F12i23* male) and the terrestrial animals but the *EF8SG* sheep.

Last but not least, methodological issues also need to be considered. The more negative $\delta^{13}C_{collagen}$ values observed at Herculaneum compared to the other Roman communities could be caused by humic acid and/or lipid contamination. This could also explain the slightly systematic enrichment of the estimated bulk $\delta^{13}C_{collagen}$ values by mass balance calculation of the amino acid compared to the observed bulk $\delta^{13}C_{collagen}$ values (Figure 4.8 a from chapter 4). The extracted collagen from Herculaneum was not considered contaminated since the darker colour, which is usually considered an indication of humic acid presence, was not detected and and all the samples fall between the the *C:N* range suggested by Van Klinken (1999). Therefore, a sodium hydroxide step to remove possible humic acid and/or a preliminary extraction of lipids from bones were not considered essential but it can not be ruled out that a small

contamination is indeed present and it is affecting the bulk $\delta^{13}C_{collagen}$ values (Sealy *et al.* 2014; Guiry *et al.* 2016). As for the $\delta^{13}C_{apatite}$ values, it is known that different acid and organic phase removal protocols alter the isotope signatures of the samples (Garvie-Lok *et al.* 2004; Pellegrini and Snoeck 2016). Nevertheless, the protocol used should minimise any fractionation during treatment (Pellegrini and Snoeck 2016). To conclude, the differences observed here between males and females - although from a small assemblage - must be related to different diets and/or metabolic mechanisms in the two groups, since they were all subjected to the same laboratory protocols.

In conclusion, the isotope analysis of bone apatite to a small sub-sample from this study seemed at first a valuable tool to detect gender related dietary differences. However, the inclusion of the animals allowed avoiding erroneous interpretations, since pre-constructed models, such as those proposed by Froehle *et al.* (2010, 2012) do not account for environmental or geographical isotope variability. It is suggested therefore that, if the measurement of $\delta^{13}C_{apatite}$ values is included in the dietary investigation, this is also carried out on the local fauna in order to guide the interpretation. In this specific case, it is difficult to explain the ^{13}C-enrichment of the $\delta^{13}C_{apatite}$ values compared to the $\delta^{13}C_{collagen}$, particularly in the group consisting of the female individuals and one male, but they seem to be at least partly influenced by the local geography.

7.1.3 Diet at Herculaneum in AD 79: the CSIA-AA approach

The analysis of carbon and nitrogen from the single amino acids which constitute bone collagen has a great potential in discriminating the food sources that contribute to the overall diet. The metabolic pathways of amino acids and more specifically the carbon and nitrogen routes in the human body have been widely explored in the past (see chapter 3 section 3.2.1). This allows the reconnection of the $\delta^{13}C_{AA}$ and $\delta^{15}N_{AA}$ values to specific fraction of diet which are more relevant in some sources than others. For example, carbon in alanine is obtained from the digestion of carbohydrates via the synthesis of pyruvate. Therefore, the $\delta^{13}C$ value of alanine in the bone collagen is informative about those food sources rich in carbohydrates, such as cereals (see chapter 3 section 3.2.2). However, a certain degree of uncertainty needs to be accepted. It was shown for example that the synthesis of non-essential amino acids, such as alanine, is inhibited when the diet is rich in protein as these will be preferentially routed (Jones 2002; Howland 2003; Howland *et al.* 2003; Jim *et al.* 2004; Corr *et al.* 2005; Jim *et al.* 2006; Webb *et al.* 2017) and that fractionation of carbon and nitrogen in amino acids can be further complicated in case of metabolic diseases or starvation (*e.g.*, Fuller and

Petzke 2017). Here, it is assumed that the diet at Herculaneum was not exceptionally high in proteins and that the individuals were not affected by severe malnutrition or metabolic diseases, as suggested by historical and archaeological evidences (see chapter 2 and section 3.1.3 from chapter 3). Moreover, isotopic fractionation of essential and source amino acids is minimal regardless of the protein quantity and quality of diet, providing a valuable tool to directly explore the protein fraction of diet without relying on any assumptions. Following, the CSIA-AA results will be discussed by answering some relevant archaeological questions.

Marine food consumption revealed

In the last few years, the carbon or nitrogen isotope values of the single amino acids have been often used to explore marine food consumption and some proxies have been considered more helpful than others (*e.g.*, Corr *et al.* 2005; Styring *et al.* 2010; Choy *et al.* 2010; Honch *et al.* 2012).

Glycine is a non-essential amino acid which was shown to be highly sensitive to the contribution of marine protein in diet. The reason why this happens has still not been fully understood but researchers believe that when a diet is relatively poor in proteins but rich in a particular amino acid, which is the case of glycine in marine fish, this amino acid will be at least in part directly routed (Corr *et al.* 2005; Webb *et al.* 2017). A recent feeding experiment has shown that the direct routing of glycine becomes significant when marine protein is $\geq 50\%$ (Webb *et al.* 2017). The $\delta^{13}C_{Gly}$ values of the bone collagen of the individuals from Herculaneum appear ^{13}C-enriched compared to the $\delta^{13}C_{Phe}$ ones. In Corr *et al.* (2005), high-marine protein consumers exhibited a $\delta^{13}C_{Gly-Phe}$ offset of $+12.0 \pm 1.9$ ‰. Individuals from Herculaneum shows a higher averaged offset, $\delta^{13}C_{Gly-Phe} = +17.2 \pm 2.7$ ‰ however, $\delta^{13}C_{Phe}$ values of human, animals and cereals are ^{13}C-depleted compared to those considered by Corr *et al.* (2005), stressing again the importance of including a local baseline in dietary investigations from archaeological populations (Choy *et al.* 2010; Honch *et al.* 2012). $\delta^{13}C_{Gly-Phe}$ values are not significantly different in males and females (Mann-Whitney U Test, p-value = 0.3028). However, phenylalanine is probably not the most suitable essential amino acid to discriminate sources in this context, since the $\delta^{13}C_{Phe}$ values largely overlap between food groups (cereals, animals and marine fish from Figure 7.4). When the carbon isotope values of a different essential amino acid, for example leucine, are used against those of glycine, it is possible to observe a much higher discrimination between food groups and gender (Figure 7.4 b). The same pattern was observed using the $\delta^{13}C$ values of valine, isoleucine and lysine. It would appear therefore that proteins

were at least in part directly routed from marine resources, particularly in the males, with the only exception of the male individuals *F7i7* and *F8i23*, both less than 30 year old.

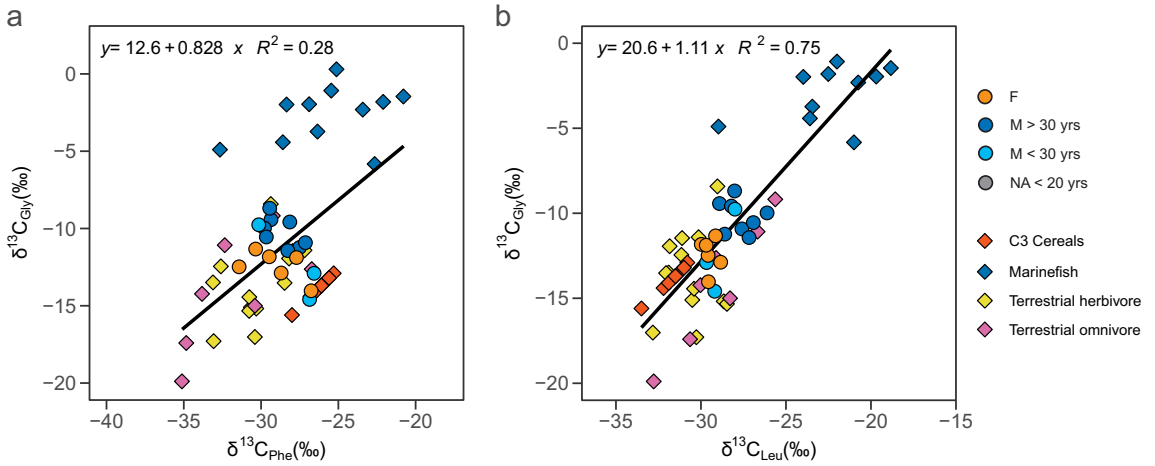

Figure 7.4 δ^{13}C values of glycine from Herculaneum human individuals, cereals, animals and marine fish from comparable contexts against the δ^{13}C values of the essential amino acids phenylalanine (a) and leucine (b).

The comparison of δ^{13}C values in phenylalanine and valine to distinguish between C_3, C_4, freshwater and marine protein consumers was first proposed by Honch *et al.* (2012) and since then applied to various archaeological populations (*e.g.*, Colonese *et al.* 2014; Mora *et al.* 2018; Jaouen *et al.* 2019). If the protein source is predominantly C_3 or C_4, phenylalanine and valine should exhibit similar values, less ^{13}C-depleted in case of C_4 consumption. If freshwater or marine protein are also present in the diet, valine should be ^{13}C-enriched compared to phenylalanine, with more ^{13}C-enriched values in case of marine protein consumption (see chapter 3 section 3.2.1). In this dataset, valine appears to be ^{13}C-enriched compared to phenylalanine not only in the marine fish group but also in the majority of the terrestrial animals and the humans (Figure 7.5 a). Such a high proportion of freshwater resources in the diet of people living at Herculaneum seems unlikely and, most importantly, unrealistic in the case of herbivore and omnivore animals. Instead, a most likely explanation is that phenylalanine at the bottom of the terrestrial animal food web is ^{13}C-enriched compared to that of the cluster which identifies C_3 protein consumptions from Honch *et al.* (2012). The $\delta^{13}C_{Phe}$ values of cereals are between those of terrestrial animals and marine fish, making the interpretation of the human data difficult but, at the same time, it has the advantage of distinguishing between two separate terrestrial food webs, one identified by the majority of the animals and one represented by the C_3 cereals, suggesting perhaps that

the diet of the male individuals *F7i7* and *F8i23* and of the female individuals *F10i11* and *F12i28* was rich of proteins with a C_3 signature different from that of the the majority of the animals (Figure 7.5 a). This could be either indicative of consumption of imported products or that these humans spent a great part of the last years of their lives in a different geographical area.

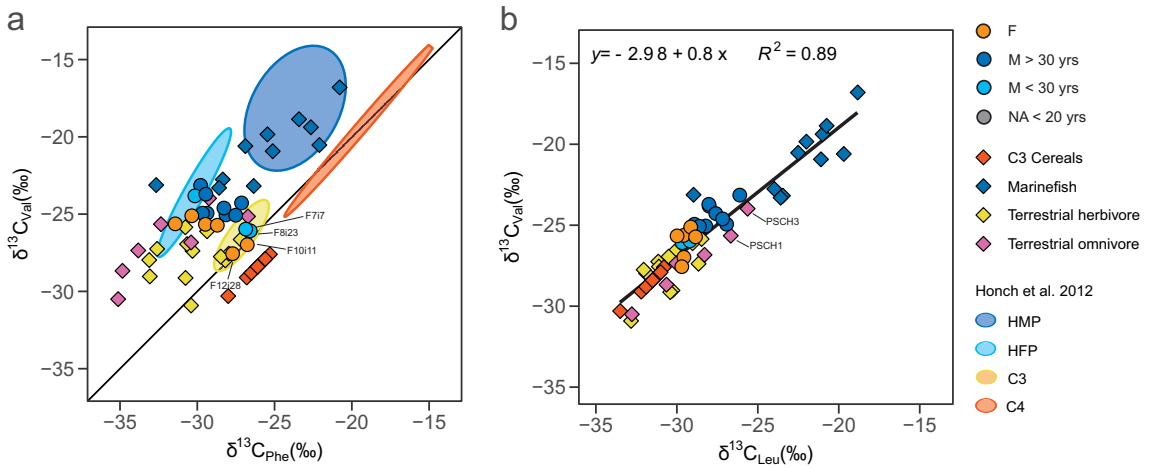

Figure 7.5 δ^{13}C values of glycine from Herculaneum human individuals, cereals, animals and marine fish from comparable contexts against the δ^{13}C values of the essential amino acids phenylalanine (a) and leucine (b).

When a different essential amino acid is used instead of phenylalanine, the marine contribution is better distinguished (Figure 7.5 b). Males at Herculaneum seem to access more marine proteins than females. Two of the chicken samples exhibit ^{13}C-enriched values of valine and leucine. Although it can not be excluded that marine proteins were part of the diet of these animals, it is more likely that they are indicative of a C_4 input, for which there are no other references in the dataset. If this is the case, a ^{13}C-enrichment of essential amino acids in the human collagen could also be caused by C_4s consumption. However, protein content of C_4 cereals is low and therefore difficult to detect from the overall protein contribution, unless the diet consists mainly of C_4 cereals, which was excluded by looking at the non-essential amino acids (see previous section 7.1.2 and Figure 7.3).

The combination of nitrogen isotope values of a trophic amino acid and of a source amino acid is nowadays one the most deployed method to explore trophic positions of organisms in ecology, sometimes also applied to archaeological contexts (*e.g.*, Styring *et al.* 2010; Naito *et al.* 2016; Jaouen *et al.* 2019). When glutamic acid and phenylalanine δ^{15}N values are compared, the humans from Herculaneum appear to be on a trophic

level above the terrestrial animals. Although this could be interpreted at first as a high consumption of animal and fish proteins, it should be noted that the majority of the C_3 cereals have $\delta^{15}N_{Glx}$ values equal if not higher to those of the terrestrial animals, probably as a result of high manuring practices (Styring *et al.* 2014b). Marine fish exhibit $\delta^{15}N_{Phe}$ values lower than those of the terrestrial animals and cereals and therefore, if the higher $\delta^{15}N_{Glx}$ values in the male group was caused by consumption of marine proteins, it would be expected that more ^{15}N-depleted $\delta^{15}N_{Phe}$ values are seen in this group. On the contrary, males have on average slightly higher $\delta^{15}N_{Phe}$ values compared to females (males: $n = 11$, mean $\pm$ 1σ= +10.6 $\pm$ 0.8 ‰; females: $n = 6$, mean $\pm$ 1σ= +10.0 $\pm$ 0.61 ‰), suggesting that the majority of the proteins in their diet was coming from C_3 cereals with perhaps a marine input, higher in some individuals than others. On the contrary, the protein fraction of the diet of the female group was most likely composed of a mixture of local terrestrial sources and highly manured C_3 cereals, perhaps with a small contribution of marine foodstuff.

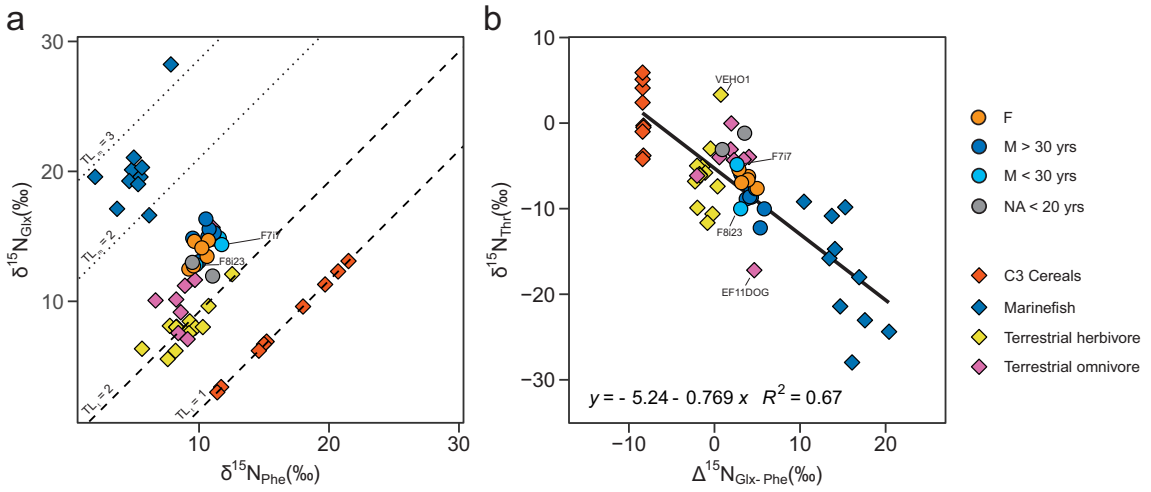

Figure 7.6 $\delta^{15}N$ values of glutamic acid against the $\delta^{15}N$ values of phenylalanine (a) and $\delta^{15}N$ values of threonine against the offset $\delta^{15}N_{Glx-Phe}$ values (b) from Herculaneum human individuals, cereals, animals and marine fish from comparable contexts.

Fuller and Petzke (2017) recently proposed that more ^{15}N-depleted $\delta^{15}N$ values of threonine are caused by an increased activity of the enzyme threonine ammonia-lyase as a response to the amount of proteins in diet, although it seems to be also reactive to protein quality (highest in case of marine proteins), starvation and diabetes. $\delta^{15}N_{Thr}$ values in total plasma of rats from the Fuller and Petzke (2017)'s feeding experiment went from -3.6 $\pm$ 1 ‰ (adequate protein, 13.8 %) to -7.9 $\pm$ 1 ‰ (high protein, 51.3 %) using casein as the only protein source. These values can not be used in their absolute terms for interpretation since nitrogen in threonine could fractionate additionally in

bone collagen compared to blood plasma and, perhaps most importantly, the diet of human individuals is most likely composed of a number of protein sources. When the $\delta^{15}N_{Thr}$ values and the offset $\delta^{15}N_{Glx-Phe}$ values from the Herculaneum individuals and the baseline are compared, the two variables are found correlated ($R^2 = 0.67$). This correlation suggests that male individuals had a diet with a higher proportion of marine proteins, and perhaps overall higher in proteins, than the female individuals.

It is also interesting to note that the two juveniles with non determined biological sex exhibit the highest $\delta^{15}N_{Thr}$ values, indicative of a diet low in proteins and with negligible marine protein sources. The female group has an average $\delta^{15}N_{Thr}$ value of -6.62 ± 0.74 ‰, which is close to the medium protein (25.7 %) value from the rat feeding experiment (Fuller and Petzke 2017). This seems to indicate that it is unlikely that the female individuals from this assemblage were under a low-protein diet and that, as the $\delta^{15}N_{Glx-Phe}$ values seem to indicate, a small but significant contribution of marine proteins was present. Among the adult individuals, the male identified with the code $F7i7$ exhibit the highest $\delta^{15}N_{Thr}$ values (-4.86 ± 0.25 ‰), indicative of a diet lower in proteins than that of other males and even of the female group. The male individual $F8i23$, which, together with $F7i7$, was often found with different carbon amino acid isotope values compared to the other males from the assemblage in the paragraphs above, exhibits one of the lowest $\delta^{15}N_{Glx}$ values among the human individuals (Figure 7.6 a) but one of the most ^{15}N-depleted $\delta^{15}N$ values of threonine (Figure 7.6 b). It is possible that in this case, the more ^{15}N-depleted $\delta^{15}N_{Thr}$ value is caused by malnutrition or other conditions.

For comparative purposes, the carbon and nitrogen isotope values of amino acids were also explored by using the Principal Component Analysis (PCA, R-function *prcomp* and R-packages *ggbiplot* and *ggplot2* for data visualisation), first considering only the source amino acids (PCA-SAA, $\delta^{15}N_{Phe}$, $\delta^{15}N_{Lys}$, $\delta^{13}C_{Val}$, $\delta^{13}C_{Leu}$, $\delta^{13}C_{Ile}$, $\delta^{13}C_{Phe}$) and then by also including the trophic amino acids (PCA-TAA, $\delta^{13}C_{Gly}$, $\delta^{13}C_{Ser}$, $\delta^{13}C_{Glx}$, $\delta^{13}C_{Ala}$, $\delta^{13}C_{Asx}$, $\delta^{13}C_{Pro}$, $\delta^{13}C_{Thr}$, $\delta^{15}N_{Gly}$, $\delta^{15}N_{Glx}$, $\delta^{15}N_{Ala}$, $\delta^{15}N_{Asx}$, $\delta^{15}N_{Pro}$, $\delta^{15}N_{Val}$, $\delta^{15}N_{Leu}$, $\delta^{15}N_{Ile}$, $\delta^{15}N_{Thr}$). Here, the terms "source" and "trophic" are used also including the $\delta^{13}C$ values of essential and non-essential amino acids, respectively. $\delta^{13}C_{Lys}$ and $\delta^{15}N_{Ser}$ were not included since it was not possible to estimate the isotopic signature of these amino acids from cereals. Carbon and nitrogen isotope values of hydroxyproline were also not considered since this amino acid is absent in cereals. Carbon and nitrogen isotope values of methionine and tyrosine were not included since they were detected only in a small number of samples. The PCA allowed

the observation of the clustering of the data considering the overall contribution of the selected amino acids. The data were standardised for the analysis. By only considering the first three principal components (PC1, PC2 and PC3) generated it was possible to explain 96% and 87% of variance in the dataset from PCA-SAA and PCA-TAA, respectively. Results are reported in Figure 7.7, with the original variables (vectors) reported in separate graphs (Figure 7.7 b and d for the results from PCA-SAA and f and h for the results from PCA-TAA) in order to help the visualisation of the data clustering (Figure 7.7 a and c for the results from PCA-SAA and Figure 7.7 e and g for the results from PCA-TAA). Ellipses represent 68% normal probability. The detailed results from the two PCA analyses are reported in Appendix F, Table F.1 and Table F.2.

Looking at the clustering generated by PCA-SAA, it is possible to see that marine fish are characterised by higher score values for $\delta^{13}C_{Val}$, $\delta^{13}C_{Leu}$, $\delta^{13}C_{Ile}$ and higher score values for $\delta^{13}C_{Phe}$, while C_3 cereals, in most cases, by higher score values for $\delta^{15}N_{Lys}$. The humans appear to have intermediate values. In particular, the males cluster slightly closer to the C_3 cereal and marine fish groups compared to the females, indicating a higher contribution of proteins from these sources in the male group.

When trophic amino acids are included in the analysis (PCA-TAA), the clustering does not change substantially. Compared to PCA-SAA, the human individuals appear to be better separated from the terrestrial animal groups, as a consequence of trophic isotope fractionation, indicating a consumption of animal products, as well as local plant food. Again, male individuals appear to be closer to the marine and C_3 cereal groups compared to the females. However the human individual values from the PCA-TAA should be interpreted with caution since the degree of trophic fractionation in the individual amino acids is here neglected. On the contrary, source amino acids are not expected to undergo isotope fractionation from protein in food to protein in the consumer; therefore, PCA-SAA is a valuable tool to explore protein contribution from isotopically distinguished trophic webs (in this case, C_3 cereals, local terrestrial and marine) in the diet of AD 79 human individuals.

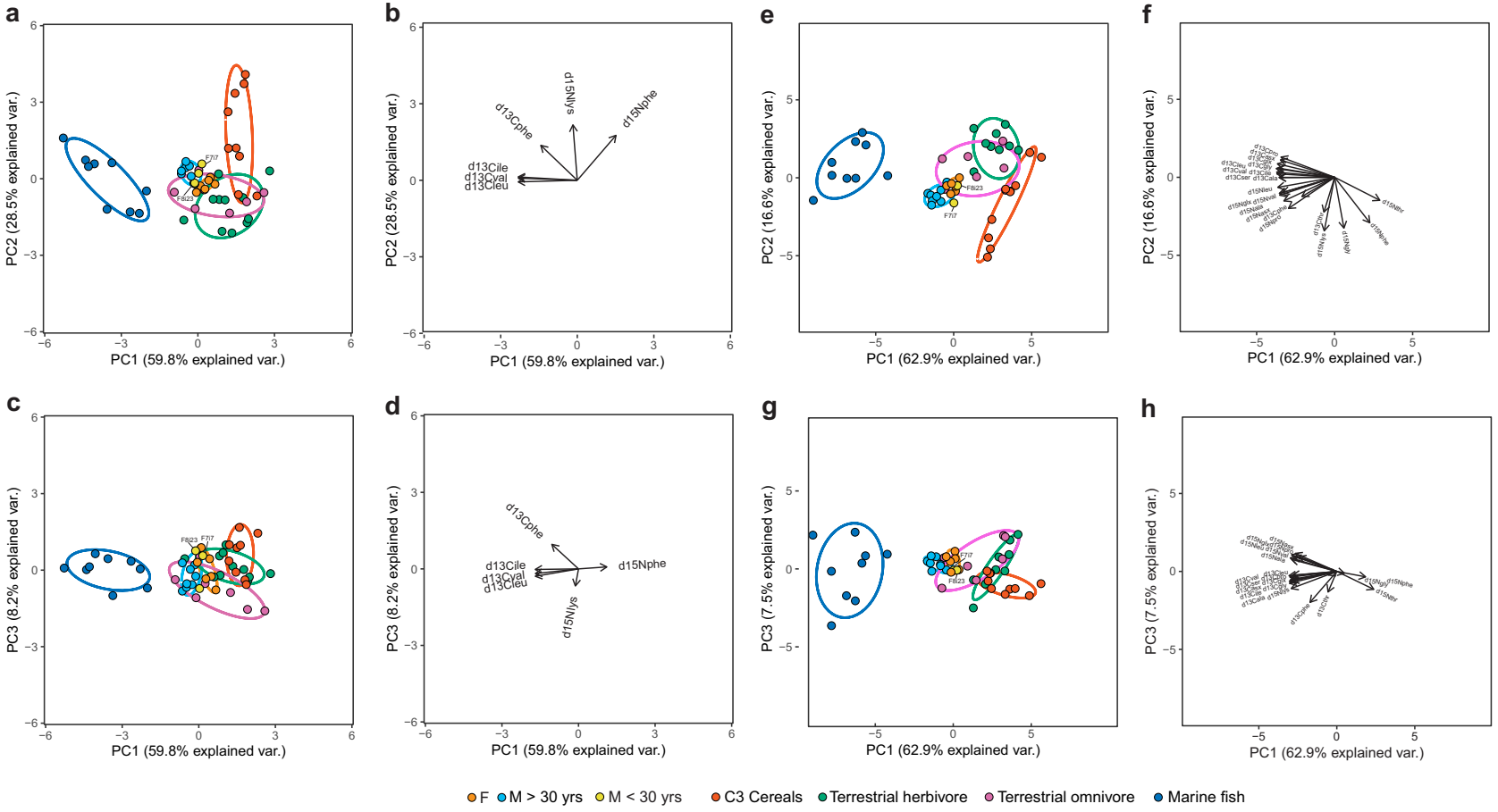

Figure 7.7 Principal component analysis of δ^{15}N and δ^{13}C of source (PCA-SAA, a, b, c and d) and source and trophic (PCA-TAA, e, f, g and h) amino acids of the human, animal and cereal samples object of this study. The principal component 1 (PC1) values are plotted against those of principal component 2 (PC2) (Figures a and b for PCA-SAA and e and f for PCA-TAA) and those of principal component 3 (PC3) (Figure c and d for PCA-SAA and g and h for PCA-TAA). To facilitate the visualisation of the data, the vectors have been plotted in separate graphs (Figures b, d, f and h).)

In conclusion, CSIA-AA was proven to be a powerful tool to detect marine product contribution in the diet of nineteen individuals living in Herculaneum. Qualitatively, this was achieved by observing the carbon and nitrogen isotope values of different amino acids which were previously applied to archaeological populations, sometimes critiquing their direct applicability and proposing other proxies which were considered to be more adequate in this specific context. The carbon and nitrogen isotope values of the single amino acids can also be used to explore the protein and calorific contribution of marine products in quantitative terms by deploying Bayesian mixing models, as proposed in chapter 6. Thanks to the application of these models, it was estimated that, in the diet of people living at Herculaneum, marine fish contributed to 26 ± 6 (%) of total proteins and 10 ± 3 (%) of total calories, which is more than three times the amount of marine fish consumed by modern Mediterranean populations (see chapter 6). Critically, this confirms previous insights that bulk SIA underestimates the contribution from subordinate but still relevant (in this case, more than 20 % of total protein) food categories from the diet of past human societies, particularly in the Mediterranean basin.

Legume consumption at Herculaneum

It is well attested that dry legumes were an important source of protein and calories in Imperial Roman times, particularly in the diet of the poor (see chapter 2 section 2.1.3). However, their contribution to the overall isotopic collagen signal of human individuals from Roman contexts has never really been explored, mainly due to the fact that legumes, being C_3 plants, show bulk $\delta^{13}C$ values similar to those of C_3 cereals or C_3 plant consumers and that their $\delta^{15}N$ values (see sections 3.1.2 and 5.2.2), although significantly lower than those of C_3 cereals, are hardly distinguishable from the overall dietary mixture using the SIA approach (see Figure 7.1 and Table 7.1.1). In this section, the potential of determining the contribution of dry legumes to the diet of the nineteen individuals from Herculaneum using CSIA-AA is explored.

As discussed in chapter 5 section 5.1.5, the calculated amino acid to bulk offsets from pulses are more variable compared to those from C_3 cereals and therefore it was suggested that more analyses of modern material are needed before being able to confidently predict amino acid isotope values from archaeological legumes. Nevertheless, here the offsets calculated from the two modern pulse samples (*MC* and *ML*) and, where possible, those available from Styring *et al.* (2014a) are used to evaluate the potential of the inclusion of legumes in the dietary mixing model analysis proposed in chapter 6 using conservative uncertainties. To do so, Model 1 (M1) and Model 2

(M2) were adapted to include the amino acid (*i.e.*, $\delta^{13}C_{Val}$, $\delta^{13}C_{Leu}$, $\delta^{13}C_{Ile}$, $\delta^{13}C_{Phe}$, $\delta^{15}N_{Phe}$ and $\delta^{15}N_{Lys}$) and fraction (*i.e.*, Whole N, Whole C and CHO C) estimated values for legumes using the bulk isotope values from the four legume samples from Herculaneum presented in chapter 5 section 5.2. The more conservative uncertainties associated with the legume values is the error propagated from the estimations, used instead of the standard error (SEM) that was used for the other food categories, in order to acknowledge the higher variability of the legume values compared to the other food categories. The macronutrient and amino acid concentration (expressed as percentage (%) of total protein in M1 and as dry weight (%) in M2) were derived from the USDA National Nutrient Database for Standard Reference[1] using the food items identified by the NDB numbers 16052, 16056, 16069, 16076 and 16085. The input values and the generated estimates are reported in Table E.6 and Table E.7 for M1 and M2, respectively. The estimates generated by M1 and M2 grouped by gender are reported in Table 7.1.3 where they are also compared to modern Mediterranean populations (Balanza *et al.* 2007).

According to M1 (Figure 7.8), legumes contributed overall 11 ± 10 % of total proteins at Herculaneum, among the four food categories considered. Legumes therefore make the lowest contribution. Women consumed on average slightly more legume proteins than men although the difference is not statistically significant (females = 17 ± 13 %, males = 13 ± 12 %; Mann-Whitney U Test, p-value = 0.145). Among the female group, individuals *F10i11* and *F12i28* have the highest legume contribution (22 ± 13 % and 18 ± 11 %, respectively), while in the male group, it is the individual F8i23 who receives the highest protein contribution from legumes (23 ± 13 %).

When the calorific contribution (M2) from the four categories sources is also considered, legumes contribute the same as marine fish to the overall total calories, although with a larger uncertainty (legumes = 10 ± 11 %, marine fish = 10 ± 3 %). The difference between gender is less pronounced and statistically not significant (females = 15 ± 14 %, males = 13 ± 13 %; Mann-Whitney U Test, p-value 0.2127).

In chapter 6, the contribution from terrestrial animal products was interpreted with caution since this was believed to potentially include locally grown plants, including legumes. However, when legumes are added to the models, despite a high degree of uncertainty associated to the estimated amino acid values, the terrestrial animal products still play a prominent role into the diet of the individuals from Herculaneum and in particular for the women (Table 7.1.3).

[1]The USDA National Nutrient Database for Standard Reference can be accessed at this link.

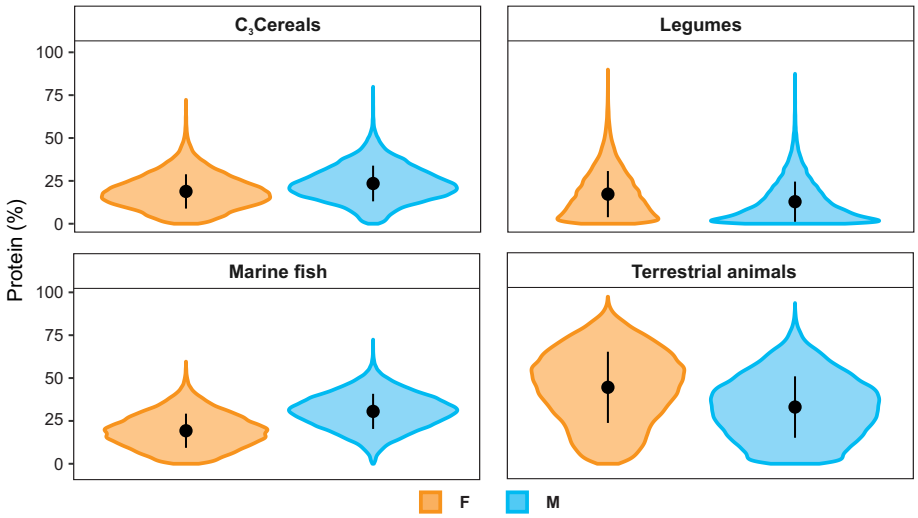

Figure 7.8 Violin plots describing the protein contribution (%) of C_3 cereals, legumes, terrestrial animals and marine fish to seventeen individuals from Herculaneum grouped by gender. The violin represents the kernel density mirrored on each side. Circles represent the mean; bars represent 1σ.

Garnsey and Scheidel (1998) criticised the general consensus around the importance of legumes in the diet of past Mediterranean societies. Indeed, although there is no doubt that the nutritional value of the legumes was known in classical antiquity, the ancient texts also report the negative effect that the consumption of legumes can cause, such as flatulence and disturbed sleep. Moreover, favism, a hereditary disorder caused by the deficiency of the red blood cell enzyme known as "G6PD", was most likely already afflicting a large proportion of the Mediterranean population (*e.g.*, Cappellini and Fiorelli 2008). It is unlikely therefore that the rich, who could afford more expensive products such as meat and bread wheat, would have consumed dry legumes in bulk, which was instead probably the case for the ordinary people (Garnsey and Scheidel 1998, 214-225).

When the data from modern Mediterranean populations (Spain, Portugal, Italy, Greece, Cyprus, France and Albania) for the years 1961-1963 and 1998-2000 provided by Balanza *et al.* (2007) are compared to the estimates generated from Herculaneum, the consumption of terrestrial animal products at Herculaneum appears to be surprisingly similar to that of modern Mediterranean populations from the early 1960s, which is generally accepted as the model "Mediterranean diet" (Balanza *et al.* 2007)(Table 7.1.3). What is also interesting to note however is that legumes play a minor but still appreciable role in the diet of people living in Herculaneum when compared to the marginal contribution that they have in the modern Mediterranean diet (Table 7.1.3). It is clear however that legumes did not constitute a staple for these individuals, whose

	Modern Mediterranean				**Herculaneum**					
	1961-1963		**1998-2000**		**all**		**female**		**male**	
					Protein contribution (%)					
	mean	1σ	**mean**	1σ	**mean**	1σ	**mean**	1σ	**mean**	1σ
Cereals	44%	8%	28%	5%	21%	7%	19%	10%	24%	10%
Terrestrial animals	45%	19%	62%	11%	43%	13%	45%	21%	33%	18%
Legumes	4%	2%	3%	1%	11%	10%	17%	13%	13%	12%
Marine fish	6%	3%	8%	3%	25%	8%	19%	10%	31%	10%
					Calorific contribution (%)					
	mean	1σ	**mean**	1σ	**mean**	1σ	**mean**	1σ	**mean**	1σ
Cereals	67%	13%	51%	9%	47%	13%	32%	17%	47%	19%
Terrestrial animals	27%	11%	44%	8%	33%	12%	45%	19%	28%	17%
Legumes	3%	2%	2%	1%	10%	11%	16%	14%	13%	13%
Marine fish	2%	1%	3%	1%	10%	3%	8%	5%	12%	5%

Table 7.3 Relative protein and calorific contribution of cereals, terrestrial animals, legumes and marine fish to the diet of modern Mediterranean populations (Balanza *et al.* 2007) and Herculaneum, the latter estimated using two Bayesian mixing models as described in the text.

diet was instead mainly based on cereals and terrestrial animal products, diverging from what had been predicted by Foxhall and Forbes (1982) and since then generally accepted by many. Following on what had been proposed by (Garnsey and Scheidel 1998, 214-225), this is perhaps indicative that at Herculaneum in the 1^{st} century AD, people could afford other equally nutritious but perhaps more palatable food items to the detriment of legumes.

Olive oil calorific contribution at Herculaneum

The Bayesian Mixing model M2 has the advantage of accounting for those food categories which are not composed of proteins, such as sugars and pure oils/fats. Applied to Roman populations, this gives the opportunity of exploring the caloric contribution from olive oil, whose economic and nutritional importance makes it part of the Mediterranean triad.

Nowadays, olive oil is consumed worldwide as a simple cooking medium in the same way as any other vegetable oil or animal fat. In Mediterranean Europe, between 1998 and 2000, olive oil contributed on average to 5.6 $\pm$ 3.9 % of the energy percentage of the total caloric value of the diet (TCV, also referred to as total available energy) per capita per day (Balanza *et al.* 2007). The most recent data from the Food Balance

Sheets (FBSs) of FAO (Food and Agriculture Organization of the United Nations) report that in 2018, Italians consumed 10 L/year of olive oil per capita[2]

On the contrary, in antiquity, olive oil was seen as a nutritious ingredient perhaps at the same extent of cereals (Horden and Purcell 2000, 211-213) and it is estimated that olive oil contributed on average to 20-50 L/year per capita, up to one-third of total calories (Mattingly 1988, 1996; Foxhall 2007). Thanks to the estimates from M2, it was possible to quantify in a direct way the consume of olive oil from a Roman Mediterranean population for the first time, although a large degree of uncertainty has to be accepted (Figure 7.9).

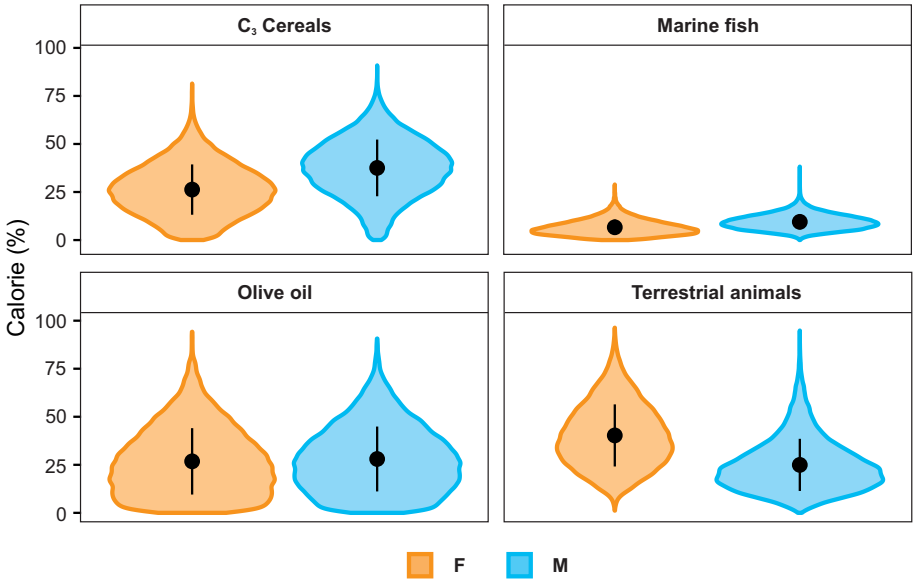

Figure 7.9 Violin plots describing the calorific contribution (%) of C_3 cereals, marine fish, olive oil and terrestrial animals to seventeen individuals from Herculaneum grouped by gender. The violin represents the kernel density mirrored on each side. Circles represent the mean; bars represent 1σ.

The relative calorific contribution (%) of olive oil in the diet of the individuals from Herculaneum is estimated to be 29 ± 17 %, in line with the prediction made previously by historians of the ancient economy. According to M2 estimates, there is no gender related difference in olive oil consumption (Mann-Whitney U Test, p-value = 0.5804), suggesting that olive oil was a staple in the diet of people living in Herculaneum. As discussed in chapter 2 section 2.1.6, olive oil was certainly produced in the area and to such an extent that the by-products of its production were used as a type of fuel (the so-called *pomace*, Rowan 2015). It can not be ruled out therefore that such a high consumption of olive oil is a reflection of the production surplus in the area and not a general trend in the Roman Mediterranean. It is hoped that in the future CSIA-AA

[2]Using a conversion factor of 0.9 from Kg to L. FBSs can be accessed at this link.

will be applied to other Roman Mediterranean communities, offering the opportunity to explore olive oil consumption across geographical areas and social strata.

7.2 New pieces to the puzzle: who was living at Herculaneum?

The new data obtained thanks to the application of CSIA-AA provide support for some previous evidence about the ancient town of Herculaneum and on the lifeways of its inhabitants prior the AD 79 Vesuvius eruption. In this section, it is assumed that the individuals who sought shelter under the *fornici* were indeed inhabitants of the ancient town and that they represent a cross section of its population (therefore not biased towards any specific social class)(see chapter 2 section 2.3 for a discussion about the human remains from Herculaneum). It is also assumed that the 19 individuals analysed are representative of the entire assemblage.

That marine fish was an important source of protein and calories for the people from Herculaneum was already determined thanks to preliminary radiocarbon dating of a sub-sample of individuals (Craig *et al.* 2013) and the estimates agree with those determined using the two novel Bayesian mixing models (*i.e.*, 26 ± 6 (%) of total proteins and 10 ± 3 (%) of total calories as reported in chapter 6). It is not possible to tell if this can be expected to be a standard trend in the Roman Mediterranean or if Herculaneum represents an exceptional case. Certainly, fishing was an important activity at Herculaneum and in general in the Bay of Naples, and it has been suggested that at least part of the population must have been involved in this industry, perhaps even some of the individuals from the Herculaneum death assemblage (Capasso 2001, 994 and 1026-1028)(see chapter 2 section 2.1.7 and 2.3.3). Fishing in the area represented a high chance of gain for the people in the area and it is likely that part of the population was organised in guilds (*collegia*) for the exploitation of marine resources, whose members were part of the same family or manumitted slaves (Bekker-Nielsen 2010). Moreover, the fish and shellfish assemblage from the Herculaneum sewer is populated by very small shellfish which makes the authors of the study suspect that people living in *Cardo V* at Herculaneum were collected seafood themselves in bulk by drag netting rather than by purchasing it from the market (Robinson and Rowan 2015). According to the Roman law in fact, anyone was free to exploit marine resources (Bekker-Nielsen 2010). However, the direct involvement of these individuals in the fishing industry on its own does not explain such a significant consumption of marine products observed through CSIA-AA. More likely, the greater access to a food category, namely marine

fish, which was certainly not among the most inexpensive sources, suggests either a surplus in the production and consequently a reduced cost of fish in the area, or higher economic possibilities of the people living in Herculaneum. It remains to be explained why women ate relatively less marine fish then men (chapter 6 and section 7.1.3 from this chapter). One reason might be the status of these women: if they were slaves or freedwomen, the husband and/or patron had by law more power in the house (Kleijwegt 2012, 117) and the diet might have been regulated according to his power, for example by keeping more of the fresh fish for himself. As discussed in section 2.2.1, the slave-driven urbanism of Herculaneum made the city mainly composed of slaves, freedmen and freedwomen, therefore it is possible that the women here analysed are in fact either slaves or freedwomen.

Interestingly, Martyn *et al.* (2018) previously observed statistically significant differences of the bulk δ^{15}N values in male individuals from Herculaneum below and above 30 years old. This observation on its own adds a new layer of knowledge around the individuals who perished under the *fornici*, witnessing a social or cultural change happening around the age of 30 for males and which is reflected in their diet. As already pointed out by Martyn *et al.* (2018), by the age of 30, men would have either received the role of *pater familias* or manumitted from their state of slave. As for the latter, out of highly commercialised zones such as the Bay of Naples and Rome, one should not assume that the new status of freedmen would signify a wealthier life and therefore also a better diet, depending on the chances of the ex-slave to find a work opportunity. However, in this area, such a suggestion seems safe (Verboven 2012). Age-related dietary differences were also observed through CSIA-AA and in the estimates generated using M1 and M2. However, the latter are not statistically significant, due to the low number of individuals ($n = 3$) below 30 years old (Mann-Whitney U Test, p-value = 0.05248 is the lowest p-value tested for marine protein consumption)(Figure 7.10). According to the estimates, these three male individuals have a diet that appears to be between that of females and older males (Figure 7.10).

By looking at the proxies explored in the previous sections, it is interesting to note that two of the three younger individuals (*F7i7* and *F8i23*) have diets that are very different from the main male group and sometimes even from the female one. They exhibit among the lowest $\delta^{15}N_{Glx-Phe}$ offsets (Figure 7.6), suggesting a diet mainly based on the consumption of lower trophic level products (*i.e.*, plants), while the $\delta^{13}C_{Phe}$ values suggest that these products might have been (possibly imported) C_3 cereals (Figure 7.5 a). The PCA analysis seems to confirm the latter, particularly in the case of the individual *F7i7* (Figure 7.7 a, c, e and g). These subtle differences are not

detectable by relying on the Bayesian mixing models M1 and M2 alone, where of course the error associated to the estimates account for the propagation of all the uncertainties around fractionation (only for M2), pre-defined food groups and macronutrient and amino acid concentration of the food items. However, *F7i7* appears to be the male individual with the highest protein and calorific contribution from cereals and with the lowest contribution of marine fish and terrestrial animals, while the estimates of the individual *F8i23* are similar to those observed from the female group. It would appear from the CSIA-AA data that at least *F7i7* was either under some sort of controlled diet based on the consumption of C_3 cereals or that their collagen signal is mirroring a different environment but still indicative of low trophic level product consumption; in both cases, it seems safe to infer that they might have been less wealthy than other individuals, and that possibly they were slaves.

Two juvenile individuals (*F8i10* aged 10-15 years old and *F8i11* aged 15-20), whose biological sex is undetermined, were probably under a even more restricted diet than that of the individuals *F7i7* and *F8i23*, certainly the ones with the lowest protein intake (Figure 7.6 b). Unfortunately, due to the lack of carbon isotope measurements, these individuals were not included in the mixing models. It is possible that the diet of children and teenagers was somehow restricted as a consequence of their subordinate role in the household (Garnsey and Saller 2014, 151-169). A recent carbon and nitrogen isotope analysis of dentine sections of Roman individuals from Bainesse, UK, suggests an increase of animal proteins in the diet of these individuals only from 7 years onwards (Cocozza *et al.* 2021). If it is assumed that this picture applies to other territories of the Empire, such as the Bay of Naples and more specifically Herculaneum, it is likely that a diet lower in animal proteins between the end of breastfeeding (around 2-5 years according to Cocozza *et al.* (2021)) and 7 years would still be in part represented in the collagen isotope values of at least the youngest individual *F8i10*, considering a collagen turnover rate of the ribs of *ca.* 3-5 years (Jørkov *et al.* 2009). However, this would not explain the nitrogen isotope values of trophic amino acids of the slightly older individual *F8i11*. Moreover, in the event that a child survived its tenth birthday (which was a rare event in Roman times, if we consider modern estimates suggesting that only 50 % would have survived this age (Carroll 2011, 102)), it is difficult to believe that the father would have risked losing his lineage and patrimony by restricting the diet (and endangering the life) of his children (Garnsey and Saller 2014, 151-169). It seems more likely therefore that these two juvenile individuals were also slaves, although this represents of course a tentative conclusion. It is no surprise to see the possible presence of slaves in the Herculaneum *fornici* assemblage since, according to the most recent

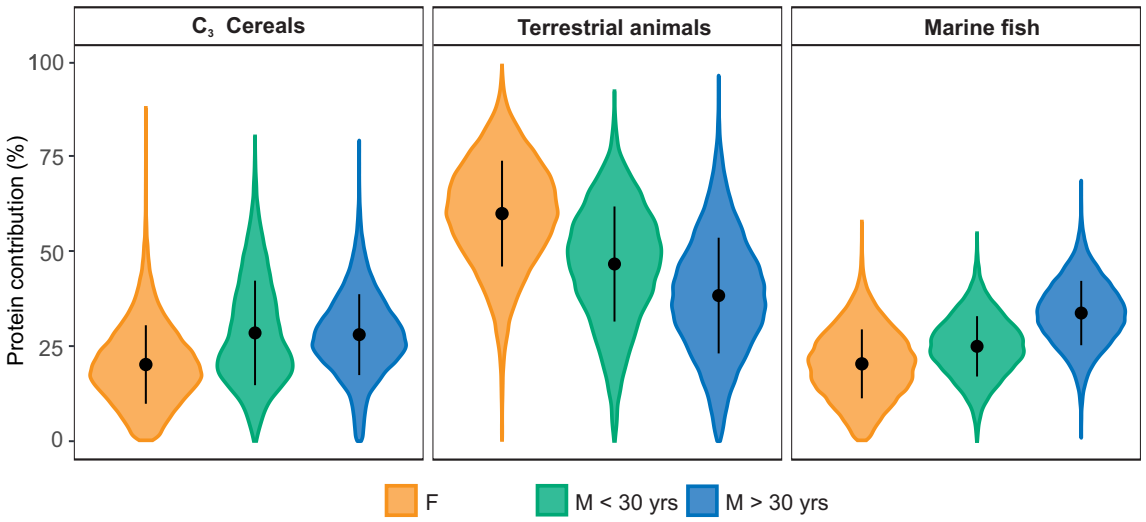

Figure 7.10 Violin plots describing the protein contribution (%) of C_3 cereals, terrestrial animals and marine fish to female, male under 30 year old and male above 30 year old individuals from Herculaneum. The violin represents the kernel density mirrored on each side. Circles represent the mean; bars represent 1σ.

analysis of the *Album of names*, just before the eruption, the majority of the population was composed by slaves (40 %) and by freedmen and freedwomen (20 %) (see chapter 2, section 2.2.1, de Ligt and Garnsey (2012)). Of course, these data on their own can not be realistically used to identify *F7i7*, *F8i23*, *F8i10* and *F8i11* as slaves, for which more evidence is essential. However, high resolution dietary reconstructions, achieved thanks to CSIA-AA in this context, could be successfully applied to explore socio-cultural differences (and inequality) in archaeological populations or single individuals which are better contextualised, for example from their burial or by their grave goods.

Perhaps, one of the most interesting outcomes of the application of CSIA-AA to this assemblage is the amount of protein and calories with an animal origin contributing to the diet of people from Herculaneum, which is comparable to that of modern Mediterranean populations (see chapter 6). The zooarchaeological evidence from Roman archaeological sites in Europe and Italy attest an increased consumption of animal products from the Late Republic to the Empire, particularly in urban sites (Jongman 2007; Ikeguchi 2017), in response to an economy that was exceeding the bare subsistence level. Apart from meat, animals such as sheep, goat, cattle and chickens could be more conveniently exploited throughout all their life for their secondary products, namely milk, cheese and eggs. The presence of sheep and cattle with the human remains within the Herculaneum *fornici* is indicative of the strong economic dependency that these individuals had on these animals. In addition, this seems to suggest that at least some of these individuals were living in close contact with the

animals, with the possibility to directly access their products. Consumption of milk and cheese at Herculaneum was already suggested by Capasso (1999), who evidenced the presence of some skeletal lesions from the individual recovered on the seashore which, according to the author, were caused by brucellosis, a bacterial disease mainly caused by the consumption of non-pasteurised dairy products (see chapter 2 section 2.3.3). Living in close contact with the animals, would make it easier to access their products. Rowan (2014) recovered a significant number of chicken (and a few goose) eggshells from the Herculaneum *Cardo V* sewer, suggesting that eggs were easily accessed at Herculaneum. Moreover, Ikeguchi (2017) has suggested that milk and milk products were more available in urban contexts in the Italian peninsula than previously thought. The contribution of animal products is relatively less important in the male individuals probably as result of the higher consumption of cereals. Certainly, people who were living in the Bay of Naples could have accessed wheat both locally grown and imported from the Provinces at a low price. However, milling and baking must have had a cost and therefore it is not difficult to imagine that the portions of wheat and wheat products such as bread were distributed in the household depending on the "needs, status and power" (Garnsey 1999, 100-112) of the individuals - therefore preferentially to the *pater familias* (Garnsey and Scheidel 1998, 237-239). Even more if these men were actively involved in working activities, such as, perhaps, fishing (see chapter 2 section 2.1.7 and 2.3.3). As a consequence, the isotope signal from other nutritious (in terms of calories and proteins) foodstuffs, such as secondary animal products, would prevail over that of cereals in the female group. In addition to this, one should consider the role of women in the Roman household. Carroll (2011) suggests that the death of women in their reproductive years was acutely felt in the family, therefore implying that their deaths had to be avoided by all means due to their role of childbearers and care of the children. A diet composed of nutritious animal products would have helped in this direction, ensuring the birth of new children in the family and their care.

In addition to this, it is essential to remember that the "terrestrial animal" food category used for the Bayesian mixing models M1 and M2 could potentially also include locally produced plant products such as nuts, rich in proteins and fats, and fruits rich in sugars such as figs and carobs, which were all available in the area and whose consumption is attested by historical and archaeological evidence (*e.g.*, Horden and Purcell 2000, 210). However, these products alone do not adequately explain the high protein and calorific contribution observed from M1 and M2 respectively, which seems therefore predominantly linked to the consumption of animal products. These results have important implications about reading gender related differences in antiquity:

clearly, at Herculaneum, men and women had different access to specific food items. These results could be used to reflect on dynamics of gender inequality.

Although up to this day there are many gaps around the ancient town of Herculaneum and its inhabitants, all the evidence so far collected seems to point towards the same direction. As many urban sites in the Bay of Naples, Herculaneum appears to be invested by the increased economy of the area since the 2^{nd} century BC which determined an increased demand for workers which was met by the importation of slaves from the newly acquired Provinces. With time, many of these slaves were manumitted and they started their own business activities, with a succession of new generations of freedmen, freedwomen and free borns, for which the *Album of names* of Herculaneum is certainly the main testimonial (de Ligt and Garnsey 2012, 2019). The spread luxury of the houses in Herculaneum was interpreted as one of the ways that these ex-slaves or free-borns had to affirm their newly acquired identity as Roman citizens (Wallace-Hadrill 1994). The analysis of the remains from the *Cardo V* sewer from Herculaneum revealed that even the ordinary people were able to access a variety of food items (Rowan 2014, 2017a,b). The new dietary information obtained thanks to the application of CSIA-AA appear to confirm that people who lived at Herculaneum just before the eruption had a wealthy standard of living comparable to that of modern times, which seems to be a reflection, rather than of their social position, of the economy of the area.

7.3 Conclusion

In conclusion, the carbon and nitrogen isotope analysis of the single amino acids applied to the exceptional death assemblage of Herculaneum was demonstrated to be a powerful tool to detect and quantify dietary differences in the Roman Mediterranean. Certainly, as outlined in section 7.1.1, the application of carbon and nitrogen isotope analysis of bulk material remains is of great help in detecting intra- and inter-populations differences in diet but it remains difficult to explain which sources are responsible for the observed isotopic values. The data available from several animal feeding experiments clearly show that interpreting the bulk SIA is extremely challenging, perhaps even more in the Roman Mediterranean, where it is commonly accepted that the majority of the calories were covered by the consumption of plants with a C_3 signal. This most likely hides the contribution from other sources, such as marine and C_4 plants, that can be relevant to investigate questions such as social or gender inequality and nutritional health status in the Roman times. A preliminary study

carried out to evaluate the potential of including the carbon isotope values of bone apatite, which could provide a perhaps more straight-forward way to explore diet than the analysis of amino acids, was also presented (section 7.1.2). However, the results obtained are ambiguous, perhaps influenced by the volcanic activity in the area before the eruption, suggesting that the carbon apatite values are potentially influenced by other factors. On the contrary, the results obtained by CSIA-AA are directly linked to specific sources in diets and they are free of assumptions in the case of source and essential amino acids. In section 7.1.3, it was shown that CSIA-AA can be used to confidently identify marine inputs in diet which is notably one of the main challenges in the Mediterranean, and potentially quantify other sources, such as legumes and olive oil, with many important implication in the study of the ancient economy. Last but not least, CSIA-AA allowed exploring group dynamics at Herculaneum, but also to frame the diet of single individuals (section 7.2). Overall, the results support previous historical and archaeological hypotheses, suggesting that the life of who was living at Herculaneum in the 1^{st} century AD was invested by the economic expansion of the Bay of Naples, and perhaps of the Empire as a whole.

Chapter 8

Conclusions and suggestions for future research

The carbon and nitrogen stable isotope analysis of amino acids (CSIA-AA) were used in this thesis to investigate the diet of a sub-sample of the Herculaneum catastrophic death assemblage, representing, to my knowledge, the first application of CSIA-AA in a historical Mediterranean context. Previous stable isotope research had struggled to identify the contribution of different dietary sources in the diet of people living in the Mediterranean basin during the Imperial Roman times, particularly that of marine fish (see chapter 3 section 3.1.3). This is due to the low-resolution and limitations of the classic bulk SIA approach, particular in a context where it is likely that the high consumption of cereals and olive oil participated in the synthesis of non-essential amino acids in collagen. Moreover, the bulk nitrogen stable isotope values of marine specimens in the Mediterranean overlap with those of terrestrial sources (see chapter 7 section 7.1.1). In this thesis, CSIA-AA was demonstrated to be extremely helpful in disentangling many of the questions that still remain to be explored about the diet of who was living at Herculaneum and, in more general, in the Mediterranean during the 1^{st} century AD. Here, the aims of the thesis presented in chapter 1 will be revisited, namely: i) what are the advantages of using CSIA-AA over bulk SIA in Mediterranean archaeological contexts? and ii) what can be said about the diet of those who lived in Herculaneum in AD 79 thanks to the application of CSIA-AA?

8.1 Advantages of using CSIA-AA over bulk SIA in Mediterranean archaeological contexts

In the last twenty years, SIA has been applied to numerous Roman communities around the Mediterranean. These studies all interpreted the bulk carbon and nitrogen values as indicative of a high C_3 cereals consumption. The access to marine fish was proposed for those individuals with ^{13}C-enriched carbon isotope values and higher nitrogen isotope values. However, only broad quantitative estimations of diet, both in terms of calories and proteins, are obtained when using mixing models, as it was shown in chapter 6.

As discussed in chapter 3 section 3.1, feeding experiments have shown that it is not possible to predict diet-to-consumer fractionation offsets without knowing the composition of the diet *a priori*. In addition to this, the study of dietary practices in the Mediterranean basin using bulk SIA is made perhaps even more difficult by two factors: i) the high consumption of cereals and olive oil hides the contribution of other sources, such as that of marine fish (see chapter 3 sections 3.1 and 3.1.3); ii) the nitrogen isotope values of fish in the Mediterranean are significantly lower than those from the Atlantic (see chapter 5 section 5.2.2) and they overlap whit those of C_3 cereals (see chapter 7 section 7.1.1).

Moreover, gender-related differences were only rarely identified by previous studies in the Roman Mediterranean and it is possible that more subtle differences are not detectable by using the bulk SIA approach (see chapter 3 section 3.1.3).

The application of CSIA-AA made it possible to clearly distinguish between cereals and terrestrial animals due to their different isotopic signatures at the amino acid level and to better identify the contribution of marine products. Thanks to CSIA-AA it was possible to see that men at Herculaneum eat more cereals compared to the women and it is possible that the higher bulk nitrogen isotope values observed in the male individuals are caused by a higher consumption of manured cereals rather than (or in conjunction with) marine fish (see chapter 6 and chapter 7 sections 7.1.3 and 7.2).

Thanks to CSIA-AA it was also possible to observe differences in farming practices. For example, it was shown that some of the herbivores were at least partly fed on cereals for human consumption, while others were most likely left to graze on the local vegetation. Some of the pigs had an herbivorous diet. It was also possible to clearly evidence a terrestrial input in the carbon isotope values of the amino acid of one *garum* sample composed of small bone elements of herrings and tarpons, suggesting that some of the fish consumed in the Roman Mediterranean was probably captured and farmed in coastal lagoons or fishponds, as the SIA data also seems to suggest for some of

the specimens here analysed and *garum* samples previously published (see chapter 5 section 5.2.2).

In conclusion, the higher resolution achieved by applying CSIA-AA to the case study of Herculaneum suggests that this approach could be successfully applied to other archaeological Mediterranean contexts for which the bulk SIA approach is equally limited. The comparison with modern populations (see chapter 6) has clearly shown that marine consumption can be dangerously underestimated using bulk SIA. A higher consumption of marine resources, although secondary to other foodstuffs, can make us reflect on the economic possibilities of an individual, their role in the society or perhaps even on their occupation. Moreover, the access to marine fish might have changed with time depending on climatic and environmental factors, cultural influences and economic scenarios. Whoever perished on the ancient seashore of Herculaneum in AD 79, was eating more than three times the amount of marine fish proteins than the people living nowadays in the Mediterranean are (see chapter 6). Is this limited to this assemblage or is it extended to the Bay of Naples? Or perhaps it characterises the entire Mediterranean Roman World? Did the consumption of marine fish change with the diffusion of Christianity? This thesis has proven for the first time that CSIA-AA can overcome this important limitation of bulk SIA also in the Mediterranean. Outside of historical periods, the detection of marine food consumption using CSIA-AA could make us understand better the diet and group and social dynamics of prehistoric communities, for which there are only limited archaeological and no written evidence.

8.2 Reconstruction of diet at Herculaneum through CSIA-AA

As introduced in section 1.1 and presented in section 2.1, historical and archaeological investigations have generated a wealth of information about how diet looked like for the people who were living in the Mediterranean basin during the Roman times. However, the estimates produced by the scholars of the ancient economy might not apply to everywhere in the Empire and it is still poorly understood how diet diverged among different socio-cultural groups and across time and space.

Thanks to CSIA-AA, it was possible to observe that C_3 cereals at Herculaneum provided most of the calories, but their contribution was estimated to be on average *ca.* 50 %, which is much lower than the commonly accepted 70 % estimate proposed by Foxhall and Forbes (1982) considering the quantity of grains that were distributed during the *frumentationes*. The remaining calories were provided by a mixture of

sources among which terrestrial animal products are almost as equally important as the C_3 cereals (on average, *ca.* 40 % of total calorific contribution). Although it can not be excluded that some of these calories might have come from local plant food (vegetables and fruits), the inclusion of non-essential and trophic amino acids in M2 suggests that these estimates are indeed indicative of a high consumption of animal products and they are comparable to those estimated from survey data of modern populations living in the Mediterranean basin (Balanza *et al.* 2007)(see chapter 6).

As mentioned in the previous section, marine fish was also clearly an important dietary component at Herculaneum. However, other items might have played an important role. When olive oil is included in M2, it was estimated to contribute to *ca.* 30 % of the total calories, despite a large error. This is six times the contribution of olive oil in the diet of modern Mediterranean populations and, although it might at first seem hard to believe, this is in line with the estimates proposed by different economic studies, supporting the idea that olive oil was indeed used as a nutritious ingredient rather than a condiment, which is probably a much later transformation (Horden and Purcell 2000, pp. 211-213).

The contribution of legumes was also preliminary investigated using a higher uncertainty due to the small number of modern samples (see chapter 5 section 5.1.5). Despite the large error of the estimates, legumes appear to be secondary to terrestrial animal products both in protein and calorific terms, supporting the proposal of Garnsey and Scheidel (1998) that legumes were most likely replaced by more refine and palatable products if the people could afford it (see chapter 7 section 7.1.3).

Of course it is impossible to tell whether this trend would be confirmed by other Roman communities living in the Mediterranean in the 1^{st} century AD, or if Herculaneum represents an exceptional case, at least until CSIA-AA is applied to other contexts. Nevertheless, these results demonstrate that the general accepted picture about the Roman diet might be not as so homogeneous as previously thought.

The results obtained from CSIA-AA also helped to understand the differences which were previously detected using SIA (Martyn *et al.* 2018). In particular, they showed that the consumption of C_3 cereal and marine products was observed to be higher in the men, while the women obtained the majority of their proteins and calories from animal products. As discussed in chapter 7 section 7.2, it is possible that larger portions of cereals and cereal products such as bread were allocated to the men in the household, perhaps because they were involved in more energy-expensive working activities. As for marine fish, it is possible that some of these individuals were involved in fishing activities which could have increased the chance to access this

type of product at a much lower price. However these results could reflect dynamics of gender-inequality, as it seems to be suggested by the $\delta^{15}N_{Thr}$ values, which suggest an overall lower consumption of proteins in the female group. Moreover, thanks to CSIA-AA, it was also possible to observe that two out of three of the younger male individuals (*i.e.*, < 30 yrs) and two juveniles (*i.e.*, < 20 yrs) were probably under a poorer diet, mainly composed of cereals and other terrestrial products. The $\delta^{15}N_{Thr}$ values of these individuals were the lowest of the entire group, which could suggest that their diet was also overall poorer of proteins.

Unfortunately, due to the circumstances of the recovery, the nature of the assemblage and perhaps even to how the study of the skeletons was organised (see chapter 2 section 2.3), very little can be told about the individuals who compose this extraordinary assemblage. First of all, it is impossible to tell for sure if these individuals were the inhabitants of the ancient town, since they could have as well sought shelter under the *fornici* while escaping from the eruption from somewhere else. It is also impossible to tell what is the social background of these individuals, although the available evidence seems to suggest that none should prevail over the others (see chapter 2 section 2.2.1 and 2.3). This can make the interpretation of the results difficult. However, accepting the most likely event that these people were indeed inhabitants of the ancient town, and considering what is known of the political and economic scenario of the Bay of Naples, the CSIA-AA results can provide a new level of knowledge around this group of individuals. The most recent analysis of the *Album of names* of Herculaneum suggests that the inhabitants of the ancient town were for the 40 % composed of slaves and for the 20 % by freedmen and freedwomen (de Ligt and Garnsey 2012, 2019). It is possible that the youngest individuals here analysed were indeed slaves, although this remains necessarily a tentative interpretation. Nevertheless, in line with other evidence from the ancient town, the CSIA-AA data seem to indicate that who was living at Herculaneum at the time of the eruption was benefiting from the political and economic scenario of the Bay of Naples, a pillar in the Mediterranean system of the production and distribution of goods.

The application of CSIA-AA on this exceptional assemblage provided new insights into the everyday life of a Roman community and, it is hoped, opened the way to new line of researches. The high resolution provided by CSIA-AA can be used to learn more from the Roman society, for example by exploring the role of the different members of the household. Indeed, this thesis has suggested that children might have been under a poorer diet compared to the adults, both men and women. Moreover, men under the age of 30 years old were eating less marine fish than the older ones at Herculaneum.

Although it is possible that the youngest individuals, including the children, were slaves, the differences in diet could also depend on the role of these individuals in their households. The application of CSIA-AA to other cemetery populations which are archaeologically better defined, for example slave mass burials (*e.g.*, Salesse *et al.* 2021) or house tombs (*e.g.*, Tacoma 2017), could help in this direction.

8.3 Future directions

This thesis has also faced some limitations that can be explored by future work. These include:

- CSIA-AA of modern domestic plant samples such as C_4 and legumes. These values will be used to estimate the isotope values of amino acids from archaeological material and evaluate their contribution in the diet of past human societies. For example, the presence of millet at Herculaneum is well attested (see chapter 2 section 2.1) and it seems important to quantify its contribution to the diet of the people who perished on the Herculaneum seashore. CSIA-AA of a larger number of legume species could also be of help to support the estimates proposed in chapter 7. The contribution of these two sources are also likely to be of interest for other contexts around the Mediterranean and beyond.

- CSIA-AA applied to other Roman communities living in the Mediterranean area could be used to compare the composition of the diet across space, with the possibility to explore the link between the diet and the complex economic and political dynamics put in place by the Empire. Thanks to the high-resolution provided by the CSIA-AA approach, as proved by this thesis, it will also be possible to investigate differences between groups (*e.g.*, by gender, age or social status) in terms of inequality.

- As for the individuals from Herculaneum, strontium isotope ($^{87}Sr/^{86}Sr$) analysis applied to the enamel could confirm whether or not these individuals were slaves or a fist generation of Roman citizens as the *Album of names* of Herculaneum seems to suggest. If the $^{87}Sr/^{86}Sr$ values will be found different from those of the local geology, it will be possible to suggest that these individuals were originally non-local, probably slaves imported from the newly acquired Provinces, adding a new layer of evidence about their lost identities. Similarly, the analysis of the ancient DNA could provide unique information about their ancestry (e.g.,

Antonio *et al.* 2019), particularly if these individuals are a second generation of Roman citizens.

- CSIA-AA showed a clear difference between the diet of the younger and older male individuals at Herculaneum. If this method will be in future applied to the dentine sections from the teeth that form later in life (M2 or M3) it could be better defined when and how young men were allowed to change their diet and potentially link the evidence to cultural or social mechanisms.

In conclusion, this thesis has shown that CSIA-AA applied to Mediterranean contexts can be of help to better define the diet of past human societies living in this area of the world. Nowadays, CSIA-AA probably represents the only opportunity to confidently quantify the relative protein and calorie contributions to the diet of the Romans, which might not have been as uniform as previously thought.

Bibliography

Abelson, P. H. and Hoering, T. (1961). Carbon isotope fractionation in formation of amino acids by photosynthetic organisms. *Proceedings of the National Academy of Sciences*, 47 (5), pp. 623–632.

Aguilera, M., Araus, J. L., Voltas, J., Rodríguez-Ariza, M. O., Molina, F., Rovira, N., Buxo, R. and Ferrio, J. P. (2008). Stable carbon and nitrogen isotopes and quality traits of fossil cereal grains provide clues on sustainability at the beginnings of Mediterranean agriculture. *Rapid Communications in Mass Spectrometry*, 22 (11), pp. 1653–1663.

Alexander, M. M., Gerrard, C. M., Gutiérrez, A. and Millard, A. R. (2015). Diet, society, and economy in late medieval Spain: stable isotope evidence from Muslims and Christians from Gandía, Valencia. *American Journal of Physical Anthropology*, 156 (2), pp. 263–273.

Allen, M., Poggiali, D., Whitaker, K., Marshall, T. R. and Kievit, R. A. (2019). Raincloud plots: a multi-platform tool for robust data visualization. *Wellcome open research*, 4.

Allen, R. C. (2009). How prosperous were the Romans? Evidence from Diocletian's price edict (AD 301). In: A. Bowman and A. Wilson (Eds.), *Quantifying the Roman economy: Methods and problems*, Oxford: Oxford University Press, pp. 327–345.

Allevato, E., Ermolli, E. R., Boetto, G. and Di Pasquale, G. (2010). Pollen-wood analysis at the Neapolis harbour site (1^{st}–3^{rd} century AD, Southern Italy) and its archaeobotanical implications. *Journal of Archaeological Science*, 37 (9), pp. 2365–2375.

Allison, E. P., Hall, A. R., Jones, A. K. G., Kenward, H. K., O'Connor, T. P., Phipps, J. and Tomlinson, P. (1990). 5 Rougier Street. In: *The Past Environment of York*, Council for British Archaeology, volume 14 of *The Archaeology of York*.

Almeida, E. R. (1984). *Il Monte Testaccio: ambiente, storia, materiali*. Rome: Quasar.

Ambrose, S. H. (1991). Effects of diet, climate and physiology on nitrogen isotope abundances in terrestrial foodwebs. *Journal of archaeological science*, 18 (3), pp. 293–317.

Ambrose, S. H. (2000). Controlled diet and climate experiments on nitrogen isotope ratios of rats. In: S. H. Ambrose and M. A. Katzenberg (Eds.), *Biogeochemical*

approaches to paleodietary analysis, New York: Kluwer Academic Publishers, pp. 243–259.

Ambrose, S. H. and Norr, L. (1993). Experimental evidence for the relationship of the carbon isotope ratios of whole diet and dietary protein to those of bone collagen and carbonate. In: J. B. Lambert and G. Grupe (Eds.), *Prehistoric human bone. Archaeology at the molecular level*, Berlin: Springer-Verlag, pp. 1–37.

Amouretti, M.-C. (1986). *Le pain et l'huile dans la Grèce antique. De l'araire au moulin*, volume 328 of *Coll. Annales littéraires de l'Université de Besançon*. Paris: Les Belles Lettres.

Anderson, M. A. and Robinson, D. (2018). *House of the Surgeon, Pompeii: Excavations in the Casa Del Chirurgo (VI 1, 9-10.23)*. Oxford: Oxbow Books.

Antonio, M. L., Gao, Z., Moots, H. M., Lucci, M., Candilio, F., Sawyer, S., Oberreiter, V., Calderon, D., Devitofranceschi, K., Aikens, R. C., Aneli, S., Bartoli, F., Bedini, A., Cheronet, O., Cotter, D. J., Fernandes, D. M., Gasperetti, G., Grifoni, R., Guidi, A., La Pastina, F., Loreti, E., Manacorda, D., Matullo, G., Morretta, S., Nava, A., Nicolai, V. F., Nomi, F., Pavolini, C., Pentiricci, M., Pergola, P., Piranomonte, M., Schmidt, R., Spinola, G., Sperduti, A., Rubini, M., Bondioli, L., Coppa, A., Pinhasi, R. and Pritchard, J. K. (2019). Ancient Rome: a genetic crossroads of Europe and the Mediterranean. *Science*, 366 (6466), pp. 708–714.

Arthur, P. (1991). *Romans in northern Campania: settlement and land-use around the Massico and the Garigliano Basin*. 1, Rome: Archaeological Monographs of the British School at Rome.

Ascough, P., Cook, G. and Dugmore, A. (2005). Methodological approaches to determining the marine radiocarbon reservoir effect. *Progress in Physical Geography*, 29 (4), pp. 532–547.

Aston, F. (1920). The constitution of the elements. *Nature*, 106 (2667), p. 468.

Aston, F. W. (1913). A new elementary constituent of the atmosphere. *Report, British Association for the Advancement of Science*, 83, p. 403.

Aston, F. W. (1919). The constitution of the elements. *Nature*, 104 (2616), p. 393.

Bada, J. L. (1985). Amino acid racemization dating of fossil bones. *Annual Review of Earth and Planetary Sciences*, 13 (1), pp. 241–268.

Balanza, R., García-Lorda, P., Pérez-Rodrigo, C., Aranceta, J., Bonet, M. B. and Salas-Salvadó, J. (2007). Trends in food availability determined by the Food and Agriculture Organization's food balance sheets in Mediterranean Europe in comparison with other European areas. *Public health nutrition*, 10 (2), pp. 168–176.

Baldoni, M., Gismondi, A., Alexander, M., D'Agostino, A., Tibaldi, D., Di Marco, G., Scano, G., Canini, A., Caserta, E., Rickards, O. and Martínez-Labarga, C. (2019). A multidisciplinary approach to investigate the osteobiography of the Roman Imperial population from Muracciola Torresina (Palestrina, Rome, Italy). *Journal of Archaeological Science: Reports*, 27.

Balzer, A., Gleixner, G., Grupe, G., Schmidt, H.-L., Schramm, S. and Turban-Just, S. (1997). In vitro decomposition of bone collagen by soil bacteria: the implications for stable isotope analysis in archaeometry. *Archaeometry*, 39 (2), pp. 415–429.

Bekker-Nielsen, T. (2010). Fishing in the Roman world. In: *Ancient nets and fishing gear. Proceedings of the international workshop on "Nets and fishing gear in classical antiquity: a first approach"*, Universidad de Cádiz, Servicio de Publicaciones; Aarhus University Press, pp. 187–203.

Bella, J. (2016). Collagen structure: new tricks from a very old dog. *Biochemical Journal*, 473 (8), pp. 1001–1025.

Bellotti, P., Mattei, M., Tortora, P. and Valeri, P. (2009). Geoarchaeological investigations in the area of the imperial harbours of Rome. *Méditerranée. Revue géographique des pays méditerranéens/Journal of Mediterranean geography*, (112), pp. 51–58.

Bentley, R. A. (2006). Strontium isotopes from the earth to the archaeological skeleton: a review. *Journal of archaeological method and theory*, 13 (3), pp. 135–187.

Bisel, C. (1991). The human skeletons of Herculaneum. *International Journal of Anthropology*, 6 (1), pp. 1–20.

Bisel, S. C. (1988). Nutrition in first century Herculaneum. *Anthropologie*, pp. 61–66.

Bland, J. M. and Altman, D. G. (2003). Applying the right statistics: analyses of measurement studies. *Ultrasound in Obstetrics and Gynecology*, 22 (1), pp. 85–93.

Boeckmann, B., Bairoch, A., Apweiler, R., Blatter, M.-C., Estreicher, A., Gasteiger, E., Martin, M. J., Michoud, K., O'Donovan, C., Phan, I., Pilbout, S. and Schneider, M. (2003). The SWISS-PROT protein knowledgebase and its supplement TrEMBL in 2003. *Nucleic acids research*, 31 (1), pp. 365–370.

Boetto, G. (2010). Fishing vessels in Antiquity: the archaeological evidence from Ostia. In: *Ancient nets and fishing gear. Proceedings of the international workshop on "Nets and fishing gear in classical antiquity: a first approach"*, Universidad de Cádiz, Servicio de Publicaciones; Aarhus University Press, pp. 243–255.

Bogaard, A., Charles, M., Twiss, K. C., Fairbairn, A., Yalman, N., Filipovic, D., Demirergi, G. A., Ertug, F., Russell, N. and Henecke, J. (2009). Private pantries and celebrated surplus: storing and sharing food at Neolithic Çatalhöyük, Central Anatolia. *Antiquity*, 83 (321), pp. 649–668.

Bogaard, A., Filipović, D., Fairbairn, A., Green, L., Stroud, E., Fuller, D. and Charles, M. (2017). Agricultural innovation and resilience in a long-lived early farming community: the 1,500-year sequence at Neolithic to early Chalcolithic Çatalhöyük, central Anatolia. *Anatolian Studies*, 67, pp. 1–28.

Bogaard, A., Henton, E., Evans, J. A., Twiss, K. C., Charles, M. P., Vaiglova, P. and Russell, N. (2014). Locating Land Use at N eolithic Ç atalhöyük, Turkey: The Implications of $^{87}Sr/^{86}Sr$ signatures in plants and sheep tooth sequences. *Archaeometry*, 56 (5), pp. 860–877.

Bogaard, A., Poulton, P. and Merbach, I. (2007). The impact of manuring on nitrogen isotope ratios in cereals: archaeological implications for reconstruction of diet and crop management practices. *Journal of Archaeological Science*, 34 (3), pp. 335–343.

Borgongino, M. and Stefani, G. (2021). Quando accadde? le diverse ipotesi sulla data dell'eruzione del 79 dC. *Studi e ricerche del Parco archeologico di Pompei*, 46, pp. 29–44.

Bosi, G., Mazzanti, M. B., Montecchi, M. C., Torri, P. and Rinaldi, R. (2017). The life of a Roman colony in Northern Italy: Ethnobotanical information from archaeobotanical analysis. *Quaternary International*, 460, pp. 135–156.

Bowersock, G. (1978). The rediscovery of Herculaneum and Pompeii. *The American Scholar*, 47 (4), pp. 461–470.

Bowes, K., Mercuri, A. M., Rattighieri, E., Rinaldi, R., Arnoldus-Huyzendveld, A., Ghisleni, M., Grey, C., Mackinnon, M. and Vaccaro, E. (2015). Palaeoenvironment and land use of Roman peasant farmhouses in southern Tuscany. *Plant Biosystems*, 149 (1), pp. 174–184.

Bownes, J. M., Ascough, P. L., Cook, G. T., Murray, I. and Bonsall, C. (2017). Using stable isotopes and a Bayesian mixing model (FRUITS) to investigate diet at the early Neolithic site of Carding Mill Bay, Scotland. *Radiocarbon*, 59 (5), pp. 1275–1294.

Brand, W. A., Coplen, T. B., Vogl, J., Rosner, M. and Prohaska, T. (2014). Assessment of international reference materials for isotope-ratio analysis (IUPAC Technical Report). *Pure and Applied Chemistry*, 86 (3), pp. 425–467.

Braun, A., Vikari, A., Windisch, W. and Auerswald, K. (2014). Transamination governs nitrogen isotope heterogeneity of amino acids in rats. *Journal of agricultural and food chemistry*, 62 (32), pp. 8008–8013.

Brenna, J. T., Corso, T. N., Tobias, H. J. and Caimi, R. J. (1997). High-precision continuous-flow isotope ratio mass spectrometry. *Mass spectrometry reviews*, 16 (5), pp. 227–258.

Brinkkemper, O., Braadbaart, F., Van Os, B., Van Hoesel, A., Van Brussel, A. and Fernandes, R. (2018). Effectiveness of different pre-treatments in recovering pre-burial isotopic ratios of charred plants. *Rapid Communications in Mass Spectrometry*, 32 (3), pp. 251–261.

Brown, T. A. and Brown, K. (2011). *Biomolecular archaeology: an introduction*. Chichester: John Wiley & Sons.

Brown, T. A., Nelson, D. E., Vogel, J. S. and Southon, J. R. (1988). Improved collagen extraction by modified Longin method. *Radiocarbon*, 30 (2), pp. 171–177.

Brunner, E. J., Jones, P. J., Friel, S. and Bartley, M. (2009). Fish, human health and marine ecosystem health: policies in collision. *International Journal of Epidemiology*, 38 (1), pp. 93–100.

Bruno, B. (2005). Le anfore da trasporto. In: D. Gandolfi (Ed.), *La ceramica e i materiali di età romana: classi, produzioni, commerci e consumi*, Istituto internazionale di studi liguri, pp. 353–394.

Buckley, M. (2016). Species identification of bovine, ovine and porcine type 1 collagen; comparing peptide mass fingerprinting and LC-based proteomics methods. *International journal of molecular sciences*, 17 (4).

Buckley, M. (2018). Zooarchaeology by mass spectrometry (ZooMS) collagen fingerprinting for the species identification of archaeological bone fragments. In: *Zooarchaeology in practice*, Cham: Springer, pp. 227–247.

Buckley, M., Collins, M., Thomas-Oates, J. and Wilson, J. C. (2009). Species identification by analysis of bone collagen using matrix-assisted laser desorption/ionisation time-of-flight mass spectrometry. *Rapid Communications in Mass Spectrometry: An International Journal Devoted to the Rapid Dissemination of Up-to-the-Minute Research in Mass Spectrometry*, 23 (23), pp. 3843–3854.

Buckley, M., Harvey, V. L. and Chamberlain, A. T. (2017). Species identification and decay assessment of Late Pleistocene fragmentary vertebrate remains from Pin Hole Cave (Creswell Crags, UK) using collagen fingerprinting. *Boreas*, 46 (3), pp. 402–411.

Buckley, M. and Kansa, S. W. (2011). Collagen fingerprinting of archaeological bone and teeth remains from Domuztepe, South Eastern Turkey. *Archaeological and Anthropological Sciences*, 3 (3), pp. 271–280.

Buckley, M., Kansa, S. W., Howard, S., Campbell, S., Thomas-Oates, J. and Collins, M. (2010). Distinguishing between archaeological sheep and goat bones using a single collagen peptide. *Journal of Archaeological Science*, 37 (1), pp. 13–20.

Camardo, D. (2006). Archaeology and conservation at Herculaneum: from the Maiuri campaign to the Herculaneum Conservation Project. *Conservation and Management of Archaeological Sites*, 8 (4), pp. 205–214.

Capasso, L. (1999). Brucellosis at Herculaneum (79 AD). *International Journal of Osteoarchaeology*, 9 (5), pp. 277–288.

Capasso, L. (2001). *I fuggiaschi di Ercolano: paleobiologia delle vittime dell'eruzione vesuviana del 79*, volume 33. Rome: L'Erma di Bretschneider.

Capasso, L. (2002). Bacteria in two-millennia-old cheese, and related epizoonoses in Roman populations. *Journal of Infection*, 45 (2), pp. 122–127.

Capasso, L. and Capasso, L. (1999). Mortality in Herculaneum before volcanic eruption in 79 AD. *The Lancet*, 354 (9192), p. 1826.

Capasso, L., D'Alessandro, A. and Bartoli, F. (2001). Analisi paleonutrizionale mediante spettroscopia ad assorbimento atomico. In: L. Capasso (Ed.), *I fuggiaschi di Ercolano*, L'Erma di Bretschneider, pp. 1065–1068.

Capasso, L. and Di Domenicantonio, L. (1998). Work-related syndesmoses on the bones of children who died at Herculaneum. *The Lancet*, 352 (9140), p. 1634.

Capasso, L. and Di Tota, G. (1998). Lice buried under the ashes of Herculaneum. *The Lancet*, 351 (9107), p. 992.

Cappellini, M. D. and Fiorelli, G. (2008). Glucose-6-phosphate dehydrogenase deficiency. *The Lancet*, 371 (9606), pp. 64–74.

Carroll, M. (2011). Infant death and burial in Roman Italy. *Journal of Roman Archaeology*, 24, pp. 99–120.

Casson, L. (1980). The role of the state in Rome's grain trade. *Memoirs of the American Academy in Rome*, 36, pp. 21–33.

Cerchiai, L. (2010). *Gli antichi popoli della Campania: archeologia e storia*. Rome: Carocci.

Chandezon, C. (2015). Animals, meat, and alimentary by-products: patterns of production and consumption. *A companion to food in the ancient world*, 89, p. 135.

Cheng, H., Bremner, J. and Edwards, A. (1964). Variations of nitrogen-15 abundance in soils. *Science*, 146 (3651), pp. 1574–1575.

Cheung, C. and Szpak, P. (2020). Interpreting Past Human Diets Using Stable Isotope Mixing Models. *Journal of Archaeological Method and Theory*, pp. 1–37.

Chikaraishi, Y., Kashiyama, Y., Ogawa, N. O., Kitazato, H. and Ohkouchi, N. (2007). Metabolic control of nitrogen isotope composition of amino acids in macroalgae and gastropods: implications for aquatic food web studies. *Marine Ecology Progress Series*, 342, pp. 85–90.

Chikaraishi, Y., Ogawa, N. O., Doi, H. and Ohkouchi, N. (2011). 15 N/14 N ratios of amino acids as a tool for studying terrestrial food webs: a case study of terrestrial insects (bees, wasps, and hornets). *Ecological research*, 26 (4), pp. 835–844.

Chikaraishi, Y., Ogawa, N. O., Kashiyama, Y., Takano, Y., Suga, H., Tomitani, A., Miyashita, H., Kitazato, H. and Ohkouchi, N. (2009). Determination of aquatic food-web structure based on compound-specific nitrogen isotopic composition of amino acids. *Limnology and Oceanography: methods*, 7 (11), pp. 740–750.

Chikaraishi, Y., Ogawa, N. O., Ohkouchi, N. *et al.* (2010). Further evaluation of the trophic level estimation based on nitrogen isotopic composition of amino acids. *Earth, life, and isotopes*, pp. 37–51.

Choy, K., Smith, C. I., Fuller, B. T. and Richards, M. P. (2010). Investigation of amino acid $\delta^{13}C$ signatures in bone collagen to reconstruct human palaeodiets using liquid chromatography–isotope ratio mass spectrometry. *Geochimica et Cosmochimica Acta*, 74 (21), pp. 6093–6111.

Choy, K., Yun, H. Y., Lee, J., Fuller, B. T. and Shin, K.-H. (2021). Direct isotopic evidence for human millet consumption in the Middle Mumun period: Implication and importance of millets in early agriculture on the Korean Peninsula. *Journal of Archaeological Science*, 129, p. 105372.

Cocozza, C., Fernandes, R., Ughi, A., Groß, M. and Alexander, M. M. (2021). Investigating infant feeding strategies at Roman Bainesse through Bayesian modelling of incremental dentine isotopic data. *International Journal of Osteoarchaeology*.

Collins, M., Waite, E. and Van Duin, A. (1999). Predicting protein decomposition: the case of aspartic–acid racemization kinetics. *Philosophical Transactions of the Royal Society of London B. Series B: Biological Sciences*, 354 (1379), pp. 51–64.

Colonese, A. C., Collins, M., Lucquin, A., Eustace, M., Hancock, Y., Ponzoni, R. d. A. R., Mora, A., Smith, C., DeBlasis, P., Figuti, L., Wesolowski, V., Plens, C. R., Eggers, S., Scunderlick Eloy de Farias, D., Glendhill, A. and Craig, O. E. (2014). Long-term resilience of late Holocene coastal subsistence system in southeastern South America. *PloS One*, 9 (4), p. e93854.

Commendador, A. S., Finney, B. P., Fuller, B. T., Tromp, M. and Dudgeon, J. V. (2019). Multiproxy isotopic analyses of human skeletal material from Rapa Nui: Evaluating the evidence from carbonates, bulk collagen, and amino acids. *American Journal of Physical Anthropology*, 169 (4), pp. 714–729.

Cooley, A. E. and Cooley, M. G. L. (2013). *Pompeii and Herculaneum: A sourcebook*. London-New York: Routledge.

Cooper, C., Lupo, K., Matson, R., Lipe, W., Smith, C. I. and Richards, M. P. (2016). Short-term variability of human diet at Basketmaker II Turkey Pen Ruins, Utah: Insights from bulk and single amino acid isotope analysis of hair. *Journal of Archaeological Science: Reports*, 5, pp. 10–18.

Coplen, T. B. (2011). Guidelines and recommended terms for expression of stable-isotope-ratio and gas-ratio measurement results. *Rapid Communications in Mass Spectrometry*, 25 (17), pp. 2538–2560.

Corbel, M. J. (1997). Brucellosis: an overview. *Emerging infectious diseases*, 3 (2), pp. 213–219.

Corr, L. T., Berstan, R. and Evershed, R. P. (2007a). Development of N-acetyl methyl ester derivatives for the determination of $\delta^{13}C$ values of amino acids using gas chromatography-combustion-isotope ratio mass spectrometry. *Analytical chemistry*, 79 (23), pp. 9082–9090.

Corr, L. T., Berstan, R. and Evershed, R. P. (2007b). Optimisation of derivatisation procedures for the determination of $\delta^{13}C$ values of amino acids by gas chromatography/combustion/isotope ratio mass spectrometry. *Rapid Communications in Mass Spectrometry*, 21 (23), pp. 3759–3771.

Corr, L. T., Sealy, J. C., Horton, M. C. and Evershed, R. P. (2005). A novel marine dietary indicator utilising compound-specific bone collagen amino acid $\delta^{13}C$ values of ancient humans. *Journal of Archaeological Science*, 32 (3), pp. 321–330.

Cowan, P. M., McGavin, S. and North, A. C. T. (1955). The polypeptide chain configuration of collagen. *Nature*, 176 (4492), pp. 1062–1064.

Craig, H. (1953). The geochemistry of the stable carbon isotopes. *Geochimica et Cosmochimica Acta*, 3 (2-3), pp. 53–92.

Craig, H. and Craig, V. (1972). Greek marbles: determination of provenance by isotopic analysis. *Science*, 176 (4033), pp. 401–403.

Craig, O. E., Allen, R. B., Thompson, A., Stevens, R. E., Steele, V. J. and Heron, C. (2012). Distinguishing wild ruminant lipids by gas chromatography/combustion/isotope ratio mass spectrometry. *Rapid Communications in Mass Spectrometry*, 26 (19), pp. 2359–2364.

Craig, O. E., Biazzo, M., O'Connell, T. C., Garnsey, P., Martínez-Labarga, C., Cristina, Lelli, R., Salvadei, L., Tartaglia, G., Nava, A., Renò, L., Fiammenghi, A., Rickards, O. and Bondioli, L. (2009). Stable isotopic evidence for diet at the Imperial Roman coastal site of Velia (1^{st} and 2^{nd} centuries AD) in Southern Italy. *American Journal of Physical Anthropology*, 139 (4), pp. 572–583.

Craig, O. E., Bondioli, L., Fattore, L., Higham, T. and Hedges, R. (2013). Evaluating marine diets through radiocarbon dating and stable isotope analysis of victims of the AD79 eruption of Vesuvius. *American Journal of Physical Anthropology*, 152 (3), pp. 345–352.

Crisp, M., Demarchi, B., Collins, M., Morgan-Williams, M., Pilgrim, E. and Penkman, K. (2013). Isolation of the intra-crystalline proteins and kinetic studies in Struthio camelus (ostrich) eggshell for amino acid geochronology. *Quaternary Geochronology*, 16, pp. 110–128.

Crowe, F., Sperduti, A., O'Connell, T. C., Craig, O. E., Kirsanow, K., Germoni, P., Macchiarelli, R., Garnsey, P. and Bondioli, L. (2010). Water-related occupations and diet in two Roman coastal communities (Italy, first to third century AD): Correlation between stable carbon and nitrogen isotope values and auricular exostosis prevalence. *American Journal of Physical Anthropology*, 142 (3), pp. 355–366.

Cubas, M., Peyroteo-Stjerna, R., Fontanals-Coll, M., Llorente-Rodríguez, L., Lucquin, A., Craig, O. E. and Colonese, A. C. (2019). Long-term dietary change in Atlantic and Mediterranean Iberia with the introduction of agriculture: a stable isotope perspective. *Archaeological and Anthropological Sciences*, 11 (8), pp. 3825–3836.

Curtis, R. I. (1991). *Garum and salsamenta*, volume 3 of *Studies in Ancient Medicine*. Leiden: Brill.

Curtis, R. I. (2009). Umami and the foods of classical antiquity. *The American Journal of Clinical Nutrition*, 90 (3), pp. 712S–718S.

De Angelis, F., Varano, S., Battistini, A., Di Giannantonio, S., Ricci, P., Lubritto, C., Facchin, G., Brancazi, L., Santangeli-Valenzani, R., Catalano, P., Gazzanica, V., Rickards, O. and Martínez-Labarga, C. (2020a). Food at the heart of the Empire: dietary reconstruction for Imperial Rome inhabitants. *Archaeological and Anthropological Sciences*, 12 (10), pp. 1–21.

De Angelis, F. D., Veltre, V., Varano, S., Romboni, M., Renzi, S., Zingale, S., Ricci, P., Caldarini, C., Giannantonio, S. D., Lubritto, C., Catalano, P., Rickards, O. and Martínez-Labarga, C. (2020b). Dietary and Weaning Habits of the Roman Community of Quarto Cappello del Prete (Rome, 1^{st}-3^{rd} Century CE). *Environmental Archaeology*, pp. 1–15.

De Jorio, A. (1827). *Notizie su gli scavi di Ercolano*. Naples: Dalla stamperia francese.

de Ligt, L. and Garnsey, P. (2012). The Album of Herculaneum and a model of the town's demography. *Journal of Roman Archaeology*, 25, pp. 69–94.

de Ligt, L. and Garnsey, P. (2019). The Album of Herculaneum revisited. In: M. Maiuro and M. Balbo (Eds.), *Popolazione, Risorse e Urbanizzazione nella Campania Antica*, Bari: Edipuglia, volume 31 of *Pragmateiai*, pp. 197–209.

De Sena, E. C. (2005). An assessment of wine and oil production in Rome's hinterland: ceramic, literary, art historical and modern evidence. *Archaeology and Science*.

De Simone, G. F. (2017). The Agricultural Economy of Pompeii. In: *The Economy of Pompeii*, Oxford: Oxford University Press, pp. 23–51.

De Vos, M., Bowman, A. and Wilson, A. (2013). The rural landscape of Thugga: farms, presses, mills and transport. In: *The Roman Agricultural Economy. Organization, Investment, and Production*, Oxford: Oxford: Oxford University Press, pp. 143–218.

Degens, E. T., Guillard, R. R. L., Sackett, W. M. and Hellebust, J. A. (1968). Metabolic fractionation of carbon isotopes in marine plankton—I. Temperature and respiration experiments. In: *Deep Sea Research and Oceanographic Abstracts*, volume 15, pp. 1–9.

Demarchi, B., Collins, M., Tomiak, P., Davies, B. J. and Penkman, K. (2013). Intra-crystalline protein diagenesis (IcPD) in Patella vulgata. Part II: breakdown and temperature sensitivity. *Quaternary Geochronology*, 16, pp. 158–172.

Demarchi, B., Hall, S., Roncal-Herrero, T., Freeman, C. L., Woolley, J., Crisp, M. K., Wilson, J., Fotakis, A., Fischer, R., Kessler, B. M., Rakownikow Jersie-Christensen, R., Olsen, J. V., Haile, J., Thomas, J., Marean, C. W., Parkington, J., Presslee, S., Lee-Thorp, J., Ditchfield, P., Hamilton, J. F., Ward, M. W., Wang, C. M., Shaw, M. D., Harrison, T., Domínguez-Rodrigo, M., MacPhee, R. D., Kwekason, A., Ecker, M., Horwitz, L. K., Chazan, M., Kröger, R., Thomas-Oates, J., Harding, J. H., Cappellini, E., Penkman, K. and Collins, M. J. (2016). Protein sequences bound to mineral surfaces persist into deep time. *elife*, 5 (e17092).

Dempster, A. (1918). A new method of positive ray analysis. *Physical Review*, 11 (4), pp. 316–325.

DeNiro, M. and Epstein, S. (1976). You are what you eat (plus a few ‰): The carbon isotope cycle in food chains. In: *Abstracts with Programs*, Geological Society of America, volume 8, pp. 834–835.

DeNiro, M. J. and Epstein, S. (1978). Influence of diet on the distribution of carbon isotopes in animals. *Geochimica et Cosmochimica Acta*, 42 (5), pp. 495–506.

DeNiro, M. J. and Epstein, S. (1981). Influence of diet on the distribution of nitrogen isotopes in animals. *Geochimica et Cosmochimica Acta*, 45 (3), pp. 341–351.

DeWitte, S. N. and Stojanowski, C. M. (2015). The osteological paradox 20 years later: past perspectives, future directions. *Journal of Archaeological Research*, 23 (4), pp. 397–450.

Diffey, C., Neef, R. and Bogaard, A. (2017). The archaeobotany of large-scale hermetic cereal storage at the Hittite capital of Hattusha. In: A. Schachner (Ed.), *Innovation versus Beharrung: Was macht den Unterschied des hethitischen Reichs im Anatolien des 2. Jahrtausends v. Chr.?*, Istanbul: Ege Yayinlari, pp. 185–202.

Diffey, C., Neef, R., Seeher, J. and Bogaard, A. (2020). The agroecology of an early state: New results from Hattusha. *Antiquity*, 94 (377).

Docherty, G., Jones, V. and Evershed, R. P. (2001). Practical and theoretical considerations in the gas chromatography/combustion/isotope ratio mass spectrometry $\delta^{13}C$ analysis of small polyfunctional compounds. *Rapid Communications in Mass Spectrometry*, 15 (9), pp. 730–738.

Dotsika, E. and Michael, D. E. (2018). Using stable isotope technique in order to assess the dietary habits of a Roman population in Greece. *Journal of Archaeological Science: Reports*, 22, pp. 470–481.

Dudd, S. N. (1999). *Molecular and isotopic characterisation of animal fats in archaeological pottery*. Ph.D. thesis, University of Bristol.

Dunn, P. J., Honch, N. V. and Evershed, R. P. (2011). Comparison of liquid chromatography–isotope ratio mass spectrometry (LC/IRMS) and gas chromatography–combustion–isotope ratio mass spectrometry (GC/C/IRMS) for the determination of collagen amino acid $\delta^{13}C$ values for palaeodietary and palaeoecological reconstruction. *Rapid Communications in Mass Spectrometry*, 25 (20), pp. 2995–3011.

Eda, M., Morimoto, M., Mizuta, T. and Inoué, T. (2020). ZooMS for birds: Discrimination of Japanese archaeological chickens and indigenous pheasants using collagen peptide fingerprinting. *Journal of Archaeological Science: Reports*, 34 (102635).

Ermolli, E. R., Romano, P., Ruello, M. R. and Lumaga, M. R. B. (2014). The natural and cultural landscape of Naples (Southern Italy) during the Graeco-Roman and Late Antique periods. *Journal of Archaeological Science*, 42, pp. 399–411.

Evershed, R. P. (2008). Organic residue analysis in archaeology: the archaeological biomarker revolution. *Archaeometry*, 50 (6), pp. 895–924.

Evershed, R. P., Arnot, K. I., Collister, J., Eglinton, G. and Charters, S. (1994). Application of isotope ratio monitoring gas chromatography–mass spectrometry to the analysis of organic residues of archaeological origin. *Analyst*, 119 (5), pp. 909–914.

Fattore, L., Bondioli, L., Garnsey, P., Rossi, P. F. and Sperduti, A. (2012). Poster: The human skeletal remains from Herculaneum: new evidence from the excavation of the fornici 7, 8, 9, 10 and 11. In: *AAPA* 81^{st} *Annual Meeting.*

Fernandes, R. (2016). A simple (r) model to predict the source of dietary carbon in individual consumers. *Archaeometry*, 58 (3), pp. 500–512.

Fernandes, R., Grootes, P., Nadeau, M.-J. and Nehlich, O. (2015). Quantitative diet reconstruction of a Neolithic population using a Bayesian mixing model (FRUITS): the case study of Ostorf (Germany). *American Journal of Physical Anthropology*, 158 (2), pp. 325–340.

Fernandes, R., Larsen, T., Knipper, C., Feng, F. and Wang, Y. (2017). IsoMemo.com: a database of isotopic data for ecology, archaeology, and environmental science; 2017.

Fernandes, R., Millard, A. R., Brabec, M., Nadeau, M.-J. and Grootes, P. (2014). Food reconstruction using isotopic transferred signals (FRUITS): a Bayesian model for diet reconstruction. *PloS One*, 9 (2).

Fernandes, R., Nadeau, M.-J. and Grootes, P. M. (2012). Macronutrient-based model for dietary carbon routing in bone collagen and bioapatite. *Archaeological and Anthropological Sciences*, 4 (4), pp. 291–301.

Fiorentino, G., Ferrio, J. P., Bogaard, A., Araus, J. L. and Riehl, S. (2015). Stable isotopes in archaeobotanical research. *Vegetation History and Archaeobotany*, 24 (1), pp. 215–227.

Fogel, M. L. and Tuross, N. (2003). Extending the limits of paleodietary studies of humans with compound specific carbon isotope analysis of amino acids. *Journal of Archaeological Science*, 30 (5), pp. 535–545.

Fogel, M. L., Tuross, N., Johnson, B. J. and Miller, G. H. (1997). Biogeochemical record of ancient humans. *Organic Geochemistry*, 27 (5-6), pp. 275–287.

Foxhall, L. (2007). *Olive cultivation in ancient Greece: seeking the ancient economy*. Oxford: Oxford University Press.

Foxhall, L. and Forbes, H. A. (1982). Sitometreia: the role of grain as a staple food in classical antiquity. *Chiron*, 12, pp. 41–90.

France, C. A., Sugiyama, N. and Aguayo, E. (2020). Establishing a preservation index for bone, dentin, and enamel bioapatite mineral using ATR-FTIR. *Journal of Archaeological Science: Reports*, 33 (102551).

Fraser, R. A., Bogaard, A., Charles, M., Styring, A. K., Wallace, M., Jones, G., Ditchfield, P. and Heaton, T. H. (2013a). Assessing natural variation and the effects of charring, burial and pre-treatment on the stable carbon and nitrogen isotope values of archaeobotanical cereals and pulses. *Journal of Archaeological Science*, 40 (12), pp. 4754–4766.

Fraser, R. A., Bogaard, A., Heaton, T., Charles, M., Jones, G., Christensen, B. T., Halstead, P., Merbach, I., Poulton, P. R., Sparkes, D. and Styring, A. K. (2011). Manuring and stable nitrogen isotope ratios in cereals and pulses: towards a new archaeobotanical approach to the inference of land use and dietary practices. *Journal of Archaeological Science*, 38 (10), pp. 2790–2804.

Fraser, R. A., Bogaard, A., Schäfer, M., Arbogast, R. and Heaton, T. H. (2013b). Integrating botanical, faunal and human stable carbon and nitrogen isotope values to reconstruct land use and palaeodiet at LBK Vaihingen an der Enz, Baden-Württemberg. *World Archaeology*, 45 (3), pp. 492–517.

Frederiksen, M. and Purcell, N. (1984). *Campania*. Rome: British school at Rome.

Frischer, B. (1984). Monumenta et arae honoris virtutisque causa: evidence of memorials for roman civic heroes. *Bullettino della Commissione Archeologica Comunale di Roma*, 88, pp. 51–86.

Froehle, A. W., Kellner, C. M. and Schoeninger, M. J. (2010). FOCUS: effect of diet and protein source on carbon stable isotope ratios in collagen: follow up to Warinner and Tuross. *Journal of Archaeological Science*, 37 (10), pp. 2662–2670.

Froehle, A. W., Kellner, C. M. and Schoeninger, M. J. (2012). Multivariate carbon and nitrogen stable isotope model for the reconstruction of prehistoric human diet. *American Journal of Physical Anthropology*, 147 (3), pp. 352–369.

Froese, R. and Pauly, D. (2000). *FishBase 2000: concepts designs and data sources*. Makati City: international Center for Living Aquatic Resources Management.

Fry, B. (2006). *Stable isotope ecology*. New York: Springer.

Fuller, B. T., Fuller, J. L., Sage, N. E., Harris, D. A., O'Connell, T. C. and Hedges, R. E. (2005). Nitrogen balance and $\delta^{15}N$: why you're not what you eat during nutritional stress. *Rapid Communications in Mass Spectrometry*, 19 (18), pp. 2497–2506.

Fuller, B. T. and Petzke, K. J. (2017). The dietary protein paradox and threonine 15N-depletion: Pyridoxal-5'-phosphate enzyme activity as a mechanism for the $\delta^{15}N$ trophic level effect. *Rapid Communications in Mass Spectrometry*, 31 (8), pp. 705–718.

Garnsey, P. (1989). *Famine and food supply in the Graeco-Roman world: responses to risk and crisis*. Cambridge: Cambridge University Press.

Garnsey, P. (1999). *Food and society in classical antiquity*. Cambridge: Cambridge University Press.

Garnsey, P. (2008). The Land. In: A. K. Bowman, P. Garnsey and D. Rathbone (Eds.), *The High Empire, AD 70–192*, Cambridge University Press, The Cambridge Ancient History, pp. 679–709.

Garnsey, P. and de Ligt, L. (2016). Migration in early-imperial Italy: Herculaneum and Rome compared. In: L. de Ligt and L. E. Tacoma (Eds.), *Migration and Mobility in the Early Roman Empire*, Leiden: Brill, pp. 72–94.

Garnsey, P. and Saller, R. (2014). *The Roman Empire: Economy, Society and Culture*. London: Bloomsbury Academic.

Garnsey, P. and Scheidel, W. (1998). *Cities, Peasants and Food in Classical Antiquity: Essays in Social and Economic History*. Cambridge: Cambridge University Press.

Garvie-Lok, S. J., Varney, T. L. and Katzenberg, M. A. (2004). Preparation of bone carbonate for stable isotope analysis: the effects of treatment time and acid concentration. *Journal of Archaeological Science*, 31 (6), pp. 763–776.

Gasteiger, E., Hoogland, C., Gattiker, A., Wilkins, M. R., Appel, R. D., Bairoch, A. *et al.* (2005). Protein identification and analysis tools on the ExPASy server. In: *The Proteomics Protocols Handbook*, Springer, pp. 571–607.

Giordano, G., Zanella, E., Trolese, M., Baffioni, C., Vona, A., Caricchi, C., De Benedetti, A., Corrado, S., Romano, C., Sulpizio, R. and Geshi, N. (2018). Thermal interactions of the AD79 Vesuvius pyroclastic density currents and their deposits at Villa dei Papiri (Herculaneum archaeological site, Italy). *Earth and Planetary Science Letters*, 490, pp. 180–192.

Gismondi, A., Baldoni, M., Gnes, M., Scorrano, G., D'Agostino, A., Di Marco, G., Calabria, G., Petrucci, M., Müldner, G., Von Tersch, M., Alexander, M. and Martínez-Labarga, C. (2020). A multidisciplinary approach for investigating dietary and medicinal habits of the Medieval population of Santa Severa (7^{th}-15^{th} centuries, Rome, Italy). *PloS One*, 15 (1).

Grimm, V. E. (2006). On Food and the Body. In: D. S. Potter (Ed.), *A companion to the Roman Empire*, Blackwell Publishing, Blackwell companions to the ancient world, pp. 354–368.

Guidobaldi, M. P., Camardo, D. and Notomista, M. (2014). I carotaggi geoarcheologici nell'area della nuova caserma dei Carabinieri di Ercolano. *Rivista di Studi Pompeiani*, 25, pp. 166–170.

Guiry, E. J., Szpak, P. and Richards, M. P. (2016). Effects of lipid extraction and ultrafiltration on stable carbon and nitrogen isotopic compositions of fish bone collagen. *Rapid Communications in Mass Spectrometry*, 30 (13), pp. 1591–1600.

Gurioli, L., Cioni, R., Sbrana, A. and Zanella, E. (2002). Transport and deposition of pyroclastic density currents over an inhabited area: the deposits of the AD 79 eruption of Vesuvius at Herculaneum, Italy. *Sedimentology*, 49 (5), pp. 929–953.

Hare, P. E. and Estep, M. L. (1983). Carbon and nitrogen isotopic composition of amino acids in modern and fossil collagens. *Carnegie Institution of Washington Yearbook*, 82, pp. 410–414.

Hare, P. E., Fogel, M. L., Stafford Jr, T. W., Mitchell, A. D. and Hoering, T. C. (1991). The isotopic composition of carbon and nitrogen in individual amino acids isolated from modern and fossil proteins. *Journal of Archaeological Science*, 18 (3), pp. 277–292.

Harvey, V. L., Daugnora, L. and Buckley, M. (2018). Species identification of ancient Lithuanian fish remains using collagen fingerprinting. *Journal of Archaeological Science*, 98, pp. 102–111.

Hayes, J., Freeman, K. H., Popp, B. N. and Hoham, C. H. (1990). Compound-specific isotopic analyses: a novel tool for reconstruction of ancient biogeochemical processes. *Organic Geochemistry*, 16 (4-6), pp. 1115–1128.

Hedges, R., Rush, E. and Aalbersberg, W. (2009). Correspondence between human diet, body composition and stable isotopic composition of hair and breath in Fijian villagers. *Isotopes in Environmental and Health Studies*, 45 (1), pp. 1–17.

Hedges, R. E. (2004). Isotopes and red herrings: comments on Milner *et al.* and Lidén *et al. Antiquity*, 78 (299), pp. 34–37.

Hedges, R. E., Clement, J. G., Thomas, C. D. L. and O'connell, T. C. (2007). Collagen turnover in the adult femoral mid-shaft: Modeled from anthropogenic radiocarbon tracer measurements. *American Journal of Physical Anthropology*, 133 (2), pp. 808–816.

Hedges, R. E. and Reynard, L. M. (2007). Nitrogen isotopes and the trophic level of humans in archaeology. *Journal of Archaeological Science*, 34 (8), pp. 1240–1251.

Heinritz, S. N., Mosenthin, R. and Weiss, E. (2013). Use of pigs as a potential model for research into dietary modulation of the human gut microbiota. *Nutrition Research Reviews*, 26 (2), pp. 191–209.

Heiss, A. G., Pouget, N., Wiethold, J., Delor-Ahü, A. and Le Goff, I. (2015). Tissue-based analysis of a charred flat bread (galette) from a Roman cemetery at Saint-Memmie (Dép. Marne, Champagne-Ardenne, north-eastern France). *Journal of Archaeological Science*, 55, pp. 71–82.

Hellevang, H. and Aagaard, P. (2015). Constraints on natural global atmospheric CO_2 fluxes from 1860 to 2010 using a simplified explicit forward model. *Scientific Reports*, 5, p. 17352.

Hoefs, J. (2008). *Stable isotope geochemistry*. Berlin: Springer-Verlag.

Hoering, T. (1955). Variations of nitrogen-15 abundance in naturally occurring substances. *Science*, 122 (3182), pp. 1233–1234.

Hoering, T. C. and Ford, H. T. (1960). The isotope effect in the fixation of nitrogen by Azotobacter. *Journal of the American Chemical Society*, 82 (2), pp. 376–378.

Holdaway, R. N., Duffy, B. and Kennedy, B. (2018). Evidence for magmatic carbon bias in ^{14}C dating of the Taupo and other major eruptions. *Nature Communications*, 9 (1), pp. 1–9.

Honch, N. V., McCullagh, J. S. and Hedges, R. E. (2012). Variation of bone collagen amino acid $\delta^{13}C$ values in archaeological humans and fauna with different dietary regimes: Developing frameworks of dietary discrimination. *American Journal of Physical Anthropology*, 148 (4), pp. 495–511.

Horden, P. and Purcell, N. (2000). *The corrupting sea: a study of Mediterranean history*. Oxford: Wiley-Blackwell.

Hou, Y. and Wu, G. (2017). Nutritionally nonessential amino acids: a misnomer in nutritional sciences. *Advances in Nutrition*, 8 (1), pp. 137–139.

Howland, M. R. (2003). *Compound-specific stable isotope investigations of the influence of diet on the stable isotope composition of body tissues*. Ph.D. thesis, University of Bristol.

Howland, M. R., Corr, L. T., Young, S. M., Jones, V., Jim, S., Van Der Merwe, N. J., Mitchell, A. D. and Evershed, R. P. (2003). Expression of the dietary isotope signal in the compound-specific $\delta^{13}C$ values of pig bone lipids and amino acids. *International Journal of Osteoarchaeology*, 13 (1-2), pp. 54–65.

Ikeguchi, M. (2017). Beef in Roman Italy. *Journal of Roman Archaeology*, 30, pp. 7–37.

Introna, F. (2018). *Apicio: antica cucina romana. Introduzione, nuova traduzione e note a cura di Federica Introna*. Ariccia: RL Classici Greci Latini.

Jackes, M. (2011). Representativeness and bias in archaeological skeletal samples. *Social Bioarchaeology*, 14, pp. 107–146.

Jaouen, K., Richards, M. P., Le Cabec, A., Welker, F., Rendu, W., Hublin, J.-J., Soressi, M. and Talamo, S. (2019). Exceptionally high $\delta^{15}N$ values in collagen single amino acids confirm Neandertals as high-trophic level carnivores. *Proceedings of the National Academy of Sciences*, 116 (11), pp. 4928–4933.

Jarman, C. L., Larsen, T., Hunt, T., Lipo, C., Solsvik, R., Wallsgrove, N., Ka'apu-Lyons, C., Close, H. G. and Popp, B. N. (2017). Diet of the prehistoric population of Rapa Nui (Easter Island, Chile) shows environmental adaptation and resilience. *American Journal of Physical Anthropology*, 164 (2), pp. 343–361.

Jay, M. and Richards, M. P. (2007). British Iron Age diet: stable isotopes and other evidence. In: *Proceedings of the Prehistoric Society.*, volume 73, pp. 169–190.

Jim, S., Ambrose, S. H. and Evershed, R. P. (2004). Stable carbon isotopic evidence for differences in the dietary origin of bone cholesterol, collagen and apatite: implications for their use in palaeodietary reconstruction. *Geochimica et Cosmochimica Acta*, 68 (1), pp. 61–72.

Jim, S., Jones, V., Ambrose, S. H. and Evershed, R. P. (2006). Quantifying dietary macronutrient sources of carbon for bone collagen biosynthesis using natural abundance stable carbon isotope analysis. *British Journal of Nutrition*, 95 (6), pp. 1055–1062.

Jones, V. (2002). *Investigating the routing and synthesis of amino acids between diet and bone collagen via feeding experiments and applications to palaeodietary reconstruction*. Ph.D. thesis, University of Bristol.

Jongman, W. M. (2007). The Early Roman Empire: Consumption. In: W. Scheidel, I. Morris and R. Saller (Eds.), *The Cambridge economic history of the Greco-Roman world*, Cambridge: Cambridge University Press, pp. 592–618.

Jørkov, M. L. S., Heinemeier, J. and Lynnerup, N. (2009). The petrous bone—A new sampling site for identifying early dietary patterns in stable isotopic studies. *American journal of physical anthropology*, 138 (2).

Kaufman, D. S. and Manley, W. F. (1998). A new procedure for determining DL amino acid ratios in fossils using reverse phase liquid chromatography. *Quaternary Science Reviews*, 17 (11), pp. 987–1000.

Keeling, C. D., Mook, W. G. and Tans, P. P. (1979). Recent trends in the $^{13}C/^{12}C$ ratio of atmospheric carbon dioxide. *Nature*, 277, pp. 121–123.

Keenleyside, A., Schwarcz, H., Stirling, L. and Lazreg, N. B. (2009). Stable isotopic evidence for diet in a Roman and Late Roman population from Leptiminus, Tunisia. *Journal of Archaeological Science*, 36 (1), pp. 51–63.

Kehoe, D. P. (2007). The Early Roman Empire: Production. In: W. Scheidel, I. Morris and R. Saller (Eds.), *The Cambridge economic history of the Greco-Roman world*, Cambridge: Cambridge University Press, pp. 543–569.

Kendall, I. P., Lee, M. R. and Evershed, R. P. (2017). The effect of trophic level on individual amino acid $\delta^{15}N$ values in a terrestrial ruminant food web. *STAR: Science & Technology of Archaeological Research*, 3 (1), pp. 135–145.

Kenward, H. K. and Williams, D. (1979). Biological Evidence from the Roman Warehouses in Coney Street. In: *The Past Environment of York*, Council for British Archaeology, volume 14 of *The Archaeology of York*.

Killgrove, K. and Tykot, R. H. (2013). Food for Rome: a stable isotope investigation of diet in the Imperial period (1^{st}–3^{rd} centuries AD). *Journal of Anthropological Archaeology*, 32 (1), pp. 28–38.

Killgrove, K. and Tykot, R. H. (2018). Diet and collapse: a stable isotope study of Imperial-era Gabii (1st–3rd centuries AD). *Journal of Archaeological Science: Reports*, 19, pp. 1041–1049.

King, A. (1983). Pottery. In: M. Henig (Ed.), *A handbook of Roman art: a comprehensive survey of all the arts of the Roman world*, Ithaca: Cornell University Press, pp. 179–190.

King, A. (1999). Diet in the Roman world: a regional inter-site comparison of the mammal bones. *Journal of Roman Archaeology*, 12 (1), pp. 168–202.

King, A. (2002). Evidence from wall paintings, sculpture, mosaics, faunal remains and ancient literary sources. *The Natural History of Pompeii*, pp. 401–450.

Kirby, D. P., Buckley, M., Promise, E., Trauger, S. A. and Holdcraft, T. R. (2013). Identification of collagen-based materials in cultural heritage. *Analyst*, 138 (17), pp. 4849–4858.

Kleijwegt, M. (2012). Deciphering Freedwomen in the Roman Empire. In: *Free at Last! The Influence of Freed Slaves on the Roman Empire*, London: Bristol Classical Press, pp. 110–129.

Kontopoulos, I., Penkman, K., Liritzis, I. and Collins, M. J. (2019). Bone diagenesis in a Mycenaean secondary burial (Kastrouli, Greece). *Archaeological and Anthropological Sciences*, 11 (10), pp. 5213–5230.

Kragten, J. (1994). Tutorial review. Calculating standard deviations and confidence intervals with a universally applicable spreadsheet technique. *Analyst*, 119 (10), pp. 2161–2165.

Kromhout, D., Bosschieter, E. B. and Coulander, C. d. L. (1985). The inverse relation between fish consumption and 20-year mortality from coronary heart disease. *New England Journal of Medicine*, 312 (19), pp. 1205–1209.

Kron, G. (2015). Agriculture. *A companion to food in the ancient world*, 89, pp. 160–172.

Kropff, A. (2016). An English translation of the Edict on Maximum Prices, also known as the Price Edict of Diocletian (*Edictum de pretiis rerum venalium*). *Academia.edu*.

Krueger, H. and Sullivan, C. (1984). Models for carbon isotope fractionation between diet and bone. In: J. F. Turnland and P. E. Johnson (Eds.), *Stable Isotopes in Nutrition*, Washington DC: American Chemical Society, volume 258 of *ACS Symposium Series*, pp. 205–220.

Lagia, A. (2015). Diet and the polis: An isotopic study of diet in Athens and Laurion during the classical, Hellenistic, and imperial Roman periods. *Hesperia Supplements*, 49, pp. 119–145.

Lamb, A. L., Evans, J. E., Buckley, R. and Appleby, J. (2014). Multi-isotope analysis demonstrates significant lifestyle changes in King Richard III. *Journal of Archaeological Science*, 50, pp. 559–565.

Lambers, H., Stuart Chapin III, F. and Pons, T. L. (2008). Photosynthesis, Respiration, and Long-Distance Transpor. In: *Plant Physiological Ecology*, New York: Springer-Verlag, pp. 11–162.

Lasztity, R. (1996). *The chemistry of cereal proteins,* 2^{nd} *edition*. Boca Raton: CRC Press.

Lazer, E. (2009). *Resurrecting Pompeii*. New York: Routledge.

Lieberman, M., Marks, A. D. and Peet, A. (2013). *Marks' basic medical biochemistry: a clinical approach,* 4^{th} *Edition*. Philadelphia: Lippincott Williams & Wilkins,.

Lightfoot, E. and O'Connell, T. C. (2016). On the use of biomineral oxygen isotope data to identify human migrants in the archaeological record: intra-sample variation, statistical methods and geographical considerations. *PloS One*, 11 (4).

Lightfoot, E., Šlaus, M. and O'Connell, T. C. (2012). Changing cultures, changing cuisines: cultural transitions and dietary change in Iron Age, Roman, and Early Medieval Croatia. *American Journal of Physical Anthropology*, 148 (4), pp. 543–556.

Lis, B. (2015). From Cooking Pots to Cuisine: Limitations and Perspectives of a Ceramic-Based Approach. In: M. Spataro and A. Villing (Eds.), *Ceramics, Cuisine and Culture: The archaeology and science of kitchen pottery in the ancient mediterranean world*, Oxford: Oxbow Books, pp. 104–14.

Longin, R. (1971). New method of collagen extraction for radiocarbon dating. *Nature*, 230, pp. 241–242.

López-Costas, O. and Müldner, G. (2016). Fringes of the empire: Diet and cultural change at the Roman to post-Roman transition in NW Iberia. *American Journal of Physical Anthropology*, 161 (1), pp. 141–154.

Ma, Y., Grimes, V., Van Biesen, G., Shi, L., Chen, K., Mannino, M. A. and Fuller, B. T. (2021). Aminoisoscapes and palaeodiet reconstruction: New perspectives on millet-based diets in China using amino acid $\delta^{13}C$ values. *Journal of Archaeological Science*, 125.

Maass, P. and Friedling, L. (2016). Scars of parturition? Influences beyond parity. *International Journal of Osteoarchaeology*, 26 (1), pp. 121–131.

MacKinnon, M. (2001). High on the hog: Linking zooarchaeological, literary, and artistic data for pig breeds in Roman Italy. *American Journal of Archaeology*, pp. 649–673.

MacKinnon, M. (2010a). Cattle 'breed' variation and improvement in Roman Italy: connecting the zooarchaeological and ancient textual evidence. *World Archaeology*, 42 (1), pp. 55–73.

MacKinnon, M. (2010b). 'Sick as a dog': zooarchaeological evidence for pet dog health and welfare in the Roman world. *World Archaeology*, 42 (2), pp. 290–309.

MacKinnon, M. (2018). Multispecies dynamics and the ecology of urban spaces in roman antiquity. In: S. E. Pilaar Birch (Ed.), *Multispecies Archaeology*, Abingdon: Routledge, pp. 170–182.

Macko, S. A., Fogel, M. L., Hare, P. E. and Hoering, T. (1987). Isotopic fractionation of nitrogen and carbon in the synthesis of amino acids by microorganisms. *Chemical Geology: Isotope Geoscience section*, 65 (1), pp. 79–92.

Maggi, G. (1998). Lo scavo dell'area suburbana meridionale di Ercolano. *Rivista di Studi Pompeiani*, 9, pp. 167–172.

Maggi, G. (2009). Ercolano, intervista a Giuseppe Maggi. Appunti di storia e riflessioni a tre secoli dalla scoperta della città di Ercolano. Accessed at vesuvioweb, http://www.vesuvioweb.com/it/wp-content/uploads/2-Giuseppe-Maggi-Ercolano-1709-2009-vesuvioweb.pdf.

Maggi, G. (2013). *Ercolano. Fine di una città*. Naples: Kairós.

Malossini, F. (2011). Gli allevamenti animali nel fondo rustico dell'antica Roma. *Atti della Accademia roveretana degli Agiati. Classe di scienze matematiche, fisiche e naturali, I.*

Mancinelli, G., Vizzini, S., Mazzola, A., Maci, S. and Basset, A. (2013). Cross-validation of $\delta^{15}N$ and FishBase estimates of fish trophic position in a Mediterranean lagoon: the importance of the isotopic baseline. *Estuarine, Coastal and Shelf Science*, 135, pp. 77–85.

Mariani Costantini, R. and Capasso, L. (2001). Sulla presenza di DNA endogeno nei resti scheletrici dei fuggiaschi di Ercolano. In: L. Capasso (Ed.), *I fuggiaschi di Ercolano*, L'Erma di Bretschneider, pp. 1069–1074.

Martyn, R., Craig, O. E., Ellingham, S. T., Islam, M., Fattore, L., Sperduti, A., Bondioli, L. and Thompson, T. (2020). A re-evaluation of manner of death at Roman Herculaneum following the AD 79 eruption of Vesuvius. *Antiquity*, 94 (373).

Martyn, R., Garnsey, P., Fattore, L., Petrone, P., Sperduti, A., Bondioli, L. and Craig, O. (2018). Capturing Roman dietary variability in the catastrophic death assemblage at Herculaneum. *Journal of Archaeological Science: Reports*, 19, pp. 1023–1029.

Marzano, A. (2013a). Agricultural production in the hinterland of Rome: wine and olive oil. In: A. Bowman (Ed.), *The Roman Agricultural Economy: Organization, Investment, and Production*, Oxford: Oxford University Press, pp. 85–106.

Marzano, A. (2013b). *Harvesting the sea: the exploitation of marine resources in the Roman Mediterranean*. Oxford: Oxford University Press.

Marzano, A. and Brizzi, G. (2009). Costly display or economic investment? A quantitative approach to the study of marine aquaculture. *Journal of Roman Archaeology*, 22, p. 215.

Mastrolorenzo, G., Petrone, P., Pappalardo, L. and Guarino, F. M. (2010). Lethal thermal impact at periphery of pyroclastic surges: evidences at Pompeii. *PloS One*, 5 (6), p. e11127.

Mastrolorenzo, G., Petrone, P. P., Pagano, M., Incoronato, A., Baxter, P. J., Canzanella, A. and Fattore, L. (2001). Herculaneum victims of Vesuvius in AD 79. *Nature*, 410 (6830), pp. 769–770.

Mattingly, D. J. (1988). Oil for export? A comparison of Libyan, Spanish and Tunisian olive oil production in the Roman empire. *Journal of Roman Archaeology*, 1, pp. 33–56.

Mattingly, D. J. (1996). First fruit? The olive in the Roman world. In: G. Shipley and J. Salmon (Eds.), *Human Landscapes in Classical Antiquity: Environment and Culture*, London: Routledge, pp. 213–253.

Mattingly, D. J. (2006). The imperial economy. In: D. S. Potter (Ed.), *A companion to the Roman Empire*, Blackwell Publishing, Blackwell companions to the ancient world, pp. 183–297.

McClelland, J. W. and Montoya, J. P. (2002). Trophic relationships and the nitrogen isotopic composition of amino acids in plankton. *Ecology*, 83 (8), pp. 2173–2180.

McCullagh, J. S., Juchelka, D. and Hedges, R. E. (2006). Analysis of amino acid 13C abundance from human and faunal bone collagen using liquid chromatography/isotope ratio mass spectrometry. *Rapid Communications in Mass Spectrometry*, 20 (18), pp. 2761–2768.

McGrath, K., Rowsell, K., St-Pierre, C. G., Tedder, A., Foody, G., Roberts, C., Speller, C. and Collins, M. (2019). Identifying archaeological bone via non-destructive ZooMS and the materiality of symbolic expression: examples from Iroquoian bone points. *Scientific Reports*, 9 (1), pp. 1–10.

McKinney, C. R., McCrea, J. M., Epstein, S., Allen, H. and Urey, H. C. (1950). Improvements in mass spectrometers for the measurement of small differences in isotope abundance ratios. *Review of Scientific Instruments*, 21 (8), pp. 724–730.

McMahon, K. W., Fogel, M. L., Elsdon, T. S. and Thorrold, S. R. (2010). Carbon isotope fractionation of amino acids in fish muscle reflects biosynthesis and isotopic routing from dietary protein. *Journal of Animal Ecology*, 79 (5), pp. 1132–1141.

McMahon, K. W. and McCarthy, M. D. (2016). Embracing variability in amino acid $\delta^{15}N$ fractionation: mechanisms, implications, and applications for trophic ecology. *Ecosphere*, 7 (12).

McMahon, K. W., Polito, M. J., Abel, S., McCarthy, M. D. and Thorrold, S. R. (2015). Carbon and nitrogen isotope fractionation of amino acids in an avian marine predator, the gentoo penguin (*Pygoscelis papua*). *Ecology and Evolution*, 5 (6), pp. 1278–1290.

Meier-Augenstein, W. (1999). Applied gas chromatography coupled to isotope ratio mass spectrometry. *Journal of Chromatography A*, 842 (1-2), pp. 351–371.

Mekota, A.-M., Grupe, G., Ufer, S. and Cuntz, U. (2006). Serial analysis of stable nitrogen and carbon isotopes in hair: monitoring starvation and recovery phases of patients suffering from anorexia nervosa. *Rapid Communications in Mass Spectrometry*, 20 (10), pp. 1604–1610.

Metges, C. C. and Petzke, K. J. (1997). Measurement of $^{15}N/^{14}N$ Isotopic Composition in Individual Plasma Free Amino Acids of Human Adults at Natural Abundance by Gas Chromatography–Combustion Isotope Ratio Mass Spectrometry. *Analytical Biochemistry*, 247 (1), pp. 158–164.

Metges, C. C., Petzke, K.-J. and Hennig, U. (1996). Gas chromatography/combustion/isotope ratio mass spectrometric comparison of N-acetyl-and N-pivaloyl amino acid esters to measure ^{15}N isotopic abundances in physiological samples: a pilot study on amino acid synthesis in the upper gastro-intestinal tract of minipigs. *Journal of Mass Spectrometry*, 31 (4), pp. 367–376.

Meyer, F. G. (1980). Carbonized food plants of Pompeii, Herculaneum, and the Villa at Torre Annunziata. *Economic Botany*, 34 (4), pp. 401–437.

Minagawa, M. and Wada, E. (1984). Stepwise enrichment of ^{15}N along food chains: further evidence and the relation between $\delta^{15}N$ and animal age. *Geochimica et Cosmochimica Acta*, 48 (5), pp. 1135–1140.

Miyake, Y. and Wada, E. (1967). The abundance ratio of $^{15}N/^{14}N$ in marine environments. *Records of Oceanographic Works in Japan*, 9, pp. 37–53.

Monteix, N. (2010). *Les lieux de métier: boutiques et ateliers d'Herculanum*. Rome: École française de Rome, Publications du Centre Jean Bérard.

Monteix, N. (2017). Urban production and the Pompeian economy. In: *The Economy of Pompeii*, Oxford: Oxford University Press, pp. 209–240.

Moore, J. W. and Semmens, B. X. (2008). Incorporating uncertainty and prior information into stable isotope mixing models. *Ecology Letters*, 11 (5), pp. 470–480.

Mora, A., Pacheco, A., Roberts, C. and Smith, C. (2018). Pica 8: Refining dietary reconstruction through amino acid $\delta^{13}C$ analysis of tendon collagen and hair keratin. *Journal of Archaeological Science*, 93, pp. 94–109.

Mora, A., Pacheco, A., Roberts, C. A. and Smith, C. (2021). Palaeopathology and amino acid $\delta^{13}C$ analysis: Investigating pre-Columbian individuals with tuberculosis at Pica 8, northern Chile (1050-500 BP). *Journal of Archaeological Science*, 129.

Morrison, D. J., Dodson, B., Slater, C. and Preston, T. (2000). ^{13}C natural abundance in the British diet: implications for ^{13}C breath tests. *Rapid Communications in Mass Spectrometry*, 14 (15), pp. 1321–1324.

Morton, J. D. and Schwarcz, H. P. (2004). Palaeodietary implications from stable isotopic analysis of residues on prehistoric Ontario ceramics. *Journal of Archaeological Science*, 31 (5), pp. 503–517.

Moses, V. (2012). *Status and meat consumption in Pompeii: Diet and its social implications through the analysis of ancient primary sources and zooarchaeological remains*. Master's thesis, Department of Archaeology, University of Michigan.

Mouritsen, O. G., Duelund, L., Calleja, G. and Frøst, M. B. (2017). Flavour of fermented fish, insect, game, and pea sauces: Garum revisited. *International Journal of Gastronomy and Food Science*, 9, pp. 16–28.

Mueller-Bieniek, A., Nowak, M., Styring, A., Lityńska-Zając, M., Moskal-del Hoyo, M., Sojka, A., Paszko, B., Tunia, K. and Bogaard, A. (2019). Spatial and temporal patterns in Neolithic and Bronze Age agriculture in Poland based on the stable carbon and nitrogen isotopic composition of cereal grains. *Journal of Archaeological Science: Reports*, 27.

Müldner, G. and Richards, M. P. (2007). Stable isotope evidence for 1500 years of human diet at the city of York, UK. *American Journal of Physical Anthropology*, 133 (1), pp. 682–697.

Murphy, C., Thompson, G. and Fuller, D. Q. (2013). Roman food refuse: urban archaeobotany in Pompeii, Regio VI, Insula 1. *Vegetation History and Archaeobotany*, 22 (5), pp. 409–419.

Naito, Y. I., Chikaraishi, Y., Drucker, D. G., Ohkouchi, N., Semal, P., Wißing, C. and Bocherens, H. (2016). Ecological niche of Neanderthals from Spy Cave revealed by nitrogen isotopes of individual amino acids in collagen. *Journal of Human Evolution*, 93, pp. 82–90.

Naito, Y. I., Chikaraishi, Y., Ohkouchi, N., Mukai, H., Shibata, Y., Honch, N. V., Dodo, Y., Ishida, H., Amano, T., Ono, H. and Yoneda, M. (2010a). Dietary reconstruction of the Okhotsk Culture of Hokkaido, Japan, based on nitrogen composition of amino acids: implications for correction of ^{14}C marine reservoir effects on human bones. *Radiocarbon*, 52 (2), pp. 671–681.

Naito, Y. I., Honch, N. V., Chikaraishi, Y., Ohkouchi, N. and Yoneda, M. (2010b). Quantitative evaluation of marine protein contribution in ancient diets based on nitrogen isotope ratios of individual amino acids in bone collagen: an investigation at the Kitakogane Jomon site. *American Journal of Physical Anthropology*, 143 (1), pp. 31–40.

Nielsen, J. M., Popp, B. N. and Winder, M. (2015). Meta-analysis of amino acid stable nitrogen isotope ratios for estimating trophic position in marine organisms. *Oecologia*, 178 (3), pp. 631–642.

Nier, A. O. (1940). A mass spectrometer for routine isotope abundance measurements. *Review of Scientific Instruments*, 11 (7), pp. 212–216.

Nier, A. O. and Gulbransen, E. A. (1939). Variations in the relative abundance of the carbon isotopes. *Journal of the American Chemical Society*, 61 (3), pp. 697–698.

Nitsch, E., Charles, M. and Bogaard, A. (2015). Calculating a statistically robust $\delta^{13}C$ and $\delta^{15}N$ offset for charred cereal and pulse seeds. *STAR: Science & Technology of Archaeological Research*, 1 (1), pp. 1–8.

O'Connell, T. (2017). 'Trophic' and 'source' amino acids in trophic estimation: a likely metabolic explanation. *Oecologia*, 184 (2), pp. 317–326.

O'Connell, T. C., Ballantyne, R. M., Hamilton-Dyer, S., Margaritis, E., Oxford, S., Pantano, W., Millett, M. and Keay, S. J. (2019). Living and dying at the Portus Romae. *Antiquity*, 93 (369), pp. 719–734.

O'Connell, T. C. and Collins, M. J. (2018). Comment on" Ecological niche of Neanderthals from Spy Cave revealed by nitrogen isotopes of individual amino acids in collagen"[J. Hum. Evol. 93 (2016) 82-90]. *Journal of Human Evolution*, 117, pp. 53–55.

O'Connell, T. C., Kneale, C. J., Tasevska, N. and Kuhnle, G. G. (2012). The diet-body offset in human nitrogen isotopic values: A controlled dietary study. *American Journal of Physical Anthropoly*, 149 (3), pp. 426–434.

Ohkouchi, N., Chikaraishi, Y., Close, H. G., Fry, B., Larsen, T., Madigan, D. J., McCarthy, M. D., McMahon, K. W., Nagata, T., Naito, Y. I., Ogawa, N. O., Popp, B. N., Steffan, S., Takano, Y., Tayasu, I., Wyatt, A. S. J., Yamaguchi, Y. T. and Yokoyama, Y. (2017). Advances in the application of amino acid nitrogen isotopic analysis in ecological and biogeochemical studies. *Organic Geochemistry*, 113, pp. 150–174.

Olcese, G. (2017). Wine and amphorae in Campania in the Hellenistic age: the case of Ischia. In: *The Economic Integration of Roman Italy*, Leiden-Boston: Brill, pp. 299–321.

Ottaway, P. (2004). *Roman York*. Cheltenham: Tempus Stroud.

Ottaway, P. (2011). Roman York, from the Core to the Periphery: an Introduction to the Big Picture. In: *Proceedings of the world class heritage conference, 2011*, PJO Archaeology.

Pagano, M. (1987). Una iscrizione elettorale da Ercolano. *Cronache ercolanesi*, 17, pp. 151–152.

Pang, P. C. and Nriagu, J. O. (1977). Isotopic variations of the nitrogen in Lake Superior. *Geochimica et Cosmochimica Acta*, 41 (6), pp. 811–814.

Pantoja, S., Repeta, D. J., Sachs, J. P. and Sigman, D. M. (2002). Stable isotope constraints on the nitrogen cycle of the Mediterranean Sea water column. *Deep Sea Research Part I: Oceanographic Research Papers*, 49 (9), pp. 1609–1621.

Paolini, M., Ziller, L., Laursen, K. H., Husted, S. and Camin, F. (2015). Compound-specific $\delta^{15}N$ and $\delta^{13}C$ analyses of amino acids for potential discrimination between organically and conventionally grown wheat. *Journal of Agricultural and Food Chemistry*, 63 (25), pp. 5841–5850.

Park, R. and Epstein, S. (1961). Metabolic fractionation of ^{13}C & ^{12}C in plants. *Plant Physiology*, 36 (2), p. 133.

Parnell, A. C., Inger, R., Bearhop, S. and Jackson, A. L. (2010). Source partitioning using stable isotopes: coping with too much variation. *PloS One*, 5 (3).

Passey, B. H., Robinson, T. F., Ayliffe, L. K., Cerling, T. E., Sponheimer, M., Dearing, M. D., Roeder, B. L. and Ehleringer, J. R. (2005). Carbon isotope fractionation between diet, breath CO_2, and bioapatite in different mammals. *Journal of Archaeological Science*, 32 (10), pp. 1459–1470.

Pate, F. D., Henneberg, R. J. and Henneberg, M. (2016). Stable carbon and nitrogen isotope evidence for dietary variability at ancient Pompeii, Italy. *Mediterranean Archaeology & Archaeometry*, 16 (1).

Pateiro, M., Munekata, P. E., Domínguez, R., Wang, M., Barba, F. J., Bermúdez, R. and Lorenzo, J. M. (2020). Nutritional profiling and the value of processing by-products from gilthead sea bream (*Sparus aurata*). *Marine Drugs*, 18 (2), p. 101.

Paterson, J. (2005). Trade and traders in the Roman world: scale, structure, and organisation. In: H. Parkins and C. Smith (Eds.), *Trade, traders and the ancient city*, Routledge, pp. 145–163.

Pauly, D. and Zeller, D. (2016). Catch reconstructions reveal that global marine fisheries catches are higher than reported and declining. *Nature Communications*, 7 (1), pp. 1–9.

Pellegrini, M. and Snoeck, C. (2016). Comparing bioapatite carbonate pre-treatments for isotopic measurements: Part 2—Impact on carbon and oxygen isotope compositions. *Chemical Geology*, 420, pp. 88–96.

Penkman, K. (2005). *Amino acid geochronology: a closed system approach to test and refine the UK model*. Ph.D. thesis, University of Newcastle upon Tyne.

Penkman, K., Kaufman, D. S., Maddy, D. and Collins, M. (2008). Closed-system behaviour of the intra-crystalline fraction of amino acids in mollusc shells. *Quaternary Geochronology*, 3 (1-2), pp. 2–25.

Peres, T. M. (2010). Methodological issues in zooarchaeology. In: *Integrating Zooarchaeology and Paleoethnobotany*, New York: Springer, pp. 15–36.

Perret, S., Merle, C., Bernocco, S., Berland, P., Garrone, R., Hulmes, D. J., Theisen, M. and Ruggiero, F. (2001). Unhydroxylated triple helical collagen I produced in transgenic plants provides new clues on the role of hydroxyproline in collagen folding and fibril formation. *Journal of Biological Chemistry*, 276 (47), pp. 43693–43698.

Peterson, B. J. and Fry, B. (1987). Stable isotopes in ecosystem studies. *Annual review of ecology and systematics*, 18 (1), pp. 293–320.

Petrone, P. (2019). The Herculaneum victims of the 79 AD Vesuvius eruption: a review. *Journal of Anthropological Sciences*, 97, pp. 69–89.

Petrone, P., Giordano, M., Giustino, S. and Guarino, F. M. (2011). Enduring fluoride health hazard for the Vesuvius area population: the case of AD 79 Herculaneum. *PloS One*, 6 (6).

Petrone, P., Graziano, V., Sastri, C., Sauvage, T., Mezzasalma, M., Paternoster, M. and Guarino, F. M. (2019). Dental fluorosis in the Vesuvius towns in AD 79: a multidisciplinary approach. *Annals of human biology*, 46 (5), pp. 388–392.

Petrone, P., Pucci, P., Vergara, A., Amoresano, A., Birolo, L., Pane, F., Sirano, F., Niola, M., Buccelli, C. and Graziano, V. (2018). A hypothesis of sudden body fluid vaporization in the 79 AD victims of Vesuvius. *PloS One*, 13 (9).

Petrone, P. P. (2011). Human corpses as time capsules: new perspectives in the study of past mass disasters. *Journal of Anthropological Sciences*, 89, pp. 3–6.

Philben, M., Billings, S. A., Edwards, K. A., Podrebarac, F. A., van Biesen, G. and Ziegler, S. E. (2018). Amino acid $\delta^{15}N$ indicates lack of N isotope fractionation during soil organic nitrogen decomposition. *Biogeochemistry*, 138 (1), pp. 69–83.

Phillips, D. L. (2001). Mixing models in analyses of diet using multiple stable isotopes: a critique. *Oecologia*, 127 (2), pp. 166–170.

Phillips, D. L. and Gregg, J. W. (2003). Source partitioning using stable isotopes: coping with too many sources. *Oecologia*, 136 (2), pp. 261–269.

Phillips, D. L. and Koch, P. L. (2002). Incorporating concentration dependence in stable isotope mixing models. *Oecologia*, 130 (1), pp. 114–125.

Pinhasi, R. and Bourbou, C. (2007). How representative are human skeletal assemblages for population analysis? *Advances in Human Palaeopathology*, pp. 31–44.

Pinhasi, R., Fernandes, D., Sirak, K., Novak, M., Connell, S., Alpaslan-Roodenberg, S., Gerritsen, F., Moiseyev, V., Gromov, A., Raczky, P., Anders, A., Pietrusewsky, M., Rollefson, G., Jovanovic, M., Trinhhoang, H., Bar-Oz, G., Oxenham, M., Matsumura, H. and Hofreiter, M. (2015). Optimal ancient DNA yields from the inner ear part of the human petrous bone. *PloS One*, 10 (6).

Privat, K. L., O'connell, T. C. and Richards, M. P. (2002). Stable isotope analysis of human and faunal remains from the Anglo-Saxon cemetery at Berinsfield, Oxfordshire: dietary and social implications. *Journal of Archaeological Science*, 29 (7), pp. 779–790.

Prowse, T., Schwarcz, H. P., Saunders, S., Macchiarelli, R. and Bondioli, L. (2004). Isotopic paleodiet studies of skeletons from the Imperial Roman-age cemetery of Isola Sacra, Rome, Italy. *Journal of Archaeological Science*, 31 (3), pp. 259–272.

Prowse, T. L. (2001). *Isotopic and dental evidence for diet from the necropolis of Isola Sacra (1^{st}–3^{rd} centuries AD), Italy.* Ph.D. thesis, University of Alberta.

Prowse, T. L., Schwarcz, H. P., Saunders, S. R., Macchiarelli, R. and Bondioli, L. (2005). Isotopic evidence for age-related variation in diet from Isola Sacra, Italy. *American Journal of Physical Anthropology*, 128 (1), pp. 2–13.

Radvanyi, P. and Villain, J. (2017). The discovery of radioactivity. *Comptes Rendus Physique*, 18 (9–10), pp. 544–550.

Reimer, P. and McCormac, F. (2002). Marine radiocarbon reservoir corrections for the Mediterranean and Aegean Seas. *Radiocarbon*, 44 (1), pp. 159–166.

Reynard, L., Henderson, G. and Hedges, R. (2010). Calcium isotope ratios in animal and human bone. *Geochimica et Cosmochimica Acta*, 74 (13), pp. 3735–3750.

Reynard, L., Pearson, J., Henderson, G. and Hedges, R. (2013). Calcium isotopes in juvenile milk-consumers. *Archaeometry*, 55 (5), pp. 946–957.

Reynard, L. M. and Hedges, R. E. (2008). Stable hydrogen isotopes of bone collagen in palaeodietary and palaeoenvironmental reconstruction. *Journal of Archaeological Science*, 35 (7), pp. 1934–1942.

Reynard, L. M., Henderson, G. M. and Hedges, R. E. (2011). Calcium isotopes in archaeological bones and their relationship to dairy consumption. *Journal of Archaeological Science*, 38 (3), pp. 657–664.

Reynard, L. M., Meltzer, D. J., Emslie, S. D. and Tuross, N. (2015). Stable isotopes in yellow-bellied marmot (*Marmota flaviventris*) fossils reveal environmental stability in the late Quaternary of the Colorado Rocky Mountains. *Quaternary Research*, 83 (2), pp. 345–354.

Reynard, L. M., Ryan, S. E., Guirguis, M., Contreras-Martínez, M., Pompianu, E., Ramis, D., van Dommelen, P. and Tuross, N. (2020). Mediterranean precipitation isoscape preserved in bone collagen δ 2 H. *Scientific reports*, 10 (1), pp. 1–6.

Ricci, P., Sirignano, C., Altieri, S., Pistillo, M., Santoriello, A. and Lubritto, C. (2016). Paestum dietary habits during the Imperial period: archaeological records and stable isotope measurement. *Acta Imeko*, 5 (2), pp. 26–32.

Richards, M. P., Fuller, B. T., Sponheimer, M., Robinson, T. and Ayliffe, L. (2003). Sulphur isotopes in palaeodietary studies: a review and results from a controlled feeding experiment. *International Journal of Osteoarchaeology*, 13 (1-2), pp. 37–45.

Richards, M. P. and Trinkaus, E. (2009). Isotopic evidence for the diets of European Neanderthals and early modern humans. *Proceedings of the National Academy of Sciences*, 106 (38), pp. 16034–16039.

Richter, K. K., McGrath, K., Masson-MacLean, E., Hickinbotham, S., Tedder, A., Britton, K., Bottomley, Z., Dobney, K., Hulme-Beaman, A., Zona, M., Fischer, R., Collins, M. J. and Speller, C. F. (2020). What's the catch? Archaeological application of rapid collagen-based species identification for Pacific Salmon. *Journal of Archaeological Science*, 116.

Richter, K. K., Wilson, J., Jones, A. K., Buckley, M., van Doorn, N. and Collins, M. J. (2011). Fish'n chips: ZooMS peptide mass fingerprinting in a 96 well plate format to identify fish bone fragments. *Journal of Archaeological Science*, 38 (7), pp. 1502–1510.

Rissech, C., Pujol, A., Christie, N., Lloveras, L., Richards, M. P. and Fuller, B. T. (2016). Isotopic reconstruction of human diet at the Roman site (1^{st}-4^{th} c. AD) of Carrer Ample 1, Barcelona, Spain. *Journal of Archaeological Science: Reports*, 9, pp. 366–374.

Roberts, P., Fernandes, R., Craig, O. E., Larsen, T., Lucquin, A., Swift, J. and Zech, J. (2017). Calling all archaeologists: guidelines for terminology, methodology, data handling, and reporting when undertaking and reviewing stable isotope applications in archaeology. *Rapid Communications in Mass Spectrometry*, 32 (5), pp. 361–372.

Robinson, M. and Rowan, E. (2015). Roman food remains in archaeology and the contents of a Roman sewer at Herculaneum. In: *A companion to food in the ancient world*, Oxford: Wiley Blackwell, volume 89, pp. 105–116.

Roffet-Salque, M., Dunne, J., Altoft, D. T., Casanova, E., Cramp, L. J., Smyth, J., Whelton, H. L. and Evershed, R. P. (2017). From the inside out: Upscaling organic residue analyses of archaeological ceramics. *Journal of Archaeological Science: Reports*, 16, pp. 627–640.

Rolandi, G., Paone, A., Di Lascio, M. and Stefani, G. (2008). The 79 AD eruption of Somma: The relationship between the date of the eruption and the southeast tephra dispersion. *Journal of Volcanology and Geothermal Research*, 169 (1-2), pp. 87–98.

Roper, A. C. (2019). *Seeds Glorious Seeds: Analysis of modern, charred, experimentally degraded and archaeological seeds*. Master's thesis, University of York.

Rowan, E. (2014). *Roman diet and nutrition in the Vesuvian region: a study of the bioarchaeological remains from the Cardo V sewer at Herculaneum*. Ph.D. thesis, Oxford University, UK.

Rowan, E. (2015). Olive oil pressing waste as a fuel source in antiquity. *American Journal of Archaeology*, 119 (4), pp. 465–482.

Rowan, E. (2017a). Bioarchaeological preservation and non-elite diet in the Bay of Naples: An analysis of the food remains from the Cardo V sewer at the Roman site of Herculaneum. *Environmental Archaeology*, 22 (3), pp. 318–336.

Rowan, E. (2017b). Sewers, Archaeobotany, and Diet at Pompeii and Herculaneum. In: *The Economy of Pompeii*, Oxford: Oxford University Press, pp. 111–133.

Sackett, W. M., Eckelmann, W. R., Bender, M. L. and Bé, A. W. (1965). Temperature dependence of carbon isotope composition in marine plankton and sediments. *Science*, 148 (3667), pp. 235–237.

Sadori, L., Allevato, E., Bellini, C., Bertacchi, A., Boetto, G., Di Pasquale, G., Giachi, G., Giardini, M., Masi, A., Pepe, C., Rullo Ermolli, E. and Lippi, M. M. (2015). Archaeobotany in Italian ancient Roman harbours. *Review of Palaeobotany and Palynology*, 218, pp. 217–230.

Sadori, L., Giardini, M. and Susanna, F. (2010). The plant landscape as inferred from a basket of the Roman town of Privernum (Latium, central Italy). *Plant Biosystems*, 144 (4), pp. 874–887.

Salesse, K., Dufour, É., Balter, V., Tykot, R. H., Maaranen, N., Rivollat, M., Kharobi, A., Deguilloux, M.-F., Pemonge, M.-H., Brůžek, J. and Castex, D. (2021). Far from home: A multi-analytical approach revealing the journey of an African-born individual to imperial Rome. *Journal of Archaeological Science: Reports*, 37.

Saller, R. (2008). Status and Patronage. In: A. K. Bowman, P. Garnsey and D. Rathbone (Eds.), *The High Empire, AD 70–192*, Cambridge: Cambridge University Press, The Cambridge Ancient History, pp. 817–854.

Santamato, E. (2014). Per una interpretazione dei graffiti privati e dell'economia quotidiana a Pompei (con particolare riguardo alle liste di prezzi). *Ancient Society*, pp. 307–341.

Sayle, K. L., Brodie, C. R., Cook, G. T. and Hamilton, W. D. (2019). Sequential measurement of $\delta^{15}N$, $\delta^{13}C$ and $\delta^{34}S$ values in archaeological bone collagen at the Scottish Universities Environmental Research Centre (SUERC): a new analytical frontier. *Rapid Communications in Mass Spectrometry*, 33 (15), pp. 1258–1266.

Scheidel, W. (2004). Human mobility in Roman Italy, I: the free population. *The Journal of Roman Studies*, 94, pp. 1–26.

Scheidel, W. (2008). Roman population size: the logic of the debate. In: *People, land, and politics: demographic developments and the transformation of Roman Italy*, Leiden-Boston: Brill, pp. 17–70.

Schmidt, C. W., Oakley, E., D'Anastasio, R., Brower, R., Remy, A. and Viciano, J. (2015). Herculaneum. In: *The analysis of burned human remains*, Cambridge Massachusetts: Academic Press, pp. 149–161.

Schoeninger, M. J. and DeNiro, M. J. (1984). Nitrogen and carbon isotopic composition of bone collagen from marine and terrestrial animals. *Geochimica et Cosmochimica Acta*, 48 (4), pp. 625–639.

Schwarcz, H. P. (2002). Some biochemical aspects of carbon isotopic paleodiet studies. In: *Biogeochemical approaches to paleodietary analysis*, New York: Springer, volume 5, pp. 189–209.

Scott, G. R. and Poulson, S. R. (2012). Stable carbon and nitrogen isotopes of human dental calculus: a potentially new non-destructive proxy for paleodietary analysis. *Journal of Archaeological Science*, 39 (5), pp. 1388–1393.

Sealy, J., Johnson, M., Richards, M. and Nehlich, O. (2014). Comparison of two methods of extracting bone collagen for stable carbon and nitrogen isotope analysis: comparing whole bone demineralization with gelatinization and ultrafiltration. *Journal of Archaeological Science*, 47, pp. 64–69.

Sealy, J. C., Van Der Merwe, N. J., Thorp, J. A. L. and Lanham, J. L. (1987). Nitrogen isotopic ecology in southern Africa: implications for environmental and dietary tracing. *Geochimica et Cosmochimica Acta*, 51 (10), pp. 2707–2717.

Segrè, A. (1950). Note sulla storia dei cereali nell'antichità. *Aegyptus*, 30 (2), pp. 161–197.

Shaw, B. D. (1996). Seasons of death: aspects of mortality in imperial Rome. *The Journal of Roman Studies*, 86, pp. 100–138.

Shoulders, M. D. and Raines, R. T. (2009). Collagen structure and stability. *Annual review of biochemistry*, 78, pp. 929–958.

Sigurdsson, H., Cashdollar, S. and Sparks, S. R. (1982). The eruption of Vesuvius in AD 79: reconstruction from historical and volcanological evidence. *American Journal of Archaeology*, pp. 39–51.

Smith, B. N. and Epstein, S. (1970). Biogeochemistry of the stable isotopes of hydrogen and carbon in salt marsh biota. *Plant Physiology*, 46 (5), pp. 738–742.

Smith, C. I., Fuller, B. T., Choy, K. and Richards, M. P. (2009). A three-phase liquid chromatographic method for $\delta^{13}C$ analysis of amino acids from biological protein hydrolysates using liquid chromatography–isotope ratio mass spectrometry. *Analytical biochemistry*, 390 (2), pp. 165–172.

Soddy, F. (1913). The radio-elements and the periodic law. *Nature*, 91, pp. 57–58.

Spangenberg, J. E. and Ogrinc, N. (2001). Authentication of vegetable oils by bulk and molecular carbon isotope analyses with emphasis on olive oil and pumpkin seed oil. *Journal of Agricultural and Food Chemistry*, 49 (3), pp. 1534–1540.

Sperduti, A., Bondioli, L., Craig, O. E., Prowse, T. and Garnsey, P. (2018). Bones, teeth, and history. In: *The science of Roman history: Biology, climate, and the future of the past*, New Jersey: Princeton University Press, pp. 123–173.

Spurr, M. S. (1986). *Arable cultivation in Roman Italy, c. 200 BC-AD 100*. 3, Society for the promotion of Roman studies.

Steele, V. J., Stern, B. and Stott, A. W. (2010). Olive oil or lard?: distinguishing plant oils from animal fats in the archeological record of the eastern Mediterranean using gas chromatography/combustion/isotope ratio mass spectrometry. *Rapid communications in Mass spectrometry*, 24 (23), pp. 3478–3484.

Stewart, J. R., Allen, R. B., Jones, A. K., Penkman, K. E. and Collins, M. J. (2013). ZooMS: making eggshell visible in the archaeological record. *Journal of Archaeological Science*, 40 (4), pp. 1797–1804.

Stock, B. and Semmens, B. (2017). MixSIAR GUI user manual v3. 1.

Stock, B. C., Jackson, A. L., Ward, E. J., Parnell, A. C., Phillips, D. L. and Semmens, B. X. (2018). Analyzing mixing systems using a new generation of Bayesian tracer mixing models. *PeerJ*, 6.

Strohalm, M., Kavan, D., Novak, P., Volny, M. and Havlicek, V. (2010). mMass 3: a cross-platform software environment for precise analysis of mass spectrometric data. *Analytical chemistry*, 82 (11), pp. 4648–4651.

Styring, A. K. (2012). *Crop $\delta^{15}N$ value expression in bone collagen of ancient fauna and humans: a new approach to palaeodietary and agricultural reconstruction*. Ph.D. thesis, University of Bristol.

Styring, A. K., Fraser, R. A., Arbogast, R.-M., Halstead, P., Isaakidou, V., Pearson, J. A., Schäfer, M., Triantaphyllou, S., Valamoti, S. M., Wallace, M. *et al.* (2015). Refining human palaeodietary reconstruction using amino acid $\delta^{15}N$ values of plants, animals and humans. *Journal of Archaeological Science*, 53, pp. 504–515.

Styring, A. K., Fraser, R. A., Bogaard, A. and Evershed, R. P. (2014a). Cereal grain, rachis and pulse seed amino acid $\delta^{15}N$ values as indicators of plant nitrogen metabolism. *Phytochemistry*, 97, pp. 20–29.

Styring, A. K., Fraser, R. A., Bogaard, A. and Evershed, R. P. (2014b). The effect of manuring on cereal and pulse amino acid $\delta^{15}N$ values. *Phytochemistry*, 102, pp. 40–45.

Styring, A. K., Kuhl, A., Knowles, T. D., Fraser, R. A., Bogaard, A. and Evershed, R. P. (2012). Practical considerations in the determination of compound-specific amino acid $\delta^{15}N$ values in animal and plant tissues by gas chromatography-combustion-isotope ratio mass spectrometry, following derivatisation to their *N*-acetylisopropyl esters. *Rapid Communications in Mass Spectrometry*, 26 (19), pp. 2328–2334.

Styring, A. K., Manning, H., Fraser, R. A., Wallace, M., Jones, G., Charles, M., Heaton, T. H., Bogaard, A. and Evershed, R. P. (2013). The effect of charring and burial on the biochemical composition of cereal grains: investigating the integrity of archaeological plant material. *Journal of Archaeological Science*, 40 (12), pp. 4767–4779.

Styring, A. K., Sealy, J. C. and Evershed, R. P. (2010). Resolving the bulk $\delta^{15}N$ values of ancient human and animal bone collagen via compound-specific nitrogen isotope analysis of constituent amino acids. *Geochimica et Cosmochimica Acta*, 74 (1), pp. 241–251.

Surovell, T. A. (2000). Radiocarbon dating of bone apatite by step heating. *Geoarchaeology*, 15 (6), pp. 591–608.

Szpak, P. (2014). Complexities of nitrogen isotope biogeochemistry in plant-soil systems: implications for the study of ancient agricultural and animal management practices. *Frontiers in plant science*, 5, p. 288.

Tacail, T., Martin, J. E., Herrscher, E., Albalat, E., Verna, C., Ramirez-Rozzi, F., Clark, G., Valentin, F. and Balter, V. (2021). Quantifying the evolution of animal dairy intake in humans using calcium isotopes. *Quaternary Science Reviews*, 256.

Tacoma, L. E. (2017). Bones, Stones, and Monica: Isola Sacra Revisited. In: E. Lo Cascio, L. E. Tacoma and M. J. Groen-Vallinga (Eds.), *The Impact of Mobility and Migration in the Roman Empire*, Leiden: Brill, pp. 132–154.

Tafuri, M. A., Goude, G. and Manzi, G. (2018). Isotopic evidence of diet variation at the transition between classical and post-classical times in Central Italy. *Journal of Archaeological Science: Reports*, 21, pp. 496–503.

Takano, Y., Kashiyama, Y., Ogawa, N. O., Chikaraishi, Y. and Ohkouchi, N. (2010). Isolation and desalting with cation-exchange chromatography for compound-specific nitrogen isotope analysis of amino acids: application to biogeochemical samples. *Rapid Communications in Mass Spectrometry*, 24 (16), pp. 2317–2323.

Tchernia, A. (2016). *The Romans and Trade*. Oxford: Oxford University Press.

Thoennessen, M. (2016). *The Discovery of Isotopes*. New York: Springer.

Thomas, R. and Wilson, A. (1994). Water supply for Roman farms in Latium and South Etruria1. *Papers of the British School at Rome*, 62, pp. 139–196.

Thurmond, D. (2006). *A handbook of food processing in classical Rome: for her bounty no winter*. Leiden: Brill.

Tieszen, L. L. (1991). Natural variations in the carbon isotope values of plants: implications for archaeology, ecology, and paleoecology. *Journal of Archaeological Science*, 18 (3), pp. 227–248.

Tieszen, L. L. and Fagre, T. (1993). Effect of diet quality and composition on the isotopic composition of respiratory CO_2, bone collagen, bioapatite, and soft tissues. In: *Prehistoric human bone*, New York: Springer, pp. 121–155.

Tomlinson, P. (1989). Plant remains from 5 Rougier Street, York. *Ancient Monuments Laboratory Report*, 57.

Torino, M. and Fornaciari, G. (1993). Analisi dei resti umani dei fornici 7 e 8 sulla marina di Ercolano. *Rivista di Studi Pompeiani*, 6, pp. 187–195.

Torino, M. and Fornaciari, G. (1995). Indagine paleodemografica su un campione di popolazione dell'antica Ercolano all'epoca dell'eruzione vesuviana del 79 dC. *Archivio per l'Antropologia e la Etnologia*, 125, pp. 99–112.

Trentacoste, A. (2020). Fodder for change: animals, urbanisation, and socio-economic transformation in protohistoric Italy. *Theoretical Roman Archaeology Journal*, 3 (1).

Trentacoste, A., Lightfoot, E., Le Roux, P., Buckley, M., Kansa, S., Esposito, C. and Gleba, M. (2020). Heading for the hills? A multi-isotope study of sheep management in first-millennium BC Italy. *Journal of Archaeological Science: Reports*, 29.

Trentacoste, A., Nieto-Espinet, A., Guimarães, S., Wilkens, B., Petrucci, G. and Valenzuela-Lamas, S. (2021). New trajectories or accelerating change? Zooarchaeological evidence for Roman transformation of animal husbandry in Northern Italy. *Archaeological and Anthropological Sciences*, 13 (1), pp. 1–22.

Tsutaya, T. and Yoneda, M. (2013). Quantitative reconstruction of weaning ages in archaeological human populations using bone collagen nitrogen isotope ratios and approximate Bayesian computation. *PloS One*, 8 (8).

Tuross, N., Fogel, M. L. and Hare, P. (1988). Variability in the preservation of the isotopic composition of collagen from fossil bone. *Geochimica et Cosmochimica Acta*, 52 (4), pp. 929–935.

Tuross, N., Reynard, L. M., Harvey, E., Coppa, A. and McCormick, M. (2017). Human skeletal development and feeding behavior: the impact on oxygen isotopes. *Archaeological and Anthropological Sciences*, 9 (7), pp. 1453–1459.

Valenzuela, A., Baker, K., Carden, R. F., Evans, J., Higham, T., Hoelzel, A. R., Lamb, A., Madgwick, R., Miller, H., Alcover, J. A., Cau, M. A. and Sykes, N. (2016). Both introduced and extinct: the fallow deer of Roman Mallorca. *Journal of Archaeological Science: Reports*, 9, pp. 168–177.

Van der Merwe, N. J. (1982). Carbon isotopes, photosynthesis, and archaeology: Different pathways of photosynthesis cause characteristic changes in carbon isotope ratios that make possible the study of prehistoric human diets. *American scientist*, 70 (6), pp. 596–606.

Van der Merwe, N. J. and Vogel, J. C. (1978). ^{13}C content of human collagen as a measure of prehistoric diet in woodland North America. *Nature*, 276, pp. 815–816.

van der Veen, M. (2018). Archaeobotany: the archaeology of human-plant interactions. In: *The science of Roman history: Biology, climate, and the future of the past*, New Jersey: Princeton University Press, pp. 53–94.

Van Klinken, G. J. (1999). Bone collagen quality indicators for palaeodietary and radiocarbon measurements. *Journal of Archaeological Science*, 26 (6), pp. 687–695.

Van Neer, W. and De Cupere, B. (1993). First archaeozoological results from the Hellenistic-Roman site of Sagalassos. In: *Sagalassos I. First general report on the survey (1986–1989) and excavations (1990–1991)*, Leuven: Leuven University Press, volume 5 of *Acta Archaeologica Lovaniensia Monographiae*, pp. 225–238.

Veit, G., Kobbe, B., Keene, D. R., Paulsson, M., Koch, M. and Wagener, R. (2006). Collagen XXVIII, a novel von Willebrand factor A domain-containing protein with many imperfections in the collagenous domain. *Journal of Biological Chemistry*, 281 (6), pp. 3494–3504.

Verboven, K. (2012). The freedman economy of Roman Italy. In: *Free at Last! The Influence of Freed Slaves on the Roman Empire*, London: Bristol Classical Press, pp. 88–109.

Viciano, J., Alemán, I., D'Anastasio, R., Capasso, L. and Botella, M. C. (2011). Odontometric sex discrimination in the Herculaneum sample (79 AD, Naples, Italy), with application to juveniles. *American Journal of Physical Anthropology*, 145 (1), pp. 97–106.

Vika, E. and Theodoropoulou, T. (2012). Re-investigating fish consumption in Greek antiquity: results from $\delta^{13}C$ and $\delta^{15}N$ analysis from fish bone collagen. *Journal of Archaeological Science*, 39 (5), pp. 1618–1627.

Vizzini, S., Savona, B., Do Chi, T. and Mazzola, A. (2005). Spatial variability of stable carbon and nitrogen isotope ratios in a Mediterranean coastal lagoon. *Hydrobiologia*, 550 (1), pp. 73–82.

Wada, E., Kadonaga, T. and Matsuo, S. (1975). ^{15}N abundance in nitrogen of naturally occurring substances and global assessment of denitrification from isotopic viewpoint. *Geochemical Journal*, 9 (3), pp. 139–148.

Wagner, I. and Musso, H. (1983). New naturally occurring amino acids. *Angewandte Chemie International Edition in English*, 22 (11), pp. 816–828.

Wallace-Hadrill, A. (1994). *Houses and society in Pompeii and Herculaneum*. Princeton New Jersey: Princeton University Press.

Wallace-Hadrill, A. (2008). *Rome's cultural revolution*, volume 10. Cambridge: Cambridge University Press.

Wallace-Hadrill, A. (2011). *Herculaneum: past and future*. London: Frances Lincoln Ltd.

Warinner, C. and Tuross, N. (2009). Alkaline cooking and stable isotope tissue-diet spacing in swine: archaeological implications. *Journal of Archaeological Science*, 36 (8), pp. 1690–1697.

Warinner, C. and Tuross, N. (2010). Brief communication: Tissue isotopic enrichment associated with growth depression in a pig: Implications for archaeology and ecology. *American Journal of Physical Anthropology*, 141 (3), pp. 486–493.

Webb, E. C., Honch, N. V., Dunn, P. J., Linderholm, A., Eriksson, G., Lidén, K. and Evershed, R. P. (2016a). Compound-specific amino acid isotopic proxies for distinguishing between terrestrial and aquatic resource consumption. *Archaeological and Anthropological Sciences*, 10 (1), pp. 1–18.

Webb, E. C., Lewis, J., Shain, A., Kastrisianaki-Guyton, E., Honch, N. V., Stewart, A., Miller, B., Tarlton, J. and Evershed, R. P. (2017). The influence of varying proportions of terrestrial and marine dietary protein on the stable carbon-isotope compositions of pig tissues from a controlled feeding experiment. *STAR: Science & Technology of Archaeological Research*, 3 (1), pp. 28–44.

Webb, E. C., Stewart, A., Miller, B., Tarlton, J. and Evershed, R. P. (2016b). Age effects and the influence of varying proportions of terrestrial and marine dietary protein on the stable nitrogen-isotope compositions of pig bone collagen and soft tissues from a controlled feeding experiment. *STAR: Science & Technology of Archaeological Research*, 2 (1), pp. 54–66.

Welker, F., Soressi, M., Rendu, W., Hublin, J.-J. and Collins, M. (2015). Using ZooMS to identify fragmentary bone from the late Middle/Early Upper Palaeolithic sequence of Les Cottés, France. *Journal of Archaeological Science*, 54, pp. 279–286.

Wilson, R. (2000). Campanaio—an agricultural settlement in Roman Sicily. *Antiquity*, 74 (284), pp. 289–290.

Wood, J. W., Milner, G. R., Harpending, H. C., Weiss, K. M., Cohen, M. N., Eisenberg, L. E., Hutchinson, D. L., Jankauskas, R., Cesnys, G., Česnys, G. *et al.* (1992). The osteological paradox: problems of inferring prehistoric health from skeletal samples [and comments and reply]. *Current anthropology*, 33 (4), pp. 343–370.

Wright, P. J. (2010). Methodological issues in paleoethnobotany: a consideration of issues, methods, and cases. In: *Integrating Zooarchaeology and Paleoethnobotany*, Springer, pp. 37–64.

Yarnes, C. T. and Herszage, J. (2017). The relative influence of derivatization and normalization procedures on the compound-specific stable isotope analysis of nitrogen in amino acids. *Rapid Communications in Mass Spectrometry*, 31 (8), pp. 693–704.

Yoshinaga, J., Minagawa, M., Suzuki, T., Ohtsuka, R., Kawabe, T., Inaoka, T. and Akimichi, T. (1996). Stable carbon and nitrogen isotopic composition of diet and hair of Gidra-speaking Papuans. *American Journal of Physical Anthropology*, 100 (1), pp. 23–34.

Young, S. M. (2003). *Metabolic mechanisms and the isotopic investigation of ancient diets with an application to human remains from Cuello, Belize.* Ph.D. thesis, Department of Anthropology, Harvard University.

Appendix A

Carbon and Nitrogen stable isotope studies from the Roman Mediterranean

This appendix presents carbon and nitrogen stable isotope data collected from published studies on Imperial Roman populations from the Mediterranean basin and discussed in chapter 3 section 3.1.3.

Site	**Sex**	$\delta^{13}C$	$\delta^{15}N$	**Publication**
AN	ND	-18.57	10.93	Prowse et al. 2004; 2005
AN	ND	-19.2	11.11	Prowse et al. 2004; 2005
AN	ND	-19.58	9.35	Prowse et al. 2004; 2005
AN	ND	-19.89	8.89	Prowse et al. 2004; 2005
AN	ND	-19.09	9.08	Prowse et al. 2004; 2005
AN	ND	-19.07	10.71	Prowse et al. 2004; 2005
AN	ND	-19.9	6.9	Prowse et al. 2004; 2005
AN	ND	-19.9	7.9	Prowse et al. 2004; 2005
AN	ND	-19.5	8.6	Prowse et al. 2004; 2005
AN	ND	-19.3	10.8	Prowse et al. 2004; 2005
AN	ND	-19	11	Prowse et al. 2004; 2005
AN	ND	-19.6	6.9	Prowse et al. 2004; 2005
AN	ND	-19	11.3	Prowse et al. 2004; 2005
AN	ND	-19.2	11.1	Prowse et al. 2004; 2005
At	F	-19.3	10.5	Lagia 2015
At	M	-19	9.9	Lagia 2015
At	M	-19.8	4	Lagia 2015
At	M	-18.8	9.6	Lagia 2015
At	M	-18.9	9.7	Lagia 2015
At	M	-19.3	9.8	Lagia 2015
At	M	-18.8	10.5	Lagia 2015
At	M	-18.7	10.7	Lagia 2015
At	ND	-18.8	10.2	Lagia 2015
Ba	F	-19.1	10.4	Rissech et al. 2016
Ba	F	-19	11.1	Rissech et al. 2016

Ba	F	-18.8	11.4	Rissech et al. 2016
Ba	F	-19.2	11.6	Rissech et al. 2016
Ba	F	-19.1	10.8	Rissech et al. 2016
Ba	M	-19	10.6	Rissech et al. 2016
Ba	M	-18.5	10.7	Rissech et al. 2016
Ba	M	-19	10.6	Rissech et al. 2016
Ba	M	-18.5	10.8	Rissech et al. 2016
Ba	M	-18.7	10.9	Rissech et al. 2016
Ba	M	-18.8	11	Rissech et al. 2016
Ba	M	-18.6	11.3	Rissech et al. 2016
Ba	M	-19.3	11.6	Rissech et al. 2016
Ba	M	-19.5	10.7	Rissech et al. 2016
Ba	M	-18.4	11.7	Rissech et al. 2016
CB	F	-19.7	8.6	Killgrove and Tykot 2013; De Angelis et al. 2020a
CB	F	-18.9	11.9	Killgrove and Tykot 2013; De Angelis et al. 2020a
CB	F	-19.6	8.4	Killgrove and Tykot 2013; De Angelis et al. 2020a
CB	F	-18.6	11.9	Killgrove and Tykot 2013; De Angelis et al. 2020a
CB	F	-18.9	11.3	Killgrove and Tykot 2013; De Angelis et al. 2020a
CB	F	-18.9	11.6	Killgrove and Tykot 2013; De Angelis et al. 2020a
CB	F	-18.6	11.3	Killgrove and Tykot 2013; De Angelis et al. 2020a
CB	F	-19.3	9.6	Killgrove and Tykot 2013; De Angelis et al. 2020a
CB	F	-19.3	10.5	Killgrove and Tykot 2013; De Angelis et al. 2020a
CB	F	-20.2	8.3	Killgrove and Tykot 2013; De Angelis et al. 2020a
CB	F	-19.5	11.4	Killgrove and Tykot 2013; De Angelis et al. 2020a
CB	F	-17.6	12.6	Killgrove and Tykot 2013; De Angelis et al. 2020a
CB	F	-18.6	11.1	Killgrove and Tykot 2013; De Angelis et al. 2020a
CB	F	-19.2	10.8	Killgrove and Tykot 2013; De Angelis et al. 2020a
CB	F	-19.1	12.6	Killgrove and Tykot 2013; De Angelis et al. 2020a
CB	F	-18.5	10.2	Killgrove and Tykot 2013; De Angelis et al. 2020a
CB	F	-18.1	9.6	Killgrove and Tykot 2013; De Angelis et al. 2020a
CB	F	-17.4	10.2	Killgrove and Tykot 2013; De Angelis et al. 2020a
CB	F	-18.6	11	Killgrove and Tykot 2013; De Angelis et al. 2020a
CB	F	-18.1	11.2	Killgrove and Tykot 2013; De Angelis et al. 2020a
CB	F	-17.7	11	Killgrove and Tykot 2013; De Angelis et al. 2020a

CB	F	-17.5	9.3	Killgrove and Tykot 2013; De Angelis et al. 2020a
CB	M	-16.5	12.1	Killgrove and Tykot 2013; De Angelis et al. 2020a
CB	M	-18.2	11.1	Killgrove and Tykot 2013; De Angelis et al. 2020a
CB	M	-20	9.3	Killgrove and Tykot 2013; De Angelis et al. 2020a
CB	M	-18.7	11.3	Killgrove and Tykot 2013; De Angelis et al. 2020a
CB	M	-20.4	11.8	Killgrove and Tykot 2013; De Angelis et al. 2020a
CB	M	-19.2	11.5	Killgrove and Tykot 2013; De Angelis et al. 2020a
CB	M	-19	11.6	Killgrove and Tykot 2013; De Angelis et al. 2020a
CB	M	-18.6	12	Killgrove and Tykot 2013; De Angelis et al. 2020a
CB	M	-19	12.4	Killgrove and Tykot 2013; De Angelis et al. 2020a
CB	M	-19	11.9	Killgrove and Tykot 2013; De Angelis et al. 2020a
CB	M	-18.3	12.2	Killgrove and Tykot 2013; De Angelis et al. 2020a
CB	M	-18.2	11.8	Killgrove and Tykot 2013; De Angelis et al. 2020a
CB	M	-18.7	11.4	Killgrove and Tykot 2013; De Angelis et al. 2020a
CB	M	-18.7	11	Killgrove and Tykot 2013; De Angelis et al. 2020a
CB	M	-18.9	11.5	Killgrove and Tykot 2013; De Angelis et al. 2020a
CB	M	-19.1	11	Killgrove and Tykot 2013; De Angelis et al. 2020a
CB	M	-18.4	12.2	Killgrove and Tykot 2013; De Angelis et al. 2020a
CB	M	-19	12.6	Killgrove and Tykot 2013; De Angelis et al. 2020a
CB	M	-18.9	10.7	Killgrove and Tykot 2013; De Angelis et al. 2020a
CB	M	-19.3	10.6	Killgrove and Tykot 2013; De Angelis et al. 2020a
CB	M	-19.3	10.3	Killgrove and Tykot 2013; De Angelis et al. 2020a
CB	M	-18.8	12	Killgrove and Tykot 2013; De Angelis et al. 2020a
CB	M	-19.2	9.4	Killgrove and Tykot 2013; De Angelis et al. 2020a
CB	M	-18.7	9.6	Killgrove and Tykot 2013; De Angelis et al. 2020a
CB	M	-19.6	7.2	Killgrove and Tykot 2013; De Angelis et al. 2020a
CB	M	-19.5	8.4	Killgrove and Tykot 2013; De Angelis et al. 2020a
CB	M	-19	8	Killgrove and Tykot 2013; De Angelis et al. 2020a

CB	M	-18.6	11.3	Killgrove and Tykot 2013; De Angelis et al. 2020a
CB	M	-18.2	11.8	Killgrove and Tykot 2013; De Angelis et al. 2020a
CB	M	-18.2	11.1	Killgrove and Tykot 2013; De Angelis et al. 2020a
CB	M	-18.1	11.6	Killgrove and Tykot 2013; De Angelis et al. 2020a
CB	M	-18.1	11.6	Killgrove and Tykot 2013; De Angelis et al. 2020a
CB	M	-18.7	7	Killgrove and Tykot 2013; De Angelis et al. 2020a
CB	M	-18.6	10.1	Killgrove and Tykot 2013; De Angelis et al. 2020a
CB	M	-17.7	10.8	Killgrove and Tykot 2013; De Angelis et al. 2020a
CB	ND	-18.5	11.3	Killgrove and Tykot 2013; De Angelis et al. 2020a
CB	ND	-18.6	11.3	Killgrove and Tykot 2013; De Angelis et al. 2020a
CB	ND	-19.1	10.6	Killgrove and Tykot 2013; De Angelis et al. 2020a
CB	ND	-18.7	11.4	Killgrove and Tykot 2013; De Angelis et al. 2020a
CB	ND	-18.8	11.6	Killgrove and Tykot 2013; De Angelis et al. 2020a
CB	ND	-18.6	11.1	Killgrove and Tykot 2013; De Angelis et al. 2020a
CB	ND	-19.1	10.8	Killgrove and Tykot 2013; De Angelis et al. 2020a
CB	ND	-18.9	9.7	Killgrove and Tykot 2013; De Angelis et al. 2020a
CB	ND	-19	10.7	Killgrove and Tykot 2013; De Angelis et al. 2020a
CB	ND	-19.1	10.6	Killgrove and Tykot 2013; De Angelis et al. 2020a
CB	ND	-18.8	11.6	Killgrove and Tykot 2013; De Angelis et al. 2020a
CB	ND	-19.3	11.8	Killgrove and Tykot 2013; De Angelis et al. 2020a
CB	ND	-19.1	8.6	Killgrove and Tykot 2013; De Angelis et al. 2020a
CB	ND	-19.2	9.8	Killgrove and Tykot 2013; De Angelis et al. 2020a
CB	ND	-20.4	8.1	Killgrove and Tykot 2013; De Angelis et al. 2020a
CB	ND	-19.7	8.6	Killgrove and Tykot 2013; De Angelis et al. 2020a
CB	ND	-19.2	10.1	Killgrove and Tykot 2013; De Angelis et al. 2020a
CB	ND	-18.9	11.3	Killgrove and Tykot 2013; De Angelis et al. 2020a
CM	F	-19.3	10.6	De Angelis et al. 2020a
CM	F	-19.3	9.3	De Angelis et al. 2020a
CM	F	-20.8	7.7	De Angelis et al. 2020a

CM	F	-20.4	8	De Angelis et al. 2020a
CM	F	-19	11.5	De Angelis et al. 2020a
CM	F	-19.2	11.7	De Angelis et al. 2020a
CM	F	-19.2	12	De Angelis et al. 2020a
CM	F	-19.1	10.5	De Angelis et al. 2020a
CM	F	-19.2	9.7	De Angelis et al. 2020a
CM	F	-19.1	11.7	De Angelis et al. 2020a
CM	F	-19.3	11.7	De Angelis et al. 2020a
CM	F	-19.1	10.9	De Angelis et al. 2020a
CM	F	-19.3	11.3	De Angelis et al. 2020a
CM	F	-18.9	11	De Angelis et al. 2020a
CM	F	-19.1	12	De Angelis et al. 2020a
CM	F	-18.8	11.4	De Angelis et al. 2020a
CM	F	-19.3	11.4	De Angelis et al. 2020a
CM	F	-19.2	11.7	De Angelis et al. 2020a
CM	F	-19.3	11.8	De Angelis et al. 2020a
CM	M	-18.7	11.2	De Angelis et al. 2020a
CM	M	-18.7	11.4	De Angelis et al. 2020a
CM	M	-19.1	11.4	De Angelis et al. 2020a
CM	M	-18.7	12.2	De Angelis et al. 2020a
CM	M	-19	9.8	De Angelis et al. 2020a
CM	M	-19.5	10.2	De Angelis et al. 2020a
CM	M	-19.8	9.2	De Angelis et al. 2020a
CM	M	-19.4	9.7	De Angelis et al. 2020a
CM	M	-19.1	11.2	De Angelis et al. 2020a
CM	M	-19.1	11	De Angelis et al. 2020a
CM	M	-19	10.5	De Angelis et al. 2020a
CM	M	-19.4	11.8	De Angelis et al. 2020a
CM	M	-20.4	7.2	De Angelis et al. 2020a
CM	M	-18.9	11.3	De Angelis et al. 2020a
CM	M	-19.6	11.1	De Angelis et al. 2020a
CM	M	-19	11.5	De Angelis et al. 2020a
CM	M	-18.8	11.1	De Angelis et al. 2020a
CM	M	-18.8	12.3	De Angelis et al. 2020a
CM	M	-19	9.7	De Angelis et al. 2020a
CM	M	-19.2	11.2	De Angelis et al. 2020a
CM	M	-18.7	9	De Angelis et al. 2020a
CM	M	-19.1	12.5	De Angelis et al. 2020a
CM	M	-18.9	12.6	De Angelis et al. 2020a
CM	M	-19.5	10.3	De Angelis et al. 2020a
CM	M	-18.7	11.9	De Angelis et al. 2020a
CM	M	-20.4	8.5	De Angelis et al. 2020a
CM	M	-14.8	11	De Angelis et al. 2020a
CM	M	-19.6	11	De Angelis et al. 2020a
CM	M	-20.4	9.1	De Angelis et al. 2020a
CM	M	-19.2	10.6	De Angelis et al. 2020a
CM	M	-19	12.9	De Angelis et al. 2020a
CM	M	-18.9	10.5	De Angelis et al. 2020a
CM	M	-19.1	11	De Angelis et al. 2020a
CM	M	-17	12.4	De Angelis et al. 2020a
CM	M	-19.8	9.2	De Angelis et al. 2020a
CM	M	-18.2	12.6	De Angelis et al. 2020a
CM	M	-19.1	9.7	De Angelis et al. 2020a
CM	M	-19.5	11.3	De Angelis et al. 2020a
CM	M	-19.3	12	De Angelis et al. 2020a

CM	M	-19.8	10.6	De Angelis et al. 2020a
CM	M	-20.6	9.3	De Angelis et al. 2020a
CM	M	-19.4	11.6	De Angelis et al. 2020a
CM	M	-20.1	12.2	De Angelis et al. 2020a
CM	M	-18.8	9.8	De Angelis et al. 2020a
CM	M	-19.8	9.3	De Angelis et al. 2020a
CM	M	-18.7	10.9	De Angelis et al. 2020a
CM	M	-19.9	10.3	De Angelis et al. 2020a
CM	ND	-20.6	8.5	De Angelis et al. 2020a
CM	ND	-19.4	11.2	De Angelis et al. 2020a
CM	ND	-19.1	11.3	De Angelis et al. 2020a
CM	ND	-19.6	11.5	De Angelis et al. 2020a
CM	ND	-19.2	10.3	De Angelis et al. 2020a
CM	ND	-19.5	11.7	De Angelis et al. 2020a
CE	F	-17.9	9.5	Killgrove and Tykot 2013
CE	F	-18.8	11	Killgrove and Tykot 2013
CE	F	-18.1	11.5	Killgrove and Tykot 2013
CE	M	-17.8	9.1	Killgrove and Tykot 2013
CE	M	-19.5	7.8	Killgrove and Tykot 2013
CE	M	-18.4	8.8	Killgrove and Tykot 2013
CE	M	-19.1	8.5	Killgrove and Tykot 2013
CE	M	-12.5	8.3	Killgrove and Tykot 2013
Cr	F	-19.41	9.37	Lightfoot et al. 2012
Cr	F	-19.18	9.96	Lightfoot et al. 2012
Cr	F	-18.71	11.17	Lightfoot et al. 2012
Cr	F	-18.71	10.82	Lightfoot et al. 2012
Cr	F	-19.11	10.66	Lightfoot et al. 2012
Cr	F	-19.26	9.78	Lightfoot et al. 2012
Cr	F	-19.05	9.83	Lightfoot et al. 2012
Cr	F	-19.11	9.67	Lightfoot et al. 2012
Cr	F	-18.28	9.83	Lightfoot et al. 2012
Cr	F	-19.06	10.5	Lightfoot et al. 2012
Cr	F	-18.63	9.96	Lightfoot et al. 2012
Cr	F	-19.03	10.12	Lightfoot et al. 2012
Cr	F	-18.91	9.05	Lightfoot et al. 2012
Cr	F	-18.13	10.42	Lightfoot et al. 2012
Cr	F	-19.17	9.58	Lightfoot et al. 2012
Cr	F	-19.11	9.53	Lightfoot et al. 2012
Cr	F	-19.28	9.22	Lightfoot et al. 2012
Cr	F	-19.16	10.46	Lightfoot et al. 2012
Cr	F	-19.08	8.74	Lightfoot et al. 2012
Cr	F	-18.63	10.26	Lightfoot et al. 2012
Cr	F	-19.41	8.51	Lightfoot et al. 2012
Cr	F	-18.47	9.87	Lightfoot et al. 2012
Cr	F	-18.68	10.53	Lightfoot et al. 2012
Cr	F	-18.95	9.64	Lightfoot et al. 2012
Cr	M	-18.93	10.84	Lightfoot et al. 2012
Cr	M	-18.52	10.29	Lightfoot et al. 2012
Cr	M	-18.23	9.3	Lightfoot et al. 2012
Cr	M	-19.01	9	Lightfoot et al. 2012
Cr	M	-19.2	9.19	Lightfoot et al. 2012
Cr	M	-19.01	9.08	Lightfoot et al. 2012
Cr	M	-18.7	10.3	Lightfoot et al. 2012
Cr	M	-18.22	10.25	Lightfoot et al. 2012
Cr	M	-19.39	10.65	Lightfoot et al. 2012

Cr	M	-19.01	10.13	Lightfoot et al. 2012
Cr	M	-18.91	9.65	Lightfoot et al. 2012
Cr	M	-18.74	10.03	Lightfoot et al. 2012
Cr	M	-18.65	12.9	Lightfoot et al. 2012
Cr	M	-18.58	10.13	Lightfoot et al. 2012
Cr	M	-18.5	10.09	Lightfoot et al. 2012
Cr	M	-19.62	10.06	Lightfoot et al. 2012
Cr	M	-18.39	10.56	Lightfoot et al. 2012
Cr	M	-18.96	9.72	Lightfoot et al. 2012
Cr	M	-19.02	9.31	Lightfoot et al. 2012
Cr	M	-19.09	9.58	Lightfoot et al. 2012
Cr	M	-18.52	9.79	Lightfoot et al. 2012
Cr	M	-18.78	9.9	Lightfoot et al. 2012
Cr	M	-18.53	10.8	Lightfoot et al. 2012
Cr	M	-19.11	9.57	Lightfoot et al. 2012
Cr	M	-19.18	10.39	Lightfoot et al. 2012
Cr	M	-18.82	10.79	Lightfoot et al. 2012
Cr	M	-17.84	10.83	Lightfoot et al. 2012
Cr	M	-19.1	8.66	Lightfoot et al. 2012
Cr	M	-18.95	9.77	Lightfoot et al. 2012
Cr	M	-18.62	10.42	Lightfoot et al. 2012
Cr	ND	-18.69	9.11	Lightfoot et al. 2012
Cr	ND	-19.23	9	Lightfoot et al. 2012
Cr	ND	-19.11	9.18	Lightfoot et al. 2012
Cr	ND	-19.29	10.01	Lightfoot et al. 2012
Cr	ND	-18.99	9.36	Lightfoot et al. 2012
Cr	ND	-18.74	9.35	Lightfoot et al. 2012
Cr	ND	-19.36	8.75	Lightfoot et al. 2012
Cr	ND	-18.84	10.4	Lightfoot et al. 2012
Cr	ND	-18.88	9.67	Lightfoot et al. 2012
Ed	F	-18.1	9.3	Dotsika and Michael 2018
Ed	F	-18.4	9.7	Dotsika and Michael 2018
Ed	F	-18	10.8	Dotsika and Michael 2018
Ed	F	-16.5	10	Dotsika and Michael 2018
Ed	F	-18.5	9.9	Dotsika and Michael 2018
Ed	F	-17.3	9.8	Dotsika and Michael 2018
Ed	F	-17	10.3	Dotsika and Michael 2018
Ed	F	-18.3	8.8	Dotsika and Michael 2018
Ed	F	-17.3	8.9	Dotsika and Michael 2018
Ed	F	-21	10.4	Dotsika and Michael 2018
Ed	F	-17.2	9.9	Dotsika and Michael 2018
Ed	F	-16.2	9.6	Dotsika and Michael 2018
Ed	F	-16.7	10.6	Dotsika and Michael 2018
Ed	F	-17.7	9.9	Dotsika and Michael 2018
Ed	M	-17.5	9.7	Dotsika and Michael 2018
Ed	M	-16.9	10.1	Dotsika and Michael 2018
Ed	M	-16.3	10.3	Dotsika and Michael 2018
Ed	M	-17.6	10.1	Dotsika and Michael 2018
Ed	M	-16.8	10	Dotsika and Michael 2018
Ga	F	-18.8	11.10	Killgrove and Tykot 2018
Ga	F	-19	8.50	Killgrove and Tykot 2018
Ga	F	-18.9	11.50	Killgrove and Tykot 2018
Ga	F	-19.3	9.90	Killgrove and Tykot 2018
Ga	F	-19.3	10.40	Killgrove and Tykot 2018
Ga	F	-19.3	9.70	Killgrove and Tykot 2018

Ga	F	-18.5	11.40	Killgrove and Tykot 2018
Ga	M	-18.8	11.50	Killgrove and Tykot 2018
Ga	M	-19.2	11.30	Killgrove and Tykot 2018
Ga	M	-19.3	11.30	Killgrove and Tykot 2018
Ga	M	-19.3	11.00	Killgrove and Tykot 2018
Ga	M	-19	11.20	Killgrove and Tykot 2018
Ga	M	-18.8	11.20	Killgrove and Tykot 2018
Ga	M	-19.3	10.70	Killgrove and Tykot 2018
Ga	M	-18.8	11.30	Killgrove and Tykot 2018
Ga	M	-15.8	8.60	Killgrove and Tykot 2018
He	F	-19.92	9.41	Craig et al. 2013; Martyn et al. 2018
He	F	-18.9	10.95	Craig et al. 2013; Martyn et al. 2018
He	F	-19.45	9.56	Craig et al. 2013; Martyn et al. 2018
He	F	-19.4	9.61	Craig et al. 2013; Martyn et al. 2018
He	F	-19.67	9.26	Craig et al. 2013; Martyn et al. 2018
He	F	-19.7	9.31	Craig et al. 2013; Martyn et al. 2018
He	F	-18.96	10.63	Craig et al. 2013; Martyn et al. 2018
He	F	-19.79	10.09	Craig et al. 2013; Martyn et al. 2018
He	F	-19.27	9.94	Craig et al. 2013; Martyn et al. 2018
He	F	-18.96	10.09	Craig et al. 2013; Martyn et al. 2018
He	F	-19.65	9.16	Craig et al. 2013; Martyn et al. 2018
He	F	-19.32	10.49	Craig et al. 2013; Martyn et al. 2018
He	F	-20.12	9.01	Craig et al. 2013; Martyn et al. 2018
He	F	-19.1	10.25	Craig et al. 2013; Martyn et al. 2018
He	F	-19.12	10.29	Craig et al. 2013; Martyn et al. 2018
He	F	-19.19	9.67	Craig et al. 2013; Martyn et al. 2018
He	F	-18.76	10.7	Craig et al. 2013; Martyn et al. 2018
He	F	-19.38	9.33	Craig et al. 2013; Martyn et al. 2018
He	F	-18.83	10.09	Craig et al. 2013; Martyn et al. 2018
He	F	-19.21	10.43	Craig et al. 2013; Martyn et al. 2018
He	F	-19.3	10.51	Craig et al. 2013; Martyn et al. 2018
He	F	-19.67	10.09	Craig et al. 2013; Martyn et al. 2018

He	F	-19.47	10.02	Craig et al. 2013; Martyn et al. 2018
He	F	-19.18	10.09	Craig et al. 2013; Martyn et al. 2018
He	F	-18.76	11.43	Craig et al. 2013; Martyn et al. 2018
He	F	-19.89	8.89	Craig et al. 2013; Martyn et al. 2018
He	F	-19.09	9.08	Craig et al. 2013; Martyn et al. 2018
He	F	-19.07	10.71	Craig et al. 2013; Martyn et al. 2018
He	M	-19.27	10.07	Craig et al. 2013; Martyn et al. 2018
He	M	-18.75	10.63	Craig et al. 2013; Martyn et al. 2018
He	M	-18.88	10.83	Craig et al. 2013; Martyn et al. 2018
He	M	-19.22	10.29	Craig et al. 2013; Martyn et al. 2018
He	M	-19.57	9.1	Craig et al. 2013; Martyn et al. 2018
He	M	-18.8	11.45	Craig et al. 2013; Martyn et al. 2018
He	M	-19.12	10.76	Craig et al. 2013; Martyn et al. 2018
He	M	-18.21	9.05	Craig et al. 2013; Martyn et al. 2018
He	M	-19.02	10.18	Craig et al. 2013; Martyn et al. 2018
He	M	-18.79	11.07	Craig et al. 2013; Martyn et al. 2018
He	M	-19.3	11.72	Craig et al. 2013; Martyn et al. 2018
He	M	-19.01	10.64	Craig et al. 2013; Martyn et al. 2018
He	M	-19.18	11.67	Craig et al. 2013; Martyn et al. 2018
He	M	-19.02	10.54	Craig et al. 2013; Martyn et al. 2018
He	M	-18.84	11.57	Craig et al. 2013; Martyn et al. 2018
He	M	-19.04	10.55	Craig et al. 2013; Martyn et al. 2018
He	M	-19.59	9.14	Craig et al. 2013; Martyn et al. 2018
He	M	-19.07	10.49	Craig et al. 2013; Martyn et al. 2018
He	M	-19.07	9.1	Craig et al. 2013; Martyn et al. 2018
He	M	-18.98	9.51	Craig et al. 2013; Martyn et al. 2018
He	M	-19.12	9.87	Craig et al. 2013; Martyn et al. 2018
He	M	-18.62	11.03	Craig et al. 2013; Martyn et al. 2018

He	M	-18.71	9.3	Craig et al. 2013; Martyn et al. 2018
He	M	-19.11	9.13	Craig et al. 2013; Martyn et al. 2018
He	M	-19.07	10.34	Craig et al. 2013; Martyn et al. 2018
He	M	-19.49	10.23	Craig et al. 2013; Martyn et al. 2018
He	M	-19.23	10	Craig et al. 2013; Martyn et al. 2018
He	M	-19.25	10.27	Craig et al. 2013; Martyn et al. 2018
He	M	-19.55	9.89	Craig et al. 2013; Martyn et al. 2018
He	M	-19.21	10.54	Craig et al. 2013; Martyn et al. 2018
He	M	-19.05	10.5	Craig et al. 2013; Martyn et al. 2018
He	M	-19.33	10.48	Craig et al. 2013; Martyn et al. 2018
He	M	-19.4	10.72	Craig et al. 2013; Martyn et al. 2018
He	M	-19.42	10.74	Craig et al. 2013; Martyn et al. 2018
He	M	-18.57	10.93	Craig et al. 2013; Martyn et al. 2018
He	M	-19.2	11.11	Craig et al. 2013; Martyn et al. 2018
He	M	-19.58	9.35	Craig et al. 2013; Martyn et al. 2018
He	ND	-19.81	8.17	Craig et al. 2013; Martyn et al. 2018
He	ND	-20.17	8.99	Craig et al. 2013; Martyn et al. 2018
He	ND	-19.38	9.46	Craig et al. 2013; Martyn et al. 2018
He	ND	-20	9.15	Craig et al. 2013; Martyn et al. 2018
IS	F	-18.7	11.1	Prowse et al. 2004; 2005
IS	F	-18.6	11.7	Prowse et al. 2004; 2005
IS	F	-18.4	12.3	Prowse et al. 2004; 2005
IS	F	-18.7	12	Prowse et al. 2004; 2005
IS	F	-18.9	11.7	Prowse et al. 2004; 2005
IS	F	-18.2	12.5	Prowse et al. 2004; 2005
IS	F	-18.6	11.7	Prowse et al. 2004; 2005
IS	F	-18.7	11.5	Prowse et al. 2004; 2005
IS	F	-18.9	11.3	Prowse et al. 2004; 2005
IS	F	-18.7	9.2	Prowse et al. 2004; 2005
IS	F	-18.6	11.8	Prowse et al. 2004; 2005
IS	F	-18.9	10.5	Prowse et al. 2004; 2005
IS	F	-18.7	12.9	Prowse et al. 2004; 2005
IS	F	-18.5	11.5	Prowse et al. 2004; 2005
IS	F	-18.2	12.2	Prowse et al. 2004; 2005
IS	F	-18.4	11.8	Prowse et al. 2004; 2005
IS	F	-18.9	11.9	Prowse et al. 2004; 2005

IS	F	-19.1	10.2	Prowse et al. 2004; 2005
IS	M	-18.7	11.6	Prowse et al. 2004; 2005
IS	M	-18	11.5	Prowse et al. 2004; 2005
IS	M	-18.5	11.4	Prowse et al. 2004; 2005
IS	M	-19.5	11.1	Prowse et al. 2004; 2005
IS	M	-18.5	11.5	Prowse et al. 2004; 2005
IS	M	-18.6	12.4	Prowse et al. 2004; 2005
IS	M	-18.3	11.9	Prowse et al. 2004; 2005
IS	M	-17.3	12.2	Prowse et al. 2004; 2005
IS	M	-18.9	12.9	Prowse et al. 2004; 2005
IS	M	-18.5	11.2	Prowse et al. 2004; 2005
IS	M	-19.2	9.6	Prowse et al. 2004; 2005
IS	M	-19.3	9.9	Prowse et al. 2004; 2005
IS	M	-18.6	12.3	Prowse et al. 2004; 2005
IS	M	-18.6	10.5	Prowse et al. 2004; 2005
IS	M	-18.1	11.4	Prowse et al. 2004; 2005
IS	M	-18.4	11.2	Prowse et al. 2004; 2005
IS	M	-18.8	11.5	Prowse et al. 2004; 2005
IS	M	-18.3	11.6	Prowse et al. 2004; 2005
IS	M	-18.6	11.4	Prowse et al. 2004; 2005
IS	M	-18.9	11	Prowse et al. 2004; 2005
IS	M	-19.9	10.4	Prowse et al. 2004; 2005
IS	M	-18.8	11.2	Prowse et al. 2004; 2005
IS	M	-18.5	11.1	Prowse et al. 2004; 2005
IS	M	-19.5	10.4	Prowse et al. 2004; 2005
IS	M	-19	12.1	Prowse et al. 2004; 2005
IS	M	-18.6	11.2	Prowse et al. 2004; 2005
IS	M	-18.9	11.9	Prowse et al. 2004; 2005
IS	M	-18.3	11.5	Prowse et al. 2004; 2005
IS	M	-18.7	10.3	Prowse et al. 2004; 2005
IS	M	-19.4	9	Prowse et al. 2004; 2005
IS	M	-18.7	11.7	Prowse et al. 2004; 2005
IS	M	-18.4	11.5	Prowse et al. 2004; 2005
IS	M	-18.6	11.6	Prowse et al. 2004; 2005
IS	M	-19.1	10	Prowse et al. 2004; 2005
IS	M	-19	9.9	Prowse et al. 2004; 2005
IS	M	-18.6	12	Prowse et al. 2004; 2005
IS	M	-18.5	11.6	Prowse et al. 2004; 2005
IS	M	-18.3	10.5	Prowse et al. 2004; 2005
IS	M	-18.5	11.6	Prowse et al. 2004; 2005
IS	M	-18.4	11.6	Prowse et al. 2004; 2005
IS	M	-18.9	11.6	Prowse et al. 2004; 2005
IS	M	-18.6	11.7	Prowse et al. 2004; 2005
IS	M	-18.7	12.5	Prowse et al. 2004; 2005
IS	M	-18.6	12.1	Prowse et al. 2004; 2005
IS	M	-18.1	11.5	Prowse et al. 2004; 2005
IS	M	-18.7	12	Prowse et al. 2004; 2005
IS	M	-18	11.5	Prowse et al. 2004; 2005
IS	M	-18.2	11.9	Prowse et al. 2004; 2005
IS	M	-19	11.6	Prowse et al. 2004; 2005
IS	M	-19	11	Prowse et al. 2004; 2005
IS	M	-18.6	11	Prowse et al. 2004; 2005
IS	M	-18.9	8.3	Prowse et al. 2004; 2005
IS	M	-18.9	10.6	Prowse et al. 2004; 2005
IS	M	-19.3	9.3	Prowse et al. 2004; 2005

IS	M	-19.3	11.2	Prowse et al. 2004; 2005
IS	M	-18.6	11.6	Prowse et al. 2004; 2005
IS	M	-18.3	11.4	Prowse et al. 2004; 2005
IS	M	-18.7	10.7	Prowse et al. 2004; 2005
IS	M	-18.9	10.5	Prowse et al. 2004; 2005
IS	M	-18.9	12	Prowse et al. 2004; 2005
IS	M	-18.9	9.7	Prowse et al. 2004; 2005
IS	M	-18.9	10.1	Prowse et al. 2004; 2005
IS	M	-18.8	11.2	Prowse et al. 2004; 2005
IS	M	-18.8	11.4	Prowse et al. 2004; 2005
IS	M	-18.9	10.9	Prowse et al. 2004; 2005
IS	M	-18.9	11.7	Prowse et al. 2004; 2005
IS	ND	-18.4	11	Prowse et al. 2004; 2005
IS	ND	-18.7	9.3	Prowse et al. 2004; 2005
IS	ND	-18.7	11.5	Prowse et al. 2004; 2005
IS	ND	-18.8	12.1	Prowse et al. 2004; 2005
IS	ND	-18.9	10.7	Prowse et al. 2004; 2005
IS	ND	-18	12.3	Prowse et al. 2004; 2005
IS	ND	-18.1	11.4	Prowse et al. 2004; 2005
Le	F	-17.6	14.5	Keenleyside et al. 2009
Le	F	-18.1	13.7	Keenleyside et al. 2009
Le	F	-17.5	14.6	Keenleyside et al. 2009
Le	F	-17.4	15.1	Keenleyside et al. 2009
Le	F	-17.4	11.3	Keenleyside et al. 2009
Le	F	-17.8	14.4	Keenleyside et al. 2009
Le	F	-18.2	11.1	Keenleyside et al. 2009
Le	F	-17.8	11.7	Keenleyside et al. 2009
Le	F	-17.6	12.9	Keenleyside et al. 2009
Le	F	-19	13.2	Keenleyside et al. 2009
Le	F	-17.1	13.2	Keenleyside et al. 2009
Le	F	-17.9	12.6	Keenleyside et al. 2009
Le	F	-19	10.7	Keenleyside et al. 2009
Le	M	-17.8	14	Keenleyside et al. 2009
Le	M	-16.5	13.9	Keenleyside et al. 2009
Le	M	-17.5	13.9	Keenleyside et al. 2009
Le	M	-18.3	11.9	Keenleyside et al. 2009
Le	M	-18.2	13.5	Keenleyside et al. 2009
Le	M	-18	13.5	Keenleyside et al. 2009
Le	M	-17.1	13	Keenleyside et al. 2009
Le	M	-18.9	14	Keenleyside et al. 2009
Le	M	-16.9	15.7	Keenleyside et al. 2009
Le	M	-17.9	12	Keenleyside et al. 2009
Le	M	-17.5	12.9	Keenleyside et al. 2009
Le	M	-17.8	12.4	Keenleyside et al. 2009
Le	M	-18.2	10	Keenleyside et al. 2009
Le	ND	-17.5	14.1	Keenleyside et al. 2009
Le	ND	-17.4	14.9	Keenleyside et al. 2009
Le	ND	-18	12.6	Keenleyside et al. 2009
Le	ND	-18.8	11.5	Keenleyside et al. 2009
Le	ND	-18.4	14.7	Keenleyside et al. 2009
Le	ND	-18	13.8	Keenleyside et al. 2009
Le	ND	-17.7	12.8	Keenleyside et al. 2009
Le	ND	-17.2	14.8	Keenleyside et al. 2009
Le	ND	-18.1	11.4	Keenleyside et al. 2009
Le	ND	-17.2	14.5	Keenleyside et al. 2009

Le	ND	-18.6	11.5	Keenleyside et al. 2009
Le	ND	-18.3	12.5	Keenleyside et al. 2009
Le	ND	-17.4	13	Keenleyside et al. 2009
Le	ND	-17.9	13.4	Keenleyside et al. 2009
Le	ND	-18.8	10.5	Keenleyside et al. 2009
Le	ND	-17.1	12.5	Keenleyside et al. 2009
Le	ND	-18.1	12	Keenleyside et al. 2009
Le	ND	-17.2	13.5	Keenleyside et al. 2009
Le	ND	-18.5	11.5	Keenleyside et al. 2009
Le	ND	-17.6	12.7	Keenleyside et al. 2009
Le	ND	-17.5	11.4	Keenleyside et al. 2009
Le	ND	-18.1	10.4	Keenleyside et al. 2009
Le	ND	-16.7	13.3	Keenleyside et al. 2009
Le	ND	-17.7	10	Keenleyside et al. 2009
Le	ND	-16.9	12.2	Keenleyside et al. 2009
Le	ND	-18.4	12.8	Keenleyside et al. 2009
Le	ND	-17.8	11.8	Keenleyside et al. 2009
Le	ND	-18	13.1	Keenleyside et al. 2009
Le	ND	-17	12.6	Keenleyside et al. 2009
Le	ND	-17.6	13.7	Keenleyside et al. 2009
LF	F	-19.61	9.09	Tafuri et al. 2018
LF	F	-19.78	8.61	Tafuri et al. 2018
LF	F	-19.47	10.2	Tafuri et al. 2018
LF	F	-19.64	10.5	Tafuri et al. 2018
LF	F	-18.67	10.83	Tafuri et al. 2018
LF	F	-19.44	11.08	Tafuri et al. 2018
LF	F	-19.38	11.79	Tafuri et al. 2018
LF	F	-19.45	11.18	Tafuri et al. 2018
LF	F	-20.11	9.65	Tafuri et al. 2018
LF	F	-20.06	8.27	Tafuri et al. 2018
LF	F	-20.44	8.82	Tafuri et al. 2018
LF	F	-20.34	8.02	Tafuri et al. 2018
LF	F	-20.17	8.96	Tafuri et al. 2018
LF	F	-19.34	10.04	Tafuri et al. 2018
LF	F	-19.77	9.54	Tafuri et al. 2018
LF	j	-19.76	8.88	Tafuri et al. 2018
LF	M	-19.07	10.9	Tafuri et al. 2018
LF	M	-17.88	12.15	Tafuri et al. 2018
LF	M	-19.71	10.34	Tafuri et al. 2018
LF	M	-19.49	10.33	Tafuri et al. 2018
LF	M	-19.52	10.27	Tafuri et al. 2018
LF	M	-19.97	10.08	Tafuri et al. 2018
LF	M	-20.34	8.81	Tafuri et al. 2018
LF	M	-19.86	8.96	Tafuri et al. 2018
LF	M	-19.45	10.23	Tafuri et al. 2018
LF	M	-20.49	6.61	Tafuri et al. 2018
LF	M	-19.49	11.48	Tafuri et al. 2018
LF	M	-19.17	11.29	Tafuri et al. 2018
LF	M	-20.47	8.43	Tafuri et al. 2018
LF	M	-19.15	11.77	Tafuri et al. 2018
LF	M	-20.34	10.91	Tafuri et al. 2018
Pa	ND	-21.9	4.7	Ricci et al. 2016
Pa	ND	-22.1	5.1	Ricci et al. 2016
Pa	ND	-19	7.8	Ricci et al. 2016
Pa	ND	-19.5	7.6	Ricci et al. 2016

Pa	ND	-19.3	8.5	Ricci et al. 2016
Pa	ND	-20.9	7.6	Ricci et al. 2016
Pa	ND	-19.4	7.9	Ricci et al. 2016
Pa	ND	-19	7.9	Ricci et al. 2016
Pa	ND	-18.5	8.2	Ricci et al. 2016
Pa	ND	-18.5	9.4	Ricci et al. 2016
Pa	ND	-19.5	8.5	Ricci et al. 2016
Pa	ND	-18.8	8.1	Ricci et al. 2016
Pa	ND	-20.1	7.6	Ricci et al. 2016
Pa	ND	-20	7.8	Ricci et al. 2016
Pa	ND	-19	7.5	Ricci et al. 2016
Pa	ND	-19.6	8	Ricci et al. 2016
Pa	ND	-20.3	8.2	Ricci et al. 2016
Pa	ND	-18.4	11.4	Ricci et al. 2016
Pa	ND	-19.9	8.8	Ricci et al. 2016
Pa	ND	-20.6	8.4	Ricci et al. 2016
Pa	ND	-19.3	8.4	Ricci et al. 2016
Pom	M	-20.1	9.3	Pate et al. 2016
Pom	M	-19.4	10.2	Pate et al. 2016
Pom	M	-19.4	9.5	Pate et al. 2016
Pom	M	-19.2	9.3	Pate et al. 2016
Pom	M	-18.9	10.4	Pate et al. 2016
Pom	M	-18.7	10.6	Pate et al. 2016
Pom	M	-18.7	10.4	Pate et al. 2016
Pom	M	-18.1	9.9	Pate et al. 2016
Pom	M	-16.1	8.6	Pate et al. 2016
Pom	M	-15.8	9.1	Pate et al. 2016
Pom	F	-19.9	10.6	Pate et al. 2016
Pom	F	-19.7	9.8	Pate et al. 2016
Pom	F	-19.7	9.6	Pate et al. 2016
Pom	F	-19.6	10.1	Pate et al. 2016
Pom	F	-19.5	10.2	Pate et al. 2016
Pom	F	-19.5	10.1	Pate et al. 2016
Pom	F	-19.5	9.8	Pate et al. 2016
Pom	F	-19.4	9.8	Pate et al. 2016
Pom	F	-19.4	9.6	Pate et al. 2016
Pom	F	-19.3	10.6	Pate et al. 2016
Pom	F	-19.3	10.2	Pate et al. 2016
Pom	F	-19.3	8.1	Pate et al. 2016
Pom	F	-19.2	10.4	Pate et al. 2016
Pom	F	-19.1	10.3	Pate et al. 2016
Pom	F	-18.9	8.2	Pate et al. 2016
Pom	F	-18.5	10.4	Pate et al. 2016
Pom	F	-18.4	9.9	Pate et al. 2016
Pr	F	-19.9	8.4	Baldoni et al. 2020
Pr	F	-19.9	8.5	Baldoni et al. 2020
Pr	F	-20	7.7	Baldoni et al. 2020
Pr	F	-19.8	9	Baldoni et al. 2020
Pr	F	-19.8	9.1	Baldoni et al. 2020
Pr	F	-20.2	8.2	Baldoni et al. 2020
Pr	F	-19.5	8.5	Baldoni et al. 2020
Pr	F	-20	7.4	Baldoni et al. 2020
Pr	F	-19.7	10.5	Baldoni et al. 2020
Pr	F	-18.9	11.3	Baldoni et al. 2020
Pr	F	-19.7	9.9	Baldoni et al. 2020

Pr	F	-19.9	9.9	Baldoni et al. 2020
Pr	F	-19.9	10.1	Baldoni et al. 2020
Pr	F	-19.4	11.1	Baldoni et al. 2020
Pr	M	-19.9	8.1	Baldoni et al. 2020
Pr	M	-19	12.2	Baldoni et al. 2020
Pr	M	-19.8	8.6	Baldoni et al. 2020
Pr	M	-19.5	8.5	Baldoni et al. 2020
Pr	M	-20.2	6.9	Baldoni et al. 2020
Pr	M	-20.3	6.7	Baldoni et al. 2020
Pr	M	-20	8.1	Baldoni et al. 2020
Pr	M	-21.6	9.2	Baldoni et al. 2020
Pr	M	-19.7	9.8	Baldoni et al. 2020
Pr	M	-20.4	8.5	Baldoni et al. 2020
Pr	ND	-19.5	9.5	Baldoni et al. 2020
Pr	ND	-19.7	9.7	Baldoni et al. 2020
Pr	ND	-21.1	6.5	Baldoni et al. 2020
Pr	ND	-19.6	8.3	Baldoni et al. 2020
Pr	ND	-19.6	10.1	Baldoni et al. 2020
Pr	ND	-20.6	9.6	Baldoni et al. 2020
Pr	ND	-20.5	8.6	Baldoni et al. 2020
Pr	ND	-19.8	9.7	Baldoni et al. 2020
Pr	ND	-22.5	9.5	Baldoni et al. 2020
QCP	F	-19.5	9.9	De Angelis et al. 2020a; 2020b
QCP	F	-19.5	8.7	De Angelis et al. 2020a; 2020b
QCP	F	-18.8	9.6	De Angelis et al. 2020a; 2020b
QCP	F	-19.1	9	De Angelis et al. 2020a; 2020b
QCP	F	-20.5	8.4	De Angelis et al. 2020a; 2020b
QCP	F	-19.8	7.7	De Angelis et al. 2020a; 2020b
QCP	F	-19.1	10.3	De Angelis et al. 2020a; 2020b
QCP	M	-18.6	11.5	De Angelis et al. 2020a; 2020b
QCP	M	-18.7	12.3	De Angelis et al. 2020a; 2020b
QCP	M	-19.3	9.7	De Angelis et al. 2020a; 2020b
QCP	M	-18.8	10.2	De Angelis et al. 2020a; 2020b
QCP	M	-19.8	8.1	De Angelis et al. 2020a; 2020b
QCP	M	-19.4	8.8	De Angelis et al. 2020a; 2020b
QCP	M	-19.6	7.7	De Angelis et al. 2020a; 2020b
QCP	M	-20	9.1	De Angelis et al. 2020a; 2020b
QCP	M	-19.3	10.2	De Angelis et al. 2020a; 2020b
QCP	M	-18.2	8.8	De Angelis et al. 2020a; 2020b
QCP	M	-18.9	11.4	De Angelis et al. 2020a; 2020b
QCP	ND	-19.5	9.7	De Angelis et al. 2020a; 2020b
Ve	F	-19.6	8.3	Craig et al. 2009
Ve	F	-19.4	8.3	Craig et al. 2009
Ve	F	-19.5	8.6	Craig et al. 2009
Ve	F	-19.4	8.3	Craig et al. 2009
Ve	F	-19.6	7.5	Craig et al. 2009
Ve	F	-20	7.5	Craig et al. 2009
Ve	F	-19.6	9.3	Craig et al. 2009
Ve	F	-19.7	9.1	Craig et al. 2009
Ve	F	-19.3	7.7	Craig et al. 2009
Ve	F	-19.1	9.4	Craig et al. 2009
Ve	F	-19.6	7.5	Craig et al. 2009
Ve	F	-19.2	8.2	Craig et al. 2009
Ve	F	-19.3	8.3	Craig et al. 2009
Ve	F	-19.6	6.6	Craig et al. 2009

Ve	F	-19.7	7.9	Craig et al. 2009
Ve	F	-19.1	10.1	Craig et al. 2009
Ve	F	-19.6	8.2	Craig et al. 2009
Ve	F	-19	8.7	Craig et al. 2009
Ve	F	-19.5	8.7	Craig et al. 2009
Ve	F	-19.5	8.2	Craig et al. 2009
Ve	F	-19.6	10.5	Craig et al. 2009
Ve	F	-19.3	8.3	Craig et al. 2009
Ve	F	-19.2	7.5	Craig et al. 2009
Ve	F	-19.7	8	Craig et al. 2009
Ve	F	-19.5	8.1	Craig et al. 2009
Ve	F	-19.7	7.5	Craig et al. 2009
Ve	F	-19.3	9.3	Craig et al. 2009
Ve	F	-19.4	8.6	Craig et al. 2009
Ve	F	-19.3	9.4	Craig et al. 2009
Ve	F	-19.2	8.8	Craig et al. 2009
Ve	F	-19.4	8.5	Craig et al. 2009
Ve	F	-19.9	7.7	Craig et al. 2009
Ve	F	-19.5	7.3	Craig et al. 2009
Ve	F	-19.8	7.6	Craig et al. 2009
Ve	F	-19.6	9.3	Craig et al. 2009
Ve	F	-19.7	6.7	Craig et al. 2009
Ve	F	-19.4	8.7	Craig et al. 2009
Ve	F	-19.4	9.8	Craig et al. 2009
Ve	F	-19.6	7.6	Craig et al. 2009
Ve	F	-19.7	7.4	Craig et al. 2009
Ve	F	-19.9	7.5	Craig et al. 2009
Ve	F	-19.9	7.4	Craig et al. 2009
Ve	F	-19.6	6.8	Craig et al. 2009
Ve	F	-19.7	8	Craig et al. 2009
Ve	F	-19.7	7.9	Craig et al. 2009
Ve	F	-19.8	7.8	Craig et al. 2009
Ve	F	-19.8	8.1	Craig et al. 2009
Ve	F	-19.7	7.7	Craig et al. 2009
Ve	F	-18.9	8.5	Craig et al. 2009
Ve	M	-20	8.6	Craig et al. 2009
Ve	M	-19.2	14	Craig et al. 2009
Ve	M	-19.6	7.7	Craig et al. 2009
Ve	M	-19.6	9.6	Craig et al. 2009
Ve	M	-19.8	8.1	Craig et al. 2009
Ve	M	-19.7	7.8	Craig et al. 2009
Ve	M	-19.5	8	Craig et al. 2009
Ve	M	-19.1	9.5	Craig et al. 2009
Ve	M	-19.5	7.6	Craig et al. 2009
Ve	M	-19.3	8.7	Craig et al. 2009
Ve	M	-19	9.2	Craig et al. 2009
Ve	M	-19.6	11.4	Craig et al. 2009
Ve	M	-19.5	8.5	Craig et al. 2009
Ve	M	-19.2	8.3	Craig et al. 2009
Ve	M	-19.4	8.5	Craig et al. 2009
Ve	M	-19.4	9.4	Craig et al. 2009
Ve	M	-19.9	8.4	Craig et al. 2009
Ve	M	-19.4	8.8	Craig et al. 2009
Ve	M	-19.4	7.9	Craig et al. 2009
Ve	M	-19.6	8.8	Craig et al. 2009

Ve	M	-19.2	8.6	Craig et al. 2009
Ve	M	-19.3	8.4	Craig et al. 2009
Ve	M	-19.5	11.3	Craig et al. 2009
Ve	M	-19	9.2	Craig et al. 2009
Ve	M	-19.5	8.9	Craig et al. 2009
Ve	M	-19.2	8.5	Craig et al. 2009
Ve	M	-19.4	8.4	Craig et al. 2009
Ve	M	-19.2	8.8	Craig et al. 2009
Ve	M	-19.4	7.2	Craig et al. 2009
Ve	M	-19.1	8.8	Craig et al. 2009
Ve	M	-19.6	7.6	Craig et al. 2009
Ve	M	-19.7	9.8	Craig et al. 2009
Ve	M	-19.6	6.4	Craig et al. 2009
Ve	M	-19.4	7.9	Craig et al. 2009
Ve	M	-19.5	7.8	Craig et al. 2009
Ve	M	-19.2	8.8	Craig et al. 2009
Ve	M	-19.5	8.5	Craig et al. 2009
Ve	M	-19.2	9.1	Craig et al. 2009
Ve	M	-19.1	10.5	Craig et al. 2009
Ve	M	-19.3	7.1	Craig et al. 2009
Ve	M	-19.6	8.2	Craig et al. 2009
Ve	M	-19.3	8.3	Craig et al. 2009
Ve	M	-19.1	10.9	Craig et al. 2009
Ve	M	-19.2	8.6	Craig et al. 2009
Ve	M	-19.1	14.1	Craig et al. 2009
Ve	M	-19.2	9.1	Craig et al. 2009
Ve	M	-19.4	9.4	Craig et al. 2009
Ve	M	-19.7	8.1	Craig et al. 2009
Ve	M	-19.4	8	Craig et al. 2009
Ve	M	-19.5	6.6	Craig et al. 2009
Ve	M	-19.7	8.3	Craig et al. 2009
Ve	M	-18.7	10	Craig et al. 2009
Ve	M	-19.4	10.2	Craig et al. 2009
Ve	M	-19.5	8.3	Craig et al. 2009
Ve	M	-19.1	10.3	Craig et al. 2009
Ve	M	-19.2	8.3	Craig et al. 2009
Ve	M	-19.4	8.4	Craig et al. 2009
Ve	M	-19	9.2	Craig et al. 2009
Ve	M	-19.2	8	Craig et al. 2009
Ve	M	-19.5	8	Craig et al. 2009
Ve	M	-19.3	11.1	Craig et al. 2009
Ve	ND	-19.4	7.3	Craig et al. 2009
Ve	ND	-19.2	7.5	Craig et al. 2009
Ve	ND	-19.2	12.3	Craig et al. 2009
Ve	ND	-19.8	11.1	Craig et al. 2009
VPS	F	-19.4	10.7	De Angelis et al. 2020a
VPS	F	-18.3	12.4	De Angelis et al. 2020a
VPS	F	-19	10.5	De Angelis et al. 2020a
VPS	F	-19.5	10.7	De Angelis et al. 2020a
VPS	F	-19.4	10.9	De Angelis et al. 2020a
VPS	F	-19	11.3	De Angelis et al. 2020a
VPS	F	-19.1	10	De Angelis et al. 2020a
VPS	F	-20	11.3	De Angelis et al. 2020a
VPS	F	-19.4	11.7	De Angelis et al. 2020a
VPS	F	-19.8	10.9	De Angelis et al. 2020a

VPS	F	-19.6	11.4	De Angelis et al. 2020a
VPS	F	-18.6	13.2	De Angelis et al. 2020a
VPS	F	-19	11.8	De Angelis et al. 2020a
VPS	F	-19.1	12.1	De Angelis et al. 2020a
VPS	M	-18.9	11.9	De Angelis et al. 2020a
VPS	M	-19.7	10.3	De Angelis et al. 2020a
VPS	M	-18.9	10.4	De Angelis et al. 2020a
VPS	M	-19.3	11.4	De Angelis et al. 2020a
VPS	M	-18.9	12	De Angelis et al. 2020a
VPS	M	-19.3	12.1	De Angelis et al. 2020a
VPS	M	-19.2	11.3	De Angelis et al. 2020a
VPS	M	-19.5	10	De Angelis et al. 2020a
VPS	M	-18.6	11.4	De Angelis et al. 2020a
VPS	M	-18.6	12.4	De Angelis et al. 2020a
VPS	M	-19.3	10.5	De Angelis et al. 2020a
VPS	M	-18.1	13.1	De Angelis et al. 2020a

Table A.1 $\delta^{13}C$ and $\delta^{15}N$ values of the human individuals from Imperial Roman Mediterranean contexts. AN: ANAS, At: Athens, Ba: Barcelona; CB: Casal Bertone, CM: Castel Malnome, CE: Castellaccio Europarco, Cr: Croatia, Ed: Edessa, Ga: Gabii, He: Herculaneum, IS: Isola Sacra, Le: Leptiminus, LF: Lucus Feroniae, Pa: Paestum, Pom: Pompeii; Pr: Praeneste, QCP: Quarto Cappello del Prete, Ve: Velia, VPS: Via di Padre Semeria.

	AN	**At**	**Ba**	**CB**	**CM**	**CE**	**Cr**	**Ed**	**Ga**	**He**	**IS**	**Le**	**LF**	**Pa**	**Pom**	**Pr**	**QCP**	**Ve**
At	1.000																	
Ba	1.000	1.000																
CB	0.338	1.000	1.000															
CM	1.000	1.000	0.929	**0.001**														
CE	0.870	1.000	1.000	1.000	0.498													
Cr	0.097	1.000	1.000	1.000	**0.002**	1.000												
Ed	**0.003**	**0.031**	**0.003**	**0.000**	**0.000**	1.000	**0.000**											
Ga	1.000	1.000	1.000	1.000	1.000	1.000	1.000	**0.017**										
He	1.000	1.000	0.416	**0.000**	1.000	0.334	**0.000**	**0.000**	1.000									
IS	**0.000**	0.957	1.000	1.000	**0.000**	1.000	**0.001**	**0.000**	0.184	**0.000**								
Le	**0.000**	**0.002**	**0.000**	**0.000**	**0.000**	1.000	**0.000**	1.000	**0.000**	**0.000**	**0.000**							
LF	1.000	0.286	**0.002**	**0.000**	**0.031**	0.062	**0.000**	**0.000**	**0.002**	**0.002**	**0.000**	**0.000**						
Pa	1.000	1.000	1.000	**0.044**	1.000	0.454	**0.049**	**0.000**	1.000	1.000	**0.000**	**0.000**	1.000					
Pom	1.000	1.000	1.000	1.000	1.000	1.000	0.849	**0.005**	1.000	1.000	**0.002**	**0.000**	0.092	1.000				
Pr	0.103	**0.014**	**0.000**	**0.000**	**0.000**	**0.006**	**0.000**	**0.000**	**0.000**	**0.000**	**0.000**	**0.000**	1.000	1.000	**0.000**			
QCP	1.000	1.000	1.000	0.617	1.000	1.000	0.486	**0.001**	1.000	1.000	**0.001**	**0.000**	1.000	1.000	1.000	**0.020**		
Ve	1.000	0.231	**0.000**	**0.000**	**0.013**	**0.014**	**0.000**	**0.000**	**0.000**	**0.002**	**0.000**	**0.000**	0.578	1.000	1.000	**0.000**	1.000	
VPS	1.000	1.000	1.000	1.000	1.000	1.000	1.000	**0.000**	1.000	1.000	**0.000**	**0.000**	**0.020**	1.000	1.000	**0.000**	1.000	0.090

Table A.2 p-values obtained by applying the non-paramentric Pairwise Wilcoxon Rank Sum Test (R version 4.0.3) adjusted by Bonferroni for multiple testing to the $\delta^{13}C$ values. Results were considered significant when $p \leq 0.05$ (highlighted in bold). AN: ANAS, At: Athens, Ba: Barcelona; CB: Casal Bertone, CM: Castel Malnome, CE: Castellaccio Europarco, Cr: Croatia, Ed: Edessa, Ga: Gabii, He: Herculaneum, IS: Isola Sacra, Le: Leptiminus, LF: Lucus Feroniae, Pa: Paestum, Pom: Pompeii; Pr: Praeneste, QCP: Quarto Cappello del Prete, Ve: Velia, VPS: Via di Padre Semeria.

	AN	At	Ba	CB	CM	CE	Cr	Ed	Ga	He	IS	Le	LF	Pa	Pom	Pr	QCP	Ve
At	1.000																	
Ba	1.000	**0.046**																
CB	1.000	1.000	1.000															
CM	0.880	1.000	1.000	1.000														
CE	1.000	1.000	1.000	1.000	0.986													
Cr	1.000	1.000	**0.000**	**0.000**	**0.000**	1.000												
Ed	1.000	1.000	**0.001**	0.103	0.068	1.000	1.000											
Ga	1.000	1.000	1.000	1.000	1.000	1.000	0.133	0.781										
He	1.000	1.000	**0.005**	**0.004**	**0.002**	1.000	1.000	1.000	1.000									
IS	**0.003**	**0.017**	1.000	0.317	0.717	**0.035**	**0.000**	**0.000**	0.639	**0.000**								
Le	**0.000**	**0.001**	**0.001**	**0.000**	**0.000**	**0.004**	**0.000**	**0.000**	**0.000**	**0.000**	**0.000**							
LF	1.000	1.000	0.700	0.509	0.171	1.000	1.000	1.000	1.000	1.000	**0.000**	**0.000**						
Pa	1.000	0.552	**0.001**	**0.000**	**0.000**	1.000	**0.000**	**0.000**	**0.001**	**0.000**	**0.000**	**0.000**	**0.000**					
Pom	1.000	1.000	**0.000**	**0.007**	**0.005**	1.000	1.000	1.000	0.200	1.000	**0.000**	**0.000**	1.000	**0.000**				
Pr	1.000	1.000	**0.000**	**0.000**	**0.000**	1.000	**0.020**	0.309	**0.015**	**0.002**	**0.000**	**0.000**	0.945	0.341	0.402			
QCP	1.000	1.000	0.056	0.191	0.055	1.000	1.000	1.000	1.000	1.000	**0.000**	**0.000**	1.000	**0.048**	1.000	1.000		
Ve	1.000	0.616	**0.000**	**0.000**	**0.000**	1.000	**0.000**	**0.000**	**0.000**	**0.000**	**0.000**	**0.000**	**0.000**	1.000	**0.000**	1.000	0.226	
VPS	0.207	**0.039**	1.000	1.000	1.000	0.279	**0.000**	**0.000**	1.000	**0.000**	1.000	**0.001**	**0.009**	**0.000**	**0.000**	**0.000**	**0.003**	**0.000**

Table A.3 p-values obtained by applying the non-paramentric Pairwise Wilcoxon Rank Sum Test (R version 4.0.3) adjusted by Bonferroni for multiple testing to the $\delta^{15}N$ values. Results were considered significant when $p \leq 0.05$ (highlighted in bold). AN: ANAS, At: Athens, Ba: Barcelona; CB: Casal Bertone, CM: Castel Malnome, CE: Castellaccio Europarco, Cr: Croatia, Ed: Edessa, Ga: Gabii, He: Herculaneum, IS: Isola Sacra, Le: Leptiminus, LF: Lucus Feroniae, Pa: Paestum, Pom: Pompeii; Pr: Praeneste, QCP: Quarto Cappello del Prete, Ve: Velia, VPS: Via di Padre Semeria.

Group	Animal	$\delta^{13}C$	$\delta^{15}N$	Site	*Publication*
Domestic herbivore	Cattle	-20.7	5.2	IS	Prowse et al. 2004; 2005
Domestic herbivore	Horse	-20.4	6	IS	Prowse et al. 2004; 2005
Domestic herbivore	Sheep/Goat	-20.9	5.8	IS	Prowse et al. 2004; 2005
Domestic herbivore	Donkey	-21.2	3.6	IS	Prowse et al. 2004; 2005
Domestic herbivore	Cattle	-22.6	2.9	Ve	Craig et al. 2009
Domestic herbivore	Horse	-20.5	3.1	Ve	Craig et al. 2009
Domestic herbivore	Horse	-21.4	4	Ve	Craig et al. 2009
Domestic herbivore	Horse	-20.5	3.5	Ve	Craig et al. 2009
Domestic herbivore	Horse	-20.6	5.7	Ve	Craig et al. 2009
Domestic herbivore	Horse	-21.6	2.3	Ve	Craig et al. 2009
Domestic herbivore	Goat	-19.1	6.5	Ve	Craig et al. 2009
Domestic herbivore	Goat	-21.2	2.6	Ve	Craig et al. 2009
Domestic herbivore	Cattle	-21.5	5.3	CM	De Angelis et al. 2020a
Domestic herbivore	Sheep	-21.1	6.7	PS	De Angelis et al. 2020a
Domestic herbivore	Cattle	-20.1	6.7	PS	De Angelis et al. 2020a
Domestic herbivore	Goat	-20.6	4.2	Col	De Angelis et al. 2020a
Domestic herbivore	Sheep	-21.8	5.4	Col	De Angelis et al. 2020a
Domestic herbivore	Cattle	-20.8	5.4	Col	De Angelis et al. 2020a
Domestic herbivore	Cattle	-21.3	5	Po	O'Connell et al., 2019
Domestic herbivore	Cattle	-21.3	2.9	Po	O'Connell et al., 2019
Domestic herbivore	Cattle	-21.3	5	Po	O'Connell et al., 2019
Domestic herbivore	Cattle	-19.6	9.5	Po	O'Connell et al., 2019
Domestic herbivore	Sheep	-20.9	4.8	Po	O'Connell et al., 2019
Domestic herbivore	Sheep	-21.1	3.3	Po	O'Connell et al., 2019
Domestic herbivore	Sheep	-20.7	7.2	Po	O'Connell et al., 2019
Domestic herbivore	Sheep/Goat	-20.3	6.2	Ba	Rissech et al. 2016
Domestic herbivore	Sheep/Goat	-20.6	3.9	Ba	Rissech et al. 2016
Domestic herbivore	Cattle	-22	1.9	Ba	Rissech et al. 2016
Domestic herbivore	Cattle	-20.7	2.8	Ba	Rissech et al. 2016
Domestic herbivore	Cattle	-21.1	3.5	Ba	Rissech et al. 2016
Domestic herbivore	Cattle	-20.6	2.8	Ba	Rissech et al. 2016
Domestic herbivore	Sheep/goat	-19.1	6	Le	Keenleyside et al. 2009
Domestic herbivore	Sheep	-21.1	10.4	Le	Keenleyside et al. 2009
Domestic herbivore	Cattle	-18.8	10.3	Le	Keenleyside et al. 2009
Domestic herbivore	Goat	-18.3	6.2	Le	Keenleyside et al. 2009
Domestic herbivore	Sheep	-19.8	12.9	Le	Keenleyside et al. 2009
Domestic herbivore	Equid	-21	6.9	Le	Keenleyside et al. 2009
Domestic herbivore	Cattle	-20.67	3.66	Cr	Lightfoot et al. 2012
Domestic herbivore	Cattle	-19.96	3.61	Cr	Lightfoot et al. 2012
Domestic herbivore	Cattle	-20.87	4.66	Cr	Lightfoot et al. 2012
Domestic herbivore	Horse/donkey	-21.4	2.52	Cr	Lightfoot et al. 2012
Domestic herbivore	Horse/donkey	-20.76	7.51	Cr	Lightfoot et al. 2012
Domestic herbivore	Cattle	-20.25	4.75	Cr	Lightfoot et al. 2012
Domestic herbivore	Cattle	-20.56	4.19	Cr	Lightfoot et al. 2012
Domestic herbivore	Cattle	-19.57	5.43	Cr	Lightfoot et al. 2012
Domestic herbivore	Cattle	-20.52	3.99	Cr	Lightfoot et al. 2012
Domestic herbivore	Cattle	-20.18	3.28	Cr	Lightfoot et al. 2012
Domestic herbivore	Cattle	-20.59	4.79	Cr	Lightfoot et al. 2012
Domestic herbivore	Cattle	-20.72	5.16	Cr	Lightfoot et al. 2012
Domestic herbivore	Sheep/goat	-21.4	5.28	Cr	Lightfoot et al. 2012
Domestic herbivore	Sheep/goat	-20.42	4.82	Cr	Lightfoot et al. 2012
Domestic herbivore	Sheep/goat	-20.78	5.6	Cr	Lightfoot et al. 2012
Domestic herbivore	Sheep/goat	-19.85	3.15	Cr	Lightfoot et al. 2012
Domestic herbivore	Sheep/goat	-19.56	4.8	Cr	Lightfoot et al. 2012

Domestic herbivore	Sheep/goat	-19.92	5.23	Cr	Lightfoot et al. 2012
Domestic herbivore	Sheep/goat	-21.15	3.71	Cr	Lightfoot et al. 2012
Domestic herbivore	Sheep/goat	-20.48	4.95	Cr	Lightfoot et al. 2012
Domestic herbivore	Sheep/goat	-20.14	4.75	Cr	Lightfoot et al. 2012
Domestic herbivore	Sheep/goat	-19.98	6.69	Cr	Lightfoot et al. 2012
Domestic herbivore	Cattle	-20.8	4.58	Cr	Lightfoot et al. 2012
Domestic herbivore	Cattle	-20.92	5.92	Cr	Lightfoot et al. 2012
Domestic herbivore	Sheep/goat	-21.23	5.16	Cr	Lightfoot et al. 2012
Domestic herbivore	Cattle	-20.36	4.73	Cr	Lightfoot et al. 2012
Domestic herbivore	Sheep/goat	-21.1	5.24	Cr	Lightfoot et al. 2012
Domestic herbivore	Sheep/goat	-20.32	3.79	Cr	Lightfoot et al. 2012
Domestic herbivore	Sheep/goat	-20.43	3.96	Cr	Lightfoot et al. 2012
Domestic herbivore	Cattle	-21.09	3.6	Cr	Lightfoot et al. 2012
Domestic herbivore	Cattle	-19.68	4.08	Cr	Lightfoot et al. 2012
Domestic herbivore	Cattle	-20.46	3.97	Cr	Lightfoot et al. 2012
Domestic herbivore	Sheep/goat	-20.84	6.05	Cr	Lightfoot et al. 2012
Domestic herbivore	Sheep/goat	-21.65	3.6	Cr	Lightfoot et al. 2012
Domestic herbivore	Sheep/goat	-21	3.5	Pom	Pate et al. 2016
Domestic herbivore	Cattle	-20.3	3.4	Pom	Pate et al. 2016
Wild herbivore	Deer	-23	2.2	Ve	Craig et al. 2009
Wild herbivore	Deer	-21.8	2	Ve	Craig et al. 2009
Wild herbivore	Deer	-22.5	2.6	Ve	Craig et al. 2009
Wild herbivore	Deer	-22	4.7	Ve	Craig et al. 2009
Wild herbivore	Deer	-22.2	5.9	CM	De Angelis et al. 2020a
Wild herbivore	Deer	-19.7	5	CM	De Angelis et al. 2020a
Wild herbivore	Hare	-21.9	3.8	Col	De Angelis et al. 2020a
Wild herbivore	Hare	-21.5	2	Pod	O'Connell et al., 2019
Wild herbivore	Red deer	-20.2	4.4	Ba	Rissech et al. 2016
Wild herbivore	Red deer	-20	2.7	Ba	Rissech et al. 2016
Wild herbivore	Red deer	-20.1	3.5	Ba	Rissech et al. 2016
Wild herbivore	Red deer	-19.9	2.2	Ba	Rissech et al. 2016
Wild herbivore	Red deer	-20.1	2.9	Ba	Rissech et al. 2016
Wild herbivore	Hare	-18.2	6	Le	Keenleyside et al. 2009
Domestic omnivore	Pig	-21	5.2	IS	Prowse et al. 2004; 2005
Domestic omnivore	Pig	-21	3.1	Ve	Craig et al. 2009
Domestic omnivore	Pig	-21.5	3.2	Ve	Craig et al. 2009
Domestic omnivore	Pig	-20.5	7.9	Ve	Craig et al. 2009
Domestic omnivore	Pig	-20.9	5.3	Ve	Craig et al. 2009
Domestic omnivore	Pig	-21.3	4	Ve	Craig et al. 2009
Domestic omnivore	Pig	-20.4	6.7	Col	De Angelis et al. 2020a
Domestic omnivore	Pig	-20.2	4.5	Col	De Angelis et al. 2020a
Domestic omnivore	Chicken	-20.8	5.4	Col	De Angelis et al. 2020a
Domestic omnivore	Pig	-20	6.3	Col	De Angelis et al. 2020a
Domestic omnivore	Pig	-21.1	8.6	Po	O'Connell et al., 2019
Domestic omnivore	Pig	-20.4	4.3	Po	O'Connell et al., 2019
Domestic omnivore	Pig	-20.8	3.5	Po	O'Connell et al., 2019
Domestic omnivore	Pig	-20.2	7	Pom	Pate et al. 2016
Domestic omnivore	Pig	-20.75	4.08	LF	Tafuri et al. 2018
Domestic omnivore	Pig	-20.93	4.61	LF	Tafuri et al. 2018
Domestic omnivore	Pig	-19.4	4.4	Ba	Rissech et al. 2016
Domestic omnivore	Pig	-20.2	8.7	Ba	Rissech et al. 2016
Domestic omnivore	Pig	-20	7.3	Ba	Rissech et al. 2016
Domestic omnivore	Pig	-19.9	4.3	Ba	Rissech et al. 2016
Domestic omnivore	Pig	-20.3	3	Ba	Rissech et al. 2016
Domestic omnivore	Pig	-20.3	4.8	Ba	Rissech et al. 2016

Domestic omnivore	Chicken	-18.6	10.3	Ba	Rissech et al. 2016
Domestic omnivore	Pig	-19	9.6	Le	Keenleyside et al. 2009
Domestic omnivore	Pig	-20.51	8.91	Cr	Lightfoot et al. 2012
Domestic omnivore	Pig	-20.62	5.59	Cr	Lightfoot et al. 2012
Domestic omnivore	Pig	-20.71	5.35	Cr	Lightfoot et al. 2012
Domestic omnivore	Pig	-19.89	5.52	Cr	Lightfoot et al. 2012
Domestic omnivore	Pig	-19.95	7.65	Cr	Lightfoot et al. 2012
Domestic omnivore	Pig	-20.25	5.48	Cr	Lightfoot et al. 2012
Marine fish	Tuna	-13.5	12.1	Ve	Craig et al. 2009
Marine fish	Tuna	-13.9	9.8	Ve	Craig et al. 2009
Marine fish	Tuna	-14.9	9.9	Ve	Craig et al. 2009
Marine fish	Fish	-12.6	9.1	Ve	Craig et al. 2009
Marine fish	Fish	-13.9	7.9	Pod	O'Connell et al., 2019
Marine fish	Fish	-15.1	9.9	Pod	O'Connell et al., 2019
Marine fish	Fish	-13.4	12.1	Pod	O'Connell et al., 2019
Marine fish	Fish	-7.6	10.1	Pod	O'Connell et al., 2019
Marine fish	Garum	-13.6	9.4	Af	Prowse 2001
Marine fish	Garum	-17.8	4.9	Ad	Prowse 2001
Marine fish	Garum	-14.3	6.2	Ad	Prowse 2001
Marine fish	Garum	-13.5	5.9	Ad	Prowse 2001
Marine fish	Garum	-10.96	8.24	Cr	Lightfoot et al. 2012
Marine fish	Garum	-12.2	4.9	Pom	Pate et al. 2016
Marine fish	Sparidae	-14.8	5.7	Pom	Craig et al. 2013
Marine fish	Sparidae	-13.9	6.1	Pom	Craig et al. 2013
Marine fish	Sparidae	-15.4	6.6	Pom	Craig et al. 2013
Marine fish	Sparidae	-14.4	6.7	Pom	Craig et al. 2013
Marine fish	Sparidae	-14.5	8.5	Pom	Craig et al. 2013
C_3 cereals	Wheat	-22.5	9.1	Po	O'Connell et al., 2019
C_3 cereals	Wheat	-23	10.1	Po	O'Connell et al., 2019
C_3 cereals	Wheat	-23.4	4	Po	O'Connell et al., 2019
C_3 cereals	Wheat	-23	10.9	Po	O'Connell et al., 2019
C_3 cereals	Barley	-23.7	0.8	Pom	Pate et al. 2016
Legumes	Peas	-26.1	2	Pom	Pate et al. 2016
Legumes	Lentils	-23	5	Pom	Pate et al. 2016

Table A.4 $\delta^{13}C$ and $\delta^{15}N$ values of animal and wheat remains analysed from Imperial Roman Mediterranean contexts. Ba: Barcelona; CM: Castel Malnome, Col: Colosseum, Cr: Croatia, IS: Isola Sacra, Le: Leptiminus, LF: Lucus Feroniae, Po: Portus Romae, Pod: $V^{th} - VI^{th}$ centuries AD Portus Romae, Pom: Pompeii, Ve: Velia, VPS: Via di Padre Semeria. Horse and donkey specimens were not included in the statistical analyses since these species were probably not preferentially consumed.

Domestic herbivores

	Ba	CM	Col	Cr	IS	Le	Po	Pom	PS
CM	1.000								
Col	1.000	1.000							
Cr	1.000	1.000	1.000						
IS	1.000	1.000	1.000	1.000					
Le	1.000	1.000	1.000	1.000	1.000				
Po	1.000	1.000	1.000	1.000	1.000	1.000			
Pom	1.000	1.000	1.000	1.000	1.000	1.000	1.000		
PS	1.000	1.000	1.000	1.000	1.000	1.000	1.000	1.000	
Ve	1.000	1.000	1.000	1.000	1.000	1.000	1.000	1.000	1.000

Domestic omnivores

	Ba	Col	Cr	IS	Le	LF	Po	Pom
Col	1.000							
Cr	1.000	1.000						
IS	1.000	1.000	1.000					
Le	1.000	1.000	1.000	1.000				
LF	1.000	1.000	1.000	1.000	1.000			
Po	0.801	1.000	1.000	1.000	1.000	1.000		
Pom	1.000	1.000	1.000	1.000	1.000	1.000	1.000	
Ve	0.205	1.000	0.848	1.000	1.000	1.000	1.000	1.000

Wild herbivores

	Ba	CM	Col	Le	Pod
CM	1.000				
Col	1.000	1.000			
Le	1.000	1.000	1.000		
Pod	1.000	1.000	1.000	1.000	
Ve	1.000	1.000	1.000	1.000	1.000

Table A.5 p-values obtained by applying the non-paramentric Pairwise Wilcoxon Rank Sum Test (R version 4.0.3) adjusted by Bonferroni for multiple testing to the $\delta^{13}C$ values of the animals divided by group. Results were considered significant when $p \leq 0.05$ (highlighted in bold). Ba: Barcelona; CM: Castel Malnome, Col: Colosseum, Cr: Croatia, IS: Isola Sacra, Le: Leptiminus, LF: Lucus Feroniae, Po: Portus Romae, Pod: $Vth - VIth$ centuries AD Portus Romae, Pom: Pompeii, Ve: Velia, VPS: Via di Padre Semeria.

Domestic herbivores

	Ba	**CM**	**Col**	**Cr**	**IS**	**Le**	**Po**	**Pom**	**PS**
CM	1.000								
Col	1.000	1.000							
Cr	1.000	1.000	1.000						
IS	1.000	1.000	1.000	1.000					
Le	0.770	1.000	**0.030**	0.839	0.672				
Po	1.000	1.000	1.000	1.000	1.000	1.000			
Pom	1.000	1.000	1.000	1.000	1.000	1.000	1.000		
PS	1.000	1.000	0.949	1.000	1.000	1.000	1.000	1.000	
Ve	1.000	1.000	1.000	1.000	1.000	0.120	1.000	1.000	1.000

Domestic omnivores

	Ba	**Col**	**Cr**	**IS**	**Le**	**LF**	**Po**	**Pom**
Col	1.000							
Cr	1.000	1.000						
IS	1.000	1.000	1.000					
Le	1.000	1.000	1.000	1.000				
LF	1.000	1.000	1.000	1.000	1.000			
Po	1.000	1.000	1.000	1.000	1.000	1.000		
Pom 1.000	1.000	1.000	1.000	1.000	1.000	1.000		
Ve	1.000	1.000	1.000	1.000	1.000	1.000	1.000	1.000

Wild herbivores

	Ba	**CM**	**Col**	**Le**	**Pod**
CM	1.000				
Col	1.000	1.000			
Le	1.000	1.000	1.000		
Pod	1.000	1.000	1.000	1.000	
Ve	1.000	1.000	1.000	1.000	1.000

Table A.6 p-values obtained by applying the non-paramentric Pairwise Wilcoxon Rank Sum Test (R version 4.0.3) adjusted by Bonferroni for multiple testing to the $\delta^{15}N$ values of the animals divided by group. Results were considered significant when $p \leq 0.05$ (highlighted in bold). Ba: Barcelona; CM: Castel Malnome, Col: Colosseum, Cr: Croatia, IS: Isola Sacra, Le: Leptiminus, LF: Lucus Feroniae, Po: Portus Romae, Pod: $Vth - VIth$ centuries AD Portus Romae, Pom: Pompeii, Ve: Velia, VPS: Via di Padre Semeria.

Appendix B

CSIA-AA protocol - BioArCh, University of York

The protocol for the hydrolysis and derivatisation of amino acids used at BioArCh, Department of Archaeology, University of York is presented below. The protocol was adapted by Alison Harris, Helen M. Talbot and the author of this thesis from Metges *et al.* (1996); Corr *et al.* (2007b); Styring (2012); Philben *et al.* (2018).

SOP Name/Title: AMINO ACIDS – Hydrolysis and NAIP derivatisation		
Document Storage Location/Source		Document Number: **M00**
SOP Originator: **Laboratory Manager**	Approving Position: **Director**	Effective Date: **09/08/2012**
Name: **Matthew von Tersch**	Name: **Oliver Craig**	Last Edited Date: **05/06/2021**
Signature:	Signature:	Other:

LOCATION:

ENV/208 and ENV/209

COSHH REF:

Refer to the attached COSHH risk assessment.

PRINCIPAL:

Analysis of single-compound amino acid isotope ratios ($\delta^{13}C$ and $\delta^{15}N$) on samples derived from humans, animals and plants can provide insight into the diet and health of individuals from pre-history to the modern day (e.g., Ohkouchi et al. 2017, Jaouen et al. 2019, Commendador et al. 2019, Grimes et al. 2021).

Collagen, previously extracted from human and animal bone, is hydrolysed using 6 M HCl to release amino acids which can be analysed for their individual $\delta^{13}C$ and $\delta^{15}N$ compound specific isotope values by comparison to a range of international and in-house reference materials of known isotopic composition.

Amino acids are small, polar and in some cases highly volatile molecules which must be derivatised before they can be analysed by gas chromatography – combustion – Isotope Ratio Mass Spectrometry (GC-c-IRMS).

The derivatisation method described below is known as the *N*-acetyl-isopropyl (NAIP) method (after Styring et al. 2015) and is utilised because it reduces the number of additional C atoms added to each amino acid during the derivatisation process compared to some other procedures in use (Corr et al. 2007). However, this, and other derivatisation processes do not add additional N atoms to the molecules and numerous alternative procedures are available (after Corr et al. 2007).

After deriviatisation, samples are re-suspended in ethylacetate and analysed in house on the Thermo Delta V plus system with

All members of BioArCh wishing to investigate amino acids in this way are responsible for ensuring that the procedures detailed in the SOP are followed precisely when carrying out collagen hydrolysis and derivatisation and when preparing aliquots of standards and samples for analysis by GC-c-IRMS.

References

Commendador, A.S., Finney, B.P., Fuller, B.T., Tromp, M. and Dudgeon, J.V., 2019. Multiproxy isotopic analyses of human skeletal material from Rapa Nui: Evaluating the evidence from carbonates, bulk collagen, and amino acids. *American journal of physical anthropology*, 169(4), pp.714-729.

Corr, L.T., Berstan, R. and Evershed, R.P., 2007. Optimisation of derivatisation procedures for the determination of $\delta^{13}C$ values of amino acids by gas chromatography/combustion/isotope ratio mass spectrometry. *Rapid Communications in Mass Spectrometry*, 21(23), pp.3759-3771.

Jaouen, K., Richards, M.P., Le Cabec, A., Welker, F., Rendu, W., Hublin, J.J., Soressi, M. and Talamo, S., 2019. Exceptionally high $\delta^{15}N$ values in collagen single amino acids confirm Neandertals as high-trophic level carnivores. *Proceedings of the National Academy of Sciences*, 116(11), pp.4928-4933.

Ma, Y., Grimes, V., Van Biesen, G., Shi, L., Chen, K., Mannino, M.A. and Fuller, B.T., 2021. Aminoisoscapes and palaeodiet reconstruction: New perspectives on millet-based diets in China using amino acid $\delta^{13}C$ values. *Journal of Archaeological Science,* 125.

Ohkouchi, N., Chikaraishi, Y., Close, H.G., Fry, B., Larsen, T., Madigan, D.J., McCarthy, M.D., McMahon, K.W., Nagata, T., Naito, Y.I. and Ogawa, N.O., 2017. Advances in the application of amino acid nitrogen isotopic analysis in ecological and biogeochemical studies. *Organic Geochemistry*, 113, pp.150-174.

Styring, A.K., Fraser, R.A., Arbogast, R.M., Halstead, P., Isaakidou, V., Pearson, J.A., Schäfer, M., Triantaphyllou, S., Valamoti, S.M., Wallace, M. and Bogaard, A., 2015. Refining human palaeodietary reconstruction using amino acid δ15N values of plants, animals and humans. *Journal of Archaeological Science*, 53, pp.504-515.

SAMPLE TYPE:

Archaeological or modern bone collagen; Archaeological or modern seeds.

REAGENTS:

Stock reagents (excluding amino acids)**:**

- Acetic Anhydride (Sigma-Aldrich 320102-100ML; Stored under fumehood in ENV/208)
- Acetone (Fisher A/0600/PB17 >99.8%; Stored under fumehood in ENV/208)
- Acetyl Chloride (Sigma-Aldrich 00990-100ML; Stored under fumehood in ENV/208)
- Dichloromethane (DCM; stored under fumehood in ENV/209)
- Ethanol (Stored under fumehood ENV/208 & 209)
- Ethyl acetate (Sigma-Aldrich 34858-2.5L for HPLC > 99.7%; Stored under fumehood in ENV/208)
- Hexane (Stored under fumehood in ENV/209)
- Methanol (Stored under fumehood ENV/208 & 209)
- Molecular sieve 0.3 nm beads (Merck 1.05704.0250 (Stored in chemicals cupboard ENV/208)
- 2-Propanol (Honeywell 603-117-00-0; Chromasolve Plus for HPLC >99.9%; Stored under fumehood in ENV/208)

- Sodium Chloride (S/3161/53 Fisher [sourced from Biology stores]; Stored in chemicals cupboard ENV/208)
- Hydrochloric Acid 12 M (Stored under fumehood in ENV/209)
- Triethylamine (Sigma-Aldrich 471283-100ML; Stored under fumehood in ENV/208)
- Water (HPLC grade; Stored under fumehood in ENV/208)

Working reagents (excluding amino acids)**:**

- Ethyl acetate (Stored in reagent bottle in Fume hood in ENV/208)
- DCM (Stored in reagent bottle in Fume hood in ENV/208)
- *n*-hexane/DCM (3:2 v/v) Stored in reagent bottle in Fume hood in ENV/208)
- Ethyl acetate wash solutions and dilution solution (Stored in individual scintillation vials in fume hood in ENV/208)
- Hydrochloric acid 6 M (Stored in 50 ml Falcon tube in Fridge F8 in ENV/208)
- 0.1 M HCL (Stored in Fridge F8 in ENV/208)

MATERIALS REQUIRED (see Figs 1 & 2) (excluding amino acids)**:**

- Sample collagen

- 20 ml scintillation vials (Ashed)
- Glass Hach tubes (test tubes) (Ashed) and black phenolic caps (washed and oven dry)
- Reactivials (Ashed) and cap (washed and oven dry)
- Short and long glass Pasteur pipettes (Ashed)
- 3.5 ml Hydrolysis vials (Ashed)
- 1.5 ml GC vials (Ashed) and caps (Sourced from lipids supplies in ENV/209)
- 1.5 ml GC vials, with integrated inserts (Ashed; Chromacol 03-FISV) and caps (Chromacol 9-SCK(B)-ST101)
- 1000 µl Gilson (or FINN) pipette or similar with flexible tube adaptor to accommodate glass Pasteur pipettes (Located in ENV/208)
- 200 µl Gilson (or FINN) pipette (Located in ENV/208)
- Long re-useable stainless steel needle
- Disposable Long (Sterican 0.80 x 80 mm, P/N 4665465) and short (BD Microlance P/N 304432) hypodermic needles (amino acids cupboard ENV/208)
- 10 ml plastic syringe (BD Emerald 10 ml Luer Tip – P/N 307736; amino acids cupboard ENV/208))
- Nanoseps (0.45 µm Bio-Inert 100/pk PALL Life Sciences ODM45C34)
- Teflon tape (sourced from B&Q; located in amino acids cupboard ENV/208)

ASHING – Items listed as "Ashed" are first wrapped tightly in Aluminium foil. Small holes are them made in the foil and Amino Acids written on each package in marker pen. Foil packages are them heated in the muffle furnace at 450°C for 6 h.

IMPORTANT:
If stocks of any of the reagents and materials listed above are running low, inform Helen Talbot (or other technician) immediately so that new supplies can be ordered.

All users are responsibility for ensuring that stocks of ashed glassware are available at all times for all users of the amino acid procedure.

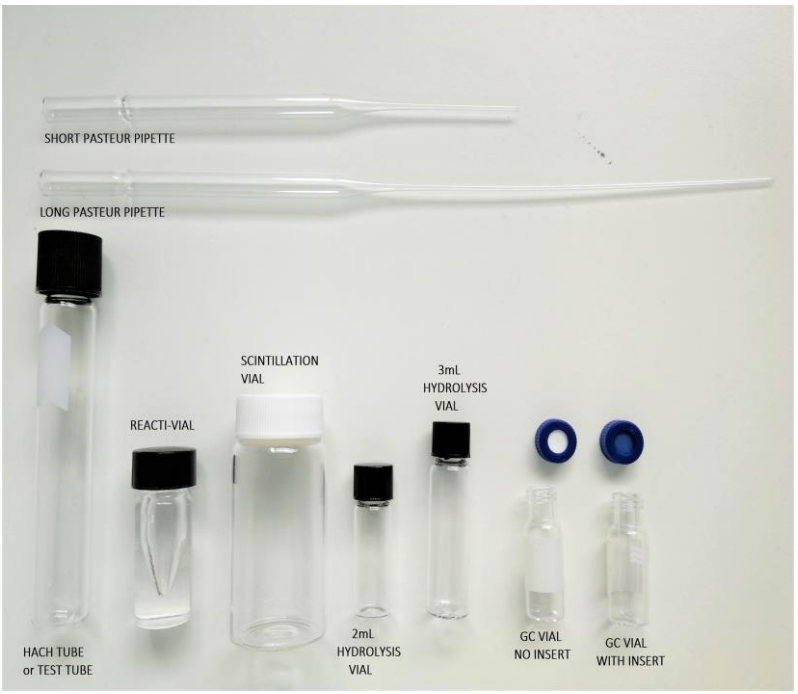

Figure 1. *Examples of glass items required for procedure. All glass items must be ashed in the muffle furnace before use. (Note: 2 ml Hydrolysis vial no longer used).*

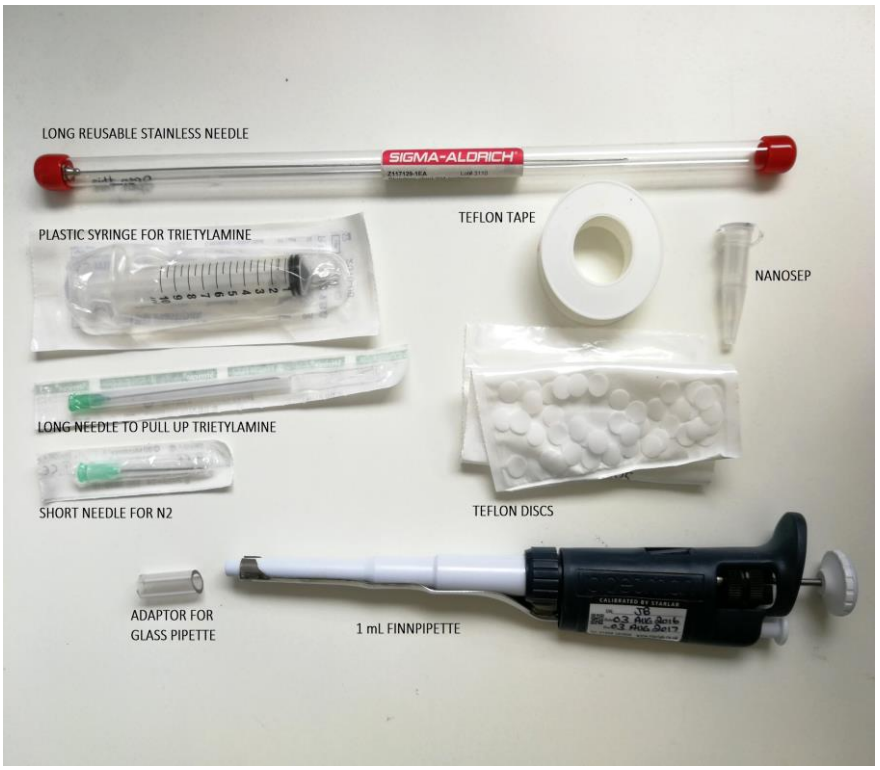

Figure 2. *Examples of other items (disposable and non-disposable) required for procedure. (Note: Teflon discs no longer used).*

EQUIPMENT TRAINING REQUIRED (please see technician)

Gilson or Finn pipettes
Magnetic stirrer
Vortex
Centrifuge
5 d.p balance
Sonic bath
Nitrogen evaporator and heating blocks
Muffle Furnace
Oven

SAFETY:

BEFORE starting any lab work, ALL users must read the attached COSHH risk assessment, complete the form at the end and return to Matthew von Tersch.

- The fumehood must be used at all times where practically possible
- Gloves, lab coat and protective spectacles must be worn at all times
- This procedure uses toxic organic solvents; always monitor the condition of gloves if splashing occurs and replace if required.

WASTES:

CHEMICALS: See attached COSHH for dealing with waste

Throughout this procedure, most of the excess chemical reagents used, in minimum possible quantities, are removed via evaporation under N_2 in the fume hood. Disposable vials containing other small volumes (<1 ml) of unused reagents or mixtures (e.g. acidified 2-propanol; Part C, sub-section 1.2 below) should be blown down under N_2 or left to evaporate in the back of the fume hood for 24 h and then placed in the yellow sharps bin (in Fume hood ENV/208) before disposal of the bin via normal waste streams (Biology Stores).

Very small volumes of solvents (e.g. ~0.6 ml/sample of Hexane/DCM [3:2 v/v] used in the de-fatting process; Part B, sub-section 2.8 and 2.9) or from needle washing (Part C, section 4) for dilutions are removed by transfer to a waste beaker containing blue roll to increase surface area and promote rapid evaporation.

For any larger volumes of liquid **CHEMICALS WASTE**, the following standard rules apply:

ALL chemical wastes should be decanted into the appropriate **PLASTIC** coated waste bottle (See example in Fig. 3 below). **NEVER** pour these wastes down the sink.

Waste	Waste Bottle
DCM only	Halogenated waste bottle
Hexane/DCM mix	Halogenated waste bottle
Methanol Only	Flammable waste bottle
Hexane Only	Flammable waste bottle
Ethyl acetate Only	Flammable waste bottle

The waste bottles can be found in the waste cabinet in ENV/209 or at the back of one of the fumehoods (ENV/209). Waste bottles should be filled to the shoulder only - **NEVER** to the very top.

Figure 3. *Example of waste solvent bottle (Located in Fume Hood ENV/209)*

When a bottle is full – notify the technician and start a new bottle, placing the appropriate label on the front. These labels can be found on the side of the waste cabinet in ENV/209.

CLEANING REUSABLE ITEMS:

PLEASE NOTE: It is your responsibility to ensure that any glassware you have used is cleaned by you.

BLACK TUBE CAPS:

The black phenolic caps used with the hach tubes and reacti vials should be washed along with the tubes in a 2-5% Decon90 bath in the large glass beakers located by sink in ENV/208. After soaking for 24 hours they should be rinsed x3 with tap water and then x3 with deionised water. Allow to dry on blue roll then wrap in foil and dry in drying oven at 45°C for ~24 h.

DIRTY REUSABLE GLASSWARE (*beakers/test tubes etc)*:

Once the procedure is concluded, all tubes and vials should be left open under the fume hood overnight to dry out any remaining organic solvent residue. Blow down possible leftover

acetyl chloride, acidified propanol, TEA and acetic anhydride under N_2 then dispose of these vials in the yellow waste bin in the fume hood.

When Hach tubes and reacti vials are dry, remove all labels with acetone, rinse with tap water in the chemicals sink and scrub with a bottlebrush to remove any residue (if required). Place tubes in 2-5% Decon90 bath for at least 24 h in large glass beakers located by chemicals sink (ENV/208.)

After 24 h scrub tubes with the bottle brush, rinse several times in normal tap water and then rinse x3 in deionised water. Leave to dry on rack next to sink or loosely wrap in aluminium foil and dry in the oven at 45°C. When dry, tightly wrap clean glassware in aluminium foil and ash in the muffle furnace (in ENV/209) at 450°C for 6 hours (*speak to the technician about this*). On the next day take the glassware out of the oven and place it in the correct boxes inside the AAs cupboard in ENV/208.

NB Larger items of dirty glassware, other than hach tubes, reacti vials and scintillation vials, should be placed into the blue glass washing bin in the lab (e.g. beakers).

CLEAN CHEMICALLY CONTAMINATED-ONLY GLASSWARE:

Any glassware that is contaminated with solvents (Hexane, dichloromethane, methanol, Ethyl acetate; e.g. Pasteur pipettes) should be placed into the red top plastic 'sweet pots' on the bench. When full, these should be emptied into the red glass bins.

BROKEN AND / OR CHEMICALLY CONTAMINATED GLASSWARE:

Any broken glassware that is contaminated with chemicals/sample that cannot be cleaned or has been used with glass wool should be place in the yellow 13 l bin in the fume cupboard (ENV/208).

CLEANING N_2 BLOW-DOWN NEEDLES: put used needles in a clean beaker and add dichloromethane sufficient to cover up to mid-height of the needles (when pouring, make the DCM going all the way inside the needles from the upper opening to the bottom of the beaker). Cover the beaker with some aluminium foil and sonicate for 15 min at room temperature. Drain off the used DCM (Halogenated waste) and repeat sonication in clean DCM. Collect the needles in a piece of aluminium foil and store them in the oven (45°C) in ENV/209.

CLEANING THE FUMEHOOD: Always ensure the fumehood is cleaned and clear of used items as soon as possible. Dispose of all foil and empty reagent vials (see above). Spray detergent (3% decon, stored under the lab sink in ENV/208) on a piece of blue roll and scrub around the fumehood, in particular on the heating/blowing down system, N2 valve, handle etc to remove any residue. To rinse away the detergent, repeat the procedure again this time with water and blue roll. Top up any solvent reagent bottles as required.

A. Preparation of Standards for derivatisation with samples

Analysis Mode	Standards required	
	International	Sigma
Carbon	Yes	Yes
Nitrogen	Yes	No

1. PREPARATION OF INDIVIDUAL AMINO ACID STANDARD STOCK SOLUTIONS

Stock solutions should be prepared according to the instructions below.

1.1 INTERNATIONAL STANDARDS

a. Using the microbalance, prepare the following individual stock standards in separate ashed scintillation vials. Add 10 ml 0.1M Hydrochloric Acid (HCl) to each vial using a 1000 µl Gilson pipette.

b. Vials should be flushed with nitrogen, capped, parafilmed and stored at -20°C in ENV/208 (F6). All vials should show the following information:
- Name and weight of Amino Acid (e.g. 6.5 mg L-Alanine in 10 ml 0.1M HCL)
- Date prepared
- Your Name or Initials

Amino Acid	Weight Required
L-Alanine	6.5 mg
Glycine	6.2 mg
L-Valine	7.3 mg
L-Leucine	7.9 mg
Norleucine (supplied by Sigma)	7.7 mg
L-Aspartic acid	9.1 mg
L-Glutamic acid	9.4 mg
L-Phenylalanine	8.6 mg
Hydroxyproline	10.2 mg

NOTE - The required weights of each amino acid are different to account for the varying amounts of nitrogen in each standard in order to produce a similar peak area for each compound at the analysis stage.

1.2 SIGMA STANDARDS

a. Using the microbalance, add the following individual stock standards into a single ashed scintillation vial. Add 16 ml 0.1M Hydrochloric Acid (HCl) using a 1000 µl Gilson pipette.

Amino Acid	Weight Required
Alanine	10 mg each
Glycine	
Valine	
Leucine	
Isoleucine	
Proline	
Aspartic acid	
Glutamic acid	
Phenylalanine	
trans-4-Hydroxy-L-Proline	
Lysine	
Tyrosine	
Serine	
Threonine	
Methionine	
Norleucine	

b. Vials should be flushed with nitrogen, capped, parafilmed and stored at -20°C in ENV/208 (F6). All vials should show the following information:

- The vial should be named **YOSS** (York Sigma Standard) and numbered incrementally (e.g., YOSS3)
- Date prepared
- Your Name or Initials

2. PREPARATION OF WORKING SOLUTIONS FOR DERIVATISATION

2.1 International Standards mix:

a. Using a 200 µl Gilson pipette, add 50 µl of each amino acid solution into glass test tube and reduce to dryness under N_2 using the blow down on the fume hood in ENV 208.

b. Several (Hach) tubes of standard can be prepared at the same time in order to save time when starting a new derivatisation. Additional mixes should be resuspended in 100 µl 0,1M HCl and stored frozen. Mixes should then be defrosted and blown down to dryness before use.

NB: The amount can be doubled (i.e., use 100 µl of each AA solution) in order to have some spare "nitrogen standards" for future use.

2.2 Sigma Standards mix:

a. add 40 µl of the stock solution (e.g., YOSS3) into glass test tubes and reduce to dryness under N_2 using the blow down in the fume hood in ENV 208.

NB Prepared working standards should be derivatised together with the samples. This is essential for Carbon analyses.

3. PREPARATION OF INTERNAL STANDARD SOLUTION

3.1 A solution of Norleucine (Nle, SIGMA N8513-100MG) is prepared and used as an internal standard added to all blanks and standards. Before use, each new bottle of Nle powder is first analysed on the EA-IRMS in order to determine the $\delta^{13}C$ and $\delta^{15}N$ values for the stock material.

3.2 Weigh out exactly 5 mg Sigma Norleucine into a sterile scintillation vial (Fig. 4).

3.3 Add 1 ml of 0.1 M HCl using 1000 µl Gilson pipette.

3.4 Flush with N_2 then seal lid with parafilm and store at +4°C (F8 in ENV 208) until required.

***NB**: Always note the Number (e.g., Nle2) of the Norleucine you are using for each batch of samples. This is written on the lid of the scintillation vial containing the solution (e.g.,"Nle 2") as this is required to identify the exact $\delta^{13}C$ and $\delta^{15}N$ for the solution in use.*

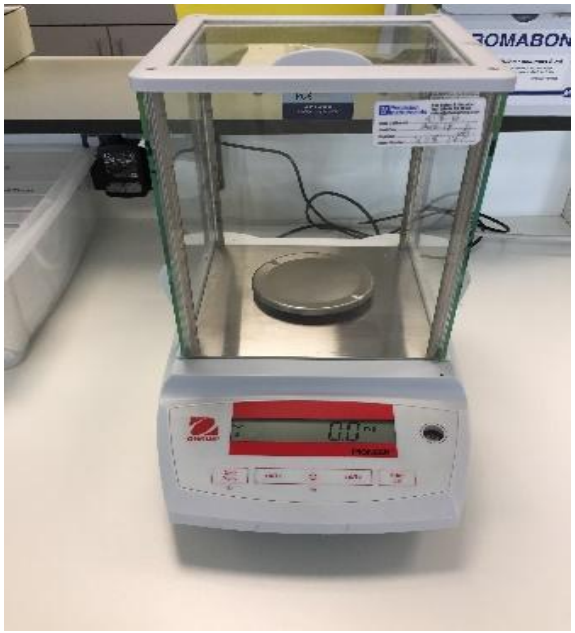

Figure 4. Use this balance (ENV/208) for weighing out samples and also for weighing exactly 5 mg of Norleucine.

B) HYDROLYSIS OF AMINO ACIDS

NOTE: *It is recommended that you weigh out samples on the day before you intend to start the hydrolysis. This means that you can add acid and start the samples heating as early as possible and therefore, 24 h later, after samples have cooled down and are ready for work-up you have the whole day to do this (Hydrolysis Day 2).*

1. Hydrolysis (Day 1)

1.1 Switch oven on and set temperature to 110°C
   a. Press **x/w** then use arrow buttons to set the temperature
   b. Put the heating block that is going to hold the reacti-vials inside the oven in order to pre-heat it.
   c. Remember to fill in details on sheet on front of oven.

1.2 Weigh out dried collagen sample into a labelled 1.0 ml reacti-vial. (Note this can be done the day before to save time.)
   a. Always carefully check that the lids for the reacti-vials fit well i.e. close tightly with no "loose movement".
   b. Weigh out 4 mg collagen per sample (but could go lower for precious samples, e.g. 2 mg for Prehistoric material) (see Fig. 3).
   c. Place large piece of foil in front of the balance, then use one smaller piece for each sample and discard after each one.
   d. Use spatula and forceps when weighing out into vial. (Collagen material is quite "fibrous" so often need forceps to remove small pieces.)
   e. To clean spatula and tweezers between samples use ethanol bottle and tissue.

1.3 Add 50 µl of Norleucine Internal standard solution (Fridge F8; ENV/208) to all samples vials and 1 blank using a 200 µl Gilson pipette.
   a. Note: add 50 µl for a 4 mg collagen sample or alter volume proportionally with starting weight of collagen (e.g. 25 µl for 2 mg).

1.4 Add 200 µl of 6M HCl to each sample using 200 µl Gilson pipette. This is made up as a stock solution (in 50 ml Falcon tube) by carefully adding 20 ml of 12 M HCl to 20 ml deionised water (do this in fume hood in ENV/209 nearest to the acid cabinet). 6 M working solution is stored in the fridge (F8) in ENV/208.

1.5 Place the reacti-vials in the oven in the heating block pre-heated at 110°C.
   a. Start heating the vials with lids slightly loose to allow any evolved gases to escape from the vial. After 1 min, close lids tightly (Note: there is a glove for holding hot vials located under Fume Hood. Remember that it has to be covered by a nitrile glove. Also use multiple gloves (2+) on the other hand to tighten the caps.
   b. Leave the vials in the oven, for exactly 24 hours. Never open the oven during the hydrolysis.

Hydrolysis (Day 2) – Filtration, de-fat and workup.

2.1 After heating for 24 h, cool the hydrolysis vials (reacti-vials) down to room temperature.

2.2 Label new batch of 1 ml reacti-vials for each sample. (Check for "good" lids.)

2.3 Transfer the hydrolysate from each sample into the inner part of a labelled nanosep using a Pasteur pipette.

a. Hold both vial and nanosep in one hand and Pasteur pipette with the other.
b. Use long pipette and allow time for the last "drop" of liquid to drip from pipette.

2.4 Filter the hydrolysate by centrifuging nanosep at 10,000 rmp for 60 s. (This should be saved as program #1 on the centrifuge; Fig. 5).

Figure 5. *Use this centrifuge (facing the lab door; ENV208). Set speed to 100 and time to 1 min/60 s. Press start. (Ensure you have a balanced number of samples in the rotor).*

2.5 Transfer filtered hydrolysate into a new clean 1 ml reacti-vial (step 2.2. above) using a Pasteur pipette, as follows:

a. Discard insert (into yellow waste bin in fume hood) from top of nanosep to access hydrolysate below.
b. Hold both vial and nanosep in one hand and pipette with the other.
c. Use long pipette and allow time for the last "drop" of liquid to drip from pipette. (You can try taking a little liquid back up into the pipette to help get the last bit out.)

2.6 Cover base of fume hood with aluminium foil and prepare 2 "foil sausages" (i.e. 2 rolls of foil of sufficient length and solidity to balance all of the Pasteur pipettes required for steps 2.8 and 2.9 below, without allowing them to touch the base of the fume hood or each other. This allows for re-use the same Pasteur pipette (one for each sample) for each of the stages below.

2.7 Using a long Pasteur pipette, add *n*-hexane/DCM (3:2 v/v) to the level of 0.4 ml of the reacti-vial and tighten the cap.

a. First tip the vial slowly a couple of times to check for leaks. If it leaks change the cap and your gloves.
b. Vortex the vial for 10-20 s.
c. Wait for separation of the two layers (upper layer organic solvent with lipophilic compounds, lower layer acidic solution containing amino acids).

2.8 Remove the upper layer with a Pasteur pipette (short form) into a solvent waste container (with paper) and carefully place each pipette onto the foil sausages (keeping track of which pipette is associated with which sample)

a. When removing the first 2 aliquots of DCM/Hexane it is ok to leave a little behind in the reacti-vial.

d. For the 3rd and final aliquot make sure you remove as much as possible but without taking any of the aqueous phase.

2.9 Repeat all steps in section 2.7 twice more (3 times in total).

2.10 Transfer remaining liquid (aqueous phase) into a new labelled Hach tube.

2.11 Blow down liquid with N_2 until completely (usually takes between 1-2 h; Fig. 6).

2.12 When dry remove from blow-down, dissolve in 100 to 200 µl of 0.1M HCl and freeze, or proceed to step one of derivatisation

a. If the derivatisation will be carried out in 24 - 48h, the samples can be stored frozen without resuspending.

2.13 If the samples were resuspended, evaporate to dryness under a gentle stream of N_2, the day before starting the derivatisation. (This allows the derivatisation to commence as early as possible the day after.)

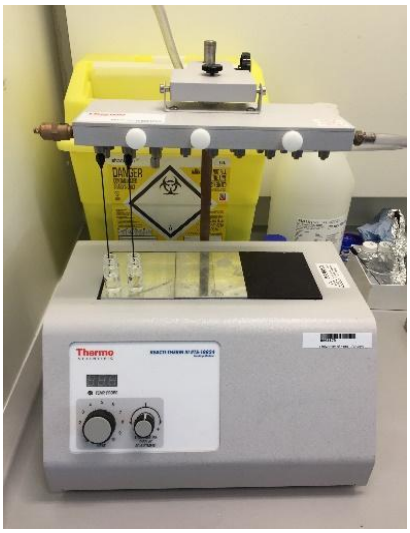

Figure. 6. *N_2 blow-down is set up in ENV 208 Fume Hood. Note 3 white plastic knobs near top. Each one can be used to isolate 9 blow-down positions if required and to control the amount of N_2 going to each tube.. Attach individual needles (the ones used only for CSIA) as required. There are blanking "screws" for positions not in use.*

C. DERIVATIZATION OF AMINO ACIDS

Before starting the procedure note the following points:

1. *The entire procedure must be carried out in the Fume Hood in ENV/208*
2. Ensure that the samples, standards and blanks were evaporated to dryness under a gentle stream of N_2 the day before and then stored in the freezer overnight.
3. Reagent quantities are for nine derivatisations (6 actual samples [typically including 1 bovine collagen control], 2 standards (1 international mix [YOS], 1 Sigma mix [YOSS]), 1 blank) and should be adjusted proportionally for different numbers of derivatisations.

1. ESTERIFICATION OF AMINO ACIDS according to *N*-acetyl-isopropyl (NAIP) method (after Styring et al. 2015)

1.1 The following steps should be performed precisely in this order to maximise time efficiency:

a. Add approximately 4 layers of molecular sieves to a clean scintillation vial (make sure the lid seal properly), and fill the vial with 2-propanol. Bubbles will form immediately as excess of water is removed into the sieves (Fig. 7). Wait until bubble formation ceases before using.
b. Store the stock bottle of 2-propanol under N_2 gas (flush for 10 s before wrapping the lid with parafilm).
c. Turn the heating block on at 100°C (always check the actual temperature with a thermometer).
d. Take the previously dried samples (to be derivatised) out of the freezer and allow to warm up to room temperature
e. Go to biology (J Block, ground floor, first lab to the left) to obtain crushed ice from ice machine. Use one of the polystyrene box (specific for amino acids users) that can be found on top of the fridges in ENV/208.
f. Monitor vial containing molecular sieves and 2-propanol for continued bubble formation
g. Wrap the threads of each of the 9 Hach tubes 2 -3 layers of white Teflon tape (stored in amino acid cupboard). Be sure that the screw thread is dry before doing so. Ensure the wrapping is in the direction you would screw on the cap to close the tube.
h. Label 1 new set of Hach tubes with permanent marker for later steps.

1.2 Make a solution of acidified 2-propanol (4:1; 2-propanol to acetyl chloride):

a. Place the magnetic stirrer plate inside the fume cupboard (Fig. 8).
b. Clean a small magnetic flea with 3 to 5 rinses of dichloromethane (DCM) using a short glass pipette. Always use clean (ashed) scintillation vial to do so, one for DCM and one for the magnetic Flea. Throw the used pipette in the yellow bin in the fume hood after use.
c. Acidified 2-propanol ***must*** be mixed in an ice bath due to exothermic reaction. Fill a glass tray with the crushed ice. The ice must be in contact with a scintillation vial

containing the clean magnetic flea. Use distilled water to solidify the ice around the outside of the vial. Place tray on magnetic stirrer plate (Fig. 6).

d. Bubbles should have stopped forming in the 2-propanol – molecular sieve mixture (continue to wait if not).
e. Using a glass pipette (long-form, with the rubber adapter for the 1000 ul Gilson pipette; Fig. 2), add **8 ml of dry 2-propanol** to the scintillation vial. Start the magnetic stirrer (gentle speed) then slowly add **2 ml of acetyl chloride** dropwise. Allow solution to mix for 1 min.
f. The acetyl chloride does not need to be stored under N_2 gas but do wrap the lid of the stock bottle with parafilm.

1.3 Add 1 ml of acidified propanol to each sample tube using a 1000 ul Gilson pipette. Mark the meniscus of the liquid in each tube so that the tubes can be checked for evaporation after heating.

1.4 Vortex each sample (move the vortex mixer under the fume hood), check the lid is tightly closed, and then place samples on heating block at 100°C. Cover the entire block and tubes with multiple layers of aluminium foil. Check for evaporation after 5 min. Check again after 10 min.

a. Evaporation at this stage is very bad as it will cause isotopic fractionation. When checking and tightening the lids, point the Hach tube away from your face into the fume hood.

1.5 After 45 min (total heating time 1 h), remove samples from the heating block and quench the reaction in a freezer (-20°C) for approximately 5 min, or until samples reach room temperature.

1.6 Remove acidified 2-propanol under a stream of N_2 (this may take 20 to 90 min so check frequently) at room temperature (Fig. 9). The heating block can be set at 40°C at this stage.

1.7 Add ~300 µl dichloromethane (DCM) and dry down under N_2 at room temperature. Repeat with 2nd aliquot of DCM. Make sure the metal blocks are back at room temperature at this stage to prevent evaporation of amino acids.

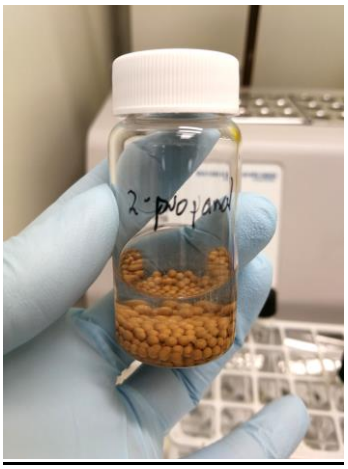

***Figure 7**. 2-Propanol with molecular sieves added – wait until bubbles stop forming before use.*

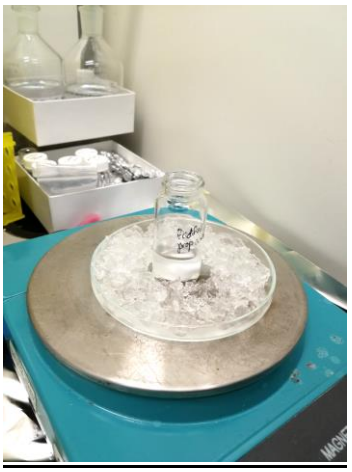

***Figure 8.** Mixing 2-propanol with Acetyl Chloride in ice-bath on magnetic stirrer plate.*

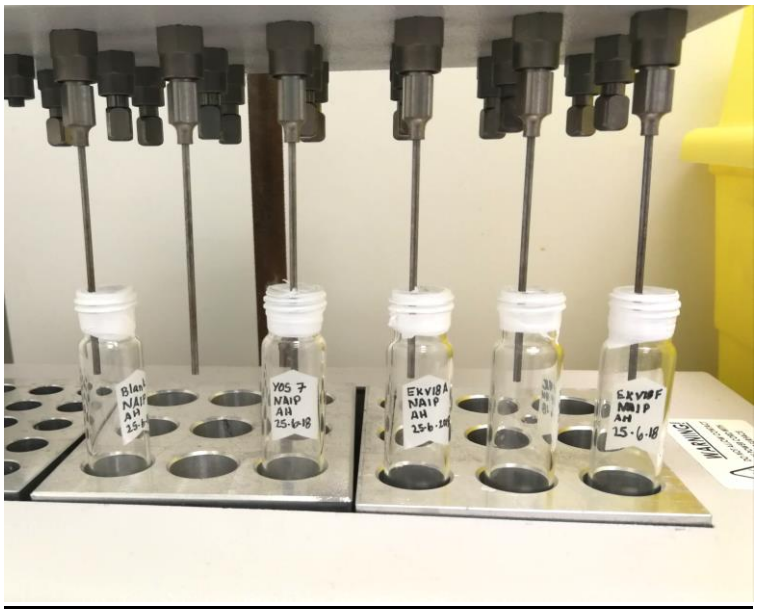

***Figure 9.** Hach tubes (with samples) blowing down (note Teflon tape).*

2. **ACETYLATION OF AMINO ACIDS** according to *N*-acetyl-isopropyl (NAIP) method (after Styring et al. 2015)

Before starting the procedure note the following points

1. The entire procedure must be carried out in the Fume Hood in ENV/208

2. Ensure that the samples have been blown down to complete dryness following the esterification step.

3. Reagent quantities are for nine derivatisations (6 actual samples [typically including 1 bovine collagen control], 2 standards (1 international mix [YOS], 1 Sigma mix [YOSS]), 1 blank) and should be adjusted proportionally for different numbers of derivatisations.

2.1 Set the heating block to 60°C

2.2 Mix acetic anhydride, triethylamine and HPLC grade acetone (1:2:5 v/v/v) in a sterile scintillation vial (=TEA mix):

a. Begin with acetone. Half fill a sterile scintillation vial (labelled appropriately) with acetone from the stock bottle, don't pipette directly from the bottle. Pipette (using long glass pipette attached to 1000 uL Gilson pipette) **6.25 ml of acetone** to the sterile scintillation vial of the mix (labelled TEA mix).

b. Do not inhale acetic anhydride!!!. Use a Pasteur Pipette to transfer acetic anhydride (only as much as you will need, approx. half full), into a 3.5 ml hydrolysis vial. Add molecular sieves (approx. 4 layers) and wait until bubbles cease. **Add 1.25 ml of acetic anhydride** to the TEA mix vial using the Gilson pipette.

c. Extract triethylamine from stock bottle (Fig. 10):

i) Secure stock bottle using clamp stand.

ii) Attach short disposable needle to N_2 gas line and secure it with parafilm.

iii) Insert needle through septum of reagent bottle, but do not allow needle to touch the liquid inside.

iv) Turn on N_2 gas so that the surface of the triethylamine just gently ripples (i.e. gas flow not too fast).

v) Secure 80 mm needle to disposable plastic syringe.

vi) Insert 80 mm needle into stock bottle. Suck up nitrogen gas, remove needle, and purge syringe. Repeat three times.

vii) Place an overturned aluminium block next to the secured stock bottle and place labelled scintillation vial for triethylamine on it.

viii) Reinsert the 80 mm needle, this time inserting into the triethylamine. If the gas flow is low enough, you should be able to gently pull up the syringe plunger until you have the correct amount of reagent (take ~3 ml for 6 samples). Carefully extract the needle from the septum, but hold the plunger as the syringe contains gas and the void inside the syringe can produce a spillage. Then, gently depress the plunger to release the solution into the labelled vial waiting on the aluminium block. (Fig. 8).

ix) *You will notice over time that you will not need any more N_2 to pull up triethylamine.*

x) *When the level of triethylamine in the bottle is low, you will also need the longer reusable stainless needle stored in the AAs' cupboard. This needs to be rinsed outside and inside twice with methanol first and DCM, before and after use.*

xi) Dispose the needles and syringe in the yellow sharps bin. Recap the triethylamine bottle, and wrap cap with parafilm.

2.3 Add **2.5 ml of triethylamine** dropwise (using Gilson pipette and long Pasteur pipette) to the reagent solution vial (TEA mix vial). You don't need to mix it with the magnetic flea, just gently swirl the solution when all reagents combined.

2.4 Add **1 ml** of the **TEA mix solution** to each sample. Vortex samples for 5 s (move the vortex mixer under the fume hood). At this point you should see a stringy white precipitate form in each sample and blank (Fig. 11).

2.5 Place samples on the pre-heated heating block at 60°C (always check the actual temperature with a thermometer) for 10 min covered with aluminium foil.

2.6 Quench reaction in freezer for 5 min then check for evaporation.

2.7 Dry down samples under N_2 (approx. 30 min).

Figure 10. *Triethylamine and "pulling up" procedure.*

Figure 11. *White precipitate formation when TEA mix is added.*

3. PHASE SEPARATION

3.1 Prepare a saturated NaCl solution by adding pure NaCl (chemicals cupboard in ENV/208) to HPLC grade water (~1/2 fill scintillation vial). Continue to add NaCl until no further solids will dissolve.

3.2 Dissolve each sample in 2 ml of ethyl acetate. The samples will likely not fully dissolve until the next step.

3.3 Add 1 ml of NaCl solution and vortex for 20 seconds. Remove the organic phase (on top) to a clean, labelled tube (prepared earlier).

3.4 Repeat the procedure but, now, adding only 1 ml of ethyl acetate to the first tube, vortex for 20 s and removing the organic phase, transferring to the same new labelled tube that contains the first part of the organic phase.

3.5 Add several layers (~3) of molecular sieves to each sample (in the new Hach tubes) and wait for the bubbles to stop forming.

a. While waiting for the bubbles to cease, label new sterilised GC vials (without insert).

3.6 When the bubbles cease, transfer as much of the sample as possible into new labelled and sterilised GC vials (no insert). Dry down the organic residue under a gentle stream of N_2 (not heated) and keep transferring the liquid until there is no more remaining in the Hach tube. This will take almost an hour to be perfectly dry (Fig. 12).

a. Be careful when using the blow down apparatus in this step. Turn the metal blocks upside down, then carefully lower the needles leaving a space to place the GC vials underneath, then place the vails. Don't do it the other way around or a rapid movement can make the vials fall and lose the sample.

3.7 Add 1 ml of DCM and dry down the organic residue under a gentle stream of N_2 to remove any remaining excess water.

3.8 When dry, cap the vials and place the samples in a GC vials box, properly labelled, in the freezer, or continue to the next step "Sample dilution".

Figure 12. *Samples transferred into GC vials then blown down under N_2.*

4. Standard and Sample DILUTION for analysis

NB: this is carried out in the fume hood in ENV/208

4.1 Syringes for dilution and aliquoting are located the Amino Acid cupboard in ENV/208.
- 500 µl "solvents only"
- 250 µl "solvents only"
- 100 µl "samples only"
- 50 µl "standards only"

4.2 Before use, and between samples/standards, each syringe is washed repeatedly with Ethyl Acetate (EtAc) using scintillation vials containing only EtAc and labelled: WASH 1, WASH 2 and FINAL WASH.

4.3 Rinse syringe x10 using vial WASH 1. Repeat x10 using vial WASH 2. Repeat x2 using vial FINAL WASH.

4.4 Be sure that the syringe does not touch the sample/standard vial, if that happens repeat the full set of syringe washes.

4.5 Repeat the washing procedure for "sample" and "standard" syringes between each sample.

4.6 **Dilution of Standard Mixtures post derivatisation**

a. Dilution of Standards for N_2 analysis ("Nitrogen dilutions"):

i) International Standards mix:
- Add 250 µl* of ethyl acetate using 250 µl GC syringe labelled "solvent only".
- Cap the vial and vortex to ensure complete dissolution.
- Split the solution into 50 µl aliquots (5 aliquots total) using 50 µl GC syringe labelled "standards only". Transfer each aliquot into a furnaced, labelled, GC vial with 300 µl fixed-insert.

**NB: if starting with 100 µl of each AA solution, dilute in 500 µl of ethyl acetate instead and prepare 10 aliquots*

ii) Sigma Standards mix:
- Add 500 µl of ethyl acetate using 500 µl GC syringe labelled "solvent only".
- Cap the vial and vortex to ensure complete dissolution.
- Take 2 x50 µl aliquots using 50 µl GC syringe labelled "standards only". Transfer each aliquot into a furnaced, labelled GC vial with 300 µl fixed-insert.

b. Dilution of Standards for C analysis:
- Take one 50 µl aliquot (at N_2 dilution; sections 4.6 a and b above) of both standard mixes and dilute by adding 250 µl EtAc to each vial using GC syringe labelled "solvent only".
- Cap the vial and vortex to ensure complete mixing.
- Split the 300 µl solution into 50 µl aliquots (6 aliquots of the Sigma Standards mix and at least 2 aliquots of the International Standards mix) using 50 µl

GC syringe labelled “standards only”. Transfer each aliquot into a furnaced, labelled GC vial with 300 µl fixed-insert.

4.7 Dilution of Samples post derivatisation

a. Dilution of Samples for N analysis:

- Take the derivatised blown down samples (GC vials without inserts) and add ethyl acetate using GC syringe labelled “Solvent only”.
- Note: The amount of ethyl acetate used is scaled to the original sample mass as follows:
  4 mg collagen samples and blank (Nle only): 300 µl EtAc
  2 mg collagen: 150 µl EtAc
- Split the solution into 50 µl aliquots using the 100 µl GC syringe labelled “samples only”. Transfer each aliquot into a furnaced, labelled GC vial with 300 µl fixed-insert.
- Prepare at least 2 x50 µl aliquots for each sample and blank; one for N analysis and 1 for further dilution for C analysis (see below).

b. Dilution of Samples for C analysis:

- Take 1 x50 µl aliquot at “N dilution” for each sample and add 250 µl EtAc and vortex to ensure complete mixing.
- Split the solution into 50 µl aliquots using the 100 µl GC syringe labelled “samples only”. Transfer each aliquot into a furnaced, labelled GC vial with 300 µl fixed-insert.
- Prepare at least 2 x50 µl aliquots for each sample and blank.

Appendix C

Standards and Bovine controls

This appendix contains the carbon and nitrogen isotope values of the standard amino acids and of the bovine collagen controls run on the GC-C-IRMS system for this project.

Product	**Supplier**	**Code**	$\delta^{13}C$ (‰)	1σ	$\delta^{15}N$ (‰)	1σ
		International standards (nitrogen mode)				
ALanine	Indiana/SI science	AZ104-01\M0R3337N40	-17.93	0.02	43.25	0.07
L-Glycine	Indiana	56-40-6	-40.81	0.04	1.76	0.06
L-Valine	Indiana	0516-06-03	-24.03	0.04	-5.21	0.05
L-Leucine	SI science	AZ200\LAH0629	-28.36		6.22	
L-(+)-Norleucine	SI science	AZ201\LAM3141mix	-28.85		18.96	
L-Aspartic Acid	SI science	AZ203\M1B6432N35	-23.95		35.2	
L-glutamic acid	USGS	USGS40	-26.39	0.04	-4.52	0.06
L-Hydroxyproline	SI science	AZ1Z0\LAM3262	-12.66		-9.17	
Phenylalanine	Indiana/SI sicence	AZ100-01\M0N1811NA	-11.2	0.02	1.7	0.06
		Sigma standards (carbon mode)				
L-Alanine	Sigma	05129-1G-1K	-19.31	0.02	-1.69	0.04
Glycine	Sigma	50050-1G-KC	-33.31	0.02	-0.36	0.07
L- Valine	Sigma	94620-1G-KC	-10.89	0.02	-1.06	0.04
L-Leucine	Sigma	L8000-1G-KC	-13.78	0.06	1.02	0.02
L-Isoleucine	Sigma	58880-1G-KC	-24.89	0.07	2.7	0.05
L-Proline	Sigma	81709-1G-KC	-12.23	0.02	-7.11	0.03
L-Aspartic acid	Sigma	11189-1G-KC	-27.52	0.12	-1.8	0.02
L-Glutamic acid	Sigma	49450-1G-KC	-28.57	0.09	-5.48	0.03
L-Phenylalanine	Sigma	P2126-1G-KC	-11.52	0.05	-0.92	0.06
trans-4-Hydroxy-L-Proline	Sigma	56250-1G-KC	-12.52	0.03	-8.07	0.04
L-Lysine	Sigma	62930-1G-KC-F	-13.7	0.11	-1.09	0.03
L-Tyrosine	Sigma	T3754-1G-KC-F	-24.85	0.02	3.84	0.06
L-Serine	Sigma	84960-1G-KC	-12.69	0.09	3.49	0.19
L-Threonine	Sigma	89180-1G-KC	-10.46	0.01	-1.72	0.05
L-Methionine	Sigma	64320-1G-KC-F	-29.88	0.14	1.17	0.04
L-Norleucine_1	Sigma	N8513-100MG	-27.59	0.02	14.31	0.23

L-Norleucine_2	Sigma	N8513-100MG	-28.16	0.03	14.55	0.04
L-Norleucine_3	Sigma	N8513-100MG	-27.7	0.02	13.77	0.6

Table C.1 List of the standards used for GC-C-IRMS analysis and their "true" values. The $\delta^{13}C$ and $\delta^{15}N$ (‰) values of the international standards are those provided by the supplier. The $\delta^{13}C$ and $\delta^{15}N$ (‰) values of the Sigma standards were measured at BioArCh by EA-IRMS. Three Sigma L-Norleucine were opened and used as internal standards for the duration of this project.

Der. date	**Run date**	**Ala** $\delta^{15}N$ (‰)	**Gly** $\delta^{15}N$ (‰)	**Val** $\delta^{15}N$ (‰)	**Leu** $\delta^{15}N$ (‰)	**Nle** $\delta^{15}N$ (‰)	**Asp** $\delta^{15}N$ (‰)	**Glu** $\delta^{15}N$ (‰)	**Hyp** $\delta^{15}N$ (‰)	**Phe** $\delta^{15}N$ (‰)
11/11/17	17/11/17	44.17	1.91	-5.02	5.51	18.25	34.27	-3.87	-13.07	1.42
11/11/17	17/11/17	41.92	2.36	-5.38	4.94	18.02	32.98	-4.54	-12.44	1.56
11/11/17	17/11/17	40.4	1.96	-5.3	5.68	16.97	31.79	-3.24	-11.86	1.15
11/11/17	17/11/17	39.07	4.87	-3.8	6.38	17.66	31.85	-0.93	-11.34	2.73
11/11/17	17/11/17	39.63	4.02	-3.29	5.78	17.96	31.63	-1.66	-11.96	2.73
11/11/17	17/11/17	38.07	4.26	-5.25	6.47	17.03	31.29	-0.49	-8.65	2.86
28/09/18	07/02/19	46.53	4.71	-2.83	7.32	13.56	34.74	-6.06	-8	1.95
28/09/18	07/02/19	46.93	5.17	-2.31	6.86	14.36	34.04	-4.61	-7.9	1.23
28/09/18	07/02/19	46.53	4.5	-2.39	6.58	14.41	34.44	-4.11	-9.32	0.26
28/09/18	07/02/19	43.13	1.99	-4.21	6.53	13.13	33.14	-3.33	-8.23	2.72
28/09/18	07/02/19	43.04	3.05	-1.28	6.67	13.55	30.9	-4.52	-8.48	0.18
28/09/18	07/02/19	43.39	2.29	-4.88	6.22	14.03	33.48	-2.29	-8.08	2.69
28/09/18	07/02/19	42.06	2.14	-5.07	6.22	13.63	32.83	-4.67	-10.23	2.61
28/09/18	07/02/19	43.2	1.97	-3.41	7.61	13.27	32.41	-2.96	-10.47	2.19
28/09/18	07/02/19	43.34	1.52	-5.52	6.89	13.72	33.76	-3.69	-7.71	2.63
03/10/18	12/02/19	43.97	1.61	-3.87	6.18	14.3	34.72	-4.35	-8.7	1.03
03/10/18	12/02/19	43.81	1.26	-3.61	6.31	14.43	33.39	-4.72	-8.97	0.84
03/10/18	12/02/19	43.03	2.29	-3.3	6.01	13.02	32.23	-4.38	-8.53	1.26
03/10/18	12/02/19	43.89	2.05	-3.04	6.15	12.21	31.46	-4.45	-7.54	1.58
03/10/18	12/02/19	44.74	2.58	-3.69	5.99	13.81	33.92	-2.85	-7.95	3
03/10/18	12/02/19	44.32	3.01	-3.34	7.23	12.95	33.63	-3.33	-8.13	1.36
03/10/18	12/02/19	43.47	1.58	-3.33	5.72	14.64	34.76	-3.82	-8.02	2.07
03/10/18	12/02/19	42.71	2.37	-4.42	6.03	13.1	33.26	-3.55	-8.86	2.73
03/10/18	12/02/19	43.38	1.31	-3.54	5.63	14.07	33.21	-3.01	-8.32	2.31
03/10/18	12/02/19	43.99	2.32	-5.28	5.95	13.7	34.49	-4.45	-7.83	1.66
17/10/18	15/05/19	41.69	2	-4.19	5.96	14.24	33.81	-3.89	-7.96	1.95
17/10/18	15/05/19	41.44	1.87	-4.47	5.8	14.05	33.66	-4.25	-9.35	1.88
17/10/18	15/05/19	41.22	1.28	-4.9	5.91	13.45	34.46	-4.11	-9.03	1.16
17/10/18	15/05/19	39.68	0.56	-6.82	5.24	12.61	31.65	-4.06	-9.69	1.11
17/10/18	15/05/19	37.83	-0.81	-7.35	4.04	12	30.86	-7.38	-10.17	1.18
17/10/18	15/05/19	37.7	-0.62	-5.99	4.62	12.13	30.86	-6	-10.66	1
17/10/18	15/05/19	37.94	-0.14	-5.42	4.76	12.89	29.91	-5.36	-10.5	1.88
17/10/18	15/05/19	37.91	0.55	-6.42	5.42	12.54	30.81	-5.18	-10.35	-0.02
17/10/18	15/05/19	37.96	0.53	-6.76	4.3	11.91	30.7	-6.17	-9.96	0.17
17/10/18	15/05/19	37.69	-0.25	-4.82	4.78	12.15	31.73	-6.76	-8.86	-1.46
17/10/18	15/05/19	37.79	1.56	-5.71	4.49	12.22	30.58	-5.82	-9.89	-1.13
18/10/18	20/05/19	42.25	1.5	-4.58	5.68	13.6	34.74	-4.21	-7	1.56
18/10/18	20/05/19	42.06	1.67	-4.71	6.53	14.02	33.86	-4.81	-8.33	1.62
18/10/18	20/05/19	42.09	0.94	-4.27	5.95	13.93	33.75	-3.84	-8.21	0.77
18/10/18	20/05/19	40.32	2.06	-4.25	5.43	13.18	32.8	-5.4	-8.61	1.09
18/10/18	20/05/19	39.37	0.64	-4.65	4.56	11.55	31.84	-5.2	-10.12	1.79
18/10/18	20/05/19	37.9	0.05	-6.31	3.68	11.58	29.98	-5.52	-7.92	1.42
18/10/18	20/05/19	37.09	0.89	-5.75	4.56	11.82	29.15	-5.63	-11.35	0.85

18/10/18	20/05/19	38.42	1.32	-5.83	4.85	11.47	30.03	-6.56	-10.02	1.59
18/10/18	20/05/19	38.88	0.74	-4.99	3.15	12.04	30.35	-6.15	-8.62	1.02
18/10/18	20/05/19	39.94	1.71	-5.39	4.05	11.43	29.82	-7.01	-6.98	1.9
18/10/18	20/05/19	39.18	1.35	-5.47	4.12	12.11	29.85	-4.91	-9.34	1.26
15/01/19	12/06/19	47.28	4.69	-2.09	7.84	16.41	34.84	-2.81	-8.2	2.53
15/01/19	12/06/19	46.68	4.56	-2.67	7.65	15.79	34.65	-2.86	-8.4	1.99
15/01/19	12/06/19	46.54	3.95	-2.24	7.78	16	35.22	-2.8	-7.67	2.28
15/01/19	12/06/19	43.69	2.99	-2.37	6.72	15.98	34.49	-3.26	-8.68	2.33
15/01/19	12/06/19	43.29	1.03	-3.5	6.83	15.84	34.85	-3.61	-8.94	1.54
15/01/19	12/06/19	41.65	-0.53	-3.71	6.09	15.41	34.65	-3.28	-8.9	1.91
15/01/19	12/06/19	40.77	-0.4	-3.26	6.81	15.2	34.41	-3.21	-8.39	1.71
15/01/19	12/06/19	40.73	-0.36	-4.42	5.89	14.94	34.36	-2.99	-8.22	1.51
15/01/19	12/06/19	44.29	2.15	-2.93	6.54	15.44	34.98	-3.16	-8.35	1.71
15/01/19	12/06/19	44.39	2.32	-2.72	7.31	15.45	34.74	-3.76	-9.05	1.9
03/10/18	08/07/19	42.07	0.92	-2.15	6.55	16.37	34.99	-2.38	-7.83	2.31
03/10/18	08/07/19	42.63	1.05	-1.36	6.46	15.89	35.18	-2.91	-7.15	2.15
03/10/18	08/07/19	42.57	0.93	-2.46	6.62	15.85	35.34	-2.88	-7.48	1.74
03/10/18	08/07/19	41.68	-1.51	-6.77	4.71	12.83	32.34	-4.84	-8.17	2.16
03/10/18	08/07/19	44.33	0.05	-4.45	6.12	15.24	33.85	-3.42	-7.37	1.7
03/10/18	08/07/19	42.01	-1.9	-5.54	5.46	14.22	33.69	-3.79	-6.97	1.95
03/10/18	08/07/19	41.41	-1.93	-7.49	4.9	12.36	32.32	-4.46	-8.29	1.34
03/10/18	08/07/19	40.01	-1.39	-6.93	4.45	11.37	32.12	-4.29	-7.81	0.31
28/09/18	08/07/19	42.45	2.36	-2.86	6.83	15.44	35.32	-2.98	-7.81	2.44
28/09/18	08/07/19	42.1	1.71	-2.63	7.54	15.63	35.03	-2.83	-7.96	2.31
28/09/18	08/07/19	43.64	3.09	-2.34	7.3	15.24	35.07	-3.47	-8.15	2.08
28/09/18	08/07/19	43.75	3.58	-1.6	7.44	15.17	35.19	-2.74	-7.74	2.23
09/07/19	15/07/19	43.51	3.19	-2.75	7.48	15.66	35.01	-2.45	-7.79	2.03
09/07/19	15/07/19	42.9	2.59	-2.8	7.85	15.22	35.04	-2.53	-7.24	2.24
09/07/19	15/07/19	42.79	2.09	-2.64	7.46	15.22	35.22	-2.72	-7.63	2.79
09/07/19	15/07/19	39.21	-1.96	-5.53	5.12	12.69	32.31	-3.55	-7.85	1.6
09/07/19	15/07/19	38.99	-2.93	-6.32	5.12	12.56	33.29	-2.64	-8.2	2.26
09/07/19	15/07/19	38.97	-2.37	-5.65	5.42	13.01	32.72	-3.09	-7.93	1.78
09/07/19	15/07/19	39.43	-2.14	-5.8	6.18	14.16	34.09	-2.6	-8.02	2.23
09/07/19	15/07/19	39.42	0.2	-3.09	7.04	15.55	34.84	-2.79	-8.11	1.43
09/07/19	15/07/19	41.42	3.11	-2.29	6.91	14.34	34.4	-2.81	-8.15	0.92
09/07/19	15/07/19	42.09	2.14	-2.56	6.51	13.73	33.79	-2.32	-6.67	1.8
09/07/19	22/07/19	42.5	2.58	-2.89	7.02	15.67	34.61	-2.81	-8.36	2.09
09/07/19	22/07/19	42.64	2.7	-2.38	7.36	15.34	35.15	-2.51	-8.49	2.62
09/07/19	22/07/19	42.34	2.67	-2.55	7.6	15.45	35.09	-2.93	-8.05	1.8
09/07/19	22/07/19	38.99	-2.8	-6.4	4.79	12.62	33.37	-3.51	-8.07	1.32
09/07/19	22/07/19	38.8	-3.09	-7.35	4.47	12.76	32.42	-3.35	-8.66	2.09
09/07/19	22/07/19	38.56	-4.1	-7.22	4.44	12.81	32.49	-4.58	-8.38	1.96
09/07/19	22/07/19	38.91	-3.59	-7.5	4.76	13.85	33.19	-3.26	-8.71	2.59
09/07/19	22/07/19	39.54	-0.91	-5.18	6.09	14.66	33.48	-2.08	-7.86	2.47
09/07/19	22/07/19	40.36	-0.08	-5.02	5.87	14.48	34.52	-3.22	-6.42	2.06
09/07/19	22/07/19	40.09	0.87	-3.03	7.54	15.76	34.66	-3.09	-7.93	1.54
09/07/19	22/07/19	39.42	0.69	-2.2	8.65	16.13	34.24	-2.66	-8.98	0.71
18/07/19	24/07/19	40.26	-1.23	-4.8	6.14	14.79	33.94	-3.59	-7.67	1.91
18/07/19	24/07/19	40.89	0.33	-3.5	7.64	15.3	34.48	-3.19	-8.14	2.05
18/07/19	24/07/19	40.82	1.18	-2.87	7.82	15.86	35.38	-3.35	-7.68	1.95
18/07/19	24/07/19	39.29	-3.87	-7.67	3.29	11.34	31.67	-4.51	-8.54	1.62
18/07/19	24/07/19	39.6	-4.15	-6.92	4.92	13.58	33.06	-2.83	-8.12	2.74
18/07/19	24/07/19	40.31	0.14	-4.71	6.52	15.62	34.56	-2.41	-7.94	2.13
18/07/19	24/07/19	39.23	-1.8	-6.62	5.25	14.38	33.9	-2.57	-8.15	2.53
18/07/19	24/07/19	39.33	-2.55	-5.76	7.81	16.84	34.8	-2.7	-8.02	2.09

18/07/19	24/07/19	39.55	-2.67	-4.33	7.98	16.47	35.17	-2.42	-7.88	2.13
18/07/19	24/07/19	42.31	2.97	-2.41	7.64	15.48	35.01	-2.5	-8.14	2.09
18/07/19	24/07/19	42.1	4.32	-1.96	8.09	16.24	35.42	-3.18	-8.34	1.48
24/07/19	30/07/19	42.21	3.13	-2.56	7.68	15.2	35.5	-2.7	-7.6	1.63
24/07/19	30/07/19	42.23	3.02	-2.13	7.03	15.71	35.18	-2.21	-8.67	1.17
24/07/19	30/07/19	42.81	3.52	-2.65	7.36	15.7	35.11	-3.1	-7.84	1.99
24/07/19	30/07/19	42.02	1.37	-4.43	5.39	13.95	33.78	-4.03	-7.6	2.36
24/07/19	30/07/19	41.6	0.24	-4.65	5.74	14.66	34.84	-2.65	-6.48	2.29
24/07/19	30/07/19	41.72	0.22	-4.34	5.85	15.34	34.56	-3.12	-7.54	2.43
24/07/19	30/07/19	41.48	0.49	-4.7	6.37	15.15	34.28	-2.89	-6.72	2.11
24/07/19	30/07/19	40.87	0.84	-4.79	6.47	14.87	34.38	-2.07	-7.33	2.64
24/07/19	30/07/19	40.76	-0.14	-5.4	5.74	14.49	33.56	-2.67	-7.62	1.78
24/07/19	30/07/19	41.38	0.87	-4.37	7.5	15.54	34.31	-2.66	-6.83	2.12
24/07/19	30/07/19	41.03	0.63	-4.87	6.48	14.93	34.69	-2.85	-7.12	1.75
24/07/19	30/07/19	39.57	-1.87	-4.53	6.24	14.05	33.87	-3.43	-7.02	2.2
24/07/19	30/07/19	41.37	1.5	-2.73	7.4	15.01	34.87	-2.65	-7.24	2.16
24/07/19	30/07/19	42.27	2.53	-1.87	7.52	15.33	34.73	-2.64	-8	1.61
26/07/19	05/08/19	43.17	2.96	-1.85	7.47	15.26	34.74	-2.48	-8.03	1.63
26/07/19	05/08/19	42.75	3.09	-2.07	7.38	15.3	35.39	-3.09	-8.03	2.21
26/07/19	05/08/19	42.43	3.23	-2.39	7.54	15.56	34.76	-2.93	-8.08	1.29
26/07/19	05/08/19	42.18	1.45	-4.06	5.87	14.69	33.82	-3.51	-7.72	2.37
26/07/19	05/08/19	41.73	0.45	-4.37	6.81	15.57	34.54	-3.3	-7.52	2.3
26/07/19	05/08/19	41.13	-1.42	-5.46	5.12	14.02	33.37	-3.44	-7.71	2.11
26/07/19	05/08/19	40.9	0	-4.13	7.05	15.49	35.12	-2.76	-6.79	2
26/07/19	05/08/19	41.82	1.18	-2.42	7.05	15.73	33.39	-2.86	-7.56	2.6
26/07/19	05/08/19	40.9	0.26	-4.34	6.14	15.36	34.27	-3.21	-7.36	2.08
26/07/19	05/08/19	41.25	0.34	-3.3	7.73	15.2	33.98	-3.26	-7.47	1.64
26/07/19	05/08/19	41.85	2.3	-2.21	7.83	15.2	34.63	-2.11	-8.44	2.31
26/07/19	05/08/19	41.63	2.2	-1.05	7.84	16.08	34.93	-2.62	-8.34	1.81
02/09/19	16/09/19	42.85	2.03	-1.48	7.92	16.16	34.75	-2.49	-8.11	2.06
02/09/19	16/09/19	42.39	1.39	-3.86	8.51	16.01	35.63	-2.67	-8.12	2.49
02/09/19	16/09/19	42.35	2.43	-3.36	7.69	15.74	35.04	-3.02	-7.48	1.82
02/09/19	16/09/19	42.7	0.91	-4.82	7.71	16.33	34.86	-2.57	-7.98	2.64
02/09/19	16/09/19	42.34	0.59	-3.52	7.29	14.5	33.95	-3.32	-8.12	1.9
02/09/19	16/09/19	42.02	0.9	-3.42	7.67	14.43	34.75	-2.99	-7.67	0.82
02/09/19	16/09/19	41.24	1.49	-3.91	6.55	14.42	34.3	-3.72	-8.26	1.46
02/09/19	16/09/19	42.71	0.94	-4.08	7.53	15.79	34.8	-2.75	-7.66	2.54
02/09/19	16/09/19	43.19	1.27	-2.81	7.77	15.34	36.12	-2.36	-8.43	2.11
02/09/19	16/09/19	44.71	1.04	-3.2	7.53	15.48	35.34	-2.95	-8.6	2.16
04/04/19	26/09/19	44.62	0.13	1.33	10.31	18.04	35.17	-3.21	-7.67	3.17
04/04/19	26/09/19	47.14	4.61	-1.29	8.49	16.52	35.07	-2.47	-7.93	2
04/04/19	26/09/19	46.46	3.24	-2.96	8.38	16.67	35.83	-3.14	-7.79	2.29
04/04/19	26/09/19	45.82	1.76	-4.46	7.37	15.49	35.23	-3.52	-8.87	2.04
04/04/19	26/09/19	48.84	4.43	-3.63	6.7	15.01	34.64	-3.56	-8.58	1.79
04/04/19	26/09/19	45.87	2.98	-4.39	6.62	15.07	35.11	-3.44	-9.03	2.38
04/04/19	26/09/19	47.22	2.35	-5.27	6.3	16.41	34.96	-3.89	-7.47	1.92
04/04/19	26/09/19	43.8	1.23	-3.62	8.17	16.36	34.8	-2.45	-9.1	2.36
04/04/19	26/09/19	43.6	1.6	-4.05	7.39	16.13	35.32	-2.68	-1.91	0.29
01/10/19	15/10/19	44.93	1.92	-2.53	7.65	15.56	35.34	-3.01	-7.9	2.07
01/10/19	15/10/19	45.1	1.63	-2.11	7.41	15.58	35.17	-2.81	-8.42	2
01/10/19	15/10/19	45.47	2.38	-2.14	7.61	16.05	35.01	-2.82	-7.7	2.1
01/10/19	15/10/19	51.7	4.81	-1.82	6.51	14.82	34.05	-2.96	-8.87	1.51
01/10/19	15/10/19	47.75	2.78	-3.19	6.56	14.46	34.11	-3.98	-9.85	1.69
01/10/19	15/10/19	51.55	3.65	-3.5	6.2	14.4	34.27	-3.21	-8.67	1.85
01/10/19	15/10/19	49.18	1.6	-4.6	7.24	15.39	35.01	-2.85	-7.91	1.99

01/10/19	15/10/19	49.65	1.39	-4.91	6.96	15.94	34.46	-3.17	-7.79	1.94
11/10/19	15/10/19	50.14	2.24	-3.8	6.25	15.26	34.37	-3.24	-8.41	2.13
11/10/19	15/10/19	47.46	1.93	-3.33	6.15	14.23	34.24	-2.46	-7.85	1.66
11/10/19	15/10/19	49.37	2.67	-3.58	6.03	14.24	33.7	-3.01	-9.06	1.65
13/11/19	09/12/19	46.18	2.81	-3.78	6.62	14.66	34.72	-2.79	-8.86	1.47
13/11/19	09/12/19	45.4	2.29	-4.21	6.52	14.39	35.33	-2.75	-8.92	1.1
13/11/19	09/12/19	45.79	2.05	-4.13	6.87	14.29	35.52	-4.12	-9.14	1.43
13/11/19	09/12/19	45.14	1.9	-3.97	6.39	14.4	34.91	-3.94	-8.68	1.43
10/10/19	09/12/19	45.41	2.54	-2.74	6.53	14.29	34.74	-3.84	-8.26	1.05
10/10/19	09/12/19	45.48	2.83	-1.6	6.8	14.69	33.9	-4.43	-9.45	2
11/10/19	09/12/19	43.33	0.94	-4.96	5.97	13.93	33.56	-4.37	-9.89	1.99
11/10/19	09/12/19	44.06	1.04	-4.79	5.77	13.84	33.65	-3.95	-9.58	1.5
11/10/19	09/12/19	44.62	1.98	-4.18	6.78	14.13	34.34	-3.72	-8.83	1.27
11/10/19	09/12/19	44.06	1.64	-5.04	6.38	13.99	34.33	-4.1	-9.03	0.87
11/10/19	09/12/19	44.2	1.39	-4.27	6.11	14.34	33.7	-4.15	-9.18	1.59
11/10/19	09/12/19	44.21	0.96	-4.39	6.56	13.59	34.15	-3.34	-8.66	1.04
18/07/19	27/01/20	43.84	0.88	-5.04	7.64	14.57	34.44	-4	-8.22	0.64
18/07/19	27/01/20	43.08	1.22	-5.56	7.07	14.25	34.86	-3.74	-8.3	1.52
18/07/19	27/01/20	43.48	1.99	-5.6	5.94	14.57	35.14	-3.86	-8.66	0.7
18/07/19	27/01/20	45.29	3.54	-1.75	7.52	14.41	33.91	-3.5	-8.41	1.32
18/07/19	27/01/20	43.96	3.42	-3.52	6.59	14.05	34.52	-3.98	-8.83	1.04
18/07/19	27/01/20	44.07	3.46	-3.1	6.69	13.75	34.51	-3.37	-10.52	1.84
18/07/19	27/01/20	45.29	4.32	-1.9	7.53	13.65	33.62	-3.87	-8.35	1
18/07/19	27/01/20	45.08	4.17	-1.92	8.01	13.54	33.85	-3.92	-8.76	0.98
24/07/19	27/01/20	45.82	3.96	-2.45	6.79	13.69	34.64	-4.05	-8.96	1.41
24/07/19	27/01/20	46.01	3.84	-1.49	6.63	13.5	34.45	-3.59	-9.27	1.19
24/07/19	27/01/20	45.68	2.9	-4.02	6.02	14.28	34.26	-3.85	-9.49	1.49
24/07/19	27/01/20	45.44	2.42	-4.61	5.79	14.23	34.36	-4.07	-9.16	1.18

Table C.2 International standards' raw $\delta^{15}N$ values. Norleucine (Nle) International was only used in the first run (17/11/17). For all the other runs, the Nle used was the one purchased from Sigma-Aldrich.

Der. date	Run date	Ala $\delta^{13}C$ (‰)	Gly $\delta^{13}C$ (‰)	Val $\delta^{13}C$ (‰)	Leu $\delta^{13}C$ (‰)	Ile $\delta^{13}C$ (‰)	Nle $\delta^{13}C$ (‰)	Thr $\delta^{13}C$ (‰)	Ser $\delta^{13}C$ (‰)	Pro $\delta^{13}C$ (‰)	Asp $\delta^{13}C$ (‰)	Met $\delta^{13}C$ (‰)	Glu $\delta^{13}C$ (‰)	Hyp $\delta^{13}C$ (‰)	Phe $\delta^{13}C$ (‰)	Lys $\delta^{13}C$ (‰)	Tyr $\delta^{13}C$ (‰)
15/08/18	14/09/18	-30.65	-36	-26.74	-26.89	-33.39	-33.14	-33.58	-34.99	-26.14	-33.08	-33.65	-32.24	-32.85	-23.44	-30.35	-35.67
15/08/18	14/09/18	-30.89	-36.47	-27.14	-26.75	-33.74	-33.51	-33.63	-35.06	-25.89	-33.01	-34.12	-32.48	-32.92	-23.75	-30.78	-35.72
15/08/18	14/09/18	-30.78	-35.86	-27.16	-26.65	-33.94	-33.2	-33.92	-35.23	-25.91	-33.04	-33.52	-32.43	-32.58	-23.24	-30.82	-35.82
15/08/18	14/09/18	-30.91	-36.15	-26.88	-26.44	-33.4	-33.56	-33.8	-35.13	-25.86	-32.84	-33.7	-32.44	-32.07	-23.4	-30.38	-35.27
15/08/18	14/09/18	-30.7	-35.89	-26.95	-26.53	-33.77	-33.63	-33.67	-35.04	-25.62	-32.67	-33.96	-32.59	-32.75	-22.9	-30.38	-35.15
15/08/18	14/09/18	-30.84	-36.08	-26.92	-26.84	-34.08	-33.67	-33.8	-35.25	-26.13	-32.93	-33.98	-32.29	-32.32	-23.25	-29.88	-35.24
15/08/18	14/09/18	-30.72	-35.88	-26.85	-27.28	-34.92	-34.4	-34.07	-35.61	-26.3	-33.18	-34.07	-32.65	-32.47	-22.36	-30.32	-35.24
15/08/18	14/09/18	-30.85	-36.51	-27.17	-26.79	-34.46	-34.02	-32.96	-35.04	-25.67	-32.73	-33.32	-32.5	-32.73	-22.66	-31.49	-35.27
15/08/18	14/09/18	-31.24	-35.94	-26.17	-26.18	-33.1	-33.21	-32.97	-34.37	-24.98	-32.28	-33.37	-32.11	-31.36	-21.74	-30.07	-34.6
15/08/18	14/09/18	-31.26	-36.22	-26.81	-26.1	-33.6	-33.22	-33.25	-34.55	-25.04	-32.47	-33.73	-31.73	-31.32	-21.58	-30.12	-34.02
15/08/18	14/09/18	-31.15	-35.86	-26.62	-26.27	-33.75	-33.11	-33.1	-34.69	-24.91	-32.34	-33.67	-32.05	-31.16	-21.47	-29.8	-34.2
15/08/18	14/09/18	-31.08	-35.77	-26.59	-25.7	-32.87	-32.95	-32.8	-34.6	-24.91	-32.13	-33.8	-31.89	-30.81	-21.75	-29.94	-35.23
15/08/18	14/09/18	-30.81	-35.46	-26.54	-25.92	-33.23	-32.99	-32.82	-34.54	-24.96	-32.23	-33.6	-31.87	-31.17	-21.64	-28.67	-35.48
15/08/18	14/09/18	-30.97	-35.67	-26.64	-26.27	-33.72	-32.71	-32.83	-34.57	-24.87	-31.97	-33.44	-32.1	-31	-21.75	-28.89	-35.41
15/08/18	14/09/18	-30.87	-35.7	-25.85	-27.11	-33.2	-33.08	-32.88	-34.97	-25.07	-32.22	-33.44	-32.2	-31.58	-23.94	-29.78	-36.86
28/09/18	27/11/18	-30.45	-36.38	-27.66	-27.13	-33.95	-34	-34.21	-35.03	-26.49	-33.69	-34.77	-33.07	-32.54	-23.28	-31.58	-34.86
28/09/18	27/11/18	-30.72	-36.77	-27.96	-27.41	-34	-34.15	-34.4	-35.04	-26.78	-33.71	-34.63	-33.21	-33.15	-23.51	-31.48	-35.2
28/09/18	27/11/18	-30.74	-36.94	-27.81	-27.27	-34.03	-34.22	-34.46	-35.17	-27.03	-33.8	-34.67	-32.95	-33.03	-23.35	-32.38	-34.93
28/09/18	27/11/18	-30.35	-36.27	-27.7	-26.86	-33.63	-33.74	-34.14	-34.69	-26.4	-33.09	-34.21	-32.56	-32.27	-22.9	-30.91	-34.54
28/09/18	27/11/18	-30.59	-36.5	-27.45	-27.21	-33.97	-33.72	-34.31	-34.94	-26.55	-33.4	-34.45	-32.99	-32.75	-23.02	-31.04	-34.68
28/09/18	27/11/18	-30.77	-36.77	-27.51	-26.86	-33.8	-33.89	-34.13	-34.61	-26.67	-33.13	-34.82	-32.93	-32.61	-23.1	-31.83	-34.38
28/09/18	27/11/18	-30.9	-36.77	-27.92	-26.97	-33.81	-34.03	-34.32	-34.98	-26.39	-33.43	-35.15	-32.97	-32.66	-23.36	-27.98	-34.39
28/09/18	27/11/18	-31.91	-37.52	-28.15	-27.39	-34.72	-34.34	-34.42	-35.72	-26.88	-33.97	-35.67	-33.45	-32.95	-24.06	-30.83	-35.65
28/09/18	27/11/18	-31.98	-37.32	-27.59	-27.32	-34.34	-33.98	-34.35	-35.39	-26.24	-33.5	-34.86	-33.25	-32.6	-23.17	-31.05	-34.41
28/09/18	27/11/18	-31.97	-37.66	-27.63	-27.46	-34.55	-34.59	-34.66	-35.78	-27.06	-34.04	-35.45	-33.57	-33.6	-23.79	-30.74	-35.29
28/09/18	27/11/18	-32.33	-37.64	-27.77	-27.77	-34.54	-34.64	-34.82	-35.99	-26.93	-34.18	-35.86	-33.62	-32.89	-23.89	-30.31	-35.55
28/09/18	27/11/18	-32.02	-36.57	-28	-27.44	-34.24	-34.01	-34.12	-35.8	-26.76	-33.66	-34.88	-33.29	-32.78	-23.38	-31.04	-34.78
03/10/18	03/12/18	-31.94	-37.48	-27.97	-27.75	-34.07	-34.05	-34.48	-36.27	-26.71	-33.57	-35.68	-33.54	-32.87	-23.21	-30.54	-34.87
03/10/18	03/12/18	-32	-37.35	-27.82	-27.44	-34.14	-34.2	-34.15	-35.43	-26.91	-33.7	-35.72	-33.28	-32.9	-23.43	-30.98	-34.87
03/10/18	03/12/18	-32.07	-37.56	-28.06	-27.59	-34.11	-34.03	-34.31	-36.31	-26.86	-33.72	-35.14	-33.39	-32.93	-23.21	-31	-34.67
03/10/18	03/12/18	-32.13	-37.51	-28.09	-27.59	-33.93	-34.21	-34.28	-35.48	-26.85	-33.56	-35.27	-33.08	-32.94	-22.81	-30.75	-34.42
03/10/18	03/12/18	-31.89	-37.34	-28.25	-27.15	-34.01	-34.11	-34.1	-35.86	-26.56	-33.41	-35.39	-32.92	-32.89	-23.15	-31.35	-34.82
03/10/18	03/12/18	-32.61	-37.61	-28.43	-27.96	-34.73	-34.81	-34.82	-36.82	-27.64	-34.63	-36.02	-34.28	-34	-24.64	-31.93	-36.67
03/10/18	03/12/18	-32.52	-37.69	-27.95	-27.73	-34.68	-34.63	-34.32	-36.3	-27.07	-34.03	-35.85	-33.28	-32.94	-23.89	-30.48	-35.38
03/10/18	03/12/18	-32.32	-37.57	-28.09	-27.66	-34.38	-34.23	-34.43	-36.57	-26.9	-33.98	-36.54	-33.26	-33.09	-23.33	-32.2	-34.98

03/10/18	03/12/18	-32.18	-37.48	-27.7	-27.31	-33.74	-34.1	-33.98	-36.1	-26.57	-33.6	-34.94	-33.03	-33	-23.11	-30.51	-34.87
03/10/18	03/12/18	-32.44	-37.71	-27.91	-27.56	-34.45	-33.78	-33.98	-36.25	-27.11	-33.98	-35.7	-33.11	-32.71	-23.22	-30.37	-35.4
03/10/18	03/12/18	-32.48	-37.73	-28.19	-27.55	-34.18	-34.36	-34.19	-35.96	-26.99	-33.81	-35.33	-33.32	-32.95	-23.32	-31.69	-35.03
03/10/18	03/12/18	-32.43	-37.86	-27.86	-27.5	-34.44	-34.24	-34.12	-36.26	-26.78	-33.59	-35.35	-33.42	-32.89	-23.04	-31.21	-34.69
17/10/18	10/12/18	-32.44	-38.08	-28.36	-27.77	-34.54	-34.75	-34.86	-36.08	-27.38	-34.2	-35.23	-33.13	-32.95	-23.64	-31.64	-34.95
17/10/18	10/12/18	-32.76	-38.19	-28.46	-28.06	-34.72	-34.87	-34.75	-36.06	-27.91	-34.5	-35.07	-33.81	-32.91	-23.73	-32.46	-35.08
17/10/18	10/12/18	-32.42	-38.36	-28.42	-27.64	-34.73	-35.09	-34.84	-36.7	-27.65	-34.06	-35.73	-34.09	-33.67	-24.25	-33.16	-35.79
17/10/18	10/12/18	-32.64	-38.22	-28.43	-27.79	-34.71	-34.77	-34.37	-36.04	-27.57	-34.09	-35.97	-33.98	-34.03	-24.24	-31.72	-35.47
17/10/18	10/12/18	-32.63	-38.1	-28.18	-27.64	-34.9	-34.91	-34.65	-36.88	-27.23	-34.03	-36.28	-33.98	-33.55	-24.2	-31.65	-35.34
17/10/18	10/12/18	-32.61	-38.1	-28.27	-27.12	-34.66	-34.57	-34.43	-36.2	-27.42	-33.66	-36.52	-33.94	-33.68	-24.28	-32.65	-35.96
17/10/18	10/12/18	-32.83	-38.19	-28.26	-27.4	-34.69	-34.73	-35.03	-37.01	-27.27	-34.31	-36.21	-33.78	-33.46	-23.75	-31.64	-35.08
17/10/18	10/12/18	-33.16	-38.49	-28.48	-27.67	-34.94	-35.11	-35.28	-36.95	-27.61	-34.5	-35.9	-33.26	-33.15	-23.25	-32.86	-34.74
17/10/18	10/12/18	-33.25	-38.76	-28.22	-27.59	-34.84	-34.89	-35.18	-37.24	-27.62	-34.48	-36.39	-33.63	-33.26	-23.81	-31.37	-35.02
17/10/18	10/12/18	-32.96	-38.19	-28	-27.3	-34.53	-34.68	-34.69	-36.84	-27.37	-33.65	-36.65	-33.88	-34	-24.17	-33.3	-35.74
17/10/18	10/12/18	-33.29	-38.87	-28.6	-27.85	-35.26	-35.06	-35.26	-37.41	-28.14	-34.73	-36.49	-33.73	-33.94	-23.96	-32.47	-35.37
17/10/18	10/12/18	-33.31	-38.29	-28.54	-27.81	-34.95	-35.13	-34.9	-36.92	-27.61	-34.46	-36.35	-33.26	-32.67	-23.45	-32	-34.45
18/10/18	13/12/18	-31.13	-36.54	-26.98	-27.78	-33.22	-34.08	-33.6	-35.2	-26.08	-33.13	-34.95	-32.61	-32.55	-23.42	-31.46	-35.56
18/10/18	13/12/18	-31.64	-36.63	-27.34	-28.31	-33.74	-34.09	-33.82	-35.02	-26.56	-33.63	-35.47	-33.41	-33.03	-23.79	-31.89	-35.84
18/10/18	13/12/18	-31.62	-36.93	-27.56	-28.4	-33.76	-34.56	-33.93	-36.23	-26.8	-33.53	-34.75	-33.5	-33.05	-23.96	-31.79	-35.3
18/10/18	13/12/18	-31.73	-36.92	-27.31	-28.3	-33.45	-34.62	-33.87	-36.12	-26.58	-33.27	-35.12	-33.09	-32.29	-23.4	-30.99	-35.45
18/10/18	13/12/18	-31.85	-36.79	-27.44	-28.23	-33.84	-34.35	-33.66	-35.43	-26.48	-33.08	-35.5	-33.22	-33.01	-23.74	-31.65	-35.16
18/10/18	13/12/18	-31.88	-36.93	-27.28	-27.95	-33.53	-34.14	-32.7	-35.39	-26.34	-33.1	-35.98	-32.76	-32.17	-23.04	-30.25	-34.67
18/10/18	13/12/18	-31.55	-36.46	-27.01	-27.78	-33.37	-33.96	-33.86	-35.82	-26.13	-32.95	-34.57	-32.46	-32.05	-22.93	-31.15	-34.7
18/10/18	13/12/18	-31.81	-36.7	-27.24	-28.21	-33.65	-34.17	-33.94	-35.96	-26.37	-33.53	-35.21	-32.92	-32.73	-23.11	-31.3	-35.05
18/10/18	13/12/18	-31.91	-36.77	-27.1	-28.25	-33.54	-34.31	-33.86	-35.58	-26.67	-33.07	-35.05	-33.17	-32.25	-23.21	-29.8	-34.64
15/08/18	14/01/19	-32.72	-37.83	-28.57	-29.94	-35.03	-34.89	-34.75	-36.77	-27.55	-34.55	-36.37	-34.21	-33.34	-24.31	-32.84	-36.06
15/08/18	14/01/19	-32.82	-37.87	-28.48	-30.15	-34.75	-34.96	-34.83	-36.79	-27.27	-34.55	-36.17	-34.19	-33.62	-23.91	-32.57	-35.72
15/08/18	14/01/19	-32.73	-38.1	-28.57	-30.21	-34.9	-34.98	-34.8	-36.9	-27.38	-34.4	-36.46	-34.24	-33.38	-24.3	-32.47	-36
15/08/18	14/01/19	-32.76	-37.75	-28.52	-29.95	-34.77	-34.95	-34.75	-36.66	-27.23	-34.55	-36.37	-34.5	-33.84	-24.15	-32.67	-35.93
15/08/18	14/01/19	-32.75	-37.93	-28.41	-30.11	-34.94	-35.11	-34.87	-37.02	-27.24	-34.42	-36.43	-34.32	-33.39	-23.61	-32.58	-36.04
15/08/18	14/01/19	-32.75	-37.93	-28.53	-30.18	-34.81	-34.81	-35.09	-36.94	-27.23	-34.44	-36.75	-34.18	-33.53	-24.02	-32.41	-35.54
15/08/18	14/01/19	-32.76	-37.63	-28.43	-30.04	-34.65	-34.7	-34.6	-36.63	-27.4	-34.66	-36.28	-34.3	-33.47	-24.4	-32.44	-35.7
15/08/18	14/01/19	-32.88	-38.12	-28.87	-30.33	-35.02	-34.88	-34.76	-36.97	-27.21	-34.41	-36.17	-34.1	-33.32	-23.94	-32.39	-35.5
15/08/18	14/01/19	-32.89	-37.99	-28.67	-30	-34.78	-34.78	-34.17	-36.23	-26.88	-34.04	-35.96	-33.58	-32.71	-23.4	-31.58	-35.21
04/04/19	14/01/19	-32.75	-37.78	-28.61	-29.81	-34.71	-34.75	-34.81	-36.98	-27.25	-34.72	-36.56	-34.24	-33.43	-24.12	-32.16	-35.94
04/04/19	14/01/19	-32.59	-37.71	-28.46	-29.43	-34.47	-34.47	-34.37	-36.59	-27.32	-34.55	-36.1	-33.87	-33.25	-23.84	-32.27	-35.65
04/04/19	14/01/19	-32.53	-37.51	-28.34	-29.87	-34.41	-34.42	-34.77	-36.86	-27.14	-34.43	-36.2	-33.66	-32.91	-23.7	-32.14	-35.42
17/08/18	14/01/19	-33.29	-38.85	-29.29	-29.11	-35.55	-35.2	-35.34	-37.56	-27.73	-34.83	-36.98	-34.6	-33.77	-24.38	-33.01	-36.22

17/08/18	14/01/19	-33.35	-38.71	-29.08	-29.26	-35.57	-35.25	-35.15	-37.3	-27.71	-34.87	-36.64	-34.72	-33.98	-24.44	-32.93	-36.09
17/08/18	14/01/19	-33.5	-38.58	-29.09	-29.09	-35.47	-35.26	-35.27	-37.06	-27.99	-34.87	-36.91	-34.55	-34.12	-24.14	-33.22	-36.25
17/08/18	14/01/19	-33.62	-38.9	-29.19	-29.22	-35.7	-35.36	-35.54	-37.22	-28.01	-35	-36.87	-34.33	-33.8	-24.34	-32.99	-36.01
17/08/18	14/01/19	-33.44	-39	-29.16	-29.14	-35.38	-35.36	-35.8	-37.68	-28	-35.27	-36.84	-34.33	-33.88	-24.27	-33.17	-36.31
17/08/18	14/01/19	-33.31	-38.93	-29.47	-29.42	-35.36	-35.57	-35.63	-37.44	-28	-35.02	-36.63	-34.52	-33.81	-24.07	-32.43	-35.73
17/08/18	14/01/19	-33.17	-38.59	-29.17	-29.03	-35.24	-35.11	-35.32	-37.39	-27.7	-34.74	-36.72	-34.17	-33.45	-24.03	-33.83	-35.64
17/08/18	14/01/19	-33.32	-38.98	-29.32	-29.29	-35.87	-35.56	-35.84	-37.93	-28.2	-35.21	-37.31	-34.83	-34.16	-24.52	-33.22	-36.59
17/08/18	14/01/19	-33.56	-38.86	-29.42	-29.05	-35.34	-35.4	-35.68	-37.81	-27.99	-35.05	-36.79	-34.36	-33.51	-24.1	-33.16	-36.05
17/08/18	14/01/19	-33.07	-38.53	-28.79	-28.72	-35.14	-34.82	-35.38	-37.3	-27.61	-34.56	-36.29	-33.85	-32.99	-23.59	-32.27	-35.15
17/08/18	14/01/19	-33.29	-38.7	-29.01	-28.92	-35.16	-35.06	-35.32	-37.3	-27.74	-34.85	-36.83	-34.01	-33.31	-23.83	-33.27	-35.74
17/08/18	14/01/19	-33.34	-38.59	-28.92	-28.79	-35.2	-35.14	-35.56	-37.56	-27.97	-34.67	-36.72	-34.19	-33.38	-23.87	-32.41	-35.84
17/08/18	14/01/19	-33.36	-38.8	-29.13	-28.94	-35.25	-35.19	-35.74	-37.54	-27.73	-34.98	-36.65	-34.43	-33.73	-24.32	-33.29	-36.38
04/04/19	05/04/19	-33.17	-37.75	-29.87	-28.34	-34.92	-35.07	-34.82	-36.67	-26.77	-34.77	-36.61	-34	-32.82	-24.25	-30.85	-35.64
04/04/19	05/04/19	-33.29	-37.99	-30.1	-28.16	-35.01	-35.42	-34.88	-36.89	-27.26	-34.5	-36.97	-34.14	-32.99	-24.37	-32.19	-35.89
04/04/19	05/04/19	-33.71	-38.47	-30.29	-28.3	-35.42	-35.66	-35.18	-37.09	-27.8	-34.88	-37.31	-34.59	-33.37	-24.55	-33.33	-36.48
04/04/19	05/04/19	-33.57	-38.18	-30.05	-28.68	-35.26	-35.75	-35.54	-37	-27.73	-34.85	-37.24	-34.52	-33.56	-24.74	-32.04	-36.02
04/04/19	05/04/19	-33.4	-38.13	-30.28	-28.27	-35.7	-35.96	-35.24	-36.93	-27.48	-34.83	-37.28	-34.58	-33.51	-24.69	-31.67	-36.34
04/04/19	05/04/19	-33.63	-38.48	-30.24	-28.18	-35.25	-35.77	-35.31	-36.95	-27.43	-34.83	-37.1	-34.14	-33.12	-24.32	-32.46	-35.99
04/04/19	05/04/19	-33.49	-38.13	-30.4	-28.33	-35.19	-35.34	-35.15	-37.15	-26.99	-34.84	-36.91	-34.14	-33.02	-24.08	-33.31	-35.46
04/04/19	05/04/19	-33.2	-38.34	-30.18	-28.22	-35.01	-35.25	-34.55	-36.77	-26.73	-34.35	-36.71	-33.47	-32.73	-23.98	-32.71	-35.36
04/04/19	05/04/19	-33.43	-38.27	-30.34	-27.86	-35.18	-35.22	-34.79	-36.64	-26.78	-34.19	-36.55	-33.81	-32.46	-23.75	-32.89	-35.37
04/04/19	05/04/19	-33.71	-38.18	-30.42	-27.86	-35.37	-35.35	-34.84	-36.8	-27.09	-34.48	-37.07	-34.06	-32.77	-24.05	-33.07	-35.83
04/04/19	05/04/19	-33.52	-38.12	-30.44	-27.92	-35.21	-35.03	-34.93	-36.92	-26.66	-34.29	-37.08	-33.8	-32.68	-23.9	-33.69	-35.56
04/04/19	05/04/19	-33.21	-38.17	-30.12	-27.6	-34.73	-35	-34.44	-36.61	-26.73	-34.16	-36.93	-33.17	-32.06	-23.48	-33.1	-35.09
04/04/19	05/04/19	-33.31	-38.3	-30.33	-28.11	-34.98	-35.51	-34.93	-36.82	-27.48	-34.78	-37.01	-34.11	-33.09	-24.06	-32.96	-35.61
04/04/19	05/04/19	-33.37	-38.21	-30.13	-27.97	-35.44	-35.34	-34.73	-36.62	-27.04	-34.3	-37	-33.93	-32.76	-23.87	-34.06	-35.56
28/09/18	15/05/19	-33.04	-37.75	-28.27	-26.71	-34.73	-34.69	-34.74	-36.45	-27.42	-34.25	-35.94	-33.82	-33.61	-23.8	-31.49	-35.96
28/09/18	15/05/19	-32.86	-37.6	-27.77	-27.59	-34.58	-34.77	-34.4	-36.3	-27.14	-33.82	-35.84	-33.28	-33.17	-23.73	-31.75	-35.64
28/09/18	15/05/19	-33.03	-37.75	-27.88	-27.58	-34.72	-34.97	-34.54	-36.38	-27.04	-33.94	-35.68	-33.33	-33.26	-23.68	-31.43	-35.68
28/09/18	15/05/19	-33.05	-37.82	-28.05	-27.75	-34.99	-34.94	-34.14	-36.77	-27.11	-33.79	-36.04	-33.44	-33.09	-23.66	-32.04	-35.48
28/09/18	15/05/19	-32.73	-37.61	-28.11	-28.14	-35.68	-35.66	-34.63	-36.09	-26.92	-34.12	-35.96	-33.54	-32.88	-24.39	-32.13	-35.19
28/09/18	15/05/19	-32.76	-37.53	-27.88	-27.79	-36.75	-36.15	-34.91	-36.3	-27.22	-34.44	-35.72	-34.22	-33.63	-26.57	-32.19	-35.5
28/09/18	15/05/19	-33.46	-38.15	-28.98	-29.25	-35.63	-35.85	-36.19	-37.62	-27.87	-35.39	-37.16	-34.99	-34.69	-25.99	-32.45	-37.71
28/09/18	15/05/19	-33.34	-37.76	-28.44	-28.44	-35.28	-35.47	-35.21	-36.75	-27.58	-34.64	-36.62	-34.4	-34.18	-25.08	-31.91	-36.64
28/09/18	15/05/19	-33.22	-37.88	-28.19	-27.97	-35.08	-35.22	-35.14	-36.73	-27.11	-34.46	-36.27	-33.81	-33.56	-24.52	-30.85	-36.19
28/09/18	15/05/19	-33.32	-37.92	-28.64	-28.2	-35.19	-35.52	-35.12	-36.95	-27.26	-34.91	-36.67	-34.05	-33.59	-24.8	-31.35	-36.5
28/09/18	15/05/19	-33.65	-38.42	-28.5	-28.85	-35.41	-35.55	-35.72	-37.59	-27.78	-35.11	-36.8	-34.67	-34.28	-25.74	-33.12	-37.32
28/09/18	15/05/19	-33.35	-38.27	-28.48	-28.15	-35.03	-35.34	-34.75	-36.83	-27.59	-34.62	-36.45	-34.4	-33.55	-24.83	-31.95	-36.89

28/09/18	15/05/19	-33.09	-37.76	-28.44	-28	-35.2	-35.04	-34.69	-37.11	-26.97	-34.2	-35.81	-34	-33.24	-24.16	-32.2	-36.13
03/10/18	31/05/19	-33.19	-38.57	-28.46	-27.7	-34.57	-34.72	-34.56	-36.72	-27.53	-34.19	-36.27	-33.61	-33.58	-23.72	-31.88	-35.86
03/10/18	31/05/19	-32.92	-38.21	-28.36	-27.38	-34.46	-34.71	-34.53	-36.71	-27.27	-34.01	-36.11	-33.56	-33.29	-23.66	-32.7	-35.8
03/10/18	31/05/19	-32.81	-38.33	-28.36	-27.33	-34.51	-34.68	-34.48	-36.56	-27.44	-34.17	-36.2	-33.71	-33.36	-23.93	-32.77	-35.88
03/10/18	31/05/19	-33.05	-38.08	-28.24	-27.46	-34.39	-34.69	-34.7	-36.81	-27.55	-34.17	-36.1	-33.56	-33.38	-23.71	-31.42	-35.42
03/10/18	31/05/19	-33.15	-38.32	-28.39	-27.85	-34.69	-34.84	-34.61	-36.81	-27.92	-34.63	-36.67	-33.75	-33.82	-24.13	-32.08	-36.27
03/10/18	31/05/19	-33.21	-38.57	-28.71	-27.99	-34.94	-34.88	-34.96	-36.67	-27.77	-34.43	-36.73	-33.56	-33.74	-24.18	-32.22	-36.33
03/10/18	31/05/19	-32.83	-38.29	-28.37	-27.68	-34.74	-34.72	-34.6	-36.69	-27.61	-34.31	-35.98	-33.86	-33.35	-23.8	-32.26	-36.07
03/10/18	31/05/19	-32.86	-38.14	-28.56	-27.7	-34.79	-34.74	-34.68	-36.44	-27.53	-33.95	-36.25	-33.3	-33.23	-23.86	-32.16	-35.84
03/10/18	31/05/19	-32.92	-38.01	-28.43	-27.76	-34.63	-34.93	-34.9	-36.9	-27.38	-34.51	-36.21	-33.83	-33.94	-23.66	-32.27	-36.31
03/10/18	31/05/19	-33.05	-38.18	-28.7	-27.59	-34.83	-34.88	-35	-36.59	-27.68	-34.53	-36.24	-34.06	-33.89	-24.02	-32.9	-36.53
03/10/18	31/05/19	-32.5	-38.22	-28.42	-27.46	-34.47	-34.68	-34.61	-36.78	-27.19	-34.11	-35.89	-33.73	-33.01	-23.87	-32.92	-35.9
03/10/18	31/05/19	-32.63	-38.22	-28.71	-27.52	-34.44	-34.81	-34.67	-36.87	-27.59	-34.04	-36.39	-33.69	-33.87	-23.81	-32.08	-36.06
03/10/18	31/05/19	-32.89	-38.22	-28.38	-27.87	-34.83	-34.51	-34.4	-36.62	-27.63	-34.08	-36.41	-33.87	-33.6	-24.16	-32.2	-36.13
17/10/18	06/06/19	-33.32	-38.89	-28.62	-27.8	-35.23	-35.21	-35.25	-37.01	-27.93	-34.52	-36.81	-33.91	-33.5	-23.89	-32.2	-35.91
17/10/18	06/06/19	-33.11	-38.82	-28.42	-27.8	-35.06	-35.03	-34.93	-36.6	-27.78	-33.87	-36.33	-33.83	-33.71	-23.92	-31.54	-35.69
17/10/18	06/06/19	-33.39	-38.82	-28.37	-27.76	-34.97	-35.08	-35.22	-37.23	-27.93	-34.51	-36.61	-34.09	-33.48	-24	-32.55	-36.02
17/10/18	06/06/19	-33.57	-39.1	-28.78	-27.95	-35.1	-35.02	-35.46	-37.37	-28.09	-34.22	-37.13	-34.05	-33.8	-24	-32.81	-35.9
17/10/18	06/06/19	-33.65	-38.88	-28.79	-28.17	-35.62	-35.41	-35.6	-37.21	-28.2	-34.85	-37.02	-34.22	-34.45	-24.61	-34.01	-36.24
17/10/18	06/06/19	-33.48	-39.18	-28.75	-28.5	-35.44	-35.53	-35.53	-37.18	-28.38	-34.71	-37.04	-34.01	-34.24	-24.43	-33.07	-36.37
17/10/18	06/06/19	-33.1	-39.12	-28.79	-28.16	-35.4	-35.37	-35.11	-37.07	-28.27	-34.68	-36.89	-34.3	-34.33	-24.22	-32.76	-35.88
17/10/18	06/06/19	-32.87	-38.7	-28.81	-27.78	-35.15	-35.07	-35.23	-37.14	-28.07	-34.46	-36.71	-34.08	-33.99	-24.19	-33.22	-36.18
17/10/18	06/06/19	-33.11	-38.72	-28.77	-27.86	-35.45	-35.41	-35.41	-37.25	-28.37	-34.38	-36.51	-33.86	-34.05	-24.36	-32.48	-36.02
17/10/18	06/06/19	-33.19	-38.58	-29.01	-27.93	-35.31	-35.41	-35.54	-37.35	-28.19	-35.06	-36.87	-34.41	-33.89	-24.26	-32.16	-36.17
17/10/18	06/06/19	-33.12	-38.9	-28.96	-28.02	-35.04	-35.23	-35.66	-37.69	-28.33	-34.56	-36.78	-34.31	-34.28	-24.62	-32.98	-36.47
17/10/18	06/06/19	-33.11	-38.83	-28.54	-27.89	-35.24	-35.16	-35.48	-37.2	-28.3	-34.78	-37.27	-34.34	-33.98	-24.26	-33.02	-36.27
17/10/18	06/06/19	-33.58	-39.29	-28.94	-28.1	-35.42	-35.44	-35.43	-37.49	-28.67	-34.5	-37.07	-33.94	-34.01	-24.32	-33.16	-36.05
17/10/18	06/06/19	-33.32	-39.09	-28.62	-28.06	-34.97	-35.24	-35.04	-36.87	-28.19	-34.59	-37.26	-33.91	-33.46	-24.26	-33.46	-35.88
02/09/19	27/11/19	-30.65	-36.32	-27.27	-26.97	-33.61	-33.51	-33.32	-35.64	-26.03	-32.77	-34.42	-32.19	-31.9	-22.7	-31.58	-34.59
02/09/19	27/11/19	-30.43	-36.38	-27.18	-26.83	-33.16	-33.34	-33.12	-34.37	-25.55	-32.56	-34.15	-32.18	-31.75	-22.71	-31.1	-34.65
02/09/19	27/11/19	-31.05	-36.67	-27	-26.49	-33.21	-34	-33.18	-35.37	-25.85	-32.56	-33.91	-32.5	-32.08	-22.58	-30.81	-34.83
02/09/19	27/11/19	-31.13	-36.5	-26.58	-26.48	-33.07	-33.61	-33.5	-35.49	-25.89	-32.76	-34.07	-32.04	-31.78	-22.69	-30.81	-34.3
02/09/19	27/11/19	-31.55	-36.74	-26.72	-26.68	-33.09	-33.74	-33.32	-34.92	-26	-32.68	-33.93	-32.23	-31.88	-22.73	-30.77	-35.04
02/09/19	27/11/19	-31.2	-36.55	-26.55	-26.44	-33.35	-33.95	-33.39	-35.01	-25.78	-32.66	-34.36	-32.46	-32.08	-22.56	-31.09	-34.45
02/09/19	27/11/19	-31.36	-36.58	-26.9	-26.32	-33.1	-33.68	-33.17	-34.89	-25.89	-32.51	-34.3	-32.21	-31.94	-22.98	-30.55	-35.11
02/09/19	27/11/19	-31.85	-36.86	-27.06	-26.71	-33.55	-34.3	-33.79	-35.73	-26.33	-33.17	-35.02	-32.96	-32.8	-23.71	-31.86	-35.98
02/09/19	27/11/19	-31.61	-36.89	-27.05	-26.76	-33.54	-34.07	-33.58	-35.27	-26.42	-33.05	-35.13	-32.43	-32.49	-23.3	-30.94	-35.8
02/09/19	27/11/19	-32.13	-36.84	-27.07	-26.89	-33.62	-34.5	-33.66	-35.4	-26.45	-33.04	-35.08	-32.86	-32.57	-23.38	-31.05	-35.28

02/09/19	27/11/19	-32.03	-36.99	-26.78	-26.79	-33.59	-34.19	-33.46	-35.21	-25.96	-32.75	-34.42	-32.65	-32.38	-23.28	-31.26	-35.82
02/09/19	27/11/19	-31.99	-36.87	-26.8	-26.67	-33.33	-33.74	-33.78	-35.7	-26.36	-32.79	-34.54	-32.57	-32.16	-23.08	-30.41	-35.18
02/09/19	27/11/19	-32.2	-37.14	-27.21	-26.95	-33.77	-34.3	-34.11	-35.87	-26.62	-33.2	-35.09	-33.08	-32.91	-23.64	-31.73	-35.85
01/10/19	27/11/19	-31.68	-37.31	-28.22	-27.87	-34.69	-35.1	-34.87	-35.62	-26.83	-33.7	-35.57	-33.66	-33.01	-23.16	-31.79	-34.85
01/10/19	27/11/19	-32.32	-38.21	-27.95	-26.74	-33.89	-34.26	-33.9	-35.4	-26.65	-33.41	-35.3	-32.98	-32.59	-22.91	-31.61	-34.73
01/10/19	27/11/19	-32.36	-37.87	-27.52	-26.81	-34.11	-34.28	-34.06	-35.52	-26.94	-33.26	-35.32	-32.91	-32.56	-22.74	-31.64	-34.65
01/10/19	27/11/19	-32.38	-37.79	-27.45	-26.75	-33.91	-34.09	-33.84	-35.36	-26.58	-33.3	-34.93	-32.83	-32.19	-22.41	-30.98	-34.69
01/10/19	27/11/19	-32.51	-37.67	-27.72	-26.79	-33.86	-34.08	-33.99	-35.87	-26.51	-33.21	-35.33	-33	-32.47	-22.85	-31.36	-34.77
01/10/19	27/11/19	-32.67	-37.87	-27.64	-27.1	-34.3	-34.36	-34.33	-36.02	-26.89	-33.46	-35.04	-33.34	-33.48	-23.26	-31.98	-35.24
01/10/19	27/11/19	-32.52	-38.05	-27.69	-27.24	-34.18	-34.56	-34.3	-36.19	-27.15	-33.75	-35.53	-33.53	-33.49	-24.29	-31.96	-36.24
01/10/19	27/11/19	-32.56	-38.04	-27.73	-27.32	-34.48	-34.49	-34.61	-36.37	-27.05	-33.68	-35.59	-33.41	-33.23	-23.59	-31.24	-35.77
01/10/19	27/11/19	-32.81	-37.93	-27.78	-27.11	-34.5	-34.6	-33.99	-35.73	-26.85	-33.72	-35.35	-33.37	-33.24	-23.58	-31.31	-35.76
01/10/19	27/11/19	-33.09	-37.93	-27.55	-27.06	-34.37	-34.58	-34.76	-36.29	-26.91	-33.64	-35.96	-33.36	-33.34	-22.74	-31.56	-35.6
01/10/19	27/11/19	-33.1	-38.1	-27.82	-27.16	-33.31	-34.6	-34.54	-36.08	-27.15	-33.75	-35.63	-33.51	-33.47	-23.72	-31.48	-36
01/10/19	27/11/19	-33.32	-37.97	-27.91	-27.35	-34.69	-34.68	-34.47	-36.25	-27.12	-33.62	-35.47	-33	-33.26	-23.77	-31.91	-35.8
01/10/19	27/11/19	-33.32	-38.17	-27.66	-27.46	-34.57	-34.67	-34.11	-36.32	-27.29	-33.57	-36.18	-32.96	-33.53	-23.55	-31.23	-35.66
11/10/19	02/12/19	-31.96	-37.75	-27.74	-26.65	-33.82	-34.04	-33.79	-35.71	-26.5	-33.17	-35.05	-33.03	-32.58	-22.98	-32.16	-34.77
11/10/19	02/12/19	-31.99	-37.57	-27.72	-26.76	-33.55	-33.96	-33.92	-35.87	-26.75	-33.3	-34.98	-32.88	-32.59	-23.04	-32.19	-34.73
11/10/19	02/12/19	-32.05	-37.59	-27.75	-26.54	-33.8	-34.01	-33.98	-36.09	-26.92	-33.4	-35.31	-33	-32.59	-22.98	-31.87	-34.82
11/10/19	02/12/19	-32.32	-37.77	-27.62	-26.81	-33.88	-34.01	-34.05	-35.99	-26.83	-33.44	-35.11	-32.91	-32.68	-23.05	-32.02	-34.89
11/10/19	02/12/19	-32.38	-37.98	-27.7	-27.02	-34.01	-33.88	-34.03	-35.95	-27.01	-33.47	-35.29	-32.93	-32.69	-23.32	-31.91	-34.75
11/10/19	02/12/19	-32.37	-37.76	-27.44	-26.69	-33.76	-33.97	-33.79	-35.66	-26.76	-33.04	-35.02	-32.84	-32.35	-22.65	-31.69	-34.64
11/10/19	02/12/19	-32.12	-37.77	-27.71	-26.85	-34.1	-34.25	-34.18	-36.23	-26.64	-33.31	-35.59	-33.1	-32.63	-23.02	-31.95	-35
11/10/19	02/12/19	-32.12	-37.66	-27.88	-26.73	-33.72	-33.92	-33.85	-35.85	-26.76	-33.26	-35.79	-33.16	-32.73	-22.87	-31.61	-34.77
11/10/19	02/12/19	-32.39	-37.91	-27.81	-26.69	-33.6	-33.71	-34.14	-36.16	-26.6	-33.38	-35.58	-33.14	-32.85	-23.07	-31.99	-34.75
11/10/19	02/12/19	-32.28	-37.71	-27.71	-26.76	-33.37	-33.71	-33.9	-36.11	-26.65	-32.96	-35.2	-32.55	-32.32	-22.72	-31.22	-34.57
11/10/19	02/12/19	-32.18	-37.61	-27.51	-26.64	-33.5	-33.99	-33.74	-35.16	-26.66	-33.25	-35.27	-32.84	-32.36	-22.63	-31.3	-34.9
11/10/19	02/12/19	-32.42	-38.13	-27.6	-26.57	-33.86	-33.92	-34.06	-36.28	-26.88	-33.24	-35.71	-33.15	-32.6	-23.13	-32.16	-34.52
09/07/19	05/12/19	-32.34	-37.13	-27.87	-27.75	-34.98	-35	-34.68	-35.7	-27.47	-33.83	-32.99	-33.25	-33.23	-23.24	-32.75	-34.72
09/07/19	05/12/19	-32.52	-37.76	-28.42	-27.59	-34.41	-34.42	-34.09	-35.66	-26.76	-33.27	-32.92	-33.33	-32.65	-23.16	-31.91	-34.52
09/07/19	05/12/19	-32.36	-38.28	-28.25	-27.28	-34.76	-34.62	-34.22	-35.55	-26.79	-33.42	-36.89	-32.88	-32.77	-23.07	-32.15	-34.68
09/07/19	05/12/19	-32.72	-38.39	-27.65	-27.09	-34.46	-34.47	-34.44	-35.6	-26.96	-33.52	-32.38	-33.21	-32.3	-23.1	-31.95	-34.9
09/07/19	05/12/19	-33.15	-38.23	-27.94	-26.94	-33.91	-34.46	-34.29	-36.29	-26.61	-33.3	-31.51	-32.74	-32.59	-22.7	-32.59	-34.76
09/07/19	05/12/19	-32.99	-38.12	-27.71	-27.08	-34.17	-34.29	-34.06	-35.79	-27.03	-33.3	-35.55	-33.06	-33.11	-22.84	-32.22	-34.75
09/07/19	05/12/19	-33.12	-38.7	-27.95	-27.71	-34.38	-34.66	-34.4	-35.94	-27.21	-33.72	-36.22	-33.68	-33.95	-24.38	-32.4	-35.7
09/07/19	05/12/19	-32.95	-38.02	-27.86	-27.43	-33.83	-34.67	-34.47	-35.76	-26.9	-33.23	-35.57	-33.15	-33.27	-23.57	-32.49	-35.34
09/07/19	05/12/19	-32.53	-38.26	-28.15	-28.07	-34.88	-34.67	-34.41	-35.97	-27.09	-33.55	-35.48	-33.01	-32.95	-23.13	-32.32	-34.76
09/07/19	05/12/19	-32.5	-38.34	-28.24	-28.13	-34.43	-34.74	-34.46	-35.8	-27.14	-33.6	-35.4	-32.76	-32.99	-22.87	-32.18	-34.76

09/07/19	05/12/19	-32.6	-38.12	-28.05	-27.66	-34.28	-34.37	-34.7	-35.69	-27.03	-33.49	-35.62	-32.9	-32.69	-22.82	-32.21	-34.64
09/07/19	05/12/19	-33.4	-38.03	-28.25	-27.95	-34.44	-34.56	-34.34	-35.66	-27.15	-33.7	-35.77	-32.73	-32.89	-22.81	-32.65	-34.94
09/07/19	05/12/19	-33.4	-38.26	-28.44	-27.38	-34.42	-34.35	-34.19	-35.91	-26.97	-33.65	-38.93	-33.03	-32.48	-22.94	-32.83	-34.72
09/07/19	05/12/19	-33.26	-37.98	-28.12	-27	-34.03	-34.31	-33.91	-35.43	-26.55	-32.59	-38.86	-33.19	-32.28	-22.6	-32.17	-34.18
11/07/19	03/01/20	-33.43	-38.53	-28.66	-29.03	-36.13	-36.44	-35.95	-37.31	-28.24	-34.79	-36.51	-33.95	-33.43	-23.87	-34.42	-35.53
11/07/19	03/01/20	-33.39	-38.71	-28.99	-29.34	-36.21	-36.25	-36.09	-37.2	-28.34	-34.56	-36.85	-33.82	-33.68	-23.76	-33.98	-35.15
11/07/19	03/01/20	-33.65	-39.05	-29.15	-29.5	-36.34	-36.66	-36.46	-37.41	-28.39	-34.95	-36.9	-34.4	-34.12	-23.89	-33.88	-35.64
11/07/19	03/01/20	-33.57	-38.87	-28.98	-29.13	-36.43	-36.64	-36.48	-37.57	-28.54	-35.06	-36.91	-34.06	-33.48	-23.86	-33.63	-35.35
11/07/19	03/01/20	-33.49	-38.83	-28.81	-28.83	-36.11	-36.45	-36.08	-37.25	-28.24	-35.01	-36.73	-34.06	-33.62	-23.82	-33.66	-35.25
11/07/19	03/01/20	-33.44	-38.87	-28.85	-28.79	-36.01	-36.37	-36.24	-37.65	-28.18	-35.02	-36.94	-34.13	-34.04	-24	-33.72	-35.16
11/07/19	03/01/20	-32.51	-38.12	-28.71	-28.61	-36.01	-36.09	-35.45	-36.87	-28.25	-34.8	-36.26	-34.37	-34.42	-24.02	-35.39	-36.03
11/07/19	03/01/20	-32.61	-37.9	-28.57	-28.17	-35.55	-35.96	-35.6	-36.85	-27.99	-34.7	-35.98	-34.44	-34.28	-23.93	-35.39	-36.03
11/07/19	03/01/20	-32.28	-38.09	-28.65	-28.59	-35.69	-35.75	-35.56	-36.57	-28.02	-34.53	-36.19	-34.46	-34.05	-23.68	-34.14	-35.43
11/07/19	03/01/20	-32.65	-38.22	-28.84	-28.33	-35.67	-35.88	-35.94	-36.72	-28.14	-34.85	-36.4	-34.44	-34.22	-24.1	-34.73	-35.83
11/07/19	03/01/20	-32.32	-38.5	-28.58	-28.48	-35.85	-36.1	-35.89	-36.97	-28.37	-34.78	-36.61	-34.61	-34.63	-24.01	-34.31	-35.63
11/07/19	03/01/20	-32.4	-37.92	-28.32	-28.13	-35.46	-36.1	-35.94	-36.51	-28.05	-34.67	-36.1	-34.9	-34.74	-23.96	-34.23	-35.56
11/07/19	03/01/20	-33.33	-38.64	-29.18	-28.86	-36.01	-36.11	-36.26	-37.46	-28.47	-34.88	-37.34	-34.31	-34.35	-23.82	-33.7	-35.49
11/07/19	03/01/20	-33.52	-38.73	-29.14	-28.79	-36.19	-36.21	-35.77	-37.39	-28.54	-35	-37.29	-34.53	-34.05	-23.9	-33.29	-35.08
13/11/19	06/01/20	-33.58	-38.43	-28.66	-28.75	-36.12	-35.88	-35.97	-37.54	-28.46	-35.15	-36.8	-34.24	-34.09	-24.25	-34.62	-35.76
13/11/19	06/01/20	-33.43	-38.96	-29.53	-28.81	-35.82	-36.13	-36.16	-37.57	-28.57	-34.89	-37.41	-34.49	-34.1	-24.11	-34.91	-35.63
13/11/19	06/01/20	-33.43	-38.69	-29.45	-28.51	-35.49	-36.05	-35.74	-37.66	-28.43	-35.08	-37.04	-34.45	-34.47	-23.96	-34.85	-35.56
13/11/19	06/01/20	-33.54	-38.79	-29.41	-28.4	-35.79	-36.01	-35.77	-37.57	-28.6	-35.04	-37.26	-34.67	-33.82	-24.12	-34.47	-35.4
13/11/19	06/01/20	-33.41	-39.07	-29.59	-28.5	-35.72	-35.8	-35.71	-37.46	-28.3	-34.96	-36.96	-34.01	-34.08	-23.69	-34.23	-35
13/11/19	06/01/20	-33.49	-39.23	-29.47	-28.6	-35.6	-35.93	-35.9	-37.97	-28.47	-34.9	-37.81	-34.48	-34.36	-24.11	-34.03	-35.46
13/11/19	06/01/20	-32.63	-38.8	-28.92	-28.32	-35.79	-35.56	-35.98	-36.84	-27.98	-34.61	-36.6	-34	-33.71	-23.89	-34.86	-35.68
13/11/19	06/01/20	-32.52	-38.28	-28.72	-28.08	-35.52	-35.63	-35.56	-37	-28.15	-34.67	-35.95	-33.94	-33.71	-23.64	-34.14	-35.42
13/11/19	06/01/20	-32.4	-38.22	-28.55	-27.89	-35.41	-35.48	-35.36	-36.68	-27.85	-34.19	-35.68	-33.89	-34.21	-23.58	-33.45	-35.25
13/11/19	06/01/20	-32.62	-38.36	-28.69	-28.27	-35.65	-35.49	-35.4	-36.69	-28.05	-34.54	-35.59	-33.89	-33.66	-23.6	-34.38	-35.85
13/11/19	06/01/20	-32.5	-38	-28.97	-28.51	-35.86	-35.8	-35.9	-36.94	-28.49	-34.77	-36.12	-34.26	-34.11	-23.98	-34.08	-35.91
13/11/19	06/01/20	-32.4	-38.08	-28.72	-28.38	-35.58	-35.21	-35.88	-36.69	-27.87	-34.56	-35.78	-33.7	-33.77	-23.75	-34.34	-35.5
13/11/19	06/01/20	-32.52	-38.17	-28.3	-28.19	-35.8	-35.5	-35.57	-36.79	-28	-34.45	-35.92	-34.17	-33.5	-23.63	-33.81	-35.4
13/11/19	06/01/20	-33.3	-38.68	-29.22	-28.99	-35.63	-35.93	-35.84	-37.59	-28.11	-34.94	-36.15	-34.18	-34.11	-23.94	-33.79	-35.82

Table C.3 Sigma standards' raw $\delta^{13}C$ values.

ID	Der. date	Run date	Gly $\delta^{13}C$ (‰)	Err.	Ser $\delta^{13}C$ (‰)	Err.	Glx $\delta^{13}C$ (‰)	Err.	Ala $\delta^{13}C$ (‰)	Err.	Asx $\delta^{13}C$ (‰)	Err.	Pro $\delta^{13}C$ (‰)	Err.	Hyp $\delta^{13}C$ (‰)	Err.	Val $\delta^{13}C$ (‰)	Err.
BVCR7117_b	28/09/18	27/11/18	-18.68	1.74	-15.17	1.64	-21.15	0.85	-29.11	1.97	-23.18	1.08	-21.78	0.58	-21.79	0.96	-29.45	0.43
BVCR71117_b	17/10/18	10/12/18	-16.29	1.06	-12.66	1.82	-21.51	0.87	-26.37	0.97	-23.65	1.06	-21.5	0.56	-22.01	1.21	-29.36	0.57
BVCR231018	15/01/19	21/01/19	-16.87	0.9	-12.11	1.53	-20.51	0.89	-26.16	0.64	-21.39	0.69	-21.05	0.56	-21.37	0.8	-28.87	0.8
BVCR231018	15/01/19	01/04/19	-15.75	0.54	-11.7	1.07	-19.63	0.73	-24.44	0.45	-20.93	0.93	-20.27	0.47	-20.38	0.85	-28.13	0.4
BVC_7_1	04/04/19	05/04/19	-20.25	0.89	-14.86	0.99	-21.6	1.06	-26.71	0.55	-22.8	0.84	-24.08	0.79	-24.41	1	-26.92	0.39
BVC_7_2	04/04/19	05/04/19	-17.7	0.72	-14.05	0.64	-21.46	1.08	-26.04	0.5	-22.93	0.85	-23.56	0.79	-23.44	0.99	-26.6	0.33
BVCR231018_1	04/04/19	05/04/19	-18.75	0.87	-14.13	0.98	-21.95	1.19	-26.62	0.57	-22.48	1.08	-22.94	0.99	-23.15	1.02	-26.78	0.4
BVCR231018_2	04/04/19	05/04/19	-20.64	0.71	-16.28	0.79	-22.04	1.05	-27.1	0.52	-22.61	0.92	-23.58	0.82	-24.21	1.02	-26.6	0.45
BVCR231018_2	04/04/19	05/04/19	-19.14	0.83	-14.97	0.61	-21.13	1.04	-25.79	0.64	-21.36	0.86	-23.13	0.82	-23.01	0.98	-25.94	0.39
BVCR71117_1	04/04/19	05/04/19	-19.83	0.97	-14.74	0.59	-21.5	1.06	-26.48	1.01	-22.03	0.99	-24.25	0.82	-25.11	1.01	-26.36	0.47
BVCR7117_b	28/09/18	15/05/19	-18.87	1.12	-14.36	1.8	-21.95	1.51	-27.6	0.81	-24.15	1.63	-22.37	0.82	-22	1.44	-31.68	0.84
BVCR71117	17/10/18	06/06/19	-15.27	0.93	-12.45	1	-21.17	0.63	-26.4	0.77	-23.31	0.88	-20.67	0.54	-21.2	0.81	-29.4	0.43
BVCR231018	02/09/19	27/11/19	-19.32	0.9	-13.55	1.44	-21.72	0.89	-27.77	1.53	-22.86	0.73	-21.75	0.64	-21.68	0.93	-29.31	0.56
BVCR220701a	11/10/19	02/12/19	-18.55	0.83	-13.72	1.04	-21.42	0.46	-27.33	0.68	-23.4	0.47	-22.02	0.3	-21.97	0.42	-29.75	0.36
BVCR21419a	09/07/19	05/12/19	-16.13	1.27	-14.65	0.78	-22.41	0.72	-26.05	1.02	-23.72	1.05	-20.33	0.51	-20.82	1.09	-29.72	0.55
BVCR1419b	11/07/19	03/01/20	-20.22	1.51	-17.46	1.43	-22.65	0.94	-29.73	1.49	-25.32	1.14	-22.53	0.55	-22.68	1.14	-31.53	0.7
BVCR220719c	13/11/19	06/01/20	-18.15	2.41	-13.96	2.06	-20.12	2.04	-28.11	2.01	-21.54	2.01	-19.97	1.37	-20.39	1.65	-28.58	1.29

ID	Leu $\delta^{13}C$ (‰)	Err.	Ile $\delta^{13}C$ (‰)	Err.	Thr $\delta^{13}C$ (‰)	Err.	Met $\delta^{13}C$ (‰)	Err.	Lys $\delta^{13}C$ (‰)	Err.	Phe $\delta^{13}C$ (‰)	Err.	Tyr $\delta^{13}C$ (‰)	Err.	Est. bulk $\delta^{13}C$ (‰)	Err.	Meas. bulk $\delta^{13}C$ (‰)	Est-meas bulk offset $\delta^{13}C$ (‰)
BVCR7117_b	-31.85	0.5	-27.17	0.7	-12.91	0.79	-28.25	2.17	-22.91	2.39	-29.79	0.68	-27.24	0.82	-22.72	1.13	-22.92	0.2
BVCR71117_b	-32.49	0.5	-26.96	0.71	-15.93	1.07	-26.3	1.91	-22.04	1.44	-30.39	0.59	-29.99	1.03	-21.98	0.86	-22.92	0.94
BVCR231018	-31.49	0.64	-28.17	0.64	-18.05	1.51	-26.83	0.79	-19.69	1.09	-31.42	0.99	-29.43	0.74	-21.59	0.78	-22.89	1.3
BVCR231018	-31.1	0.37	-27.47	0.41	-14.19	0.72	-24.27	0.84	-19.44	1.53	-29.63	0.44	-27.12	1.05	-20.61	0.61	-22.89	2.28
BVC_7_1	-32.44	0.52	-28.11	0.59	-15.07	0.88	-26.43	0.77	-21.86	2.26	-31.95	0.59	-28.67	0.81	-23.54	0.87	-23.24	-0.3
BVC_7_2	-32.29	0.57	-28.5	0.5	-14.49	0.83	-25.61	0.63	-21.41	1.85	-31.69	0.61	-28.45	0.82	-22.74	0.8	-23.24	0.5
BVCR231018_1	-31.91	0.53	-28.49	0.47	-15.35	1.13	-25.62	1.09	-21.31	1.97	-32.17	0.61	-28.8	0.87	-22.85	0.95	-22.89	0.04
BVCR231018_2	-31.88	0.53	-28.44	0.57	-16.47	0.85	-26	0.62	-22.92	1.86	-32.62	0.64	-29.6	0.69	-23.67	0.82	-22.89	-0.78
BVCR231018_2	-31.33	0.53	-28.08	0.47	-15.43	0.89	-25.03	0.62	-21.85	1.86	-31.91	0.58	-28.77	0.74	-22.75	0.84	-22.89	0.14
BVCR71117_1	-31.96	0.62	-27.73	0.47	-15.06	1.04	-25.8	1.23	-21.51	1.87	-32.03	0.92	-28.69	0.92	-23.37	0.93	-22.92	-0.45
BVCR7117_b	-33.35	1.25	-28.23	1.17	-15.84	1.93	-29.59	1.15	-23.89	1.45	-30.26	1.54	-26.99	1.41	-23.19	1.13	-22.92	-0.27
BVCR71117	-33.04	0.43	-27.61	0.39	-14.04	0.73	-27.54	0.84	-21.5	1.35	-30.27	0.48	-28.71	0.52	-21.42	0.72	-22.92	1.5

BVCR231018	-31.97	0.39	-27.92	0.46	-14.65	1	-26.58	1.77	-22.18	1.16	-29.68	0.64	-27.9	1.21	-22.7	0.86	-22.89	0.19
BVCR220701a	-32.55	0.28	-28.76	0.56	-15.28	0.7	-24.4	1.35	-21.62	0.88	-30.55	0.31	-28.9	0.32	-22.68	0.53	-22.89	0.21
BVCR21419a	-31.74	0.77	-28.05	0.69	-14.54	0.72			-20.12	1.25	-30.85	0.72	-29.75	0.76	-21.58	0.83	-22.72	1.14
BVCR1419b	-32.19	0.93	-29.53	0.71	-21.14	1.7	-28.12	1.36	-19.01	1.55	-33.79	0.23	-26.49	1.7	-23.83	1.02	-22.72	-1.11
BVCR220719c	-30.24	1.15	-26.83	1.24	-13.54	1.98			-18.17	1.48	-32.86	0.96	-30.15	1.84	-21.5	1.75	-22.89	1.39

Table C.4 Carbon amino acid values ($\delta^{13}C_{AA}$) of modern cattle samples used as controls during the analysis (referred to as "bovine controls")."Err." refers to the measurement uncertainty as explained in the main text. The bulk values were measured by EA-IRMS. The estimated bulk values were derived by mass balance calculations as explained in the main text and the error associated (Err.) is the error propagated from all the amino acid measurements.

ID	**Der. date**	**Run date**		**Err.**	**Ser** $\delta^{15}N$ (‰)	**Err.**	**Glx** $\delta^{15}N$ (‰)	**Err.**	**Ala** $\delta^{15}N$ (‰)	**Err.**	**Asx** $\delta^{15}N$ (‰)	**Err.**	**Pro** $\delta^{15}N$ (‰)	**Err.**	**Hyp** $\delta^{15}N$ (‰)	**Err.**	**Val** $\delta^{15}N$ (‰)	**Err.**
BCR090212	11/11/2017	17/11/2017	3.86	0.06	3.54	0.05	9.63	0.07	6.42	0.03	8.24	0.05	9.79	0.23	10.31	0.38	13.36	0.52
BVCR71117	17/10/2018	15/05/2019	4.18	0.08	4.74	0.82	10.63	0.18	7.28	0.14	9.23	0.38	10.25	0.14	10.6	0.43	12.34	1.51
BVCR231018	15/01/2019	12/06/2019	4.14	0.73	5.07	0.6	11.12	0.4	8.34	0.53	11.16	0.51	9.07	0.2	10.21	0.24	14.96	0.61
BVCR1419	09/07/2019	15/07/2019	3.83	1.12	4.09	0.96	9.73	0.3	7.49	0.54	10.6	0.68	8.37	0.26	9.1	0.41	16.81	0.88
BVCR1419b	11/07/2019	22/07/2019	3.77	0.26	3.84	0.3	9.61	0.03	7.26	1.03	10.18	0.41	8.43	0.21	9.13	0.19	16.31	0.99
BVCR1419c	18/07/2019	24/07/2019	4.49	0.8	5.88	0.62	9.65	0.17	8.38	0.65	9.68	0.4	8.94	0.15	9.39	0.31	15.21	1.25
BVCR1419c	18/07/2019	24/07/2019	4.43	0.98	4.07	0.2	9.44	0.37	6.57	1.07	9.89	0.7	8.46	0.26	8.45	0.57	16.46	0.41
BVCR1419d	24/07/2019	30/07/2019	3.74	0.45	4.46	0.39	9.69	0.26	8.03	0.46	10.55	0.33	8.76	0.3	8.94	0.13	16	0.82
BVCR1419e	26/07/2019	05/08/2019	3.46	0.45	3.85	0.57	9.44	0.25	8.04	0.56	9.83	0.61	8.29	0.45	8.37	0.09	15.48	0.8
BVC231018	02/09/2019	10/09/2019	3.97	0.37	4.45	0.38	9.92	0.22	6.5	0.24	9.42	0.17	8.72	0.53	9.43	0.52	13.71	0.73
BVCR71117	03/10/2018	10/09/2019	2.69	0.16	3.52	1.15	9.01	0.52	6.55	0.17	9.52	0.41	7.6	0.28	8.71	0.62	13.57	0.68
BVC231018	02/09/2019	16/09/2019	4.63	0.62	4.02	0.35	9.38	0.14	6.76	0.14	9.28	0.18	8.36	0.11	8.97	0.6	13.48	0.5
BVCR71117	17/10/2018	26/09/2019	3.5	0.42	3.56	0.22	8.75	0.41	8.4	0.12	8.72	0.19	7.58	0.2	8.15	0.43	13.14	0.72
BVCR220719b	11/10/2019	15/10/2019	4.28	0.09	5.53	0.15	10.48	0.26	8.66	0.66	10.32	0.34	9.68	0.1	10.41	0.31	14.89	0.39
BVCR220719a	11/10/2019	09/12/2019	4.33	0.47	5.54	0.59	10.52	0.35	8.14	0.7	9.42	0.36	9.81	0.19	9.6	0.47	12.03	0.58
BVCR220719c	13/11/2019	27/01/2020	4.61	0.34	5.52	0.33	10.73	0.7	8.31	1.22	9.35	0.09	9.87	0.2	11.31	0.26	12.4	0.93

ID	**Leu** $\delta^{15}N$ (‰)	**Err.**	**Ile** $\delta^{15}N$ (‰)	**Err.**	**Thr** $\delta^{15}N$ (‰)	**Err.**	**Lys** $\delta^{15}N$ (‰)	**Err.**	**Phe** $\delta^{15}N$ (‰)	**Err.**	**Est. bulk** $\delta^{15}N$ (‰)	**Err.**	**Meas. bulk** $\delta^{15}N$ (‰)	**Est-meas bulk offset** $\delta^{15}N$ (‰)

BCR090212	9.51	1.12	11.45	0.29	-2.17	1.12			8.75	0.28	6.73	0.16	6.18	0.55
BVCR71117	8.63	0.1	13.55	0.4	-3.72	1.78	1.88	0.68	10.04	0.54	6.83	0.27	6.06	0.77
BVCR231018	11.5	0.44	13.64	0.46	-1.81	0.97	3.26	1.05	9.77	0.36	7.07	0.56	6.23	0.84
BVCR1419	12.65	0.1	12.6	1.38	-3.12	0.74	2.55	0.87	9.42	0.91	6.54	0.72	6.16	0.38
BVCR1419b	12.14	0.54	12.62	1.13	-3.39	0.66	3.27	0.54	9.69	0.77	6.49	0.4	6.16	0.33
BVCR1419c	10.15	0.61	12.39	0.86	-4.16	0.42	2.47	0.65	9.99	0.58	6.89	0.55	6.16	0.73
BVCR1419c	12.31	0.97	12.73	1.43	-2.47	0.87	2.59	0.55	8.99	0.8	6.6	0.7	6.16	0.44
BVCR1419d	11.33	0.7	12.17	0.25	-2.66	0.45	3.23	0.75	8.91	0.39	6.66	0.43	6.16	0.5
BVCR1419e	11.82	0.65	10.76	0.12	-3.05	1.3	3.37	0.33	9.34	0.68	6.38	0.48	6.16	0.22
BVC231018	10.59	0.23	10.92	0.2	-4.26	0.81	2.88	0.44	9.37	0.4	6.37	0.39	6.23	0.14
BVCR71117	10.33	0.42	10.88	0.52	-5.55	0.19	1.96	0.14	9.43	0.72	5.5	0.29	6.06	-0.56
BVC231018	10.64	0.43	12.35	0.56	-4.87	0.41	2.96	0.44	9.83	0.14	6.5	0.35	6.23	0.27
BVCR71117	10.54	0.44	12.64	1.56	-4.7	0.44	3.03	1.27	9.49	0.35	6.03	0.4	6.06	-0.03
BVCR220719b	11.8	0.37	12.75	0.55	-1.64	0.45	3.44	0.72	9.51	0.35	7.23	0.26	6.3	0.93
BVCR220719a	10.34	0.57	11.37	0.99	-4.1	0.31	3.19	0.27	8.22	0.04	6.98	0.41	6.3	0.68
BVCR220719c	10.65	0.51	10.37	1.83	-3.21	0.87	4.13	0.28	8.7	0.81	7.21	0.47	6.3	0.91

Table C.5 Nitrogen amino acid values ($\delta^{15}N_{AA}$) of modern cattle samples used as controls during the analysis (referred to as "bovine controls")."Err." refers to the measurement uncertainty as explained in the main text. The bulk values were measured by EA-IRMS. The estimated bulk values were derived by mass balance calculations as explained in the main text and the error associated (Err.) is the error propagated from all the amino acid measurements.

Appendix D

Bulk SIA and CSIA results

Information about the material analysed for this thesis as well as the bulk SIA and CSIA-AA results are reported in this appendix.

D.1 Archaeological grains

Cereals from Roman York

The barley and spelt caryopses from Roman York analysed in this thesis were sampled from two deposits of cereal grains discovered at 39-41 Coney Street and 5 Rougier Street (Ottaway 2004).
The site located at 39-41 Coney Street was excavated during 1974-75 by the York Archaeological Trust and coded 1974.18. The excavation brought to light a Roman warehouse first built in 70-90 AD, then probably set on fire, and later rebuilt between the 1^{st} and the 2^{nd} century AD (Kenward and Williams 1979). The warehouse is close to a Roman military fort and therefore it is believed that it was used by the soldiers to store cereals (Kenward and Williams 1979). The samples here analysed belong to the second phase of the store-building, particularly from context 2098, one of a series of slots filled with a cereal deposit coded 2077. The deposit was composed of *Triticum spelta* (54.8-61.0 %), *Hordeum vulgare* (23.2-25.0 %) *Secale cereale* (9.4-17.8 %), *Bromus* sp. (6.6-7.6 %), *Avena fatua* and *Avena sativa* (3.6-5.6 %), even though difficulties arose during classification due to spread germination and charring that had altered the seeds' morphology (Kenward and Williams 1979). Rye (*Secale cereale*), oat (*Avena* sp.) and brome (*Bromus* sp.) are not considered to be local, thus it is probable that the warehouse was an off-loading point, also suggested from its position, located nearby the River Ouse (Ottaway 2011).

The excavations at 5 Rougier Street, coded 1981.12, were also directed by the York Archaeological Trust. The area, which was located next to the main access road to York coming from south-west, started to be explored in 1981 (Ottaway 2004). The trench excavated revealed a thick deposit of burnt material, mainly charcoal and grains, interpreted as a warehouse destroyed by fire and dated to the late 2^{nd} century AD (Allison *et al.* 1990). Samples here analysed are from context 1205 of the burnt deposit, which was also found to be partially, if not completely, waterlogged (Allison *et al.* 1990). The deposit consisted of *Triticum spelta* (88 %) and *Hordeum vulgare* (11 %), with small proportions of other wheat grains (less than 1 %) and *Avena* sp. (less than 0.5 %) and few *Bromus* sp. grains. Tomlinson (1989) also recounts some spelt grains being in their glumes (4-6 %). Around 50 % of spelt and 20 % of barley and oat had sprouted (Allison *et al.* 1990).

Grains from Bronze Age and Neolithic Turkey

Barley, "new type" wheat and pea from Çatalhöyük were sampled from different burnt buildings from the East Mound of the famous megasite in central Anatolia, dated *ca.* 7400-6000 cal BC. Botanical material from Çatalhöyük has been extensively explored in the past few years (*e.g.*, Bogaard *et al.* 2009, 2014, 2017)
The emmer and barley from Bronze Age Hattusha were sampled from the largest archaeobotanical assemblage in the world. Hattusha, the capital of the Hittite state, was discovered in the 19^{th} century and in 1999 a grain storage was excavated, which contained enough grains to feed *ca.* 20000-30000 people/year and that was partially burnt down during the early 16^{th} century BC. The material has been recently subjected to archaeobotanical and carbon and nitrogen stable isotope analysis to investigate cultivation strategies in the Easter Mediterranean Bronze Age (Diffey *et al.* 2017, 2020).

ID	*Taxa*		Provenance	Chronology	Element	Sex	Age
	Latin name	**Common name**					
			Humans				
F10I11	*Homo sapiens*	Human	*Fornici* (Herculaneum)	79 AD	rib	F	30-40
F10I14	*Homo sapiens*	Human	*Fornici* (Herculaneum)	79 AD	rib	M	30-40
F10I16	*Homo sapiens*	Human	*Fornici* (Herculaneum)	79 AD	rib	F	30-40
F10I17	*Homo sapiens*	Human	*Fornici* (Herculaneum)	79 AD	rib	M	30-40
F10i20	*Homo sapiens*	Human	*Fornici* (Herculaneum)	79 AD	rib	M	40-50
F10I22	*Homo sapiens*	Human	*Fornici* (Herculaneum)	79 AD	tarsal bone	M	20-30
F10I28	*Homo sapiens*	Human	*Fornici* (Herculaneum)	79 AD	rib	F	30-40
F12I23	*Homo sapiens*	Human	*Fornici* (Herculaneum)	79 AD	rib	M	40-50
F12i28	*Homo sapiens*	Human	*Fornici* (Herculaneum)	79 AD	rib	F	30-40
F12I3	*Homo sapiens*	Human	*Fornici* (Herculaneum)	79 AD	rib	F	20-30
F7i10	*Homo sapiens*	Human	*Fornici* (Herculaneum)	79 AD	rib	M	30-40
F7I7	*Homo sapiens*	Human	*Fornici* (Herculaneum)	79 AD	rib	M	20-30
F8i10	*Homo sapiens*	Human	*Fornici* (Herculaneum)	79 AD	rib	IND	10-15
F8i11	*Homo sapiens*	Human	*Fornici* (Herculaneum)	79 AD	rib	IND	15-20
F8I23	*Homo sapiens*	Human	*Fornici* (Herculaneum)	79 AD	rib	M	20-30
F8I6	*Homo sapiens*	Human	*Fornici* (Herculaneum)	79 AD	rib	F	20-30

F8I7	*Homo sapiens*	Human	*Fornici* (Herculaneum)	79 AD	rib	M	40-50
F9I13	*Homo sapiens*	Human	*Fornici* (Herculaneum)	79 AD	rib	M	40-50
F9I9	*Homo sapiens*	Human	*Fornici* (Herculaneum)	79 AD	rib	M	40-50
			Cereals and Legumes				
1703b	*Hordeum vulgare*	Barley	Herculaneum	79 AD	Grain		
1703w	*Triticum* sp.	Wheat	Herculaneum	79 AD	Grain		
1895e	*Triticum dicoccum*	Emmer	Herculaneum	79 AD	Grain		
723w	*Triticum* sp.	Wheat	Herculaneum	79 AD	Grain		
MB	*Hordeum vulgare*	Barley	Italy	Modern	Grain		
MDW	*Triticum durum*	Macaroni wheat grain	Italy	Modern	Grain		
MF	*Triticum monococcum*	Einkorn	Italy	Modern	Grain		
MO	*Ave sativa*	Oat	Italy	Modern	Grain		
BarleyP	*Hordeum vulgare*	Barley	Pompeii	79 AD	Grain		
LBCFA16F	*Triticum durum/aestivum*	Free-threshing wheat grain	*Portus Romae*	Early II AD	Grain		
LBCFD16E	*Triticum durum*	Macaroni wheat grain	*Portus Romae*	Early II AD	Grain		
LBTA1012I	*Triticum aestivum*	Bread wheat grain	*Portus Romae*	Early II AD	Grain		
LBTD1012H&I	*Triticum durum*	Macaroni wheat grain	*Portus Romae*	Early II AD	Grain		
2327m	*Panicum miliaceum*	Millet	Herculaneum	79 AD	Grain		
MM	*Panicum miliaceum*	Millet	Italy	Modern	Grain		
200b	*Vicia faba*	Broadbean	Herculaneum	79 AD	Pulse		
2314c	*Cicer arietinum*	Chickpea	Herculaneum	79 AD	Pulse		
2317p	*Vicia faba*	Pea	Herculaneum	79 AD	Pulse		
692l	*Lens culiris*	Lentil	Herculaneum	79 AD	Pulse		
MC	*Cicer arietinum*	Chickpea	Italy	Modern	Pulse		
ML	*Lens culiris*	Lentil	Italy	Modern	Pulse		
			Terrestrial herbivores				
EF10OC	*Ovis*	Sheep	*Fornici* (Herculaneum)	79 AD	vertebra		

EF7DOG?	*Bos*	Cow	*Fornici* (Herculaneum)	79 AD	fragments
EF7OC	*Ovis*	Sheep	*Fornici* (Herculaneum)	79 AD	vertebra
EF8BOS?	*Bos*	Cow	*Fornici* (Herculaneum)	79 AD	tooth
EF8SG	*Ovis*	Sheep	*Fornici* (Herculaneum)	79 AD	long bone
PSC1	*Bos*	Cow	Porta Stabia (Pompeii)	Early I BC	phalanx
PSC2	*Bos*	Cow	Porta Stabia (Pompeii)	Early I BC	phalanx
PSFE1	*Capra*	Goat	Porta Stabia (Pompeii)	Early I AD	rib
PSG2	Herbivore	Herbivore	Porta Stabia (Pompeii)	Early I AD	metacarpal
PSSG3	*Capreolus*	Roe deer	Porta Stabia (Pompeii)	Early I AD	phalanx
VEDE1	*Capreolus*	Roe deer	Velia	I - II AD	
VEHO1	*Equus*	Horse	Velia	I - II AD	
VEHO2	*Equus*	Horse	Velia	I - II AD	
VEHO3	*Equus*	Horse	Velia	I - II AD	
VEHO4	*Equus*	Horse	Velia	I - II AD	
VESH1	*Capra*	Goat	Velia	I - II AD	
VPHO	*Equus*	Horse	Villa dei Papiri (Herculaneum)	79 AD	
		Terrestrial omnivores			
EF11DOG	*Canis*	Dog	*Fornici* (Herculaneum)	79 AD	vertebra
EF12DOG1	*Canis*	Dog	*Fornici* (Herculaneum)	79 AD	atlante
EF12DOG2	*Canis*	Dog	*Fornici* (Herculaneum)	79 AD	vertebra
PSB1	Columbiformes	Pigeon/dove	Porta Stabia (Pompeii)	Early I AD	fragments
PSCH1	*Gallus*	Chicken	Porta Stabia (Pompeii)	Early I AD	humerus

PSCH2	*Gallus*	Chicken	Porta Stabia (Pompeii)	Early I AD	tibio tarsus
PSCH3	*Gallus*	Chicken	Porta Stabia (Pompeii)	Early I AD	femur
PSG1	*Sus*	Pig	Porta Stabia (Pompeii)	Early I AD	femur
PSG3	*Sus*	Pig	Porta Stabia (Pompeii)	Early I AD	tibia
PSP1	*Sus*	Pig	Porta Stabia (Pompeii)	Early I AD	tibia
PSP2	*Sus*	Pig	Porta Stabia (Pompeii)	Early I AD	tibia
PSP3	*Sus*	Pig	Porta Stabia (Pompeii)	Early I AD	tibia
PSP4	*Sus*	Pig	Porta Stabia (Pompeii)	Early I AD	jaw
PSP5	*Sus*	Pig	Porta Stabia (Pompeii)	Early I AD	jaw
PSP6	*Sus*	Pig	Porta Stabia (Pompeii)	Early I AD	radius
PSP7	*Sus*	Pig	Porta Stabia (Pompeii)	Early I AD	radius cap
PSS1	*Sus*	Pig	Porta Stabia (Pompeii)	Early I AD	humerus
PSSG1	*Sus*	Pig	Porta Stabia (Pompeii)	Early I AD	pelvis
PSSG2	*Sus*	Pig	Porta Stabia (Pompeii)	Early I AD	phalanx
			Marine fish		
ABF3	Sciaenidae	Meagre	Albarracín	X-XII AD	vertebra
TU17058	Scombridae	Tuna	Castro Marim	Roman	vertebra
TU17059	Scombridae	Tuna	Castro Marim	Roman	vertebra
HSCC	Congridae	Congridae	House of the Surgeon (Pompeii)	III BC - I AD	Posterior abd. vertebra

HSG1	Garum	Herrings and tarpons	House of the Surgeon (Pompeii)	III BC - I AD	mixed elements
HSG3	Garum	Herrings and tarpons	House of the Surgeon (Pompeii)	III BC - I AD	mixed elements
HSLA	Labridae	Wrasses	House of the Surgeon (Pompeii)	III BC - I AD	Premaxilla
HSMM	Merlucciidae	European hake	House of the Surgeon (Pompeii)	III BC - I AD	Caudal vertebra
HSSP1	Sparidae	Sea breams and porgies	House of the Surgeon (Pompeii)	III BC - I AD	Caudal vertebra
HSSP2	Sparidae	Sea breams and porgies	House of the Surgeon (Pompeii)	III BC - I AD	Posterior abd. vertebra
HSSP3	Sparidae	Sea breams and porgies	House of the Surgeon (Pompeii)	III BC - I AD	Caudal vertebra
HSSSA	Scombridae	Atlantic bonito	House of the Surgeon (Pompeii)	III BC - I AD	Caudal vertebra
HSSSQ	Squatinidae	Angelshark	House of the Surgeon (Pompeii)	III BC - I AD	Posterior abd. vertebra
HSTT	Carangidae	Atlantic horse mackerel	House of the Surgeon (Pompeii)	III BC - I AD	Posterior abd. vertebra
PSM1	Merlucciidae	European hake	Porta Stabia (Pompeii)	Early I AD	vertebra
PSMU1	Muraenidae	Mediterranean moray	Porta Stabia (Pompeii)	Early I AD	mandibola
PSPL1	Pleuronectidae	European plaice	Porta Stabia (Pompeii)	Early I AD	Preopercular
PSSC1	Scombridae	Scombridae	Porta Stabia (Pompeii)	Early I AD	vertebra

PSSC2	Scombridae	Bonito or frigate tuna	Porta Stabia (Pompeii)	Early I AD	vertebra
PSSC3	Scombridae	Bonito or frigate tuna	Porta Stabia (Pompeii)	Early I AD	Hyomandibular
PSSC5	Scombridae	Atlantic chub mackerel	Porta Stabia (Pompeii)	Early I AD	Dentary
PSSC6	Scombridae	Horse mackrel, bonito, tuna	Porta Stabia (Pompeii)	Early I AD	Quadrate
PSSC7	Scombridae	Bonito or frigate tuna	Porta Stabia (Pompeii)	Early I AD	vertebra
PSSP1	Sparidae	Sea breams and porgies	Porta Stabia (Pompeii)	Early I AD	vertebra
PSSP2	Sparidae	Gilt-head bream	Porta Stabia (Pompeii)	Early I AD	mandibola
PSSP3	Sparidae	Sea breams and porgies	Porta Stabia (Pompeii)	Early I AD	
PST1	Carangidae	Mediterranean horse mackerel	Porta Stabia (Pompeii)	Early I AD	vertebra
TU17050	Scombridae	Tuna	Punta Camaril	II BC	vertebra
SSF2	Triakidae	School shark	Santa Severa	VII-XV AD	
SSF3+4	Sparidae	Sea breams and porgies	Santa Severa	VII-XV AD	
SSF5	Labridae	Ballan wrasse	Santa Severa	VII-XV AD	
SSFsb	Sparidae	Sea bream	Santa Severa	VII-XV AD	

Table D.1 Information about the material analysed in this thesis. Sex and age determination of the human remains from AD79 Herculaneum were provided by Dr Luca Bondioli. The classification of the terrestrial animals by their Latin name is the one obtained using ZooMS while the common name is sometimes more specific depending on the morphological identification or archaeological context. The morphological identification of the marine fish and the estimation of their total length (cm) was carried out by Dr H. K. Robson, for the remains from the House of the Surgeon (Pompeii), and by Dr J. K. Bakker, for those from Porta Stabia (Pompeii).

ID	**Collagen yield** %	%C	%N	C:N	$\delta^{13}C$ (‰)	Err.	$\delta^{13}C_{apa}$ (‰)	Err.	$\delta^{15}N$ (‰)	Err.	$\delta^{18}O_{apa}$ (‰)	Err.
						Humans						
F10I11		41.9	14.7	3.3	-19.7	0.03	-8.65	0.3	9.31	0.5*		
F10I14		42.2	15.3	3.2	-19.02	0.5			10.54	0.5		
F10I16		43.7	15.3	3.3	-19.79	0.1	-9.23	0.3	10.09	0.2		

F10I17		41.4	15.2	3.2	-18.84	0.5			11.57	0.5		
F10i20		43.1	15.6	3.2	-19.59	0.5			9.14	0.5	-1.44	0.4
F10I22		43.1	15.8	3.2	-19.07	0.5			10.49	0.5		
F10I28		41.6	15	3.2	-19.65	0.03			9.16	0.2		
F12I23		43.7	15.5	3.3	-18.57	0.1	-8.61	0.3	10.93	0.12	-1.34	0.4
F12i28	14.84%	40.57	14.9	3.2	-19.08	0.07	-8.44	0.3	10.39	0.25		
F12I3		43.8	15.5	3.3	-19.67	0.19	-7.5	0.3	10.09	0.3		
F7i10	13.15%	39.77	14.5	3.2	-18.91	0.14	-10.71	0.3	9.73	0.23		
F7I7		41.7	15.2	3.2	-19.27	0.5			10.07	<0.5	-1.24	0.4
F8i10		42.2	15.5	3.2	-19.77	0.5			9.5	0.5		
F8i11		43.4	16	3.2	-19.81	0.5			8.17	0.5		
F8I23		42	15.4	3.2	-19.57	0.5			9.1	<0.5		
F8I6		35.6	12.6	3.3	-19.92	0.5			9.41	0.5		
F8I7		42.4	15.5	3.2	-18.88	0.5			10.83	<0.5		
F9I13					-19.12	0.1	-10.24	0.3	10.76	0.2		
F9I9					-18.8	0.1	-10.22	0.3	11.45	0.2		
Cereals and Legumes												
1703b		73.69	20.82	4.13	-22.4	0.12			7.1	0.19		
1703w		73.83	18.54	4.65	-22.7	0.12			4.1	0.2	-1.25	0.4
1895e		79.56	22.11	4.2	-25	0.17			0.8	0.27	-0.17	0.4
723w		65.2	18.64	4.08	-23.2	0.13			4.3	0.19		
MB		44.54	2.34	22.18	-27.67	0.07			6.18	0.24		
MDW		44.42	2.79	18.61	-24.39	0.05			9.5	0.19		
MF		43.62	2.29	22.2	-27.03	0.05			7.35	0.18		
MO		44.74	1.92	27.22	-28.09	0.06			3.64	0.3		
BarleyP					-23.8				0.8			
LBCFA16F					-22.6				9.1	0.2		
LBCFD16E					-23.1				10.1	0.2	1.05	0.4
LBTA1012I					-23.5				4	0.2		
LBTD1012H&I					-23.1				10.9	0.2		
2327m		76.86	22.56	3.97	-11.1	0.07			1.76	0.23		
MM		43.65	1.66	30.75	-13.92	0.03			2.67	0.25		
200b		60.69	9.77	7.25	-26.53	0.17			0.6	0.23		
2314c		69.55	10.57	7.68	-22.21	0.17			0.92	0.23		
2317p		61.74	6.64	10.85	-21.21	0.04			0.35	0.21		
692l		63.86	11.18	6.66	-22.18	0.16			-0.49	0.25		
MC		40.67	1.12	42.27	-21.84	0.1			-1.58	0.31		

ML		41.36	1.91	25.33	-24.6	0.13			-0.36	0.24		
						Terrestrial herbivores						
EF10OC	9.21%	39.34	14.4	3.19	-19.8	0.08			3.68	0.29	0.06	0.4
EF7DOG?	9.43%	40.89	14.77	3.23	-20.91	0.06			4.88	0.28		
EF7OC	13.19%	30.06	10.82	3.24	-20.06	0.13			3.15	0.21		
EF8BOS?	5.59%	38.35	14.2	3.15	-21.52	0.12			5.6	0.2	-0.05	0.4
EF8SG	46.70%	38.74	14.2	3.18	-21.2	0.07	-10.24	0.3	7.29	0.17		
PSC1	14.36%	42.83	15.66	3.19	-19.35	0.05			5.78	0.18		
PSC2	31.13%	43.86	15.98	3.2	-20.22	0.11	-4.61	0.3	6.17	0.18		
PSFE1	12.15%	43.61	15.84	3.21	-21.31	0.12			3.91	0.2		
PSG2	4.65%	41.03	14.94	3.2	-21.32	0.05			6.64	0.17		
PSSG3	19.19%	42.54	14.99	3.31	-20.57	0.06	-5.36	0.3	3.66	0.3		
VEDE1				3.14	-21.96	0			4.66	0.05		
VEHO1		41.02	14.84	3.22	-17.84	0.03			1.5	0.23		
VEHO2				3.28	-21.4	0.04			8.1	0.43		
VEHO3				3.16	-21.64	0.01			2.34	0.04		
VEHO4				3.21	-21.36	0.06			3.96	0.06		
VESH1				3.22	-21.24	0.1			2.57	0.09		
VPHO	49.39%	33.77	12.43	3.17	-20.94	0.09			2.69	0.2		
						Terrestrial omnivores						
EF11DOG	17.21%	40.19	14.79	3.17	-18.7	0.08			8.78	0.25		
EF12DOG1	15.94%	42.56	15.64	3.18	-18.8	0.06			8.76	0.24		
EF12DOG2	12.57%	41.52	15.07	3.21	-19.16	0.08			8.88	0.24		
PSB1	7.21%	42.41	15.04	3.29	-13.42	0.06			5.42	0.18		
PSCH1	11.15%	43.88	6.99	3.24	-17.14	0.05	-5.68	0.3	6.99	0.17		
PSCH2	16.04%	39.11	14.16	3.22	-18.18	0.04			5.61	0.18		
PSCH3	7.49%	42.73	15.34	3.25	-15.6	0.06			6.44	0.17		
PSG1	16.94%	29.27	10.6	3.22	-20.61	0.06	-8.11	0.3	4.56	0.29		
PSG3	11.90%	43.94	16.12	3.18	-18.54	0.09			4.18	0.19		
PSP1	19.15%	40.91	14.5	3.29	-19.03	0.05			7.88	0.17		
PSP2	10.89%	40.15	14.99	3.13	-21.02	0.06			6.18	0.26		
PSP3	13.49%	41.31	14.99	3.22	-20.81	0.04	-7.92	0.3	6.32	0.17		
PSP4	10.88%	43.59	16	3.18	-20.05	0.04			3.08	0.2	-0.31	0.4
PSP5	13.49%	41.44	14.82	3.26	-21.44	0.04			7.93	0.16		
PSP6	14.86%	41.9	15.25	3.2	-20.89	0.04			3.06	0.2		

PSP7	12.04%	43.26	15.82	3.19	-20.6	0.05			2.36	0.21		
PSS1	5.08%	30.15	10.71	3.29	-21.05	0.06			3.15	0.3		
PSSG1	3.02%	35.42	12.93	3.2	-20.78	0.06			3.63	0.32		
PSSG2	14.52%	41.54	15.39	3.15	-20.86	0.06			3.24	0.3		
					Marine fish							
ABF3	16.53%	45.62	16.85	3.16	-11.43	0.08	-5.96	0.3	9.79	0.17		
TU17058	4.09%	44.17	16.32	3.16	-12.28	0.12			9.83	0.15	-4.34	
TU17059	4.51%	46.81	16.67	3.27	-12.29	0.37			10.08	0.16		
HSCC	4.22%	44.41	15.9	3.26	-14.17	0.23			9.18	0.16		
HSG1	11.63%	41.34	14.69	3.28	-16.22	0.21			8.09	0.16		
HSG3	5.78%	41	13.96	3.43	-15.51	0.25			4.83	0.18		
HSLA	11.45%	42.96	15	3.34	-12.9	0.41			9.19	0.16		
HSMM	1.03%	39.07	14.09	3.23	-13.65	0.16			10.76	0.16		
HSSP1	6.13%	45.08	16.27	3.23	-12.87	0.08			6.97	0.16		
HSSP2	3.77%	42.72	15.78	3.16	-13.14	0.09			8	0.16		
HSSP3	51.29%	40.6	14.42	3.29	-15.67	0.13			11.86	0.18		
HSSSA	17.59%	44.32	15.85	3.26	-12.41	0.12			12.2	0.17	-3.4	0.4
HSSSQ	10.39%	39.56		3.51	-11.87	0.1	-1.55	0.3	9.45	0.16		
HSTT	9.70%	49.93	17.71	3.29	-13.85	0.11			9.21	0.16		
PSM1	3.64%	35.26	13.25	3.1	-12.18	0.09			11.81	0.23		
PSMU1	9.35%	36.58	10.58	3.22	-11.04	0.06			10.58	0.15	-5.3	0.4
PSPL1	9.03%	38.23	13.96	3.2	-13.81	0.18			8.65	0.16		
PSSC1	13.27%	39.22	13.28	3.45	-14.32	0.13			7.72	0.25		
PSSC2	13.48%	42.41	15.65	3.16	-12.77	0.09			7.16	0.25		
PSSC3	10.18%	39.18	14.29	3.2	-13.09	0.23			8.06	0.25	-4.22	0.4
PSSC5	9.01%	41.84	15.7	3.11	-13.21	0.08			8.78	0.24		
PSSC6	11.17%	42.1	15.42	3.18	-13.57	0.16			9.11	0.23	-2.81	0.4
PSSC7	10.50%	42.88	15.68	3.19	-13.93	0.09			6.46	0.26	-5.69	0.4
PSSP1	7.63%	40.72	15.25	3.12	-12.62	0.06			9.54	0.16		
PSSP2	2.81%	40.33	13.97	3.37	-13.86	0.12			9.24	0.24		
PSSP3	10.80%	36.33	13.8	3.07	-12.85	0.08			5.69	0.27		
PST1	10.97%	37.29	14.19	3.07	-13.34	0.08			8.42	0.25		
TU17050	4.00%	37.79	13.4	3.29	-13.07	0.21			10.79	0.15	-3.99	
SSF2	15.13%	43.05	15.46	3.25	-11.73	0.08	-5.36	0.3	14.42	0.18		
SSF3+4	13.18%	42.93	15.85	3.16	-8.66	0.1			9.79	0.16		
SSF5	8.44%	42.95	15.11	3.32	-10.34	0.18			10.41	0.16	-5.25	0.4

SSFsb	3.39%	42.8	15.3	3.26	-7.95	0.1		9.99	0.16

Table D.2 Bulk carbon and nitrogen values from human and animal collagen and plant material ($\delta^{13}C$ ‰ and $\delta^{15}N$ ‰) and carbon and oxygen isotope values of bone apatite ($\delta^{13}C_{apa}$ ‰ and $\delta^{18}O_{apa}$ ‰) from a small sub-sample of human and faunal remains. From only two human individuals the collagen was extracted and measured via EA-IRMS (*F12i28* and *F7i10*) for this thesis. For all the others, the data are those generated by Craig *et al.* (2013) and Martyn *et al.* (2018). $\delta^{13}C$ ‰ and $\delta^{15}N$ ‰ values of the barley samples from Pompeii (*BarleyP*) and the grains from *Portus Romae* (*LBCFA16F*, *LBCFD16E*, *LBTA1012I*, *LBTD1012H&I*) are from Pate *et al.* (2016) and O'Connell *et al.* (2019), respectively, and they are corrected for charring after Nitsch *et al.* (2015).

ID	**Gly** $\delta^{13}C$ (‰)	**Err.**	**Ser** $\delta^{13}C$ (‰)	**Err.**	**Glx** $\delta^{13}C$ (‰)	**Err.**	**Ala** $\delta^{13}C$ (‰)	**Err.**	**Asx** $\delta^{13}C$ (‰)	**Err.**	Pro $\delta^{13}C$ (‰)	**Err.**	**Hyp** $\delta^{13}C$ (‰)	**Err.**	**Val** $\delta^{13}C$ (‰)	**Err.**
Humans																
F10i11	-14.03	1.06	-9.45	1.22	-19.23	0.92	-21.52	0.64	-20.18	1.25	-20.12	1.14	-19.5	1.85	-26.98	0.77
F10i14	-9.43	0.95	-7	1.92	-19.08	0.88	-20.15	0.88	-20.88	1.03	-18.08	0.57	-19.02	1.31	-24.94	0.37
F10i16	-12.48	1.05	-8.64	1.38	-19.72	1	-21.07	0.68	-21.12	0.68	-19.9	0.72	-21.41	0.92	-25.63	0.53
F10i17	-9.98	1.15	-6.48	1.45	-17.58	1.03	-19.66	0.9	-19.01	0.91	-18.52	0.54	-19.43	1.07	-23.14	0.56
F10i20	-9.58	0.69	-8.08	1.1	-19.23	0.47	-18.45	0.35	-21.44	0.54	-19.69	0.55	-19.46	1.38	-25.05	0.24
F10i22	-9.76	0.71	-7.15	1.1	-18.31	0.64	-18.47	0.4	-19.47	0.6	-19.32	0.63	-20.34	0.48	-23.82	0.18
F10i28	-11.83	0.9	-8.85	1.17	-19.16	0.91	-20.35	0.58	-21.26	1.02	-20	0.68	-21.94	0.81	-25.66	0.58
F12i23	-8.69	0.84	-6.05	1.29	-18.52	1.28	-19.8	0.56	-19.84	1.04	-18.93	0.64	-20.45	1.18	-23.71	0.41
F12i28	-11.88	1.31	-9.81	0.92	-19.83	0.74	-20.4	1.05	-21.27	1.12	-18.93	0.51	-19.22	1.08	-27.56	0.54
F12i3	-11.33	0.95	-8.07	1.33	-18.58	1.06	-20.3	0.64	-19.78	0.83	-19.3	0.75	-20.97	0.9	-25.11	0.47
F7i10	-11.23	1.26	-9.63	1	-20.29	0.74	-19.71	1.01	-20.94	0.93	-19.39	0.51	-19.71	1.1	-25.07	0.52
F7i7	-12.9	1.99	-11.16	1.87	-19.18	1.05	-21.93	2.13	-20.99	1.3	-19.62	0.71	-20.3	1.13	-26.08	0.78
F8i23	-14.59	1.78	-11.76	1.62	-18.95	0.95	-22.48	2.01	-20.99	1.08	-19.48	0.73	-19.93	0.98	-25.97	0.47
F8i6	-12.88	0.69	-9.14	1.37	-18.69	0.96	-19.33	0.69	-20.47	1.04	-19.73	0.59	-19.89	0.82	-25.72	0.42
F8i7	-10.92	0.92	-7.96	1.52	-18.63	0.99	-19.81	0.82	-20.15	1.12	-19.13	0.75	-18.94	0.95	-24.28	0.69
F9i13	-10.55	0.64	-8.62	0.9	-18.64	0.73	-20.8	0.43	-19.63	0.68	-18.94	0.37	-20.98	0.84	-24.94	0.55
F9i9	-11.43	0.6	-9.84	1.17	-18	0.75	-20.82	0.49	-19.58	0.68	-18.96	0.38	-19.26	0.82	-24.61	0.58
Cereals and Legumes																
1703b	-12.9	1.7	-10.5	1.9	-22.9	1.3	-22.4	1.7	-23.9	1.2	-21.9	1			-27.6	1.3
1703w	-13.3	1.7	-10.8	1.9	-23.2	1.3	-22.7	1.7	-24.2	1.2	-22.3	1			-28	1.3
1895e	-15.6	1.7	-13.2	1.9	-25.6	1.3	-25.1	1.7	-26.6	1.2	-24.6	1			-30.3	1.3
723w	-13.8	1.7	-11.3	1.9	-23.7	1.3	-23.2	1.7	-24.8	1.2	-22.8	1			-28.5	1.3
MB	-19.73	1.12	-16.16	1.84	-28.08	1.23	-27.62	1.54	-29.24	1.05	-27.46	0.8			-32.07	0.63

MDW	-14.39	1.12	-11.85	1.67	-25.49	1	-24.44	1.67	-26.59	0.82	-24	0.87			-30.99	0.6
MF	-16.68	1.07	-15.49	1.46	-27.1	1.14	-27.06	1.54	-27.91	0.77	-26.33	1			-31.9	0.62
BarleyP	-14.4	1.7	-11.9	1.9	-24.3	1.3	-23.8	1.7	-25.4	1.2	-23.4	1			-29.1	1.3
LBCFA16F	-13.2	1.7	-10.7	1.9	-23.1	1.3	-22.6	1.7	-24.2	1.2	-22.2	1			-27.9	1.3
LBCFD16E	-13.7	1.7	-11.2	1.9	-23.6	1.3	-23.1	1.7	-24.7	1.2	-22.7	1			-28.4	1.3
LBTA1012I	-14.1	1.7	-11.6	1.9	-24	1.3	-23.5	1.7	-25.1	1.2	-23.1	1			-28.8	1.3
LBTD1012H&I	-13.7	1.7	-11.2	1.9	-23.6	1.3	-23.1	1.7	-24.7	1.2	-22.7	1			-28.4	1.3
MM	-8.72	0.96	-0.89	1.82	-13.03	0.88	-13.89	1.55	-12.46	0.79	-12	1.31			-17.96	0.62
200b	-19.5	3.1	-13.4	2.6	-27.0	0.6	-25.3	1.7	-26.1	0.9	-24.1	0.6			-32.4	2.0
2314c	-15.2	3.1	-9.0	2.6	-22.6	0.6	-21.0	1.7	-21.7	0.9	-19.8	0.6			-28.1	2.0
2317p	-15.2	3.1	-9.1	2.6	-22.7	0.6	-21.0	1.7	-21.7	0.9	-19.8	0.6			-28.1	2.0
692l	-14.2	3.1	-8.1	2.6	-21.7	0.6	-20.0	1.7	-20.7	0.9	-18.8	0.6			-27.1	2.0
MC	-16.81	0.89	-10.32	2.86	-22.2	0.55	-21.72	0.61	-21.59	0.48	-19.12	1.06			-29.05	0.32
ML	-15.62	1.29	-9.83	1.19	-25.17	0.57	-22.34	0.75	-23.9	0.88	-22.52	0.34			-29.14	0.66
Terrestrial herbivores																
EF10OC	-14.44	1.9	-16.68	2.27	-20.33	1.01	-26.55	1.89	-23.22	0.79	-19.7	0.7	-19.54	1.54	-29.13	1.13
EF7OC	-11.46	1.3	-9.81	0.84	-19.25	0.9	-21.46	1.02	-19.44	1.27	-19.64	0.63	-19.02	1.13	-27.56	1.26
EF8BOS?	-17.29	1.68	-20.21	1.97	-22.79	0.98	-29.14	1.64	-25.45	0.65	-19.16	0.56	-19.91	1.28	-29.03	0.92
EF8SG	-17.02	0.85	-13.51	1.25	-23.97	0.78	-27.88	1.26	-23.8	0.61	-22.34	0.51	-23.11	1.11	-30.91	0.55
PSC1	-15.18	1.75	-16.97	1.39	-21.18	0.82	-25.89	1.68	-23.82	0.54	-17.37	0.58	-17.32	1.33	-27.38	1.05
PSC2	-11.41	1.51	-11.32	1.03	-19.27	0.81	-21.76	1.08	-20.35	1.03	-17.77	0.6	-18.38	1.17	-26.64	0.72
PSG2	-13.52	1.01	-9.43	1.17	-22.18	0.46	-25.29	0.7	-23.25	0.51	-19.97	0.31	-20.52	0.43	-27.75	0.55
VEDE1	-13.49	0.91	-11.16	1.65	-21.64	0.92	-25.24	0.89	-19.43	1.35	-19.79	0.53	-21.75	1.09	-27.97	0.35
VEHO1	-8.42	1.64	-9.32	2.32	-18.5	1.62	-19.91	1.32	-17.62	1.85	-14.94	1.08	-17.63	1.68	-26.11	1.2
VEHO2	-11.94	0.83	-11.91	0.99	-20.66	0.53	-23.83	0.69	-21.24	0.89	-17.62	0.51	-18.79	0.83	-27.99	0.42
VEHO3	-15.1	1.05	-14.21	1.32	-21.08	0.77	-23.34	0.9	-20.04	1.1	-21.13	0.71	-22.6	0.61	-26.94	0.65
VEHO4	-15.33	0.71	-12.89	1.55	-19.02	0.96	-23.94	0.67	-18.55	0.98	-20.52	0.51	-20.39	0.97	-25.85	0.39
VESH1	-12.45	1.01	-7.83	1.76	-21.5	0.98	-24.81	0.93	-20.16	1.13	-19.61	0.62	-21.84	1.17	-27.25	0.43
Terrestrial omnivores																
EF11DOG	-12.63	0.76	-9.8	0.6	-19.72	0.55	-21.44	0.72	-20.73	0.8	-18.91	0.49	-18.89	0.72	-25.15	0.69
PSCH1	-11.08	1.5	-15.8	1.51	-19.14	0.82	-19.68	1.39	-20.49	0.96	-15.74	0.56	-16.07	0.83	-25.65	0.94
PSCH2	-15	1.38	-10.85	1.57	-19.38	0.77	-22.43	1.32	-20.55	0.88	-19.33	0.54	-20.12	0.69	-26.83	0.86
PSCH3	-9.18	1.41	-11.64	2.3	-15.55	0.74	-16.01	1.36	-16.61	0.95	-14.22	0.59	-14.06	0.91	-23.98	1.09
PSP3	-17.41	1.39	-13.31	1.69	-22.42	0.77	-26.58	1.35	-24.02	0.96	-20.78	0.54	-21.12	0.73	-28.67	0.88
PSP4	-14.23	1.41	-11.94	1.52	-22.26	0.74	-24.39	1.35	-23	1.1	-19.11	0.56	-19.53	0.7	-27.35	0.88
PSP5	-19.89	1.63	-16.1	1.6	-21.36	0.94	-27.13	1.49	-22.8	1.27	-20.84	0.77	-22.11	0.84	-30.5	0.99

Marine fish																
ABF3	-1.81	0.98	0.41	1.58	-13.58	1.4	-12.03	0.74	-13.84	1.55	-13.49	0.62	-13.6	1.3	-20.53	0.74
HSG1	-4.9	0.91	-3.39	0.97	-16.1	0.92	-18.5	0.78	-17.66	0.98	-15.98	0.64	-18.3	1.1	-23.12	0.64
HSLA	-5.83	1.74	-3.19	1.67	-11.48	0.87	-14.77	1.98	-12.24	1.09	-11.87	0.56	-12.77	0.91	-19.38	0.55
HSSP1	0.3	0.65	2.02	1.42	-13.01	0.98	-15.62	0.8	-14.64	0.99	-13.59	0.65	-12.89	0.8	-20.93	0.55
HSSP2	-3.73	0.98	-2.99	0.89	-13.65	0.84	-16.56	0.67	-15.17	0.88	-14.62	0.49	-13.98	0.78	-23.18	0.39
HSSSA	-1.08	0.6	-1.84	1.19	-12.66	0.73	-15.62	0.47	-15.23	0.97	-13.25	0.37	-13.25	0.87	-19.84	0.51
HSSSQ	-2.31	0.55	3.27	1.42	-11.57	0.91	-13.59	0.77	-11.32	1.41	-12.12	0.58	-11.86	0.83	-18.86	0.43
PSSC2	-1.98	1.55	-4.75	1.34	-15.09	0.85	-17.71	1.59	-16.86	0.61	-11.81	0.45	-12.29	1.11	-22.76	0.88
PSSP1	-4.42	1.58	-4.22	1.27	-15.73	0.78	-18.84	1.63	-19.55	0.66	-15.28	0.4	-16.07	1.08	-23.3	0.72
SSF2	-1.96	0.88	3.26	1.01	-14.05	0.78	-14.23	0.36	-14.02	0.69	-13.68	0.45	-15.38	0.84	-20.6	0.29
SSF5	-1.46	0.68	3.3	1.43	-9.26	0.97	-11.07	0.71	-9.45	1.03	-9.89	0.59	-9.33	0.78	-16.8	0.48

ID	**Leu** $\delta^{13}C$ (‰)	**Err.**	**Ile** $\delta^{13}C$ (‰)	**Err.**	**Thr** $\delta^{13}C$ (‰)	**Err.**	**Met** $\delta^{13}C$ (‰)	**Err.**	**Lys** $\delta^{13}C$ (‰)	**Err.**	**Phe** $\delta^{13}C$ (‰)	**Err.**	**Tyr** $\delta^{13}C$ (‰)	**Err.**	**Est. bulk** $\delta^{13}C$ (‰)	**Err.**	**Est-meas bulk offset** $\delta^{13}C$ (‰)
Humans																	
F10i11	-29.56	0.87	-22.37	1	-9.47	1.7	-25.73	1.08	-23.03	1.55	-26.76	1.44	-25.62	1.36	-19.62	1.08	0.08
F10i14	-28.91	0.54	-22.03	0.63	-7.45	1.78	-24.77	1.59	-19.21	1.48	-29.36	1.29	-22.69	1.14	-17.61	0.87	1.41
F10i16	-29.58	0.61	-23.76	0.47	-10.97	0.78	-23.21	1.81	-21.09	1.13	-31.42	0.88	-22.13	0.77	-19.3	0.84	0.5
F10i17	-26.11	0.54	-22.34	0.66	-9.46	1.29			-19.42	1.91	-29.78	0.57	-20.52	1.84	-17.4	0.9	1.44
F10i20	-28.21	0.28	-22.77	0.59	-10.04	0.76	-21.93	1.22	-20.1	1.15	-28.14	1.02	-22.35	0.67	-18.1	0.6	1.49
F10i22	-28	0.25	-23.52	0.68	-8.66	0.76	-17.79	0.56	-18.63	1.21	-30.15	0.42	-22.25	0.45	-17.71	0.63	1.39
F10i28	-29.98	0.56	-23.55	0.49	-12.05	0.65	-28.14	0.62	-21.22	0.99	-29.47	1.23	-24.05	0.77	-19.09	0.79	0.56
F12i23	-28.02	0.6	-21.12	0.49	-8.94	1.03	-23.44	0.88	-18.45	1.44	-29.44	0.9	-20.78	1.62	-17.43	0.84	1.14
F12i28	-29.69	0.81	-22.95	0.63	-7.34	0.83			-19.03	1.38	-27.71	0.73	-25.41	1.62	-18.65	0.87	0.43
F12i3	-29.14	0.61	-23.1	0.31	-10.98	0.46	-27.3	0.59	-20.48	1.03	-30.35	0.94	-24.14	1.05	-18.52	0.83	1.15
F7i10	-28.6	0.78	-21.53	0.63	-6.39	0.83			-19.79	0.95	-27.51	0.75	-25.89	1.45	-18.49	0.83	0.42
F7i7	-29.67	0.65	-22.56	0.85	-5.1	1.02	-27.77	2.18	-22.47	2.46	-26.57	1.25	-21.69	1.45	-19.18	1.33	0.09
F8i23	-29.19	0.59	-22.03	0.71	-5.36	0.71			-20.79	2.49	-26.86	0.83	-20.56	0.85	-19.37	1.21	0.2
F8i6	-28.84	0.4	-21.91	0.71	-5.84	0.72			-22.18	1.69	-28.7	0.92	-20.08	2.11	-18.82	0.78	1.1
F8i7	-27.59	0.51	-21.19	0.63	-3.44	0.86	-26.31	0.89	-19.69	1.32	-27.13	0.77	-23.1	1.24	-17.91	0.88	0.97
F9i13	-26.92	0.42	-22.14	0.44	-9.3	0.81	-25.15	1.66	-18.64	1.15	-29.66	0.69	-20.02	0.83	-17.99	0.58	1.13
F9i9	-27.17	0.49	-22.15	0.46	-9	0.67	-25.13	1.45	-17.8	0.97	-28.27	0.62	-18.11	0.91	-18.02	0.58	0.78

Cereals and Legumes																
1703b	-30.8	1.2	-24.3	1.2	-8	1.1					-25.3	2	-23.5	1.4		
1703w	-31.1	1.2	-24.7	1.2	-8.3	1.1					-25.7	2	-23.8	1.4		
1895e	-33.5	1.2	-27	1.2	-10.6	1.1					-28	2	-26.2	1.4		
723w	-31.6	1.2	-25.2	1.2	-8.8	1.1					-26.2	2	-24.3	1.4		
MB	-35.32	0.71	-28.53	0.53	-13.17	1.01	-28	1.33			-30.18	1.84	-28.73	1.08		
MDW	-33.86	0.5	-27.29	0.54	-10.33	0.86	-33.11	2.18			-28.21	1.25	-26.3	1.09		
MF	-35.15	0.57	-29.2	0.6	-12.4	0.93	-37.15	1.42			-29.63	1.12	-27.47	1.24		
BarleyP	-32.2	1.2	-25.8	1.2	-9.4	1.1					-26.8	2	-24.9	1.4		
LBCFA16F	-31	1.2	-24.6	1.2	-8.2	1.1					-25.6	2	-23.7	1.4		
LBCFD16E	-31.5	1.2	-25.1	1.2	-8.7	1.1					-26.1	2	-24.2	1.4		
LBTA1012I	-31.9	1.2	-25.5	1.2	-9.1	1.1					-26.5	2	-24.6	1.4		
LBTD1012H&I	-31.5	1.2	-25.1	1.2	-8.7	1.1					-26.1	2	-24.2	1.4		
MM	-21.55	0.44	-13.8	0.52	-1.25	1.16	-18.53	0.94			-17.53	0.64	-13.38	1.43		
200b	-36.0	1.4	-30.3	0.6	-15.8	1.0					-30.7	0.6	-31.3	1.8		
2314c	-31.6	1.4	-25.9	0.6	-11.5	1.0					-26.4	0.6	-27.0	1.8		
2317p	-31.6	1.4	-26.0	0.6	-11.5	1.0					-26.4	0.6	-27.0	1.8		
692l	-30.6	1.4	-25.0	0.6	-10.5	1.0					-25.4	0.6	-26.0	1.8		
MC	-32.21	0.53	-25.36	0.48	-11.25	0.56	-36.8	1.99			-26.27	0.48	-27.85	0.7		
ML	-33.08	0.39	-28.58	0.54	-13.78	0.98	-15.93	1.23			-28.59	0.52	-28.19	0.46		
Terrestrial herbivores																
EF10OC	-30.41	1.1	-26.7	0.58	-18.51	1.44	-26.47	0.98	-15.62	1.43	-30.76	0.61	-29.42	1.19	-20.64	1.22	-0.84
EF7OC	-31.11	0.88	-25.59	0.89	-11.76	0.7			-16.81	1.01	-27.96	0.78	-25.4	0.79	-18.81	0.93	1.25
EF8BOS?	-30.27	0.99	-27.7	0.62	-18.68	1.46	-27.28	2.26	-17.13	1.69	-33.07	0.19	-27.73	1.84	-21.9	1.08	-0.38
EF8SG	-32.83	0.61	-28.53	0.77	-14.27	0.94	-29.21	1.29	-21.53	0.86	-30.4	1.11	-29.26	1.24	-22.83	0.77	-1.63
PSC1	-28.66	1.19	-25.71	1.17	-17.08	0.97			-14.22	1.46	-30.31	0.78	-28.35	0.72	-19.83	1.07	-0.48
PSC2	-30.14	0.86	-25.82	0.82	-9.63	0.95			-16.07	0.78	-27.19	0.79	-25.05	1.22	-18.15	0.92	2.07
PSG2	-32.05	0.49	-25.88	0.38	-11.04	0.55			-18.02	0.73	-28.48	0.34	-26.46	1.86	-20.29	0.59	1.03
VEDE1	-31.9	0.57	-26.83	0.4	-13.32	1.76	-25.47	1.3	-20.33	1.44	-33.11	0.54	-28.65	0.95	-20.41	0.83	1.59
VEHO1	-29.03	1.16	-19.66	0.81	-10.65	2.13	-22.58	1.76	-16.09	1.61	-29.37	1	-20.4	0.97	-16.12	1.39	1.72
VEHO2	-31.84	0.57	-23.63	0.46	-12.05	0.65	-26.65	0.65	-20.63	1.43	-28.19	0.42	-25.67	0.51	-19.05	0.68	2.35
VEHO3	-30.51	0.3	-24.93	0.69	-17.49	1.89	-25.84	1.25	-21.22	1.58	-30.66	0.61	-23.35	2.14	-20.88	0.9	0.72
VEHO4	-28.47	0.44	-24.87	0.5	-13.88	1.21	-21	1.03	-19.98	1.59	-30.77	0.57	-24.54	0.83	-20.21	0.74	1.15
VESH1	-31.15	0.65	-24.87	0.62	-11.59	0.89	-25.83	2.55	-20.29	1.52	-32.6	0.66	-25.13	0.87	-19.85	0.88	1.35
Terrestrial omnivores																
EF11DOG	-29.11	0.53	-23.56	0.45	-8.7	0.56	-25.32	2.31	-20.5	1.27	-26.72	0.37	-19.96	2.45	-18.76	0.66	0.36

PSCH1	-26.67	0.99	-22.92	0.87	-15.59	2.22			-15.9	1.03	-32.35	0.48	-26.68	1.34	-18.39	1	-1.28
PSCH2	-28.29	0.62	-22.74	0.54	-5	0.72			-20.26	1.07	-30.4	0.57	-27.89	0.96	-20.01	0.9	-1.83
PSCH3	-25.63	0.55	-21.66	0.49	-14.16	1.21			-15.09	1.16	-29.24	0.56	-26.64	2.18	-16.22	0.98	-0.62
PSP3	-30.64	0.57	-26.15	0.39	-17.56	0.73			-18.91	1.03	-34.84	0.55	-29.48	1.64	-22	0.91	-1.19
PSP4	-30.03	0.7	-24.22	0.45	-17.2	0.92			-17.32	0.97	-33.82	0.61	-28.65	1.13	-20.3	0.93	-0.25
PSP5	-32.78	0.95	-26.04	0.85	-9.5	0.91			-21.75	1.54	-35.12	1.1	-27.36	0.63	-22.6	1.14	-1.16
Marine fish																	
ABF3	-22.51	1.15	-14.96	1.03	-5.02	1.56	-19.96	1.11	-14.29	1.75	-22.1	1.49	-18.97	1.41	-10.68	1.06	0.75
HSG1	-28.97	0.79	-21.44	0.75	-12.23	1.09	-25.71	0.69	-17.5	1.18	-32.66	0.51	-22.1	1.9	-14.48	0.84	1.74
HSLA	-21	0.53	-15.78	0.95	-3.18	0.73	-20.3	1.41	-13.84	2.47	-22.65	0.59	-18.43	1.49	-11.17	1.23	0.92
HSSP1	-21.1	0.59	-18.26	0.71	-25.46	0.77	-25.4	1.64	-14.77	1.51	-25.12	0.82	-17.32	1.32	-11.17	0.83	1.7
HSSP2	-23.45	0.58	-18.6	0.78	-10.89	0.68	-24.92	1	-14.88	0.85	-26.35	0.5	-19.26	2.55	-12.61	0.75	0.53
HSSSA	-22	0.4	-16.15	0.78	-8.59	0.87	-21.85	0.82	-13.16	1.1	-25.46	0.77	-16.22	2.24	-11.01	0.65	1.4
HSSSQ	-20.75	0.42	-15.62	0.58	-17.69	0.7	-21.39	1.54	-13.26	1.91	-23.42	0.76	-17.95	1.94	-10.28	0.82	1.59
PSSC2	-23.98	0.79	-17.87	0.72	-12.45	0.99	-26.84	1.96	-11.04	1.86	-28.35	0.63	-23.45	0.77	-11.89	1.05	0.42
PSSP1	-23.59	1.64	-19.42	0.75	-8.96	1.16	-21.86	1.86	-12.17	1.46	-28.59	0.82	-22.16	1.89	-13.59	1.06	-0.97
SSF2	-19.69	0.51	-17.22	0.46	-8.32	0.67	-24.7	0.57	-15.24	1.13	-26.89	0.5	-16.33	1.23	-11.08	0.67	0.65
SSF5	-18.83	0.4	-14.98	0.75	-3.39	0.99	-23.04	1.87	-11.41	1.43	-20.79	0.9	-14.31	1.97	-8.18	0.81	2.16

Table D.3 Carbon amino acid values ($\delta^{13}C_{AA}$) of human and animal collagen and plant material. The amino acid values of archaeological plant material (*1703b*, *1703w*, *1895e*, *723w*, *200b*, *2314c*, *2317p*, *692l*, *LBCFA16F*, *LBCFD16E*, *LBTA1012I*, *LBTD1012H&I*) were estimated using calculated $\Delta^{13}C_{AA-bulk}$ offsets determined by measuring the bulk and amino acid values of modern grains and pulses. The *Err.* associated to the estimated amino acid values of the archaeological plant material is the propagated error which accounts for the highest measurement uncertainty of the modern samples and their standard deviation. The estimated bulk values were derived by mass balance calculations as explained in the main text; in this case, Err. is the error propagated from all the amino acid measurements.

ID	**Gly** $\delta^{15}N$ (‰)	**Err.**	**Ser** $\delta^{15}N$ (‰)	**Err.**	**Glx** $\delta^{15}N$ (‰)	**Err.**	**Ala** $\delta^{15}N$ (‰)	**Err.**	**Asx** $\delta^{15}N$ (‰)	**Err.**	**Pro** $\delta^{15}N$ (‰)	**Err.**	**Hyp** $\delta^{15}N$ (‰)	**Err.**	**Val** $\delta^{15}N$ (‰)	**Err.**
Humans																
F10i11	4.15	0.3	6.55	0.78	12.5	0.35	9.24	0.5	12.46	0.49	12.37	0.33	12.51	0.76	16.17	0.21
F10i14	8.41	0.38	10.32	0.56	14.87	0.82	12.53	0.21	13.65	0.06	15.08	0.24	16.13	0.3	14.07	0.52
F10i16	6.76	0.3	12.78	0.42	14.7	0.16	12.22	0.72	13.95	0.4	14.21	0.24	14.78	0.26	17.05	0.62
F10i17	7.61	0.54	9.06	0.7	15.1	0.21	12.54	0.76	14.63	0.61	14.89	0.31	15.26	0.16	20.22	0.62
F10i20	4.97	0.24	7.54	0.56	13.07	0.46	10.32	0.78	12.53	0.39	13.15	0.17	13.68	0.29	18.6	0.45
F10i22	8.78	0.25	5.97	0.77	14.88	0.29	12.24	0.68	12.67	0.29	15.23	0.25	15.44	0.32	15.47	0.26

F10i28	5.08	0.63	8.3	0.2	13.47	0.22	10.02	1.11	14.45	0.44	13.04	0.08	14.09	0.02	18.18	0.55
F12i23	6.7	0.23	13.08	0.19	14.81	0.54	11.92	0.59	15.38	0.8	14.54	0.26	16.22	0.42	19.92	0.25
F12i28	7.02	0.76	8.09	0.84	14.63	0.05	9.67	0.78	14.78	0.6	14.12	0.43	15.04	0.24	18.31	0.54
F12i3	6.57	0.17	9.19	0.63	14.13	0.35	10.88	0.64	14.3	0.45	14.55	0.34	15.94	0.36	18.27	0.78
F7i10	7.18	0.33	8.72	0.67	14.96	0.18	11.66	0.22	15.4	0.78	13.91	0.32	14.77	0.39	20.24	1.16
F7i7	7.2	0.16	5.07	0.6	14.38	0.11	11.7	0.49	13.91	0.16	13.95	0.15	15.12	0.1	17.79	0.56
F8i10	7.08	0.12	7.62	0.25	13.01	0.03	10.08	0.06	11.5	0.17	13.02	0.08	14.93	0.24	11.95	0.87
F8i11	5.73	0.01	7.52	0.12	11.96	0.34	9.39	0.24	10.68	0.07	13.84	0.04	14.36	0.33	11.35	0.25
F8i23	5.96	0.62	7.59	1.25	12.83	0.65	11.48	0.78	12.36	0.52	12.3	0.47	12.27	0.33	16.05	0.79
F8i6	6.11	0.35	8.08	0.78	12.74	0.46	11.09	0.7	12.37	0.34	12.54	0.43	12.86	0.25	16.62	1.1
F8i7	7.02	0.48	13.21	0.55	15.29	0.33	12.39	1.07	14.95	0.67	15.21	0.2	15.99	0.83	19.82	0.3
F9i13	7.83	0.32	4.71	0.49	15.57	0.29	13.26	0.6	15.96	0.52	15.26	0.27	15.31	0.18	17.83	0.37
F9i9	8.98	0.31	5.28	0.73	16.35	0.49	13.9	0.42	15.83	0.67	16.2	0.35	16.13	0.24	19.34	0.27
Cereals and Legumes																
1703b	7.7	1.8			9.6	0.9	9.3	0.9	11.5	1	10.7	0.7			12	1.1
1703w	4.8	1.8			6.7	0.9	6.3	0.9	8.6	1	7.8	0.7			9	1.1
1895e	1.5	1.8			3.4	0.9	3	0.9	5.3	1	4.5	0.7			5.8	1.1
723w	5	1.8			6.9	0.9	6.5	0.9	8.8	1	8	0.7			9.3	1.1
MB	8.08	0.07	6.08	0.25	8.91	0.02	8.2	0.59	10.67	0.32	10.03	0.12			11.3	0.9
MDW	8.56	1.03	7.45	1.07	11.41	0.69	11.16	0.7	13.19	0.67	12.67	0.51			14.23	1.06
MF	8.39	0.62	6.86	0.55	10.35	0.37	10.2	1.03	12.54	0.81	11.31	0.47			12.31	0.76
BarleyP	1.2	1.8			3	0.9	2.7	0.9	4.9	1	4.2	0.7			5.4	1.1
LBCFA16F	9.5	1.8			11.3	0.9	11	0.9	13.2	1	12.5	0.7			13.7	1.1
LBCFD16E	10.5	1.8			12.3	0.9	12	0.9	14.2	1	13.5	0.7			14.7	1.1
LBTA1012I	4.4	1.8			6.2	0.9	5.9	0.9	8.1	1	7.4	0.7			8.6	1.1
LBTD1012H&I	11.3	1.8			13.1	0.9	12.8	0.9	15	1	14.3	0.7			15.5	1.1
MM	5.21	0.18	1.61	0.62	4.89	0.14	5.1	0.5	6.86	0.28	6.86	0.35			8.38	0.88
200b	3.9	3.0			2.5	2.0	1.6	2.0	3.4	2.0	6.2	3.0			3.1	4.0
2314c	4.2	3.0			2.8	2.0	1.9	2.0	3.8	2.0	6.5	3.0			3.4	4.0
2317p	3.7	3.0			2.2	2.0	1.3	2.0	3.2	2.0	5.9	3.0			2.9	4.0
692l	2.8	3.0			1.4	2.0	0.5	2.0	2.3	2.0	5.1	3.0			2.0	4.0
MC	-0.21	1.16	-4.64	0.61	2.06	0.82	1.68	1.09	3.15	0.85	8.54	0.46			6.45	0.3
ML	0.55	0.31	-2.91	1.24	3.73	0.6	3.37	0.62	4.41	0.25	8.37	0.21			5.56	0.85
Terrestrial herbivores																
EF10OC	0.36	0.67	3.13	0.72	8.02	0.08	2.88	0.64	9.49	0.55	5.77	0.22	6.98	0.69	11.81	0.52
EF7DOG?	2.85	0.52	2.77	0.38	7.86	0.4	4.37	0.98	8.38	0.12	6.71	0.35	6.68	0.16	14.02	0.55

EF7OC	-0.79	1	2.39	0.51	7.55	0.23	3.68	0.39	9.01	0.54	5.29	0.42	6.22	0.88	11.81	1.45
EF8BOS?	4.17	0.13	3.29	0.33	8.11	0.12	3.94	0.63	8.71	0.12	6.94	0.42	7.75	0.25	15.67	0.55
EF8SG	4.55	0.1	8.26	0.73	12.09	0.53	9.8	0.99	13.11	0.78	9.97	0.45	10.97	0.36	14	1.24
PSC1	3.56	0.36	2.61	0.65	8.04	0.3	5.5	0.65	8.63	0.38	7.42	0.14	7.99	0.22	15.94	1.39
PSC2	4.13	0.45	-0.51	0.58	9.64	0.04	6.44	0.81	9.74	0.26	8.32	0.21	8.86	0.49	15.82	0.78
PSSG3	-0.05	0.19	1.52	0.71	6.19	0.46	4.19	0.78	7.1	0.41	7.06	0.31	7.4	0.52	13.01	1.04
VEDE1	3.56	0.64	3.11	0.78	8.46	0.56	5.97	0.5	8.29	0.4	9.59	0.49	9.39	0.59	7.4	0.39
VEHO1	-1.3	0.26	0.3	0.25	6.35	0.08	3.15	0.25	6.06	0.64	8.32	0.19	8.06	0.39	4.55	0.59
VEHO3	-1.58	0.06	0.74	0.39	5.56	0.25	3.96	0.89	6.66	0.35	5.24	0.3	5.96	0.81	9.39	0.6
VEHO4	-0.21	0.26	0.07	0.38	7.98	0.42	4.6	0.34	8.14	0.62	9.22	0.14	8.41	0.42	8.21	0.98
VESH1	0	0.23	-0.73	0.34	8.01	0.22	4.36	0.15	7.42	0.22	7.81	0.26	8.37	0.36	5.97	0.92
Terrestrial omnivores																
EF11DOG	5.88	0.37	8.43	0.56	15.69	0.66	12.92	0.1	14.5	0.12	14.48	0.07	15.5	0.21	15.23	0.6
EF12DOG2	5.73	0.08	7.1	0.1	14.83	0.09	11.84	0.07	12.89	0.01	13.71	0.29	15.03	0.03	14.69	0.29
PSCH1	6.22	0.25	5.48	0.6	10.07	0.65	9.73	0.6	9.11	0.34	9.97	0.2	9.73	0.38	11.4	0.91
PSCH2	5.34	0.55	6.49	0.84	9.16	0.41	9.99	1.28	9.4	0.42	9.78	0.24	9.77	0.47	10.57	0.34
PSCH3	6.67	0.28	6.39	0.55	10.14	0.34	9.58	0.59	10.69	0.5	10.4	0.4	9.79	0.16	11.58	0.68
PSG1	1.18	1.13	2.74	0.82	7.56	0.08	3.26	0.8	9.24	0.82	7.74	0.11	8.43	0.61	12.69	1.27
PSP3	3.55	0.19	5.31	0.73	11.2	0.06	8.97	0.61	10.39	0.52	10.42	0.28	10.49	0.13	11.09	0.97
PSP4	-0.28	0.04	4.98	0.54	7.09	0.34	4.63	0.08	7.38	0.19	8.11	0.22	7.65	0.51	8.88	0.11
PSP5	4.65	0.27	2.26	0.88	11.65	0.44	10.42	0.42	11.91	0.34	12.24	0.23	12.8	0.82	13.7	0.45
Marine fish																
ABF3	1.17	0.18	3.78	0.24	20.12	0.43	19.57	1.43	17.54	0.53	13.63	0.28	15.14	0.99	27.44	0.52
HSLA	5.22	0.5	8.31	0.35	17.12	0.65	16.22	0.4	14.89	0.66	15.2	0.36	16.5	0.38	18.47	1.48
HSSP1	2.25	0.22	3.14	0.64	18.8	0.49	18.22	0.17	15.95	0.74	12.74	0.11	12.72	0.04	19.06	0.63
HSSP2	-2.57	0.45	2.35	0.59	19.58	0.06	18.44	0.87	16.64	0.33	13.27	0.6	14.57	0.8	26.71	0.22
HSSSQ	2.76	0.23	0.79	0.08	20.3	0.48	21.66	0.47	17.7	0.28	17.43	0.11	17.48	0.09	19.42	1.45
PSMU1	3.58	1.16	5.75	0.74	19.26	0.38	16.61	0.73	22.07	0.06	17.25	0.21	18.01	1.02	26.14	0.62
PSPL1	-0.82	0.87	3.88	0.41	19.57	0.34	18.75	0.86	19.19	0.37	12.46	0.21	14.65	0.15	27.49	0.6
PSSC2	-7.16	0.27	-1.47	0.96	21.06	0.83	21.32	1.22	22.69	0.59	15.05	0.83	16.86	0.57	29.12	0.54
PSSP1	1.62	0.29	3.81	0.23	19.02	0.33	17.26	0.56	19.64	0.35	12.71	0.34	14.55	0.59	26.63	0.54
SSF2	1.96	0.21	3.58	0.36	28.23	0.33	27.6	0.65	24.37	0.07	22.65	0.06	23.44	0.38	33.79	0.38
SSF5	2.5	0.45	5.97	0.33	16.62	0.44	15.05	1.21	15.24	0.34	13.33	0.44	14.23	0.73	24.57	1.14

ID	Leu $\delta^{15}N$ (‰)	Err.	Ile $\delta^{15}N$ (‰)	Err.	Thr $\delta^{15}N$ (‰)	Err.	Lys $\delta^{15}N$ (‰)	Err.	Phe $\delta^{15}N$ (‰)	Err.	Est. bulk $\delta^{15}N$ (‰)	Err.	Est-meas bulk offset $\delta^{15}N$ (‰)
Humans													
F10i11	14.06	0.13	12.05	1.3	-6.74	0.75	1.59	1.24	9.22	1.05	8	0.45	-1.31
F10i14	12.7	0.72	10.72	0.76	-12.26	1.01	2.83	0.49	9.52	1.06	10.69	0.4	0.15
F10i16	14.56	0.29	13.92	0.68	-6.26	0.51	3.29	0.77	10.72	0.45	10.31	0.38	0.21
F10i17	17.05	0.48	16.85	0.62	-8.67	0.52	3.73	0.75	10.79	0.36	10.88	0.51	-0.69
F10i20	14.74	0.47	13.81	0.47	-5.96	0.8	2.21	0.21	10	0.12	8.83	0.34	-0.31
F10i22	13.35	0.31					3.66	1.23	11.56	1.13	10.91	0.4	0.42
F10i28	14.14	0.31	13.67	0.84	-5.44	1.06	3.28	0.74	10.62	0.35	9.02	0.51	-0.18
F12i23	16.22	0.78	15.19	1	-8.88	0.84	4.12	0.43	11.1	0.91	10.56	0.38	-0.37
F12i28	16.97	0.12	15.52	0.56	-7.66	0.8	2.56	0.7	9.65	0.67	9.96	0.6	-0.43
F12i3	15.28	0.76	15.14	0.44	-6.65	0.44	2.38	1.2	10.22	1.39	9.99	0.43	-0.1
F7i10	16.5	0.38	16.9	1.16	-7.77	1.23	3.68	0.55	10.68	0.4	10.42	0.4	0.69
F7i7	14.85	0.2	14.62	0.76	-4.86	0.25	3.09	0.48	11.75	0.21	10.09	0.25	0.02
F8i10	10.53	0.14	4.55	0.52	-1.2	0.27			9.49	1.41	9.67	0.15	0.17
F8i11	10.15	0.32	6.1	1.23	-3.11	0.75			11.05	0.21	9.13	0.13	0.96
F8i23	13.64	0.72	12.94	1.07	-10.03	0.6	1.71	0.61	9.77	0.18	8.87	0.63	-0.23
F8i6	14.45	0.78			-6.98	0.48	1.46	1.15	9.58	0.85	8.87	0.53	-0.54
F8i7	16.39	0.68	15.39	0.92	-8.63	1.34	2.65	1.17	11.17	1.18	10.8	0.56	-0.03
F9i13	15.82	0.51	15.8	0.7	-7.68	1.14	3.4	0.63	10.78	0.09	10.94	0.4	0.18
F9i9	17.06	0.32	16.56	0.2	-10.04	0.32	4.7	0.49	10.53	0.24	11.82	0.39	0.37
Cereals and Legumes													
1703b	8.3	1.1	9.2	1.1	2.4	1.2	6.3	1.3	18	1.1			
1703w	5.4	1.1	6.2	1.1	-0.5	1.2	3.3	1.3	15	1.1			
1895e	2.1	1.1	2.9	1.1	-3.8	1.2	0	1.3	11.7	1.1			
723w	5.6	1.1	6.4	1.1	-0.3	1.2	3.5	1.3	15.2	1.1			
MB	7.64	0.24	8.59	0.17	1.34	0.44	4.86	0.38	17.58	0.37			
MDW	10.46	1.1	11.51	1.03	5.52	1.08	9.82	0.73	19.31	0.56			
MF	8.69	0.35	9.17	0.75	2.21	0.36	5.98	0.87	18.85	0.36			
BarleyP	1.7	1.1	2.6	1.1	-4.2	1.2	-0.3	1.3	11.4	1.1			
LBCFA16F	10	1.1	10.9	1.1	4.1	1.2	8	1.3	19.7	1.1			
LBCFD16E	11	1.1	11.9	1.1	5.1	1.2	9	1.3	20.7	1.1			
LBTA1012I	4.9	1.1	5.8	1.1	-1	1.2	2.9	1.3	14.6	1.1			
LBTD1012H&I	11.8	1.1	12.7	1.1	5.9	1.2	9.8	1.3	21.5	1.1			
MM	3.89	0.38	5.11	0.44	3.83	0.4	4.29	0.55	10.03	0.61			

200b	-1.3	3.0	3.0	1.0	-3.1	1.0	1.1	2.0	3.9	4.0			
2314c	-1.0	3.0	3.4	1.0	-2.8	1.0	1.5	2.0	4.2	4.0			
2317p	-1.5	3.0	2.8	1.0	-3.3	1.0	0.9	2.0	3.6	4.0			
692l	-2.4	3.0	2.0	1.0	-4.2	1.0	0.0	2.0	2.8	4.0			
MC	0.03	1.05	1.03	1.32	-4.81	1.28	-2.24	1.13	9.01	0.96			
ML	1.34	0.34	1.9	0.63	-4.46	0.76	1.35	0.33	5.47	0.25			
Terrestrial herbivores													
EF10OC	8.69	0.62	10.11	0.49	-6.81	0.83	1.71	0.07	10.29	0.58	3.66	0.47	-0.02
EF7DOG?	11.79	0.3	11.06	1.08	-5.1	0.89	0.36	1.06	9.27	0.8	4.89	0.55	0.01
EF7OC	9.38	0.59	10.48	0.67	-6.13	0.91	0.5	0.87	9.23	1.18	3.1	0.7	-0.1
EF8BOS?	11.27	0.24	12.13	0.73	-7.39	0.57	0.82	1.11	7.75	0.85	5.41	0.36	-0.19
EF8SG	10.49	0.76	10.34	0.67	-2.98	0.93	3.93	0.79	12.55	0.17	7.83	0.48	0.54
PSC1	11.77	0.54	11.02	1.84		0.15	2.11	0.49	8.27	0.61	5.79	0.4	0.01
PSC2	11.59	0.46	11.46	0.87	-5.79	0.64	2.73	0.21	10.73	0.77	6.22	0.41	0.05
PSSG3	8.37	0.77	7.83	0.46	-9.9	0.63	0.37	0.79	8.19	0.49	3.48	0.43	-0.18
VEDE1	6.42	0.57	4.21	1.19	-11.65	1.83	0.54	0.32	9.28	1.2	5.52	0.58	0.82
VEHO1	3.5	0.36	2.43	0.56	3.32	0.6	0.01	0.99	5.61	0.8	2.91	0.33	1.41
VEHO3	6.85	0.42	5.72	0.85	-4.99	0.96	-1.47	1.03	7.59	0.16	2.22	0.37	-0.08
VEHO4	5.41	0.17	3.56	0.86	-5.97	0.68	1.63	0.59	9.73	1.01	4.01	0.34	0.01
VESH1	4.74	1.05	5.67	1.97	-10.62	0.42	-1.08	0.07	8.24	0.35	3.33	0.28	0.73
Terrestrial omnivores													
EF11DOG	14.5	0.09	11.27	0.52	-17.19	1.41	2.72	0.28	11.04	0.51	9.78	0.3	0.9
EF12DOG2	12.88	0.09	7.77	0.61	-3.96	0.6			10.8	0.38	9.89	0.15	1.11
PSCH1	9.02	0.06	9.22	0.82	-4.26	0.24	2.5	0.61	6.65	0.37	7.29	0.37	0.3
PSCH2	8.64	0.41	9.13	0.41	-3.99	1.37	3.08	1.68	8.59	0.34	7.02	0.64	1.41
PSCH3	9.12	0.79	10.17	0.52	-3.08	1.42	2.34	0.09	8.24	0.48	7.73	0.4	1.29
PSG1	10.6	0.09					1.77	0.99	8.4	0.68	4.56	0.69	0
PSP3	9.75	0.32	9.9	0.59	-4.33	0.3	3.63	0.57	8.91	0.39	7.01	0.34	0.69
PSP4	6.34	0.35	7.86	0.43	-6.15	0.45	1.56	0.56	9.12	0.39	3.89	0.19	0.81
PSP5	11.13	0.19	11.41	0.54	-0.04	0.73	4.57	0.55	9.68	0.2	8.23	0.35	0.3
Marine fish													
ABF3	22.85	0.42	22.45	1.51	-9.83	0.71	3.8	0.61	4.84	0.5	8.88	0.45	-0.91
HSLA	22.61	0.73	1.26	0.47	-15.8	0.37	5.06	0.48	3.69	0.53	9.77	0.49	0.58
HSSP1	20.37	0.28	1.23	0.27	-18.01	0.62	1.01	0.56	1.89	0.21	7.92	0.31	0.95
HSSP2	24.21	0.38	24.55	0.25	-23.04	0.85	1.23	0.62	2	1.14	6.63	0.52	-1.37

HSSSQ	28.49	0.88	18.36	0.54	-21.42	0.49	3.74	0.54	5.61	0.85	9.83	0.32	0.38
PSMU1	22.55	0.33	23.41	1.4		0.26	3.11	1.71	4.63	0.96	10.77	0.8	0.19
PSPL1	24.11	0.37	24.12	0.47	-14.72	0.86	3.57	0.22	5.49	0.14	7.82	0.59	-0.83
PSSC2	24.45	0.22	24.41	0.7	-27.97	0.53	0.59	0.89	4.98	0.49	5.63	0.63	-1.53
PSSP1	22.11	0.31			-10.85	1.16	3.43	0.87	5.31	0.79	8.45	0.4	-1.09
SSF2	29.92	0.46	29.06	0.3	-24.38	1.22	4.93	1.13	7.83	0.61	12.64	0.35	-1.78
SSF5	20.35	0.73	19.59	1.11	-9.19	0.92	5.79	0.76	6.16	1.19	8.63	0.59	-1.78

Table D.4 Nitrogen amino acid values ($\delta^{15}N_{AA}$) of human and animal collagen and plant material. *Err.* represents the measurement uncertainty. The amino acid values of archaeological plant material (*1703b*, *1703w*, *1895e*, *723w*, *200b*, *2314c*, *2317p*, *692l*, *LBCFA16F*, *LBCFD16E*, *LBTA1012I*, *LBTD1012H&I*) were estimated using calculated $\Delta^{15}N_{AA-bulk}$ offsets determined by measuring the bulk and amino acid values of modern grains and pulses. The *Err.* associated to the estimated amino acid values of the archaeological plant material is the propagated error which accounts for the highest measurement uncertainty of the modern samples and their standard deviation. The estimated bulk values were derived by mass balance calculations as explained in the main text; in this case, Err. is the error propagated from all the amino acid measurements.

Appendix E

Supplementary Material to Soncin *et al.* 2021 - Chapter 6

This Appendix contains the supplementary figures and tables to chapter 6 and the input parameters and the generated estimates of the Bayesian mixing models discussed in chapter 6 and chapter 7.

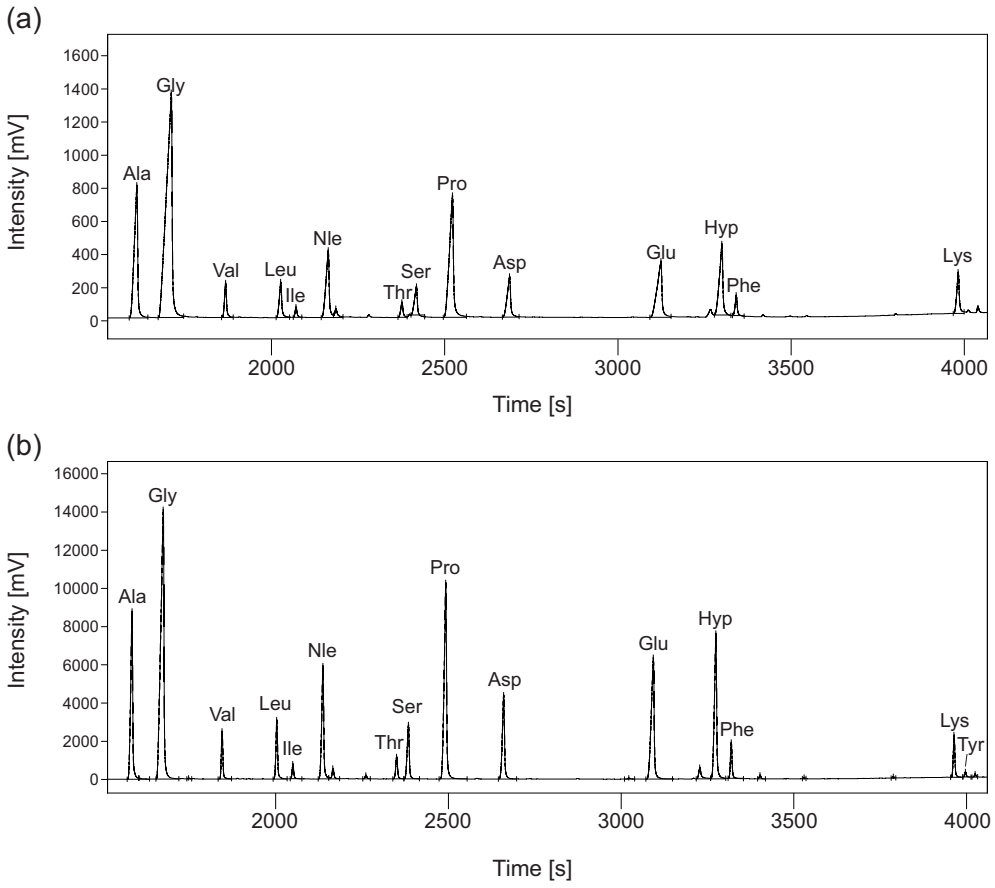

Figure E.1 GC-C-IRMS chromatograms of amino acids from archaeological bone collagen, in nitrogen mode (a) and carbon mode (b). See section 6.2.4 "Materials and Methods" for details. Ala: alanine, Gly: glycine, Val: valine, Leu: leucine, Ile: isoleucine, Nle: norleucine, Thr: threonine, Ser: serine, Pro: proline, Asp: aspartic acid, Glu: glutamic acid, Hyp: hydroxyproline, Phe: phenylalanine, Lys: lysine, Tyr: tyrosine.

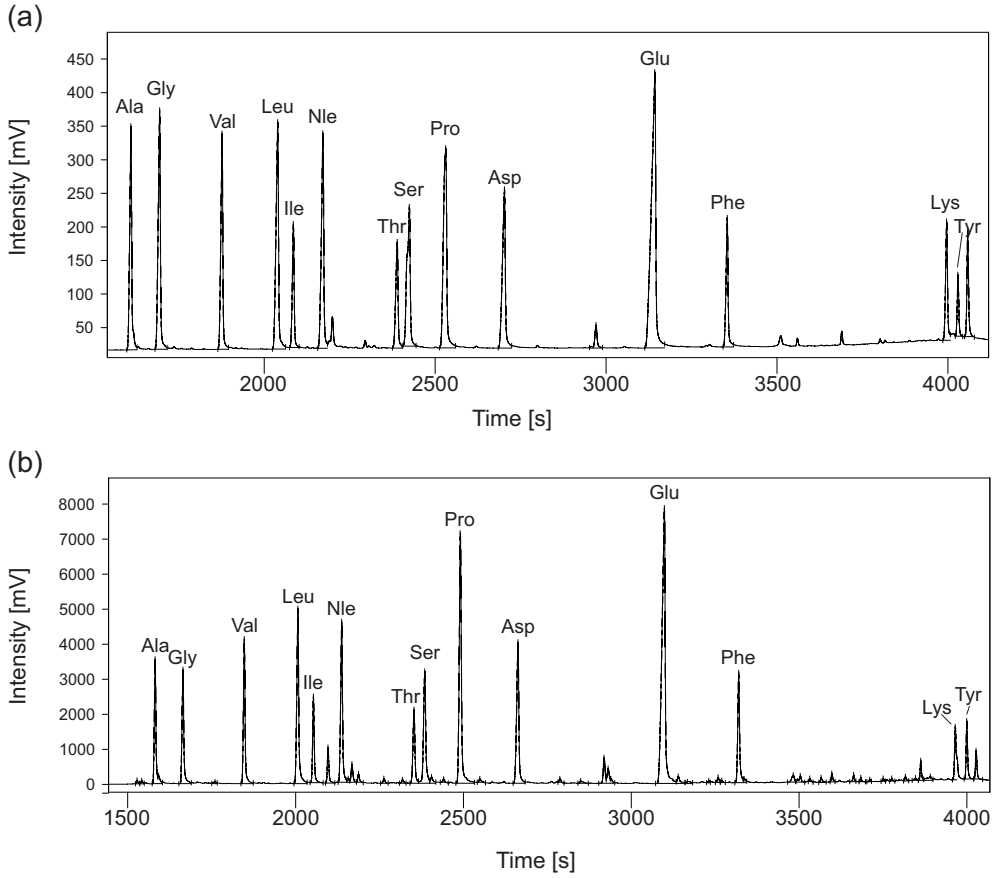

Figure E.2 GC-C-IRMS chromatograms of amino acids from modern grains, in nitrogen mode (a) and carbon mode (b). See section 6.2.4 "Materials and Methods" for details. Ala: alanine, Gly: glycine, Val: valine, Leu: leucine, Ile: isoleucine, Nle: norleucine, Thr: threonine, Ser: serine, Pro: proline, Asp: aspartic acid, Glu: glutamic acid, Hyp: hydroxyproline, Phe: phenylalanine, Lys: lysine, Tyr: tyrosine.

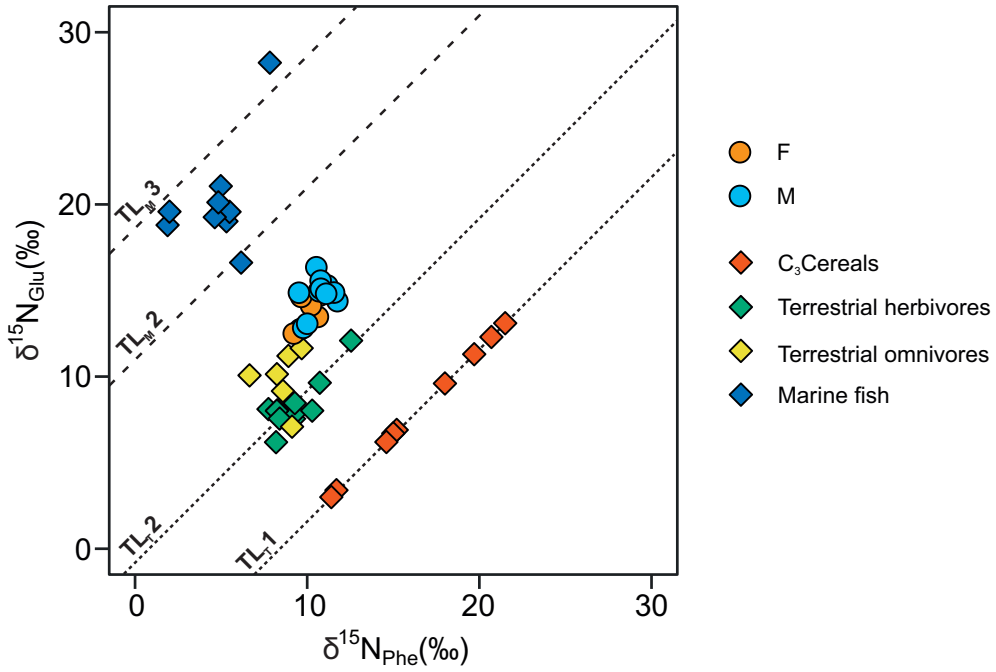

Figure E.3 Scatter plot of nitrogen isotope ratios of phenylalanine and glutamic acid. Predicted values for terrestrial and marine trophic levels are shown.

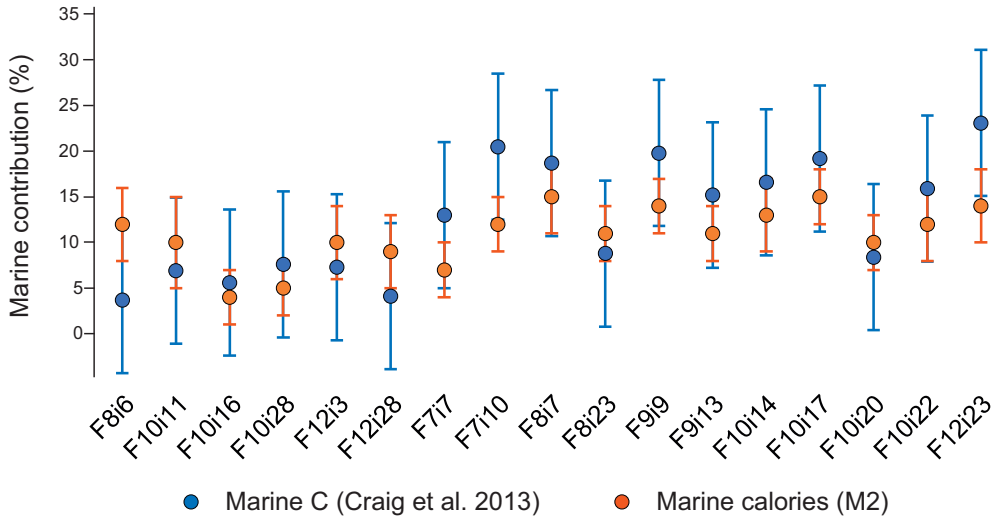

Figure E.4 Comparison of dietary marine contribution estimates from CSIA and AMS dating. Orange - % contribution of dietary calories derived from marine source, estimated using Model 2 above. Blue - % contribution of collagen carbon derived from a marine source, estimated from the measured and predicted marine reservoir ages (Craig *et al.* 2013; Martyn *et al.* 2018). Error bars represent 1σ. The errors for the marine carbon estimations are based on the error of the maximum marine reservoir age for the region (*i.e.*, 390 $\pm$ 30 years from Craig *et al.* (2013).

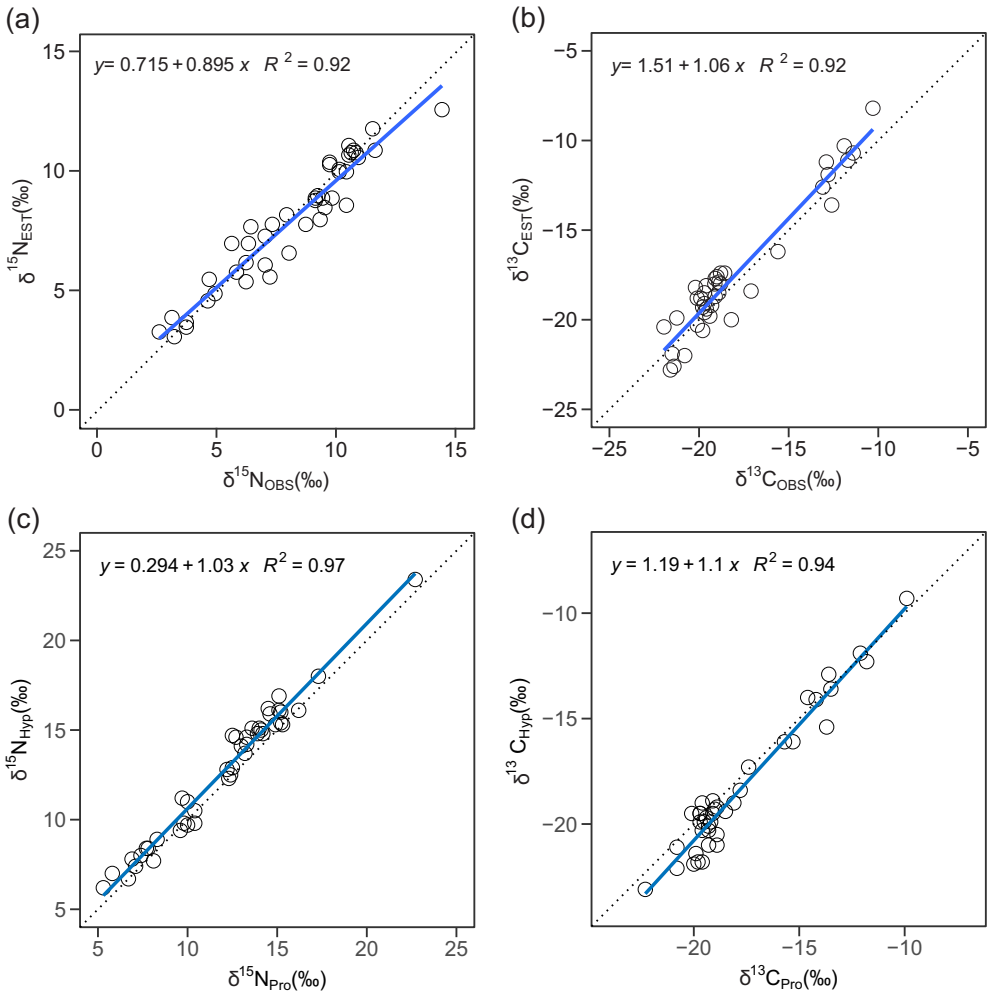

Figure E.5 Quality control assessment. Bivariate plots showing correlations between bulk collagen stable isotope values estimated (EST) based on the proportional contribution of each amino acid determined by GC-C-IRMS and observed (OBS) by bulk EA-IRMS for $\delta^{15}N$ (a) and $\delta^{13}C$ (b). Bivariate plots showing the relationship between proline and hydroxyproline measured in the same samples for $\delta^{15}N$ (c) and $\delta^{13}C$ (d).

A.

Sample name	*Fornici*	Date	Sex	Age	Gly δ^{15}N (‰)	Err.	Ser δ^{15}N (‰)	Err.	Glu δ^{15}N (‰)	Err.	Ala δ^{15}N (‰)	Err.	Asp δ^{15}N (‰)	Err.	Pro δ^{15}N (‰)	Err.	Hyp δ^{15}N (‰)	Err.	Val δ^{15}N (‰)	Err.
F8i6	8	79 AD	F	20-30	6.1	0.4	8.1	0.8	12.7	0.5	11.1	0.7	12.4	0.3	12.5	0.4	12.9	0.3	16.6	1.1
F10i11	10	79 AD	F	30-40	4.2	0.3	6.6	0.8	12.5	0.4	9.2	0.5	12.5	0.5	12.4	0.3	12.5	0.8	16.2	0.2
F10i16	10	79 AD	F	30-40	6.8	0.3	12.8	0.4	14.7	0.2	12.2	0.7	14.0	0.4	14.2	0.2	14.8	0.3	17.1	0.6
F10i28	10	79 AD	F	30-40	5.1	0.6	8.3	0.2	13.5	0.2	10.0	1.1	14.5	0.4	13.0	0.1	14.1	0.0	18.2	0.6
F12i3	12	79 AD	F	20-30	6.6	0.2	9.2	0.6	14.1	0.4	10.9	0.6	14.3	0.5	14.6	0.3	15.9	0.4	18.3	0.8
F12i28	12	79 AD	F	30-40	7.0	0.8	8.1	0.8	14.6	0.1	9.7	0.8	14.8	0.6	14.1	0.4	15.0	0.2	18.3	0.5
F7i7	7	79 AD	M	20-30	7.2	0.2	5.1	0.6	14.4	0.1	11.7	0.5	13.9	0.2	14.0	0.2	15.1	0.1	17.8	0.6
F7i10	7	79 AD	M	30-40	7.2	0.3	8.7	0.7	15.0	0.2	11.7	0.2	15.4	0.8	13.9	0.3	14.8	0.4	20.2	1.2
F8i7	8	79 AD	M	40-50	7.0	0.5	13.2	0.6	15.3	0.3	12.4	1.1	15.0	0.7	15.2	0.2	16.0	0.8	19.8	0.3
F8i23	8	79 AD	M	20-30	6.0	0.6	7.6	1.3	12.8	0.7	11.5	0.8	12.4	0.5	12.3	0.5	12.3	0.3	16.1	0.8
F9i9	9	79 AD	M	40-50	9.0	0.3	5.3	0.7	16.4	0.5	13.9	0.4	15.8	0.7	16.2	0.4	16.1	0.2	19.3	0.3
F9i13	9	79 AD	M	40-50	7.8	0.3	4.7	0.5	15.6	0.3	13.3	0.6	16.0	0.5	15.3	0.3	15.3	0.2	17.8	0.4
F10i14	10	79 AD	M	30-40	8.4	0.4	10.3	0.6	14.9	0.8	12.5	0.2	13.7	0.1	15.1	0.2	16.1	0.3	14.1	0.5
F10i17	10	79 AD	M	30-40	7.6	0.5	9.1	0.7	15.1	0.2	12.5	0.8	14.6	0.6	14.9	0.3	15.3	0.2	20.2	0.6
F10i20	10	79 AD	M	40-50	5.0	0.2	7.5	0.6	13.1	0.5	10.3	0.8	12.5	0.4	13.2	0.2	13.7	0.3	18.6	0.5
F10i22	10	79 AD	M	20-30	8.8	0.3	6.0	0.8	14.9	0.3	12.2	0.7	12.7	0.3	15.2	0.3	15.4	0.3	15.5	0.3
F12i23	12	79 AD	M	40-50	6.7	0.2	13.1	0.2	14.8	0.5	11.9	0.6	15.4	0.8	14.5	0.3	16.2	0.4	19.9	0.3

Sample name	*Fornici*	Date	Sex	Age	Leu δ^{15}N (‰)	Err.	Ile δ^{15}N (‰)	Err.	Thr δ^{15}N (‰)	Err.	Lys δ^{15}N (‰)	Err.	Phe δ^{15}N (‰)	Err.	Est. Bulk δ^{15}N (‰)	Err.	C:N	Meas. Bulk δ^{15}N (‰)	Err.	Est-Meas (‰)
F8i6	8	79 AD	F	20-30	14.5	0.8			-7.0	0.5	1.5	1.2	9.6	0.9	8.9	0.5	3.3**	9.4**	<0.5**	-0.5
F10i11	10	79 AD	F	30-40	14.1	0.1	12.1	1.3	-6.7	0.8	1.6	1.2	9.2	1.1	8.0	0.5	3.3*	9.3*	0.5*	-1.3

F10i16	10	79 AD	F	30-40	14.6	0.3	13.9	0.7	-6.3	0.5	3.3	0.8	10.7	0.5	10.3	0.4	3.2	9.7	0.2	0.2
F10i28	10	79 AD	F	30-40	14.1	0.3	13.7	0.8	-5.4	1.1	3.3	0.7	10.6	0.4	9.0	0.5	3.2*	9.2*	0.2*	-0.2
F12i3	12	79 AD	F	20-30	15.3	0.8	15.1	0.4	-6.7	0.4	2.4	1.2	10.2	1.4	10.0	0.4	3.3*	10.1*	0.3*	-0.1
F12i28	12	79 AD	F	30-40	17.0	0.1	15.5	0.6	-7.7	0.8	2.6	0.7	9.7	0.7	10.0	0.6	3.2	10.4	0.3	-0.4
F7i7	7	79 AD	M	20-30	14.9	0.2	14.6	0.8	-4.9	0.3	3.1	0.5	11.8	0.2	10.1	0.3	3.2**	10.1**	<0.5**	0.0
F7i10	7	79 AD	M	30-40	16.5	0.4	16.9	1.2	-7.8	1.2	3.7	0.6	10.7	0.4	10.4	0.4	3.2	9.7	0.2	0.7
F8i7	8	79 AD	M	40-50	16.4	0.7	15.4	0.9	-8.6	1.3	2.7	1.2	11.2	1.2	10.8	0.6	3.2**	10.8**	<0.5**	0.0
F8i23	8	79 AD	M	20-30	13.6	0.7	12.9	1.1	-10.0	0.6	1.7	0.6	9.8	0.2	8.9	0.6	3.2**	9.1**	<0.5**	-0.2
F9i9	9	79 AD	M	40-50	17.1	0.3	16.6	0.2	-10.0	0.3	4.7	0.5	10.5	0.2	11.8	0.4	3.3	11.5	0.2	0.4
F9i13	9	79 AD	M	40-50	15.8	0.5	15.8	0.7	-7.7	1.1	3.4	0.6	10.8	0.1	10.9	0.4	3.2	10.7	0.2	0.2
F10i14	10	79 AD	M	30-40	12.7	0.7	10.7	0.8	-12.3	1.0	2.8	0.5	9.5	1.1	10.7	0.4	3.2**	10.5**	<0.5**	0.2
F10i17	10	79 AD	M	30-40	17.1	0.5	16.9	0.6	-8.7	0.5	3.7	0.8	10.8	0.4	10.9	0.5	3.2**	11.6**	<0.5**	-0.7
F10i20	10	79 AD	M	40-50	14.7	0.5	13.8	0.5	-6.0	0.8	2.2	0.2	10.0	0.1	8.8	0.3	3.2**	9.1**	<0.5**	-0.3
F10i22	10	79 AD	M	20-30	13.4	0.3					3.7	1.2	11.6	1.1	11.2	0.4	3.2**	10.5**	<0.5**	0.7
F12i23	12	79 AD	M	40-50	16.2	0.8	15.2	1.0	-8.9	0.8	4.1	0.4	11.1	0.9	10.6	0.4	3.3*	10.9*	0.12*	-0.4

B.

Sample name	***Fornici***	**Date**	**Sex**	**Age**	**Gly** $\delta^{13}C$ (‰)	**Err.**	**Ser** $\delta^{13}C$ (‰)	**Err.**	**Glu** $\delta^{13}C$ (‰)	**Err.**	**Ala** $\delta^{13}C$ (‰)	**Err.**	**Asp** $\delta^{13}C$ (‰)	**Err.**	**Pro** $\delta^{13}C$ (‰)	**Err.**	**Hyp** $\delta^{13}C$ (‰)	**Err.**	**Val** $\delta^{13}C$ (‰)	**Err.**
F8I6	6	79 AD	F	20-30	-12.9	0.7	-9.1	1.4	-18.7	1.0	-19.3	0.7	-20.5	1.0	-19.7	0.6	-19.9	0.8	-25.7	0.4
F10i11	10	79 AD	F	30-40	-14.0	1.1	-9.5	1.2	-19.2	0.9	-21.5	0.6	-20.2	1.3	-20.1	1.1	-19.5	1.9	-27.0	0.8
F10i16	10	79 AD	F	30-40	-12.5	1.1	-8.6	1.4	-19.7	1.0	-21.1	0.7	-21.1	0.7	-19.9	0.7	-21.4	0.9	-25.6	0.5
F10i28	10	79 AD	F	30-40	-11.8	0.9	-8.9	1.2	-19.2	0.9	-20.4	0.6	-21.3	1.0	-20.0	0.7	-21.9	0.8	-25.7	0.6
F12I3	12	79 AD	F	20-30	-11.3	1.0	-8.1	1.3	-18.6	1.1	-20.3	0.6	-19.8	0.8	-19.3	0.8	-21.0	0.9	-25.1	0.5
F12i28	12	79 AD	F	30-40	-11.9	1.3	-9.8	0.9	-19.8	0.7	-20.4	1.1	-21.3	1.1	-18.9	0.5	-19.2	1.1	-27.6	0.5
F7I7	7	79 AD	M	20-30	-12.9	2.0	-11.2	1.9	-19.2	1.1	-21.9	2.1	-21.0	1.3	-19.6	0.7	-20.3	1.1	-26.1	0.8

F7i10	7	79 AD	M	30-40	-11.2	1.3	-9.6	1.0	-20.3	0.7	-19.7	1.0	-20.9	0.9	-19.4	0.5	-19.7	1.1	-25.1	0.5
F8I7	8	79 AD	M	40-50	-10.9	0.9	-8.0	1.5	-18.6	1.0	-19.8	0.8	-20.2	1.1	-19.1	0.8	-18.9	1.0	-24.3	0.7
F8I23	8	79 AD	M	20-30	-14.6	1.8	-11.8	1.6	-19.0	1.0	-22.5	2.0	-21.0	1.1	-19.5	0.7	-19.9	1.0	-26.0	0.5
F9i9	9	79 AD	M	40-50	-11.4	0.6	-9.8	1.2	-18.0	0.8	-20.8	0.5	-19.6	0.7	-19.0	0.4	-19.3	0.8	-24.6	0.6
F9i13	9	79 AD	M	40-50	-10.6	0.6	-8.6	0.9	-18.6	0.7	-20.8	0.4	-19.6	0.7	-18.9	0.4	-21.0	0.8	-24.9	0.6
F10I14	10	79 AD	M	30-40	-9.4	1.0	-7.0	1.9	-19.1	0.9	-20.2	0.9	-20.9	1.0	-18.1	0.6	-19.0	1.3	-24.9	0.4
F10I17	10	79 AD	M	30-40	-10.0	1.2	-6.5	1.5	-17.6	1.0	-19.7	0.9	-19.0	0.9	-18.5	0.5	-19.4	1.1	-23.1	0.6
F10I20	10	79 AD	M	40-50	-9.6	0.7	-8.1	1.1	-19.2	0.5	-18.5	0.4	-21.4	0.5	-19.7	0.6	-19.5	1.4	-25.1	0.2
F10I22	10	79 AD	M	20-30	-9.8	0.7	-7.2	1.1	-18.3	0.6	-18.5	0.4	-19.5	0.6	-19.3	0.6	-20.3	0.5	-23.8	0.2
F12I23	12	79 AD	M	40-50	-8.7	0.8	-6.1	1.3	-18.5	1.3	-19.8	0.6	-19.8	1.0	-18.9	0.6	-20.5	1.2	-23.7	0.4

Sample name	***Fornici***	**Date**	**Sex**	**Age**	**Leu**		**Ile**		**Thr**		**Lys**		**Phe**		**Tyr**		**Est. Bulk**		**C:N**	**Meas. Bulk**		**Est-Meas**
					$\delta^{13}C$ (‰)	**Err.**	**$\delta^{13}C$ (‰)**	**Err.**	**$\delta^{13}C$ (‰)**	**Err.**	**$\delta^{13}C$ (‰)**	**Err.**	**$\delta^{13}C$ (‰)**	**Err.**	**$\delta^{13}C$ (‰)**	**Err.**	**$\delta^{13}C$ (‰)**	**Err.**		**$\delta^{13}C$ (‰)**	**Err.**	(‰)
F8I6	6	79 AD	F	20-30	-28.8	0.4	-21.9	0.7	-5.8	0.7			-22.2	1.7	-28.7	0.9	-20.1	2.1	3.3*	-19.9**	<0.5**	1.1
F10i11	10	79 AD	F	30-40	-29.6	0.9	-22.4	1.0	-9.5	1.7	-25.7	1.1	-23.0	1.6	-26.8	1.4	-25.6	1.4	3.3*	-19.7*	0.03*	0.1
F10i16	10	79 AD	F	30-40	-29.6	0.6	-23.8	0.5	-11.0	0.8	-23.2	1.8	-21.1	1.1	-31.4	0.9	-22.1	0.8	3.2	-19.8*	0.1	0.5
F10i28	10	79 AD	F	30-40	-30.0	0.6	-23.6	0.5	-12.1	0.7	-28.1	0.6	-21.2	1.0	-29.5	1.2	-24.1	0.8	3.2*	-19.7*	0.03*	0.6
F12I3	12	79 AD	F	20-30	-29.1	0.6	-23.1	0.3	-11.0	0.5	-27.3	0.6	-20.5	1.0	-30.4	0.9	-24.1	1.1	3.3*	-19.7*	0.19*	1.1
F12i28	12	79 AD	F	30-40	-29.7	0.8	-23.0	0.6	-7.3	0.8			-19.0	1.4	-27.7	0.7	-25.4	1.6	3.2	-19.1	0.1	0.4
F7I7	7	79 AD	M	20-30	-29.7	0.7	-22.6	0.9	-5.1	1.0	-27.8	2.2	-22.5	2.5	-26.6	1.3	-21.7	1.5	3.2*	-19.3**	<0.5**	0.1
F7i10	7	79 AD	M	30-40	-28.6	0.8	-21.5	0.6	-6.4	0.8			-19.8	1.0	-27.5	0.8	-25.9	1.5	3.2	-18.9	0.1	0.4
F8I7	8	79 AD	M	40-50	-27.6	0.5	-21.2	0.6	-3.4	0.9	-26.3	0.9	-19.7	1.3	-27.1	0.8	-23.1	1.2	3.2*	-18.9**	<0.5**	1.0
F8I23	8	79 AD	M	20-30	-29.2	0.6	-22.0	0.7	-5.4	0.7			-20.8	2.5	-26.9	0.8	-20.6	0.9	3.2*	-19.6**	<0.5**	0.2
F9i9	9	79 AD	M	40-50	-27.2	0.5	-22.2	0.5	-9.0	0.7	-25.1	1.5	-17.8	1.0	-28.3	0.6	-18.1	0.9	3.3	-18.80*	0.1	0.6

F9i13	9	79 AD	M	40-50	-26.9	0.4	-22.1	0.4	-9.3	0.8	-25.2	1.7	-18.6	1.2	-29.7	0.7	-20.0	0.8	3.2	-19.12*	0.1	1.1
F10I14	10	79 AD	M	30-40	-28.9	0.5	-22.0	0.6	-7.5	1.8	-24.8	1.6	-19.2	1.5	-29.4	1.3	-22.7	1.1	3.2*	-19.0**	<0.5**	1.4
F10I17	10	79 AD	M	30-40	-26.1	0.5	-22.3	0.7	-9.5	1.3			-19.4	1.9	-29.8	0.6	-20.5	1.8	3.2*	-18.8**	<0.5**	1.4
F10I20	10	79 AD	M	40-50	-28.2	0.3	-22.8	0.6	-10.0	0.8	-21.9	1.2	-20.1	1.2	-28.1	1.0	-22.4	0.7	3.2*	-19.6**	<0.5**	1.5
F10I22	10	79 AD	M	20-30	-28.0	0.3	-23.5	0.7	-8.7	0.8	-17.8	0.6	-18.6	1.2	-30.2	0.4	-22.3	0.5	3.2*	-19.1**	<0.5**	1.4
F12I23	12	79 AD	M	40-50	-28.0	0.6	-21.1	0.5	-8.9	1.0	-23.4	0.9	-18.5	1.4	-29.4	0.9	-20.8	1.6	3.3*	-18.57*	0.10*	1.1

Table S1. Stable nitrogen (A) and carbon isotope (B) values of amino acids and bulk collagen of the human individuals from Herculaneum. Err. refers to the measurement uncertainty. The estimated (est.) bulk isotope value is derived by summing the proportional contribution of nitrogen and carbon in each amino acid to collagen. Measured (meas.) bulk values were analyzed via EA-IRMS. *Data previously reported in Craig *et al.* (2013), **Data previously reported in Martyn *et al.* (2018).

A.

Sample name	Site	Chronology (year or century)	Animal Group	Taxa
EF7OC	Herculaneum	79 AD	Terrestrial herbivore	*Ovis*
EF7DOG	Herculaneum	79 AD	Terrestrial herbivore	*Bos*
F8SG	Herculaneum	79 AD	Terrestrial herbivore	*Ovis*
EF8BOS	Herculaneum	79 AD	Terrestrial herbivore	*Bos*
EF10OC	Herculaneum	79 AD	Terrestrial herbivore	*Ovis*
PSC1	Porta Stabia - Pompeii	Early I BC	Terrestrial herbivore	*Bos*
PSC2	Porta Stabia - Pompeii	Early I BC	Terrestrial herbivore	*Bos*
PSSG3	Porta Stabia - Pompeii	Early I AD	Terrestrial herbivore	*Capreolus*
VESH1	Velia	I - II AD	Terrestrial herbivore	*Capra*
VEDE1	Velia	I - II AD	Terrestrial herbivore	*Capreolus*
PSG1	Porta Stabia - Pompeii	Early I AD	Terrestrial herbivore	*Sus*
PSP3	Porta Stabia - Pompeii	Early I AD	Terrestrial omnivore	*Sus*
PSP4	Porta Stabia - Pompeii	Early I AD	Terrestrial omnivore	*Sus*
PSP5	Porta Stabia - Pompeii	Early I AD	Terrestrial omnivore	*Sus*
PSCH1	Porta Stabia - Pompeii	Early I AD	Terrestrial omnivore	*Gallus*
PSCH2	Porta Stabia - Pompeii	Early I AD	Terrestrial omnivore	*Gallus*
PSCH3	Porta Stabia - Pompeii	Early I AD	Terrestrial omnivore	*Gallus*
HSSPI	House of the Surgeon - Pompeii	III BC - I AD	Marine fish	Sparidae
HSSPII	House of the Surgeon - Pompeii	III BC - I AD	Marine fish	Sparidae
PSSPI	Porta Stabia - Pompeii	Early I AD	Marine fish	Sparidae
PSSC2	Porta Stabia - Pompeii	Early I AD	Marine fish	Scombridae
PSPL1	Porta Stabia - Pompeii	Early I AD	Marine fish	*Pleuronectes platessa*

PSMU1	Porta Stabia - Pompeii	Early I AD	Marine fish	*Muraena helena*
SSF2	Santa Severa, Italy	VII-XV AD	Marine fish	*Galeorhinus galeus*
SSF5	Santa Severa, Italy	VII-XV AD	Marine fish	*Labrus bergylta*
ABF3	Albarracín, Spain	X-XII AD	Marine fish	*Argyrosomus regius*

B.

Sample name	Gly		Ser		Glu		Ala		Asp		Pro		Hyp		Val	
	$\delta^{15}N$ (‰)	Err.	$\delta^{15}N$ (‰)	Err.	$\delta^{15}N$ (‰)	Err.	$\delta^{15}N$ (‰)	Err.	$\delta^{15}N$ (‰)	Err.	$\delta^{15}N$ (‰)	Err.	$\delta^{15}N$ (‰)	Err.	$\delta^{15}N$ (‰)	Err.
EF7OC	-0.8	1.0	2.4	0.5	7.6	0.2	3.7	0.4	9.0	0.5	5.3	0.4	6.2	0.9	11.8	1.5
EF7DOG	2.9	0.5	2.8	0.4	7.9	0.4	4.4	1.0	8.4	0.1	6.7	0.4	6.7	0.2	14.0	0.6
F8SG	4.6	0.1	8.3	0.7	12.1	0.5	9.8	1.0	13.1	0.8	10.0	0.5	11.0	0.4	14.0	1.2
EF8BOS	4.2	0.1	3.3	0.3	8.1	0.1	3.9	0.6	8.7	0.1	6.9	0.4	7.8	0.3	15.7	0.6
EF10OC	0.4	0.7	3.1	0.7	8.0	0.1	2.9	0.6	9.5	0.6	5.8	0.2	7.0	0.7	11.8	0.5
PSC1	3.6	0.4	2.6	0.7	8.0	0.3	5.5	0.7	8.6	0.4	7.4	0.1	8.0	0.2	15.9	1.4
PSC2	4.1	0.5	-0.5	0.6	9.6	0.0	6.4	0.8	9.7	0.3	8.3	0.2	8.9	0.5	15.8	0.8
PSSG3	-0.1	0.2	1.5	0.7	6.2	0.5	4.2	0.8	7.1	0.4	7.1	0.3	7.4	0.5	13.0	1.0
VESH1	0.0	0.2	-0.7	0.3	8.0	0.2	4.4	0.2	7.4	0.2	7.8	0.3	8.4	0.4	6.0	0.9
VEDE1	3.6	0.6	3.1	0.8	8.5	0.6	6.0	0.5	8.3	0.4	9.6	0.5	9.4	0.6	7.4	0.4
PSG1	1.2	1.1	2.7	0.8	7.6	0.1	3.3	0.8	9.2	0.8	7.7	0.1	8.4	0.6	12.7	1.3
PSP3	3.6	0.2	5.3	0.7	11.2	0.1	9.0	0.6	10.4	0.5	10.4	0.3	10.5	0.1	11.1	1.0
PSP4	-0.3	0.0	5.0	0.5	7.1	0.3	4.6	0.1	7.4	0.2	8.1	0.2	7.7	0.5	8.9	0.1
PSP5	4.7	0.3	2.3	0.9	11.7	0.4	10.4	0.4	11.9	0.3	12.2	0.2	12.8	0.8	13.7	0.5
PSCH1	6.2	0.3	5.5	0.6	10.1	0.7	9.7	0.6	9.1	0.3	10.0	0.2	9.7	0.4	11.4	0.9
PSCH2	5.3	0.6	6.5	0.8	9.2	0.4	10.0	1.3	9.4	0.4	9.8	0.2	9.8	0.5	10.6	0.3
PSCH3	6.7	0.3	6.4	0.6	10.1	0.3	9.6	0.6	10.7	0.5	10.4	0.4	9.8	0.2	11.6	0.7

HSSPI	-1.2	0.0	1.8	0.6	16.9	0.3	16.0	0.9	15.5	0.5	9.7	0.2	11.2	0.3	24.5	1.3
HSSPII	-2.6	0.5	2.4	0.6	19.6	0.1	18.4	0.9	16.6	0.3	13.3	0.6	14.6	0.8	26.7	0.2
PSSPI	1.6	0.3	3.8	0.2	19.0	0.3	17.3	0.6	19.6	0.4	12.7	0.3	14.6	0.6	26.6	0.5
PSSC2	-7.2	0.3	-1.5	1.0	21.1	0.8	21.3	1.2	22.7	0.6	15.1	0.8	16.9	0.6	29.1	0.5
PSPL1	-0.8	0.9	3.9	0.4	19.6	0.3	18.8	0.9	19.2	0.4	12.5	0.2	14.7	0.2	27.5	0.6
PSMU1	3.6	1.2	5.8	0.7	19.3	0.4	16.6	0.7	22.1	0.1	17.3	0.2	18.0	1.0	26.1	0.6
SSF2	2.0	0.2	3.6	0.4	28.2	0.3	27.6	0.7	24.4	0.1	22.7	0.1	23.4	0.4	33.8	0.4
SSF5	2.5	0.5	6.0	0.3	16.6	0.4	15.1	1.2	15.2	0.3	13.3	0.4	14.2	0.7	24.6	1.1
ABF3	1.2	0.2	3.8	0.2	20.1	0.4	19.6	1.4	17.5	0.5	13.6	0.3	15.1	1.0	27.4	0.5

Sample name	**Leu** $\delta^{15}N$ (‰)	**Err.**	**Ile** $\delta^{15}N$ (‰)	**Err.**	**Thr** $\delta^{15}N$ (‰)	**Err.**	**Lys** $\delta^{15}N$ (‰)	**Err.**	**Phe** $\delta^{15}N$ (‰)	**Err.**	**Est. Bulk** $\delta^{15}N$ (‰)	**Err.**	**C:N**	**Meas. Bulk** $\delta^{15}N$ (‰)	**Err.**	**Est-Meas (‰)**
EF7OC	9.4	0.6	10.5	0.7	-6.1	0.9	0.5	0.9	9.2	1.2	3.1	0.7	3.2	3.2	0.2	-0.1
EF7DOG	11.8	0.3	11.1	1.1	-5.1	0.9	0.4	1.1	9.3	0.8	4.9	0.6	3.2	4.9	0.3	0.0
F8SG	10.5	0.8	10.3	0.7	-3.0	0.9	3.9	0.8	12.6	0.2	7.8	0.5	3.2	7.3	0.2	0.5
EF8BOS	11.3	0.2	12.1	0.7	-7.4	0.6	0.8	1.1	7.8	0.9	5.4	0.4	3.2	6.2	0.3	-0.2
EF10OC	8.7	0.6	10.1	0.5	-6.8	0.8	1.7	0.1	10.3	0.6	3.7	0.5	3.2	3.7	0.3	0.0
PSC1	11.8	0.5	11.0	1.8	-1.0	0.2	2.1	0.5	8.3	0.6	5.8	0.4	3.2	5.8	0.2	0.0
PSC2	11.6	0.5	11.5	0.9	-5.8	0.6	2.7	0.2	10.7	0.8	6.2	0.4	3.2	6.2	0.2	0.1
PSSG3	8.4	0.8	7.8	0.5	-9.9	0.6	0.4	0.8	8.2	0.5	3.5	0.4	3.3	3.7	0.3	-0.2
VESH1	4.7	1.1	5.7	2.0	-10.6	0.4	-1.1	0.1	8.2	0.4	3.3	0.3	3.2***	2.57***	0.09***	0.7
VEDE1	6.4	0.6	4.2	1.2	-11.7	1.8	0.5	0.3	9.3	1.2	5.5	0.6	3.1***	4.66***	0.05***	0.8
PSG1	10.6	0.1					1.8	1.0	8.4	0.7	4.6	0.7	3.2	4.6	0.3	0.0
PSP3	9.8	0.3	9.9	0.6	-4.3	0.3	3.6	0.6	8.9	0.4	7.0	0.3	3.2	6.3	0.2	0.7

PSP4	6.3	0.4	7.9	0.4	-6.2	0.5	1.6	0.6	9.1	0.4	3.9	0.2	3.2	3.1	0.2	0.8
PSP5	11.1	0.2	11.4	0.5	0.0	0.7	4.6	0.6	9.7	0.2	8.2	0.4	3.3	7.9	0.2	0.3
PSCH1	9.0	0.1	9.2	0.8	-4.3	0.2	2.5	0.6	6.7	0.4	7.3	0.4	3.2	7.0	0.2	0.3
PSCH2	8.6	0.4	9.1	0.4	-4.0	1.4	3.1	1.7	8.6	0.3	7.0	0.6	3.2	5.6	0.2	1.4
PSCH3	9.1	0.8	10.2	0.5	-3.1	1.4	2.3	0.1	8.2	0.5	7.7	0.4	3.3	6.4	0.2	1.3
HSSPI	19.7	0.6	20.6	1.0	-13.1	0.2	1.2	0.6	2.5	0.4	6.1	0.3	3.2	7.0	0.2	-0.9
HSSPII	24.2	0.4	24.6	0.3	-23.0	0.9	1.2	0.6	2.0	1.1	6.6	0.5	3.2	8.0	0.2	-1.4
PSSPI	22.1	0.3			-10.9	1.2	3.4	0.9	5.3	0.8	8.5	0.4	3.1	9.5	0.2	-1.1
PSSC2	24.5	0.2	24.4	0.7	-28.0	0.5	0.6	0.9	5.0	0.5	5.6	0.6	3.2	7.2	0.3	-1.5
PSPL1	24.1	0.4	24.1	0.5	-14.7	0.9	3.6	0.2	5.5	0.1	7.8	0.6	3.2	8.7	0.2	-0.8
PSMU1	22.6	0.3	23.4	1.4			3.1	1.7	4.6	1.0	10.8	0.8	3.2	10.6	0.2	0.2
SSF2	29.9	0.5	29.1	0.3	-24.4	1.2	4.9	1.1	7.8	0.6	12.6	0.4	3.3	14.4	0.2	-1.8
SSF5	20.4	0.7	19.6	1.1	-9.2	0.9	5.8	0.8	6.2	1.2	8.6	0.6	3.3	10.4	0.2	-1.8
ABF3	22.9	0.4	22.5	1.5	-9.8	0.7	3.8	0.6	4.8	0.5	8.9	0.5	3.2	9.8	0.2	-0.9

C.

Sample name	Gly		Ser		Glu		Ala		Asp		Pro		Hyp		Val	
	$\delta^{13}C$ (‰)	Err.	$\delta^{13}C$ (‰)	Err.	$\delta^{13}C$ (‰)	Err.	$\delta^{13}C$ (‰)	Err.	$\delta^{13}C$ (‰)	Err.	$\delta^{13}C$ (‰)	Err.	$\delta^{13}C$ (‰)	Err.	$\delta^{13}C$ (‰)	Err.
EF7OC	-11.5	1.3	-9.8	0.8	-19.3	0.9	-21.5	1.0	-19.4	1.3	-19.6	0.6	-19.0	1.1	-27.6	1.3
F8SG	-17.0	0.9	-13.5	1.3	-24.0	0.8	-27.9	1.3	-23.8	0.6	-22.3	0.5	-23.1	1.1	-30.9	0.6
EF8bos	-17.3	1.7	-20.2	2.0	-22.8	1.0	-29.1	1.6	-25.5	0.7	-19.2	0.6	-19.9	1.3	-29.0	0.9
EF10OC	-14.4	1.9	-16.7	2.3	-20.3	1.0	-26.6	1.9	-23.2	0.8	-19.7	0.7	-19.5	1.5	-29.1	1.1
PSC1	-15.2	1.8	-17.0	1.4	-21.2	0.8	-25.9	1.7	-23.8	0.5	-17.4	0.6	-17.3	1.3	-27.4	1.1
PSC2	-11.4	1.5	-11.3	1.0	-19.3	0.8	-21.8	1.1	-20.4	1.0	-17.8	0.6	-18.4	1.2	-26.6	0.7
PSG2	-13.5	1.0	-9.4	1.2	-22.2	0.5	-25.3	0.7	-23.3	0.5	-20.0	0.3	-20.5	0.4	-27.8	0.6

VESH1	-12.5	1.0	-7.8	1.8	-21.5	1.0	-24.8	0.9	-20.2	1.1	-19.6	0.6	-21.8	1.2	-27.3	0.4
VEDE1	-13.5	0.9	-11.2	1.7	-21.6	0.9	-25.2	0.9	-19.4	1.4	-19.8	0.5	-21.8	1.1	-28.0	0.4
PSP3	-17.4	1.4	-13.3	1.7	-22.4	0.8	-26.6	1.4	-24.0	1.0	-20.8	0.5	-21.1	0.7	-28.7	0.9
PSP4	-14.2	1.4	-11.9	1.5	-22.3	0.7	-24.4	1.4	-23.0	1.1	-19.1	0.6	-19.5	0.7	-27.4	0.9
PSP5	-19.9	1.6	-16.1	1.6	-21.4	0.9	-27.1	1.5	-22.8	1.3	-20.8	0.8	-22.1	0.8	-30.5	1.0
PSCH1	-11.1	1.5	-15.8	1.5	-19.1	0.8	-19.7	1.4	-20.5	1.0	-15.7	0.6	-16.1	0.8	-25.7	0.9
PSCH2	-15.0	1.4	-10.9	1.6	-19.4	0.8	-22.4	1.3	-20.6	0.9	-19.3	0.5	-20.1	0.7	-26.8	0.9
PSCH3	-9.2	1.4	-11.6	2.3	-15.6	0.7	-16.0	1.4	-16.6	1.0	-14.2	0.6	-14.1	0.9	-24.0	1.1
PSSPI	-4.4	1.6	-4.2	1.3	-15.7	0.8	-18.8	1.6	-19.6	0.7	-15.3	0.4	-16.1	1.1	-23.3	0.7
PSSC2	-2.0	1.6	-4.8	1.3	-15.1	0.9	-17.7	1.6	-16.9	0.6	-11.8	0.5	-12.3	1.1	-22.8	0.9
HSSSQ	-2.3	0.6	3.3	1.4	-11.6	0.9	-13.6	0.8	-11.3	1.4	-12.1	0.6	-11.9	0.8	-18.9	0.4
HSSPI	0.3	0.7	2.0	1.4	-13.0	1.0	-15.6	0.8	-14.6	1.0	-13.6	0.7	-12.9	0.8	-20.9	0.6
HSSPII	-3.7	1.0	-3.0	0.9	-13.7	0.8	-16.6	0.7	-15.2	0.9	-14.6	0.5	-14.0	0.8	-23.2	0.4
HSSSA	-1.1	0.6	-1.8	1.2	-12.7	0.7	-15.6	0.5	-15.2	1.0	-13.3	0.4	-13.3	0.9	-19.8	0.5
HSLA	-5.8	1.7	-3.2	1.7	-11.5	0.9	-14.8	2.0	-12.2	1.1	-11.9	0.6	-12.8	0.9	-19.4	0.6
SSF2	-2.0	0.9	3.3	1.0	-14.1	0.8	-14.2	0.4	-14.0	0.7	-13.7	0.5	-15.4	0.8	-20.6	0.3
SSF5	-1.5	0.7	3.3	1.4	-9.3	1.0	-11.1	0.7	-9.5	1.0	-9.9	0.6	-9.3	0.8	-16.8	0.5
ABF3	-1.8	1.0	0.4	1.6	-13.6	1.4	-12.0	0.7	-13.8	1.6	-13.5	0.6	-13.6	1.3	-20.5	0.7

Sample name	**Leu**		**Ile**		**Thr**		**Lys**		**Phe**		**Tyr**		**Est. Bulk**			**Meas. Bulk**		**Est-Meas bulk offset (‰)**
	$\delta^{13}C$ (‰)	**Err.**	**$\delta^{13}C$ (‰)**	**Err.**	**$\delta^{13}C$ (‰)**	**Err.**	**$\delta^{13}C$ (‰)**	**Err.**	**$\delta^{13}C$ (‰)**	**Err.**	**$\delta^{13}C$ (‰)**	**Err.**	**$\delta^{13}C$ (‰)**	**Err.**	**C:N**	**$\delta^{13}C$ (‰)**	**Err.**	
EF7OC	-31.1	0.9	-25.6	0.9	-11.8	0.7	-16.8	1.0	-28.0	0.8	-25.4	0.8	-18.8	0.9	3.2	-20.1	0.1	1.3
F8SG	-32.8	0.6	-28.5	0.8	-14.3	0.9	-21.5	0.9	-30.4	1.1	-29.3	1.2	-22.8	0.8	3.2	-21.6	0.1	-1.6
EF8bos	-30.3	1.0	-27.7	0.6	-18.7	1.5	-17.1	1.7	-33.1	0.2	-27.7	1.8	-21.9	1.1	3.2	-21.5	0.1	-0.4

EF10OC	-30.4	1.1	-26.7	0.6	-18.5	1.4	-15.6	1.4	-30.8	0.6	-29.4	1.2	-20.6	1.2	3.2	-19.8	0.1	-0.8
PSC1	-28.7	1.2	-25.7	1.2	-17.1	1.0	-14.2	1.5	-30.3	0.8	-28.4	0.7	-19.8	1.1	3.2	-19.4	0.1	-0.5
PSC2	-30.1	0.9	-25.8	0.8	-9.6	1.0	-16.1	0.8	-27.2	0.8	-25.1	1.2	-18.2	0.9	3.2	-20.2	0.1	2.1
PSG2	-32.1	0.5	-25.9	0.4	-11.0	0.6	-18.0	0.7	-28.5	0.3	-26.5	1.9	-20.3	0.6	3.2	-21.3	0.1	1.0
VESH1	-31.2	0.7	-24.9	0.6	-11.6	0.9	-20.3	1.5	-32.6	0.7	-25.1	0.9	-19.9	0.9	3.22***	21.24***	0.1	1.4
VEDE1	-31.9	0.6	-26.8	0.4	-13.3	1.8	-20.3	1.4	-33.1	0.5	-28.7	1.0	-20.4	0.8	3.14***	21.96***	0.0	1.6
PSP3	-30.6	0.6	-26.2	0.4	-17.6	0.7	-18.9	1.0	-34.8	0.6	-29.5	1.6	-22.0	0.9	3.2	-20.8	0.0	-1.2
PSP4	-30.0	0.7	-24.2	0.5	-17.2	0.9	-17.3	1.0	-33.8	0.6	-28.7	1.1	-20.3	0.9	3.2	-20.1	0.0	-0.3
PSP5	-32.8	1.0	-26.0	0.9	-9.5	0.9	-21.8	1.5	-35.1	1.1	-27.4	0.6	-22.6	1.1	3.3	-21.4	0.0	-1.2
PSCH1	-26.7	1.0	-22.9	0.9	-15.6	2.2	-15.9	1.0	-32.4	0.5	-26.7	1.3	-18.4	1.0	3.2	-17.1	0.1	-1.3
PSCH2	-28.3	0.6	-22.7	0.5	-5.0	0.7	-20.3	1.1	-30.4	0.6	-27.9	1.0	-20.0	0.9	3.2	-18.2	0.0	-1.8
PSCH3	-25.6	0.6	-21.7	0.5	-14.2	1.2	-15.1	1.2	-29.2	0.6	-26.6	2.2	-16.2	1.0	3.3	-15.6	0.1	-0.6
PSSPI	-23.6	1.6	-19.4	0.8	-9.0	1.2	-12.2	1.5	-28.6	0.8	-22.2	1.9	-13.6	1.1	3.1	-12.6	0.1	-1.0
PSSC2	-24.0	0.8	-17.9	0.7	-12.5	1.0	-11.0	1.9	-28.4	0.6	-23.5	0.8	-11.9	1.1	3.2	-12.8	0.1	0.4
HSSSQ	-20.8	0.4	-15.6	0.6	-17.7	0.7	-13.3	1.9	-23.4	0.8	-18.0	1.9	-10.3	0.8	3.5	-11.9	0.1	1.6
HSSPI	-21.1	0.6	-18.3	0.7	-25.5	0.8	-14.8	1.5	-25.1	0.8	-17.3	1.3	-11.2	0.8	3.2	-12.9	0.1	1.7
HSSPII	-23.5	0.6	-18.6	0.8	-10.9	0.7	-14.9	0.9	-26.4	0.5	-19.3	2.6	-12.6	0.8	3.2	-13.1	0.1	0.5
HSSSA	-22.0	0.4	-16.2	0.8	-8.6	0.9	-13.2	1.1	-25.5	0.8	-16.2	2.2	-11.0	0.7	3.3	-12.4	0.1	1.4
HSLA	-21.0	0.5	-15.8	1.0	-3.2	0.7	-13.8	2.5	-22.7	0.6	-18.4	1.5	-11.2	1.2	3.3	-12.1	0.4	0.9
SSF2	-19.7	0.5	-17.2	0.5	-8.3	0.7	-15.2	1.1	-26.9	0.5	-16.3	1.2	-11.1	0.7	3.3	-11.7	0.1	0.7
SSF5	-18.8	0.4	-15.0	0.8	-3.4	1.0	-11.4	1.4	-20.8	0.9	-14.3	2.0	-8.2	0.8	3.3	-10.3	0.2	2.2
ABF3	-22.5	1.2	-15.0	1.0	-5.0	1.6	-14.3	1.8	-22.1	1.5	-19.0	1.4	-10.7	1.1	3.2	-11.4	0.1	0.8

Table S2. Information (A) and stable nitrogen (B) and carbon isotope (C) values of amino acids and bulk collagen of the faunal remains analysed in this study. Err. refers to the measurement uncertainty. The estimated (est.) bulk isotope value is derived by

summing the proportional contribution of nitrogen and carbon in each amino acid to collagen. Measured (meas.) bulk values were analysed via EA-IRMS. ***Data previously reported in Craig *et al.* (2009)**.**

A.

Sample name	Provenance	Chronology	Common name	Latin name
MDW	Italy	Modern	Macaroni wheat grain	*Triticum durum*
MB	Italy	Modern	Barley	*Hordeum vulgare*
MF	Italy	Modern	Einkorn	*Triticum monococcum*
1703b	Herculaneum	79 AD	Barley	*Hordeum vulgare*
1895e	Herculaneum	79 AD	Emmer	*Triticum dicoccum*
723w	Herculaneum	79 AD	Wheat	*Triticum* sp.
1703w	Herculaneum	79 AD	Wheat	*Triticum* sp.
BarleyP*****	Pompeii	79 AD	Barley	*Hordeum vulgare*
LBCFA16F****	*Portus Romae*	Early second	Free-threshing wheat grain	*Triticum durum/aestivum*
LBCFD16E****	*Portus Romae*	Early second	Macaroni wheat grain	*Triticum durum*
LBTA1012I****	*Portus Romae*	Early second	Bread wheat grain	*Triticum aestivum*
LBTD1012H&I****	*Portus Romae*	Early second	Macaroni wheat grain	*Triticum durum*

B.

Sample name	Gly	Err.	Glu	Err.	Ala	Err.	Asp	Err.	Pro	Err.	Val	Err.
	$\delta^{15}N$ (‰)		$\delta^{15}N$ (‰)		$\delta^{15}N$ (‰)		$\delta^{15}N$ (‰)		$\delta^{15}N$ (‰)		$\delta^{15}N$ (‰)	
MDW	8.6	1.0	11.4	0.7	11.2	0.7	13.2	0.7	12.7	0.5	14.2	1.1
MB	8.1	0.1	8.9	0.0	8.2	0.6	10.7	0.3	10.0	0.1	11.3	0.9
MF	8.4	0.6	10.4	0.4	10.2	1.0	12.5	0.8	11.3	0.5	12.3	0.8
1703b	7.7	1.8	9.6	0.9	9.3	0.9	11.5	1.0	10.7	0.7	12.0	1.1
1895e	1.5	1.8	3.4	0.9	3.0	0.9	5.3	1.0	4.5	0.7	5.8	1.1
723w	5.0	1.8	6.9	0.9	6.5	0.9	8.8	1.0	8.0	0.7	9.3	1.1
1703w	4.8	1.8	6.7	0.9	6.3	0.9	8.6	1.0	7.8	0.7	9.0	1.1

BarleyP*****	1.2	1.8	3.0	0.9	2.7	0.9	4.9	1.0	4.2	0.7	5.4	1.1
LBCFA16F****	9.5	1.8	11.3	0.9	11.0	0.9	13.2	1.0	12.5	0.7	13.7	1.1
LBCFD16E****	10.5	1.8	12.3	0.9	12.0	0.9	14.2	1.0	13.5	0.7	14.7	1.1
LBTA1012I****	4.4	1.8	6.2	0.9	5.9	0.9	8.1	1.0	7.4	0.7	8.6	1.1
LBTD1012H&I****	11.3	1.8	13.1	0.9	12.8	0.9	15.0	1.0	14.3	0.7	15.5	1.1

Sample name	**Leu $\delta^{15}N$ (‰)**	**Err.**	**Ile $\delta^{15}N$ (‰)**	**Err.**	**Thr $\delta^{15}N$ (‰)**	**Err.**	**Lys $\delta^{15}N$ (‰)**	**Err.**	**Phe $\delta^{15}N$ (‰)**	**Err.**	**Tyr $\delta^{15}N$ (‰)**	**Err.**	**Meas. Bulk $\delta^{15}N$ (‰)**	**Err.***	**Meas. Bulk $\delta^{15}N$ corrected for charring (-0.31‰) (‰)**
MDW	10.5	1.1	11.5	1.0	5.5	1.1	9.8	0.7	19.3	0.6	9.8	0.7	9.5	0.2	
MB	7.6	0.2	8.6	0.2	1.3	0.4	4.9	0.4	17.6	0.4	4.9	0.4	6.2	0.2	
MF	8.7	0.3	9.2	0.7	2.2	0.4	6.0	0.9	18.8	0.4	6.0	0.9	7.4	0.2	
1703b	8.3	1.1	9.2	1.1	2.4	1.2	6.3	1.3	18.0	1.1	6.3	1.3	7.4	0.2	7.1
1895e	2.1	1.1	2.9	1.1	-3.8	1.2	0.0	1.3	11.7	1.1	0.0	1.3	1.2	0.3	0.8
723w	5.6	1.1	6.4	1.1	-0.3	1.2	3.5	1.3	15.2	1.1	3.5	1.3	4.6	0.2	4.3
1703w	5.4	1.1	6.2	1.1	-0.5	1.2	3.3	1.3	15.0	1.1	3.3	1.3	4.4	0.2	4.1
BarleyP*****	1.7	1.1	2.6	1.1	-4.2	1.2	-0.3	1.3	11.4	1.1	-0.3	1.3	0.8*****		0.5
LBCFA16F****	10.0	1.1	10.9	1.1	4.1	1.2	8.0	1.3	19.7	1.1	8.0	1.3	9.1****	0.2****	8.8
LBCFD16E****	11.0	1.1	11.9	1.1	5.1	1.2	9.0	1.3	20.7	1.1	9.0	1.3	10.1****	0.2****	9.8
LBTA1012I****	4.9	1.1	5.8	1.1	-1.0	1.2	2.9	1.3	14.6	1.1	2.9	1.3	4.0****	0.2****	3.7
LBTD1012H&I****	11.8	1.1	12.7	1.1	5.9	1.2	9.8	1.3	21.5	1.1	9.8	1.3	10.9****	0.2****	10.6

C.

Sample name	**Gly $\delta^{13}C$ (‰)**	**Err.**	**Ser $\delta^{13}C$ (‰)**	**Err.**	**Glu $\delta^{13}C$ (‰)**	**Err.**	**Ala $\delta^{13}C$ (‰)**	**Err.**	**Asp $\delta^{13}C$ (‰)**	**Err.**	**Pro $\delta^{13}C$ (‰)**	**Err.**	**Val $\delta^{13}C$ (‰)**	**Err.**
MDW	-14.4	1.1	-11.9	1.7	-25.5	1.0	-24.4	1.7	-26.6	0.8	-24.0	0.9	-31.0	0.6

MB	-19.7	1.1	-16.2	1.8	-28.1	1.2	-27.6	1.5	-29.2	1.1	-27.5	0.8	-32.1	0.6
MF	-16.7	1.1	-15.5	1.5	-27.1	1.1	-27.1	1.5	-27.9	0.8	-26.3	1.0	-31.9	0.6
1703b	-12.9	1.7	-10.5	1.9	-22.9	1.3	-22.4	1.7	-23.9	1.2	-21.9	1.0	-27.6	1.3
1895e	-15.6	1.7	-13.2	1.9	-25.6	1.3	-25.1	1.7	-26.6	1.2	-24.6	1.0	-30.3	1.3
723w	-13.8	1.7	-11.3	1.9	-23.7	1.3	-23.2	1.7	-24.8	1.2	-22.8	1.0	-28.5	1.3
1703w	-13.3	1.7	-10.8	1.9	-23.2	1.3	-22.7	1.7	-24.2	1.2	-22.3	1.0	-28.0	1.3
BarleyP*****	-14.4	1.7	-11.9	1.9	-24.3	1.3	-23.8	1.7	-25.4	1.2	-23.4	1.0	-29.1	1.3
LBCFA16F****	-13.2	1.7	-10.7	1.9	-23.1	1.3	-22.6	1.7	-24.2	1.2	-22.2	1.0	-27.9	1.3
LBCFD16E****	-13.7	1.7	-11.2	1.9	-23.6	1.3	-23.1	1.7	-24.7	1.2	-22.7	1.0	-28.4	1.3
LBTA1012I****	-14.1	1.7	-11.6	1.9	-24.0	1.3	-23.5	1.7	-25.1	1.2	-23.1	1.0	-28.8	1.3
LBTD1012H&I****	-13.7	1.7	-11.2	1.9	-23.6	1.3	-23.1	1.7	-24.7	1.2	-22.7	1.0	-28.4	1.3

Sample name	**Leu**		**Ile**		**Thr**		**Phe**		**Tyr**		**Meas. Bulk**		**Meas. Bulk $\delta^{13}C$**
	$\delta^{13}C$ (‰)	**Err.**	**$\delta^{13}C$ (‰)**	**Err.**	**$\delta^{13}C$ (‰)**	**Err.**	**$\delta^{13}C$ (‰)**	**Err.**	**$\delta^{13}C$ (‰)**	**Err.**	**$\delta^{13}C$ (‰)*** **	**Err.**	**corrected for charring (-0.11‰) (‰)**
MDW	-33.9	0.5	-27.3	0.5	-10.3	0.9	-28.2	1.3	-26.3	1.1	-24.4	0.2	
MB	-35.3	0.7	-28.5	0.5	-13.2	1.0	-30.2	1.8	-28.7	1.1	-27.7	0.2	
MF	-35.2	0.6	-29.2	0.6	-12.4	0.9	-29.6	1.1	-27.5	1.2	-27.0	0.2	
1703b	-30.8	1.2	-24.3	1.2	-8.0	1.1	-25.3	2.0	-23.5	1.4	-22.2	0.1	-22.4
1895e	-33.5	1.2	-27.0	1.2	-10.6	1.1	-28.0	2.0	-26.2	1.4	-24.9	0.2	-25.0
723w	-31.6	1.2	-25.2	1.2	-8.8	1.1	-26.2	2.0	-24.3	1.4	-23.1	0.1	-23.2
1703w	-31.1	1.2	-24.7	1.2	-8.3	1.1	-25.7	2.0	-23.8	1.4	-22.6	0.1	-22.7
BarleyP*****	-32.2	1.2	-25.8	1.2	-9.4	1.1	-26.8	2.0	-24.9	1.4	-23.7*****		-23.8
LBCFA16F****	-31.0	1.2	-24.6	1.2	-8.2	1.1	-25.6	2.0	-23.7	1.4	-22.5****	0.2****	-22.6

LBCFD16E****	-31.5	1.2	-25.1	1.2	-8.7	1.1	-26.1	2.0	-24.2	1.4	-23.0****	0.2****	-23.1
LBTA1012I****	-31.9	1.2	-25.5	1.2	-9.1	1.1	-26.5	2.0	-24.6	1.4	-23.4****	0.2****	-23.5
LBTD1012H&I****	-31.5	1.2	-25.1	1.2	-8.7	1.1	-26.1	2.0	-24.2	1.4	-23.0****	0.2****	-23.1

Table S3. Information (A) and stable nitrogen (B) and carbon (C) isotope values of bulk and amino acids of cereals. Nitrogen isotope and carbon isotope bulk and amino acid values were measured from modern cereals (MDW, MB and MF). The offset between each amino acid and their corresponding bulk value was then added to the bulk isotope values of grains from Herculaneum (1703b, 1895e, 723w and 1703w) and other Roman cereals obtained from the literature: **** data from Pate *et al.* (2016), ***** data from O'Connell *et al.* (2019).

Target	Source	Meas. Protein M1 (%)	1SD	Est. Protein M2 (%)	Meas-Est
F8i6	C3cereals	17.1	8.9	11.9	5.3
F8i6	TAnimals	56.2	11.8	64.8	-8.7
F8i6	MFish	26.7	7.2	23.3	3.4
F10i11	C3cereals	22.1	12.7	13.0	9.1
F10i11	TAnimals	53.2	15.6	66.8	-13.5
F10i11	MFish	24.7	9.0	20.2	4.5
F10i16	C3cereals	18.3	7.4	14.9	3.4
F10i16	TAnimals	70.1	10.7	76.0	-5.9
F10i16	MFish	11.6	6.4	9.0	2.5
F10i28	C3cereals	24.7	8.5	20.4	4.2
F10i28	TAnimals	59.0	12.5	66.6	-7.7
F10i28	MFish	16.4	7.2	12.9	3.4
F12i3	C3cereals	14.1	9.6	8.6	5.5
F12i3	TAnimals	65.4	12.1	70.8	-5.5
F12i3	MFish	20.6	7.8	20.6	0.0
F12i28	C3cereals	23.7	9.9	17.6	6.1
F12i28	TAnimals	55.1	12.4	63.8	-8.7
F12i28	MFish	21.2	7.4	18.6	2.6
F7i7	C3cereals	43.1	9.9	39.2	3.9
F7i7	TAnimals	34.5	13.1	41.9	-7.3
F7i7	MFish	22.4	8.0	19.0	3.4
F7i10	C3cereals	33.7	8.3	29.9	3.7
F7i10	TAnimals	32.9	11.2	40.5	-7.5
F7i10	MFish	33.4	7.4	29.6	3.8
F8i7	C3cereals	35.4	11.3	28.1	7.3
F8i7	TAnimals	24.9	12.1	34.7	-9.8
F8i7	MFish	39.8	7.7	37.2	2.5
F8i23	C3cereals	23.5	7.2	19.1	4.4
F8i23	TAnimals	47.0	10.9	56.0	-9.0
F8i23	MFish	29.6	7.0	25.0	4.6
F9i9	C3cereals	31.9	7.8	29.3	2.6
F9i9	TAnimals	31.2	11.1	35.7	-4.5
F9i9	MFish	37.0	7.0	35.0	2.0

F9i13	C3cereals	28.0	6.3	27.7	0.4
F9i13	TAnimals	41.2	9.7	42.6	-1.4
F9i13	MFish	30.8	6.8	29.7	1.0
F10i14	C3cereals	15.1	9.5	9.2	6.0
F10i14	TAnimals	57.1	12.3	65.9	-8.8
F10i14	MFish	27.8	7.7	25.0	2.8
F10i17	C3cereals	27.4	7.2	25.2	2.2
F10i17	TAnimals	35.5	11.4	40.9	-5.4
F10i17	MFish	37.1	7.6	33.8	3.3
F10i20	C3cereals	22.1	6.7	17.8	4.2
F10i20	TAnimals	49.9	11.3	58.9	-8.9
F10i20	MFish	28.0	7.0	23.3	4.7
F10i22	C3cereals	18.8	9.2	12.2	6.6
F10i22	TAnimals	58.3	10.6	63.0	-4.7
F10i22	MFish	22.9	6.7	24.8	-1.9
F12i23	C3cereals	30.6	10.6	24.3	6.3
F12i23	TAnimals	33.7	13.0	42.1	-8.4
F12i23	MFish	35.7	7.6	33.6	2.1
AVG	C3cereals	25.2	7.1	22.5	2.6
AVG	TAnimals	48.8	9.7	53.4	-4.7
AVG	MFish	26.1	6.2	24.0	2.0

Table S4. Comparison between the estimates from Model 1 and the protein estimates from Model 2. Protein contribution for each source from *Model 2* was calculated by multiplying the estimates from *Model 2* (express as % calorie contribution) by the protein content (% dry weight) of the source and then by normalizing the values.

Wilcox test

M1	**W**	**p-value**
C_3 Cereals	12	0.03937
Terrestrial Animals	60	0.007737
Marine Fish	4	0.004179

M2	**W**	**p-value**
C_3 Cereals	12	0.03937
Terrestrial Animals	59	0.01038
Marine Fish	8	0.0138

Table S5. Non-parametric Wilcox test (two-sided) applied to *Model 1* (M1) and *Model 2* (M2) to explore differences between genders for each food source. The test was run on the median values of the Markov chains generated by the model for each individual using the R function *wilcox.test* (R version 4.0.3). A significance level of 0.05 was used.

A.

				Dry weight (%)			
		AVG (*g*/100*g*)	1SD	AVG	1SD	SEM	carbon content (%)
	water	13.92	12.02				
	Protein	12.57	3.15	15.36	3.85	0.38	17.64
C_3 Cereals	Total lipid	2.72	2.31				
	Carbohydrate	69.25	10.18	84.64	12.44	1.24	82.36
	water	61.24	19.98				
	Protein	16.08	7.97	44.64	22.12	0.92	35.49
Terrestrial Animals	Total lipid	19.95	19.91	55.36	55.28	2.30	64.51
	Carbohydrate	1.52	1.58				
	water	75.61	6.38				
	Protein	17.72	2.93	79.43	13.13	1.01	72.49
Marine Fish	Total lipid	4.59	4.48	20.57	20.10	1.55	27.51
	Carbohydrate	1.39	0.21				

B.

				Per protein (%)			Dry weight (%)		
	Amino Acids	AVG (*g*/100*g*)	1SD	AVG	1SD	SEM	AVG	1SD	SEM
	Tryptophan	0.18	0.07	1.41	0.55	0.17	0.21	0.08	0.03
	Threonine	0.38	0.10	3.05	0.83	0.26	0.46	0.12	0.04
	Isoleucine	0.46	0.16	3.70	1.27	0.40	0.55	0.19	0.06
	Leucine	0.88	0.29	7.09	2.33	0.74	1.06	0.35	0.11
	Lysine	0.40	0.19	3.22	1.53	0.48	0.48	0.23	0.07
	Methionine	0.22	0.07	1.77	0.55	0.17	0.26	0.08	0.03
	Cystine	0.32	0.13	2.60	1.02	0.32	0.39	0.15	0.05
C_3 Cereals	Phenylalanine	0.66	0.18	5.32	1.43	0.45	0.79	0.21	0.07
	Tyrosine	0.37	0.14	3.00	1.14	0.36	0.45	0.17	0.05
	Valine	0.59	0.22	4.74	1.77	0.56	0.71	0.27	0.08
	Arginine	0.65	0.32	5.24	2.57	0.81	0.78	0.38	0.12
	Histidine	0.29	0.08	2.31	0.66	0.21	0.34	0.10	0.03
	Alanine	0.50	0.21	4.00	1.69	0.53	0.60	0.25	0.08
	Aspartic acid	0.78	0.40	6.23	3.25	1.03	0.93	0.49	0.15
	Glutamic acid	3.49	1.01	28.02	8.08	2.55	4.19	1.21	0.38
	Glycine	0.52	0.22	4.16	1.73	0.55	0.62	0.26	0.08
	Proline	1.17	0.32	9.42	2.55	0.81	1.41	0.38	0.12
	Serine	0.59	0.17	4.73	1.36	0.43	0.71	0.20	0.06

	Tryptophan	0.21	0.06	1.17	0.32	0.07	0.58	0.16	0.03
	Threonine	0.80	0.19	4.53	1.08	0.22	2.23	0.53	0.11
	Isoleucine	0.87	0.21	4.94	1.20	0.24	2.43	0.59	0.12
	Leucine	1.43	0.33	8.16	1.90	0.39	4.01	0.93	0.19
	Lysine	1.58	0.38	9.02	2.18	0.44	4.43	1.07	0.22
	Methionine	0.49	0.12	2.79	0.66	0.13	1.37	0.32	0.07
	Cystine	0.22	0.05	1.25	0.28	0.06	0.61	0.14	0.03
	Phenylalanine	0.72	0.16	4.10	0.91	0.19	2.02	0.45	0.09
	Tyrosine	0.63	0.15	3.58	0.88	0.18	1.76	0.43	0.09
Terrestrial Animals	Valine	0.90	0.20	5.15	1.14	0.23	2.53	0.56	0.11
	Arginine	1.17	0.26	6.66	1.47	0.30	3.28	0.72	0.15
	Histidine	0.61	0.16	3.48	0.91	0.19	1.71	0.45	0.09
	Alanine	1.06	0.22	6.05	1.25	0.26	2.98	0.62	0.13
	Aspartic acid	1.67	0.37	9.51	2.12	0.43	4.68	1.04	0.21
	Glutamic acid	2.79	0.66	15.89	3.74	0.76	7.81	1.84	0.37
	Glycine	0.98	0.20	5.56	1.16	0.24	2.73	0.57	0.12
	Proline	0.80	0.16	4.58	0.92	0.19	2.25	0.45	0.09
	Serine	0.70	0.16	3.99	0.89	0.18	1.96	0.44	0.09
	Tryptophan	0.20	0.03	1.20	0.16	0.04	0.94	0.13	0.03
	Threonine	0.78	0.12	4.59	0.71	0.20	3.60	0.55	0.15
	Isoleucine	0.81	0.13	4.77	0.79	0.22	3.74	0.62	0.17
	Leucine	1.40	0.26	8.28	1.53	0.43	6.50	1.20	0.33
	Lysine	1.56	0.33	9.22	1.92	0.53	7.24	1.51	0.42
	Methionine	0.51	0.10	3.01	0.60	0.17	2.36	0.47	0.13
	Cystine	0.20	0.03	1.16	0.16	0.04	0.91	0.12	0.03
	Phenylalanine	0.68	0.12	4.02	0.71	0.20	3.15	0.55	0.15
	Tyrosine	0.60	0.09	3.56	0.53	0.15	2.79	0.41	0.11
Marine Fish	Valine	0.88	0.18	5.19	1.04	0.29	4.07	0.82	0.23
	Arginine	1.13	0.12	6.68	0.73	0.20	5.24	0.57	0.16
	Histidine	0.46	0.15	2.73	0.86	0.24	2.14	0.68	0.19
	Alanine	1.06	0.18	6.26	1.06	0.29	4.91	0.83	0.23
	Aspartic acid	1.80	0.30	10.61	1.74	0.48	8.32	1.37	0.38
	Glutamic acid	2.62	0.43	15.47	2.54	0.70	12.14	1.99	0.55
	Glycine	0.87	0.15	5.15	0.89	0.25	4.04	0.70	0.19
	Proline	0.64	0.10	3.75	0.57	0.16	2.94	0.45	0.12
	Serine	0.74	0.10	4.37	0.58	0.16	3.43	0.45	0.13

Table S6. Macronutrient (A) and amino acid (B) composition of foodstuff divided by group. Cereals, *n* = 10; Terrestrial animals, *n* = 24; Marine fish, *n* = 13. **A.** Dry weight (%) was calculated by removing water content and by multiplying the resulting value by 100. Carbohydrates were considered to be negligible in the dry weight (%) calculation for terrestrial animals and marine fish, while lipids were negligible in cereals. Carbon content (%) was calculated by multiplying the dry weight (%) for specific carbon content factors as described in the text by the values then normalized. **B.** Dry weight (%) was calculated by dividing the amino

acid content (g/100g) by the total dry weight (%) reported in A. Dry weight per protein (%) was obtained for each amino acid by dividing the amino acid content (g/100g) by the total amino acid content (g/100g) which correspond to protein (g/100g) in A).

Model 0$_{wd}$ - **FRUITS INPUTS**

Proxies

$\delta^{13}C$
$\delta^{15}N$

Target values

ID	$\delta^{13}C$ bulk	**Unc**	$\delta^{15}N$ bulk	Unc
F8i6	-19.9	0.5	9.4	0.5
F10i11	-19.7	0.5	9.3	0.5
F10i16	-19.8	0.5	9.7	0.5
F10i28	-19.7	0.5	9.2	0.5
F12i3	-19.7	0.5	10.1	0.5
F12i28	-19.1	0.5	10.4	0.5
F7i7	-19.3	0.5	10.1	0.5
F7i10	-18.9	0.5	9.7	0.5
F8i7	-18.9	0.5	10.8	0.5
F8i23	-19.6	0.5	9.1	0.5
F9i9	-18.8	0.5	11.5	0.5
F9i13	-19.1	0.5	10.7	0.5
F10i14	-19	0.5	10.5	0.5
F10i17	-18.8	0.5	11.6	0.5
F10i20	-19.6	0.5	9.1	0.5
F10i22	-19.1	0.5	10.5	0.5
F12i23	-18.6	0.5	10.9	0.5
AVG	-19.3	0.2	10.2	0.2

Sources

C3cereals
TAnimals
MFish

Source fractions

Protein
CarbsLipids

Offset/Weights

	Offset	**Unc.**	**Protein**	**Unc.**	**CarbsLipids**	Unc.
$\delta^{13}C$	4.8	0.5	74	4	26	4
$\delta^{15}N$	5.5	0.5	100		0	

Source values

	^{13}C	**Unc.**	^{15}N	**Unc.**
C3cereals Protein	-25.3	1	5.5	1.5
C3cereals CarbsLipids	-22.8	1		
TAnimals Protein	-22	1	5.2	1
TAnimals CarbsLipids	-28	1		
MFish Protein	-14.1	1	11	1
MFish CarbsLipids	-19.1	1		

Source concentrations

	Protein	**Unc.**	**CarbsLipids**	**Unc.**

C3cereals	15.4	0.4	84.6	1.2
TAnimals	44.6	0.9	55.4	2.3
MFish	79.4	1	20.6	1.5

Model 0 $_{wd}$ **- FRUITS ESTIMATES**

Target	Source	Mean	sd	2.5pc	median	97.5pc	16pc	84pc
F8i6	C3cereals	0.4718	0.3322	0.01265	0.4222	0.9713	0.0895	0.8899
F8i6	TAnimals	0.509	0.3277	0.01476	0.561	0.9655	0.0951	0.8841
F8i6	MFish	0.01921	0.01847	0.0005205	0.01372	0.06952	0.0036	0.0347
F10i11	C3cereals	0.4762	0.3163	0.01605	0.4434	0.9681	0.1047	0.8703
F10i11	TAnimals	0.5035	0.311	0.01571	0.5335	0.9578	0.1164	0.8648
F10i11	MFish	0.02028	0.01911	0.0006249	0.01483	0.07204	0.0042	0.036
F10i16	C3cereals	0.4738	0.3243	0.01239	0.4447	0.9707	0.0986	0.8786
F10i16	TAnimals	0.5056	0.3187	0.01687	0.5369	0.9632	0.1077	0.8723
F10i16	MFish	0.02055	0.01995	0.0005621	0.01446	0.07369	0.0039	0.0377
F10i28	C3cereals	0.4571	0.3158	0.01151	0.4093	0.9677	0.1068	0.8571
F10i28	TAnimals	0.524	0.3114	0.01367	0.5777	0.9665	0.1259	0.8715
F10i28	MFish	0.01891	0.01845	0.0004346	0.01339	0.06703	0.0034	0.0345
F12i3	C3cereals	0.4629	0.3078	0.01625	0.4329	0.9583	0.1106	0.8484
F12i3	TAnimals	0.5136	0.3018	0.02235	0.5443	0.9559	0.1341	0.8564
F12i3	MFish	0.02349	0.0224	0.0007502	0.01702	0.08245	0.0046	0.042
F12i28	C3cereals	0.4298	0.2784	0.01558	0.3979	0.9373	0.114	0.767
F12i28	TAnimals	0.5387	0.271	0.03565	0.5679	0.9488	0.2111	0.8403
F12i28	MFish	0.03156	0.02758	0.001098	0.02432	0.1023	0.0069	0.0558
F7i7	C3cereals	0.4375	0.2953	0.01467	0.4005	0.9531	0.1032	0.8073
F7i7	TAnimals	0.5357	0.2886	0.0292	0.5748	0.9579	0.1752	0.8553
F7i7	MFish	0.02679	0.02448	0.000807	0.02006	0.09253	0.0055	0.0484
F7i10	C3cereals	0.4341	0.2836	0.01909	0.4054	0.947	0.116	0.773
F7i10	TAnimals	0.5384	0.2782	0.02755	0.5696	0.9512	0.2057	0.8466
F7i10	MFish	0.02747	0.02442	0.000901	0.02094	0.09168	0.006	0.0492
F8i7	C3cereals	0.4302	0.2847	0.01556	0.3952	0.9317	0.1059	0.7824
F8i7	TAnimals	0.5319	0.2763	0.03978	0.5671	0.9403	0.1882	0.8395
F8i7	MFish	0.03788	0.03227	0.001278	0.02984	0.1214	0.0085	0.0672
F8i23	C3cereals	0.4547	0.3155	0.01441	0.4227	0.965	0.0882	0.8487
F8i23	TAnimals	0.5258	0.3104	0.0203	0.5609	0.9649	0.1376	0.8833
F8i23	MFish	0.01942	0.01884	0.0005412	0.01398	0.06919	0.0036	0.0346
F9i9	C3cereals	0.4455	0.2858	0.01671	0.4244	0.9373	0.1134	0.7881
F9i9	TAnimals	0.5074	0.2748	0.02945	0.53	0.9347	0.1806	0.8222
F9i9	MFish	0.04708	0.03747	0.002124	0.03835	0.1444	0.0125	0.081
F9i13	C3cereals	0.4413	0.2881	0.01553	0.4133	0.9416	0.1148	0.7973
F9i13	TAnimals	0.5237	0.2795	0.03294	0.5552	0.9429	0.1775	0.8369
F9i13	MFish	0.03497	0.03082	0.001119	0.02668	0.1153	0.0077	0.0627
F10i14	C3cereals	0.4489	0.2901	0.01677	0.4271	0.9431	0.1099	0.8031
F10i14	TAnimals	0.5177	0.2818	0.02975	0.5393	0.9474	0.1728	0.838
F10i14	MFish	0.03347	0.02975	0.001023	0.02586	0.1109	0.0074	0.0592
F10i17	C3cereals	0.4316	0.2762	0.01508	0.4109	0.9176	0.1169	0.7609
F10i17	TAnimals	0.521	0.2654	0.0462	0.5446	0.933	0.2078	0.8181
F10i17	MFish	0.0474	0.03762	0.001989	0.03879	0.1427	0.0118	0.0823
F10i20	C3cereals	0.4547	0.3155	0.01441	0.4227	0.965	0.0882	0.8487
F10i20	TAnimals	0.5258	0.3104	0.0203	0.5609	0.9649	0.1376	0.8833
F10i20	MFish	0.01942	0.01884	0.0005412	0.01398	0.06919	0.0036	0.0346
F10i22	C3cereals	0.4283	0.2869	0.01455	0.3895	0.9447	0.1063	0.7814
F10i22	TAnimals	0.5388	0.279	0.03411	0.5791	0.9474	0.1929	0.8467
F10i22	MFish	0.03285	0.02909	0.00111	0.02487	0.1104	0.0071	0.0585

F12i23	C3cereals	0.4338	0.2729	0.01731	0.4134	0.9185	0.1224	0.7627
F12i23	TAnimals	0.5227	0.2634	0.04647	0.5439	0.9389	0.2057	0.816
F12i23	MFish	0.04359	0.03507	0.001761	0.03569	0.1323	0.011	0.0754
AVG	C3cereals	0.4562	0.3102	0.01143	0.4423	0.9559	0.0854	0.8397
AVG	TAnimals	0.5205	0.3048	0.02352	0.5409	0.9612	0.1486	0.8787
AVG	MFish	0.02322	0.02071	0.0007426	0.01777	0.07704	0.0047	0.0413

Table E.1 *Model 0_{wd}* input parameters and the generated estimates.

***Model 0_p* - FRUITS INPUTS**

Proxies

$\delta^{13}C$
$\delta^{15}N$

Target values

ID	$\delta^{13}C$ bulk	**Unc**	$\delta^{15}N$ bulk	Unc
F8i6	-19.9	0.5	9.4	0.5
F10i11	-19.7	0.5	9.3	0.5
F10i16	-19.8	0.5	9.7	0.5
F10i28	-19.7	0.5	9.2	0.5
F12i3	-19.7	0.5	10.1	0.5
F12i28	-19.1	0.5	10.4	0.5
F7i7	-19.3	0.5	10.1	0.5
F7i10	-18.9	0.5	9.7	0.5
F8i7	-18.9	0.5	10.8	0.5
F8i23	-19.6	0.5	9.1	0.5
F9i9	-18.8	0.5	11.5	0.5
F9i13	-19.1	0.5	10.7	0.5
F10i14	-19	0.5	10.5	0.5
F10i17	-18.8	0.5	11.6	0.5
F10i20	-19.6	0.5	9.1	0.5
F10i22	-19.1	0.5	10.5	0.5
F12i23	-18.6	0.5	10.9	0.5
AVG	-19.3	0.2	10.2	0.2

Sources

C3cereals
TAnimals
MFish

Source fractions

Protein

Offset/Weights

	Offset	**Unc.**	**Protein**
$\delta^{13}C$	5	2.3	100
$\delta^{15}N$	5.5	0.5	100

Source values

	^{13}C	**Unc.**	^{15}N	**Unc.**
C3cereals Protein	-25.3	1	5.5	1.5

TAnimals Protein	-22	1	5.2	1
MFish Protein	-14.1	1	11	1

Source concentrations

	Protein	Unc.
C3cereals	100	0
TAnimals	100	0
MFish	100	0

***Model 0_p* - FRUITS ESTIMATES**

Target	Source	Mean	sd	2.5pc	median	97.5pc	16pc	84pc
F8i6	C3cereals	0.534	0.2624	0.03818	0.5746	0.9275	0.2096	0.8165
F8i6	TAnimals	0.3976	0.268	0.0175	0.3577	0.9102	0.1044	0.7219
F8i6	MFish	0.06838	0.05808	0.002309	0.05363	0.2169	0.0147	0.1241
F10i11	C3cereals	0.5378	0.2695	0.03209	0.5881	0.9366	0.2004	0.82
F10i11	TAnimals	0.3952	0.2746	0.01503	0.3445	0.9185	0.0983	0.7401
F10i11	MFish	0.06699	0.05687	0.002107	0.05222	0.211	0.014	0.1231
F10i16	C3cereals	0.5353	0.256	0.03864	0.5692	0.9298	0.2335	0.8085
F10i16	TAnimals	0.3909	0.2619	0.01574	0.3557	0.9063	0.1054	0.6978
F10i16	MFish	0.07385	0.06238	0.002353	0.05836	0.2316	0.0156	0.1337
F10i28	C3cereals	0.5302	0.2715	0.03295	0.5733	0.9415	0.1945	0.8228
F10i28	TAnimals	0.4009	0.2771	0.01492	0.3551	0.9207	0.0942	0.7406
F10i28	MFish	0.0689	0.05839	0.002165	0.05438	0.215	0.0143	0.1259
F12i3	C3cereals	0.5083	0.2537	0.04292	0.5314	0.9169	0.2069	0.7862
F12i3	TAnimals	0.4071	0.26	0.0183	0.376	0.9006	0.1171	0.7134
F12i3	MFish	0.08465	0.06957	0.002797	0.06697	0.257	0.019	0.1544
F12i28	C3cereals	0.479	0.2449	0.03769	0.4889	0.9001	0.1963	0.7476
F12i28	TAnimals	0.4252	0.2553	0.0205	0.4078	0.9009	0.1334	0.7176
F12i28	MFish	0.09577	0.07306	0.003745	0.08031	0.2717	0.0239	0.1695
F7i7	C3cereals	0.4963	0.2506	0.03742	0.5186	0.9103	0.2011	0.7696
F7i7	TAnimals	0.4175	0.2631	0.02097	0.3918	0.9006	0.12	0.7291
F7i7	MFish	0.08621	0.06986	0.002882	0.06921	0.2583	0.0193	0.1546
F7i10	C3cereals	0.5023	0.2589	0.03295	0.526	0.9154	0.1913	0.7817
F7i10	TAnimals	0.4168	0.2679	0.0191	0.3933	0.9163	0.1146	0.7312
F7i10	MFish	0.08089	0.06843	0.002544	0.06283	0.2558	0.0174	0.1479
F8i7	C3cereals	0.4512	0.2498	0.02484	0.4585	0.8956	0.1577	0.7278
F8i7	TAnimals	0.4364	0.2578	0.02508	0.4238	0.9023	0.138	0.7345
F8i7	MFish	0.1124	0.08388	0.004376	0.09621	0.3089	0.0279	0.198
F8i23	C3cereals	0.5313	0.2725	0.02851	0.5762	0.9375	0.1912	0.8233
F8i23	TAnimals	0.4014	0.2791	0.01433	0.3531	0.9258	0.096	0.7474
F8i23	MFish	0.06726	0.05756	0.002195	0.05274	0.2188	0.0141	0.1224
F9i9	C3cereals	0.4494	0.2394	0.03348	0.4512	0.8783	0.1775	0.7154
F9i9	TAnimals	0.4045	0.2476	0.02026	0.3869	0.8817	0.127	0.6835
F9i9	MFish	0.1461	0.1004	0.008013	0.1304	0.3771	0.0442	0.2488
F9i13	C3cereals	0.4679	0.2526	0.03197	0.4745	0.9032	0.1709	0.7471
F9i13	TAnimals	0.4236	0.2612	0.02069	0.4081	0.8909	0.1228	0.7283
F9i13	MFish	0.1085	0.08258	0.004499	0.09181	0.3043	0.0261	0.1913
F10i14	C3cereals	0.4527	0.2488	0.0285	0.4543	0.8942	0.1677	0.7307
F10i14	TAnimals	0.4474	0.2568	0.02629	0.4383	0.8987	0.1526	0.7402
F10i14	MFish	0.09985	0.07876	0.00375	0.08203	0.2889	0.0238	0.1781
F10i17	C3cereals	0.459	0.2369	0.04302	0.4646	0.8785	0.1872	0.7208
F10i17	TAnimals	0.3961	0.2446	0.02144	0.3795	0.8665	0.1217	0.6737
F10i17	MFish	0.1449	0.09845	0.007794	0.1307	0.3705	0.0443	0.2445
F10i20	C3cereals	0.5313	0.2725	0.02851	0.5762	0.9375	0.1912	0.8233

F10i20	TAnimals	0.4014	0.2791	0.01433	0.3531	0.9258	0.096	0.7474
F10i20	MFish	0.06726	0.05756	0.002195	0.05274	0.2188	0.0141	0.1224
F10i22	C3cereals	0.4641	0.2514	0.02739	0.4738	0.8997	0.1706	0.7418
F10i22	TAnimals	0.4355	0.2592	0.02297	0.4188	0.9067	0.1398	0.7331
F10i22	MFish	0.1004	0.07929	0.003755	0.08239	0.2931	0.0241	0.1784
F12i23	C3cereals	0.4341	0.2467	0.02665	0.4361	0.8779	0.1433	0.7124
F12i23	TAnimals	0.4436	0.255	0.02461	0.4399	0.8996	0.1525	0.7371
F12i23	MFish	0.1223	0.08886	0.004924	0.1054	0.3247	0.0323	0.2157
AVG	C3cereals	0.5393	0.2413	0.04558	0.5704	0.9151	0.2677	0.7937
AVG	TAnimals	0.3781	0.2495	0.01564	0.3487	0.8841	0.1083	0.659
AVG	MFish	0.0826	0.06646	0.00288	0.06742	0.2515	0.0193	0.1465

Table E.2 *Model 0_p* input parameters and the generated estimates.

***Model 1* - FRUITS INPUTS**

Proxies

d15NPhe
d13CPhe
d15NLys
d13CVal
d13CLeu
d13CIle

Target values

ID	d15Nphe	Unc	d13Cphe	Unc	d15Nlys	Unc	d13Cval	Unc	d13Cleu	Unc	d13Cile	Unc
F8i6	9.6	0.8	-28.7	0.9	1.5	1.1	-25.7	0.4	-28.8	0.4	-21.9	0.7
F10i11	9.2	1.1	-26.8	1.4	1.6	1.2	-27	0.8	-29.6	0.9	-22.4	1
F10i16	10.7	0.5	-31.4	0.9	3.3	0.8	-25.6	0.5	-29.6	0.6	-23.8	0.5
F10i28	10.6	0.4	-29.5	1.2	3.3	0.7	-25.7	0.6	-30	0.6	-23.5	0.5
F12i3	10.2	1.4	-30.4	0.9	2.4	1.2	-25.1	0.5	-29.1	0.6	-23.1	0.3
F12i28	9.7	0.7	-27.7	0.7	2.6	0.7	-27.6	0.5	-29.7	0.8	-23	0.6
F7i7	11.7	0.2	-26.6	1.2	3.1	0.5	-26.1	0.8	-29.7	0.7	-22.6	0.9
F7i10	10.7	0.4	-27.5	0.7	3.7	0.5	-25.1	0.5	-28.6	0.8	-21.5	0.6
F8i7	11.2	1.2	-27.1	0.8	2.7	1.2	-24.3	0.7	-27.6	0.5	-21.2	0.6
F8i23	9.8	0.2	-26.9	0.8	1.7	0.6	-26	0.5	-29.2	0.6	-22	0.7
F9i9	10.5	0.2	-28.3	0.6	4.7	0.5	-24.6	0.6	-27.2	0.5	-22.2	0.5
F9i13	10.8	0.1	-29.7	0.7	3.4	0.6	-24.9	0.6	-26.9	0.4	-22.1	0.4
F10i14	9.5	1.1	-29.4	1.3	2.8	0.5	-24.9	0.4	-28.9	0.5	-22	0.6
F10i17	10.8	0.4	-29.8	0.6	3.7	0.8	-23.1	0.6	-26.1	0.5	-22.3	0.7
F10i20	10	0.1	-28.1	1	2.2	0.2	-25.1	0.2	-28.2	0.3	-22.8	0.6
F10i22	11.6	1.1	-30.1	0.4	3.7	1.2	-23.8	0.2	-28	0.2	-23.5	0.7
F12i23	11.1	0.9	-29.4	0.9	4.1	0.4	-23.7	0.4	-28	0.6	-21.1	0.5
AVG	10.5	0.4	-28.7	0.5	3	0.4	-25.2	0.3	-28.5	0.3	-22.4	0.3

Sources

C3cereals
TAnimals
MFish

Source fractions

Phe
Lys
Val
Leu
Ile

Offset/Weights

	Offset	Unc	Phe	Unc	Lys	Unc	Val	Unc	Leu	Unc	Ile	Unc
15NPhe	0.1	0.2	100	0	0	0	0	0	0	0	0	0
13CPhe	0	0.4	100	0	0	0	0	0	0	0	0	0
15NLys	0.8	0.4	0	0	100	0	0	0	0	0	0	0
13CVal	-0.1	1.1	0	0	0	0	100	0	0	0	0	0
13CLeu	-0.3	0.8	0	0	0	0	0	0	100	0	0	0
13CIle	-0.7	1.5	0	0	0	0	0	0	0	0	100	0

Source values

	d15Nphe	Unc	d13Cphe	Unc	d15Nlys	Unc	d13Cval	Unc	d13Cleu	Unc	d13Cile	Unc.
C3cereals Phe	16.4	1.5	-26.2	1								
C3cereals Lys					4.7	1.5						
C3cereals Val							-28.6	1				
C3cereals Leu									-30.7	1		
C3cereals Ile											-25.2	1
Tanimals Phe	9	0.3	-31.3	0.6								
Tanimals Lys					1.9	0.4						
Tanimals Val							-27.8	0.5				
Tanimals Leu									-30.2	0.5		
Tanimals Ile											-25.4	0.5
MFish Phe	4.9	0.6	-25	0.8								
MFish Lys					3.1	0.6						
MFish Val							-20.6	0.7				
MFish Leu									-21.7	0.5		
MFish Ile											-16.9	0.5

Concentrations

	Phe	Unc	Lys	Unc	Val	Unc	Leu	Unc	Ile	Unc
C3cereals	5.3	0.5	3.2	0.5	4.7	0.6	7.1	0.7	3.7	0.4
Tanimals	4.1	0.2	9	0.4	5.1	0.2	8.2	0.4	4.9	0.2
MFish	4	0.2	9.2	0.5	5.2	0.3	8.3	0.4	4.8	0.2

***Model 1* - FRUITS ESTIMATES**

Target	Source	Mean	sd	2.5pc	median	97.5pc	16pc	84pc
F8i6	C3cereals	0.1712	0.08872	0.0216	0.1644	0.3633	0.0826	0.2578
F8i6	TAnimals	0.5616	0.1178	0.3293	0.5644	0.7812	0.4474	0.68
F8i6	MFish	0.2671	0.07182	0.1236	0.2687	0.4041	0.1961	0.3386
F10i11	C3cereals	0.2209	0.1265	0.02164	0.2063	0.5091	0.0924	0.3464
F10i11	TAnimals	0.5322	0.1564	0.2065	0.5397	0.8135	0.3764	0.6913
F10i11	MFish	0.247	0.09047	0.07273	0.2462	0.4234	0.1551	0.3381
F10i16	C3cereals	0.1833	0.07401	0.05683	0.1767	0.3472	0.1124	0.2546
F10i16	TAnimals	0.7011	0.1066	0.4791	0.7056	0.8924	0.5934	0.8091
F10i16	MFish	0.1156	0.06443	0.009379	0.1108	0.2543	0.0476	0.1825
F10i28	C3cereals	0.2469	0.08534	0.109	0.2371	0.4478	0.1656	0.3277

F10i28	TAnimals	0.5895	0.1246	0.324	0.5953	0.816	0.469	0.7136
F10i28	MFish	0.1636	0.07201	0.02592	0.1614	0.3069	0.0895	0.2368
F12i3	C3cereals	0.1409	0.09645	0.008038	0.1257	0.3613	0.0433	0.239
F12i3	TAnimals	0.6535	0.121	0.3875	0.6632	0.8661	0.5336	0.7719
F12i3	MFish	0.2056	0.0781	0.05535	0.2052	0.359	0.1265	0.2833
F12i28	C3cereals	0.237	0.09902	0.07035	0.2277	0.4606	0.1408	0.3334
F12i28	TAnimals	0.5511	0.1237	0.288	0.5583	0.7726	0.4268	0.6747
F12i28	MFish	0.2119	0.07414	0.06708	0.2122	0.359	0.1377	0.2859
F7i7	C3cereals	0.4311	0.09886	0.2696	0.4211	0.6508	0.3318	0.5323
F7i7	TAnimals	0.3452	0.1314	0.0824	0.347	0.5899	0.2084	0.4799
F7i7	MFish	0.2237	0.07952	0.06773	0.2248	0.3817	0.1424	0.3032
F7i10	C3cereals	0.3367	0.083	0.1957	0.329	0.5232	0.2559	0.4172
F7i10	TAnimals	0.3294	0.1122	0.09708	0.3324	0.5443	0.2169	0.4395
F7i10	MFish	0.3339	0.07438	0.1908	0.3331	0.4782	0.2585	0.4103
F8i7	C3cereals	0.3535	0.1126	0.138	0.3505	0.5797	0.2389	0.4674
F8i7	TAnimals	0.249	0.1211	0.03228	0.2448	0.498	0.1226	0.3724
F8i7	MFish	0.3975	0.07684	0.2489	0.3962	0.5458	0.3219	0.4748
F8i23	C3cereals	0.2347	0.07231	0.1181	0.2253	0.4001	0.1682	0.3022
F8i23	TAnimals	0.4696	0.1091	0.248	0.4734	0.6766	0.3638	0.5769
F8i23	MFish	0.2957	0.06983	0.1605	0.2953	0.4371	0.2261	0.3634
F9i9	C3cereals	0.3185	0.07842	0.1873	0.3085	0.5003	0.2437	0.3953
F9i9	TAnimals	0.3115	0.111	0.08107	0.3161	0.5155	0.1991	0.4223
F9i9	MFish	0.37	0.06951	0.2349	0.3697	0.5076	0.3016	0.4373
F9i13	C3cereals	0.2804	0.06262	0.1885	0.2702	0.4347	0.2236	0.3361
F9i13	TAnimals	0.4118	0.09687	0.2157	0.4124	0.5881	0.3138	0.5112
F9i13	MFish	0.3078	0.06788	0.175	0.3067	0.4444	0.2414	0.3767
F10i14	C3cereals	0.1512	0.0945	0.009067	0.1408	0.3656	0.054	0.2442
F10i14	TAnimals	0.5709	0.1227	0.318	0.5755	0.7987	0.4505	0.6931
F10i14	MFish	0.2778	0.0772	0.1252	0.2798	0.4277	0.1988	0.3548
F10i17	C3cereals	0.274	0.0719	0.1554	0.2666	0.4318	0.2041	0.3453
F10i17	TAnimals	0.355	0.1141	0.1171	0.3598	0.5675	0.241	0.4675
F10i17	MFish	0.371	0.07605	0.225	0.3697	0.522	0.2949	0.4473
F10i20	C3cereals	0.2206	0.06708	0.1174	0.2109	0.3855	0.1572	0.2825
F10i20	TAnimals	0.4991	0.1128	0.2598	0.5023	0.7039	0.3936	0.6074
F10i20	MFish	0.2803	0.0703	0.1405	0.2796	0.4232	0.2132	0.3479
F10i22	C3cereals	0.1883	0.09164	0.03392	0.1792	0.3969	0.0982	0.2787
F10i22	TAnimals	0.5828	0.1058	0.3629	0.5874	0.7802	0.4768	0.686
F10i22	MFish	0.2289	0.06669	0.09915	0.2276	0.3636	0.1631	0.2942
F12i23	C3cereals	0.3064	0.1062	0.1224	0.2982	0.5355	0.2007	0.4115
F12i23	TAnimals	0.3366	0.1296	0.07111	0.3405	0.5783	0.2053	0.4676
F12i23	MFish	0.357	0.07629	0.2091	0.3563	0.5101	0.2822	0.4321
AVG	C3cereals	0.2516	0.07146	0.1357	0.2442	0.4165	0.1848	0.3157
AVG	TAnimals	0.4877	0.09737	0.2898	0.4953	0.6705	0.3904	0.5795
AVG	MFish	0.2606	0.06153	0.1452	0.2601	0.3831	0.1988	0.3228

Table E.3 *Model 1* input parameters and the generated estimates.

Proxies

15NPhe
13CPhe
15NLys
13CVal
13CLeu
13CIle
15NGlu
13CGlu
13CAsp
13CAla

Target values

ID	d15Nphe	Unc	d13Cphe	Unc	d15Nlys	Unc	d13Cval	Unc	d13Cleu	Unc	d13Cile	Unc	d15Nglu	Unc	d13Cglu	Unc	d13Casp	Unc	d13Cala	Unc
F8i6	9.6	0.8	-28.7	0.9	1.5	1.1	-25.7	0.4	-28.8	0.4	-21.9	0.7	12.7	0.5	-18.7	1	-20.5	1	-19.3	0.7
F10i11	9.2	1.1	-26.8	1.4	1.6	1.2	-27	0.8	-29.6	0.9	-22.4	1	12.5	0.4	-19.2	0.9	-20.2	1.3	-21.5	0.6
F10i16	10.7	0.5	-31.4	0.9	3.3	0.8	-25.6	0.5	-29.6	0.6	-23.8	0.5	14.7	0.2	-19.7	1	-21.1	0.7	-21.1	0.7
F10i28	10.6	0.4	-29.5	1.2	3.3	0.7	-25.7	0.6	-30	0.6	-23.5	0.5	13.5	0.2	-19.2	0.9	-21.3	1	-20.3	0.6
F12i3	10.2	1.4	-30.4	0.9	2.4	1.2	-25.1	0.5	-29.1	0.6	-23.1	0.3	14.1	0.4	-18.6	1.1	-19.8	0.8	-20.3	0.6
F12i28	9.7	0.7	-27.7	0.7	2.6	0.7	-27.6	0.5	-29.7	0.8	-23	0.6	14.6	0.1	-19.8	0.7	-21.3	1.1	-20.4	1.1
F7i7	11.7	0.2	-26.6	1.2	3.1	0.5	-26.1	0.8	-29.7	0.7	-22.6	0.9	14.4	0.1	-19.2	1	-21	1.3	-21.9	2.1
F7i10	10.7	0.4	-27.5	0.7	3.7	0.5	-25.1	0.5	-28.6	0.8	-21.5	0.6	15	0.2	-20.3	0.7	-20.9	0.9	-19.7	1
F8i7	11.2	1.2	-27.1	0.8	2.7	1.2	-24.3	0.7	-27.6	0.5	-21.2	0.6	15.3	0.3	-18.6	1	-20.2	1.1	-19.8	0.8
F8i23	9.8	0.2	-26.9	0.8	1.7	0.6	-26	0.5	-29.2	0.6	-22	0.7	12.8	0.7	-19	0.9	-21	1.1	-22.5	2
F9i9	10.5	0.2	-28.3	0.6	4.7	0.5	-24.6	0.6	-27.2	0.5	-22.2	0.5	16.4	0.5	-18	0.7	-19.6	0.7	-20.8	0.5
F9i13	10.8	0.1	-29.7	0.7	3.4	0.6	-24.9	0.6	-26.9	0.4	-22.1	0.4	15.6	0.3	-18.6	0.7	-19.6	0.7	-20.8	0.4
F10i14	9.5	1.1	-29.4	1.3	2.8	0.5	-24.9	0.4	-28.9	0.5	-22	0.6	14.9	0.8	-19.1	0.9	-20.9	1	-20.2	0.9
F10i17	10.8	0.4	-29.8	0.6	3.7	0.8	-23.1	0.6	-26.1	0.5	-22.3	0.7	15.1	0.2	-17.6	1	-19	0.9	-19.7	0.9
F10i20	10	0.1	-28.1	1	2.2	0.2	-25.1	0.2	-28.2	0.3	-22.8	0.6	13.1	0.5	-19.2	0.5	-21.4	0.5	-18.5	0.3
F10i22	11.6	1.1	-30.1	0.4	3.7	1.2	-23.8	0.2	-28	0.2	-23.5	0.7	14.9	0.3	-18.3	0.6	-19.5	0.6	-18.5	0.4
F12i23	11.1	0.9	-29.4	0.9	4.1	0.4	-23.7	0.4	-28	0.6	-21.1	0.5	14.8	0.5	-18.5	1.3	-19.8	1	-19.8	0.6
AVG	10.5	0.4	-28.7	0.5	3	0.4	-25.2	0.3	-28.5	0.3	-22.4	0.3	14.4	0.2	-18.9	0.4	-20.4	0.5	-20.3	0.5

Sources

cerealsC3
TAnimals
Mfish

Source fractions

Phe
Lys
Val
Leu
Ile
WholeN
WholeC
CarbC

Offset/Weights

	Offset	Unc	Phe	Unc	Lys	Unc	Val	Unc	Leu	Unc	Ile	Unc	WholeN	Unc	WholeC	Unc	CarbC	Unc
15NPhe	0.1	0.2	100	0	0	0	0	0	0	0	0	0	0	0	0	0	0	0
13CPhe	0	0.4	100	0	0	0	0	0	0	0	0	0	0	0	0	0	0	0
15NLys	0.8	0.4	0	0	100	0	0	0	0	0	0	0	0	0	0	0	0	0
13CVal	-0.1	1.1	0	0	0	0	100	0	0	0	0	0	0	0	0	0	0	0
13CLeu	-0.3	0.8	0	0	0	0	0	0	100	0	0	0	0	0	0	0	0	0
13CIle	-0.7	1.5	0	0	0	0	0	0	0	0	100	0	0	0	0	0	0	0
15NGlu	9.7	2.5	0	0	0	0	0	0	0	0	0	0	100	0	0	0	0	0
13CGlu	8.7	3	0	0	0	0	0	0	0	0	0	0	0	0	100	0	0	0
13CAsp	4.7	1.5	0	0	0	0	0	0	0	0	0	0	0	0	100	0	0	0
13CAla	4	1.5	0	0	0	0	0	0	0	0	0	0	0	0	0	0	100	0

Source values

	d15Nphe	Unc	d13Cphe	Unc	d15Nlys	Unc	d13Cval	Unc	d13Cleu	Unc	d13Cile	Unc	d15Nglu	Unc	d13Cglu	Unc	d13Casp	Unc	d13Cala	Unc
C3cereals Phe	16.4	1.5	-26.2	1																
C3cereals Lys					4.7	1.5														
C3cereals Val							-28.6	1												
C3cereals Leu									-30.7	1										
C3cereals Ile											-25.2	1								

C3cereals WholeN													5.5	1.5		
C3cereals WholeC															-23.3	0.3
C3cereals CarbC																
Tanimals Phe	9	0.3	-31.3	0.6												
Tanimals Lys					1.9	0.4										
Tanimals Val							-27.8	0.5								
Tanimals Leu									-30.2	0.5						
Tanimals Ile											-25.4	0.5				
Tanimals WholeN													5.2	0.5		
Tanimals WholeC															-25.9	0.5
Tanimals CarbC																
MFish Phe	4.9	0.6	-25	0.8												
MFish Lys					3.1	0.6										
MFish Val							-20.6	0.7								
MFish Leu									-21.7	0.5						
MFish Ile											-16.9	0.5				
MFish WholeN													11	1		
MFish WholeC															-14	1
MFish CarbC																

C3cereals CarbC															-22.8	1
Tanimals Phe	9	0.3	-31.3	0.6												
Tanimals Lys					1.9	0.4										
Tanimals Val							-27.8	0.5								
Tanimals Leu									-30.2	0.5						
Tanimals Ile											-25.4	0.5				
Tanimals CarbC															0	0
MFish Phe	4.9	0.6	-25	0.8												
MFish Lys					3.1	0.6										
MFish Val							-20.6	0.7								
MFish Leu									-21.7	0.5						
MFish Ile											-16.9	0.5				
MFish CarbC															0	0

Concentrations

	Phe	**Unc**	**Lys**	**Unc**	**Val**	**Unc**	**Leu**	**Unc**	**Ile**	**Unc**	**WholeN**	**Unc**	**WholeC**	**Unc**	CarbC	Unc.
cerealsC3	0.8	0.1	0.5	0.1	0.7	0.1	1.1	0.3	0.6	0.2	15.4	0.4	100	0	84.6	1.2
TAnimals	2	0.1	4.4	0.2	2.5	0.1	4	0.2	2.4	0.1	44.6	0.9	100	0	0	0
Mfish	3.2	0.2	7.2	0.4	4.1	0.2	6.5	0.3	3.7	0.2	79.4	1	100	0	0	0

***Model 2* - FRUITS ESTIMATES**

Target	**Source**	**Mean**	**sd**	**2.5pc**	**median**	**97.5pc**	**16pc**	**84pc**

F8i6	C3cereals	0.3057	0.1581	0.02835	0.3043	0.6206	0.1327	0.4706
F8i6	TAnimals	0.5776	0.1529	0.2762	0.5796	0.8552	0.4216	0.7391
F8i6	MFish	0.1166	0.04141	0.04213	0.1144	0.2059	0.0757	0.157
F10i11	C3cereals	0.3255	0.181	0.02204	0.3183	0.6807	0.1263	0.5197
F10i11	TAnimals	0.5765	0.1758	0.2359	0.5831	0.884	0.3876	0.7658
F10i11	MFish	0.09805	0.04602	0.01667	0.09491	0.1983	0.0525	0.1439
F10i16	C3cereals	0.3481	0.1256	0.08911	0.3525	0.5857	0.2213	0.4728
F10i16	TAnimals	0.6112	0.1302	0.3697	0.6062	0.8801	0.4798	0.7422
F10i16	MFish	0.04078	0.0259	0.002492	0.03785	0.09907	0.0137	0.0676
F10i28	C3cereals	0.4448	0.118	0.1939	0.4471	0.6668	0.3318	0.5627
F10i28	TAnimals	0.5005	0.1271	0.2655	0.498	0.7741	0.3714	0.6241
F10i28	MFish	0.05464	0.02944	0.005597	0.05287	0.1165	0.0236	0.085
F12i3	C3cereals	0.2321	0.1513	0.01278	0.2105	0.5563	0.0699	0.3945
F12i3	TAnimals	0.6601	0.1411	0.3605	0.6753	0.8852	0.5141	0.8073
F12i3	MFish	0.1078	0.04443	0.02815	0.1058	0.2005	0.0628	0.1534
F12i28	C3cereals	0.4078	0.1523	0.07201	0.4156	0.6928	0.2592	0.5564
F12i28	TAnimals	0.5088	0.1518	0.2307	0.5073	0.84	0.3552	0.6524
F12i28	MFish	0.08333	0.03671	0.02089	0.08034	0.1638	0.0466	0.1206
F7i7	C3cereals	0.6838	0.08606	0.5268	0.6834	0.8479	0.5929	0.776
F7i7	TAnimals	0.2521	0.09224	0.08423	0.2532	0.4319	0.1536	0.3434
F7i7	MFish	0.06412	0.02749	0.01364	0.06235	0.1213	0.0366	0.0922
F7i10	C3cereals	0.6028	0.1013	0.4004	0.6068	0.7931	0.498	0.7049
F7i10	TAnimals	0.2816	0.1007	0.09519	0.278	0.4865	0.1807	0.3839
F7i10	MFish	0.1156	0.03173	0.0573	0.1142	0.1841	0.0849	0.1462
F8i7	C3cereals	0.5935	0.1516	0.2235	0.6144	0.828	0.4523	0.7379
F8i7	TAnimals	0.2538	0.1306	0.05218	0.2378	0.568	0.1254	0.3783
F8i7	MFish	0.1527	0.04548	0.07757	0.1484	0.2546	0.1084	0.197
F8i23	C3cereals	0.4408	0.1065	0.2256	0.4425	0.6409	0.3343	0.5472
F8i23	TAnimals	0.4471	0.1145	0.2456	0.4396	0.6869	0.3327	0.5626
F8i23	MFish	0.1121	0.0332	0.04754	0.1114	0.1798	0.0793	0.1448
F9i9	C3cereals	0.6053	0.08554	0.4465	0.6074	0.7779	0.5134	0.6907
F9i9	TAnimals	0.2544	0.08408	0.09583	0.25	0.4179	0.1706	0.3429
F9i9	MFish	0.1404	0.03155	0.08179	0.1395	0.2037	0.109	0.1724
F9i13	C3cereals	0.5748	0.07951	0.4247	0.574	0.7452	0.4967	0.6504
F9i13	TAnimals	0.3054	0.08393	0.1277	0.3029	0.4683	0.2265	0.3915
F9i13	MFish	0.1198	0.02975	0.06395	0.1188	0.1812	0.0906	0.1492
F10i14	C3cereals	0.2493	0.1594	0.01278	0.2319	0.5952	0.0787	0.4192
F10i14	TAnimals	0.6189	0.1521	0.301	0.6322	0.8689	0.4556	0.7788

F10i14	MFish	0.1318	0.04674	0.04486	0.1296	0.2293	0.0862	0.1777
F10i17	C3cereals	0.5495	0.103	0.3433	0.5503	0.7529	0.4492	0.652
F10i17	TAnimals	0.3077	0.1041	0.1079	0.3056	0.5223	0.2038	0.4113
F10i17	MFish	0.1428	0.03432	0.07946	0.1415	0.2137	0.1096	0.1769
F10i20	C3cereals	0.4175	0.09244	0.2268	0.4174	0.5994	0.3278	0.5097
F10i20	TAnimals	0.4763	0.1079	0.2753	0.4748	0.7013	0.3704	0.5806
F10i20	MFish	0.1061	0.03387	0.04246	0.1051	0.1751	0.0726	0.1407
F10i22	C3cereals	0.315	0.161	0.02304	0.3226	0.6175	0.136	0.4814
F10i22	TAnimals	0.5608	0.1445	0.2852	0.5537	0.8276	0.4146	0.7214
F10i22	MFish	0.1242	0.04275	0.0517	0.1196	0.2161	0.0822	0.1685
F12i23	C3cereals	0.5364	0.1477	0.1982	0.5508	0.7914	0.3885	0.6801
F12i23	TAnimals	0.32	0.1356	0.08898	0.3057	0.6346	0.1907	0.4519
F12i23	MFish	0.1436	0.04002	0.07381	0.1409	0.2308	0.1044	0.1824
AVG	C3cereals	0.4938	0.103	0.2786	0.4984	0.6837	0.3923	0.5961
AVG	TAnimals	0.4041	0.1029	0.2156	0.3969	0.6218	0.3031	0.508
AVG	MFish	0.1021	0.02951	0.04541	0.1014	0.1625	0.073	0.1307

Table E.4 *Model 2* input parameters and the generated estimates.

***Model 2* with olive oil - FRUITS INPUTS**

Proxies
15NPhe
13CPhe
15NLys
13CVal
13CLeu
13CIle
15NGlu
13CGlu
13CAsp
13CAla

Target values

ID	**d15Nphe**	**Unc**	**d13Cphe**	**Unc**	**d15Nlys**	**Unc**	**d13Cval**	**Unc**	**d13Cleu**	**Unc**	**d13Cile**	**Unc**	**d15Nglu**	**Unc**	**d13Cglu**	**Unc**	**d13Casp**	**Unc**	**d13Cala**	**Unc**
F8i6	9.6	0.8	-28.7	0.9	1.5	1.1	-25.7	0.4	-28.8	0.4	-21.9	0.7	12.7	0.5	-18.7	1	-20.5	1	-19.3	0.7
F10i11	9.2	1.1	-26.8	1.4	1.6	1.2	-27	0.8	-29.6	0.9	-22.4	1	12.5	0.4	-19.2	0.9	-20.2	1.3	-21.5	0.6

F10i16	10.7	0.5	-31.4	0.9	3.3	0.8	-25.6	0.5	-29.6	0.6	-23.8	0.5	14.7	0.2	-19.7	1	-21.1	0.7	-21.1	0.7
F10i28	10.6	0.4	-29.5	1.2	3.3	0.7	-25.7	0.6	-30	0.6	-23.5	0.5	13.5	0.2	-19.2	0.9	-21.3	1	-20.3	0.6
F12i3	10.2	1.4	-30.4	0.9	2.4	1.2	-25.1	0.5	-29.1	0.6	-23.1	0.3	14.1	0.4	-18.6	1.1	-19.8	0.8	-20.3	0.6
F12i28	9.7	0.7	-27.7	0.7	2.6	0.7	-27.6	0.5	-29.7	0.8	-23	0.6	14.6	0.1	-19.8	0.7	-21.3	1.1	-20.4	1.1
F7i7	11.7	0.2	-26.6	1.2	3.1	0.5	-26.1	0.8	-29.7	0.7	-22.6	0.9	14.4	0.1	-19.2	1	-21	1.3	-21.9	2.1
F7i10	10.7	0.4	-27.5	0.7	3.7	0.5	-25.1	0.5	-28.6	0.8	-21.5	0.6	15	0.2	-20.3	0.7	-20.9	0.9	-19.7	1
F8i7	11.2	1.2	-27.1	0.8	2.7	1.2	-24.3	0.7	-27.6	0.5	-21.2	0.6	15.3	0.3	-18.6	1	-20.2	1.1	-19.8	0.8
F8i23	9.8	0.2	-26.9	0.8	1.7	0.6	-26	0.5	-29.2	0.6	-22	0.7	12.8	0.7	-19	0.9	-21	1.1	-22.5	2
F9i9	10.5	0.2	-28.3	0.6	4.7	0.5	-24.6	0.6	-27.2	0.5	-22.2	0.5	16.4	0.5	-18	0.7	-19.6	0.7	-20.8	0.5
F9i13	10.8	0.1	-29.7	0.7	3.4	0.6	-24.9	0.6	-26.9	0.4	-22.1	0.4	15.6	0.3	-18.6	0.7	-19.6	0.7	-20.8	0.4
F10i14	9.5	1.1	-29.4	1.3	2.8	0.5	-24.9	0.4	-28.9	0.5	-22	0.6	14.9	0.8	-19.1	0.9	-20.9	1	-20.2	0.9
F10i17	10.8	0.4	-29.8	0.6	3.7	0.8	-23.1	0.6	-26.1	0.5	-22.3	0.7	15.1	0.2	-17.6	1	-19	0.9	-19.7	0.9
F10i20	10	0.1	-28.1	1	2.2	0.2	-25.1	0.2	-28.2	0.3	-22.8	0.6	13.1	0.5	-19.2	0.5	-21.4	0.5	-18.5	0.3
F10i22	11.6	1.1	-30.1	0.4	3.7	1.2	-23.8	0.2	-28	0.2	-23.5	0.7	14.9	0.3	-18.3	0.6	-19.5	0.6	-18.5	0.4
F12i23	11.1	0.9	-29.4	0.9	4.1	0.4	-23.7	0.4	-28	0.6	-21.1	0.5	14.8	0.5	-18.5	1.3	-19.8	1	-19.8	0.6
AVG	10.5	0.4	-28.7	0.5	3	0.4	-25.2	0.3	-28.5	0.3	-22.4	0.3	14.4	0.2	-18.9	0.4	-20.4	0.5	-20.3	0.5

Sources

cerealsC3
TAnimals
Mfish
oliveoil

Source fractions

Phe
Lys
Val
Leu
Ile
WholeN
WholeC
CarbC

Offset/Weights

	Offset	Unc	Phe	Unc	Lys	Unc	Val	Unc	Leu	Unc	Ile	Unc	WholeN	Unc	WholeC	Unc	CarbC	Unc
15NPhe	0.1	0.2	100	0	0	0	0	0	0	0	0	0	0	0	0	0	0	0
13CPhe	0	0.4	100	0	0	0	0	0	0	0	0	0	0	0	0	0	0	0
15NLys	0.8	0.4	0	0	100	0	0	0	0	0	0	0	0	0	0	0	0	0
13CVal	-0.1	1.1	0	0	0	0	100	0	0	0	0	0	0	0	0	0	0	0
13CLeu	-0.3	0.8	0	0	0	0	0	0	100	0	0	0	0	0	0	0	0	0
13CIle	-0.7	1.5	0	0	0	0	0	0	0	0	100	0	0	0	0	0	0	0
15NGlu	9.7	2.5	0	0	0	0	0	0	0	0	0	0	100	0	0	0	0	0
13CGlu	8.7	3	0	0	0	0	0	0	0	0	0	0	0	0	100	0	0	0
13CAsp	4.7	1.5	0	0	0	0	0	0	0	0	0	0	0	0	100	0	0	0
13CAla	4	1.5	0	0	0	0	0	0	0	0	0	0	0	0	0	0	100	0

Source values

	d15Nphe	Unc	d13Cphe	Unc	d15Nlys	Unc	d13Cval	Unc	d13Cleu	Unc	d13Cile	Unc	d15Nglu	Unc	d13Cglu	Unc	d13Casp	Unc	d13Cala	Unc
C3cereals Phe	16.4	1.5	-26.2	1																
C3cereals Lys					4.7	1.5														
C3cereals Val							-28.6	1												
C3cereals Leu									-30.7	1										
C3cereals Ile											-25.2	1								
C3cereals WholeN													5.5	1.5						
C3cereals WholeC															-23.3	0.3	-23.3	0.3		
C3cereals CarbC																			-22.8	1
Tanimals Phe	9	0.3	-31.3	0.6																
Tanimals Lys					1.9	0.4														
Tanimals Val							-27.8	0.5												
Tanimals Leu									-30.2	0.5										
Tanimals Ile											-25.4	0.5								
Tanimals WholeN													5.2	0.5						
Tanimals WholeC															-25.9	0.5	-25.9	0.5		
Tanimals CarbC																			0	0
MFish Phe	4.9	0.6	-25	0.8																

MFish Lys					3.1	0.6												
MFish Val							-20.6	0.7										
MFish Leu									-21.7	0.5								
MFish Ile											-16.9	0.5						
MFish WholeN													11	1				
MFish WholeC															-14	1	-14	1
MFish CarbC																	0	0
oliveoil Phe	0	0	0	0														
oliveoil Lys					0	0												
oliveoil Val							0	0										
oliveoil Leu									0	0								
oliveoil Ile											0	0						
oliveoil WholeN													0	0				
oliveoil WholeC															-30	1.3	-30	1.3
oliveoil CarbC																	0	0

Concentrations

	Phe	**Unc**	**Lys**	**Unc**	**Val**	**Unc**	**Leu**	**Unc**	**Ile**	**Unc**	**WholeN**	**Unc**	**WholeC**	**Unc**	CarbC	Unc.
cerealsC3	0.8	0.1	0.5	0.1	0.7	0.1	1.1	0.3	0.6	0.2	15.4	0.4	100	0	84.6	1.2
TAnimals	2	0.1	4.4	0.2	2.5	0.1	4	0.2	2.4	0.1	44.6	0.9	100	0	0	0
Mfish	3.2	0.2	7.2	0.4	4.1	0.2	6.5	0.3	3.7	0.2	79.4	1	100	0	0	0
oliveoil	0	0	0	0	0	0	0	0	0	0	0	0	100	0	0	0

***Model 2* with olive oil - FRUITS ESTIMATES**

Target	**Source**	**Mean**	**sd**	**2.5pc**	**median**	**97.5pc**	**16pc**	**84pc**
F8i6	C3cereals	0.2381	0.1242	0.02668	0.2293	0.5071	0.1111	0.364
F8i6	TAnimals	0.3964	0.151	0.1354	0.3844	0.7048	0.2431	0.5564
F8i6	Mfish	0.09389	0.03892	0.0297	0.09	0.1809	0.0555	0.1316
F8i6	Olive	0.2716	0.1723	0.01728	0.2524	0.664	0.0889	0.4483
F10i11	C3cereals	0.2566	0.1505	0.01989	0.2431	0.5748	0.0971	0.4162
F10i11	TAnimals	0.4062	0.1714	0.1113	0.393	0.7604	0.2291	0.589

F10i11	Mfish	0.07975	0.04001	0.01639	0.07558	0.1731	0.0405	0.1181
F10i11	Olive	0.2574	0.1706	0.01263	0.2369	0.633	0.0763	0.437
F10i16	C3cereals	0.2646	0.1086	0.07105	0.2614	0.4845	0.1529	0.3761
F10i16	TAnimals	0.4272	0.1507	0.1545	0.4228	0.7352	0.2731	0.5792
F10i16	Mfish	0.03444	0.0223	0.002158	0.03122	0.0853	0.0119	0.0566
F10i16	Olive	0.2738	0.1807	0.01462	0.246	0.6836	0.0855	0.4678
F10i28	C3cereals	0.3306	0.1082	0.132	0.3257	0.555	0.2234	0.441
F10i28	TAnimals	0.3517	0.1324	0.1347	0.3386	0.6439	0.2149	0.4871
F10i28	Mfish	0.04228	0.02265	0.004919	0.0398	0.09177	0.0196	0.0653
F10i28	Olive	0.2753	0.1635	0.01682	0.2651	0.6085	0.0955	0.4495
F12i3	C3cereals	0.202	0.1313	0.01128	0.1837	0.4975	0.063	0.339
F12i3	TAnimals	0.5048	0.1564	0.2161	0.5042	0.8065	0.3427	0.668
F12i3	Mfish	0.08763	0.0401	0.0216	0.08392	0.1756	0.0481	0.1275
F12i3	Olive	0.2056	0.147	0.008489	0.1794	0.5346	0.0558	0.3592
F12i28	C3cereals	0.2842	0.1213	0.07262	0.2739	0.5374	0.1609	0.4091
F12i28	TAnimals	0.3308	0.1447	0.1143	0.3109	0.6694	0.1863	0.4767
F12i28	Mfish	0.06099	0.02991	0.01239	0.05752	0.1293	0.0322	0.0899
F12i28	Olive	0.3241	0.179	0.0264	0.3098	0.6913	0.1323	0.52
F7i7	C3cereals	0.4888	0.1227	0.2472	0.4888	0.7237	0.3663	0.6153
F7i7	TAnimals	0.1796	0.0829	0.04354	0.1713	0.3634	0.0977	0.2614
F7i7	Mfish	0.05259	0.02317	0.01322	0.05037	0.1053	0.0305	0.0754
F7i7	Olive	0.279	0.1619	0.02247	0.2688	0.6265	0.1076	0.4448
F7i10	C3cereals	0.3969	0.1239	0.171	0.3942	0.6567	0.2697	0.5207
F7i10	TAnimals	0.1558	0.08187	0.03088	0.1418	0.348	0.0772	0.2378
F7i10	Mfish	0.07828	0.03036	0.02717	0.07497	0.1444	0.0486	0.1087
F7i10	Olive	0.369	0.1803	0.04739	0.3618	0.7312	0.1779	0.5587
F8i7	C3cereals	0.4157	0.1404	0.1534	0.411	0.6926	0.2741	0.5614
F8i7	TAnimals	0.1729	0.1027	0.02794	0.1543	0.423	0.0761	0.2702
F8i7	Mfish	0.1161	0.04292	0.0494	0.1105	0.2108	0.0738	0.1593
F8i7	Olive	0.2952	0.1621	0.02417	0.2859	0.628	0.1197	0.4689
F8i23	C3cereals	0.328	0.1126	0.1261	0.3235	0.5592	0.213	0.4408
F8i23	TAnimals	0.2707	0.111	0.09058	0.2609	0.5112	0.1558	0.3828
F8i23	Mfish	0.08291	0.03043	0.03128	0.08066	0.1514	0.0522	0.1126
F8i23	Olive	0.3184	0.1809	0.02335	0.3032	0.6954	0.1295	0.5099
F9i9	C3cereals	0.4638	0.1114	0.2422	0.466	0.6765	0.3499	0.5761
F9i9	TAnimals	0.1777	0.07737	0.04757	0.1718	0.3487	0.1005	0.2512
F9i9	Mfish	0.1119	0.03104	0.0557	0.1106	0.1771	0.0807	0.1429
F9i9	Olive	0.2466	0.1509	0.01759	0.2287	0.5837	0.0892	0.4039

F9i13	C3cereals	0.4253	0.09977	0.2253	0.4265	0.6204	0.3293	0.5254
F9i13	TAnimals	0.2479	0.08142	0.1093	0.2448	0.4193	0.1612	0.3291
F9i13	Mfish	0.09538	0.02899	0.04432	0.0942	0.1543	0.0651	0.1249
F9i13	Olive	0.2314	0.1482	0.01402	0.2104	0.5684	0.0781	0.3846
F10i14	C3cereals	0.1905	0.1275	0.01119	0.1687	0.4793	0.0605	0.326
F10i14	TAnimals	0.4053	0.1595	0.1272	0.4	0.7267	0.2351	0.5707
F10i14	Mfish	0.1008	0.04067	0.03211	0.09806	0.1916	0.0599	0.141
F10i14	Olive	0.3034	0.1802	0.02027	0.2873	0.6931	0.1138	0.4897
F10i17	C3cereals	0.4423	0.1073	0.2311	0.4428	0.654	0.3351	0.5502
F10i17	TAnimals	0.224	0.08864	0.0687	0.2185	0.4145	0.1364	0.3133
F10i17	Mfish	0.1231	0.03486	0.05933	0.1211	0.1966	0.0886	0.1574
F10i17	Olive	0.2106	0.1442	0.01057	0.1899	0.5451	0.0615	0.3526
F10i20	C3cereals	0.3045	0.08543	0.1557	0.2964	0.4975	0.2211	0.3908
F10i20	TAnimals	0.2838	0.1018	0.1165	0.2739	0.5207	0.1824	0.38
F10i20	Mfish	0.07793	0.029	0.02913	0.07431	0.143	0.0498	0.1067
F10i20	Olive	0.3337	0.1471	0.03827	0.3413	0.6037	0.1775	0.4819
F10i22	C3cereals	0.2734	0.1348	0.03183	0.2714	0.5535	0.1299	0.4128
F10i22	TAnimals	0.4038	0.1462	0.1425	0.3959	0.6945	0.2539	0.5579
F10i22	Mfish	0.09341	0.03745	0.03372	0.08892	0.1806	0.0564	0.1295
F10i22	Olive	0.2294	0.1603	0.01132	0.2002	0.6141	0.0675	0.3951
F12i23	C3cereals	0.4006	0.137	0.1452	0.3971	0.6732	0.2642	0.5412
F12i23	TAnimals	0.2234	0.1125	0.04677	0.2086	0.4894	0.1137	0.33
F12i23	Mfish	0.1102	0.03762	0.04599	0.1066	0.1928	0.0729	0.1483
F12i23	Olive	0.2657	0.162	0.01656	0.2498	0.6161	0.0934	0.4376
AVG	C3cereals	0.3666	0.1099	0.1664	0.3612	0.5802	0.256	0.4788
AVG	TAnimals	0.2628	0.09429	0.095	0.2584	0.4561	0.1673	0.357
AVG	Mfish	0.07791	0.02715	0.02943	0.07609	0.1335	0.0509	0.1069
AVG	Olive	0.2927	0.1654	0.02713	0.279	0.6339	0.1186	0.4627

Table E.5 Input parameters and the generated estimates of *Model 2* with olive oil included.

Model 1 **with legumes - FRUITS INPUTS**

Proxies

d15NPhe
d13CPhe
d15NLys
d13CVal
d13CLeu
d13CIle

Target values

ID	d15Nphe	Unc	d13Cphe	Unc	d15Nlys	Unc	d13Cval	Unc	d13Cleu	Unc	d13Cile	Unc
F8i6	9.6	0.8	-28.7	0.9	1.5	1.1	-25.7	0.4	-28.8	0.4	-21.9	0.7
F10i11	9.2	1.1	-26.8	1.4	1.6	1.2	-27	0.8	-29.6	0.9	-22.4	1
F10i16	10.7	0.5	-31.4	0.9	3.3	0.8	-25.6	0.5	-29.6	0.6	-23.8	0.5
F10i28	10.6	0.4	-29.5	1.2	3.3	0.7	-25.7	0.6	-30	0.6	-23.5	0.5
F12i3	10.2	1.4	-30.4	0.9	2.4	1.2	-25.1	0.5	-29.1	0.6	-23.1	0.3
F12i28	9.7	0.7	-27.7	0.7	2.6	0.7	-27.6	0.5	-29.7	0.8	-23	0.6
F7i7	11.7	0.2	-26.6	1.2	3.1	0.5	-26.1	0.8	-29.7	0.7	-22.6	0.9
F7i10	10.7	0.4	-27.5	0.7	3.7	0.5	-25.1	0.5	-28.6	0.8	-21.5	0.6
F8i7	11.2	1.2	-27.1	0.8	2.7	1.2	-24.3	0.7	-27.6	0.5	-21.2	0.6
F8i23	9.8	0.2	-26.9	0.8	1.7	0.6	-26	0.5	-29.2	0.6	-22	0.7
F9i9	10.5	0.2	-28.3	0.6	4.7	0.5	-24.6	0.6	-27.2	0.5	-22.2	0.5
F9i13	10.8	0.1	-29.7	0.7	3.4	0.6	-24.9	0.6	-26.9	0.4	-22.1	0.4
F10i14	9.5	1.1	-29.4	1.3	2.8	0.5	-24.9	0.4	-28.9	0.5	-22	0.6
F10i17	10.8	0.4	-29.8	0.6	3.7	0.8	-23.1	0.6	-26.1	0.5	-22.3	0.7
F10i20	10	0.1	-28.1	1	2.2	0.2	-25.1	0.2	-28.2	0.3	-22.8	0.6
F10i22	11.6	1.1	-30.1	0.4	3.7	1.2	-23.8	0.2	-28	0.2	-23.5	0.7
F12i23	11.1	0.9	-29.4	0.9	4.1	0.4	-23.7	0.4	-28	0.6	-21.1	0.5
AVG	10.5	0.4	-28.7	0.5	3	0.4	-25.2	0.3	-28.5	0.3	-22.4	0.3

Sources

C3cereals
Legumes
TAnimals
MFish

Source fractions

Phe
Lys
Val
Leu
Ile

Offset/Weights

	Offset	Unc	Phe	Unc	Lys	Unc	Val	Unc	Leu	Unc	Ile	Unc
15NPhe	0.1	0.2	100	0	0	0	0	0	0	0	0	0
13CPhe	0	0.4	100	0	0	0	0	0	0	0	0	0
15NLys	0.8	0.4	0	0	100	0	0	0	0	0	0	0
13CVal	-0.1	1.1	0	0	0	0	100	0	0	0	0	0
13CLeu	-0.3	0.8	0	0	0	0	0	0	100	0	0	0

13CIle	-0.7	1.5	0	0	0	0	0	0	0	0	100	0

Source values

	d15Nphe	**Unc**	**d13Cphe**	**Unc**	**d15Nlys**	**Unc**	**d13Cval**	**Unc**	**d13Cleu**	**Unc**	**d13Cile**	Unc.
C3cereals Phe	16.4	1.5	-26.2	1								
C3cereals Lys					4.7	1.5						
C3cereals Val							-28.6	1				
C3cereals Leu									-30.7	1		
C3cereals Ile											-25.2	1
Legumes Phe	3.6	4.5	-27.2	2.5								
Legumes Lys					0.9	2.1						
Legumes Val							-28.9	3.1				
Legumes Leu									-32.5	2.8		
Legumes Ile											-26.8	2.5
Tanimals Phe	9	0.3	-31.3	0.6								
Tanimals Lys					1.9	0.4						
Tanimals Val							-27.8	0.5				
Tanimals Leu									-30.2	0.5		
Tanimals Ile											-25.4	0.5
MFish Phe	4.9	0.6	-25	0.8								
MFish Lys					3.1	0.6						
MFish Val							-20.6	0.7				
MFish Leu									-21.7	0.5		
MFish Ile											-16.9	0.5

Concentrations

	Phe	**Unc**	**Lys**	**Unc**	**Val**	**Unc**	**Leu**	**Unc**	**Ile**	**Unc**
C3cereals	5.3	0.5	3.2	0.5	4.7	0.6	7.1	0.7	3.7	0.4
Legumes	1.5	0.1	2.1	0.1	1.4	0.1	2.4	0.3	1.4	0.2
Tanimals	4.1	0.2	9	0.4	5.1	0.2	8.2	0.4	4.9	0.2
MFish	4	0.2	9.2	0.5	5.2	0.3	8.3	0.4	4.8	0.2

***Model 1* with legumes - FRUITS ESTIMATES**

Target/Consumer	**Source/Food**	**Mean**	**sd**	**2.5pc**	**median**	**97.5pc**	**16pc**	**84pc**
F8i6	C3Cereals	0.1981	0.1058	0.02205	0.1911	0.4267	0.0886	0.2998
F8i6	Legumes	0.1314	0.1104	0.005264	0.1034	0.4162	0.0307	0.2335
F8i6	TAnimals	0.3966	0.1703	0.04283	0.4097	0.7052	0.2109	0.5683
F8i6	Mfish	0.2739	0.08021	0.1174	0.2733	0.4325	0.1938	0.3525
F10i11	C3Cereals	0.2539	0.1327	0.02844	0.2467	0.53	0.1151	0.3933
F10i11	Legumes	0.2151	0.1279	0.01935	0.1979	0.5136	0.0872	0.3409
F10i11	TAnimals	0.292	0.1807	0.01679	0.2761	0.6749	0.0964	0.4854
F10i11	Mfish	0.239	0.09796	0.04967	0.2388	0.4277	0.1372	0.3387
F10i16	C3Cereals	0.2013	0.09319	0.03563	0.1948	0.4079	0.1091	0.2906
F10i16	Legumes	0.1095	0.1297	0.001703	0.05748	0.4826	0.0127	0.2195
F10i16	TAnimals	0.564	0.1805	0.109	0.5938	0.8401	0.3914	0.7325
F10i16	Mfish	0.1252	0.07188	0.009408	0.1204	0.2782	0.0497	0.1973
F10i28	C3Cereals	0.2823	0.105	0.08966	0.275	0.5045	0.1808	0.3884
F10i28	Legumes	0.1129	0.1019	0.003713	0.08494	0.3865	0.0243	0.1984
F10i28	TAnimals	0.4345	0.1722	0.06947	0.4474	0.735	0.2574	0.6092
F10i28	Mfish	0.1703	0.08015	0.0263	0.1676	0.3343	0.0874	0.252
F12i3	C3Cereals	0.1481	0.1029	0.006766	0.1336	0.3887	0.0422	0.2494
F12i3	Legumes	0.1164	0.1164	0.002788	0.08012	0.441	0.0196	0.2154
F12i3	TAnimals	0.5238	0.1723	0.1177	0.5438	0.8031	0.3505	0.6933
F12i3	Mfish	0.2116	0.08312	0.05138	0.2111	0.3754	0.1264	0.2962

F12i28	C3Cereals	0.2709	0.1187	0.05036	0.2648	0.5237	0.1541	0.3867
F12i28	Legumes	0.1756	0.1128	0.01251	0.1579	0.4403	0.0638	0.2867
F12i28	TAnimals	0.3565	0.1686	0.04027	0.3636	0.6724	0.1698	0.5279
F12i28	Mfish	0.1969	0.08318	0.03632	0.1944	0.3628	0.1126	0.2815
F7i7	C3Cereals	0.456	0.09528	0.2735	0.4568	0.6466	0.3599	0.5505
F7i7	Legumes	0.1128	0.08801	0.004506	0.0924	0.3253	0.0282	0.1987
F7i7	TAnimals	0.2253	0.1379	0.01136	0.2133	0.5137	0.0737	0.3727
F7i7	Mfish	0.2058	0.08284	0.04195	0.2053	0.3651	0.1225	0.2905
F7i10	C3Cereals	0.3584	0.08791	0.1923	0.3576	0.5308	0.2702	0.4476
F7i10	Legumes	0.09579	0.07954	0.003551	0.07573	0.2968	0.0233	0.1708
F7i10	TAnimals	0.2149	0.1258	0.01539	0.2018	0.4815	0.0803	0.3471
F7i10	Mfish	0.331	0.07894	0.1717	0.3314	0.4859	0.2535	0.4089
F8i7	C3Cereals	0.3288	0.1154	0.09222	0.3308	0.5501	0.2136	0.4426
F8i7	Legumes	0.09671	0.08756	0.0029	0.0722	0.3319	0.0202	0.1706
F8i7	TAnimals	0.1801	0.1168	0.008487	0.1681	0.4271	0.0539	0.3032
F8i7	Mfish	0.3944	0.07882	0.2371	0.3959	0.5432	0.3168	0.473
F8i23	C3Cereals	0.2804	0.1123	0.04592	0.2786	0.5016	0.1736	0.3938
F8i23	Legumes	0.2269	0.1258	0.02621	0.2116	0.5078	0.1005	0.3518
F8i23	TAnimals	0.222	0.1376	0.01497	0.2054	0.5203	0.0745	0.3669
F8i23	Mfish	0.2707	0.09045	0.08007	0.2743	0.4407	0.1814	0.3602
F9i9	C3Cereals	0.328	0.08981	0.1714	0.3221	0.5229	0.2456	0.4138
F9i9	Legumes	0.07445	0.07571	0.001813	0.04861	0.2893	0.0125	0.1394
F9i9	TAnimals	0.2289	0.1229	0.01474	0.2322	0.4643	0.0893	0.3577
F9i9	Mfish	0.3687	0.07419	0.2227	0.369	0.5187	0.2958	0.44
F9i13	C3Cereals	0.3014	0.08714	0.08795	0.3001	0.4617	0.2268	0.3885
F9i13	Legumes	0.08449	0.1019	0.001388	0.04538	0.3831	0.0096	0.1684
F9i13	TAnimals	0.2987	0.1426	0.01727	0.3084	0.5608	0.1409	0.4424
F9i13	Mfish	0.3154	0.07858	0.1688	0.3124	0.4815	0.238	0.3936
F10i14	C3Cereals	0.1779	0.1083	0.01249	0.1667	0.4179	0.0652	0.2883
F10i14	Legumes	0.134	0.1085	0.005614	0.1077	0.4079	0.0319	0.2362
F10i14	TAnimals	0.3906	0.1756	0.05107	0.3995	0.7037	0.1959	0.5733
F10i14	Mfish	0.2976	0.08626	0.1262	0.2987	0.4625	0.2099	0.3846
F10i17	C3Cereals	0.2448	0.1089	0.02394	0.2531	0.4484	0.124	0.3485
F10i17	Legumes	0.1452	0.1579	0.001855	0.07066	0.5174	0.0124	0.3366
F10i17	TAnimals	0.237	0.1414	0.01186	0.2357	0.5123	0.0757	0.3881
F10i17	Mfish	0.3729	0.08087	0.2098	0.3745	0.5281	0.2922	0.4536
F10i20	C3Cereals	0.2723	0.1048	0.04361	0.2704	0.4862	0.1736	0.3782
F10i20	Legumes	0.1562	0.1106	0.006316	0.137	0.4102	0.0435	0.2692
F10i20	TAnimals	0.2764	0.1714	0.0139	0.2688	0.6036	0.0815	0.4707
F10i20	Mfish	0.2951	0.07653	0.1475	0.2945	0.4462	0.2173	0.3734
F10i22	C3Cereals	0.1597	0.1031	0.009985	0.1482	0.4018	0.0533	0.262
F10i22	Legumes	0.1804	0.1883	0.002177	0.09159	0.6148	0.0136	0.404
F10i22	TAnimals	0.4234	0.2112	0.02607	0.4708	0.7453	0.1517	0.6362
F10i22	Mfish	0.2365	0.08286	0.06521	0.234	0.4074	0.1586	0.3178
F12i23	C3Cereals	0.2997	0.1093	0.07729	0.2985	0.5172	0.1925	0.408
F12i23	Legumes	0.07941	0.09101	0.001878	0.04802	0.3537	0.0119	0.1433
F12i23	TAnimals	0.2574	0.1353	0.01843	0.2554	0.5287	0.1098	0.396
F12i23	Mfish	0.3635	0.08076	0.2034	0.3638	0.5191	0.2826	0.4436
AVG	C3Cereals	0.2681	0.0829	0.1219	0.2612	0.4406	0.1881	0.3511
AVG	Legumes	0.09775	0.0913	0.002647	0.07071	0.3426	0.0181	0.1763
AVG	TAnimals	0.3695	0.1378	0.07614	0.3855	0.6125	0.2246	0.504
AVG	Mfish	0.2646	0.07022	0.1265	0.2648	0.4016	0.1961	0.3326

Table E.6 *Model 1* input parameters and the generated estimates with legumes included.

Model 2 **with legumes - FRUITS INPUTS**

Proxies

15NPhe
13CPhe
15NLys
13CVal
13CLeu
13CIle
15NGlu
13CGlu
13CAsp
13CAla

Target values

ID	d15Nphe	Unc	d13Cphe	Unc	d15Nlys	Unc	d13Cval	Unc	d13Cleu	Unc	d13Cile	Unc	d15Nglu	Unc	d13Cglu	Unc	d13Casp	Unc	d13Cala	Unc
F8i6	9.6	0.8	-28.7	0.9	1.5	1.1	-25.7	0.4	-28.8	0.4	-21.9	0.7	12.7	0.5	-18.7	1	-20.5	1	-19.3	0.7
F10i11	9.2	1.1	-26.8	1.4	1.6	1.2	-27	0.8	-29.6	0.9	-22.4	1	12.5	0.4	-19.2	0.9	-20.2	1.3	-21.5	0.6
F10i16	10.7	0.5	-31.4	0.9	3.3	0.8	-25.6	0.5	-29.6	0.6	-23.8	0.5	14.7	0.2	-19.7	1	-21.1	0.7	-21.1	0.7
F10i28	10.6	0.4	-29.5	1.2	3.3	0.7	-25.7	0.6	-30	0.6	-23.5	0.5	13.5	0.2	-19.2	0.9	-21.3	1	-20.3	0.6
F12i3	10.2	1.4	-30.4	0.9	2.4	1.2	-25.1	0.5	-29.1	0.6	-23.1	0.3	14.1	0.4	-18.6	1.1	-19.8	0.8	-20.3	0.6
F12i28	9.7	0.7	-27.7	0.7	2.6	0.7	-27.6	0.5	-29.7	0.8	-23	0.6	14.6	0.1	-19.8	0.7	-21.3	1.1	-20.4	1.1
F7i7	11.7	0.2	-26.6	1.2	3.1	0.5	-26.1	0.8	-29.7	0.7	-22.6	0.9	14.4	0.1	-19.2	1	-21	1.3	-21.9	2.1
F7i10	10.7	0.4	-27.5	0.7	3.7	0.5	-25.1	0.5	-28.6	0.8	-21.5	0.6	15	0.2	-20.3	0.7	-20.9	0.9	-19.7	1
F8i7	11.2	1.2	-27.1	0.8	2.7	1.2	-24.3	0.7	-27.6	0.5	-21.2	0.6	15.3	0.3	-18.6	1	-20.2	1.1	-19.8	0.8
F8i23	9.8	0.2	-26.9	0.8	1.7	0.6	-26	0.5	-29.2	0.6	-22	0.7	12.8	0.7	-19	0.9	-21	1.1	-22.5	2
F9i9	10.5	0.2	-28.3	0.6	4.7	0.5	-24.6	0.6	-27.2	0.5	-22.2	0.5	16.4	0.5	-18	0.7	-19.6	0.7	-20.8	0.5
F9i13	10.8	0.1	-29.7	0.7	3.4	0.6	-24.9	0.6	-26.9	0.4	-22.1	0.4	15.6	0.3	-18.6	0.7	-19.6	0.7	-20.8	0.4
F10i14	9.5	1.1	-29.4	1.3	2.8	0.5	-24.9	0.4	-28.9	0.5	-22	0.6	14.9	0.8	-19.1	0.9	-20.9	1	-20.2	0.9
F10i17	10.8	0.4	-29.8	0.6	3.7	0.8	-23.1	0.6	-26.1	0.5	-22.3	0.7	15.1	0.2	-17.6	1	-19	0.9	-19.7	0.9
F10i20	10	0.1	-28.1	1	2.2	0.2	-25.1	0.2	-28.2	0.3	-22.8	0.6	13.1	0.5	-19.2	0.5	-21.4	0.5	-18.5	0.3
F10i22	11.6	1.1	-30.1	0.4	3.7	1.2	-23.8	0.2	-28	0.2	-23.5	0.7	14.9	0.3	-18.3	0.6	-19.5	0.6	-18.5	0.4
F12i23	11.1	0.9	-29.4	0.9	4.1	0.4	-23.7	0.4	-28	0.6	-21.1	0.5	14.8	0.5	-18.5	1.3	-19.8	1	-19.8	0.6
AVG	10.5	0.4	-28.7	0.5	3	0.4	-25.2	0.3	-28.5	0.3	-22.4	0.3	14.4	0.2	-18.9	0.4	-20.4	0.5	-20.3	0.5

Sources

cerealsC3

Legumes
TAnimals
Mfish

Source fractions

Phe
Lys
Val
Leu
Ile
WholeN
WholeC
CarbC

Offset/Weights

	Offset	Unc	Phe	Unc	Lys	Unc	Val	Unc	Leu	Unc	Ile	Unc	WholeN	Unc	WholeC	Unc	CarbC	Unc
15NPhe	0.1	0.2	100	0	0	0	0	0	0	0	0	0	0	0	0	0	0	0
13CPhe	0	0.4	100	0	0	0	0	0	0	0	0	0	0	0	0	0	0	0
15NLys	0.8	0.4	0	0	100	0	0	0	0	0	0	0	0	0	0	0	0	0
13CVal	-0.1	1.1	0	0	0	0	100	0	0	0	0	0	0	0	0	0	0	0
13CLeu	-0.3	0.8	0	0	0	0	0	0	100	0	0	0	0	0	0	0	0	0
13CIle	-0.7	1.5	0	0	0	0	0	0	0	0	100	0	0	0	0	0	0	0
15NGlu	9.7	2.5	0	0	0	0	0	0	0	0	0	0	100	0	0	0	0	0
13CGlu	8.7	3	0	0	0	0	0	0	0	0	0	0	0	0	100	0	0	0
13CAsp	4.7	1.5	0	0	0	0	0	0	0	0	0	0	0	0	100	0	0	0
13CAla	4	1.5	0	0	0	0	0	0	0	0	0	0	0	0	0	0	100	0

Source values

	d15Nphe	Unc	d13Cphe	Unc	d15Nlys	Unc	d13Cval	Unc	d13Cleu	Unc	d13Cile	Unc	d15Nglu	Unc	d13Cglu	Unc	d13Casp	Unc	d13Cala	Unc
C3cereals Phe	16.4	1.5	-26.2	1																
C3cereals Lys					4.7	1.5														
C3cereals Val							-28.6	1												
C3cereals Leu									-30.7	1										
C3cereals Ile											-25.2	1								

C3cereals WholeN											5.5	1.5						
C3cereals WholeC													-23.3	0.3	-23.3	0.3		
C3cereals CarbC																	-22.8	1
Legumes Phe	3.6	4.5	-27.2	2.5														
Legumes Lys					0.9	2.1												
Legumes Val							-28.9	3.1										
Legumes Leu									-32.5	2.8								
Legumes Ile											-26.8	2.5						
Legumes WholeN													0.3	1				
Legumes WholeC															-23	2.5	-23	2.5
Legumes CarbC																	-22.9	2.5
Tanimals Phe	9	0.3	-31.3	0.6														
Tanimals Lys					1.9	0.4												
Tanimals Val							-27.8	0.5										
Tanimals Leu									-30.2	0.5								
Tanimals Ile											-25.4	0.5						
Tanimals WholeN													5.2	0.5				
Tanimals WholeC															-25.9	0.5	-25.9	0.5
Tanimals CarbC																	0	0
MFish Phe	4.9	0.6	-25	0.8														
MFish Lys					3.1	0.6												
MFish Val							-20.6	0.7										
MFish Leu									-21.7	0.5								
MFish Ile											-16.9	0.5						
MFish WholeN													11	1				
MFish WholeC															-14	1	-14	1

MFish
CarbC

0 0

Concentrations

	Phe	**Unc**	**Lys**	**Unc**	**Val**	**Unc**	**Leu**	**Unc**	**Ile**	**Unc**	**WholeN**	**Unc**	**WholeC**	**Unc**	CarbC	Unc.
cerealsC3	0.8	0.1	0.5	0.1	0.7	0.1	1.1	0.3	0.6	0.2	15.4	0.4	100	0	84.6	1.2
Legumes	1.5	0.1	2.1	0.1	1.4	0.1	2.4	0.3	1.4	0.2	44.6	0.9	100	0	68.7	0.5
TAnimals	2	0.1	4.4	0.2	2.5	0.1	4	0.2	2.4	0.1	44.6	0.9	100	0	0	0
Mfish	3.2	0.2	7.2	0.4	4.1	0.2	6.5	0.3	3.7	0.2	79.4	1	100	0	0	0

***Model 2* with legumes - FRUITS ESTIMATES**

Target	**Source**	**Mean**	**sd**	**2.5pc**	**median**	**97.5pc**	**16pc**	**84pc**
F8i6	C3cereals	0.3131	0.1561	0.02924	0.3183	0.6184	0.1385	0.4724
F8i6	Legumes	0.1374	0.1192	0.004227	0.1052	0.4413	0.0282	0.2514
F8i6	TAnimals	0.4359	0.1757	0.09306	0.4298	0.7734	0.2609	0.6182
F8i6	Mfish	0.1137	0.04115	0.03873	0.1114	0.2	0.0728	0.1541
F10i11	C3cereals	0.308	0.1776	0.01868	0.2982	0.6543	0.108	0.5053
F10i11	Legumes	0.2586	0.1565	0.01833	0.2368	0.6149	0.0987	0.4216
F10i11	TAnimals	0.3421	0.1891	0.03368	0.318	0.7338	0.1465	0.5489
F10i11	Mfish	0.09136	0.04489	0.01438	0.08766	0.19	0.0464	0.1351
F10i16	C3cereals	0.3299	0.1472	0.0404	0.3369	0.6131	0.1735	0.4745
F10i16	Legumes	0.09916	0.1083	0.002543	0.06344	0.4238	0.0145	0.1834
F10i16	TAnimals	0.5275	0.1524	0.1988	0.5379	0.8192	0.3732	0.6738
F10i16	Mfish	0.04343	0.02887	0.002495	0.03931	0.1124	0.0143	0.0713
F10i28	C3cereals	0.4238	0.1529	0.08433	0.4363	0.687	0.2711	0.5775
F10i28	Legumes	0.1158	0.1192	0.002669	0.0744	0.4593	0.0198	0.2288
F10i28	TAnimals	0.4071	0.1522	0.08448	0.408	0.7149	0.2625	0.5541
F10i28	Mfish	0.05323	0.02904	0.005211	0.05106	0.1151	0.0231	0.0825
F12i3	C3cereals	0.2268	0.1426	0.01113	0.209	0.5365	0.0763	0.3765
F12i3	Legumes	0.1034	0.09042	0.003322	0.07899	0.337	0.0207	0.1906
F12i3	TAnimals	0.5672	0.1552	0.2467	0.5803	0.8331	0.4011	0.7246
F12i3	Mfish	0.1026	0.04317	0.02488	0.09996	0.1931	0.0597	0.1461
F12i28	C3cereals	0.3587	0.1628	0.03526	0.3752	0.6502	0.1792	0.5214
F12i28	Legumes	0.1825	0.1182	0.01144	0.1683	0.4541	0.0574	0.3069
F12i28	TAnimals	0.3861	0.1646	0.09066	0.3713	0.7186	0.2171	0.5642
F12i28	Mfish	0.0727	0.03634	0.01073	0.06972	0.1522	0.0366	0.109
F7i7	C3cereals	0.6584	0.09044	0.4494	0.6679	0.8141	0.5721	0.7419

F7i7	Legumes	0.1007	0.07698	0.00398	0.07923	0.2875	0.0233	0.1816
F7i7	TAnimals	0.1789	0.08784	0.02031	0.1783	0.3663	0.0871	0.2644
F7i7	Mfish	0.06207	0.02694	0.01301	0.06078	0.1212	0.0354	0.088
F7i10	C3cereals	0.5854	0.1109	0.3314	0.5969	0.7663	0.4848	0.6905
F7i10	Legumes	0.09322	0.08552	0.003203	0.06883	0.3316	0.0203	0.1643
F7i10	TAnimals	0.213	0.0991	0.0327	0.2134	0.4149	0.109	0.3113
F7i10	Mfish	0.1084	0.03307	0.04894	0.1072	0.1781	0.0763	0.14
F8i7	C3cereals	0.5386	0.1688	0.1143	0.5665	0.7921	0.3789	0.6977
F8i7	Legumes	0.1172	0.1091	0.003639	0.08789	0.4302	0.023	0.2087
F8i7	TAnimals	0.1911	0.1192	0.01869	0.175	0.481	0.0729	0.3017
F8i7	Mfish	0.1531	0.04767	0.07376	0.1477	0.2641	0.1067	0.1985
F8i23	C3cereals	0.3998	0.1609	0.04809	0.4229	0.6726	0.2281	0.5529
F8i23	Legumes	0.2471	0.1595	0.01333	0.2186	0.5987	0.0886	0.4201
F8i23	TAnimals	0.2566	0.1378	0.02876	0.2435	0.5593	0.1198	0.3973
F8i23	Mfish	0.09645	0.04017	0.02432	0.09332	0.1834	0.0571	0.1358
F9i9	C3cereals	0.5847	0.1078	0.3478	0.589	0.7761	0.4932	0.6874
F9i9	Legumes	0.07957	0.09015	0.001632	0.04841	0.3525	0.0123	0.1408
F9i9	TAnimals	0.1995	0.09866	0.01931	0.2011	0.3879	0.0885	0.3012
F9i9	Mfish	0.1363	0.03133	0.07593	0.1355	0.2	0.1054	0.1676
F9i13	C3cereals	0.5538	0.09132	0.347	0.5545	0.7282	0.4761	0.6417
F9i13	Legumes	0.05951	0.0736	0.001402	0.03502	0.2881	0.0092	0.1036
F9i13	TAnimals	0.2734	0.08881	0.08902	0.2752	0.4343	0.1832	0.3645
F9i13	Mfish	0.1133	0.03051	0.05847	0.1121	0.1778	0.0828	0.1429
F10i14	C3cereals	0.25	0.1523	0.0197	0.2333	0.5822	0.0897	0.4146
F10i14	Legumes	0.1113	0.09488	0.003774	0.08718	0.3543	0.0242	0.2014
F10i14	TAnimals	0.5106	0.1641	0.1739	0.5193	0.8001	0.3397	0.6787
F10i14	Mfish	0.1281	0.04581	0.04681	0.126	0.2228	0.082	0.1741
F10i17	C3cereals	0.4605	0.1776	0.04059	0.4993	0.7112	0.2762	0.6264
F10i17	Legumes	0.1762	0.2013	0.00201	0.08147	0.6944	0.0139	0.4099
F10i17	TAnimals	0.2119	0.1146	0.01458	0.208	0.4527	0.0899	0.3283
F10i17	Mfish	0.1514	0.04046	0.07978	0.1482	0.239	0.1129	0.191
F10i20	C3cereals	0.4438	0.1309	0.1424	0.4445	0.6938	0.3224	0.5723
F10i20	Legumes	0.1339	0.1157	0.004121	0.103	0.4364	0.0281	0.2507
F10i20	TAnimals	0.3216	0.1379	0.03678	0.331	0.5674	0.1812	0.4604
F10i20	Mfish	0.1007	0.03327	0.04019	0.09953	0.1698	0.0677	0.1322
F10i22	C3cereals	0.3164	0.1533	0.0403	0.3086	0.6089	0.1546	0.4763
F10i22	Legumes	0.08226	0.0995	0.001777	0.04549	0.3495	0.0111	0.1611
F10i22	TAnimals	0.4872	0.1528	0.1511	0.4884	0.7849	0.3403	0.6396

F10i22	Mfish	0.1141	0.04197	0.04014	0.1108	0.2059	0.0737	0.1539
F12i23	C3cereals	0.5114	0.1593	0.1389	0.5293	0.7757	0.3563	0.6674
F12i23	Legumes	0.08146	0.09206	0.0019	0.05127	0.3725	0.0127	0.1444
F12i23	TAnimals	0.2658	0.1365	0.03258	0.2506	0.5728	0.1303	0.3974
F12i23	Mfish	0.1413	0.04177	0.07073	0.1374	0.232	0.0999	0.1832
AVG	C3cereals	0.4428	0.1326	0.1342	0.4582	0.6615	0.3158	0.5684
AVG	Legumes	0.1027	0.1125	0.001661	0.06254	0.4188	0.015	0.2002
AVG	TAnimals	0.3561	0.1157	0.1275	0.3567	0.5788	0.2437	0.4718
AVG	Mfish	0.09845	0.03286	0.03691	0.09713	0.1651	0.0662	0.131

Table E.7 Input parameters and the generated estimates of *Model 2* with legumes included.

Appendix F

Principal Component Analysis

This appendix contains the outputs of the Principal Component Analysis (PCA) presented in chapter 7.

Importance of components

	PC1	PC2	PC3	PC4	PC5	PC6
Eingenvalue	3.5884	1.7093	0.4914	0.1042	0.0769	0.0299
Cumulative Proportion	0.5981	0.8830	0.9648	0.9822	0.9950	1.0000

Coordinates of the variables

	PC1	PC2	PC3	PC4	PC5	PC6
d13Cval	-0.97	0.03	-0.10	0.19	-0.07	-0.09
d13Cleu	-0.97	-0.03	-0.17	-0.02	-0.13	0.12
d13Cile	-0.97	0.05	-0.01	0.02	0.23	0.03
d13Cphe	-0.60	0.57	0.55	-0.08	-0.04	-0.02
d15Nlys	-0.07	0.91	-0.38	-0.13	0.01	-0.04
d15Nphe	0.64	0.74	0.04	0.21	0.01	0.07

Samples scores

	PC1	PC2	PC3	PC4	PC5	PC6
ABF3	-4.05	0.58	0.64	-0.39	0.43	-0.14
HSLA	-4.40	0.73	0.02	-0.58	-0.04	-0.34
HSSP1	-3.56	-1.20	0.45	-0.30	-0.45	0.09
HSSP2	-2.65	-1.30	0.35	-0.63	0.02	0.06
SSF2	-3.37	0.62	-1.00	0.14	-0.23	0.58
SSF5	-5.27	1.60	0.08	0.03	-0.41	-0.24
PSSC2	-2.29	-1.36	0.05	0.23	0.37	0.34
PSSP1	-2.01	-0.48	-0.70	-0.36	0.00	0.16
HSSSQ	-4.29	0.48	0.13	0.13	-0.03	-0.03
EF8BOS?	1.93	-1.72	-0.40	-0.34	-0.51	0.08
PSC1	0.84	-0.81	-0.20	-0.36	-0.48	0.04
PSC2	0.81	0.19	0.56	-0.15	-0.51	-0.30
VESH1	1.33	-2.13	0.15	0.48	0.15	-0.01
VEDE1	1.98	-1.57	-0.27	0.22	-0.14	-0.19
VEHO1	-0.55	-1.62	0.45	-0.09	0.91	0.04
VEHO3	0.95	-2.06	0.68	0.35	-0.09	-0.03
VEHO4	0.60	-0.80	-0.27	0.31	-0.38	0.05

EF10OC	1.76	-0.74	0.02	-0.27	-0.32	0.21
EF7OC	1.07	-0.83	0.99	-0.09	-0.24	-0.19
EF8SG	2.81	0.30	-0.14	-0.68	-0.30	-0.05
EF11DOG	0.04	0.33	0.53	0.19	-0.21	-0.22
PSCH1	-0.11	-1.17	-1.08	-0.17	-0.08	0.13
PSCH2	0.25	-0.44	-0.53	-0.32	0.19	0.12
PSCH3	-0.92	-0.53	-0.37	0.21	-0.19	0.18
PSP3	1.91	-0.91	-1.54	-0.41	0.03	-0.09
PSP4	1.24	-1.35	-0.88	0.21	0.26	0.10
PSP5	2.59	-0.54	-1.60	-0.76	0.52	-0.17
1703b	1.18	2.62	0.36	0.07	0.03	0.11
1895e	2.31	-0.68	1.45	-0.13	-0.04	0.06
723w	1.50	1.20	0.88	0.02	-0.02	0.12
1703w	1.20	1.19	0.99	0.08	-0.03	0.14
BarleyP	1.59	-0.62	1.67	0.03	-0.07	0.12
LBCFA16F	1.45	3.35	-0.08	0.00	0.05	0.11
LBCFD16E	1.81	3.72	-0.38	-0.09	0.07	0.08
LBTA1012I	1.63	0.88	0.98	-0.01	-0.02	0.11
LBTD1012H&I	1.86	4.09	-0.57	-0.10	0.09	0.08
F10I11	0.10	-0.28	0.88	-0.23	0.27	0.04
F10I14	-0.12	-0.21	-0.24	0.20	0.25	-0.21
F10I16	0.67	-0.21	-0.78	0.31	0.08	-0.19
F10I17	-0.65	0.19	-0.82	0.57	-0.30	0.01
F10i20	-0.16	-0.17	0.20	0.24	-0.08	-0.03
F10I22	0.03	0.21	-0.72	0.61	-0.27	-0.20
F10I28	0.49	0.06	-0.24	0.15	0.09	-0.31
F12I23	-0.48	0.43	-0.68	0.47	0.30	-0.19
F12i28	0.42	-0.06	0.45	-0.38	0.25	0.05
F12I3	0.28	-0.41	-0.34	0.42	0.08	-0.15
F7i10	-0.33	0.50	0.03	0.07	0.27	-0.13
F7I7	0.16	0.58	0.57	0.07	0.19	-0.07
F8I23	-0.13	-0.17	0.76	0.05	0.24	-0.01
F8I6	-0.06	-0.54	0.31	0.25	0.29	0.08
F8I7	-0.64	0.30	0.29	0.45	0.13	0.08
F9I13	-0.26	0.09	-0.57	0.28	-0.01	0.23
F9I9	-0.47	0.67	-0.53	-0.03	-0.07	-0.08

Table F.1 Principal component analysis output using source amino acids (PCA-SAA).

Importance of components

	PC1	PC2	PC3	PC4	PC5	PC6	PC7	PC8	PC9	PC10	PC11	PC12	PC13	PC14	PC15	PC16	PC17	PC18	PC19	PC20	PC21
Eingenvalue	13.2030	3.4786	1.5662	0.7285	0.6493	0.3446	0.2483	0.1944	0.1246	0.1132	0.0932	0.0789	0.0511	0.0341	0.0233	0.0194	0.0152	0.0128	0.0099	0.0070	0.0045
Cumulative Proportion	0.6287	0.7944	0.8689	0.9036	0.9346	0.9510	0.9628	0.9720	0.9780	0.9834	0.9878	0.9916	0.9940	0.9956	0.9967	0.9977	0.9984	0.9990	0.9995	0.9998	1.0000

Coordinates of the variables

	PC1	PC2	PC3	PC4	PC5	PC6	PC7	PC8	PC9	PC10	PC11	PC12	PC13	PC14	PC15	PC16	PC17	PC18	PC19	PC20	PC21
d13Cgly	-0.92	0.15	-0.16	0.03	-0.21	0.03	-0.07	0.16	-0.07	0.11	-0.01	0.10	-0.02	0.02	0.00	0.02	-0.02	0.05	0.03	0.02	0.00
d13Cser	-0.90	-0.01	-0.19	-0.05	-0.18	0.17	-0.24	0.01	0.10	-0.06	-0.12	0.08	-0.03	-0.01	0.01	-0.02	0.03	-0.03	-0.01	-0.01	0.00
d13Cglx	-0.93	0.22	-0.12	0.13	0.15	-0.05	0.08	-0.06	0.10	0.00	0.02	0.01	0.01	0.03	-0.07	0.04	0.04	-0.02	0.05	-0.01	0.00
d13Cala	-0.91	0.00	-0.34	0.05	0.02	0.06	-0.02	0.17	0.01	0.04	0.06	-0.04	0.12	-0.08	0.00	0.03	0.01	-0.01	-0.02	0.00	0.00
d13Casx	-0.88	0.28	-0.19	0.14	0.14	-0.01	-0.06	-0.16	0.15	0.00	0.08	0.03	0.05	0.03	0.02	-0.03	-0.03	0.05	-0.02	-0.01	0.00
d13Cpro	-0.87	0.33	-0.07	0.18	0.12	-0.17	0.04	-0.04	-0.12	0.09	0.07	0.10	-0.04	-0.02	0.04	-0.04	0.02	-0.04	-0.01	0.00	0.00
d13Cval	-0.94	0.08	-0.20	0.12	0.08	0.08	0.00	-0.02	0.04	0.10	-0.07	-0.11	-0.05	0.00	-0.02	-0.02	-0.06	-0.03	0.00	0.03	0.00
d13Cleu	-0.95	0.14	-0.09	0.16	0.01	-0.05	0.05	-0.03	-0.06	0.01	-0.12	-0.10	0.02	0.08	0.04	0.02	0.05	0.02	-0.03	0.00	0.00
d13Cile	-0.94	0.06	-0.24	0.00	0.07	-0.03	-0.06	0.06	-0.11	-0.10	0.04	-0.09	-0.09	-0.02	-0.03	-0.02	-0.01	0.02	0.00	-0.04	-0.01
d13Cthr	-0.17	-0.57	-0.41	-0.53	0.42	-0.11	-0.07	-0.03	-0.03	0.03	-0.04	0.03	0.01	0.01	0.00	0.00	0.01	0.01	0.00	0.01	0.00
d13Cphe	-0.53	-0.31	-0.61	-0.19	-0.35	0.08	0.24	-0.09	-0.01	-0.07	0.07	0.01	-0.02	0.02	0.02	0.01	-0.01	-0.01	0.00	0.00	0.01
d15Ngly	0.15	-0.83	-0.04	0.29	0.28	0.29	0.18	0.08	-0.03	0.00	-0.05	0.07	0.00	0.02	-0.01	-0.02	0.00	0.01	0.00	-0.02	0.00
d15Nglx	-0.90	-0.26	0.33	-0.04	-0.01	0.01	-0.01	0.01	0.01	-0.04	0.02	0.04	0.00	0.03	0.03	0.03	-0.02	-0.02	0.00	0.00	-0.05
d15Nala	-0.89	-0.29	0.24	-0.02	-0.09	0.00	-0.06	-0.03	-0.12	-0.11	0.00	-0.02	0.12	0.03	-0.01	-0.06	-0.01	-0.01	0.03	0.01	0.01
d15Nasx	-0.83	-0.38	0.36	-0.09	-0.09	-0.07	-0.01	0.05	0.01	0.03	0.06	0.02	-0.02	0.06	-0.08	0.01	0.00	-0.01	-0.05	0.00	0.02
d15Npro	-0.75	-0.51	0.29	0.04	0.17	0.15	-0.13	-0.02	0.00	-0.01	0.11	-0.05	-0.05	-0.01	0.06	0.04	0.01	0.00	0.02	0.01	0.02
d15Nval	-0.85	-0.25	0.30	-0.18	-0.05	-0.18	0.14	0.14	0.11	0.07	-0.06	-0.02	0.01	-0.01	0.04	-0.01	-0.02	-0.01	0.02	-0.03	0.01
d15Nleu	-0.92	-0.16	0.27	-0.06	-0.03	-0.03	0.14	-0.01	0.07	-0.06	-0.01	0.00	-0.04	-0.08	-0.01	-0.04	0.04	0.04	-0.01	0.03	-0.01
d15Nthr	0.73	-0.37	-0.36	0.26	0.04	-0.23	-0.06	0.21	0.09	-0.11	0.04	-0.01	-0.02	0.04	0.02	-0.02	0.00	-0.01	0.00	0.02	0.00
d15Nlys	-0.17	-0.87	-0.07	0.30	-0.12	-0.24	-0.06	-0.16	-0.03	-0.01	-0.08	0.03	0.00	-0.06	-0.01	0.04	-0.02	0.01	0.00	0.00	0.00
d15Nphe	0.57	-0.74	-0.11	0.01	-0.24	0.04	-0.10	-0.05	0.03	0.17	0.07	-0.07	0.00	0.02	0.00	-0.04	0.04	0.01	0.01	-0.01	-0.02

Samples scores

	PC1	PC2	PC3	PC4	PC5	PC6	PC7	PC8	PC9	PC10	PC11	PC12	PC13	PC14	PC15	PC16	PC17	PC18	PC19	PC20	PC21
ABF3	-6.85	-0.04	-1.72	-0.72	-0.35	-0.85	0.03	0.65	0.06	-0.53	-0.02	0.03	0.20	-0.07	0.07	-0.12	-0.35	0.00	-0.02	-0.09	-0.14
HSLA	-6.28	-0.03	-2.05	0.17	1.27	-0.18	0.61	-1.16	-0.43	-0.29	-0.21	0.08	-0.20	-0.20	-0.10	0.17	-0.04	0.13	-0.11	0.15	0.03
HSSP1	-5.86	2.91	0.37	1.98	-2.03	1.34	0.39	0.52	-0.06	-0.60	-0.20	0.34	-0.06	0.38	-0.05	0.11	-0.07	-0.09	0.09	-0.08	0.04
HSSP2	-5.63	2.11	0.84	-1.23	-0.53	-0.39	0.29	-0.13	0.02	-0.28	-0.14	0.15	0.34	-0.23	0.07	0.21	-0.01	0.25	0.25	-0.10	-0.02
SSF2	-9.00	-1.45	2.17	-0.69	-0.56	0.02	-0.90	-0.19	-0.04	0.16	-0.15	-0.24	0.36	0.16	0.54	0.05	0.18	0.02	-0.07	-0.03	-0.05

SSF5	-7.81	0.16	-3.64	0.58	0.32	-1.01	0.01	-0.51	0.56	0.45	-0.51	0.05	-0.12	0.07	0.14	-0.05	-0.02	-0.25	-0.04	-0.10	0.09
PSSC2	-6.29	2.32	2.35	-1.79	-1.26	-1.04	-0.42	-0.08	-0.73	0.73	0.70	-0.17	-0.05	0.01	-0.24	-0.13	-0.01	-0.09	0.00	0.01	0.14
PSSP1	-4.23	0.13	0.94	-0.46	-0.25	-1.14	0.01	0.82	-0.20	-0.08	-0.69	0.25	-0.19	0.32	-0.33	0.02	0.10	0.01	-0.09	0.18	-0.04
HSSSQ	-7.81	0.98	-0.15	1.40	-1.17	1.09	-0.02	-0.83	0.06	-0.49	0.33	-0.18	-0.18	-0.39	-0.13	-0.34	0.22	0.08	-0.01	0.13	-0.01
EF8BOS?	4.15	1.77	2.21	0.59	0.14	-0.54	1.63	0.03	-0.25	0.23	-0.39	-0.05	-0.47	0.02	0.33	-0.26	-0.01	0.02	0.02	-0.01	0.05
PSC2	1.29	0.38	-0.70	-0.15	-0.08	-0.37	0.72	-0.17	0.36	0.59	-0.04	0.63	0.15	-0.19	0.20	-0.11	0.00	-0.09	0.16	0.11	0.00
VESH1	2.73	2.83	-0.05	-0.59	0.38	0.68	-1.19	-0.30	0.06	0.23	-0.23	0.41	-0.20	0.17	0.01	-0.17	0.00	0.00	-0.05	-0.05	-0.15
VEDE1	2.92	1.81	0.76	0.14	0.57	0.83	-0.63	-0.64	0.12	0.42	0.00	0.63	0.19	0.02	0.08	-0.14	-0.16	0.23	0.01	-0.05	0.09
VEHO1	1.29	3.17	-2.50	0.60	0.76	-0.73	-1.11	0.61	-0.33	-0.35	0.82	0.27	-0.58	0.12	0.25	0.08	-0.01	0.06	0.07	0.08	0.00
VEHO3	3.31	3.43	-0.13	0.04	-0.35	-0.03	0.23	0.11	0.59	-0.18	0.24	-0.70	0.21	0.05	-0.05	-0.25	-0.23	0.14	-0.08	0.06	0.00
VEHO4	2.39	2.00	-0.27	0.48	0.22	-0.22	-0.43	-0.91	0.54	0.17	0.12	-0.73	0.05	0.35	0.03	0.38	-0.09	0.04	0.02	0.08	0.00
EF10OC	3.58	2.04	0.92	0.50	-0.87	-0.75	0.80	-0.37	0.15	0.40	0.10	0.03	-0.26	0.08	-0.20	0.26	0.21	0.07	0.05	-0.13	-0.17
EF7OC	2.06	2.20	-0.97	-0.65	-0.61	-0.34	0.13	-0.05	0.82	0.28	0.12	0.47	0.26	-0.16	-0.22	0.04	0.09	0.07	-0.09	0.06	-0.09
EF8SG	3.63	-0.85	1.85	-0.01	-0.81	-0.41	0.13	-0.41	0.30	-0.47	0.08	0.56	0.18	0.30	0.13	-0.08	-0.12	-0.08	-0.19	0.06	0.05
EF11DOG	-0.59	-0.74	0.72	-0.78	0.11	0.99	0.37	-0.84	-0.39	0.28	0.31	-0.01	0.06	-0.05	0.00	0.15	-0.19	-0.28	-0.08	0.07	-0.11
PSCH1	0.92	1.37	0.18	1.90	0.98	-0.26	0.44	0.53	-0.93	0.22	0.05	-0.14	0.47	-0.11	0.13	0.02	-0.10	0.10	-0.01	0.06	-0.05
PSCH2	1.47	0.06	-0.73	-0.17	1.42	-0.35	-0.32	-0.35	-0.37	-0.42	-0.52	-0.02	0.31	0.14	-0.17	-0.10	0.18	0.03	0.00	-0.08	0.05
PSCH3	-0.73	1.22	-1.24	2.06	0.88	-0.01	0.38	0.44	-0.24	0.51	0.56	0.01	0.63	0.14	-0.12	-0.03	0.15	-0.12	-0.10	-0.10	0.02
PSP3	3.23	0.62	2.14	1.13	0.07	-0.40	-0.44	-0.22	-0.12	-0.55	-0.44	-0.13	-0.04	-0.20	0.01	0.08	-0.04	-0.21	-0.07	0.04	-0.08
PSP4	3.15	2.36	0.64	0.74	-0.20	-0.32	-0.78	-0.01	-0.28	0.16	-0.28	-0.41	-0.33	-0.42	0.12	-0.02	0.05	-0.09	-0.04	-0.13	-0.03
PSP5	3.34	-0.80	2.06	0.25	1.36	-1.30	-0.50	-0.39	0.15	-0.79	0.12	0.19	0.21	-0.13	-0.11	-0.02	0.04	-0.06	0.14	-0.01	0.09
1703b	2.45	-2.68	-1.26	0.22	-0.94	-0.14	-0.12	-0.10	-0.19	0.11	0.04	-0.06	-0.04	0.05	-0.01	-0.06	0.01	0.01	0.02	-0.02	-0.02
1895e	5.62	1.32	-0.95	-1.34	-0.84	0.51	0.04	0.20	-0.30	-0.24	-0.31	-0.08	0.17	-0.10	0.03	0.07	0.00	0.01	-0.02	0.05	0.08
723w	3.62	-0.90	-1.30	-0.45	-0.85	0.15	-0.04	0.03	-0.23	-0.01	-0.12	-0.08	0.04	0.02	0.00	0.00	0.04	-0.01	0.00	0.00	0.02
1703w	3.33	-0.73	-1.63	-0.47	-0.80	0.17	-0.04	0.00	-0.24	0.04	-0.11	-0.10	0.01	0.06	0.00	-0.02	0.06	-0.02	-0.01	0.00	0.01
BarleyP	4.88	1.62	-1.72	-1.34	-0.72	0.55	0.06	0.14	-0.34	-0.10	-0.32	-0.15	0.11	0.00	0.02	0.04	0.07	-0.04	-0.01	0.02	0.07
LBCFA16F	2.24	-3.85	-0.78	0.60	-1.01	-0.29	-0.18	-0.12	-0.12	0.09	0.11	-0.01	-0.02	0.02	-0.01	-0.04	0.01	0.04	0.03	-0.02	-0.02
LBCFD16E	2.35	-4.55	-0.30	0.81	-1.10	-0.38	-0.22	-0.12	-0.08	0.04	0.15	0.03	0.00	-0.03	-0.01	-0.02	-0.02	0.08	0.04	-0.01	-0.01
LBTA1012I	3.97	-0.50	-1.26	-0.60	-0.85	0.23	-0.04	0.05	-0.25	-0.04	-0.16	-0.09	0.07	-0.01	0.01	0.02	0.04	0.00	0.01	0.01	0.04
LBTD1012H&I	2.17	-5.09	-0.14	1.00	-1.14	-0.46	-0.25	-0.14	-0.06	0.05	0.19	0.05	0.00	-0.04	-0.01	-0.02	-0.03	0.09	0.04	-0.01	-0.02
F10I11	0.37	0.00	-0.05	-0.69	0.18	0.24	0.40	-0.01	0.43	-0.60	0.42	-0.13	-0.18	0.02	0.11	0.06	0.11	-0.08	-0.07	-0.18	0.07
F10I14	-0.82	-0.79	0.29	-0.10	0.90	1.09	-0.37	0.11	-0.58	0.21	-0.08	0.45	-0.10	-0.07	-0.11	0.15	-0.09	-0.12	0.10	-0.03	-0.02
F10I16	0.11	-0.86	1.13	0.35	0.51	0.34	-0.41	0.37	0.30	-0.01	-0.09	-0.02	0.11	-0.13	-0.07	-0.06	-0.05	-0.13	0.05	0.09	-0.07
F10I17	-1.66	-1.00	0.49	0.49	0.62	0.39	-0.10	0.20	0.43	0.43	-0.48	-0.23	-0.05	0.07	0.03	-0.09	0.09	0.05	0.05	0.05	0.01
F10i20	-0.44	-0.28	-0.06	-0.19	0.01	0.33	0.07	0.84	0.27	0.12	-0.05	-0.23	0.06	-0.24	0.20	0.19	0.08	-0.02	0.13	0.18	0.03
F10I28	0.13	-0.55	0.66	0.20	-0.08	0.06	-0.07	0.48	0.54	0.06	0.12	-0.07	-0.04	-0.22	-0.19	0.19	-0.10	-0.21	-0.01	0.01	0.08
F12I23	-1.47	-1.12	0.37	0.14	0.28	0.27	-0.41	0.36	0.22	0.39	-0.31	-0.05	-0.33	-0.18	-0.24	-0.01	-0.17	0.15	0.05	-0.14	0.05
F12i28	-0.19	-1.04	0.47	-0.68	0.56	0.25	0.48	0.41	0.11	-0.17	0.41	0.45	-0.18	-0.22	0.15	0.19	0.24	0.08	-0.26	-0.06	0.01

F12I3	-0.45	-0.51	0.78	0.25	0.55	0.47	-0.18	0.50	0.58	0.12	0.15	-0.01	-0.07	-0.04	-0.03	-0.04	0.02	-0.05	0.05	0.02	0.09
F7i10	-0.82	-1.52	0.20	-0.57	0.47	0.09	0.33	0.39	-0.04	0.07	0.02	-0.13	-0.15	-0.18	-0.01	0.00	-0.25	0.12	-0.27	-0.07	-0.02
F7I7	0.01	-1.62	-0.08	-0.75	0.68	0.04	0.47	0.02	0.09	-0.17	0.40	0.00	-0.17	0.26	0.04	-0.09	-0.04	-0.04	0.19	0.09	-0.07
F8I23	0.24	-0.50	-0.08	-1.11	0.91	0.30	0.68	-0.37	-0.22	-0.28	0.19	-0.23	-0.08	0.20	-0.09	-0.19	-0.01	-0.13	0.16	-0.11	-0.04
F8I6	-0.14	-0.38	-0.21	-0.75	1.03	0.38	0.11	0.43	0.17	-0.19	0.05	-0.21	0.22	-0.08	-0.11	-0.16	0.20	-0.03	0.02	-0.05	-0.08
F8I7	-1.38	-1.48	-0.15	-1.00	0.92	0.36	0.09	0.22	0.07	0.16	0.02	-0.23	-0.20	0.18	0.07	-0.07	0.06	0.02	0.02	0.05	-0.04
F9I13	-1.09	-1.20	0.78	0.31	0.63	0.38	-0.11	0.22	0.03	0.10	0.01	-0.08	-0.06	0.37	-0.08	-0.01	0.09	0.18	-0.12	0.03	0.02
F9I9	-1.41	-1.75	0.83	0.36	0.66	0.39	0.39	-0.23	-0.02	0.03	0.01	-0.11	-0.05	0.10	-0.05	0.21	-0.12	0.13	0.05	-0.05	0.08

Table F.2 Principal component analysis output using source and trophic amino acids (PCA-TAA).